

On the Origin of Extraterrestrial Industrial Civilizations

Steven Suan Zhu

June 23, 2018

Washington University in Saint Louis

suan.zhu@wustl.edu

Abstract

The emergence of intelligence is likely a relatively recent phenomena throughout the cosmos. The total number of habitable extraterrestrial planets within the Milky Way capable of supporting advanced, intelligent life within the next 500 Myr is $<10,799$. Almost all of which are earth-like orbiting around a single star with mass ranges from 0.628 to 1 solar mass. No exomoons are capable of supporting advanced life, and a negligible number of low mass binary systems (<0.628 solar mass) are habitable. The nearest extraterrestrial industrial civilization lies at least 88.7 million light years away, and possibly 111 million light years beyond. No extraterrestrial civilization arises before 232.74 Mya within the observable universe, and no extraterrestrial civilization arises before 270.95 Mya within the universe by co-moving distance. Despite great distances between the nearest civilizations and the low probability of emergence within our vicinity, given the sheer size of the universe, the total number of intelligent extraterrestrial civilizations likely approaches infinity or $\left(\frac{1}{4.4 \cdot 10^7}\right)^3 \cdot 3.621 \cdot 10^6 \cdot 10^{10^{122}}$ if the universe is finitely bounded. Based on incentives for economic growth, all civilizations tend to expands near the speed of light and will eventually universally connect with each other via wormhole networks. Within such a network, the furthest distances traversable from earth can be either infinite or $3.621 \cdot 10^6 \cdot 10^{10^{122}}$ light years in radius if the universe is finitely bounded.

Keywords: Principle of Mediocrity, Paradigm Hierarchy, Gaussian Distribution, Log-Normal Distribution, Uniform Distribution, Darwinian Biological Evolution, Biological Complexity, Complexity Equivalence, Complexity Factor Transformation, Law of Accelerating Return, Special Relativity, General Relativity, Hubble Constant, Relativistic Finance, Nash Equilibrium, Worm Holes, Alcubierre Drive, Phase Transition, GFK spectral class, Exoplanets, Exomoons

Contents

1	Introduction	5
1.1	New Understanding Sharpens the Fermi Paradox	5
1.2	Assumptions in the Solution to the Fermi Paradox	6
1.3	Reconciliation of the Principles of Mediocrity with the Rare Human Hypothesis	10
1.4	Our limited Observation Window	13
2	Number of Terrestrial Planets in Habitable Zone	15
2.1	Temporal Window and Galactic Habitable Zone	15
2.2	Definition of Stellar Habitable Zone	16
2.3	Definition of Sun-like Stars	18
2.4	Number of Stars	20
2.5	Peak of Terrestrial Planet formation	23
2.6	Excluding Over-counted Binaries and Multiples	24
2.7	Habitability of Low Mass Binaries	56
2.8	Red Dwarves' Habitability	60
2.9	Habitability of Exomoon	68
3	Number of Earth	72
3.1	Orbital Eccentricity	72
3.2	Orbital Period	73
3.3	Earth & Moon Separation	75
3.4	Earth-Moon Collision Probability Explanation	82
3.5	The Right Rotational Speed	90
3.6	Moon's Obliquity Evolution	94
3.7	Earth Size	95
3.8	The Chance of Getting Watered	97
3.9	Total Water Budget of Earth	101
3.10	Right Ocean & Land Mix	105
3.11	Plate Tectonics	112
4	Evolution	115
4.1	Water vs. Other Solvents	115
4.2	Biocomplexity Explanation	116
4.3	Probability on the Emergence of Prokaryotes from Amino Acids	117
4.4	Probability on the Emergence of Eukaryotes, Sex, and Multicellularity	121
4.5	Speed of Multicellular Evolution	125
4.6	BER	135
4.7	Continent Cycle	135

4.8	Continental Movement Speed	140
5	Homo Sapien Emergence Probability	143
5.1	Why Human Did not Appear Earlier	143
5.2	Ice Age as an Accelerator and Its Causes	144
5.3	Expected Ice Age Interval	146
5.4	Supercontinent Cycle and Ice Age	164
5.5	The Probability of the Hominid Lineage	171
5.5.1	Binocular Vision	172
5.5.2	Large Cranial Capacity	173
5.5.3	Language	173
5.5.4	Bipedal	174
5.5.5	Thumbs	174
5.5.6	Social	175
5.5.7	Omnivorous Feeding	175
5.6	The Probability of Alternative Intelligence	186
5.7	Probability of the Emergence of Homo Sapiens within the Genus Homo	191
5.8	Probability of Fruit Trees	192
5.9	Probability of Crop Plants	193
5.10	Probability of Angiosperm	195
6	The Distribution Model	196
6.1	Mathematical Model for Human Evolution	196
6.2	Background Rate	198
6.3	Counting YAABER	204
6.4	YAABER for Evolution of Homo Sapiens	209
6.5	YAABER for Hunter Gatherer	211
6.6	YAABER for Feudal Society	213
6.7	YAABER for Industrial Society	221
7	Model Predictions	229
7.1	Number of Habitable Earth	229
7.2	The Model	231
7.3	The Wall of Semi-Invisibility	237
7.3.1	Base Case:	244
7.3.2	Inductive Step:	247
7.4	Complexity Equivalence	264
7.5	Complexity Transformation	268
7.6	Darwin's Great-Great Grandson's Cosmic Voyage	270
7.7	Upper Bound & Lower Bound	272

7.8	Subluminal Expansion	275
7.9	Observational Equations	276
8	Relativistic Economics	280
8.1	Overview	280
8.2	Earthbound Democracy	294
8.3	Earthbound Investing Nearest Galaxy	295
8.4	Galaxy Bound Investing Nearest Galaxy	297
8.5	Earthbound Ruling Class	298
8.6	Shipbound with Energy Gathering Case	300
8.7	Shipbound as Lottery Winners Case	302
8.8	Post-Singularity	303
8.9	Expansion Speed from Outsider's Perspective	306
8.10	Worm Hole	309
8.11	Worm Hole Maintenance Cost	319
9	The Principle of Universal Contacts	326
9.1	$E(d, v)$ Derivation and the Limit of Our Reach	326
9.2	Connected/Disconnected	337
9.3	Cosmic Nash Equilibrium	343
9.4	Looking Back in Time	345
10	Conclusion	351
10.1	Extra-terrestrials vs. Time	351
10.2	Final Thoughts	353

1 Introduction

1.1 New Understanding Sharpens the Fermi Paradox

The recent discovery by Kepler Exoplanet hunting mission revealed that Earth-like planets within the habitable zones of main sequence stars in the Milky Way galaxy might well be within the range of billions.[22] On the other hand, a practical technique to achieve nuclear fusion using the project PACER approach, which was further refined upon using small yield hydrogen detonation device with minimal fissioning plutonium underground concrete cavity[27][91] has guaranteed a cheap, sustainable energy budget for industrial use into the indefinite future.[47] Therefore, a Hubbert like peak of resource exhaustion due to falling EROEI for fossil fuel based industrial civilization can be avoided technically speaking.[47][46][57][92] Though energy conservation must be enacted in the future for such scenario to hold and to avoid Jevon's Paradox as a planet based civilization.[43] Furthermore, city-sized spaceship based on nuclear fusion power plants based on Project PACER model, also enable human interstellar travel in less than geological timescale and magnitudes lower than astronomical scales.[89] Based on the calculation, nuclear fusion powered vessels are capable of carrying the total population of human race to any predetermined destinations in a few generations with fully furnished and self-sustaining life quarters at up to a small fraction the speed of light c . If nuclear fusion inter-stellar vessels project is initiated, populations magnitudes higher than the current population can be migrated to predetermined destinations. Assuming every extraterrestrial industrial civilization arise in the Milky Way follow a similar developmental pattern of earth based on the Principle of Mediocrity, we should expect them to discover at least project PACER model of nuclear fusion. They should also be able to confirm the existence of billions of habitable planets scattered in their galaxy. Then, a strong case is presented for their preference to expand and explore the galaxies less than geologic time and bounded by the speed of light from stationary observers on earth at a maximum of 10^5 years for the diameter of the entire galaxy disk. (10^5 yrs $<$ $x < 10^9$ yrs) However, no overwhelming scientific evidence since the inception of SETI project has proved that any star in the Milky Way host an industrial civilization. Given the age of Milky Way Galaxy at 10^{11} yrs and the Principle of Mediocrity applying to the temporal aspect of cosmic biological evolution, then the chance that all extraterrestrial industrial civilization evolved at around the margin of 10^4 yrs so that they currently remain undetectable is $\frac{10^4 \text{ Yrs}}{10^{11} \text{ Yrs}} = 10^{-7}$ for each habitable planet. With 10^9 habitable planets within the galaxy, the chance is 10^{-16} in Milky Way alone. This chance can also be argued as the chance of success of extraterrestrial industrial civilization arising in our galaxy yet we failed to observe them so far. Indeed, this hope crushing number can be interpreted as such that our chance to colonize the galaxy is not much greater than 0. Assuming intelligent life can be evolved easily and transforms into an industrial civilization and all intelligent life destroys themselves eventually regardless their worldview and culture. However, I have just shown that cosmic expansion

is the predicted outcome of industrial civilization. Furthermore, the recent analysis that an average earth-like habitable planet has a median age of 78 Gyr, that is 25 Gyr ahead of earth in development. Paradoxically, advocates of Technological Singularity argues for accelerating return generalized from the Moore's Law and expect machine intelligence overtaking human intelligence around mid-century. [58][93] Robotic successors to biological humans, capable of greater endurance in all types of environments deemed hostile to biological life, can accelerate industrial civilization expansion faster and by more economical means. This is shown as rover opportunity still roaming on Mars at the temperature and atmospheric pressure significantly lower than earth after a decade following the assumed lifespan for its exploratory mission. On one hand, we have shown the predicted expansion trajectory for the future of human or human-machine industrial civilization. On the other hand, an eerily silent sky filled with billions of Earth-like planets in the Milky Way galaxy yet no detectable sign of industrial civilization comparable to our current epoch and earlier. The immense discrepancy between two sides sharpens the Fermi Paradox more than at any time before. Even more disturbingly, billions of galaxies exist within the observable universe, assuming the universe is isotropic, then each of these galaxies should hold billions of Earth-like planets as well. A study done in late 2014 to detect infrared emission proposed by Freeman Dyson and hunting for galaxy wide Dyson sphere energy harvesting civilization from the most promising and suspicious 100,000 galaxies within a light cone of $2 \cdot 10^8$ light years found nothing unusual. [48]

It is then of paramount importance and urgency to resolve this paradox with every tool and piece of knowledge we currently have, though probably still incomplete or never will be truly complete. The most significant central concern of Fermi Paradox is to address the problem of sustainability of industrial civilization; therefore, the resolution of an astrophysical-biological question has an immediate terrestrial interest.[18]

1.2 Assumptions in the Solution to the Fermi Paradox

We shall make some assumptions before our further discussion.

First, any intelligent civilization, no matter how efficient they are at energy manipulation, even down to Planck scale or beyond, still expands until it meets another extra-terrestrial civilization's sphere of influence or had grabbed all possible resources reachable. After that point in time, whether the extraterrestrial civilization will continue to consume its energy in an exponential growth based model and collapse or resort to energy conservation is not a concern for this assumption to hold. British economist Jevon in 1865 made a strong case that more efficient use of coal in Britain led to more rapid and greater consumption of the same resource. This is called the Jevon's Paradox.[10] This is further elaborated in scenarios of post-singularity civilization. Other compelling reasons for expansion will be discussed in later sections but should not be mentioned here, because these reasons are derived from this basic

assumption.

Secondly, no overwhelming evidence of any extraterrestrial industrial civilization based on our current observation of the Milky Way and beyond implies the non-existence of human comparable or beyond at that point in time where the information transmitted from that original source point. That is, we do not see evidence of extraterrestrial civilization from a star 2,000 light years away implies that there is no emerged extraterrestrial industrial civilization from that star 2,000 years ago or earlier. A natural looking galaxy lying 20 million light years away implies that no emerged extraterrestrial industrial civilization from that galaxy 20 million years ago or earlier based on the speed of light to a stationary observer on earth.

Thirdly, our current knowledge and understanding regarding harnessing nuclear fusion is sufficient evidence or a counterexample to suggest that physics and nature do not impose a ceiling on the amount of available energy a civilization can achieve before it reaches an interplanetary and a galactic scale. Once it does, it can expand at sub geological time scale and bounded by the speed of light. Our local derivations of physical laws apply universally throughout the universe. It is still possible that the civilization destroys itself through nuclear wars, biological warfare or self-decay. However, such scenarios are social and culturally specific, it does not universally apply to all possible emerging civilizations given the sheer number of Earth-like planets in the entire observable universe.

Lastly, all potentially habitable planets within the habitable zones of their parent star contain a hospitable environment for life. The low eccentricities of planet orbit, the presence of moon is not considered to be essential to the emergence of intelligent life. (Furthermore, it is assumed earth and moon type of binary planetary system are common. The reasoning behind this will be further explained in section Reconciliation of Principles of Mediocrity with Rare Human Hypothesis. Calculation is presented to explain why moons are common in Chapter 2) This is a possible overstatement since Mars, also lie on the outer edge of the habitable zone is currently inhabitable. The motive behind the assumption that all potentially habitable planet with at most one magnitude within the range of earth's condition such as water presence, atmospheric pressure, oxygen abundance is to accommodate the principle of Mediocrity, showing mathematically an upper bound on the shortest possible temporal time span and spatial distance to find nearest extra-terrestrial industrial civilization.

These assumptions led us to case scenarios. If we consider $pq=w$. Where w is the probability that expanding industrial civilization exists in a given region excluding earth, and p is the probability that intelligent life evolves in somewhere other than earth and q is the probability that laws of physics permits such intelligent species eventually expands. Then, from assumption 3), we know that $q=1$. Yet we know from assumption 2), that $w \leq 10^{-16}$ for region occupying the Milky Way galaxy with a temporal range between $13.2 \cdot 10^9 > x > 10^5$ years ago. This implies that $p \leq 10^{-16}$ for region occupying the Milky Way galaxy. This concludes that there is an extremely high probability ($1 - 10^{-16}$) that intelligent life does not exist somewhere other than earth within the Milky Way region with a temporal range between $13.2 \cdot 10^9 > x > 10^5$

years ago. We do not know the more recent 10^5 years because signals from the outermost regions of the galaxies take 10^5 light years to reach observers on earth. However, given the sheer size of the observable universe, which makes up with $> 10^{11}$ galaxies, then $p \leq 10^{-5}$ for region occupying the observable universe. This concludes that there is a good probability ($1 - 10^{-5}$) that intelligent life does not exist somewhere other than earth within the observable universe region with a temporal range between $13.2 \cdot 10^9 > x > 10^5$ years ago. It will take a stationary observer on earth at most $13.2 \cdot 10^9$ more years to verify the validity of the prediction because signals from the outermost edges of the observable universe take $13.2 \cdot 10^9$ light years to reach observers on earth. Furthermore, given the sheer size of the entire universe, which can be infinite in size, then $p \leq 1$ for region occupying the universe is possible but it can take a stationary observer infinite amount time to verify apart from observational limitation due to the expansion of the universe and redshifts.

This all suggests that intelligent life evolved on earth is rare both in space and time since the Big Bang.

However, further extrapolation leads into 4 case scenarios.

First, the earth continues to be rare or even rarer in space and time. In this scenario, events observed on earth are almost never repeated anywhere in the universe for an infinite amount of time into the future. Then, the chance of encountering any intelligent civilization infinitely approaches 0 from now to infinitely long future periods.

Secondly, earth-like cases become more frequent in space but not in time. This case is slightly optimistic but similar to the first case, where intelligent life forms evolve on Earth-like planets can repeatedly happen in the same galaxy or even neighboring stars many times, but each is separated by billions and trillions of years apart. In this case, communication can be unidirectional where an ancient civilization communicates to the younger through ancient remains and assuming symbols can endure such long epochs, but such communication is irrelevant to bidirectional communications shall be concerned in this paper.

Thirdly, earth-like cases become more frequent in time but not in space. This case is similar to the second and also slightly more optimistic than the first. Whereas each extraterrestrial civilization is emerging only by 10^5 years or less apart from each other but given the sheer size of the universe, each is separated from each other by billions or trillion light years apart. Whereas it is possible that every galaxy can guarantee the emergence of intelligent industrial civilization but only at an infinite amount of time assuming the infinite size of the universe.

Finally and most interestingly, earth-like cases become both frequent in space and time. This scenario requires particular attention because it implies encountering with extraterrestrial civilization is bounded by a limited temporal range and limited spatial distance. We shall model and abstract all scenarios of encountering behaviors based on this case. Since the first case is trivial to show or derive (it simply states that earth is a sporadic event and never repeated again), then we can show that scenario 2 and scenario 3 falls between scenario 1 and scenario 4. Models from scenario 4 can also be applied to scenario 2 and 3. If scenario 4 is true where life is

assumed to exist and abundant starting now and into the future yet its evolutionary trajectory has to satisfy our current understanding of biology, chemistry, and physical constraints. Then *these constraints create an illusion that we are alone as far as our current observation dictates yet it can be shown mathematically that they must exist*. Any intelligent life in the universe arising should be well-aware of their “neighbors” well before they ever detect them through physical means.

Fortunately, existing literature suggests that scenario 4 is possible. Two camps, the catastrophic camp and bio-complexity camp supports scenario 4. The great concerns and differences have been raised by two different camps, but both arrived at the same conclusion. That is, complex, intelligent, and technological life has only recently begun to appear in the universe.

The catastrophic camp argues that a cosmic phase transition is taking place because cosmic regulating mechanisms such as Gamma Ray Bursts, and Quasar-like super black holes were dominant in the cosmic past since the Big Bang. Prior to the formation of galaxy spiral arms, stars are much closely packed and Supernovae explosion causes great havoc on potentially life-bearing planets. If only the simplest and the sturdiest survives from each holocaust, each event disrupts biological evolution and systematically resets regional and global fauna complexity and diversity. The frequency of cataclysmic global events guarantees the universe remains silent. In the recent epoch, the evolution of spiral arms in galaxies and an exponential decrease in the large energetic release of cosmic events contributes to the growth of biological complexity and diversity guaranteeing the emergence of industrial civilization.

On the other hand, the bio-complexity camp argues that the biological complexity encoded in DNA, RNA, and epigenetics, and functional modularity increases over geological time.[87] If all genome complexity is considered and follows the Law of Accelerating Return of complexity doubling over a period $3.75 \cdot 10^8$ yrs as observed on earth from the prokaryotes to mammalian lineage, then, prokaryotes dispersed to earth by panspermia must be formed before the formation of the sun. Reaching prokaryotes level of biological complexity from a single pair of DNA requires another 5 Gyr prior to the formation of the sun. Thus, life evolved before earth. This camp also frequently cites the contradiction between rapid emergence of Prokaryote life following the Late Heavy Bombardment, yet it is never synthetically replicated in laboratory settings as an evidence supporting their hypothesis. A weaker argument can also be used to support their view given the metallicity of older stars belong to generation II are about 1~2 magnitudes lower than the sun, it has been shown that metal-poor stars offer a lower chance of planet formation and life on earth demonstrates the necessity of elements higher than Helium. However, a careful analysis of host star age and its metallicity shows a weak positive correlation, where metal-rich stars exist among the very old, and metallicity buildup of stars following the first 10^9 yrs is slow compares to the earliest times. Therefore, enough metallicity is sufficient to sustain life 10^9 yrs after the big bang, which nevertheless is consistent with their hypothesis that life evolves early.

Both camps agree that the universe is undergoing a cosmic phase transition where a lifeless

universe is transitioning toward one filled with life.[98][66] However, a crucial difference exists where the catastrophic camp believes that life is easy to evolve at any time and at anywhere as long as global cataclysmic regulatory mechanisms cease. The biological complexity camp holds that evolution of life was a slow and hard process, complexity doubling was slow from the very start; therefore, even if the universe were conducive to the evolution of life from very early on, the universe would still be lifeless until very recently. In this paper, the author is inclined toward the catastrophic camp, mainly persuaded by the mathematical models (including derivations from molecular biology, confirming punctuated equilibrium which formed as one of the pillars of the entire model) build in order to resolve this paradox.

1.3 Reconciliation of the Principles of Mediocrity with the Rare Human Hypothesis

If extraterrestrial life is now becoming abundant in all possible earth-like exoplanet candidates given in scenario 4, we still need to analyze the median and mean average level of bio-complexity of the highest form of life currently attained for each of these planets. In order to solve this problem, we need to reconcile the rare human hypothesis (that human-like intelligent life with opposable thumbs, bipedal locomotion, big brain, omnivorous diet, binocular vision, land residing, and complex language to grow knowledge in successive generations) to a weaker form of rare earth hypothesis with the Principle of Mediocrity. It basically states that if an item is drawn at random from one of several sets or categories, it's likelier to come from the most numerous category than from any one of the less numerous categories.[56] The principle has been taken to suggest that there is nothing unusual about the evolution of the Solar System, Earth's history, the evolution of biological complexity, human evolution, or the developmental path of civilization leading to expanding cosmic civilization. It is a heuristic in the vein of the Copernican principle and is sometimes used as a philosophical statement about the place of humanity. The idea is to assume mediocrity, rather than starting with the assumption that a phenomenon is special, privileged, exceptional, or even superior.[19, 75]

Before the discovery of exoplanets and Kepler's mission for exoplanets, a rare earth hypothesis generally assumed that Earth-like planets and possibly even planets are rare in the galaxy and the universe. However, it is now believed that as many as 40 billion Earth-sized planets orbiting in the habitable zones of sun-like stars and red dwarf stars within the Milky Way Galaxy alone, based on Kepler space mission data.[22] 11 billion of these estimated planets may be orbiting sun-like stars.[41] The nearest such planet may be 12 light-years away, according to the scientists. However, it is equally erroneous to assume that all life-bearing planets underwent exact or very similar evolution happened here on earth where intelligent creatures similar to human in almost every aspect. This over-generalization is in direct contradiction with the evidence obtained from our local neighborhood with a high confidence. For the delay in light

signal transmission between $0 < x < 10^5$ years, there is a low probability that all intelligent life evolved recently within a window of $0 < x < 10^5$ years in the Milky Way and not earlier. Even under the same solar radiation and environmental factors, human civilization diverged since the great exodus from Africa 100,000 years ago have evolved socially at different rates, where hunter-gatherers in Amazon forests are $10^2 < x < 10^3$ years apart in complexity from the advanced industrial nations. Therefore, the standard deviation is likely higher than $> 10^3$ years for different intelligent civilization within the Milky Way at different stages of development even if global regulating mechanisms persisted in the past suppressing the early emergence of complex life or genomic complexity and functional complexity of life and just recently enabled human level observers to exist. It is much more likely, that all extra-terrestrial beings, humans included are nearly identical in the physical, chemical, even biological aspects, but with differences mainly in subtle details and variations. These variations, then, prevented extra-terrestrial from cosmic expansion.

To understand this argument better, we need to introduce the following thought experiment. Imagine you are Nicolas Copernicus in the early 16th century living in celibacy. For some reason, the Pope, through prophetic dream knowing that you are going to disrupt the Catholic church when you grow up, imprisoned you since you are a baby and food is delivered to your prison cell. Separating yourself from any other human since you are born, except you are able to view the night sky from your cell. (the Pope does not know prior what kind of idea you comes up to disrupt the church, so he did not know your disruptive idea stems from astronomy) You are oblivious and unaware of your surroundings and people around you. While you are in the cell, you viewed the sky, made observations, and come up with the Heliocentric model of the universe. You, for a long time, thought that the Pope, the prison guard, and yourself are the only three people in Europe, which makes you 1 in 3 chance as the only one comes up with Heliocentrism if you follow the Principle of Mediocrity. Curiously enough, you then ask the prison guard if there are as many people in Europe as there are the number of visible stars. When the prison guard replied that there are tens of millions, your jaw dropped because you never expected these many people. Then, you start to ask yourself, if I come up with this theory, based on the Principle of Mediocrity, tens of millions must have done the same in Europe, so the chance that I am the first to write about it is 1 out of tens of millions. Because there are tens of millions of Europeans, then each of them, viewed the sky will have similar thoughts and worldviews. However, any outsider observer or us from the future will laugh at his conclusion. So how was his reasoning leading himself to the conclusion and where did the reasoning go wrong?

First of all, he assumed that everywhere in Europe, people use the same mathematics principle and equations, which is true. He assumed everyone lives on land just like himself and subjected to the laws of physics and electromagnetism, which is true. Then, he assumed that everyone is made of chemical composition with Carbon, hydrogen, oxygen atoms, which is also true.

Then, he further narrows down his assumptions that everyone is made of flesh and blood if the biological condition is universal among all humans: they all subject to the laws of biology, they follow specific developmental patterns, they grow hair, has two pairs of eyes, ears, legs, and arms. They are capable of self-cognition, comprehension, and language communication. This is again also true. Then, he even narrowed his assumption further and reasoned that everyone in Europe drinks beer and lives in a temperate climate like that of Poland if ecological conditions are same throughout Europe. This is only partially true because Italians, Greeks, and Spaniards enjoy a Mediterranean climate and frequently drinks wine. Then, he further reasoned that all European speak the Polish language if cultural is universal. This is assumption starts to deviate from the objective truth because only Polish people speak the Polish Language. Then, he further assumes that everyone in Europe bears the last name Copernicus if everyone descended from the same family. This over-generalization does not even apply to most Polish people. Finally, he reasoned that all Europeans have an unquenchable curiosity for astronomy and did extensive analysis of motions of heavenly bodies and came up with the Heliocentric model. In reality, only himself came up with the theory.

The conclusion from the thought experiment is significant because one should not be alarmed by the discovery of billions of Earth-like planets in the Milky Way galaxy. This does not imply every planet currently hosts an earth-like expanding industrial civilization. However, based on the evolutionary paradigm hierarchy, it is certain without a doubt these planets use the same mathematical formula just like on earth, and are subject to the same physical laws with more or less gravitational effect. Their biological body made up of oxygen, hydrogen, carbon, and maybe few different atoms not abundant here on earth. Even possibly we all share many similiar biological characteristics such as DNA blueprint, sexual reproduction, and multi-cellularity. However, it is likely that they evolved bipedal locomotion, opposable thumbs but no big brain. Or Having all the attributes of human but lived on an exclusively carnivorous diet so that agricultural revolution is not possible and civilization can only be maintained at a low level of complexity. Or they are omnivorous like human but lacks the essential crop plants to usher themselves into an agriculture revolution and creates a civilization with high population density. Therefore, we could even refine our hypothesis as *Many-earth to fewer habitable to fewer hunter-gatherer to rarer agricultural to industrial to an exceptionally rare cosmic expanding human hypothesis*, which truly captures the essence of the Fermi Paradox. It is then not surprising, to predict that intelligent life forms may already present, if not abundant in the Milky way under scenario 4 complied with the Principle of Mediocrity but lacks some trivial yet essential ingredients to usher themselves into a full-blown cosmic expanding industrial civilization.

1.4 Our limited Observation Window

To put our current lack of observation of extra-terrestrial civilization into perspective, the temporal window that is visible currently to us is very limited, yet we are looking for a resolution. By plotting the graph of all possible signals ever reachable from earth, we can compute the fraction of all possible signals we are receiving.

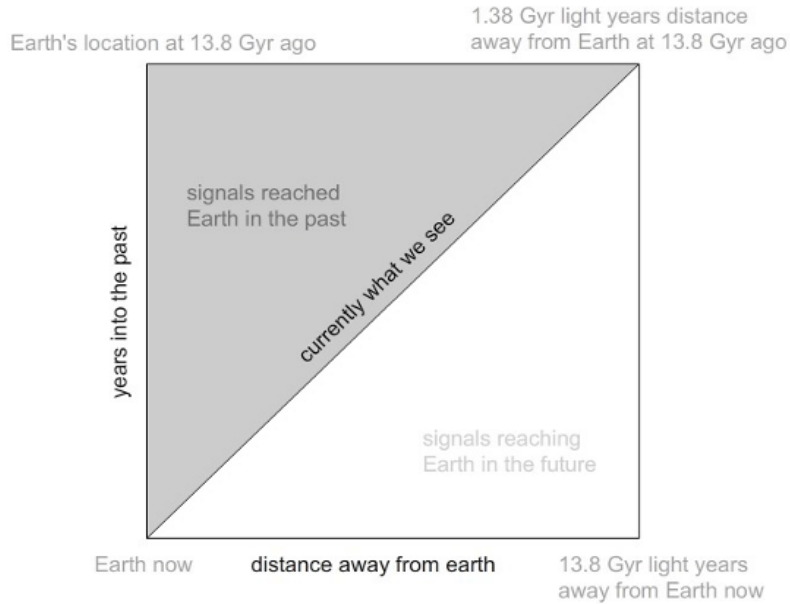


Figure 1.1: Signal detection landscape of time vs distance

From the graph, one can see that the vertical axis indicates the passage of time where the past 13.8 Gyr ago starts from the top and reaches the bottom which is the current present time. The horizontal axis represents the distance away from earth in units of light years, whereas the leftmost point represents 0 light years away from earth, the rightmost point represents 13.8 billion light-years away. The diagonal line represents the signals we are currently experiencing. That is, signals from 13.8 billion light years away had just had enough time to reach us and all remaining signals from 13.8 billion years ago up to today had yet to be received. Somewhere along the diagonal, say 6.5 billion light years away, any signals sent from earlier than 6.5 billion years ago had passed earth and signals emitted from 6.5 billion years ago is reaching earth right now, and signals emitted later than 6.5 billion years ago yet to reach us. At the leftmost point along the diagonal, which is 0 light years away from earth, all signals emitted before the present time had passed earth except the current signals and only signals yet to be emitted from the future will be captured.

Based on this graph, we can make the following logical deduction:

$$wh \geq \frac{wh}{2} \geq \sqrt{w^2 + h^2} \quad (1.1)$$

where the signals we are receiving from different types and distances away from earth is a subset of signals ever received by earth, which in turn is half all of the signals ever emitted. From a purely observational point of view, seeing the probability of extraterrestrial civilization is tiny because we can only observe a very narrow window of the range of all possible signals.

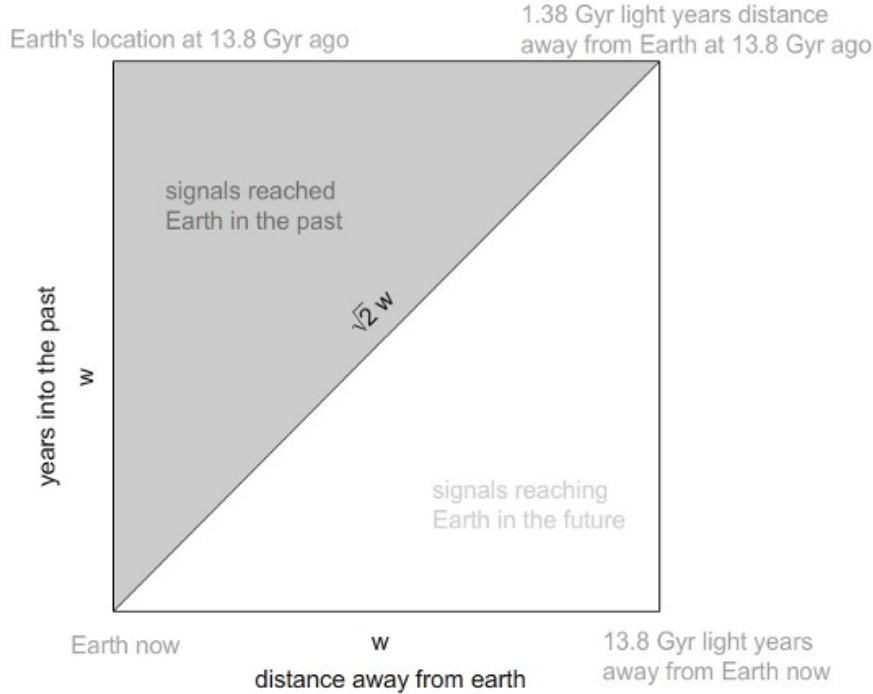


Figure 1.2: Signal detection landscape of time vs distance quantified

If we simplify the equation and assume that both the height and width of the box are of the same length, which is a reasonable assumption excluding the expansion of the universe, then the equation can be simplified as:

$$\frac{\frac{\sqrt{2}w}{2}}{\frac{w^2}{2}} = \frac{2\sqrt{2}}{w} \Rightarrow \lim_{w \rightarrow \infty} \frac{2\sqrt{2}}{w} = 0 \quad (1.2)$$

and taking the limit, we found that the observation window at the current time is diminishingly small. Of course, one can argue if extraterrestrial civilization ever expanded to include the earth from the past the earth will be transformed. The lack of evidence of artificial alteration of earth, the solar system, and the Milky Way, is an indication, that at least half the signals ever reachable since the Big Bang can be excluded from our search space, and one should focus on the remaining half. Nevertheless, the narrowness of the observational window at current time does give some solace to SETI which is complaining the eerie silence.

2 Number of Terrestrial Planets in Habitable Zone

2.1 Temporal Window and Galactic Habitable Zone

Out of the total number of earth like terrestrial planets within the habitable zones of stars with the mass range from 0.63 to 1.04 solar mass, the planets have to be formed between 5 Gyr ago and 4 Gyr ago. Prior to 5 Gyr, episodes of short Gamma-Ray Bursts, at the earlier epoch of galaxy formation, are dominant and sterilize the emergence of life from those planets.[95][94][25] The formation of terrestrial planets is correlated in both space and time. Earlier generations of planets formed closer to the galactic core, where numerous supernovae and other energetic cosmic events, as well as excessive cometary impacts caused by perturbations of the host star's Oort cloud persisted. Therefore, even if Gamma Ray Bursts becomes less frequent as the Galactic Metallicity increases (which still only reaches -0.2 near the center), earlier generations of terrestrial planets are vulnerable. Milky Way's spiral arms, constituting the Galactic Goldilocks zone with less density and higher metallicity to minimize life-threatening conditions, only start to form 8 Gya. Therefore, life favoring conditions in the galaxy only start after the start of the formation of spiral arms. It cannot be later than 4 Gyr ago because merely 500 Myr headstart on earth will give the planet a headstart of 500 million years. We have shown in our chapter 4 that at early stages of evolution it takes billions of years for the cyanobacteria fills all the major oxygen sinks on earth before free oxygen will become available throughout the ocean and the atmosphere. Therefore, having an additional 500 million years headstart means cyanobacteria have extra half billion years to transform the planet, implying a 500 Myr headstart into every other later stage of evolution of life. Moreover, the oxygen concentration can only reach an even higher level and enables the emergence of multicellular eukaryotes after another billion years of geoengineering by biologic life. Furthermore, a head start of 500 million years can be translated into 2.78^5 , or 166 fold increase in biological complexity in the evolutionary history of multicellular life, as evidenced by earth's history. Therefore, everything being equal, the chance of intelligent life emergence at the current epoch on a planet formed 4.4 Gyr ago is 36% of earth formed 4.5 Gyr ago. The chance of intelligent life emergence at the current epoch on a planet formed 4.3 Gyr ago is 12.9% of earth formed 4.5 Gyr ago. Intelligent life emergence at the current epoch on a planet formed 4.2 Gyr ago is 4.65% of earth formed 4.5 Gyr ago. On the other hand, intelligent life emergence at the current epoch on a planet formed 4.6 Gyr ago is not 278% of earth formed 4.5 Gyr ago because the average metallicity the systems of an earlier epoch is lower. Finally, we compute the total probability of planets within so-called the galactic habitable zone. The thickness of the galaxy disk averaged 2,000 light years. However, the thickness is non-uniform, the disk is thicker near the galactic center and tapers off near the galactic edge. Therefore, we modeled the galactic height by a decreasing linear function which decreases to 0 at unit 165 (representing 165,000 ly), which is the estimated edge of the galactic disk. It is speculated that 50,000 to 90,000 light years from the galactic

center lies the galactic habitable zone. The entire zone is hospitable to life except the deepest layer, where the stellar density rivals the galactic center.

$$y_0(x) = -0.02212(x - 165) \quad (2.1)$$

$$\frac{2\pi \int_{50}^{90} y_0(x) x dx}{2\pi \int_0^{165} y_0(x) x dx} \cdot 0.74 \quad (2.2)$$

$$\approx 25.76\% \quad (2.3)$$

The integration sums up each value of $y_0(x)$ for $50 \leq x \leq 90$ as the height of the disc multiplied with each successive perimeter size $2\pi x$ to yield the total volume of the galactic habitable zone. It is multiplied by 2 because the disc is symmetric above and below the disc central plane. The volume of the galactic habitable zone is then divided by the volume of the entire galaxy to yield the probabilistic percentage.

2.2 Definition of Stellar Habitable Zone

Various definitions of the stellar habitable zone have been proposed, we shall define habitable zone more rigorously. It is known that the increasing luminosity of the Sun will render earth to be uninhabitable. The rate of weathering of silicate minerals will increase as rising temperatures speed up chemical processes. This in turn will decrease the level of carbon dioxide in the atmosphere, as these weathering processes convert carbon dioxide gas into solid carbonates. Within the next 600 million years from the present, the concentration of CO_2 will fall below the critical threshold needed to sustain C_3 photosynthesis: about 50 parts per million. At this point, trees and forests in their current forms will no longer be able to survive. C_4 carbon fixation can continue at much lower concentrations, down to above 10 parts per million. Thus plants using C_4 photosynthesis may be able to survive for at least 0.8 billion years and possibly as long as 1.2 billion years from now, after which rising temperatures will make the biosphere unsustainable. Therefore, we set the distance at which earth currently will receive the equivalent of Sun's luminosity in 1 billion years into the future as the threshold of the inner edge of the habitable zone. Since luminosity increased in a nearly linear fashion to the present, rising by 1% per 110 myr, then, the total solar output experienced by the inner edge should be 9.091% more than at earth at its current location. Since the Sun's radiant power decrease by the inverse squared as celestial objects move away from them, *the inner edge must occur at 0.840278 AU*, about the midpoint between Venus and earth's current orbit.[35] The outer edge, on the other hand, is that earth's temperature does not fall below the freezing point of water at 273.15 K. Currently, with moderate greenhouse effect, earth's temperature is at 285 K, slightly warmer than predicted by the solar radiation model alone at 279 K. We use 285 K as our reference and find that *1.0887 AU as the outer edge of the habitable zone*. From these edges, we found the

midpoint at 0.964489 AU, earth's current position lies somewhat on the colder side and it is expected to cross into the warmer side 166 Myr into the future. If one computes the effective habitable window within the habitable zone, then the habitable zone of the parent star can only support 2.3 Gyr of habitability. Beyond the definition of the habitable zone, there is also the definition of a continuously habitable zone. Since the host star increases its luminosity throughout its lifespan, in the most stringent case, a planet has to be continuously within the habitable zone in order to nurture life. If this requirement is necessary, then, the earth was beyond the outer edge of the habitable zone 1.3 Gya. The earth was nevertheless active and liquid water was present from the very beginning. Now it is commonly understood that early earth has as much as three times the heat budget as it is today with completely different atmospheric composition composing mostly greenhouse gasses such as CO₂ and Methane. A thicker atmosphere also enabled the warming of the earth beyond the outer edge of the habitable zone. Prior to 2.5 Gya, the earth was also covered by ocean, a lower albedo also helped maintain the absorption of solar insolation. Most importantly, the moon was much closer to earth at the earlier times and heat generated from tidal heating was much more significant. We will see in our later chapters that the aforementioned condition applies to many terrestrial planets early in its evolution. Therefore, it is typical that as terrestrial planets formed, can lie outside the outer edge of the habitable zone and as its heat budget dwindled the increasingly warmer sun continues to maintain a stable temperature for the planet by including the planet into its edge of habitability. However, the planet cannot lie too far from the host star, as the case of Mars, which was geologically active but turned dead and frozen as its internal heat budget is exhausted. Under such scenario, the planet can only be warmed up again when sun increases its luminosity in a few billion years, but then life has to restart on such planet after billions of years of hiatus. In general, the more massive planet can retain its heat for longer than its smaller cousins so they can lie further beyond the outer habitable edge to start with. Since all planetary system's total mass budget is distributed from a central median value, earth's value can be used as the weighted average over all possible scenarios and combinations, with planets more massive and less massive included into consideration as well as its stable distance from the host star.

At the same time, for stars at solar mass, a planet lies at the outer edge or inside the habitable zone when the planet is first formed will experience higher heat budget every point in its evolutionary history. It will less likely enter an ice age, and most importantly shorter effective habitable period of no more than 2.3 Gyr. Whereas the habitability extendable by its own internal heat complemented by solar heating completely overlapped the host stars'. For earth, the continuous habitability spans 5.5 Gyr (the first 3.2 Gyr of habitability is maintained by earth's itself in addition to insufficient solar insolation, and the later 2.3 Gyr in which we are currently residing is maintained by sufficient solar insolation with limited internal heat budget and tidal heating. With minimal overlapping between the two stages).

Solar mass stars increase its luminosity quickly in contrasts to stars with smaller mass and

habitable zone shifts relatively quickly, and the effective continuous habitable zone is much smaller than the definition of the habitable zone. Luckily, our potential candidate pool includes stars ranges in mass from 0.628 to 1 solar mass. Therefore, the habitable zone shifts up to 3.2 times slower, or 7.36 Gyr. If one sets the definition of maximum temporal range for the continuously habitable zone for solar mass stars to be 500 Myr longer than earth's, then the planet experience a period of cool temperature lower than earth's geologic past with almost no to very minimal overlapping between the two stages. On the other hand, if one sets the minimum requirement for continuous habitability window to be 500 Myr shorter than earth's, then a planet experience at most only 500 million additional years for all life's habitability with more overlapping between the two stages. Then, only 40% of the currently defined habitable zone falls into the continuously habitable zone. Stars with 0.628 to 0.73 solar mass will guarantee a continuously habitable zone of 5 Gyr or longer by stellar insolation alone; therefore, 100% of the currently defined habitable zone falls into the continuously habitable zone. Stars with 0.73 to 1 solar mass will have continuously habitable zone from 5 Gyr to 2.3 Gyr; therefore, 100% to 40% of the currently defined habitable zone falls into the continuously habitable zone. Taking the weighted average of all cases, 75.73% of the currently defined habitable zone falls into the continuously habitable zone. However, stars with lower mass still allow all terrestrial planets to form beyond the outer edge of habitability. As a result, the continuous habitability zone miraculously matches the currently defined habitable zone 100% if not a bit more. *Therefore, the habitable zone restricts planets to be between 0.840278 AU and 1.0887 AU, out of a total radius of 2.7 AU radius (inside the snow line) in which terrestrial planet can form. The chance is therefore 9.20 percent.*

2.3 Definition of Sun-like Stars

By sunlike stars, one meant stars that are not too massive so that it provides ample time for evolution to take place for the emergence of intelligent species. The sun is a boundary case because it has shown that in just another 500 million years the increasing luminosity of the sun will accelerate the carbon cycle, and just another 1 billion years will increase the surface temperature high enough rendering the planet uninhabitable. Since the evolution of intelligent life on earth, as it is demonstrated in this paper, is currently ahead most of the earth like planets, therefore, setting our selection criteria stringent, 1 solar mass is the upper bound chosen for sunlike stars. Then, how low can the stellar mass go to be hospitable to intelligent life? We have shown in our section discussing red dwarfs with 0.35 solar mass or smaller is unsuitable candidates due to strong magnetic fields. Then, it leaves us mass between 0.35 solar mass to 1 solar mass for our current investigation. The greatest challenge facing intelligent life is then tidally locking to their host star. Once tidal locking completes, the planet faces one hemisphere around its star in its daylight and another half in perpetual darkness. The weather would be

extreme on such a planet. In addition, much slower rotation rate reduces the magnetic field strength of the planet, though the interference from the cosmic stellar magnetic storm is not as catastrophic as those observed on red dwarves, it is nevertheless grave compared to earth. We define a planet is tidally locked if 4.5 Gyr after its formation, it currently completes a day and night cycle every 7 days or greater. The first step is to find the habitable zone for a given stellar mass, and then assuming a habitable planet of 1 earth mass revolves at such distance from their star and the time it takes to tidally lock to their star. Finally, based on the remaining time to lock to their host star, deriving the current number of rotational days of their planet.

$$j = \sqrt{x^{3.5}} \quad (2.4)$$

$$T_{exolockingtoitsun} = \frac{\left(\frac{1}{13750}\right) \cdot (j \cdot a_{earth})^6 \cdot I_{earth} \cdot M_{earth} \cdot 909.0909}{3G(x \cdot M_{sun})^2 \cdot R_{earth}^3 \cdot 60 \cdot 60 \cdot 24 \cdot 365 \cdot 10^9} \quad (2.5)$$

$$d = \frac{4.5}{\left(\frac{T_{exolockingtoitsun}}{1}\right)} \quad (2.6)$$

$$m = \frac{1}{(1 - d)} \quad (2.7)$$

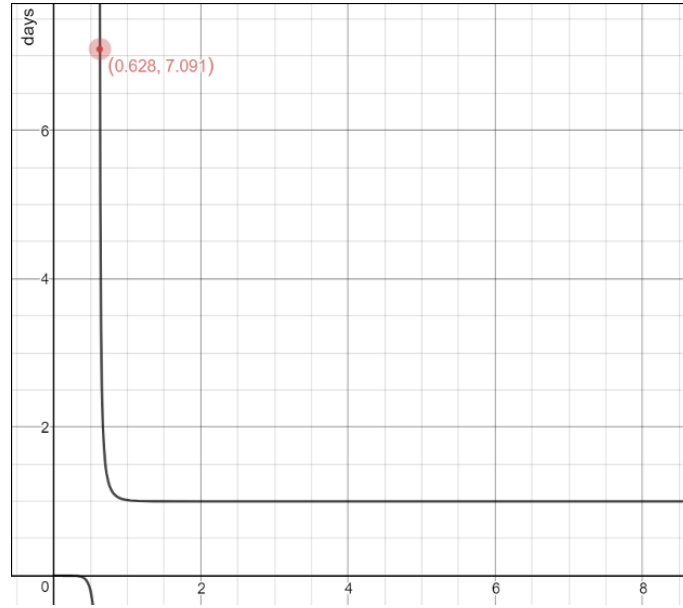


Figure 2.1: Rotational speed of terrestrial planets within the habitable zone of their parent star vs the parent star's stellar mass

Based on the derivation, a star with 0.628 solar mass or smaller will have a rotational period of 7 days or more, mimicking tidal locking condition. As a result, we will set star from 0.628 solar mass to 1 solar mass as what we call a sun-like star.

2.4 Number of Stars

To compute the total number of stars in the Milky Way, we first obtain the mass of the Milky Way galaxy which ranges from $0.8 \cdot 10^{12}$ solar mass to $1.5 \cdot 10^{12}$ solar mass. We take the median mass value at $1.15 \cdot 10^{12}$ solar mass. Then, we multiply by 0.1546 because visible matter occupies 15.46% of matter (The universe contains 26.8% dark matter and 4.9% ordinary matter). We end up with $2.319 \cdot 10^{11}$ solar mass.

$$1.15 \cdot 10^{12} \cdot 0.1546 = 2.319 \cdot 10^{11} M_{sol} \quad (2.8)$$

This is mass that made up all the stars, nebulae, and the interstellar medium. The mass of interstellar medium and nebulae occupies roughly 1% of the total mass of ordinary matter, so we can just ignore it. Then, we compute the number of stars in the stellar mass range from 0.6315 to 1 solar mass based on initial mass function [55][24] and given in the table below:

Percentage by Mass	Spectral Class	Stars in Billions	Percentage by Number
0.00%	O	0.0001433	0.00%
2.89%	B	0.6209666667	0.13%
2.58%	A	2.866	0.60%
8.99%	F	14.33	3.00%
17.18%	G	36.3026666667	7.60%
18.58%	K	57.7976666667	12.10%
49.78%	M	365.1761666667	76.45%
100.00%	Total	477.0936099668	100.00%

Table 2.1: Star distributions of Milky Way

The total number of stars in the Milky Way galaxy is 477.093 billion. The total number of stars that is between 0.628 to 1 solar mass is then 65.2 billion. However, only 1 in 5 sun-like stars can host terrestrial planets with their metallicity higher than -0.4. Many of the earlier stars are born when the cosmic neighborhood is deficient in elements heavier than helium (Population II and Population III stars). Even at the era when the Sun was born from 5 Gya to 4 Gya, the average metallicity of the sun like stars is -0.4 and only 1 in 3.8 sunlike (derived based on the stellar formation and earth formation rate of Lineweaver's approach) stars can host terrestrial planets. The number of stars formed between 5 Gya to 4 Gya is found using Lineweaver's approach at 34.348 billion, and the total number of stars is 477.093 billion.

$$N_{Earthbetween5Gyato4Gya} = \frac{k_{starsbetween5Gyato4Gya}}{k_{TotalStars}} \cdot \frac{65,201,500,000}{3.79576312764} \quad (2.9)$$

$$= 1.2366805534 \cdot 10^9$$

We shall derive the lower bound using Lineweaver's approach.

Lineweaver[60] has computed the earth formation rate through time based on the stellar formation rate of the Milky Way and using metallicity as the selection criteria. He has shown that the rate of terrestrial planet formation increases linearly as the metallicity of the stellar system increases from -0.4. A system with metallicity below -0.4 lack substantial heavy elements heavier than helium to form terrestrial planets. A system with a metallicity of 0 or higher has an increasing chance of hosting hot Jupiters (which swept through terrestrial planets' orbit and destroy them). Therefore, the rate of terrestrial planet formation is the probability of creating earth times the probability of destroying the earth, and one found that terrestrial planet formation is greatest at metallicity of 0.1, slightly higher than the sun. Lineweaver only produced the final earth formation rate curve but did not include the equation for the curve. As a result, a carefully matched curve is produced as the starting point of our derivation.

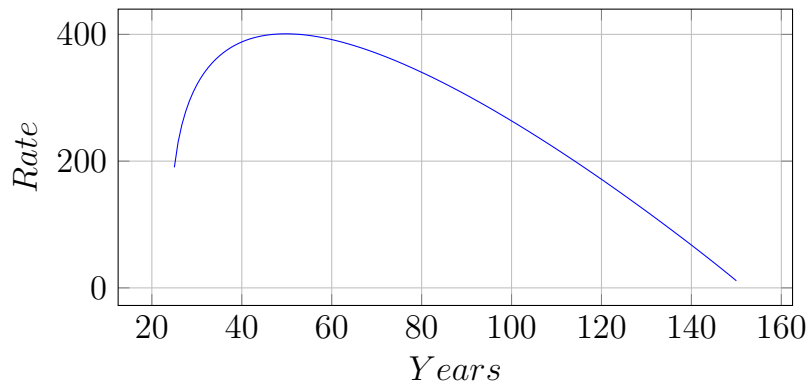


Figure 2.2: Earth formation rates through time

Using this equation above, one can derive the number of terrestrial planets formed from 5 Gya to 4 Gya. However, nowhere did Lineweaver mention about the habitability of these planets. Therefore, a factor is added for those planets that formed within the habitable zone of their host star. Furthermore, we also reproduced the equation for the stellar formation also given by Lineweaver. However, integrating the equation over the whole range of stellar formation time window from 0.4 Gyr post big bang until today less the number of stars that already died did not match the total number of stars we derived earlier.

$$f_{earth}(x) = 7.7 \cdot 2.655 \ln \left(1.1814 \cdot \left(-1.0454(x-24) + (7020.3(x-24))^{\frac{1}{2.8}} \right) \right) \quad (2.10)$$

$$f_{star}(x) = 175 \cdot 7.58 \cdot 2.655 \ln \left(1.1814 \cdot \left(-1.0036(x-5) + (7020.3(x-5))^{\frac{1}{2.8}} \right) \right) \quad (2.11)$$

$$N_{stars} = \int_5^{138} f_{star}(x) dx \cdot 10^8 \cdot \frac{1}{(D_{pa})^3} \cdot \frac{1}{10^3} \cdot 10 \cdot 2.7313 \cdot 0.958 \quad (2.12)$$

$$N_{earth} = \int_{82.25}^{92.25} f_{earth}(x) dx \cdot \frac{10^8}{(D_{pa})^3} \cdot 10 \cdot 2.7313 \cdot \frac{13.6664}{5} \cdot 1.99 \quad (2.13)$$

$$D_{pa} = 3.26156 \text{ ly} \quad (2.14)$$

$$= 1.3472610983 \cdot 10^9$$

By parameterization, we found that the actual stellar formation rate is, in fact, $2.7313 \cdot 10$ times higher than the star formation curve given. Only when the stellar formation rate increased by $2.7313 \cdot 10$, the total number of stars in the galaxy match the total number we found earlier. This factor is at least partially justified because Lineweaver was calculating star formation rate only within the galactic habitable zone, not the star formation rate of the entire galaxy. The earth formation rate is, $2.7313 \cdot 10 \cdot 1.99 \cdot \frac{13.6664}{5}$ times higher than the earth formation curve given. The $\frac{13.6664}{5}$ factor can be explained as we further taking into consideration those stars with stellar mass from 0.628 to 0.8, part of the more massive Spectral K class. We have to revise the mass range of stars represented in the selection criteria, instead of 0.8 solar mass to 1.2 solar mass, we specified 0.628 solar mass to 1 solar mass instead. Finally, The 1.99 factor can be explained as rescaled star distribution over metallicity. Lineweaver originally assumed that star formation between 5 Gya to 4 Gya follows a uniform distribution density based on metallicity, that is, there is an equally likely number of stars born with low metallicity as those with mean metallicity. In reality, the distribution of stars follows a nearly normal distribution centered on the mean with a metallicity of -0.4, therefore, we increase the earth formation factor by 2. The final result is the number of terrestrial planets within the habitable zone of their host star arose from 5 Gya to 4 Gya. The cross-examined results from our earliest derivation show that these two numbers closely match each other. We shall adopt the Lineweaver's final number as the more accurate one because it takes into account the differential rate of earth production against time. In conclusion, the total number of terrestrial planets formed between 5 Gya to 4 Gya is 1.347 billion.

2.5 Peak of Terrestrial Planet formation

Follow up from the previous calculation regarding the number of terrestrial planets between the temporal window of 5 Gya to 4 Gya, the earth was formed at the time when the total number of terrestrial planets are just falling off the peak. Once the star enters its main sequence lifespan, the terrestrial planet enters its window of habitability, but its habitability is increasingly being eroded by the increasing luminosity of the host star. Because the sun is a more massive yellow dwarf of the spectral class G, its main sequence is considerably shorter than most of the stars within spectral class G and K, the yellow and orange dwarves respectively. The amount of fuel available for nuclear fusion is proportional to the mass of the star. Thus, the lifetime of a star on the main sequence can be estimated by comparing it to solar evolutionary models. The Sun has been a main-sequence star for about 4.5 billion years, and it will become a red giant in 6.5 billion years, for a total main sequence lifetime of roughly 10^{10} years. Hence:

$$T_{MS} \approx 10^{10} \left[\frac{M}{M_{sol}} \right] \left[\frac{L_{sol}}{L} \right] = 10^{10} \left[\frac{M}{M_{sol}} \right]^{-2.5} \quad (2.15)$$

where M and L are the mass and luminosity of the star, respectively, M_{sol} is a solar mass, L_{sol} is the solar luminosity, and T_{MS} is the star's estimated main sequence lifetime. It then can be estimated that most of the orange dwarves with less than 0.74895 solar mass are still in their main sequence since their formation at the earliest times. Their window of habitability are still open because the current age of universe subtracted from the age of first possible terrestrial planet formation is still too short compares to the lower mass stars' habitability window, which ranges from 11 Gyr years up to 40 Gyr years. In fact, an orange dwarf with 0.5 solar mass will remain on the main sequence for $5.65 \cdot 10^{10}$ years, about five and half times longer than the sun. Taking the window of habitability into considerations and assuming a weighted stellar mass of 1 M_{sol} and the window of habitability of 5.3 Gyr, we have come up with a model which indicates that a peak of a number of habitable terrestrial planets 8.7~8.8 Gyr after the Big Bang. Weighted stellar mass of 1 M_{sol} is justified, because at earlier epoch, we are more concerned with the synthesis of complex organic molecules or the evolution of single cell life. As a result, stars more massive than the sun with shorter window of habitability is also considered and, overall, increased the weighted stellar mass to 1 M_{sol} .

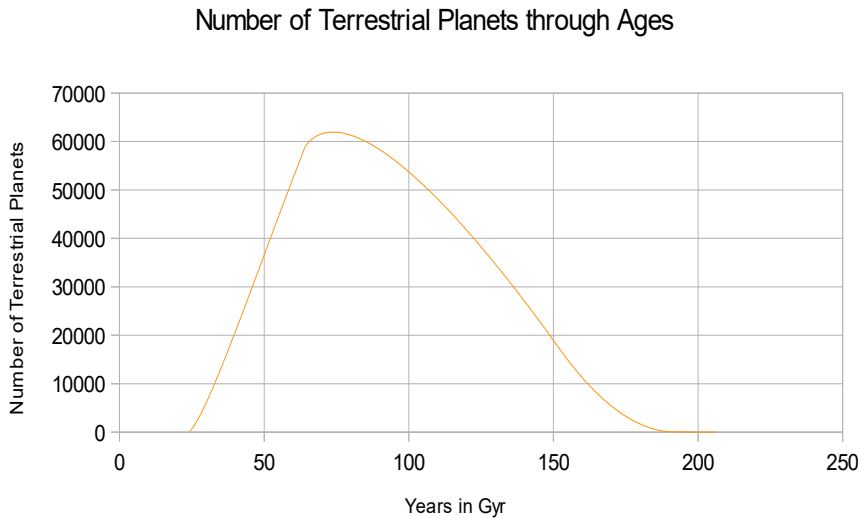


Figure 2.3: The total number of terrestrial planet through time

This result has strengthened both the panspermia theory and the catastrophic theory on the origin of life on earth. Since the formation of the first terrestrial planet occurred around 2.5 gyr after the Big Bang, or 11.3 Gyr ago, this closely matches Sharov and Gordon’s back-extrapolation of DNA complexity’s exponential doubling with a starting point around 9.7 Gyr ago. It further strengthened their arguments that life arise before earth’s formation and the Prokaryotes may have evolved much earlier on other terrestrial planets. They possibly formed long before earth, and the bacteria themselves may have survived and scattered to earth since the formation stage of the solar system but was only able to get stronghold after the cooling and the presence of water followed the late heavy bombardment 3.8 Gyr ago. Both the catastrophic theory and the panspermia model is strengthened by the fact that the total number of habitable planets reaches a maximum at the time of earth’s formation. Regardless whether the simplicity of life back then was constrained by cataclysmic cosmic events such as Gamma Ray bursts or simply a matter of slow information doubling rate at the early stages of evolution, it suggests that panspermia reaches its greatest chance of success in terms of contamination during the formation age of the earth. It has been decreasing quasi exponentially as the star formation rate slows down. This contamination could be as complex as prokaryotes surviving interstellar journey as the panspermia theory suggests or could be much more modest as an enrichment of interstellar medium with complex organic molecules which facilitated the emergence of life based on the catastrophic theory once the persistence of life becomes possible at 5 Gya.

2.6 Excluding Over-counted Binaries and Multiples

Although binary stars are not the majority of all stars within the Milky Way galaxy, they are more likely to occur around sun-like stars (GFK spectral class). The probability of binary stars

forming increases with stellar mass. Between 0.7 to 1.3 solar mass, 44 percent of all stars are binaries. The original paper does not intend to formulate further detailed model for correlation between stellar mass and multiplicity due to inadequate data. Therefore, we take 44 percent as the weighted average value for all stellar mass ranging from 0.7 to 1.3 where stellar mass at the lower mass end tends to formulate multiples with lower value closer to 35% while stars at the higher mass end tends to formulate multiples with 47% or more. Based on existing literature, binaries stars, in most cases, do not impede life formation. The general formula for multiples follow the formula:

where Triple and higher-order systems represent

$$N(n) \propto 2.5^{-n} [40]$$

25% of all solar-type multiple systems, with a distribution of systems with n components that roughly follows a geometric distribution. Knowing the frequency of multiplicity among solar mass stars and using this equation, one finds that binary represents 75% of all multiple star systems.

The habitability of binaries strongly depends on the configurations of the system. In general, four cases of binary configurations are possible. In the first case, the average separation between the stars has to be small enough so that the minimum distance required for a stable orbit for any planets revolving around the binary pairs can fall on the combined stars' luminosity's habitable zone. Research has shown that planets orbiting binaries have to be between 3 to 5 times the distance between the distance of the pairs in order to be stable and we take the mid value at 4. The computed results show binary separation between 0 AU to 0.428 AU.

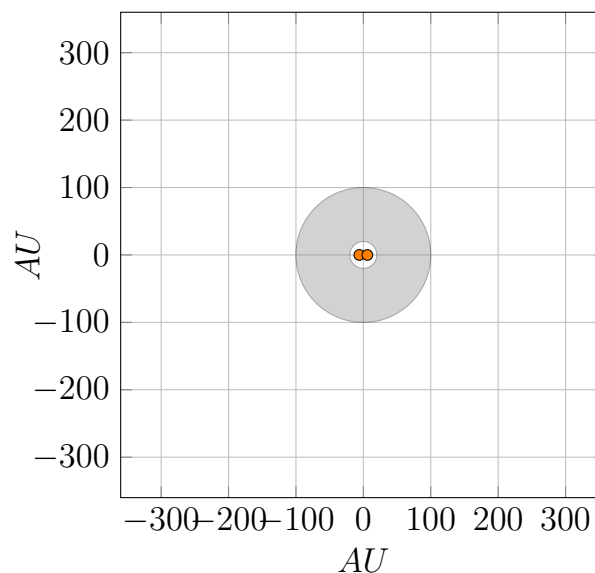


Figure 2.4: Binary pair with separation < 0.486 AU

For close orbiting binaries, one also have to find the percentage of binary companions are 0.628 solar mass or above. For lower-mass companions are not included in our original tally of stars and are deemed inhabitable (a very small portion of binaries with mass lower than 0.628 solar mass is discussed in the later section); therefore, we need to exclude them from our tally for those stars that are over-counted to be habitable. By taking the integration of the binary companion mass distribution function (which is not the initial mass function observed among single stars), we found the percentage to be 40%. That is, for closely orbiting binaries 40 percent of which hosts a companion with a mass greater than 0.628 solar mass.

We then compute the probability of binaries with separation between 0 AU to 0.428 AU. We derived a composite distribution function that closely matches the empirical data from a catalog of thousands of binaries and shall use this equation for the remainder of the multiple system habitability calculations.

$$D_0(x) = \frac{58}{1.35 \cdot \sqrt{2\pi}} e^{-0.5 \left(\frac{x-2.2}{1.35} \right)^2} \quad (2.16)$$

$$d(x) = 7(1 - 1 \cdot \tanh 1(x - 2.45)) \quad (2.17)$$

$$D(x) = D_0(x) \cdot \frac{d(x)}{14} \quad (2.18)$$

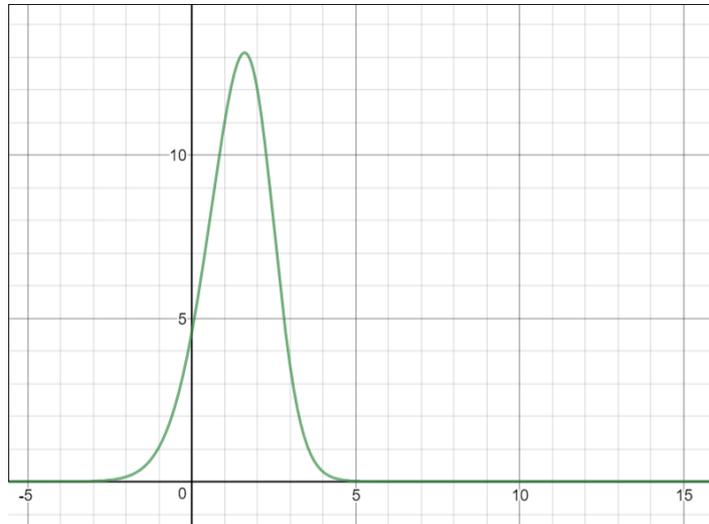


Figure 2.5: Probability Distribution Function of binary stars by separation distance

$$S_1 = \frac{\left(\int_{\log(0.001)}^{\log(0.486)} D(x) dx \right)}{\left(\int_{-\infty}^{\infty} D(x) dx \right)} \quad (2.19)$$

$$= 0.055537328824$$

$$S_{1inner} = 0.40864 \cdot S_1 = 0.0226947740506 \quad (2.20)$$

The final results show that 5.5% of all binaries have tight orbits and 2.27% of them have companions of 0.628 solar mass or above.

In the second case, the separation between the pairs is between 0.408 AU to 100 AU. Both stars in the pair in this category can not host habitable planets. As the pair separation increases, the stable orbit moves beyond the habitable zone of the pairs so no habitable planet can revolve around both stars. As the separation widens, one may speculate that planetary system can revolve around one of the two stars. However, we set a very rigorous standard for planetary habitability. We define a planetary system to be habitable if no major astronomical objects comparable to solar mass lies within 100 AU from the habitable planet. Although Pluto, Neptune lies around 30 AU from the sun, the outermost dwarf planet Sedna within the solar system lies at 506 AU, Eris, and Makemake lies at 50 AU on average. If a solar mass object lies close to the planetary system, then, over the course of millions of years, a significant number of additional comets and disturbances can be brought to the inner planets from the outer rings. Therefore, binaries with separation between 0.408 AU to 100 AU constitute the dead zone of habitability.

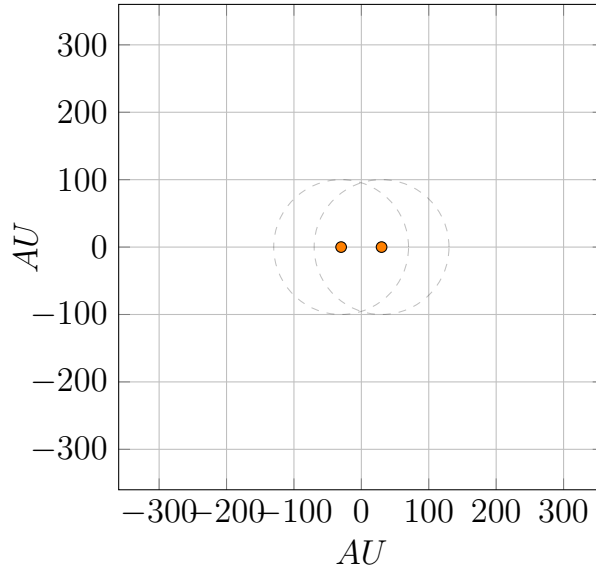


Figure 2.6: Binary pair with separation $0.486 \text{ AU} < x < 100 \text{ AU}$

Because binaries within the dead zone can host companions with different mass, we have to exclude those binaries in which the central star has a mass above 0.638 solar mass and those binaries in which both pairs have a mass above 0.638 solar mass. Using the previous binary mass distribution equation, we found that 37.36% of all pairs have companions with mass 0.628 or greater. Using the binary probability distribution based on separation distance, we found that 34% of all binaries fall into this dead zone. Therefore, we over-counted 5.36% of these

binaries by both stars and over counted 4% of these binaries by one star.

$$S_2 = \frac{\left(\int_{\log(0.486)}^{\log(100 \cdot 1.7)} D(x) dx \right)}{\left(\int_{-\infty}^{\infty} D(x) dx \right)} \quad (2.21)$$

$$= 0.734445462472$$

$$S_{2voidzone2} = 0.3732 \cdot S_2 = 0.274095046595 \quad (2.22)$$

In the third case, binaries are separated by a distance between 100 AU to 200 AU and are capable of hosting one planetary system around one of the stars. We compute the probability of binaries within this range of separation and compute the percentage of companions with a mass greater than 0.628 solar mass and found that we overcounted the number of stars habitable by 3.12%.

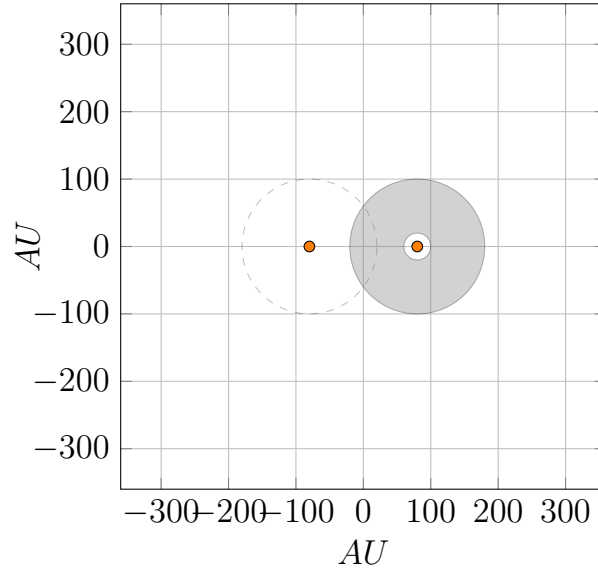


Figure 2.7: Binary pair with separation $100 \text{ AU} < x < 200 \text{ AU}$

$$S_3 = \frac{\left(\int_{\log(100 \cdot 1.7)}^{\log(200 \cdot 1.7)} D(x) dx \right)}{\left(\int_{-\infty}^{\infty} D(x) dx \right)} \quad (2.23)$$

$$= 0.0837179170749$$

$$S_{3voidzone1} = 0.3732 \cdot S_3 = 0.0312435266523 \quad (2.24)$$

Finally, in the fourth case, binaries are separated by a distance of 200 AU or greater. Under this scenario, both stars can host habitable planetary systems. Since both are capable hosting life,

we just treat them, conceptually, as two separate life hosting stars and no star is over-counted from the number of our existing habitable systems.

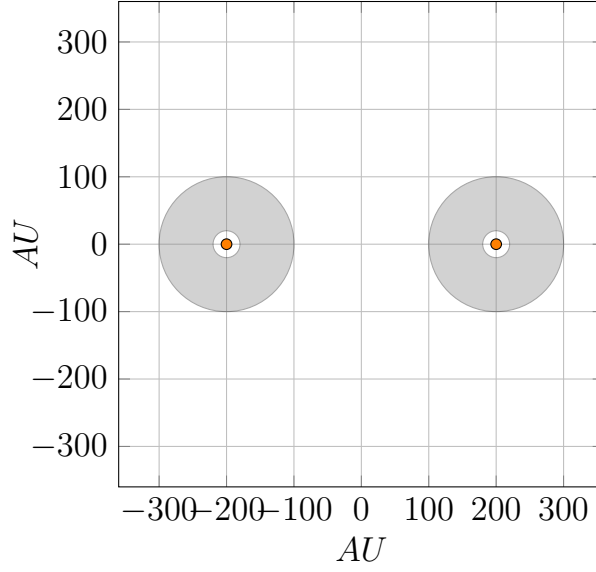


Figure 2.8: Binary pair with separation > 200 AU

$$\begin{aligned}
 S_4 &= \frac{\left(\int_{\log(200 \cdot 1.7)}^{\infty} D(x) dx \right)}{\left(\int_{-\infty}^{\infty} D(x) dx \right)} \\
 &= 0.126194963279
 \end{aligned} \tag{2.25}$$

Our calculation is simplified by excluding taking binary pairs' eccentricity into account. The eccentricity of binaries is minimal in tightly orbiting pairs due to mutual tidal interaction but can become significant in binaries with greater separation. Luckily, binaries with eccentricity up to 0.5 do not significantly alter our previous derived results and likely to reduce the number of habitable systems by 10% at most. Star eccentricity mostly affect those binary systems with separation between 100 AU to 250 AU, where the slightest deviation from perfect circular orbits can result in diminishing chance of life. We excluded this calculation from our binaries computation to ease our later computation on ternary, quaternary, quintenary, sextenary, and higher order systems.

By deriving all possible cases for binaries, we can now sum up our results and obtain the following conclusion. This shows that 69% of binaries can host potential life-bearing planets with the remaining 31% can not.

$$\begin{aligned}
 A_1 &= \left(\frac{S_{1inner}}{2S_1} \right) S_1 + \left(\frac{S_{2voidzone2}}{S_2} \right) S_2 + \left(\frac{S_{3voizone1}}{2S_3} \right) S_3 \\
 &= 0.301064196946
 \end{aligned} \tag{2.26}$$

$$1 - \frac{1}{100} \left(\frac{100(A_1)}{T} \right) = 0.698904390246 \quad (2.27)$$

Having derived our results for the binaries, we move to ternary systems consisting of three stars.

For ternary star systems, all possible cases can be reduced to two independent scenarios interacting with each other. The first independent scenario determines the characteristics of the inner two stars. If the inner two stars are in a tight orbit, then they are circling each other. Otherwise, one star orbits another at some distance away. The innermost two stars among the triples and their probabilistic distribution can be modeled based on the binary probability distribution over separation distance. Conceptually, we treat the inner two stars as a pair of binary. We can then treat the inner two stars system as a single star, and its separation between the third stars circling around them constitute another pair of binary.

Now, a prudent reader may point out that there exists a case in which a pair of binary circles around a central star. This case, however, is symmetrical to the condition we just described above, except that we would start our computation around the outer pair of stars, but the final probability stays the same as if the binary pair stayed at the center. Therefore, this extra step of computation is not necessary.

For the first case, the inner two pairs have a separation between 0 to 0.486 AU. The probability of forming such pair is multiplied by the chance of having a binary separation between $\frac{0.486}{2} \cdot 4$ AU or greater for the third star circling the first two. $\frac{0.486}{2}$ because we take the weighted average of all possible distance ranges from 0 to 0.486 and times a factor of 4 because only stars circling around the inner two stars with 4 times the separation distance away are stable.

$$S_1 = \frac{\left(\int_{\log(0.001)}^{\log(0.486)} D(x) dx \right)}{\left(\int_{-\infty}^{\infty} D(x) dx \right)} \cdot \frac{\left(\int_{\log\left(\frac{0.486}{2} \cdot 4\right)}^{\infty} D(x) dx \right)}{\left(\int_{-\infty}^{\infty} D(x) dx \right)} \quad (2.28)$$

$$= 0.0505486546584$$

Within this scenario, a dead zone occurs if the outermost third-star circles around the first two between the minimal stable orbit distance up to 100 AU. This configuration does not allow either habitable planet circling around the inner two stars nor circling around the third star.

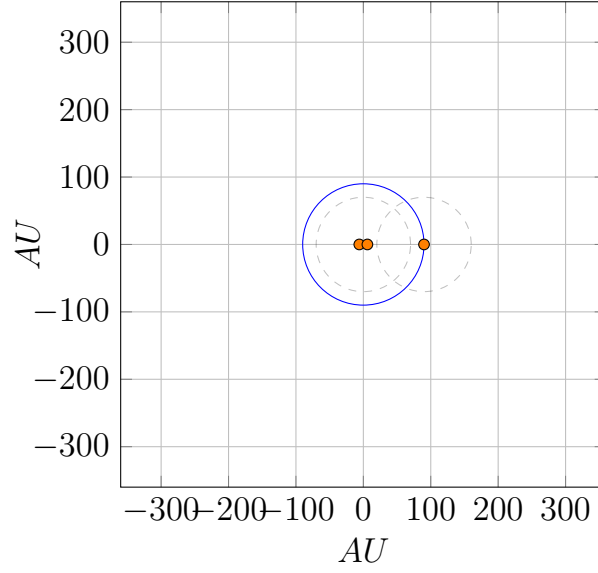


Figure 2.9: Ternary system with the inner pair < 0.486 AU and the outer third star < 100 AU

$$S_{1deadzone} = \frac{\left(\int_{\log(0.001)}^{\log(0.486)} D(x) dx \right)}{\left(\int_{-\infty}^{\infty} D(x) dx \right)} \cdot \frac{\left(\int_{\log\left(\frac{0.486}{2}\right)}^{\log(100 \cdot 1.7)} D(x) dx \right)}{\left(\int_{-\infty}^{\infty} D(x) dx \right)} \quad (2.29)$$

$$= 0.0388906539978 \quad (2.30)$$

Beyond the dead zone, when the outermost third-star circles around the first two between the 100 AU and 200 AU, one planetary system can exist around either the inner pair or around the outermost star.

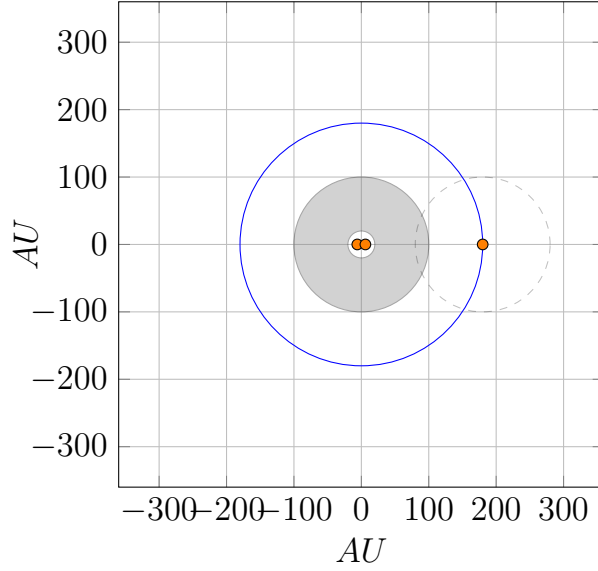


Figure 2.10: Ternary system with the inner pair < 0.486 AU and the outer third star 100 AU $< x < 200$ AU

$$S_{1o} = \frac{\left(\int_{\log(0.001)}^{\log(0.486)} D(x) dx \right)}{\left(\int_{-\infty}^{\infty} D(x) dx \right)} \cdot \frac{\left(\int_{\log(100 \cdot 1.7)}^{\log(200 \cdot 1.7)} D(x) dx \right)}{\left(\int_{-\infty}^{\infty} D(x) dx \right)} \quad (2.31)$$

$$= 0.00464946948905$$

When the outermost third-star circles around the first two with 200 AU or greater, planetary systems can exist around both the inner pair and the outermost star. Therefore, the outermost star are not over-counted from the number of our existing habitable systems.

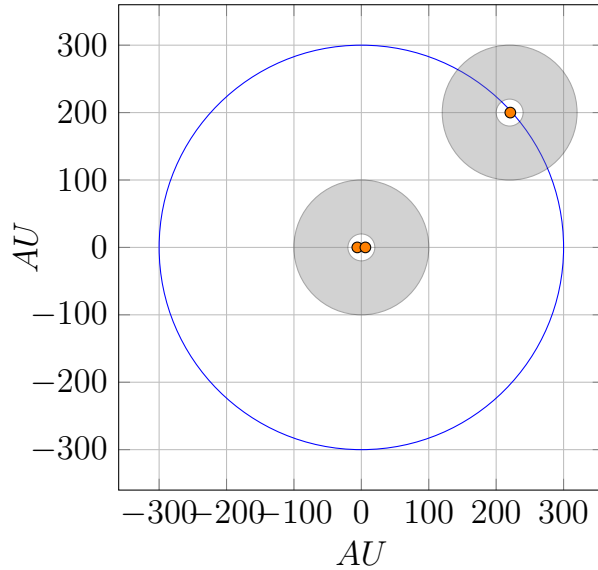


Figure 2.11: Ternary system with the inner pair < 0.486 AU and the outer third star > 200 AU

For our second case, the inner pair with separation between 0.486 AU to 25 AU, the outer ring can only be stable if it lies at $\frac{(25+0.486)}{2}$ (the weighted average distance between pairs fall within this range) times 4 (in order for the orbit to be stable)

$$S_3 = \frac{\left(\int_{\log(0.486)}^{\log(25 \cdot 1.7)} D(x) dx \right)}{\left(\int_{-\infty}^{\infty} D(x) dx \right)} \cdot \frac{\left(\int_{\log\left(\frac{(25 \cdot 1.7 + 0.486)}{2} \cdot 4\right)}^{\infty} D(x) dx \right)}{\left(\int_{-\infty}^{\infty} D(x) dx \right)} \quad (2.32)$$

$$= 0.16003294474$$

A dead zone occurs if the outermost third-star circles around the first two between the minimal stable orbit distance up to 100 AU. This configuration does not allow either habitable planet circling around the inner two stars nor circling around the third stars.

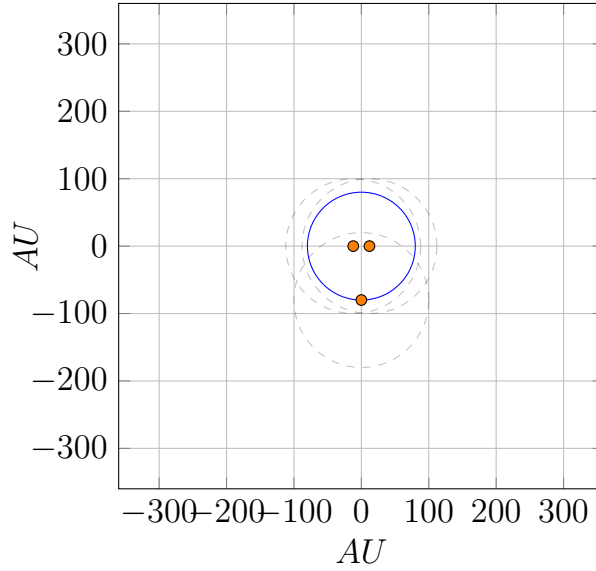


Figure 2.12: Ternary system with the inner pair $0.486 \text{ AU} < x < 25 \text{ AU}$ and the outer third star $< 100 \text{ AU}$

$$S_{3\text{deadzone}} = \frac{\left(\int_{\log(0.486)}^{\log(25 \cdot 1.7)} D(x) dx \right)}{\left(\int_{-\infty}^{\infty} D(x) dx \right)} \cdot \frac{\left(\int_{\log\left(\frac{(25 \cdot 1.7 + 0.486)}{2} \cdot 4\right)}^{\log(100 \cdot 1.7)} D(x) dx \right)}{\left(\int_{-\infty}^{\infty} D(x) dx \right)} \quad (2.33)$$

$$= 0.0531765275501$$

Beyond the dead zone, when the outermost third-star circles around the first two between the 100 AU and 200 AU, one planetary system can exist only around the outermost star.

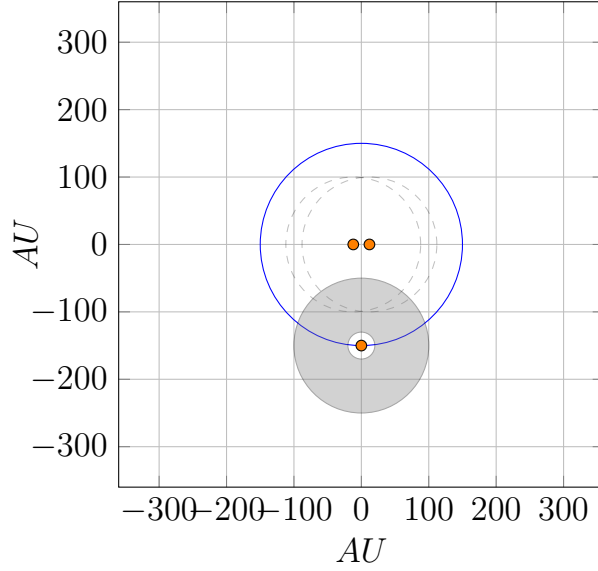


Figure 2.13: Ternary system with the inner pair $0.486 \text{ AU} < x < 25 \text{ AU}$ and the outer third star $100 \text{ AU} < x < 200 \text{ AU}$

$$S_{3o} = \frac{\left(\int_{\log(0.486)}^{\log(25 \cdot 1.7)} D(x) dx \right)}{\left(\int_{-\infty}^{\infty} D(x) dx \right)} \cdot \frac{\left(\int_{\log(100 \cdot 1.7)}^{\infty} D(x) dx \right)}{\left(\int_{-\infty}^{\infty} D(x) dx \right)} \quad (2.34)$$

$$= 0.106856417189$$

When the outermost third-star circles around the first two with 200 AU or greater, planetary system can exist around the outermost star. Therefore, two stars are over-counted from the number of our existing habitable systems.

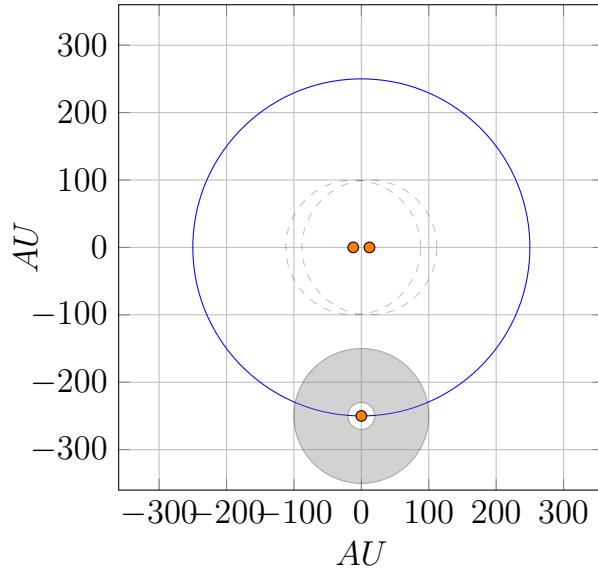


Figure 2.14: Ternary system with the inner pair $0.486 \text{ AU} < x < 25 \text{ AU}$ and the outer third star $> 200 \text{ AU}$

In the third case for ternary star systems, the inner two stars are separated between 25 AU to 100 AU, and a stable orbit for the outermost star can only exist beyond 100 AU. As a result, no dead zone exists for such configurations.

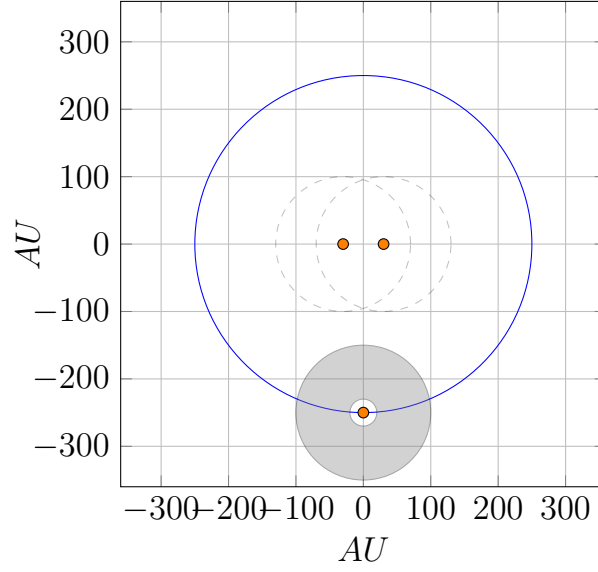


Figure 2.15: Ternary system with the inner pair $25 \text{ AU} < x < 100 \text{ AU}$ and the outer third star $> 200 \text{ AU}$

$$S_4 = \frac{\left(\int_{\log(25 \cdot 1.7)}^{\log(100 \cdot 1.7)} D(x) dx \right)}{\left(\int_{-\infty}^{\infty} D(x) dx \right)} \cdot \frac{\left(\int_{\log\left(\frac{125 \cdot 1.7 \cdot 4}{2}\right)}^{\infty} D(x) dx \right)}{\left(\int_{-\infty}^{\infty} D(x) dx \right)} \quad (2.35)$$

$$= 0.0236349640269$$

$$S_{4inner} = 0.3732 \cdot S_4 = 0.00882056857484 \quad (2.36)$$

In the fourth case, the inner two stars are separated between 100 AU to 200 AU, and a stable orbit for the outermost star can only exist beyond 400 AU. As a result, no dead zone exists for such configurations.

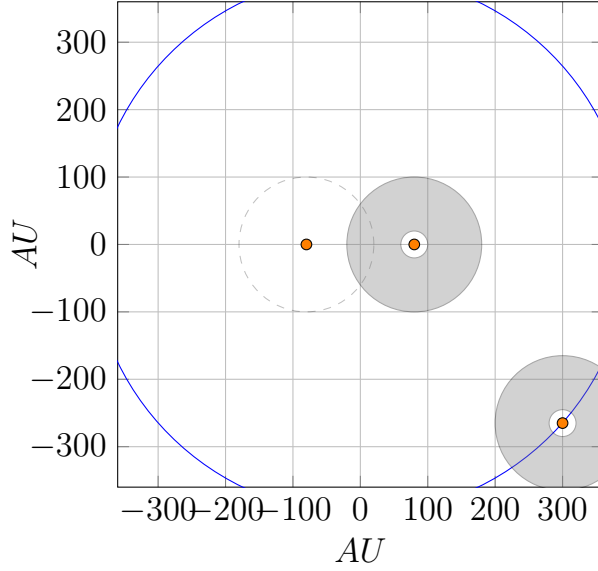


Figure 2.16: Ternary system with the inner pair $100 \text{ AU} < x < 200 \text{ AU}$ and the outer third star $> 400 \text{ AU}$

$$S_5 = \frac{\left(\int_{\log(100 \cdot 1.7)}^{\log(200 \cdot 1.7)} D(x) dx \right)}{\left(\int_{-\infty}^{\infty} D(x) dx \right)} \cdot \frac{\left(\int_{\log\left(\frac{300 \cdot 1.7}{2} \cdot 4\right)}^{\infty} D(x) dx \right)}{\left(\int_{-\infty}^{\infty} D(x) dx \right)} \quad (2.37)$$

$$= 0.00385801802965$$

$$S_{5inner} = 0.3732 \cdot S_5 = 0.00143981232866 \quad (2.38)$$

In the final case, the inner two stars are separated by greater than 200 AU, and the stable orbit for the outer circling star can only exist beyond 800 AU. As a result, no dead zone exists for such configurations. Furthermore, the great separation distance between the inner pairs allows habitable planetary system circling around both inner stars as well as the outermost one. As a result, the final case is the only case where all three stars are not over-counted from the number of our existing habitable systems. Since all three are capable hosting life, we just treat them, conceptually, as three separate life-capable hosting stars.

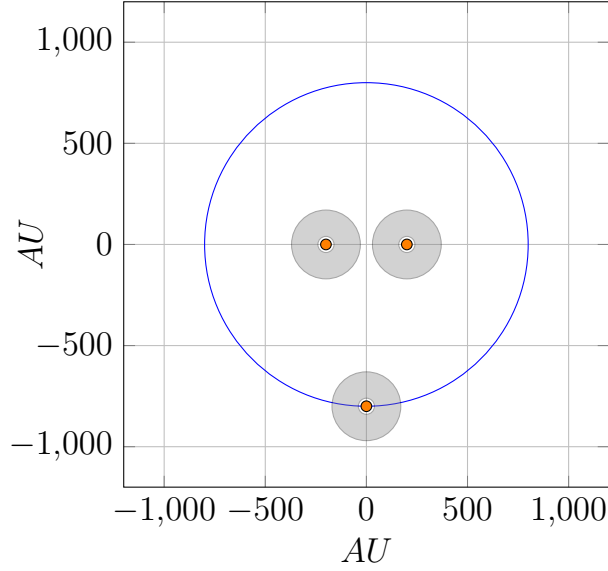


Figure 2.17: Ternary system with the inner pair > 200 AU and the outer third star > 800 AU

$$S_6 = \frac{\left(\int_{\log(200 \cdot 1.7)}^{\infty} D(x) dx \right)}{\left(\int_{-\infty}^{\infty} D(x) dx \right)} \cdot \frac{\left(\int_{\log(200 \cdot 1.7 \cdot 4)}^{\infty} D(x) dx \right)}{\left(\int_{-\infty}^{\infty} D(x) dx \right)} \quad (2.39)$$

$$= 0.00430369400515$$

$$A_0 = \left(\left(\frac{S_{1voidzone0}}{3} + \frac{2S_{1voidzone1}}{3} + \frac{3S_{1voidzone2}}{3} \right) + \frac{S_{1tight1}}{3} + \frac{2S_{1tight2}}{3} + \frac{S_{2inner}}{S_1 \cdot 3} \right) S_1 \quad (2.40)$$

$$A_1 = \left(\left(\frac{S_{3voidzone0}}{3} + \frac{2S_{3voidzone1}}{3} + \frac{3S_{3voidzone2}}{3} \right) + \frac{2 \cdot S_{3inner}}{S_3 \cdot 3} \right) S_3$$

$$+ \left(\frac{2S_{4inner}}{S_4 \cdot 3} \right) S_4 + \left(\frac{S_{5inner}}{S_5 \cdot 3} \right) S_5 \quad (2.41)$$

$$A_0 = 0.027477962409347 \quad A_1 = 0.0663464593803$$

$$1 - \frac{1}{100} \left(\frac{100(A_0 + A_1)}{T} \right) = 0.612900860807 \quad (2.42)$$

By deriving all possible cases for binaries, we can now sum up our results and obtain the following conclusion. It shows that 61.29% of binaries can host potentially life-bearing planets with the remaining 38.71% can not. This decreasing trend is not hard to interpret because as

more bodies are capable of disturbing the zone of habitability, the chance of hosting habitable planets decreases.

We then shift our attention to Quaternary star systems, the quaternary system is more complicated because not only we have to consider cases where two innermost pairs can be treated as a binary pair while the two remaining outermost stars can be treated as two separate stars circling the inner pair as a single star. We also have to consider that a pair of binary can circle another pair of binary. Therefore, we have two major cases to cover.

The first major case is basically all the cases covered under the ternary star system scenario with an additional star circling beyond the orbit of the third star. We can then treat the inner three stars system as a single star, and its separation between the fourth circling around them constitute another pair of binary. No new dead zone for habitability arises other than the one existed from the ternary system. Because in order for the fourth star to be stable, it has to circle the other three stars in a wide orbit 4 times the separation distance between the innermost star and the third, resulting in even the closest orbiting fourth star to be 200 AU away.

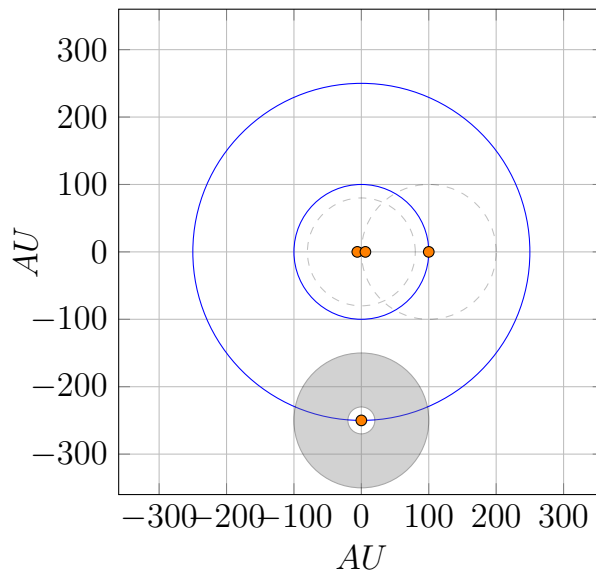


Figure 2.18: Quadruple system with one possible ternary system and the outer fourth star > 250 AU

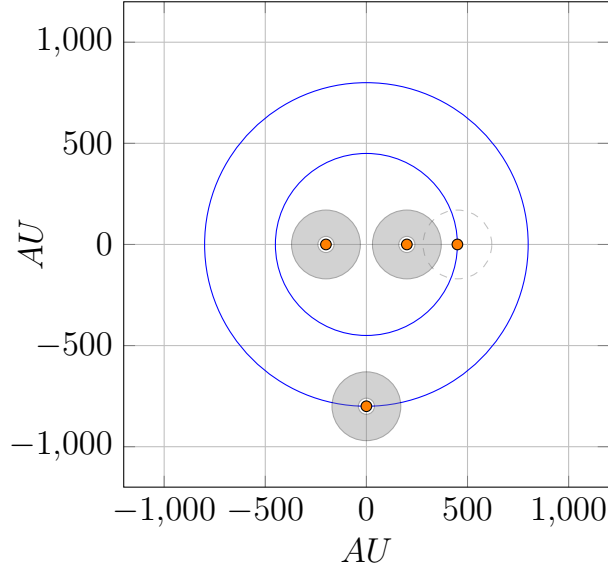


Figure 2.19: Quadruple system with one possible ternary system and the outer fourth star > 800 AU

$$A_0 = \left(\left(\frac{S_{1voidzone0}}{4} + \frac{2S_{1voidzone1}}{4} + \frac{3S_{1voidzone2}}{4} \right) + \frac{S_{1tight1}}{4} + \frac{2S_{1tight2}}{4} + \frac{S_{2inner}}{S_1 \cdot 4} \right) S_1 \quad (2.43)$$

$$A_1 = \left(\left(\frac{S_{3voidzone0}}{4} + \frac{2S_{3voidzone1}}{4} + \frac{3S_{3voidzone2}}{4} \right) + \frac{2S_{3inner}}{4S_3} \right) S_3 + \left(\frac{2S_{4inner}}{4S_4} \right) S_4 + \left(\frac{S_{5inner}}{S_5 \cdot 4} \right) S_5 \quad (2.44)$$

$$A_0 = 0.00244228290102 \quad A_1 = 0.00372429430183$$

$$P_0 = 1 - \frac{1}{100} \left(\frac{100(A_0 + A_1)}{T} \right) = 0.898708299249 \quad (2.45)$$

We obtained a result of 89.87% of the quaternary system can host potential life-bearing planets with the remaining 10.13% can not. This increasing trend is not hard to interpret because as more bodies are added the system. In order for the system to be stable, their placements have to be at a distance of 16 times the distance between the innermost pair, and 4 times in length of the semi-major axis of the third star. As a result, the additional star virtually does not affect the habitability of the inner stars at all, then the chance of habitability of planets increases. From this point onward, the habitability for multiple systems only increases.

The second major case consists of all possible combinations of two pairs of binaries where each

has separation ranges from 0 AU to beyond 200 AU.

In the first case, one computes the probability of two binary pairs separating less than 0.486 AU apart in tight orbits hosting habitable planets.

The total possible configurations range from 4 times the weighted average separation between the binary pairs in order to form stable orbits, which turns out to be $0.484 \cdot 4 = 1.944$ AU, up to the theoretical maximum separation between any pair.

$$P_{case1all} = S_1 \cdot S_1 \frac{\left(\int_{\log(0.486 \cdot 4)}^{\infty} D(x) dx \right)}{\left(\int_{-\infty}^{\infty} D(x) dx \right)} \quad (2.46)$$

$$= 0.00265630539327$$

Where S_1 , S_2 , S_3 , S_4 , S_5 , and S_6 is defined as:

$$S_1 = \frac{\left(\int_{\log(0.001)}^{\log(0.486)} D(x) dx \right)}{\left(\int_{-\infty}^{\infty} D(x) dx \right)} \quad S_3 = \frac{\left(\int_{\log(0.486)}^{\log(25 \cdot 1.7)} D(x) dx \right)}{\left(\int_{-\infty}^{\infty} D(x) dx \right)} \quad (2.47)$$

$$S_4 = \frac{\left(\int_{\log(25 \cdot 1.7)}^{\log(100 \cdot 1.7)} D(x) dx \right)}{\left(\int_{-\infty}^{\infty} D(x) dx \right)} \quad S_5 = \frac{\left(\int_{\log(100 \cdot 1.7)}^{\log(200 \cdot 1.7)} D(x) dx \right)}{\left(\int_{-\infty}^{\infty} D(x) dx \right)} \quad (2.48)$$

$$S_6 = \frac{\left(\int_{\log(200 \cdot 1.7)}^{\infty} D(x) dx \right)}{\left(\int_{-\infty}^{\infty} D(x) dx \right)} \quad (2.49)$$

$$S_1 = 0.055537328824 \quad S_3 = 0.509051264549$$

$$S_4 = 0.225394197923 \quad S_5 = 0.0837179170749$$

$$S_6 = 0.126194963279$$

With $P_{case1w1pair}$, the binary pairs can only host a single planetary system when they are separated between 100 AU and 200 AU apart.

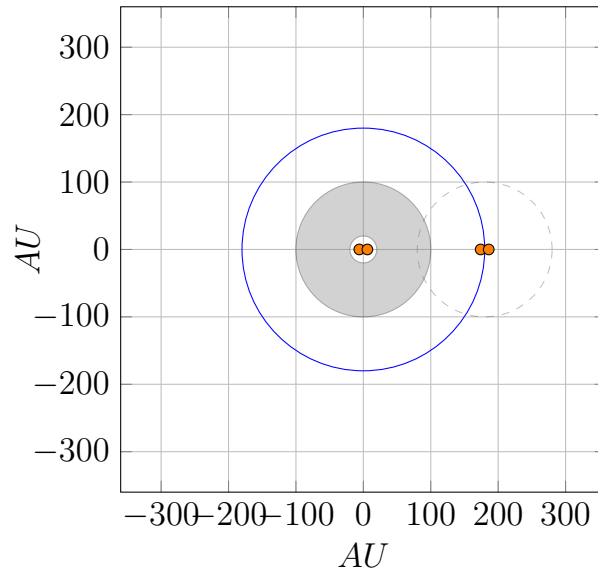


Figure 2.20: Quadruple system with the inner pair < 0.486 AU and the outer pair < 0.486 AU and a separation $100 \text{ AU} < x < 200 \text{ AU}$

With $P_{\text{case1w2pair}}$, the binary pairs can host two planetary systems when they are separated by greater than 200 AU.

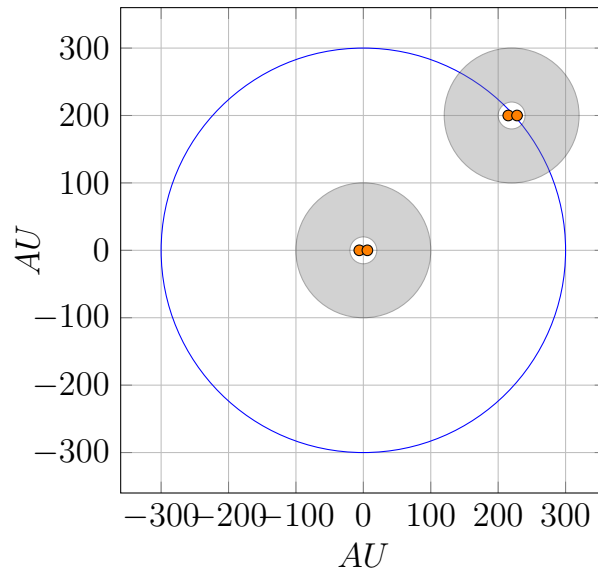


Figure 2.21: Quadruple system with the inner pair < 0.486 AU and the outer pair < 0.486 AU and a separation $> 200 \text{ AU}$

In addition, a dead zone of habitability occurs from the distance of minimum stable orbit of 1.944 AU up to 100 AU.

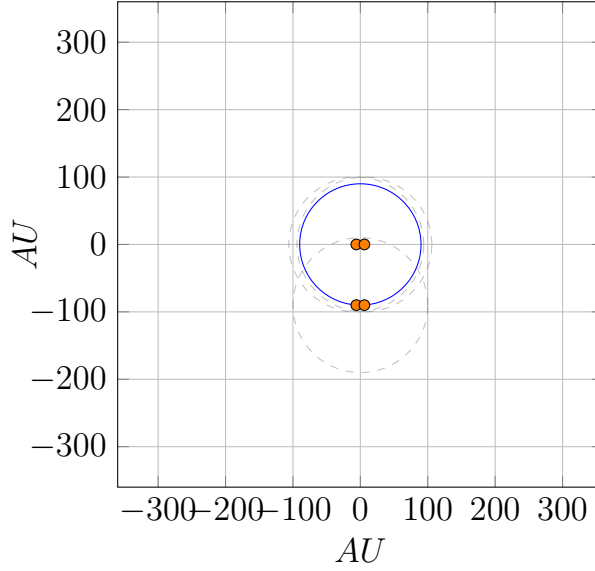


Figure 2.22: Quadruple system with the inner pair < 0.486 AU and the outer pair < 0.486 AU and a separation < 100 AU

$$\begin{aligned}
 P_{case1dead} &= S_1 \cdot S_1 \frac{\left(\int_{\log(0.486 \cdot 4)}^{\log(100 \cdot 1.7)} D(x) dx \right)}{\left(\int_{-\infty}^{\infty} D(x) dx \right)} \cdot 0.40864 \\
 &= 0.000820896945033
 \end{aligned} \tag{2.50}$$

In the second case, the inner pair has a separation between 0.486 to 25 AU, and the outer pair has a separation less than 0.486 AU. The total possible configurations range from 4 times the weighted average separation between the binary pairs in order to form stable orbits, which turns out to be $12.74 \cdot 4 = 50.97$ AU, up to the theoretical maximum separation between any pair.

$$\begin{aligned}
 P_{case2all} &= S_3 \cdot S_1 \frac{\left(\int_{\log\left(\frac{(0.486+25) \cdot 1.7}{2} \cdot 4\right)}^{\infty} D(x) dx \right)}{\left(\int_{-\infty}^{\infty} D(x) dx \right)} \\
 &= 0.0088510164068
 \end{aligned} \tag{2.51}$$

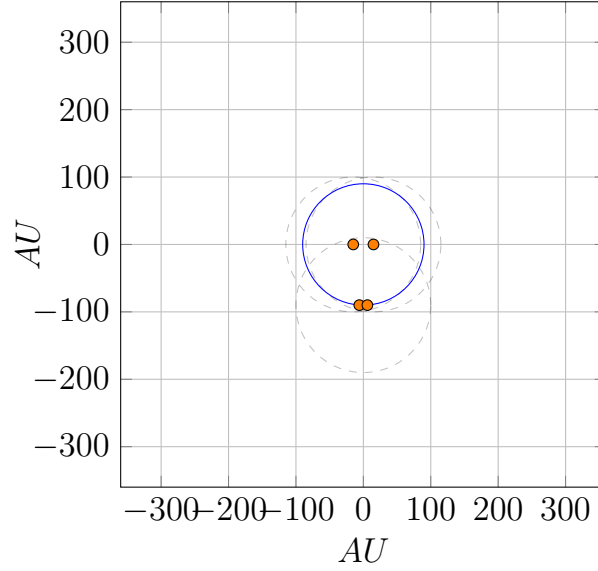


Figure 2.23: Quadruple system with the inner pair $0.486 \text{ AU} < x < 25 \text{ AU}$ and the outer pair $< 0.486 \text{ AU}$ and a separation $< 100 \text{ AU}$

A dead zone occurs when pairs separation ranges from the minimum stable orbit of 50.97 AU up to 100 AU , where the distance between the pairs disallows habitable planetary systems.

$$P_{case2dead} = S_3 \cdot S_1 \cdot \frac{\left(\int_{\log\left(\frac{(0.486+25) \cdot 1.7}{2}\right)}^{\log(100 \cdot 1.7)} D(x) dx \right)}{\left(\int_{-\infty}^{\infty} D(x) dx \right)} \cdot \frac{(0.3732 + 0.40864)}{2} \quad (2.52)$$

$$= 0.00114011678379$$

The pairs can only host a single planetary system when they are separated by 100 AU or greater. It is not possible to host two planetary systems when the pair is separated by 200 AU or greater because the separation distance of the inner pair itself creates a dead zone.

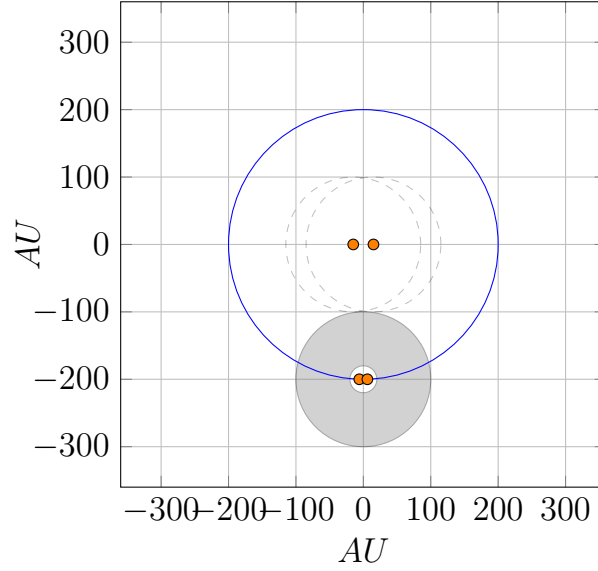


Figure 2.24: Quadruple system with the inner pair $0.486 \text{ AU} < x < 25 \text{ AU}$ and the outer pair $< 0.486 \text{ AU}$ and a separation $> 100 \text{ AU}$

$$\begin{aligned}
 P_{case2w1pair} &= S_3 \cdot S_1 \cdot \frac{\left(\int_{\log(100 \cdot 1.7)}^{\infty} D(x) dx \right)}{\left(\int_{-\infty}^{\infty} D(x) dx \right)} \cdot \frac{(0.3732 + 0.40864)}{2} \quad (2.53) \\
 &= 0.00231992254996
 \end{aligned}$$

When the inner pair has a separation between 0.486 to 25 AU, and the outer pair also has a separation between 0.486 to 25 AU, all possible cases constitute dead zones because both pairs neither permits habitable planets circling around any one of the stars within the pair nor permits habitable planets circling around the pair.

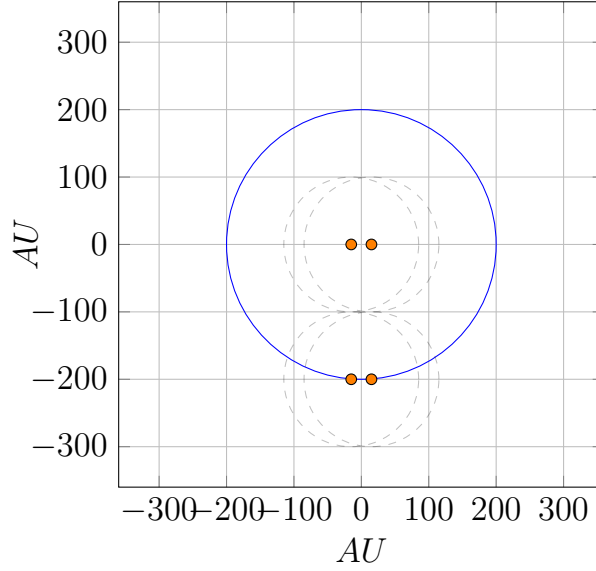


Figure 2.25: Quadruple system with the inner pair $0.486 \text{ AU} < x < 25 \text{ AU}$ and the outer pair $0.486 \text{ AU} < x < 25 \text{ AU}$ and a separation $> 100 \text{ AU}$

$$\begin{aligned}
 P_{case3dead} &= S_3 \cdot S_3 \frac{\left(\int_{\log\left(\frac{(0.486+25) \cdot 1.7}{2} \cdot 4\right)}^{\infty} D(x) dx \right)}{\left(\int_{-\infty}^{\infty} D(x) dx \right)} \cdot 0.3732 \quad (2.54) \\
 &= 0.0302768935426
 \end{aligned}$$

The third case composes cases where the inner pair has a separation between 25 AU to 100 AU. If the outer pair has a separation less than 0.486 AU, then the total possible configurations range from 4 times the weighted average separation between the binary pairs in order to form stable orbits, which turns out to be 250 AU, up to the theoretical maximum separation between any pair. Because the minimum stable orbit lies beyond the 100 AU space requirement for the habitable planetary system, no dead zone is observed under this configuration. When they are separated by 100 AU or more, one habitable system is possible to orbit around the outer pair.

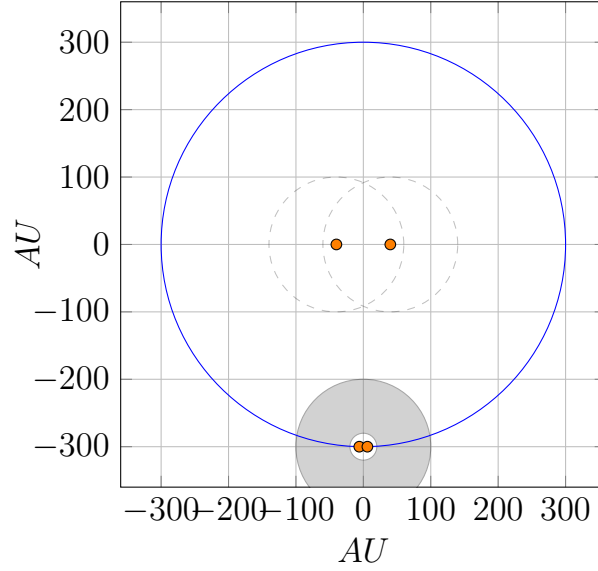


Figure 2.26: Quadruple system with the inner pair $25 \text{ AU} < x < 100 \text{ AU}$ and the outer pair $< 0.486 \text{ AU}$ and a separation $> 250 \text{ AU}$

If the outer pair has a separation between 0.486 AU to 25 AU , then all possible configurations lead to dead zones because the separation distance for both binary pairs alone results in dead zones for habitability.

$$P_{case5dead} = S_4 \cdot S_3 \frac{\left(\int_{\log(75.243 \cdot 1.7 \cdot 4)}^{\infty} D(x) dx \right)}{\left(\int_{-\infty}^{\infty} D(x) dx \right)} \cdot 0.3732 \quad (2.55)$$

$$= 0.00381948218057$$

If the outer pair has a separation between 25 AU to 100 AU , again, all possible configurations lead to dead zones because the separation distance for both binary pairs alone results in dead zones for habitability.

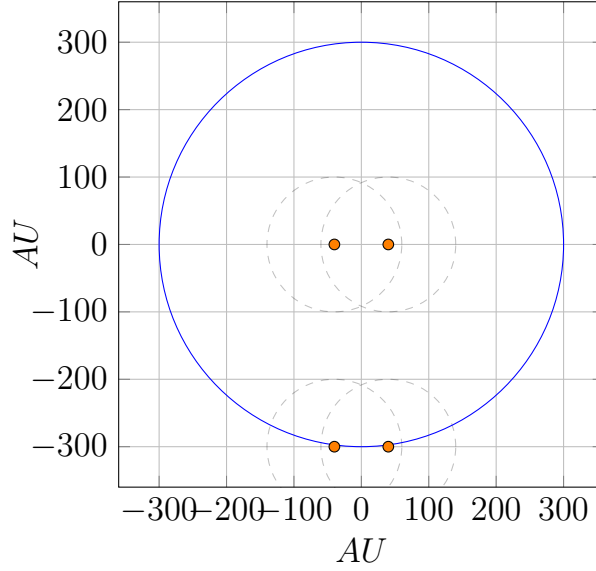


Figure 2.27: Quadruple system with the inner pair $25 \text{ AU} < x < 100 \text{ AU}$ and the outer pair $25 \text{ AU} < x < 100 \text{ AU}$ and a separation $> 250 \text{ AU}$

$$\begin{aligned}
 P_{\text{case6dead}} &= S_4 \cdot S_4 \frac{\left(\int_{\log(125 \cdot 1.7 \cdot 4)}^{\infty} D(x) dx \right)}{\left(\int_{-\infty}^{\infty} D(x) dx \right)} \cdot 0.3732 & (2.56) \\
 &= 0.00104941456592
 \end{aligned}$$

The fourth case composes scenarios where the inner pair has a separation between 100 AU to 200 AU. If the outer pair has a separation less than 0.486 AU, then the total possible configurations range from 4 times the weighted average separation between the binary pairs in order to form stable orbits, which turns out to be 300 AU, up to the theoretical maximum separation between any pair. Because the minimum stable orbit lies beyond 100 AU, the space requirement for the habitable planetary system, no dead zone is observed under this configuration, and the inner pair can host one planetary system around one of its stars, and the outer pair can host planets around the pair.

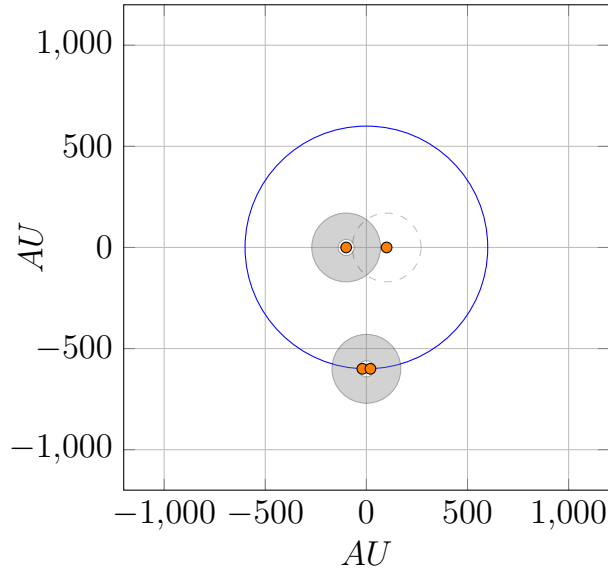


Figure 2.28: Quadruple system with the inner pair $100 \text{ AU} < x < 200 \text{ AU}$ and the outer pair $< 0.486 \text{ AU}$ and a separation $> 400 \text{ AU}$

$$P_{case7all} = S_5 \cdot S_1 \frac{\left(\int_{\log(150 \cdot 1.7 \cdot 4)}^{\infty} D(x) dx \right)}{\left(\int_{-\infty}^{\infty} D(x) dx \right)} \quad (2.57)$$

$$= 0.000214264015921$$

If the outer pair has a separation between 0.486 AU and 25 AU , again there is no dead zone, but only the inner pair can host one planetary system around one of its stars because the outer pair with such a separation falls under the binary dead zone list.

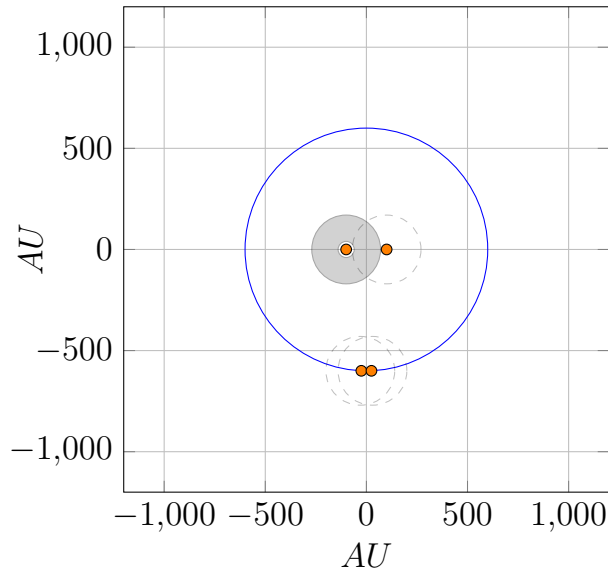


Figure 2.29: Quadruple system with the inner pair $100 \text{ AU} < x < 200 \text{ AU}$ and the outer pair $0.486 \text{ AU} < x < 25 \text{ AU}$ and a separation $> 400 \text{ AU}$

$$P_{case8all} = S_5 \cdot S_3 \frac{\left(\int_{\log(162.743 \cdot 1.7 \cdot 4)}^{\infty} D(x) dx \right)}{\left(\int_{-\infty}^{\infty} D(x) dx \right)} \quad (2.58)$$

$$= 0.00180593434059$$

If the outer pair has a separation between 25 AU and 100 AU, again there is no dead zone, but only the inner pair can host one planetary system around one of its stars because the outer pair with such a separation falls under the binary dead zone list.

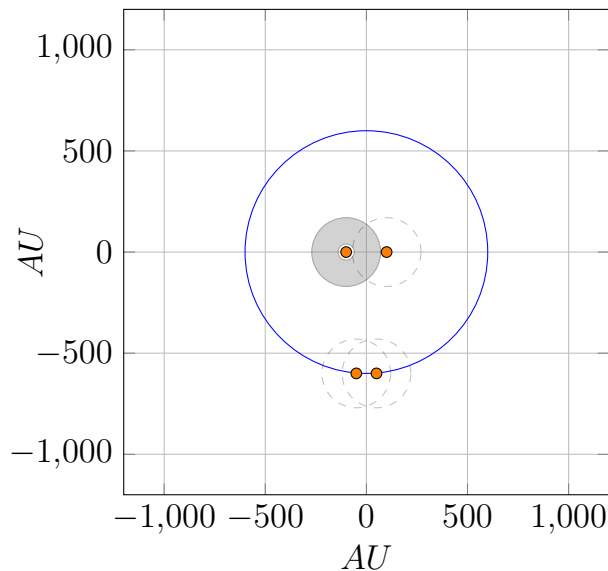


Figure 2.30: Quadruple system with the inner pair $100 \text{ AU} < x < 200 \text{ AU}$ and the outer pair $25 \text{ AU} < x < 100 \text{ AU}$ and a separation $> 400 \text{ AU}$

$$P_{case9all} = S_5 \cdot S_4 \frac{\left(\int_{\log(212.5 \cdot 1.7 \cdot 4)}^{\infty} D(x) dx \right)}{\left(\int_{-\infty}^{\infty} D(x) dx \right)} \quad (2.59)$$

$$= 0.000602874366204$$

If the outer pair has a separation between 100 AU and 200 AU, again there is no dead zone, and the inner pair can host one planetary system around one of its stars, and the outer pair can host one planetary system around one of its stars.

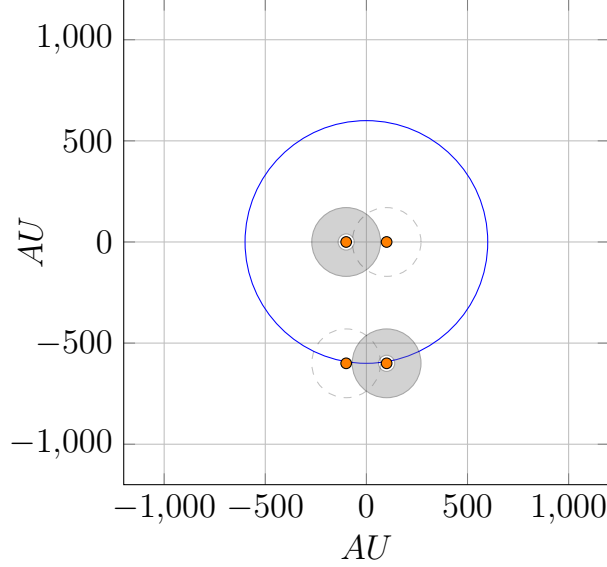


Figure 2.31: Quadruple system with the inner pair $100 \text{ AU} < x < 200 \text{ AU}$ and the outer pair $100 \text{ AU} < x < 200 \text{ AU}$ and a separation $> 400 \text{ AU}$

$$P_{case10all} = S_5 \cdot S_5 \frac{\left(\int_{\log(300 \cdot 1.7 \cdot 4)}^{\infty} D(x) dx \right)}{\left(\int_{-\infty}^{\infty} D(x) dx \right)} \quad (2.60)$$

$$= 0.000152762333122$$

The fifth case composes scenarios where the inner pair has a separation greater than 200 AU. If the outer pair has a separation less than 0.486 AU, then the total possible configurations range from 4 times the weighted average separation between the binary pairs in order to form stable orbits, which turns out to be 800 AU, up to the theoretical maximum separation between any pair. Because the minimum stable orbit lies beyond 100 AU, the space requirement for the habitable planetary system, no dead zone is observed under this configuration, and the inner pair can host two planetary systems around both of its stars, and the outer pair can host planets around the pair.

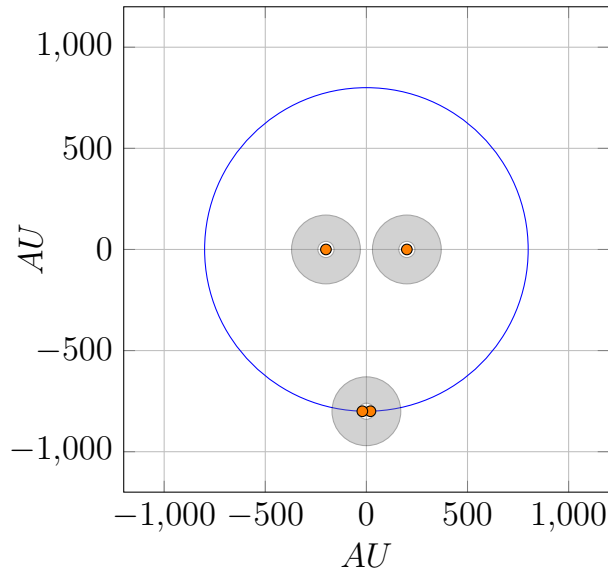


Figure 2.32: Quadruple system with the inner pair > 200 AU and the outer pair < 0.486 AU and a separation > 800 AU

$$\begin{aligned}
 P_{case11all} &= S_6 \cdot S_1 \frac{\left(\int_{\log(200 \cdot 1.7 \cdot 4)}^{\infty} D(x) dx \right)}{\left(\int_{-\infty}^{\infty} D(x) dx \right)} & (2.61) \\
 &= 0.000239015669122
 \end{aligned}$$

If the outer pair has a separation between 0.486 AU and 25 AU, there is no dead zone but only the inner pair can host two planetary systems around both of its stars because the outer pair with such separation falls under the binary dead zone list.

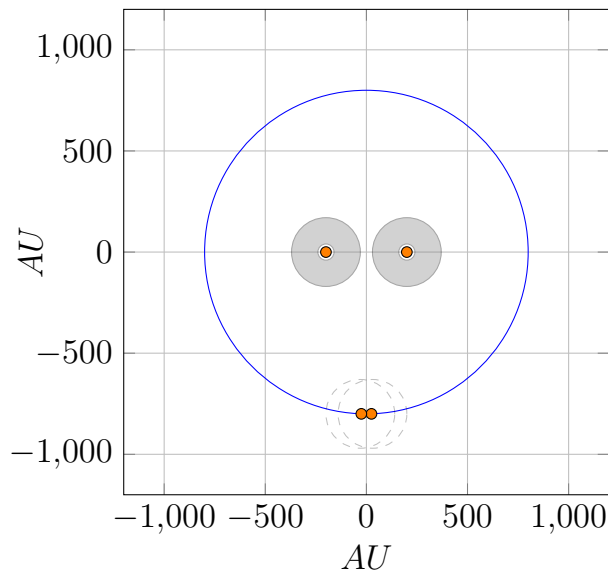


Figure 2.33: Quadruple system with the inner pair > 200 AU and the outer pair 0.486 AU $< x < 25$ AU and a separation > 800 AU

$$P_{case12all} = S_6 \cdot S_3 \frac{\left(\int_{\log(212.743 \cdot 1.7 \cdot 4)}^{\infty} D(x) dx \right)}{\left(\int_{-\infty}^{\infty} D(x) dx \right)} \quad (2.62)$$

$$= 0.00204989931341$$

If the outer pair has a separation between 25 AU and 100 AU, again there is no dead zone but only the inner pair can host two planetary systems around both of its stars because outer pair with such separation falls under the binary dead zone list.

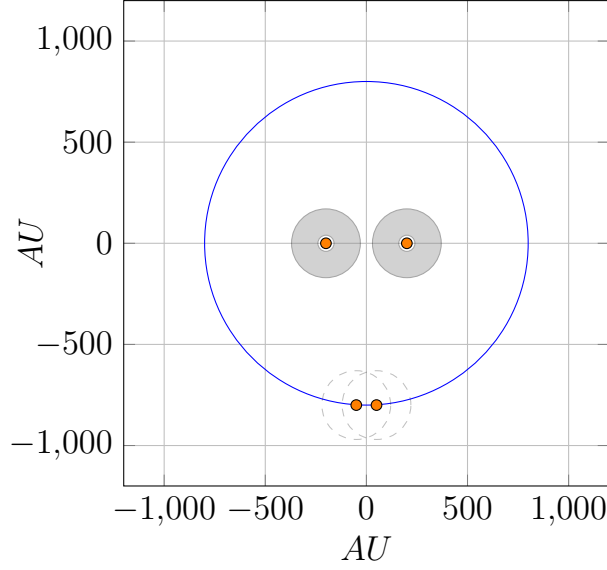


Figure 2.34: Quadruple system with the inner pair > 200 AU and the outer pair $25 \text{ AU} < x < 100 \text{ AU}$ and a separation > 800 AU

$$P_{case13all} = S_6 \cdot S_4 \frac{\left(\int_{\log(262.5 \cdot 1.7 \cdot 4)}^{\infty} D(x) dx \right)}{\left(\int_{-\infty}^{\infty} D(x) dx \right)} \quad (2.63)$$

$$= 0.000720527978655$$

If the outer pair has a separation between 100 AU and 200 AU, there is no dead zone and the inner pair can host two planetary systems around both of its stars, and the outer pair can host one planetary system around one of its stars.

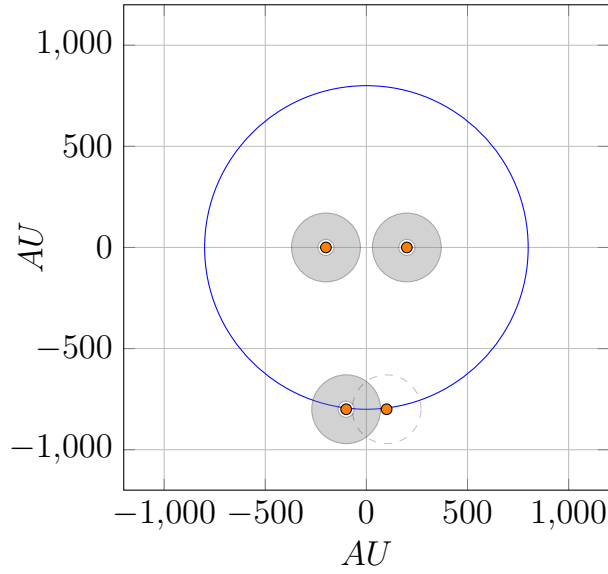


Figure 2.35: Quadruple system with the inner pair > 200 AU and the outer pair $100 \text{ AU} < x < 200 \text{ AU}$ and a separation > 800 AU

$$\begin{aligned}
 P_{case14all} &= S_6 \cdot S_5 \frac{\left(\int_{\log(350 \cdot 1.7 \cdot 4)}^{\infty} D(x) dx \right)}{\left(\int_{-\infty}^{\infty} D(x) dx \right)} & (2.64) \\
 &= 0.000192928173016
 \end{aligned}$$

If the outer pair has a separation greater than 200 AU, there is no dead zone, and planetary systems can orbit around all four-star system. This is the only case where all four stars are not over-counted from the number of our existing habitable systems. Since all four are capable of hosting life, we just treat them, conceptually, as four separate life-capable hosting stars.

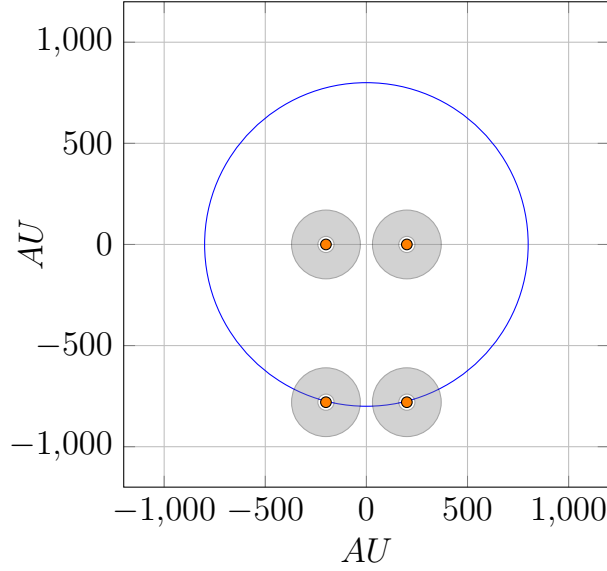


Figure 2.36: Quadruple system with the inner pair > 200 AU and the outer pair > 200 AU and a separation > 800 AU

$$P_{case15all} = S_6 \cdot S_6 \frac{\left(\int_{\log(400 \cdot 1.7 \cdot 4)}^{\infty} D(x) dx \right)}{\left(\int_{-\infty}^{\infty} D(x) dx \right)} \quad (2.65)$$

$$= 0.000248778237301$$

By deriving all possible cases for pairs of binaries, we can now sum up our results and obtain the following conclusion. This shows that 64.05% of the quaternary system with binary pairs can host potentially life-bearing planets with the remaining 25.95% can not.

$$P_{7dis} = P_{case7all} \cdot \frac{(0.40864 + 0.3732)}{2} \quad (2.66)$$

$$P_{8dis} = P_{case8all} \cdot 0.3732 \quad (2.67)$$

$$P_{9dis} = P_{case9all} \cdot 0.3732 \quad (2.68)$$

$$P_{10dis} = P_{case10all} \cdot 0.3732 \quad (2.69)$$

$$P_{11dis} = P_{case11all} \cdot 0.40864 \quad (2.70)$$

$$P_{12dis} = P_{case12all} \cdot 0.3732 \quad (2.71)$$

$$P_{13dis} = P_{case13all} \cdot 0.3732 \quad (2.72)$$

$$P_{14dis} = P_{case14all} \cdot 0.3732 \quad (2.73)$$

$$F_5 = \left(\frac{P_{14dis}}{4} \right) + \left(\frac{2P_{13dis}}{4} \right) + \left(\frac{2P_{12dis}}{4} \right) + \left(\frac{P_{11dis}}{4} \right) \quad (2.74)$$

$$F_4 = \left(\frac{2P_{10dis}}{4} \right) + \left(\frac{3P_{9dis}}{4} \right) + \left(\frac{3P_{8dis}}{4} \right) + \left(\frac{2P_{7dis}}{4} \right) \quad (2.75)$$

$$F_3 = \left(\frac{4P_{case6dead}}{4} \right) + \left(\frac{4P_{case5dead}}{4} \right) + \left(\frac{3P_{case4w1pair}}{4} \right) \quad (2.76)$$

$$F_2 = \left(\frac{4P_{case3dead}}{4} \right) + \left(\frac{3P_{case2w1pair}}{4} \right) + \left(\frac{4P_{case2dead}}{4} \right) \quad (2.77)$$

$$F_1 = \left(\frac{3P_{case1w1pair}}{4} \right) + \left(\frac{2P_{case1w2pair}}{4} \right) + \left(\frac{4P_{case1dead}}{4} \right) \quad (2.78)$$

$$P_0 = 1 - \frac{1}{100} \left(\frac{100(F_5 + F_4 + F_3 + F_2 + F_1)}{T} \right) \quad (2.79)$$

$$= 0.640577047181$$

A prudent reader may point out that we should also include the cases where the outer pair is placed at the center. Again, such case is symmetrical to our current computed case, since our earlier calculation for the quaternary system computation part 1 did not include the symmetrical case for the sake of computational simplicity, we will leave it out here as well. Finally, we take the weighted average of the two parts and arrive at the final habitability of the quaternary system at 73.08%.

$$P_{quad} = \frac{(0.0547128152559 + T \cdot P_0)}{(T + 0.0608793924588)} \quad (2.80)$$

$$= 0.730840297312$$

Once we have derived the probability for the ternary and the quaternary system, we can deduce the probability of the habitability of the sextuple system based on the results of the quaternary system. For a sextuple system with two additional stars orbiting quaternary system, all additional stars form stable orbit beyond the 200 AU limit for planetary habitability for both the circling star and the circled. As a result, all additional stars orbiting around an inner 4-star system can be treated, conceptually, as separate life hosting stars. For a sextuple system with an additional pair surrounds a pair of binary configuration, again, the outermost pair form stable orbit beyond the 200 AU limit for planetary habitability for both the circling star and the circled. As a result, all additional pairs orbiting around inner two pairs system can be treated, conceptually, as separate cases of binaries which would be already counted in our earlier calculation. Consequently, the probability of hosting habitable planets increases to 79.4%. There is a general trend of increasing habitability as the number of stars in the system goes up as more stars circling around a group of inner stars in stable orbits. We will use this number to back-extrapolate the habitable probability for a 5-star system, and 7, 8, 9, 10, and 11 star systems when the habitability approaches 100%. A system with greater than 11 stars are possible but are not counted toward the final calculation because the results do not alter the conclusion to several digits of precision. Based on the computed table, one can see that 69.28% of all multiple systems are habitable.

Multiple System	Percentage	Habitability
2*	80.00%	69.89%
3*	12.00%	61.29%
4*	4.80%	73.08%
5	1.92%	76.25%
6*	0.77%	79.41%
7	0.31%	82.70%
8	0.12%	86.13%
9	0.05%	89.70%
10	0.02%	93.42%
11	0.01%	97.29%

Table 2.2: Multiple stars systems habitability breakdown

2.7 Habitability of Low Mass Binaries

There remains the case where binary pairs with lower masses can match and provide enough heating for planets in their habitable zone and avoiding tidally lock at the same time with their combined luminosity. Multiple star system can be simply ruled out because all stable multiple systems come in a hierarchy, that is, a stable pair of binary revolves around another pair of binaries or single stars and their separation have to be at least 3 times the separation distance from the binary pairs they revolve. In essence, the habitable zone is an applicable definition only to single or binaries. Multiple star system can host habitable planet, but it must be revolving around one of its subunit consisting of a single or a binary star.

Since luminosity increases to the 3.5thpower of the stellar mass, luminosity drops to the inverse of 3.5thpower as the stellar mass decreases. This indicates that only stars from 0.5613 solar mass to 0.628 solar mass have enough mass to shed enough luminosity and when combined in pairs (assuming the secondary has a mass 81.99% of the primary) gives enough heat that provides a tidal locking free habitable zone.

$$j_{luminosity} = (0.8199 \cdot x)^{3.5} + (x)^{3.5} \quad (2.81)$$

$$j_{luminosity} = x^{3.5} \quad (2.82)$$

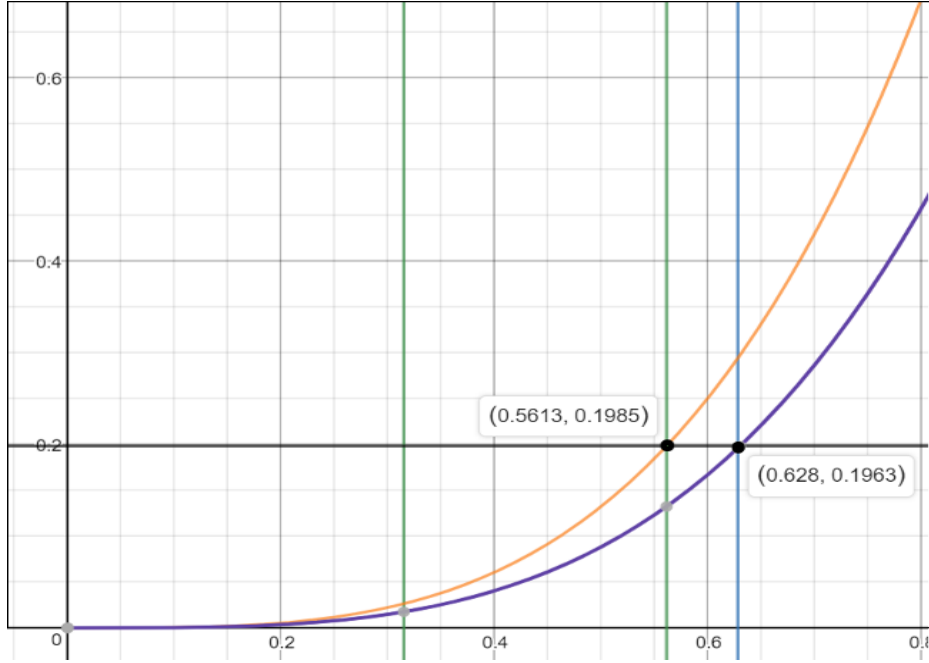


Figure 2.37: The minimum binary stars' primary stellar mass threshold requirement for the pair's combined luminosity output matches the luminosity the smallest single star

Stars with 0.628 solar mass or greater alone, without pairs, can provide a tidal locking free habitable zone and it is already counted toward our total number of habitable planets. However, by stricter definition, the chance of two equal mass closely paired binaries are rare. In fact, the primary to the secondary mass ratio in closely paired binaries do not follow the stellar mass power law distribution. There is an observed little spike in the probability distribution for secondary mass and the q number closely matching 1, but in general, the secondary companion can have all possible mass from 1 primary mass to 0.1 primary mass. An approximate distribution is given below:

$$f_{nearpeak}(x) = \frac{0.012}{Q\sqrt{2\pi}} e^{-\frac{\ln(-x+2)^2}{2(Q)^2}} \quad (2.83)$$

$$f_{near}(x) = (x^{0.1} - 0.1) + f_{nearpeak}(x) \quad (2.84)$$

$$Q = 0.05 \quad (2.85)$$

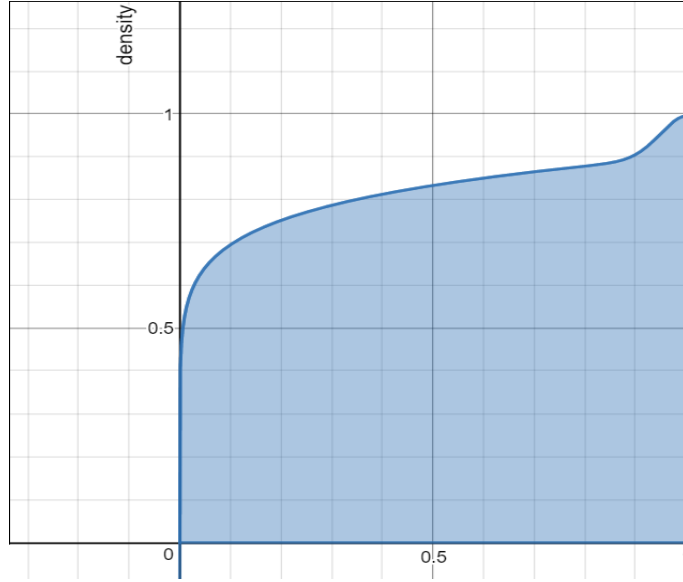


Figure 2.38: The cumulative probability distribution function of the secondary stellar mass to the primary stellar mass ratio

Now, the weighted average expected mass of the two pairs is then 1.4261, shy of the twice of the primary mass. Out of tightly orbiting binaries, only 40% of which has companions of mass 62.8% or greater relative to the primary.

$$\frac{\left(\int_{0.628}^1 f_{near}(x) dx\right)}{\int_0^1 f_{near}(x) dx} \quad (2.86)$$

$$= 0.408640496059 \quad (2.87)$$

and their companions weighted average mass is 81.99% of the primary which is the benchmark we have set earlier.

$$\frac{\left(\int_{0.628}^1 f_{near}(x) \cdot g(x) dx\right)}{\int_{0.628}^1 f_{near}(x) dx} \quad (2.88)$$

$$= 0.819943306914 \quad (2.89)$$

Based on this assumption, only stars from 0.5612 solar mass to 0.628 solar mass fit our criteria. Based on the spectral class and the initial mass function, 4% of the stars range from 0.5612 to 0.628 solar mass. Out of these stars, 36% of which are binaries or multiples. Out of the binaries and multiples, one needs to find those in tight orbits that allowed a tidal locking free habitable zone. It is difficult to compute the total luminosity of two sources of light when they are separated by a distance. However, we can approximately treat those two sources of light as a single point light source since we are only interested in closely paired binaries. In order for a planet to be in a stable orbit around a binary pair the separation distance between the

planet and binary pair has to be at least 3 times or greater (preferentially 5 times or greater) than the distance between the binary pairs. Therefore, if we treat the midpoint between the two closely paired binaries as the source of the emitting light, then the margin of error of total energy received at the stable orbit boundary ranges from 16% to 4.94% and the margin of error decreases as the planet revolves in orbit further away from the pairs.

Then, the separation distance between the pairs has to be approximately a third of the distance from the binary to the edge of the habitable zone. With pair separation greater than a third of binary's habitable edge distance, all stable orbits lie beyond the outer edge of the habitable zone. With pair separation less than a third of binary habitable edge distance, some stable orbits lie beyond the outer edge of the habitable zone, and one orbit lies on the habitable zone and some lies beyond the inner edge of the habitable zone.

$$w = 3 \cdot \frac{\dot{J}_{dist2}}{3} \tag{2.90}$$

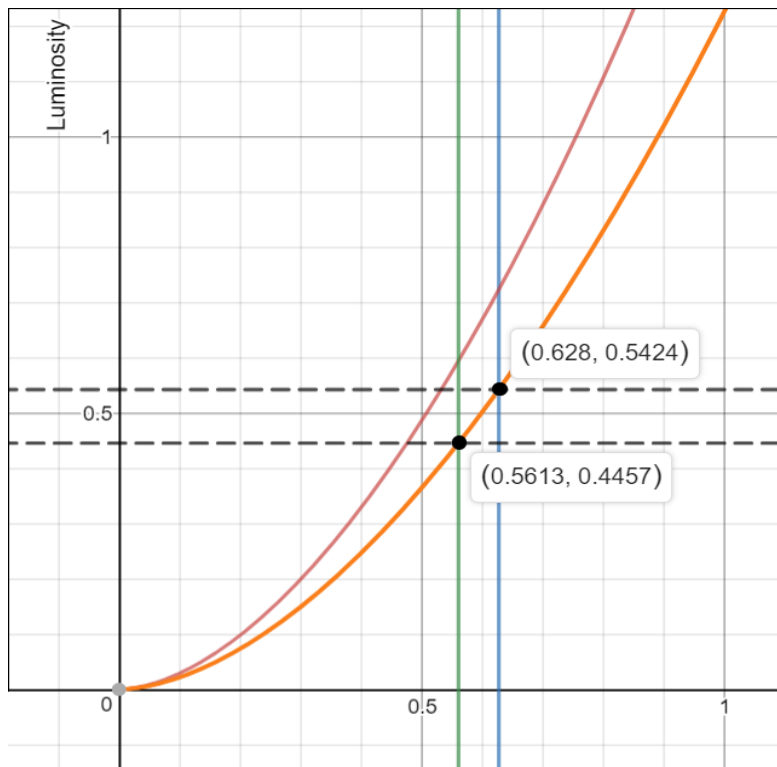


Figure 2.39: The plot for pair separation at an exact one third of the their habitable zone so that the minimum stable orbit of habitable planet falls on the habitable zone

If we assume that the average separation of 0.494 AU (taking the upper and the lower bound in the graph above) between the binary star and its habitable zone for binary primary mass ranges from 0.5613 to 0.628 solar mass, then the probability of binaries with a separation at or less than 0.1647 AU is 3.12%. (based on statistical data on the probabilistic distribution of binaries of comparable mass) Plugging into the tidal locking equation, one can see that if we treat two stars as a single source for locking effect, then any planets revolving around them

would be tidally locked in 4.58 Gyr, therefore, no planets are habitable by earth's standards.

$$T_{binlocktosun} = \frac{\left(\frac{1}{13,750}\right) \cdot (0.5424 \cdot a_{earth})^6 \cdot I_{earth} \cdot M_{earth} \cdot 909.0909}{3G \left((1.8199 \cdot 0.628M_{sun})^2\right) R_{earth}^3 \cdot 60 \cdot 60 \cdot 24 \cdot 365} \quad (2.91)$$

$$= 4.4040499657 \cdot 10^9 \text{ years}$$

If we treat two stars as completely separate sources for locking effect, then the primary star has to be 0.588 solar mass or above in order to provide a planet with a rotational day faster than one week.

$$T_{binlocktosun} = \frac{\left(\frac{1}{13750}\right) \cdot (0.4834 \cdot a_{earth})^6 \cdot 0.344 \cdot M_{earth} \cdot 909.0909}{3G \left((0.588M_{sun})^2 + (0.8199 \cdot 0.588M_{sun})^2\right) R_{earth}^3 \cdot 60 \cdot 60 \cdot 24 \cdot 365} \quad (2.92)$$

$$= 5.1863329085 \cdot 10^9 \text{ years}$$

Since the distance between the planet and the star is at least 3 times the distance between the pair (so the two mass can almost be treated as one), therefore, the first result is weighted at least 88.89% more accurate compares to the second one. The weighted results indicate that even in the most realistic case, only binary stars from 0.623 to 0.628 solar mass is what we are interested in counting, which accounts for 0.1728% of all stars.

This added up to a total of 3,201,646 extra habitable exoplanets to our list for all time period regardless of metallicity. With metallicity taking into consideration, there are only 843,478 extra exoplanets to be added to the total.

2.8 Red Dwarves' Habitability

Red dwarves are the most abundant stars in the universe, due to their smaller mass, their absolute luminosity are a small fraction compares to that of orange and yellow dwarves such as the Sun. Red dwarves are known for their long stability once it starts its nuclear fusion process which lasts for trillions of years. As a result, they form a large pool of potential candidates for habitable planets.[16] The drawbacks of the Red dwarf system are also self-evident. Because of its low luminosity, a planet has to be significantly closer to the host star compares to the Sun in order to gain the same level of radiation as it is received on Earth. As a result, all potentially habitable planets around red dwarves are tidally locked. With one side of the planet permanently facing daylight and the other perpetually stares into the darkness, the temperature difference becomes extreme. Prolonged exposure to radiation on the dayside brings extreme temperature variations between the day and night side. This is easily verified by seasonal changes on earth, where even a few extra hours of sunlight during the summer month significantly increases the temperature and fewer hours of sunlight during the winter

month significantly increases frigid cold storm events. Many have argued that life can be harsh and probably restricted to the dim light zone sandwiched between the hot inferno and the cold dead world, offering very limited adaptive radiation opportunity by the local fauna if any exists at all. Many argue that liquid water may not be sustainable because the water completely evaporates on the dayside and condenses into ice on the night side. Some have argued that an atmosphere which is dense enough can distribute the heat more uniformly throughout the planet. Others argued that an atmosphere may be maintained if the red dwarf does not follow a circular orbit around its host star. Eccentric orbit creates tidal heating which in turn generates a magnetic field strong enough to protect the planetary atmosphere from blowing away.[6] Another serious consequence is the loss of its magnetic field. Venus has a similar mass to earth, and its slow rotation and its lack of internal thermal convection, any liquid metallic portion of its core could not be rotating fast enough to generate a measurable global magnetic field. Without a magnetosphere, Venus with an atmosphere comparable to the thickness of earth with a composition of O₂ and N₂ can deplete. A thick atmosphere can reduce depletion loss, as observed on Venus, through its ionosphere.[34] The ionosphere separates the atmosphere from the outer space and the solar wind. This ionized layer excludes the solar magnetic field, giving Venus a distinct magnetic environment. Maintaining such a dense atmosphere seem to give life a chance despite a lack of magnetic field. Even hypothetically a dense O₂ atmosphere can be maintained, it will be extremely flammable, and secondly, life adapted to such dense atmosphere will evolve with higher similarity to aquatic adaptation than terrestrial adaptation. It is known that no opposable thumb and bipedalism is observed in any aquatic species, reducing the chance of the emergence of intelligent tool-using species.

All these assumptions can be valid even if they are not the universal representation of the reality on all terrestrial planets formed around red dwarves. What really separates red dwarves from their more massive cousins are their strong magnetic fields.[7] According to the standard dynamo theory, the magnitude of a magnetic field generated by a heavenly body is proportional to its temperature, its convecting mass, and its rotational rate, and the empirical law can be used to extrapolate the magnetic field strength of different heavenly bodies by its size. The sun, though 10 times greater in mass than Red dwarves, 99 percent of its mass is condensed into such a high density that the heat is transferred through conduction and radiation. The remaining 1% upper layer of the sun, separated from the sun's core by the Tachocline, composed of plasma, is where the convection taking place. Red dwarves with mass smaller than 0.36 solar mass are fully convective. As a result, they produce a magnetic field with strength hundreds of times stronger than that of the Sun. Furthermore, any habitable planets around red dwarves are hundred times closer to their host star than that of the earth. The field strength of magnetic field decreases as the inverse of the cubed of the separation distance from the magnetic field. As a result, the stellar magnetic field strength around such terrestrial planet is a million times stronger than the stellar magnetic field strength observed around the earth, which is around 10⁻⁹ Tesla. This implies that the stellar magnetic field strength is at 10⁻³ Tesla. If the planet

does have its own magnetic field to shield itself from the stellar field to protect its atmosphere like in earth's case, its own magnetic field has to be about three magnitudes stronger, which implies the planet magnetic field strength has to reach 1 Tesla. Studies have shown that large organism such as human cannot tolerate magnetic field strength of 1 Tesla for too long, this has been demonstrated by clinical studies done on patients undergoing MRI scans. This is especially true when one is exposed to a changing field. Organisms can hardly survive in such strong field because all animals move around frequently, as it moves fast, they are subject to moving magnetic fields.

On the other hand, it seems unlikely an Earth-like planet can produce a magnetic field with such strong strength. It is more likely that the planet is vulnerably exposed to the onslaught of the stellar field. Even if the atmosphere is dense enough to be maintained, two major problems arise. First of all, all stars periodically enter active periods. In sun's case, periodic appearance of sun spots and flares which increases the stellar magnetic strength by three orders of magnitude, this is observed on Earth in 1858 during the Carrington Event. Since the field strength can vary from time to time and a solar storm can last from hours to days, a changing field with strength around 1 Tesla inflicts significant damage on organisms even if they assume a sedentary lifestyle. Furthermore, a planet without a magnetic field can no longer divert cosmic rays and radiation particles from reaching the surface of the planet. From earth's polar data, where solar winds strike at the poles, the radiation level reaches 15 msvet, which in a dosage-dependent manner, can render organism sterilized and is lethal to continual exposure for more than three hundred days. Furthermore, in an extremely long stretched imaginative scenario, somehow an extremely radiation resisting organism emerges on such a planet, it may never able to utilize telecommunication technology given the magnetic storm bombardment on a daily basis. In conclusion, every other thing being equal, organisms cannot survive on red dwarves' planets due to the presence of strong magnetic field created by their host star.

To fully appreciate the strength and power of red dwarves' magnetic fields, the detailed calculation is performed.

The measured magnetic field strength of a given location is directly proportional to the total mass of the conducting fluid, its temperature, its speed of rotation in radians, and is proportional to the inverse cubed of its distance from the generating dynamo.

$$S = \frac{M \cdot T \cdot \omega}{r^3} \quad (2.93)$$

We shall start by using the field strength of earth as a reference. [39][96]

The Earth, like other planets in the Solar System, as well as the Sun and other stars, all generate magnetic fields through the motion of electrically conducting fluids. The Earth's field originates in its core. This is a region of iron alloys extending to about 3,400 km. It is divided into a solid inner core, with a radius of 1,220 km, and a liquid outer core. The motion of the liquid in the outer core is driven by heat flow from the inner core, which is about 6,000 K, to

the core-mantle boundary, which is about 3,800 K. The average density of outer core is $11.5 \frac{\text{kg}}{\text{m}^3}$, and average temperature is at 4,900 K. The total mass of the outer core amounts to 0.11538 Earth mass. The total strength of the magnetic field can be expressed as 1,179.1217 earth mass temperature unit. This value is further reduced by 56 folds at the surface of the planet as the strength of magnetic field decreases from the generating dynamo toward the surface. The distance from the generating dynamo to the surface of the planet is 2,970 km. Finally, the value is multiplied by a factor of 1, indicating a rotational speed of $1,674.4 \frac{\text{km}}{\text{h}}$. Therefore, the magnetic field strength at the surface of the planet amounts to 21.22 earth mass temperature unit, which is comparable to 21.22 microtesla, as it is observed.

$$\begin{aligned}
 u_{earth} &= \frac{\left(\frac{4}{3}\pi \left(\frac{34}{63.7}\right)^3 - \frac{4}{3}\pi \left(\frac{12.2}{63.7}\right)^3\right) \cdot \left(\frac{11.5}{5.514}\right)}{\frac{4}{3}\pi} \cdot 4,900 \cdot \frac{1}{55.5555} \quad (2.94) \\
 &= 21.2242111102
 \end{aligned}$$

The sun's magnetic field is generated by the fluid convection generated by the convection zone. The convection zone extends from 0.7 solar radii to 0.9992820136 radii. There is a 500 km deep photosphere covering above the convection zone. For approximation purpose, one can consider the convection zone extends from 0.7 solar radii to 1 solar radii. The density of the convection zone ranges from $0.2 \frac{\text{g}}{\text{cm}^3}$ at the bottom to $0.2 \frac{\text{g}}{\text{m}^3}$ (about $\frac{1}{6,000}$ th the density of air at sea level), a total drop by a million fold. The temperature rises from 5,700 K (9,100K) at the surface to 1.5 million K at the base. The total mass of the convection zone is subject to debate. If the average density of the convection zone lies at 1,000 times the density compares to the surface and 1,000 times less than the density at the bottom of the layer, then, then it is approximately 31 earth mass. However, if this is true, then the sun's magnetic field must be 200 times stronger than what we observed assuming an average temperature of 100,000 K. One can match the observed results by reducing the average temperature to 1,492 K, which is equally absurd because a star with a convective zone of 1,492 K temperature is effectively a brown dwarf. This points out that the average density must be much lower, and density drops exponentially fast away from the core. For our data analysis, we chose the convection zone with 4.625 earth mass and an average temperature of 100,000 K, together with a 500 km photosphere and a drop of field strength multiplied by a factor of $\frac{1}{29.89}$ (the rotation speed of sun is 4.293 times faster than earth but translated into radians per second it is only $\frac{1}{30}$ th of earth) yields 681.75 earth mass temperature unit. The value is comparable to what is observed on the sun by taking the weighted averages in units of 700 microteslas (sun's polar field strength at 1~2 gauss, sunspot 3,000 gauss, and 10-100 gauss in solar prominences.)

$$\begin{aligned}
u_{sun} &= \frac{\left(\frac{4}{3}\pi \left(\frac{R_{sun} \cdot 0.99928}{1}\right)^3 - \frac{4}{3}\pi \left(\frac{R_{sun} \cdot 0.7}{1}\right)^3\right) \left(\frac{0.2}{5.514 \cdot 6700}\right) 10^5 \left(\frac{1}{\left(\frac{500}{9}\right)}\right)^{\left(\frac{\log 500}{\log 2,970}\right)} \left(\frac{1}{29.89}\right)}{\frac{4}{3}\pi} \\
&= 681.748989893
\end{aligned} \tag{2.95}$$

Using the above equations, we can also set the upper limit on the mass of the convection layer. If the temperature of the entire zone is merely slightly higher than the surface temperature of the sun at 10,000 K, then, at most, convection zone contains 46.25 earth mass at the density of 1 out of 670th of the density at the bottom of the convective layer.

For Jupiter, we find that its dynamo, from literature, is generated from 0.25 to 0.79 radii region, where metallic hydrogen is able to conduct magnetic field sitting above the core and below the liquid and gas hydrogen layers above. The average temperature of this region amounts to 23,000 K. The rotational speed of 45,000 $\frac{\text{km}}{\text{h}}$, is 26.88 times faster than earth, translated into 2.41 times the speed of the earth in terms of radians per second.

However, the final result does not match the observed results. In order to match observation, the layer of the dynamo that generates the field has to be lowered to 0.735 radii. The strength at the surface of the planet is then 462.82 earth mass temperature unit, comparable to what we observed. The mass of the dynamo generating region of Jupiter is then 112 earth mass, much larger than the sun's 4.625 earth mass.

$$\begin{aligned}
v_{juptermagnetic} &= \frac{\left(\frac{4}{3}\pi \left(\frac{R_{jupiter} \cdot 0.735}{1}\right)^3 - \frac{4}{3}\pi \left(\frac{R_{jupiter} \cdot 0.25}{1}\right)^3\right) \left(\frac{1.2258}{5.514}\right) 23,000 \left(\frac{1}{13,484.42}\right) \left(\frac{24}{9.925}\right)}{\frac{4}{3}\pi} \\
&= 462.140742196
\end{aligned} \tag{2.96}$$

Finally, we check the value for Saturn. Saturn's generating dynamo arises from approximately 0.42 radii to 0.8 radii with an average temperature of 7,475 K. The rotational speed of 35,500 $\frac{\text{km}}{\text{h}}$, is 21.2 times faster than earth, or 2.25 times the rotational speed of the earth in terms of radians per second. However, the value is again larger than what is observed. In reality, the strength of Saturn's magnetic field at the surface is observed to be slightly less than earth's. Again, we fine-tuned the radii of the layer generating the dynamo so that the new results match our observation. (the upper reaches changed from 0.8 radii to 0.67 radii) The mass of the dynamo generating region of Saturn is then 19.167 earth mass, much larger than the sun's 4.625 earth mass but much smaller than Jupiter's. It is still much weaker than the sun's because its average temperature is much lower.

$$\begin{aligned}
m_{saturn} &= \frac{\left(\frac{4}{3}\pi \left(\frac{R_{saturn} \cdot 0.67}{1}\right)^3 - \frac{4}{3}\pi \left(\frac{R_{saturn} \cdot 0.4293}{1}\right)^3\right) \left(\frac{0.62449}{5.514}\right) 7475 \left(\frac{1}{15048.22}\right) \left(\frac{24}{10.55}\right)}{\frac{4}{3}\pi} \\
&= 21.6592062736
\end{aligned} \tag{2.97}$$

The mismatch of values derived based on existing literature for Jupiter and Saturn’s magnetic field strength and the observed one can be explained in many ways. It is possible that metallic hydrogen’s conductivity is lower than its equivalent at a much higher temperature in the plasma state by a magnitude or less, which is not accounted by our existing model and assumption. It is also possible that the dynamo generating effect does not start at all layers of metallic hydrogen. It is more likely to generate from either the bottom layer, middle, or upper layers. The adjustment requires further analysis, the validity of the model is not jeopardized because by fine-tuning the parameters within a reasonable range of error of tolerance, the observed and computed values do match.

We then apply our model to that of the red dwarf stars. The model composed the extent of the semi-major axis of planets for stars of different masses. In general, the smaller the star, the less material is required to create one. As a result, the smaller semi-major axis for the stars’ hosted planets. The habitable zone model illustrates how does the region where liquid water can form shifts for stars of different mass. Luckily and surprisingly, those two graphs coincide fairly well with each other at every possible stellar mass. That is, we can say that if Spectral G class like the sun can host a planet within its habitable zone, so can the rest of the stars regardless of its spectral class.

Then, we model the strength of the interplanetary magnetic field strength as observed in the solar system. From the existing literature, it states that the surface of the sun’s polar field is around 0.0002 T, but significantly higher at the sunspots and solar prominences. One takes the weighted average and chose a value of 0.0006 T. This field strength decreases to the inverse cubed from its distance away from the surface. If space were a vacuum, one should observe that the field strength at the earth, theoretically, drops to $1 \cdot 10^{-11}$ Tesla. However, satellite observations show that it is about 100 times greater at around 10^{-9} Tesla.[96] Magnetohydrodynamic (MHD) theory predicts that the motion of a conducting fluid (the interplanetary medium) in a magnetic field, induces electric currents which in turn generates magnetic fields, and in this respect, it behaves like a MHD dynamo. Based on observation, we model our field strength as it decreases away from the source. We stopped at 0.00390625 AU because when we back extrapolate, this value reaches parity with the sun’s surface value. This is interesting because the magnetic field strength decreases much faster if it is shielded within much higher density space such as inside the sun or the earth. Apparently, the magnetic field strength decreases much less in a nearly vacuum space.

Lastly, we use our earlier model to predict each celestial sphere’s generating magnetic field

strength to predict the magnetic field strength of red dwarves. Since red dwarves, those with less than 0.35 solar mass are fully convective. Its entire mass is used to generate a dynamo, at 0.35 solar mass, there is 116,550 earth masses are used to generate the magnetic field inside the star instead of 4.625 earth mass as observed for the sun. The other parameter one has to consider is the internal temperature of the star. Because currently there is a lack of data regarding the internal temperature of other star systems, we have to guesstimate. For the sun, at the bottom of the convective layer, the temperature reaches 1.5 million K, the temperature increases to 7 million K at the boundary of the core, and the core itself reaches a temperature of 15.7 million K. If one is to be conservative and downplay the field strength of the red dwarves, the average internal temperature of a red dwarf at the 0.35 solar mass should be no less than 1.5 million K, and this value decreases with the luminosity function as the stellar mass decreases. In reality, the average temperature can be much higher. 99% of sun's nuclear fusion occurred at its core, and the core temperature is 15.7 million K. We treat the rotation rate for all stars nearly the same or within the range of the error of tolerance. Then, we can almost immediately find that the strength of magnetic field on a 0.35 solar mass red dwarf is 108,000 times stronger than the sun at its surface. This is not surprising because this result has been confirmed by observation. On April 23, 2014, NASA's Swift satellite detected the strongest, hottest, and longest-lasting sequence of stellar flares ever seen from a nearby red dwarf. The initial blast from this record-setting series of explosions was as much as 10,000 times more powerful than the largest solar flare ever recorded.

$$s = \frac{333000 \cdot x}{4.625} \left(j_{luminosity} \cdot \frac{944}{10} \right) \cdot h \quad (2.98)$$

$$h = 0.0006 \cdot \left(\frac{y_{habitablezone}}{0.00390625} \right)^{-3} \cdot 100 \quad (2.99)$$

$$y_{habitablezone} = \frac{1}{1.1547} \sqrt{\left(\frac{4}{3} x^3 \right)} \quad (2.100)$$

$$j_{luminosity} = \sqrt{x^{3.5}} \quad (2.101)$$

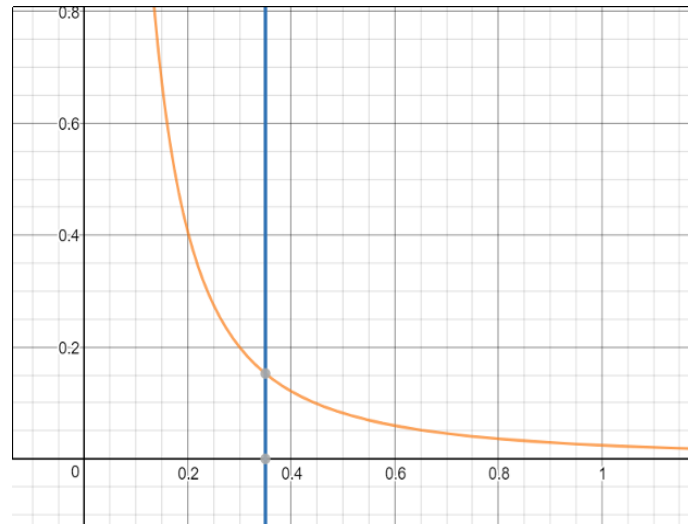


Figure 2.40: Magnetic field strength vs stellar mass

We combine the above equation to yield the strength of the stellar magnetic field experienced by red dwarf's planets. It can be shown, then, that the strength of the interplanetary magnetic field increases as the stellar mass decreases as the habitable zone has to move ever closer to the star. At 0.35 solar mass, the field strength is 0.1526 Tesla. This is significantly higher than earth's magnetic field strength at $4.5 \cdot 10^{-5}$ Tesla. Since solar magnetic field around the earth was only $4.5 \cdot 10^{-9}$ Tesla, the earth's magnetic field protects life from solar storm comfortably. However, this is not possible on any red dwarfs. It is impossible for a planet at the size of earth or slightly larger to generate a field not just 0.1526 Tesla, but significantly larger by 3 orders of magnitude to shield away from the red dwarf's. As a result, the planet will experience the onslaught of the stellar storm on a daily basis. It is still possible that the atmosphere of the planet maintained as the case of Venus, but certainly, the radiation level can be 3 to 4 times higher than observed on the surface of the earth. It has been shown that space station at low earth orbit, inside the earth's magnetic shield, receives a dosage of 140 millisievert unit of radiation. In the interplanetary space, this value increases to 480 millisieverts. Life could adapt to be more resistant to radiation on such a planet.

However, a compressed magnetic field is not the only problem planets around red dwarf has to deal with. The deadliest is the stellar prominences and stellar flares. it is frequently observed that red dwarfs frequently increases its luminosity in a matter of days and months. In the case of the sun, even a much milder version compares to the red dwarves, creates a major storm every few years. Some notable ones recorded are the Carrington Event (occurred between August 28 to September 2nd, 1859), at the time field strength has increased to 1600 nT, which is 1600 times the average strength observed around the earth. The November 1882, May 1921 geomagnetic storm, March 1989 geomagnetic storm (with minimum Dst of -589 nT, or 589 times than normal.), July 14, 2000 event (with minimum Dst of -301 nT), and October 2003 storm (with a minimum Dst of -383 nT). Since on average, each storm was 2 orders of magnitude above the average strength, the strength of storm experienced on a planet within the red dwarf's

habitable zone, even the least affected ones, will be at least 15.26 Tesla strong.

Studies have shown that large organism such as human cannot tolerate magnetic field strength of 1 Tesla or greater for more than a few hours before nausea symptoms occur, this has been demonstrated by clinical studies done on patients undergoing MRI scans. [100][90][78][79] This is especially true when one is exposed to a changing field. Organisms can hardly survive in such a strong field because all animals move around frequently, as it moves fast, they are subject to moving magnetic field and can generate electricity. At the same time, the field strength itself also shifts and fluctuates during the storm. Since an average storm each lasts for days at a time, unless organisms stop all activities during these times and hide under extremely thick layers of rocks, it is impossible for them to survive the onslaught of the storm.

2.9 Habitability of Exomoon

Having completed the tally for the number of Earth-like terrestrial planets around their host star and excluded the habitability of red dwarves, now we turn our attention to the number of habitable exomoons.

The existence of moons orbiting around planets within the solar system has been observed. It is, therefore, also hypothesized that such moons must be common in other stellar systems, though no conclusive evidence yet observed.[59]The most interesting or relevant to our assumption are those exo-moons comparable to the size of earth orbiting gas giants within the habitable zones of GFK spectral class stars. (in fact, the exo-moons have to be at least 0.4 earth mass or greater in order to hold enough oxygen concentration, and with mass less than 2 earth mass otherwise it would have enough gravity to accumulate hydrogen in its atmosphere). Studies have shown that earth massed exomoons are indeed possible, many of those can be captured by inward migrating gas giants from further out based on simulation. However, if such exomoons pre-existed as earth analogs, then they are already counted into our existing habitable exoplanet count. What we are really interested is the chance of co-evolving exomoons with the host planet within its orbit. Since no observations are yet available and research under such topic is rare, we have to resort to an observation made within the solar system. We will make certain assumptions; that is, the total mass of all moons orbiting a host planet is proportional to the hosting planet's mass. We also assume the total mass of all moons as just 1 moon orbiting within the habitable zone of the hosting planet where the radiation is low enough to cause no harm to biological life and the moon is non-tidally locked. We know from our experience within the solar system that only Saturn's moon system approximately fulfills the above assumptions; nevertheless, we shall establish an upper bound on the number of exomoons habitable.

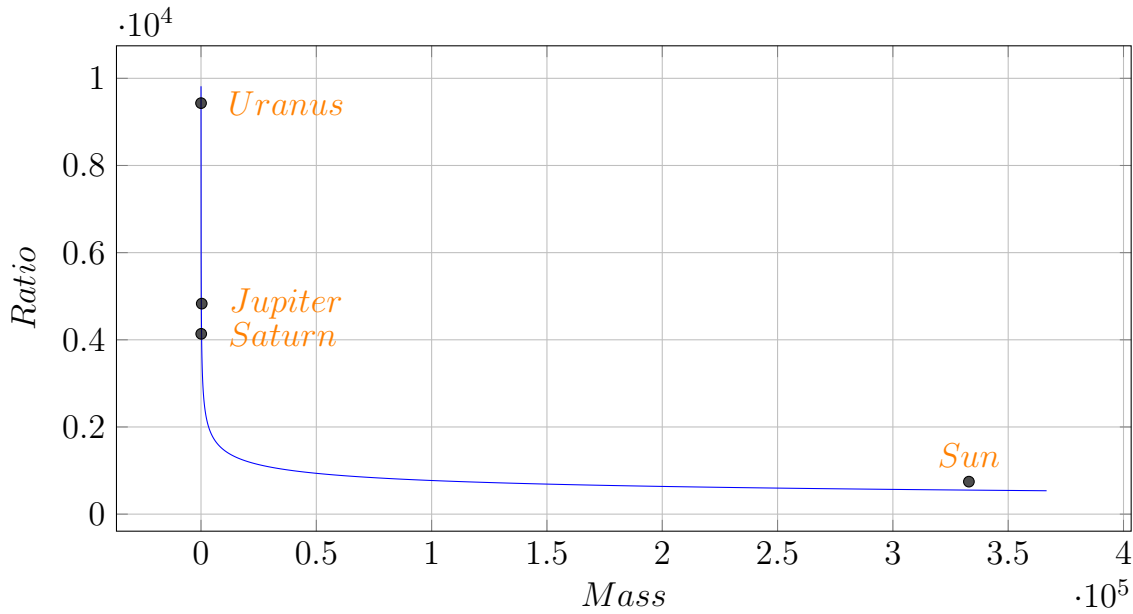


Figure 2.41: Primary to satellite mass ratio

The graph above is the ratio of the total mass of the Jovian Gas giants within the solar system to that of the total mass of moons orbiting them respectively. (except Neptune, whose moon Triton exhibits retrograde motion and is suspected to be captured from the Kuiper belt) And the Sun itself in relation to the total mass of the rest of the planets. It is noted that the lighter the planet, the lower the total mass of moons orbiting them. A linear regression is not possible under this model because it would imply that at some point the mass of the moons/planets is greater than that of the planet or the star itself. A power fit is plotted where the equation is obtained. The power fit is further refined by including the mass ratio of exoplanets and its hosting stars. This is called the stellar to planetary mass ratio.[103] The derived empirical law can predict the planetary mass budget or satellite mass budget for any given star mass or planet mass.

To solve for cases where 1 earth mass sized moon is possible, we use equation

$$y = \frac{x}{17,520x^{-0.2315}} \quad (2.102)$$

The solution indicates that only a planet with 2,793.87 earth masses or 8.78 Jovian masses (2,793.87 earth mass, 0.839% solar mass) or above can produce a satellite with a mass equivalent to earth. (see Chapter 11)

$$\begin{aligned} y &= 0.00839 \cdot M_{sol} \left(17,520 (0.00839 \cdot M_{sol})^{-0.2315}\right)^{-1} \\ &= 1.00108009577 M_{earth} \end{aligned} \quad (2.103)$$

If we lower the constraints and allow the formation of a satellite with 0.4 earth mass, then we need 1,332 earth masses, or 4.189 Jovian mass to produce a satellite hospitable to life. Since

the mass of Jupiter accounted for 70% of all the planetary mass within the solar system, we can assume that for a 4.189 Jovian mass planet to exist, we need at least 5.984 Jovian mass for any stellar system hosting such massive exomoons. An increase in the total mass of planets also indicates an increase in the mass of the hosting star, as the power law indicates. As a result, we need a star at least 3.857 times the mass of the sun. Even if we take 4.189 Jovian mass as the total mass of the planets (there is only one Jovian planet in the stellar system), the hosting star still has to have a mass 2.888 times the mass of the sun.

Based on the amount of time a star stays on the main sequence:

$$T_{MS} \approx 10^{10} \left[\frac{M}{M_{sol}} \right] \left[\frac{L_{sol}}{L} \right] = 10^{10} \left[\frac{M}{M_{sol}} \right]^{-2.5} \quad (2.104)$$

we know that such star will stay on main sequence 7.055% of the time compares to our sun. That means, that the stars stay on the main sequence for only 0.7055 Gyr. If the earth serves a model, the habitable zone will likely stay stable for half as long as the main sequence age, as a result, only 0.3527 Gyr, about as long as late Devonian up to now. If bacteria has emerged on such a system, then there is an insufficient time to evolve into complex biological creatures because the geological transformation of earth's environment with free oxygen takes 2 billion years of the photosynthetic process from cyanobacteria. This rules out the possibility of an advanced life arising from the exomoons. Even if life can emerge in less than 0.1% of all stars that are greater than 2.888 solar masses, there are at most 9,049,061 exomoons with a marginal habitability within the Milky Way with metallicity and the temporal window taking into consideration. This compares to 123,958,998 exoplanets with great habitability does not alter our calculation and assumptions at all.

Furthermore, gas giants, by their intrinsic nature, are formed beyond the snow line as a consequence of runaway gas accretion. Therefore, even if an Earth-sized moon can be possibly formed around a Jupiter sized planet circling around a solar mass star, it will not locate in the habitable zone of the stellar system.

Secondly, if such gas giants migrate inward, but then stops at the habitable zone of the star, the exomoon will then be covered in water. All planets formed beyond the snow line holds a significant amount of water in their composition. This is observed in Europa, Enceladus, Pluto, and Charon. All of their density is close to $1 \frac{\text{g}}{\text{cm}^3}$, the density of water, implying a significant percentage of its mass is composed of water. The upper limit for water budget for the solar system is 1.1342 earth mass. (10,112 pairs of water molecule per 1 million atoms and if oxygen is counted toward the composition of terrestrial planet formation), 1.1342 earth mass is translated into 1 out of 98.89 of the planetary mass, or 44.5 times in proportion to earth's ocean, which is merely 1 out 4400 of earth's mass if solar system's water is uniformly distributed. Since the water distribution of the solar system is non-uniform, all outer planets' moons get a greater share of water than the solar system average. As a result, the depth of the ocean must be indeed very high. It is possible to evolve life on such a planet but definitely not

intelligent tool using species we are concerned with.

Finally, exomoons formed around gas giants through the accretion process have a semi-major axis well within 5 million km, as a result, all non-captured exomoons tidally lock to their parent gas giants by 0.537 Gyr, in which one side permanently faces the gas giant in a shade of moonlight at the best. The 1.723 factor is the calculated result for the accretion disc size growth for 4.189 Jovian mass planet compares to 1 Jovian mass gas giant.

$$\begin{aligned}
 T_{moon2jupiter} &= \frac{\left(\frac{1}{13750}\right) \cdot (1.7239760 \cdot 5 \cdot 10^6 \cdot 10^3)^6 \cdot I_{earth} \cdot M_{earth} \cdot 909.0909}{3G (1332 \cdot M_{earth})^2 \cdot R_{earth}^3 \cdot 60 \cdot 60 \cdot 24 \cdot 365} & (2.105) \\
 &= 5.1662962 \cdot 10^8 \text{ years}
 \end{aligned}$$

Therefore, we can confidently predict that all arising extra-terrestrial life originates from habitable terrestrial planets rather than any extra-terrestrial moons.

Very lastly, we can also rule out the rogue planets. Some of the rogue planets may host microbial life, but those lives can not transition to bacteria capable of photosynthesis. Without photosynthesis and its by-product waste oxygen, eukaryotes which based their energy extraction on oxygen and energy-consuming multi-cellular organisms cannot form. Even if it somehow succeeds in so in some unimaginable way, it is impossible for an intelligent, multicellular being to change its mode of living from hunter-gathering, scavenging, to an agricultural one, which depends on the influx of solar energy. It is also predicted that the majority of the rogue planets are ejected early during the formation phase of the stellar system, as a result, cast further doubt on its ability to host complex form of life let alone its maintenance of habitability of complex life after it is ejected from the parent star.

3 Number of Earth

3.1 Orbital Eccentricity

The orbital eccentricity is another major selection criteria for the number of potentially habitable planets. For planets with higher orbital eccentricity, the planets can venture beyond its habitable zone so that liquid ocean freeze given a period of time of the year and creating snowball earth. It can also venture further closer to their sun and go through an annual period of unbearable heat, which generates an extreme level of humidity from evaporating ocean at the best and a runaway greenhouse at the worst. Though studies have been done to show that a terrestrial planet with extreme orbital eccentricity can still be habitable under the extraordinary circumstances. If a planet's eccentricity falls within the habitable zone we defined in chapter 2 between 0.840278 AU and 1.0887 AU, we will count them as habitable.

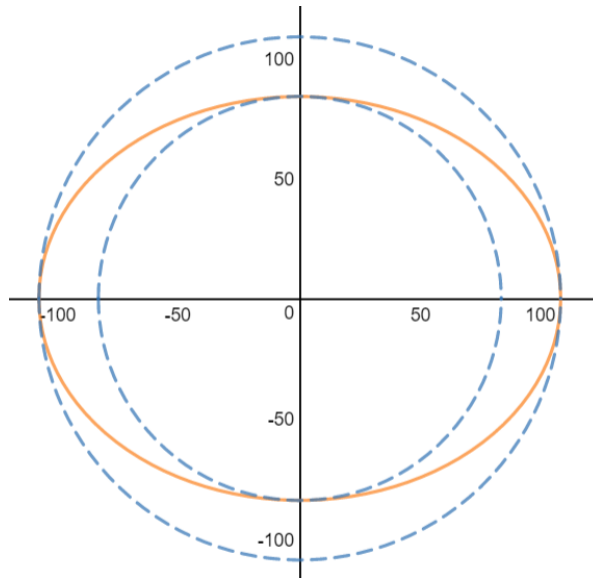


Figure 3.1: The inner and outer edge of the habitable zone

As a result, we exclude any planet with an orbital eccentricity greater than 0.6355 from the list of habitable planets.

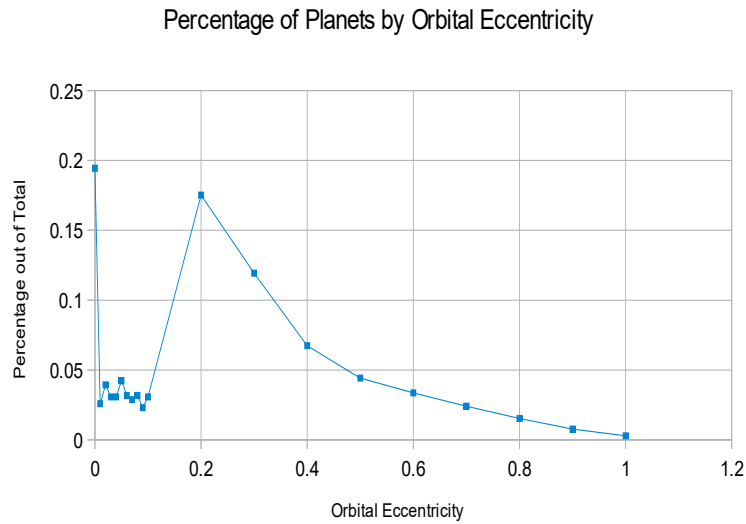


Figure 3.2: Percentage of Planets by Orbital Eccentricity

Based on 1,100 exoplanet's data points, *one finds that 95.76% of the exoplanet has eccentricity less than 0.6355*. The data is plotted below:

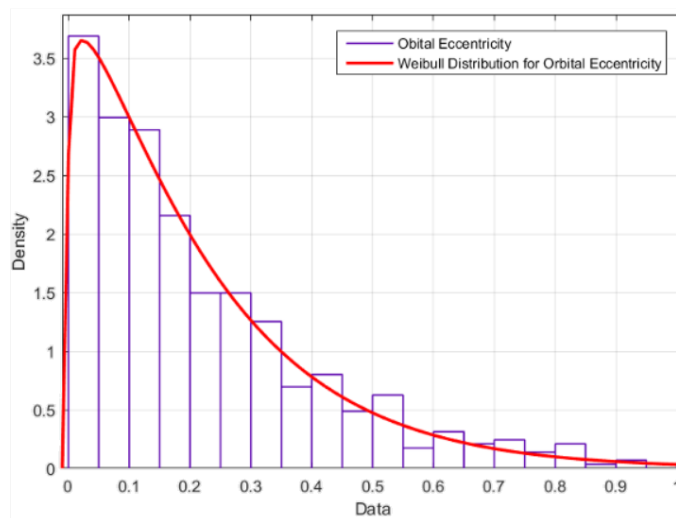


Figure 3.3: Weibull distribution for orbital eccentricity

3.2 Orbital Period

Some may also question the orbital period of the earth is unique that it revolves around the sun in 365 days. Planets revolve around the host star in faster or slower orbit may not be stable over the cosmic time scale, or it could be stable but not habitable for certain reason. However, orbital period vs. semi-major axis data derived from Kepler data indicates clearly that

earth's orbital period is typical. In fact, plugging into the regression derived from thousands of exoplanets' orbital period yield a result of 356 days for the semi-major axis of 1 AU, which is just 9 days shorter than earth's value. To demonstrate that based on the physical characteristics of earth, the earth is typical as it is evolved from the proto-planetary disk, we have two important properties now observed from thousands of exoplanets. The orbital period vs. its semi-major axis and orbital eccentricity. The graph and its computed best fit power curve predicates that an exoplanet's semi-major axis with a distance of 1 AU has an orbital period of 356 days, closely match earth's value.

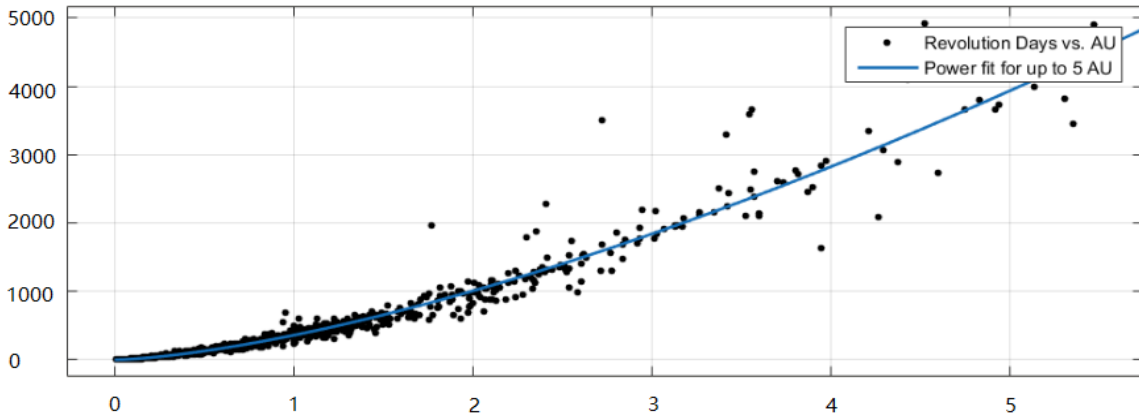


Figure 3.4: Orbital period vs. AU

To further instantiate our claim, we find that the orbital speed of all solar system bodies follows the following set of inequality:

¹

$$v_{orbit} \approx \sqrt{\frac{GM}{r}} \leq v_{orbitalactual} < v_{escape} = \sqrt{\frac{2GM}{r}} \quad (3.1)$$

One finds that all solar system bodies' orbital period closely matches the orbit speed, that is, the minimum speed at which the body stays in a circular orbit. This is not a surprise because, after all, all bodies within the solar system has very low eccentricities.

¹In order for an object to remain in orbit there must be a centrifugal force balancing the gravitational force. It is expressed in the relationship in the orbital equation

$F_g = F_c$ where F_g is the gravitation force and F_c is the centrifugal force.

In other words, $\frac{GM_1M_2}{r^2} = \frac{M_2v^2}{r}$. Solving for v gives $v = \sqrt{\frac{GM_1}{r}}$

So, in order to maintain an orbit at a distance of r above the center of the Earth, the object must maintain an orbital speed of v given here.

Planet	Orbital Speed Period≈	Escape Speed Period	Actual Period
Mercury	87.967 d	62.202 d	87.969 d
Venus	224.698 d	158.886 d	224.701 d
Earth	365.252 d	258.272 d	365.256 d
Mars	686.963 d	485.756 d	686.971 d
Jupiter	11.873 yr	8.401 yr	11.862 yr
Saturn	29.663 yr	20.975 yr	29.457 yr
Uranus	84.250 yr	59.574 yr	84.02q yr
Neptune	165.222 yr	116.830 yr	164.800 yr

Table 3.1: The orbital speed period, escape speed period, and actual period of solar system's planets

3.3 Earth & Moon Separation

The moon is moving slowly away from the earth due to tidal locking. Earth is slowed down and consequently, the moment of inertia decreases. Because earth and the moon system is a closed system where its total energy and momentum is conserved, the decrease of the moment of inertia of earth is transferred to that of the moon, increasing its distance from earth and its angular momentum. The equation is stated as the following:

$$s = \frac{\left[\left(0.3307 \cdot M_{earth} \cdot R_{earth}^2 \cdot \frac{2\pi}{24} \right) + \left(M_{moon} \sqrt{G \cdot M_{earth} \cdot a_{earthmoondist}} \right) \right]^2}{M_{moon}^2 \cdot G \cdot M_{earth}} \quad (3.2)$$

This is true because if we rearrange the equation:

$$s \cdot M_{moon}^2 \cdot G \cdot M_{earth} = \left[\left(0.3307 \cdot M_{earth} \cdot R_{earth}^2 \cdot \frac{2\pi}{24} \right) + \left(M_{moon} \sqrt{G \cdot M_{earth} \cdot a_{earthmoondist}} \right) \right]^2 \quad (3.3)$$

and taking square root at the same time:

$$M_{moon} \sqrt{G \cdot M_{earth} \cdot s} = \left(0.3307 \cdot M_{earth} \cdot R_{earth}^2 \cdot \frac{2\pi}{24} \right) + \left(M_{moon} \sqrt{G \cdot M_{earth} \cdot a_{earthmoondist}} \right) \quad (3.4)$$

The left term is the total angular momentum of the earth and moon system relative to the axis of the center of mass of the earth and moon system when all remainder of earth's moment of inertia is transferred to the orbit of the moon and pushes it into a higher orbit until earth's rate of rotation synchronized with the moon's orbital period. The first term on the right-hand

side is the moment inertia of earth at the current rotational speed multiplied by the moment of inertia. 0.3307 is the moment of inertia factor of the earth. Since earth's density is non-uniformly distributed within, the coefficient of the moment of inertia for a sphere (0.4) can not be used. The second term is the angular momentum of the moon relative to the axis of the center of mass of the earth and moon system. The left and right-hand sides must be equal. Hence, we have shown that the equation is valid.

$$s = \frac{\left[\left(0.3307 \cdot M_{earth} \cdot R_{earth}^2 \cdot \frac{2\pi}{24 \cdot 60 \cdot 60} \right) + \left(M_{moon} \sqrt{G \cdot M_{earth} \cdot a_{earthmoon}} \right) \right]^2}{M_{moon}^2 \cdot G \cdot M_{earth} \cdot 1000} \quad (3.5)$$

$$= 556,585.837834 \text{ km}$$

By plugging the equation, the final separation distance between earth and moon is found to be 556,585.84 km, well within the Hill Sphere of the earth. Thus, the moon can be maintained perpetually.

$$T_{earthlockingtomoon} = \frac{\left(\frac{1}{13.750} \right) (a_{moon})^6 \cdot I_{earth} \cdot M_{earth} \cdot 909.0909}{3 \cdot G \cdot (M_{moon})^2 \cdot R_{earth}^3 \cdot 60 \cdot 60 \cdot 24 \cdot 365} \quad (3.6)$$

$$= 4.7701691912 \cdot 10^{10} \text{ years}$$

Furthermore, the time to tidal locking between the two objects is determined to be 47.7 billion years into the future.[37] At that time, one side of the earth and one side of the moon will constantly face each other and one earth day will take 39.56 days (19.78 days of light and 19.78 days of nights on average), exactly the same as the time to take the moon orbit the earth at that point in time. For such a long timescale, it seems to be irrelevant to our discussion on the emergence and development of intelligent life; however, the final collision and merging of protoplanets can be different sizes and mass ratios. For the merging and forming planets with similar mass sizes, the mass of the moon can be significantly larger than earth's moon. In such cases, tidal locking happens much sooner, less than the time it takes (4.5 Gyr) for the history of life on earth. This does have some if not a serious challenge for the evolution of life on such a planet. If the process of tidal locking starts after the emergence of life on such a planet, life can gradually adapt to such slow rotation, including a sleep cycle every other month and might function similar to hibernation on earth. The most problematic cases are those massive moons that are quickly tidally locked to their parent planet before the emergence of life, long, cold nights can possibly freeze ocean and long, hot days can literally boil water away. These are some of the consequences of such tidally locked planet with its moon. As a result, planets locked to their moons within 0.5 Gyr of its formation are not counted as candidates for potentially intelligent life inhabiting planets. Here we show planets with different sized moons, their locking time, and their final separation distance from their host planet. We shall set stringent selection,

any planets' rotation slower than 7 earth days after 4.5 Gyr following its formation will not be counted toward our final list of habitable planets. Denominator used a factor 1.2204 to rescale earth-lunar pair value to 1. $a = 1$, $M_{earth} = x, G = 1$. Whereas $R_{earth}^2 = \left(\frac{3}{4\pi}x\right)^{\frac{2}{3}}$ because earth's mass can be modeled as:

$$\frac{4}{3}\pi R_{earth}^3 = x \quad (3.7)$$

$$R_{earth}^3 = \frac{3}{4\pi}x \quad (3.8)$$

$$R_{earth} = \left(\frac{3}{4\pi}x\right)^{\frac{1}{3}} \quad (3.9)$$

and $\frac{2}{5} \cdot \frac{3x}{4\pi} \cdot \frac{2\pi}{24} = \frac{\pi}{30}$.

$$y_{earth1moon} = \frac{\left(\frac{\pi}{30}x \cdot \left(\frac{3}{4\pi}x\right)^{\frac{2}{3}} + 1\sqrt{x}\right)^2}{1^2(x) \cdot 1.2204} \quad (3.10)$$

$$y_{earth2moon} = \frac{\left(\frac{\pi}{30}x \cdot \left(\frac{3}{4\pi}x\right)^{\frac{2}{3}} + 2\sqrt{x}\right)^2}{2^2(x) \cdot 1.2204} \quad (3.11)$$

$$y_{earth3moon} = \frac{\left(\frac{\pi}{30}x \cdot \left(\frac{3}{4\pi}x\right)^{\frac{2}{3}} + 3\sqrt{x}\right)^2}{3^2(x) \cdot 1.2204} \quad (3.12)$$

$$y_{earth4moon} = \frac{\left(\frac{\pi}{30}x \cdot \left(\frac{3}{4\pi}x\right)^{\frac{2}{3}} + 4\sqrt{x}\right)^2}{4^2(x) \cdot 1.2204} \quad (3.13)$$

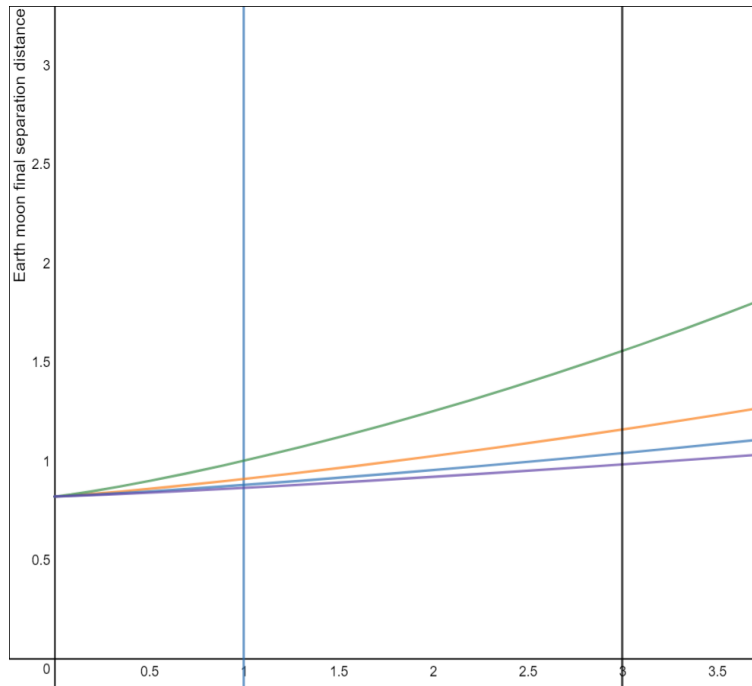


Figure 3.5: Terrestrial mass vs final separation

This graph shows the relationship between planet mass and their moon mass and the final separation distance between them when they lock into synchronous orbits. Planets ranges from 1 to 1.6 earth masses are placed within the vertical bars. (typical terrestrial planets arose 5 to 4 Gyr ago does not have metallicity above 0.2, therefore, within each star’s habitable zone the mean planetary mass cannot exceed 1.585 earth mass, see “Earth Size”). The green curve represents the locking separation distance for different earth masses with 1 lunar mass satellite, at one earth mass and 1 lunar mass, the separation distance is a unit of 1, represents 556,585.84 km of separation between the earth and moon in a synchronous orbit 47.7 Gyr into the future. One can easily see that as the planet’s mass increase, its moment of inertia also increases, and the final separation distance for a moon of the same mass increases. The orange curve represents the locking separation for different earth mass with 2 lunar mass satellite. The blue curve represents the locking separation for different earth mass with 3 lunar mass satellite. The indigo curve represents the locking separation for different earth mass with 4 lunar mass satellite. It can be clearly seen that as the satellite mass increases, the locking time shortens and the separation distance decreases, though earth with greater mass (higher moment of inertia) still maintains a greater relative separation compares to earth with smaller mass with any given fixed lunar mass satellite.

$$T_{earthlockingtomoon} = \frac{\left(\frac{1}{0.63 \cdot 13750}\right) (0.775 \cdot a_{moon})^6 I_{earth} (M_{earth}) \cdot 909.0909}{3 \cdot G \cdot (x \cdot M_{moon})^2 \cdot (R_{earth})^3 \cdot 60 \cdot 60 \cdot 24 \cdot 365 \cdot 10^9} \quad (3.14)$$

$$d = \frac{4.5}{(T_{earthlockingtomoon})} \quad (3.15)$$

$$m = \frac{1}{(1 - d)} \quad (3.16)$$

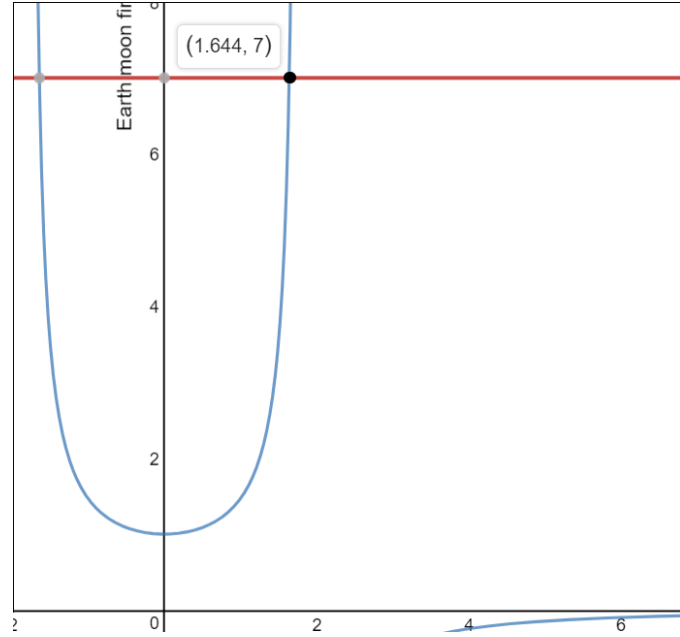


Figure 3.6: Satellite mass vs. planet rotation speed for earth mass planet

Then, we run the equation to find for 1 earth mass with differently sized satellites, and we find that at 1.644 lunar mass, after 4.5 Gyr since its formation, the tidal locking effect becomes significant in which it takes 7 days for a full rotation of the planet, where the day and night are 3.5 days each. We also compute the upper bound whereas earth with a mass of 1.6 earth mass, and we find that at 1.3 lunar mass or above the earth rotation slows down significantly for the tidal locking effect to occur.

$$T_{earthlockingtomoon} = \frac{\left(\frac{1}{0.63 \cdot 13750}\right) (0.775 \cdot a_{moon})^6 I_{earth} (1.6M_{earth}) \cdot 909.0909}{3 \cdot G \cdot (x \cdot 1.6M_{moon})^2 \cdot (R_{earth})^3 \cdot 60 \cdot 60 \cdot 24 \cdot 365 \cdot 10^9} \quad (3.17)$$

$$d = \frac{4.5}{(T_{earthlockingtomoon})} \quad (3.18)$$

$$m = \frac{1}{(1 - d)} \quad (3.19)$$

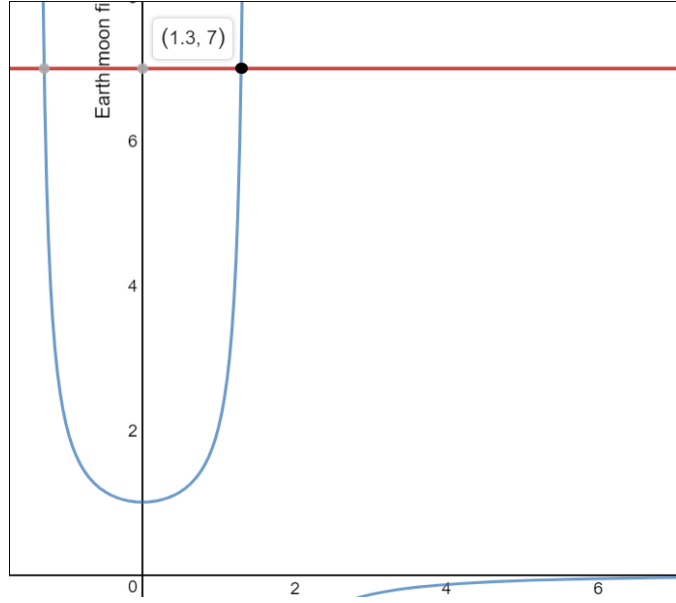


Figure 3.7: Satellite mass vs. planet rotation speed for 1.6 earth mass planet

The 1.3 lunar mass for the 1.6 earth mass planet case, is actually $1.3 \cdot 1.6 = 2.08$ lunar mass. Since the final planet gains more mass, the mass of its moon, as a consequence violent impact, also grows linearly along with the mass of the planet. Then, a satellite with 2.08 lunar mass is satisfied, because its relative mass ratio to its parent planet remain fixed despite mass gain compares to 1 earth mass planet. The lunar mass is allowed to grow beyond 1.644 lunar mass to 2.08 lunar mass because a larger earth's moment of inertia takes a larger moon to transfer into the angular momentum of the system within 4.5 Gyr.

Finally, we compute the lower bound when earth with a mass of 0.43 (why see section Earth-Size), and we find that at 2.507 ($2.507 \cdot 0.43 = 1.07801$) lunar mass or above the earth rotation slows down significantly for tidal locking effect to occur.

$$T_{earthlockingtomoon} = \frac{\left(\frac{1}{0.63 \cdot 13750}\right) (0.775 \cdot a_{moon})^6 I_{earth} (0.43 M_{earth}) \cdot 909.0909}{3 \cdot G \cdot (x \cdot 0.43 M_{moon})^2 \cdot (R_{earth})^3 \cdot 60 \cdot 60 \cdot 24 \cdot 365 \cdot 10^9} \quad (3.20)$$

$$d = \frac{4.5}{(T_{earthlockingtomoon})} \quad (3.21)$$

$$m = \frac{1}{(1 - d)} \quad (3.22)$$

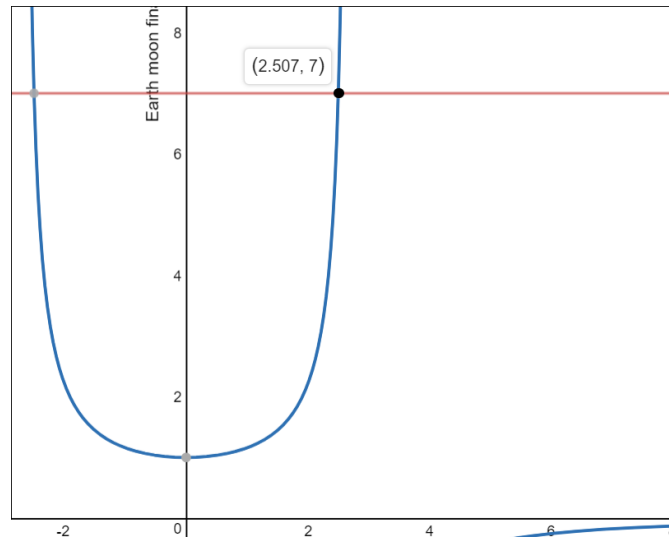


Figure 3.8: Satellite mass vs. planet rotation speed for 0.43 earth mass planet

We take the average of the three values $\frac{(1.644+2.08+1.0781)}{3}$ and arrive at 1.6 lunar mass. It shows that for terrestrial planets formed from 5 Gyr to 4 Gyr ago, its moon mass have to be 1.6 lunar mass or smaller in relation to its parent planet in order to minimize the effect of tidal locking on terrestrial life. Once we found the upper bound, we can find the final separation distance between 1 earth mass and moons of various sizes.

$$y_{moon} = \frac{\left(\frac{\pi}{30} + x\right)^2}{(x)^2 \cdot 1.2204} \tag{3.23}$$

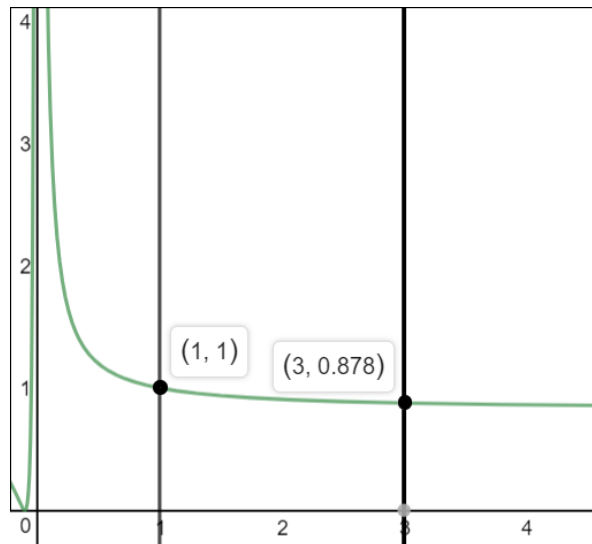


Figure 3.9: The final separation distance for tidally locked moons from 0 to 3 lunar mass

For moon's sizes ranging from 0 to 3 lunar mass, the final separation distance for tidal locking decreases sharply from 0 to 0.5 lunar mass and decreases more gently thereafter. The general

trend is clear that as the size of the moon increases the separation distance between the bodies decreases.

3.4 Earth-Moon Collision Probability Explanation

Some argued that the earth and moon system is unique in such a way that binary planetary system which stabilizes the tilt of the planet and reduces climatic shifts and swings which can drastically alter evolutionary trajectories and resets the biodiversity is rare. As a result, the preliminary condition to enable the great diversification of life is rare; and therefore an advanced life with intelligence and manipulative power is also rare. However, the formation of the earth and moon system, following the predominant giant impact hypothesis, is a physical phenomenon, that is subject the classical laws of physics. Since the classical laws of physics are universally applicable everywhere, the formation of a binary planetary system cannot be ruled as a single, past local event. Most significantly, the Pluto and Charon system, another pair of a binary planetary system, located within the solar system, has been simulated and hypothesized to be formed through impact collision.[67][21] Physical simulation concerning material composition, the final angular velocity, and the momentum yields consistent results with the observational data obtained from the Pluto Charon system, confirming the likelihood of a giant impact formation in the past.

Since all terrestrial planets form by a series of collisions and mergers with protoplanets with smaller sizes and masses, simplified mathematical model and simulation can model the probability of the mass ratio of the last major collision between the last remaining protoplanets. It is hypothesized that the origin of the moon is a consequence of a protoplanet Theia smashed into the protoplanet earth. The planet Theia has 10 percent mass of the earth, and 10 percent of which eventually coalesced into two moons and one of the moon pancaked onto the far side of our current moon. Studies and simulation have shown that a single moon and earth system is by far the most stable configuration even if collision creates more than one moon initially. By simulating the final merging process occurred to earth, one can determine the likelihood of terrestrial planet formation with a moon of significant size, and the range of moon mass possible as it is compared to earth.

In order to simulate such results, we assume that earth was formed by the merging of no more than a hundred protoplanets around its orbit. The total mass of all protoplanets amounts to the total mass of both earth and moon system. Only the very last collision and merging results in the formation of the moon because earlier merging and collision is between masses of significantly smaller sizes. For the simplicity of our model, we simply model the very last of such collision. We then developed three different mathematical models to show the likelihood and the chance of moon formation.

$$\begin{aligned} \text{total} &= \frac{1}{2}n(n-1) \cdot \frac{1}{2}(n-1)(n-2) \cdot \frac{1}{2}(n-2)(n-3) \cdot \frac{1}{2}(n-3)(n-4) \cdots \\ &\quad \cdots \frac{1}{2}(n-k)(n-(k+1)) \cdots 3 \cdot 1 \quad (3.24) \end{aligned}$$

$$\text{total} = \frac{n!}{2!(n-2)!} \cdot \frac{(n-1)!}{2!(n-3)!} \cdot \frac{(n-2)!}{2!(n-4)!} \cdots \frac{(n-k)!}{2!(n-(k+1))!} \cdots \frac{2!}{2!0!} \quad (3.25)$$

$$\text{case 1, case 2, case 3, case 4 ... case k ... case n-3, case n-2:} \quad (3.26)$$

$$n, n-2, n-3, n-4, \cdots n-(k+1) \cdots 2, 1 \quad (3.27)$$

$$\begin{aligned} &\frac{n(n-1)(n-2)(n-3) \cdots (n-k) \cdots 2 \cdot 1}{\frac{1}{2}n(n-1) \cdot \frac{1}{2}(n-1)(n-2) \cdot \frac{1}{2}(n-2)(n-3) \cdots \frac{1}{2}(n-k)(n-(k+1)) \cdots 3 \cdot 1} \\ \Rightarrow &\quad (3.28) \end{aligned}$$

$$\Rightarrow \frac{1}{\left(\frac{1}{2}\right)^{n-1} (n-1)(n-1)(n-2)(n-3) \cdots (n-k) \cdots 3 \cdot 2} \quad (3.29)$$

$$\Rightarrow \frac{1}{\left(\frac{1}{2}\right)^{n-1} (n-1)^2 (n-2)!} \Rightarrow \frac{1}{\left(\frac{1}{2}\right)^{n-1} (n-1)^2 \cdot \frac{(n-2)^n}{e^n}} \quad (3.30)$$

Test for convergence:

$$\lim_{n \rightarrow \infty} \left| \frac{\frac{1}{\left(\frac{1}{2}\right)^n n^2 \frac{(n-1)^{n+1}}{e^{n+1}}}}{\frac{1}{\left(\frac{1}{2}\right)^{n-1} (n-1)^2 \frac{(n-2)^n}{e^n}}} \right| \quad (3.31)$$

$$\Rightarrow \lim_{n \rightarrow \infty} \left| \frac{\left(\frac{1}{2}\right)^{n-1} (n-1)^2 \frac{(n-2)^n}{e^n}}{\left(\frac{1}{2}\right)^n n^2 \frac{(n-1)^{n+1}}{e^{n+1}}} \right| \quad (3.32)$$

$$\Rightarrow \lim_{n \rightarrow \infty} \left| \frac{1 \cdot (n-1)^2 \frac{(n-2)^n}{e^n}}{\left(\frac{1}{2}\right)^n n^2 \frac{(n-1)^{n+1}}{e^{n+1}}} \right| \quad (3.33)$$

$$\Rightarrow \lim_{n \rightarrow \infty} \left| \frac{(n-2)^n}{\frac{1}{2} \cdot e^n} \cdot \frac{e^{(n+1)}}{(n-1)^{(n+1)}} \right| \quad (3.34)$$

$$\Rightarrow \lim_{n \rightarrow \infty} \left| 2 \cdot \frac{e}{n-1} \right| = 0 \quad (3.35)$$

In our first model, we simply assume that a hundred protoplanet each with one-hundredth mass of the earth is free to merge with any other in a combinatorial way, from combinatorial derivation, one can see that the protoplanet merges each time with another protoplanet about one-hundredth of the earth mass is very small. In fact, as the number of protoplanets merges toward infinity from the mathematical perspective, the probability that the resulting moon comes from successive rounds of merging between the larger protoplanet with an increasing mass and another protoplanet with a mass of just $\frac{1}{100}$ th of the earth approaches 0. This implies that under a majority of the cases, during the merging process, at least one or more times, frequently toward the later stages of merging, merging takes place between two masses of comparable sizes, resulting in Theia and Earth type of collision, resulting in the creation of a moon.

$$\begin{aligned} \text{total} = & \frac{1}{2}n(n-1) \cdot \frac{1}{2}(n-1)(n-2) \cdot \frac{1}{2}(n-2)(n-3) \cdot \frac{1}{2}(n-3)(n-4) \cdots \\ & \cdots \frac{1}{2}(n-k)(n-(k+1)) \cdots \frac{1}{2} \cdot 3 \cdot 2 \cdot \frac{1}{2} \cdot 2 \cdot 1 \quad (3.36) \end{aligned}$$

$$\text{total} = \frac{n!}{2!(n-2)!} \cdot \frac{(n-1)!}{2!(n-3)!} \cdot \frac{(n-2)!}{2!(n-4)!} \cdots \frac{(n-k)!}{2!(n-(k+1))!} \cdots \frac{2!}{2!0!} \quad (3.37)$$

$$\text{case 1, case 2, case 3, case 4 ... case k ... case n-3, case n-2:} \quad (3.38)$$

$$n, 2, 2, 2, \dots \cdot 2 \cdots \cdot 2 \quad (3.39)$$

$$\Rightarrow \frac{n \cdot 2 \cdot 2 \cdot 2 \cdots 2 \cdots 2 \cdot 1}{\frac{1}{2}n(n-1) \cdot \frac{1}{2}(n-1)(n-2) \cdots \frac{1}{2}(n-k)(n-(k+1)) \cdots \frac{1}{2} \cdot 3 \cdot 2 \cdot \frac{1}{2} \cdot 2 \cdot 1} \quad (3.40)$$

$$\Rightarrow \frac{2^{n-3}}{\left(\frac{1}{2}\right)^{n-1} [(n-1)(n-2) \cdots (n-k) \cdots 4 \cdot 3 \cdot 2] [(n-1)(n-2) \cdots (n-k) \cdots 4 \cdot 3 \cdot 2]} \quad (3.41)$$

$$\Rightarrow \frac{2^{n-3}}{\left(\frac{1}{2}\right)^{n-1} \cdot (n-1)! \cdot (n-1)!} \Rightarrow \frac{2^{n-3}}{\left(\frac{1}{2}\right)^{n-1} \cdot \frac{(n-1)^n}{e^n} \cdot \frac{(n-1)^n}{e^n}} \quad (3.42)$$

Test for convergence:

$$\lim_{n \rightarrow \infty} \left| \frac{\frac{2^{n-2}}{\left(\frac{1}{2}\right)^n \cdot \frac{n^{n+1}}{e^{n+1}} \cdot \frac{n^{n+1}}{e^{n+1}}}}{\frac{2^{n-3}}{\left(\frac{1}{2}\right)^{n-1} \cdot \frac{(n-1)^n}{e^n} \cdot \frac{(n-1)^n}{e^n}}} \right| \quad (3.43)$$

$$\Rightarrow \lim_{n \rightarrow \infty} \left| \frac{2^{n-2}}{\left(\frac{1}{2}\right)^n \cdot \frac{n^{(n+1)}}{e^{(n+1)}} \cdot \frac{n^{(n+1)}}{e^{(n+1)}}} \cdot \frac{\left[\left(\frac{1}{2}\right)^{n-1} \cdot \frac{(n-1)^n}{e^n} \cdot \frac{(n-1)^n}{e^n}\right]}{2^{n-3}} \right| \quad (3.44)$$

$$\Rightarrow \lim_{n \rightarrow \infty} \left| \frac{2}{\left(\frac{1}{2}\right)} \cdot \frac{(n-1)^n}{e^n} \cdot \frac{(n-1)^n}{e^n} \cdot \frac{e^{n+1}}{n^{n+1}} \cdot \frac{e^{n+1}}{n^{n+1}} \right| \quad (3.45)$$

$$\Rightarrow \lim_{n \rightarrow \infty} \left| 4 \cdot \frac{(e \cdot e)}{n \cdot n} \right| \quad (3.46)$$

$$\Rightarrow \lim_{n \rightarrow \infty} \left| 4 \cdot \frac{e^2}{n^2} \right| \quad (3.47)$$

$$\Rightarrow \lim_{n \rightarrow \infty} \left| 4 \cdot \left(\frac{e}{n}\right)^2 \right| = 0 \quad (3.48)$$

In our second model, we simply assume that each protoplanet can only merge with its neighbor from the left or right. As a result, we derive several possible cases.

Much like the first model where each protoplanet can merge freely with their neighbors, in the

more restricted case that each protoplanet can only merge with their left or right neighbors. Based on combinatorial derivation, the protoplanet merges each time with another protoplanet about one-hundredth of the earth mass is very small, in fact, as the number of protoplanet increases toward infinity, the probability approaches 0. However, careful comparison with the earlier model shows that the n to n matching model without restriction converges to 0 faster, which is not surprising since the restricted case contains fewer choices out of the total number of combinatorial choices given n number of choices, so it takes more rounds to decrease the probability down to zero. In summary, we have demonstrated mathematically that the creation of moon through giant impact between protoplanets with a mass ratio less than 100 to 1 is very common.

$$y_{ntonmatch} = \frac{1 \cdot 100}{(x - 1)^2 (x - 2)! \cdot \left(\frac{1}{2}\right)^{(x-1)}} \quad (3.49)$$

$$y_{lefttrightmatch} = \frac{2^{(x-3)} \cdot 100}{(x - 1)! (x - 1)! \left(\frac{1}{2}\right)^{(x-1)}} \quad (3.50)$$

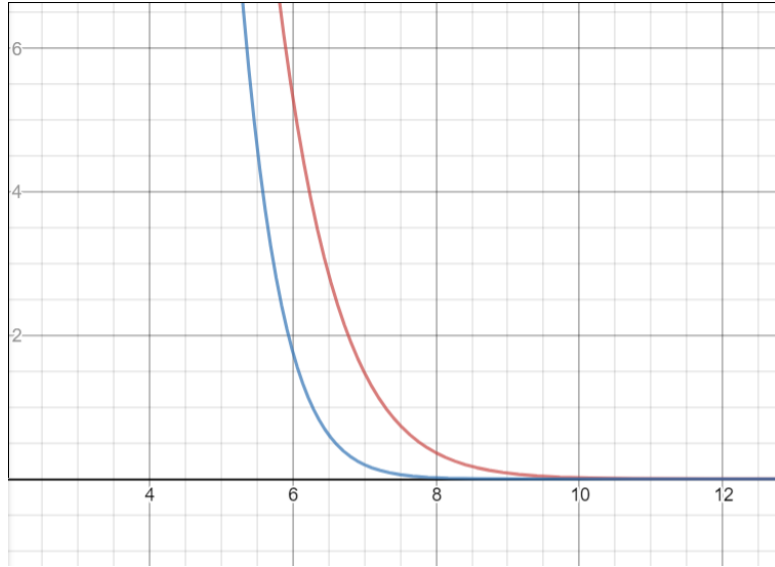


Figure 3.10: The probability that the entire oligarchic merging process is non-violent is 0 as the number of mergers increases.

Then, we need to find the mass distribution of the moons created through impact. We first model the protoplanet growth by applying the binomial distribution model, assuming each protoplanet can randomly pair with any other protoplanet. Then the formulas for calculating the mass distribution, our current model uses the case of $n = 10$, the number of merging protoplanets equals to 10, this number can be increased to a range of values to increase precision and accuracy.

$$f(1) = \Pr(X = 1) = 2 \binom{10}{1} 0.5^1 (1 - 0.5)^{10-1} = 1.953125\% \quad (3.51)$$

$$f(2) = \Pr(X = 2) = 2 \binom{10}{2} 0.5^2 (1 - 0.5)^{10-2} = 8.7890625\% \quad (3.52)$$

$$f(3) = \Pr(X = 3) = 2 \binom{10}{3} 0.5^3 (1 - 0.5)^{10-3} = 23.4375\% \quad (3.53)$$

$$f(4) = \Pr(X = 4) = 2 \binom{10}{4} 0.5^4 (1 - 0.5)^{10-4} = 41.015625\% \quad (3.54)$$

$$f(5) = \Pr(X = 5) = 1 \binom{10}{5} 0.5^5 (1 - 0.5)^{10-5} = 24.609375\% \quad (3.55)$$

From the results, the probability of 1 lunar mass satellite creation is 1.95%. The probability of 2 lunar mass satellite creation is 8.79%. The probability of 3 lunar mass satellite creation is 23.44%. The probability of 4 lunar mass creation is 41.02%. The probability of 5 lunar mass creation is 24.61%.

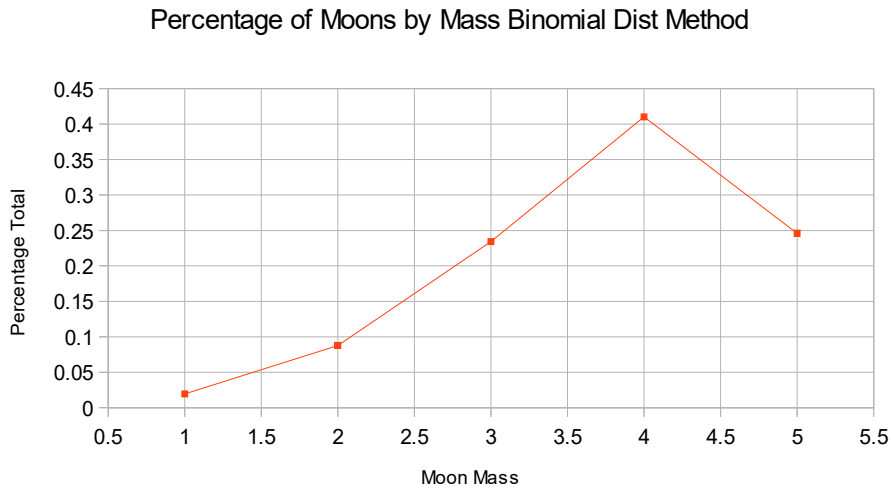


Figure 3.11: Percentage of moons by mass binomial distribution method

Next, we model the protoplanet growth by applying the binomial distribution model using restriction, assuming each protoplanet can only pair with its left or right neighbor, our current model uses the case of $n = 10$, the number of merging protoplanets equals to 10. The formula for calculating the mass distribution for the restricted case is listed below:

$$f(1) = 1 \quad (3.56)$$

$$f(2) = 1 \quad (3.57)$$

$$f(3) = 3 \quad (3.58)$$

$$f(4) = 4 [f(1) f(3) + f(2)^2] = 16 \quad (3.59)$$

$$f(5) = 5 [f(1) f(4) + f(2) f(3)] = 95 \quad (3.60)$$

$$f(6) = 6 [f(1) f(5) + f(2) f(4) + f(3)^2] = 720 \quad (3.61)$$

$$f(7) = 7 [f(1) f(6) + f(2) f(5) + f(3) f(4)] = 6,041 \quad (3.62)$$

$$f(8) = 8 [f(1) f(7) + f(2) f(6) + f(3) f(4) + f(4)^2] = 58,416 \quad (3.63)$$

$$f(9) = 9 [f(1) f(8) + f(2) f(7) + f(3) f(6) + f(4) f(5)] = 613,233 \quad (3.64)$$

$$f(10) = 10 [f(1) f(9) + f(2) f(8) + f(3) f(7) + f(4) f(6) + f(5)^2] = 7,103,170 \quad (3.65)$$

$$f(n) = \begin{cases} \text{even} & n [f(1) f(n-1) + f(2) f(n-2) + f(3) f(n-3) + \dots + f(\frac{n}{2})^2] \\ \text{odd} & n [f(1) f(n-1) + f(2) f(n-2) + f(3) f(n-3) + \dots + f(\lfloor \frac{n}{2} \rfloor) \cdot f(\lceil \frac{n}{2} \rceil)] \end{cases} \quad (3.66)$$

Using the formula, one can count the number of satellites formed with mass from 1 lunar mass to $\frac{n}{2}$ lunar mass. Whereas n is the initial starting number of protoplanets. In our case, n=10. The final results are plotted.

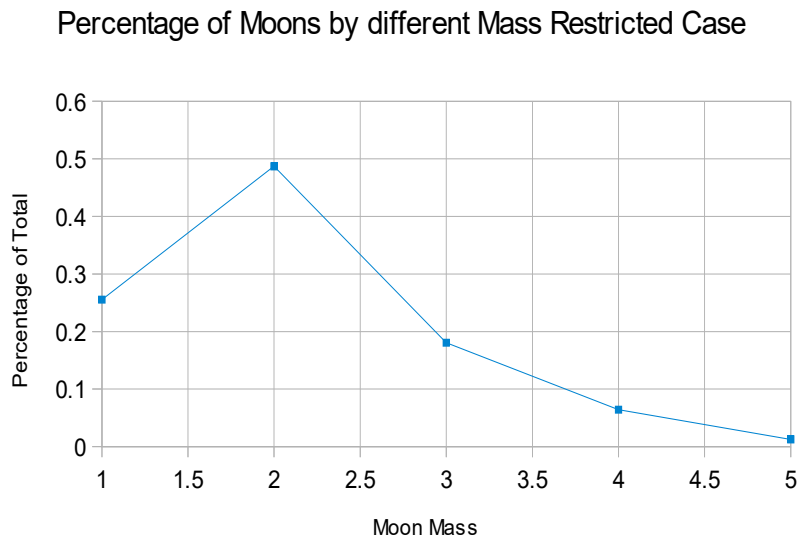


Figure 3.12: Percentage of moons by different mass using restricted case

Finally, we shall simulate the growth of protoplanet sizes by gravitational attraction. We start

by placing each protoplanet along an orbit with an equal distance between each other. Since each protoplanet is equal in mass and each is separated by an equal distance, no mass moves toward any other all are in a precarious balance. Then, merging two of the protoplanets results in an imbalance of gravitational force between protoplanets, and the merging process proceeds until all protoplanets merge into one single planet. Although, in reality, it is possible that simultaneous merging of more than two protoplanets is possible, we simplify the simulation by breaking the tie between two simultaneous mergings and ordering them in two successive steps. Simulation loops through the steps until all protoplanets merged for protoplanets numbered from 5 up to 100. The results of the simulation are graphed below:

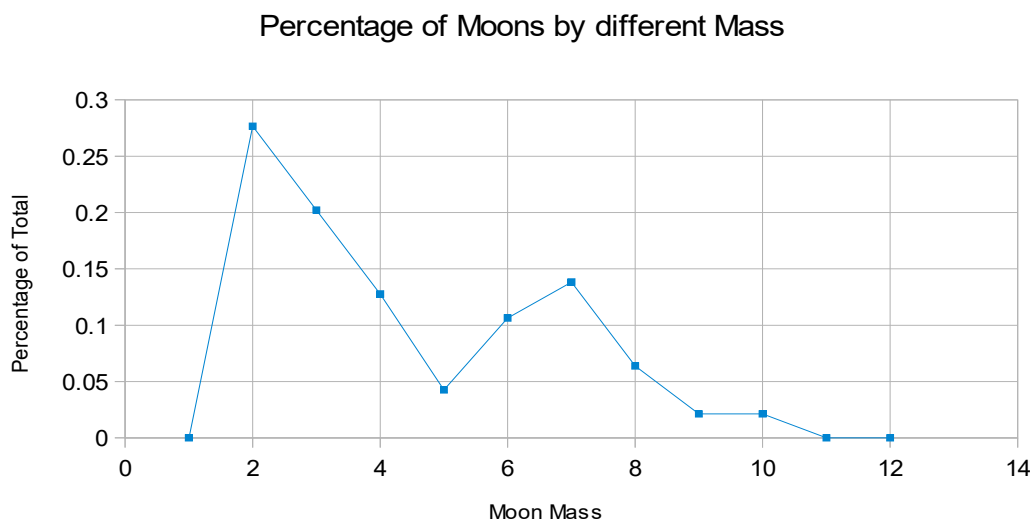


Figure 3.13: Percentage of moons of different mass by gravitational simulation

If we summarize the results from our simulation, one can predict the average size of moons created by the terrestrial planet merging process. The final graph shows the composite results of moon creation from the previous three distribution models, whereas the mean lies around 3 lunar mass. It shows that the creation of satellite with 1 lunar mass happens around 9.17 percent of the time. Since it takes another 47.7 billion years for our moon to tidally lock with earth, we found that any moon with a mass greater than 1.635 lunar mass will tidally lock within the timeframe of biological evolution starting with the weighted average of initial spin rate (see section 3.5 “Right Rotational Speed”). In the strictest sense, we exclude those terrestrial planets with large moons and exclude those moons with a mass significantly smaller than ours. *One can conclude that about 21.90% of the terrestrial planet formed in the universe have moons that bring similar effect to that we observed on earth.* That is, the moon is large enough to stabilize the axis of tilt of the planet so axial wobbling (orbital resonance) observed on Mars is minimized and small enough so that tidal locking does not occur within the timeframe of biological evolution.

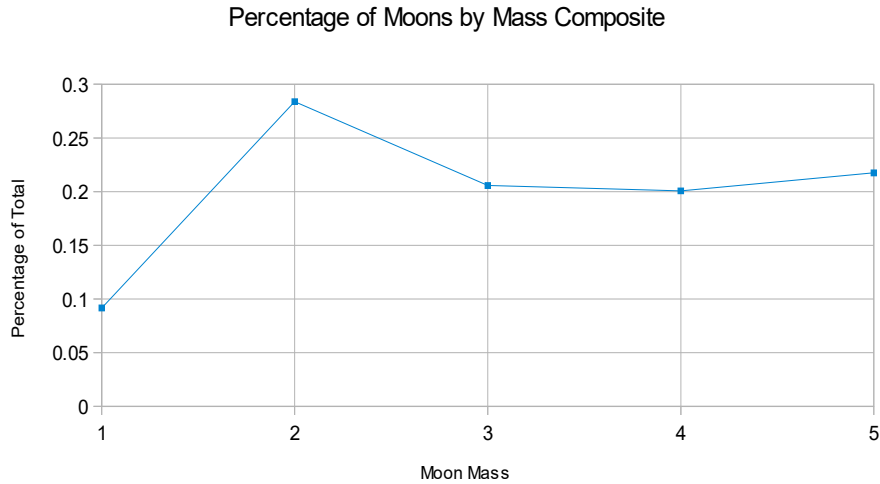


Figure 3.14: Percentage of moons of different mass by composite effects

In the final plot, the probability of the creation of moons of various sizes is taken as the average of the three cases. In reality, the real results may be a weighted average of the three cases or some additional factors unaccounted for. The protoplanets may not all occupy the exact same path, eccentricity, and distance from the sun and may well move at different speeds so that every protoplanet does have a chance to merge with every other. At the same time, each protoplanet does have its own well-defined neighborhood zone, and unbounded interaction with neighboring protoplanet is restricted. The final mass distribution is the compromise between each of these possible scenarios and requires further analysis in the future.

3.5 The Right Rotational Speed

The initial rotational speed of the consolidated planet after several successive mergers with mars sized protoplanets is also an important criterion for habitability. It is important that the initial spin rate of the planet is fast enough to generate earth-like days and nights at the time when intelligent species appears. If a planet starts with a slow rotation, it will quickly tidally lock with its satellite about the earth's moon size, or it could be moonless and retain a slow rotation as Venus. In order to calculate the final spin rate of merged planets, one needs to take into account how much linear momentum, upon collision, is transferred into the angular momentum in either the prograde or the retrograde motion, which in turn, can be either enhanced or partially canceled by the magnitude of existing angular momentum both bodies possess. We assume that upon each collision, both the prograde and the retrograde spin can exist and the magnitude of the linear momentum transferred into the angular momentum is determined by the hitting angle between the two merging mass. During the giant impact stage, the thickness of a protoplanetary disk is far larger than the size of planetary embryos, so

collisions are equally likely to come from any direction in a three dimensional space. Therefore, one has to consider the hitting angle in both horizontal and vertical plane.

$$P_{prograde}(x) = \left(\frac{(M_1 \cdot V_{escape0} \cdot (\sin x - \cos x)^2 \cdot (\sin x)^2 \cdot R_0)}{I_{earth} \cdot M_0 \cdot R_0^2} \right)^{-1} \quad (3.67)$$

$$P_{retrograde}(x) = \left(\frac{(M_1 \cdot V_{escape0} \cdot (\sin x - \cos x)^2 \cdot (\cos x)^2 \cdot R_0)}{I_{earth} \cdot M_0 \cdot R_0^2} \right)^{-1} \quad (3.68)$$

$$P_{final} = P_{prograde}(x) + P_{retrograde}(x) \quad (3.69)$$

The prograde equation minimizes the angular momentum of an object striking greater than but near the 0 degrees angle clockwise and results in a clockwise rotation. The retrograde equation minimizes the angular momentum of an object striking smaller than but near the 90 degrees angle clockwise and results in a counter-clockwise rotation. When one takes the sum of both equations, we have all cases covered between 0 to 90 degrees angle clockwise, and the remaining 270 degrees repeats itself in the same pattern. Based on the equation, one can see that, within a hitting angle of 0 to 90 degrees, the greatest transfer of angular momentum occurs when two bodies collide in 22.5 degrees and 67.5 respectively. Whereas collision in 22.5 degrees results in the retrograde(counter-clockwise) motion while the 67.5 degrees hitting angle results in the prograde (clockwise) motion. A collision with 45 degrees hitting angle results in a zero angular momentum because there is an equal magnitude of the prograde and the retrograde spin generated in an equal amount and the energy is released in the form of heat and light instead of conserving as the angular momentum. The spin rate from a single collision occurs within a hitting angle of 0 to 90 degrees is plotted. One can see that at 22.5 degrees the final rotational speed can be as fast as 0.156 days, or 3 hours 45 minutes and as the hitting angle approaches 45 degrees, the rotational spin slowed down significantly toward infinity.

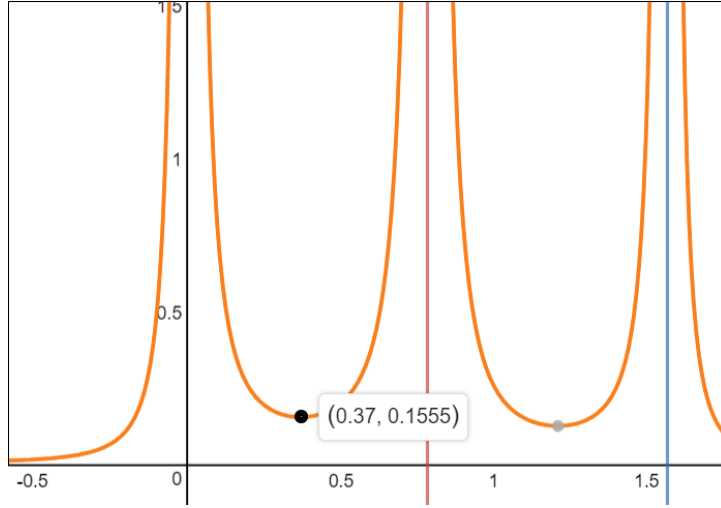


Figure 3.15: Rotational speed post-merging for different hitting angles in radians

Next, we need to generalize and compute the final rotational spin rate based on successive collisions of varying masses. In our simple model, we assume that earth is formed by merging with 9 mars sized bodied protoplanets. We will simulate the process through a few rounds of iterations.

Colliding Mass 1	Colliding Mass 2	Final Mass
0.1 M_{earth}	0.1 M_{earth}	0.2 M_{earth}
0.2 M_{earth}	0.1 M_{earth}	0.3 M_{earth}
0.3 M_{earth}	0.1 M_{earth}	0.4 M_{earth}
0.4 M_{earth}	0.2 M_{earth}	0.6 M_{earth}
0.6 M_{earth}	0.3 M_{earth}	0.9 M_{earth}

Table 3.2: The merging mass size for each step for the merging process

In the first round, two colliding masses each have only 0.1 earth mass. In the next three rounds, each colliding mass 2 will have 0.1 earth mass while the colliding mass 1 accumulates. Starting at round 4, colliding mass 2 increases to 0.2 earth mass and then to 0.3 earth mass, to reflect the weighted average colliding body size during the final merging process based on the previous merging simulation whereas the weighted average mass for 5 lunar mass satellite merging process results in 3 lunar mass (see Section 3.4). Whereas each of Colliding Mass 2's final spin rate is also calculated independently before merging with Colliding Mass 1. We assume that the initial spin, as a result of the protoplanetary disc, is normally distributed around the mean of half a day and then generate the random collision angles and plug into the following equation to generate the raw spin rate post each collision. The moment of inertia factor is set to 0.39307 instead of 0.3307 because it is determined that the moon formed 50 Myr after the formation of the earth and it takes 500 Myr for planetary differentiation to take

place. Yet, some level of differentiation did take place because moon's density is lower than earth with an exceptionally small iron core while the earth has a larger core than a typical terrestrial planet. We substitute the mass of the protoplanet hitting earth ranges from 0.1, 0.2, to 0.3 earth mass respectively, substitute the earth mass before merger ranges from 0.1, 0.2, 0.3, 0.4, and 0.6 earth mass respectively. We substitute the escape velocity of the earth as the final striking speed before the merger ranges from 0.1, 0.2, 0.3, 0.4, and 0.6 times of earth's escape velocity respectively, and the radius of earth ranges from 0.4642, 0.5848, 0.6694, 0.7368, and 0.8434 times of earth's radii respectively. We only randomly generate angles within 0 to 45 degrees clockwise for the prograde motion because all other cases repeat the pattern. A numerical example with a substitution for a 0.6 earth mass proto-Earth combining with a 0.3 earth mass protoplanet is given below:

$$P_1(x) = \frac{\left(\frac{\left(\frac{3}{10} \cdot M_{earth} \cdot (0.6 \cdot V_{escape} V_{earth}) \cdot (|\sin x - \cos x|)^2 \cdot (\sin x)^2 \cdot (0.8434 \cdot R_{earth}) \right)}{0.39307 \cdot \left(\frac{6}{10} \cdot M_{earth} \right) \cdot (0.8434 \cdot R_{earth})^2} \right)}{\frac{1}{24 \cdot 60 \cdot 60}} \quad (3.70)$$

$(\sin x - \cos x)(\sin x)$ is raised to the power of 2 because the final force is minimized by both hitting angles at the vertical and the horizontal plane. We then compute the weighted average of the raw spin rate generated by the Colliding Mass 2 by its hitting angle, the Colliding Mass 2's own initial spin rate, and the Colliding Mass 1's own initial spin rate. We use the weighted average to proceed to the next round of computation.

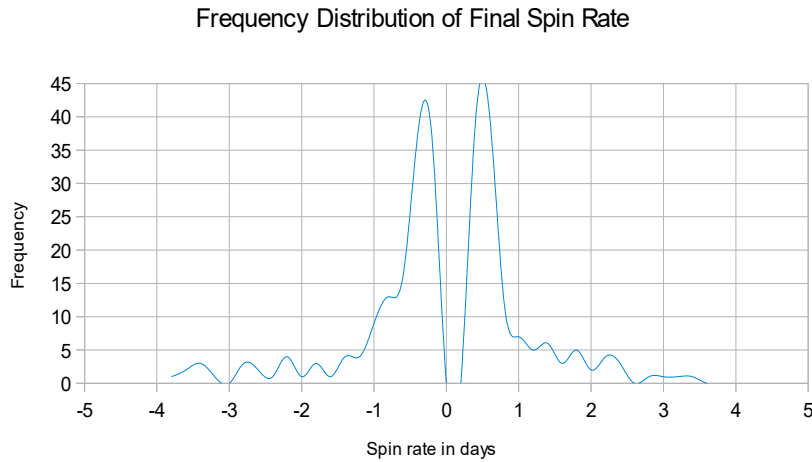


Figure 3.16: Frequency distribution of final spin rate

The final spin rate distribution is plotted above. No spin rate faster than 6 hours 8 minutes in either prograde or retrograde motion has been observed because initially there is already a limit on the transfer of angular momentum from linear momentum upon collision. We take the absolute value in either spin direction and exclude those slower spin rate which inevitably leads tidal locking (sideral rotation longer than 168 hour days) for one lunar mass within 4.5 Gyr.

Out of the remaining 78.0% of possible spin rate (ranges from 1.63 days to 6 hours 8 minutes), one takes the average of all spin rates (0.6079 days or 14 hours 35 minutes) and plugs into our tidal locking equation. We found that *satellites up to 1.635 lunar mass are tidal locking free from their host planet, that is 21.90% of all satellites' possible lunar mass configurations.*

3.6 Moon's Obliquity Evolution

The merging of protoplanets and the creation of satellites are common, but not all moons stay with their planet. If the merging occurs without a direct impact, as we have shown earlier that non-direct impact is the norm, then moon formation is inevitable in each case. The evolutionary trajectory of the moon depends both on its obliquity and its mass as well as stellar tidal forces. According to simulation and model run by Keiko and Ida, it is shown that five possible fates await moons formed around their host planet[13]. In the first case A1(which includes moons range from 0.01 Earth mass to 0.05 Earth mass, equivalent to less than 1 lunar mass up to 4 lunar mass with varying degrees of obliquity), the moon gradually gains angular momentum and separation from its host planet and decreases the host planet's moment of inertia until both bodies obtain a synchronous rotation and orbits around each other. This is the well-known case we have observed between the Earth and the moon.

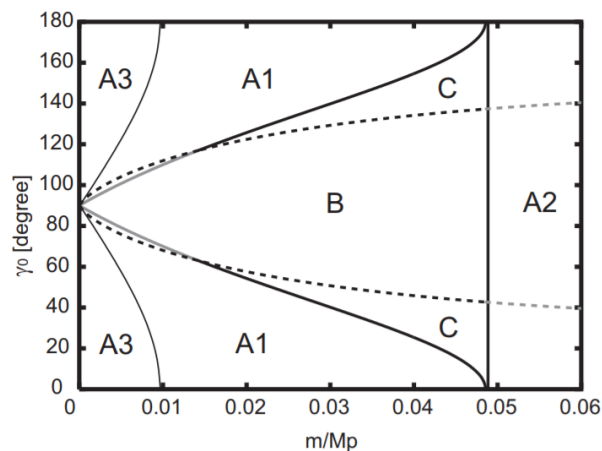


Figure 3.17: Lunar mass & obliquity and their ultimate evolution trajectory

In case A2, the satellite with more than 4 lunar mass achieves synchronization before the occurrence of the precession transition. In this case, the obliquity angle are almost conserved as the initial values. In other words, tidally locked to their home planet.

In case A3, the satellite has less than a lunar mass. The stellar tidal torques dominate over the satellite torques. In this case, Ω becomes smaller than n before the obliquity becomes zero, then the satellite begins to decay toward planet very slowly. The subsequent reduction of the planetary spin leads to a synchronous state with planetary mean motion.

In case B which includes scenarios with no less than 40 degrees of initial obliquity, the moon gradually loses angular momentum and turns back onto the host planet. In case C, the satellite follows the same evolutionary trajectory as B, but it is locked in a synchronous state before falling onto the planet at a distance of 5~10 earth radii. The timescale of this occurrence happens at (10^6 years), because the satellite orbit turns back at a relatively small radius A_{crit} , resulting in moon and earth experiencing 3.396 earth days per day and no tidal heating contributing to plate tectonics. Therefore, we can only treat case C as marginal habitable.

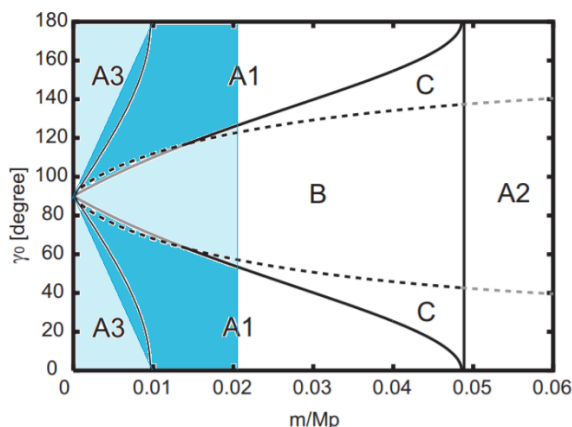


Figure 3.18: Lunar mass & obliquity which evolves toward earth-moon relationship

From earlier calculations, we have shown that a satellite with a lunar mass greater than 1.635 will form a synchronous orbit with their host planet within 4.6 Gyr. Therefore, we will include a partial region of A3 (closer to 1 lunar mass) and A1 and exclude region B and C up to 1.635 lunar mass. As a result, *around 54.767 percent cases, the moon is stabilized around its host planet with various initial obliquity and mass*, this shows that a planet with a stable moon is relatively common though not a universal characteristics of all terrestrial planet. Within the solar system, the earth is the only terrestrial planet hosting a moon of a massive size. On the other hand, dwarf planets such as Pluto and Charon, Eris, Makemake all have moons of significant mass relative to their host planet. In the case of Makemake, the collision occurred relatively recently. This can be implied from the non tidal-locking orbits of their moons and its own fast spin rate.

3.7 Earth Size

The stellar to planetary mass ratio indicates that the mass of terrestrial planets likely follows a lognormal, or skewed normal distribution where terrestrial planets ranges from 0.1 to 10 earth masses are possible within the stellar habitable zone. [103] Then the question is, what is the lowest and highest possible limit for a terrestrial planet to be habitable. Lopez and Fortney worked off of data from Kepler and modeled the radii of planets. They determined

that planets with radii of less than 1.5 Earth radii will become super-Earths, and planets with radii of greater than 2 Earth radii will become mini-Neptunes. That suggests a radius limit of 2 Earth radii, though most terrestrial planets will probably be under 1.5 Earth radii. The study has been confirmed since there is a lack of exoplanets found between 1.5 earth radii to 2 earth radii. 1.5 earth radii can be translated into 3.375 earth mass assuming similar density. However, a planet does not need to be much larger to start to retain hydrogen gas. According to one study, planets with 1.3 earth mass likely to start capture hydrogen atoms as the planet's escape velocity catching up with the atom's escape velocity at 285 K. Though hydrogen is not poisonous. It is flammable and explosive with oxygen. It is hard to imagine a super earth with a mixed hydrogen and oxygen atmosphere will not burn in flames with the slightest spark of lightning. Another group focused on planets losing their hydrogen envelopes, the gaseous layers of hydrogen that accrete during the early parts of their lives. Their calculations indicate that planets of less than one Earth Mass would accumulate envelopes of masses between 2.5×10^{16} and 1.5×10^{23} kg. The latter is about one-tenth of Earth's mass. Planets with masses between 2 Earth Mass and 5 Earth Mass could accumulate a peak envelope mass between 7.5×10^{20} and 1.5×10^{28} kg, which is substantially more massive than Earth's. The group calculated that planets with masses less than 1 earth mass would lose their envelopes within 100 Myr. They found that planets with masses greater than 2 earth mass retains their envelopes, and so become mini-Neptunes. [29] We take the average of these two results and arrived at 2.6875 Earth mass, which is used as the upper limit of the habitability of terrestrial planets. On the other hand, the lower bound for habitability is cut off at 0.43 earth mass. [50] This is done by a study based on the temperature within the habitable zone and the expected gas loss composing oxygen, carbon dioxide, and nitrogen over the course of evolutionary timescale and have shown that planet with 0.43 earth mass or above can retain an atmosphere. Taking the lower and the upper bound into considerations and using the distribution samples generated based on Kepler's exoplanet data for the exoplanet mass for one solar mass star. ²

²(See Special Chapter: Stellar to Planetary Mass ratios)

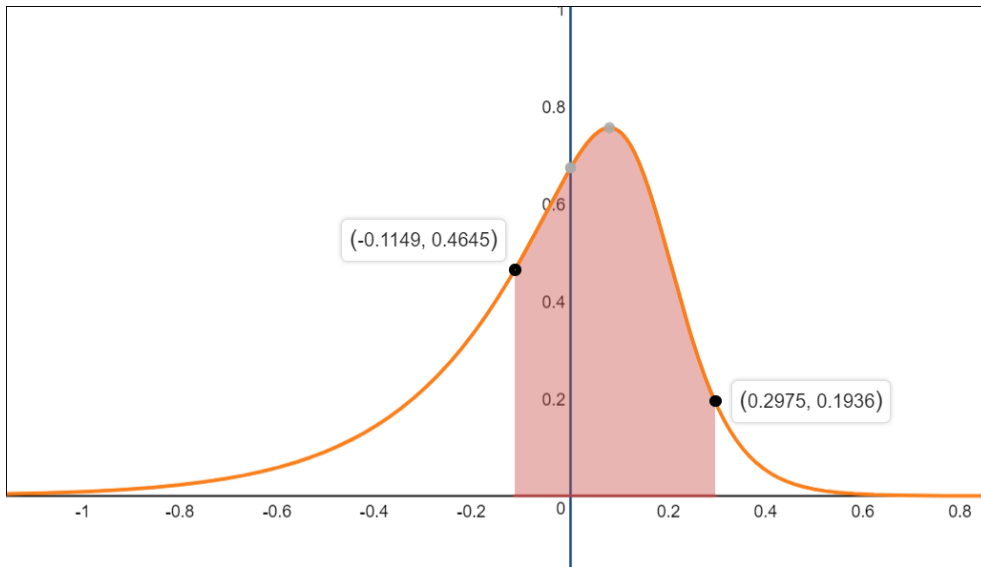


Figure 3.19: CDF of terrestrial planets between 0.43 and 2.6875 earth mass

One can compute the probability of planets falling within this range. *The final probability is obtained to be 65.18%.*

$$\frac{\int_{-0.1149}^{0.2975} P(x) dx}{\int_{-\infty}^{\infty} P(x) dx} \quad (3.71)$$

$$= 0.651812345182$$

3.8 The Chance of Getting Watered

Studies show that terrestrial planet formed linearly as the metallicity increases but then drops sharply as the rate of hot Jupiters also increases sharply as the metallicity rises. The combined effect brings the peak of terrestrial planet creation at the metallicity index of 0.2. Metallicity not only affects the likelihood of terrestrial planet formation. More importantly, depending on the metallicity, the number of hot Jupiter attempts increases between metallicity of -0.4 at 0 percent to 100 percent at metallicity of 0.4. For metallicity 0.4 or greater, an overwhelming majority of the systems hosts hot Jupiters. Therefore, the number of failed hot Jupiter increases with increasing metallicity. This is important because our own Jupiter is also a failed hot Jupiter. The Grand Tack theory posits that Jupiter originated around 3.5 AU, just beyond the snowline of the solar system at its early day of formation (at 2.7 AU). As its protoplanetary embryo gained mass and started a runaway hydrogen accretion, it slowly migrated inward toward the sun due to strong gravitational forces. The migration came to a halt when Saturn formed and began resonate in a 2:3 orbital synchronization with Jupiter. Jupiter ventured as far as 1.5 AU from the sun before being pulled eventually to its current orbit at 5 AU. The theory is proposed to explain the low mass observed for Mars, the void of any planets in the asteroid belt, and

the presence of water on earth. The theory is one of many possible fine detailed explanation of how hot Jupiter fails its migration. The true nature and complexity of the possibilities are currently not available. However, the lack of knowledge does not prevent us from arriving at our conclusion. On a system where no hot Jupiters ever arises, the inner terrestrial planets are likely to remain dry given by the understanding of the solar system formation. On a system with hot Jupiters, the inner terrestrial planets are destroyed because every protoplanet is either perturbed by the gravitational effect of the gas giant and ejected, captured, and simply absorbed. Only in cases where hot Jupiters with their migration attempts can possibly disturb the orbits of the inner planets can bring a bombardment of a significant amount of water. This gave us a clue regarding the likelihood of terrestrial planet covered by water. The chart of the percentage of hot Jupiters, failed hot Jupiters, dry terrestrial planet, and wet terrestrial planet vs. metallicity is plotted below.

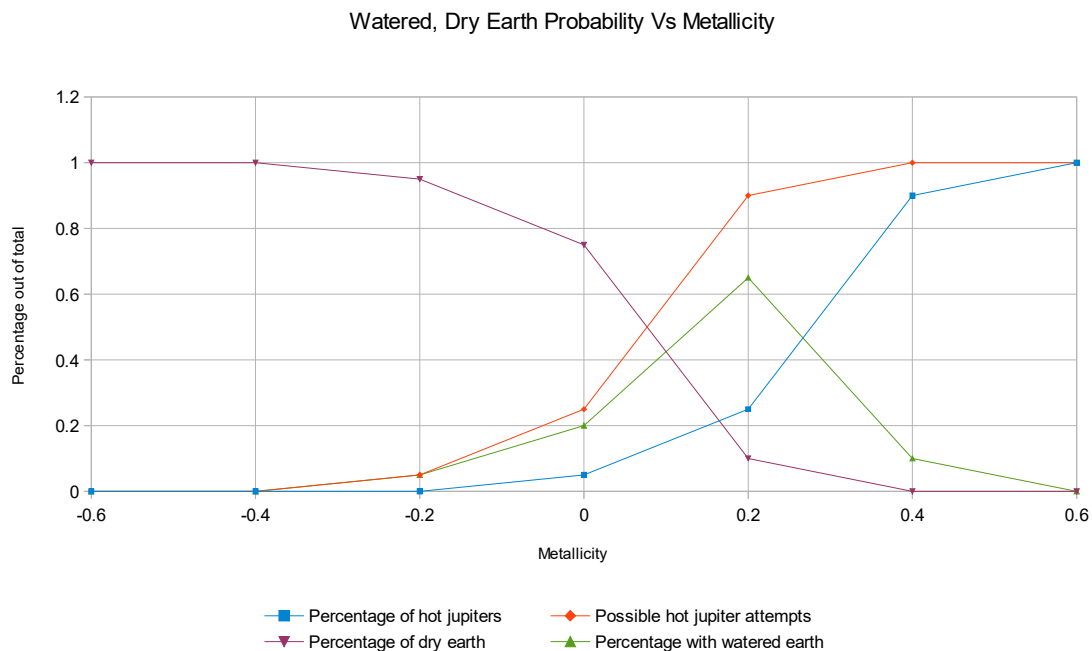


Figure 3.20: Watered, dry earth probability vs metallicity

Since the rate of failed Jupiter increases with metallicity and peaks at the metallicity of 0.2, we are able to compute the probability of a terrestrial planet gets watered over all possible ranges of metallicity which permits the creation of terrestrial planets in the first place. The average metallicity of terrestrial planets changes over the course of cosmic history. For our current investigation, we are only interested in the metallicity distribution from 5 Gyr ago to 4 Gyr ago. Metallicity of stars at any given age is normally distributed, and we can use existing observational data to compute the proportion of stars that will give rise to terrestrial planets. The average metallicity of the galaxy can be obtained from this graph, assuming the metallicity is normally distributed[49] :

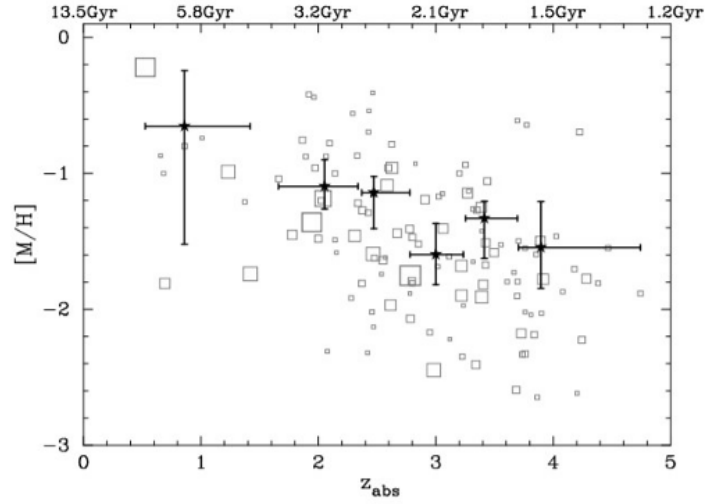


Figure 3.21: Average metallicity profile of cosmic historical past

$$f_{metallicity}(x, y) = \frac{1}{q\sqrt{2\pi}} e^{-\frac{(x+0.26+y)^2}{2q^2}} \quad (3.72)$$

$$q = 0.2$$

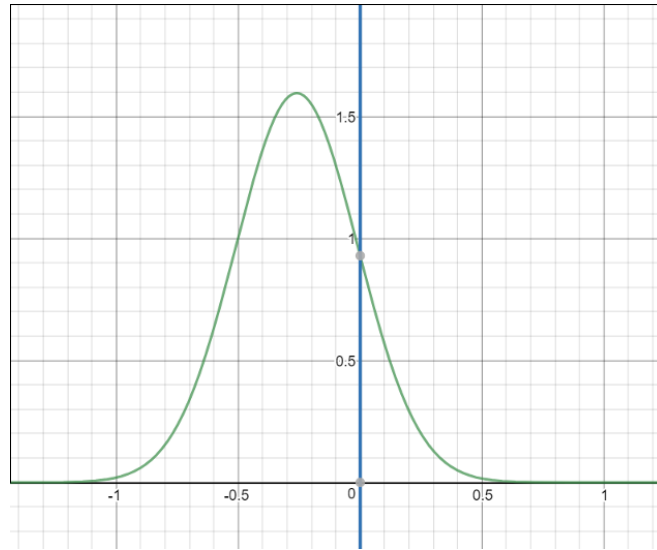


Figure 3.22: Observed metallicity PDF 4.6 Gya

Now, as we have obtained the probability distribution of stars by metallicity, we combine this distribution to our existing distribution for the percentage of failed hot Jupiters over a range of metallicity and the final percentage of wet terrestrial planets can be computed from the chart below:

$$f_{wetearth}(x) = \frac{0.1935}{(-x + 1.205) \cdot q_0 \sqrt{2\pi}} e^{-\frac{\ln(-x+1.205)^2}{2(q_0)^2}} \quad (3.73)$$

$$q_0 = 0.2$$

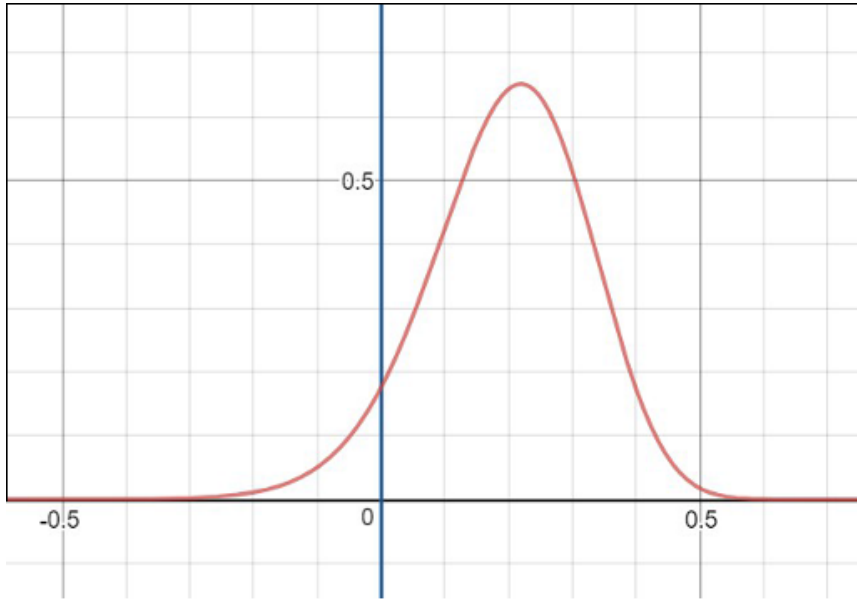


Figure 3.23: Metallicity PDF for wet earths

$$f_{composite}(x, y) = f_{metallicity}(x, y) \cdot f_{wetearth}(x) \quad (3.74)$$

$$\frac{\int_{-0.066666}^{0.066666} \int_{-\infty}^{\infty} f_{composite}(x, y) dx dy}{\int_{-0.066666}^{0.066666} \int_{-\infty}^{\infty} f_{metallicity}(x, y) dx dy} = 0.0768103434623 \quad (3.75)$$

Whereas the integration along the y -axis with values between -0.067 to 0.067 is the change of the mean metallicity of the galaxy between 5 Gya and 4 Gya. Based on this result, we need an additional round of computation. Lineweaver's original counting[60] for the number of terrestrial planets used metallicity as the selection criterion. Since the metallicity selection range is more lenient for the terrestrial planets than the wet terrestrial planets, the final percentage of the terrestrial planets is higher. We reproduced Lineweaver's distribution with metallicity as a selection criterion with the following composite equations:

$$f_{metal0}(x) = \frac{4.5}{(x - 1.4) \cdot q_0 \sqrt{2\pi}} e^{-\frac{\ln(-x+1.9)^2}{2(q_0)^2}} \quad (3.76)$$

$$d(x) = 0.9 (1 - 1 \cdot \tanh 8(x - 0.16)) \quad (3.77)$$

$$t(x) = f_{metal0}(x)^{0.4} \cdot d(x) \quad (3.78)$$

$$\int_{-\infty}^{\infty} t(x) dx \quad (3.79)$$

$$= 0.250803902373$$

with the plotted result:

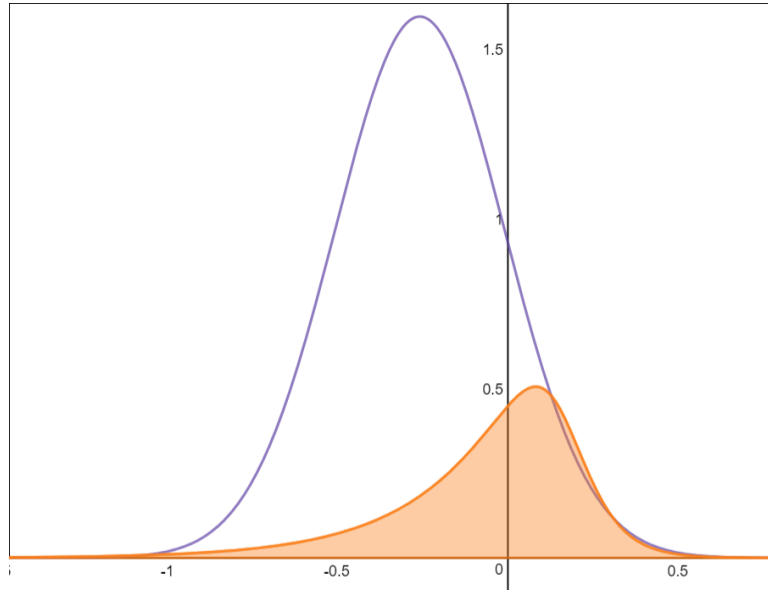


Figure 3.24: Metallicity PDF for terrestrial planets overlaying metallicity PDF 4.6 Gya

and a final 25% of all stars distribution falls within the Lineweaver’s selection criteria.

$$\frac{0.0768103434623}{0.250803902373} \tag{3.80}$$

$$= 0.306256572308$$

Finally, *prediction indicates that 30.625% of all terrestrial planets created from 5 Gyr to 4 Gyr ago is covered by ocean.*

3.9 Total Water Budget of Earth

We also need to find the average water budget on the surface of terrestrial Earth-like planets. Is earth’s ocean depth typical of all Earth-like planets or is it an anomaly? We have shown earlier the importance of water to foster and create a sustainable environment for the emergence of life. For the rise of intelligent species in particular, the ocean should cover a significant amount of planetary surface to provide a relatively stabilizing climate, yet the total mass of the oceans has to strike a delicate balance enabling continental plates elevated above the sea. If a planet is covered in tens of thousands of meters depth of oceans, intelligent, land-based life manipulating tools and fire will be utterly impossible.

To answer this question, we need to deduce the water budget from several lines of reasoning.³ First of all, from our previous discussions concerning the average mass budget leftover availability for planet formation for stars of different masses, we know that given one solar mass, the average mass budget available for planet creation is 400 earth masses. Given the metallicity of the sun, we know that 72 percent of the solar nebulae composed hydrogen, and 1.2 percent composed oxygen. Since water molecule composed of one oxygen and two hydrogen molecules, and oxygen reacts with almost every element available, we shall assume that oxygen during the formation of the solar system is readily bonded with some other element, and in particular abundantly with hydrogen. Moreover, helium is a noble gas, and not readily bond with oxygen, so the remaining elements readily bond with oxygen are carbon, iron, sulfur..etc. By finding the percentage of oxygen, as a limiting quantity and the fraction of oxygen that bonds only with hydrogen to form water, we found that the upper limit for the solar system's water budget is 4.373 earth mass (Taking the average of all of the oxygen used in the creation of water and a significant portion used in the construction of terrestrial planets). It is derived based on the solar system's planetary budget empirical law and 1.897 earth mass based on the generalized planetary budget empirical law. We take the mean, and the total water budget available to earth is 3.13485 earth masses.

Secondly, we need to settle the issue of the origin of earth's water. Some argue that earth's water was readily available during the formation phase of the earth and is rapidly rose to the surface of the planet as a consequence of planetary differentiation. They further argued that the isotope ratio of earth's ocean differs from meteorite samples, consequently, earth's water cannot be delivered from the outer space. A drawback of indigenous water formation theory is that if water was present during the initial phase of planetary formation, then the total water budget of the earth today will be roughly three percent of earth mass, which is 150 times the total water budget we have, including the underground water reservoirs. Furthermore, all dwarf planets, moons of outer planets beyond the snowline have significant water content higher than the average 3 percent of their body mass. This is easily reflected from the density of Jupiter's moon Europa, Ganymede, Saturn's moon Titan ($1.8798 \frac{\text{g}}{\text{cm}^3}$), Pluto and its moon Charon, which are all close to the density of water. All of this has shown that the distribution of water in the solar system is non-uniform. During the initial phase of solar system formation, the temperature of gas and debris of inner planets exceeded the boiling point of water, as a consequence, a significant amount of water molecules have gained enough energy and momentum and moved beyond the snowline, and rendered the inner terrestrial planets dry.[1] If inner planets were initially dry, then the majority of the water must have been delivered to earth from beyond the snow line. Substantial evidence shows that asteroid from the inner asteroid belt is dry, while dwarf planet Ceres from the outer asteroid belt is icy. Geological evidence has shown that water was present on earth before the late heavy bombardment at 3.8 Gyr ago, then the only other origin of earth's water must come from the asteroid belt. Indeed, the isotopic

³(See Special Chapter: Stellar to Planetary Mass ratios)

ratio of earth's ocean closely resembles those of the water found from asteroids of the asteroid belt. The mechanism for this delivery is explained by the migration of Jupiter into the inner solar system and its later migration outward by the pull of Saturn, which was also migrating inward. This is not atypical, in fact, it has been found that around 5% of planetary systems with solar metallicity contains hot Jupiters, and the formation of failed hot Jupiters are more likely, just like in the solar system. As Jupiter migrated toward the sun, it perturbed the protoplanets, asteroids within the asteroid belt and they either gained speed and are ejected from the solar system or lost speed and start to fall into the sun. As the debris falls toward the sun, it intercepts and crosses earth's orbit around the sun. Though a majority of cases, the debris crosses and without gravitationally attracted by the earth, on closer approaches, with a distance at or shorter than the effective Hill radius, and especially shorter than the Roche limit, the debris hit earth, thus delivering water to the surface. Computing the circumference of earth's orbit and weighted effective distance that asteroid can be captured and hit earth, we obtain the final total water budget of the earth.

From this line of reasoning, we can calculate the total amount of water budget the earth can obtain. The total water budget of the solar system beyond the snowline 2.7 AU at the formation of the solar system is 3.13485 earth masses. We adopt the Nice planetary formation model so that we assume the total water budget is dispersed between 2.7 AU to 26 AU unit, beyond the orbit of Uranus at 20 AU and stretch into the Kuiper belt. Then, we assume that a migrating gas giant could arise from any arbitrary distance away from their star. In the solar system's case, Jupiter started to migrate inward from 3.5 AU and Saturn from 6 AU. We assume that icy comets and asteroids can only be captured and impact earth when they approached 1.5 million km or closer to earth. Twice the Hill sphere distance over the circumference of earth's revolutionary path around the sun is the fraction of water can be captured by the earth. We find the total deliverable water budget to the planet earth by assuming a gas giant started its migration from the Kuiper belt, then the entire water budget of the solar system can potentially be diverted toward the sun. In the most extreme case, at most 20 times the mass of current ocean will be available to earth.

However, it is estimated an additional 1.5 to eleven times the amount of water in the oceans is contained in the Earth's interior [44] and some have hypothesized that the water in the mantle is part of a "whole-Earth water cycle." [99] The water in the mantle is dissolved in various minerals near the transition zone between Earth's upper and lower mantle. Direct evidence of the water was found in 2014 based on tests on a sample of ringwoodite. Liquid water is not present within the ringwoodite, rather the components of water (hydrogen and oxygen) are held within as hydroxide ions.

$$\begin{aligned}
 w &= \frac{26^2}{26^2} \cdot \frac{(1.1342 + 1.897)}{2} \cdot \frac{(1,500,000\text{km} \cdot 2)}{2\pi \cdot 149,597,870\text{km}} \\
 &= 0.00483727271819
 \end{aligned}
 \tag{3.81}$$

$$\frac{w}{\left(\left(\frac{1}{4,400}\right)\right) \cdot 2} \tag{3.82}$$

$$= 10.64199998$$

We will assume that the total water budget on earth currently is twice of the mass of the ocean, then we arrived a range from 0 to 10.64 times of water deliverable to earth. Since most inward migration of gas giants likely originated near or closer to the snow line because a higher concentration of ice material blown from less than 2.7 AU concentrated just beyond the snow line, it is likely that the total mass of water deliverable to earth is skewed to the left. We used a lognormal distribution to simulate the distribution of water deliverable to earth.

$$g_{ocean}(x) = \frac{5}{.95xQ_1\sqrt{2\pi}} e^{-\frac{(\ln 0.587x^{0.8})^2}{2(Q_1)^2}} \tag{3.83}$$

$$Q_1 = .63$$

Now based on estimates of continental plates and the different surface area percentage relative to the oceanic plates, the right amount of water which will enable the emergence of a shallow sea which smoothes the transition from subduction zone to dry land ranges from 0.1 earth ocean mass to 1.75 earth ocean mass. So we can integrate this region and find the probability of such ocean budget formation.

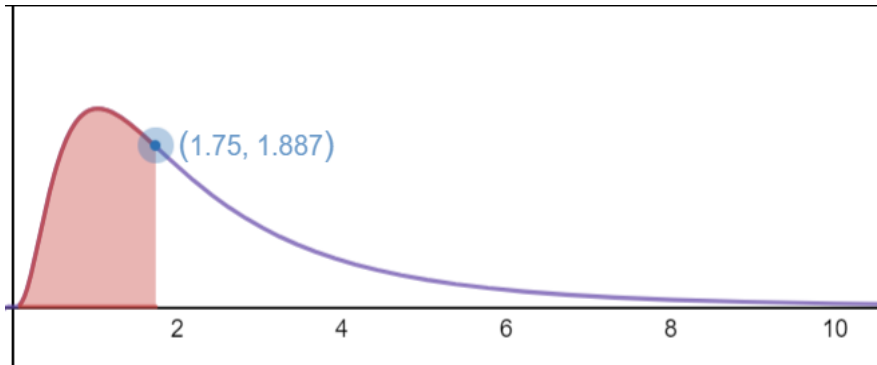


Figure 3.25: PDF for various final ocean size on a terrestrial planet

$$\frac{\int_{0.1}^{1.75} g_{ocean}(x) dx}{\int_0^{\infty} g_{ocean}(x) dx} \tag{3.84}$$

$$= 0.453252928864$$

It is now shown earth at *45.33% chance gets water delivered in the right proportion* that can potentially enable the emergence of dry land and the possibility of land-based life forms.

3.10 Right Ocean & Land Mix

Is earth's water and land ratio typical of any earth-like planet? In order to answer this question adequately, conclusions can only be settled when several different fields and their effects on earth's geologic process is thoroughly analyzed. First of all, the dry part of earth above the sea level, or the continents, are actually cratons made of lighter composition mostly of granite, that semi-floats over the ocean cratons with higher density. Continental plates are thicker in which its upper edges rises above the oceanic plates, and its lower edges sink deeper than the oceanic plates. During the early formation period of earth, planetary differentiation ensured that water, which has much lower density than the crust, covered the entire surface of the earth. Studies have shown that earth's surface temperature was nearly the same compared to that of today, despite the sun with only 75 percent of the luminosity compares to today. In what's being labeled as the Faint Young Sun paradox, the earth was supposed to be frozen as an ice ball. Some have argued that the earth's temperature was much higher as a consequence of higher methane and carbon dioxide level, but equally important, the low albedo of an early ocean planet ensured an absolute higher energy absorption rate. The emergence of continents was not evident until the Archean epoch. During the Hadean phase of earth's development, the leftover heat from radioactivity was three times higher than that of today. The rate of new crust creation along volcanic faults and the rate of existing crust destruction were too quickly for any cratons accretion to take place. By 2.5 Gyr ago, the rate of internal heat has cooled enough enabling the accretion of volcanic arcs (probably similar to the Hawaii islands chains). If the rate of accretion was faster than the rate of destruction, then continental cratons began to form and increases in size until the creation rate significantly slows down as the mantle continues to cool. This trend is clearly observed in earth's geologic history in which 30% of land mass first appeared in the Archean era and 50% in the Proterozoic era and 20% in the Paleozoic. In earth's cases, over 40 % of the surface area is covered by continental cratons, orogenic belts, and platforms. However, this percentage can easily be greater or less depending on the initial endowment of the radioactive leftover of the molecular cloud forming the planet. [28][20][81][12] The primary sources of radioactivity observed on earth come from Uranium 235, Thorium 238, and Potassium 40. On some other planets, each of the radioactive material endowment could be higher or lower than we found on earth which in turn generates different mantle cooling curves and eventually contributing to different continental plate formation sizes. Furthermore, the moon (with a separation distance of 40,000 km when it first formed) was significantly closer to earth in its early days, and must have significantly contributed to tidal heating of the early earth and enabled the accelerated emergence of the growth of the continental plates. Moreover, we have shown that though the moon formation around terrestrial planets is common, the final mass of the moon varies, which again contributes to differential growth and development of the continental plates sizes. In summary, one can conclude that the percentage of continental plates covering any planet which owns one moon and is initially covered by an entire ocean can

range from a few percentage of the surface area to completely covering the surface.

We can then formulate a mathematical model to delineate the ratio of drylands to ocean surface for different proportion of continent size. We reinstated the equation describing the continental plates [70][20] in the form of polynomial functions. The initial drop curvature to the right of y-axis in height represents mountain and high plateau, the horizontal leveling portion represents open plains or platforms, and the final drop before hitting the x-axis represents the continental shelf and continental plates' cliff. (i.e. Mariana trenches observed on earth)

We formulate a list of curves to mimic the continental plates size from covering a few percentage of the planetary surface to that of the entire surface.

$$y_{smallplate} = - \left(\frac{x - 2}{9} \right)^{29} + \frac{4}{x + 0.4} + 6.596 \quad (3.85)$$

$$y_{mediumplate} = - \left(\frac{x - 8.717}{9} \right)^{11} + \frac{13}{x + 0.4} + 6.596 \quad (3.86)$$

$$y_{bigplate} = - \left(\frac{x - 13.717}{9} \right)^5 + \frac{24}{x + 0.4} + 6.596 \quad (3.87)$$

We also need to reinstate the oceanic plate curve. For the simplicity of the model, we adopt the linear equation that slopes gradually from the dividing trenches toward the boundary between the continental and oceanic plates.

$$y_{oceanplate} = 0.3(x - 11.621) \quad (3.88)$$

The plot results are represented below:

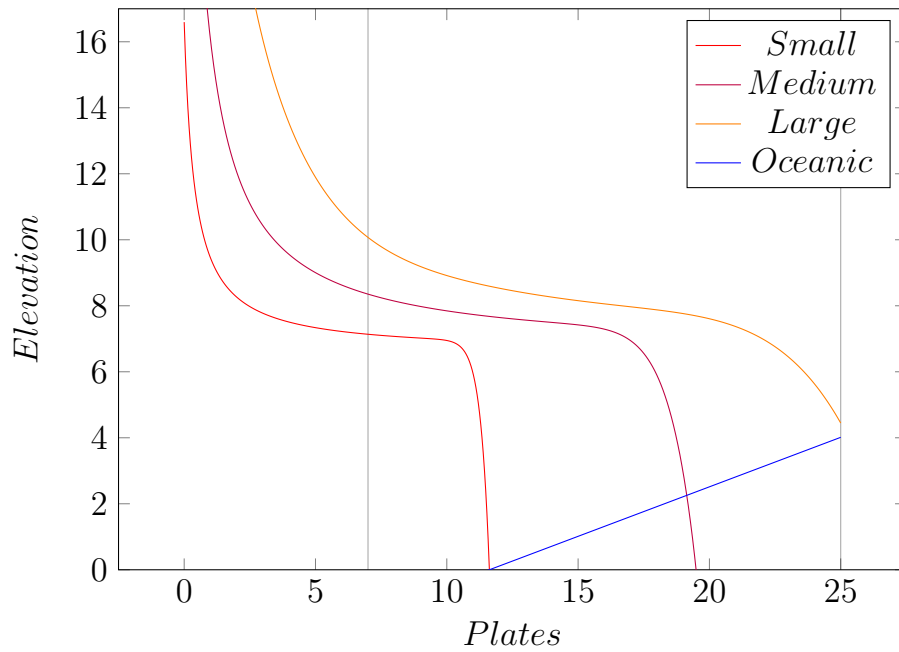


Figure 3.26: Planet with small, medium, and large sized continental plates

The blue vertical line $x = 7$ represents the proportion of the land and the ocean, where 7 units to the left of vertical line represent 29% of the land surface area and 18 units to the right represent 71% of water surface area. We will integrate and find the area enclosed by the ocean, which represents the total mass of water at the surface of the earth.

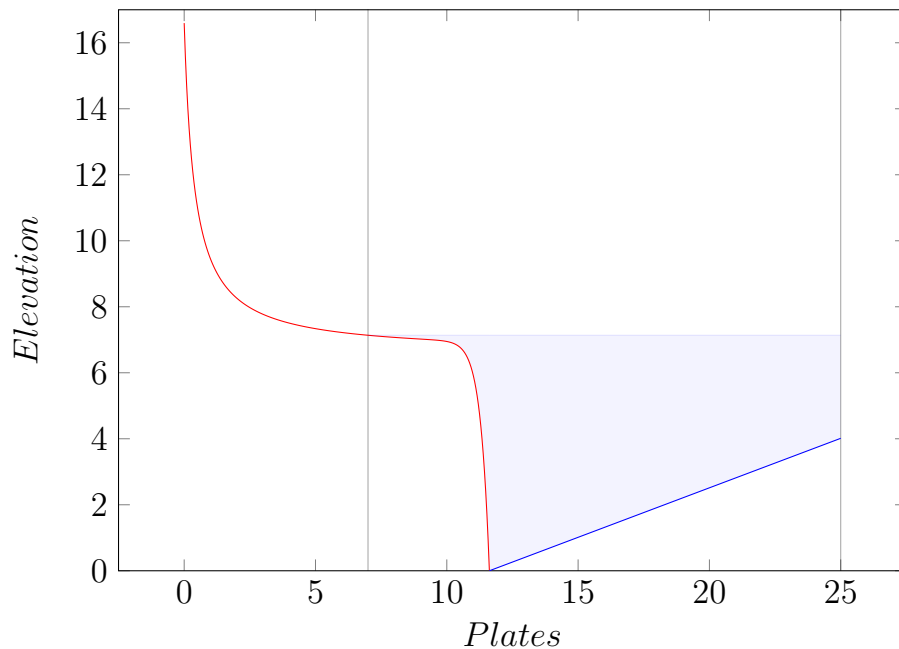


Figure 3.27: Earth's case by the model

Using integration, one obtains the final value of 71.4161. We will use this value to compute the

shoreline of different configurations of plates and oceans. In order to proceed, we need to find the equation which defines the water level for continental plates at different depth and height. The general idea of the equality is expressed as:

The minimal rectangular bounding box of the ocean - the portion occupied by the continental plate - the portion occupied by the oceanic plate = the ocean size

Where h_0 is the x coordinate of the intersection between the oceanic plate and the continental plate, x is the x coordinate of the shoreline ranges between 0 to 25 and is the value we are solving for.

$$[f_{plates}(x) - f_{plates}(h_0)](25 - x) - \left[\int_x^{h_0} f_{plates}(x) dx - f_{plates}(h_0)(h_0 - x) \right] - \left[\int_{h_0}^{25} f_{ocean}(x) dx - f_{ocean}(h_0)(25 - h_0) \right] = 71.141 \quad (3.89)$$

and the equation as:

$$[f_{plates}(x) - f_{plates}(h_0)](25 - x) - \left[\int_x^{h_0} f_{plates}(x) dx - f_{plates}(h_0)(h_0 - x) \right] - \left[\int_{h_0}^{25} f_{ocean}(x) dx - f_{ocean}(h_0)(25 - h_0) \right] = 71.141 \quad (3.90)$$

$$f_{plates}(h_0) = f_{ocean}(h_0) \quad (3.91)$$

The equation simplifies to:

$$[f_{plates}(x) - f_{plates}(25)](25 - x) - \left[\int_x^{25} f_{plates}(x) dx - f_{plates}(25)(25 - x) \right] = 71.141 \quad (3.92)$$

When ocean completely floats over the continental plates in the most extreme scenarios.

Using this equation, one can then derive the water level and the shoreline and the proportion of ocean and dry land surface ratio.

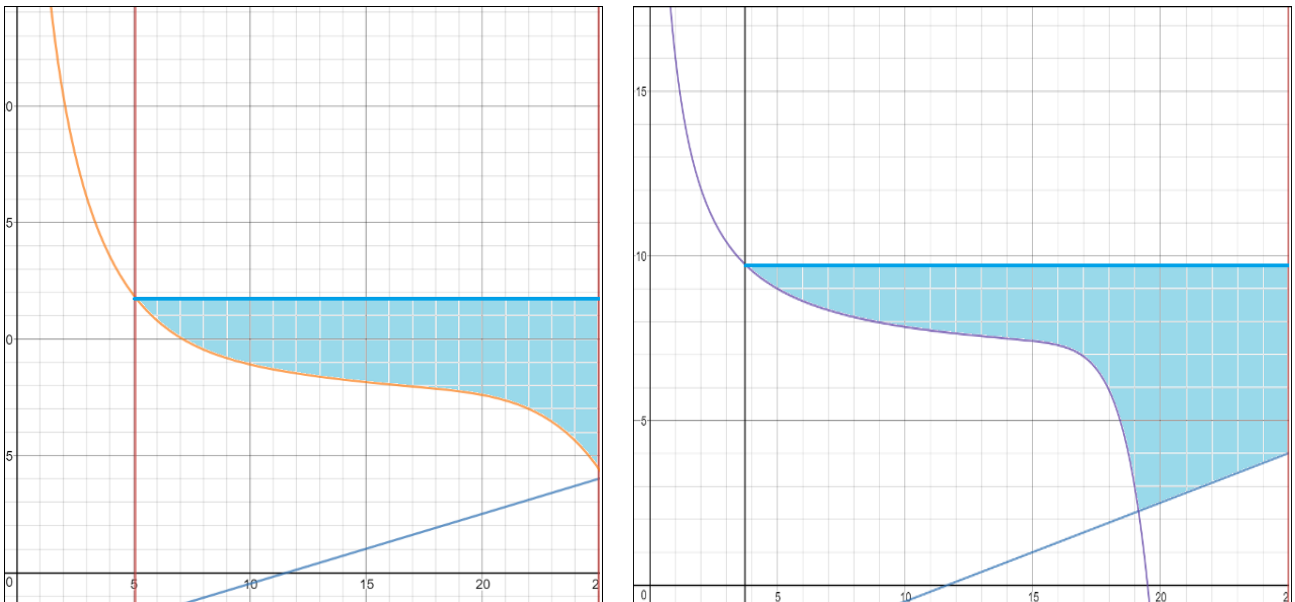


Figure 3.28: Water level for 2 different possible continental configurations

We set a total set of 9 equations, mimicking the share of continental crust in proportion to the earth's total surface area from 100%, 77.97%, 53.72%, 49.43%, 46.48%, 44.42%, 38.34%, 33.05%, to 18.08% respectively. Then we find the surface to ocean ratio.

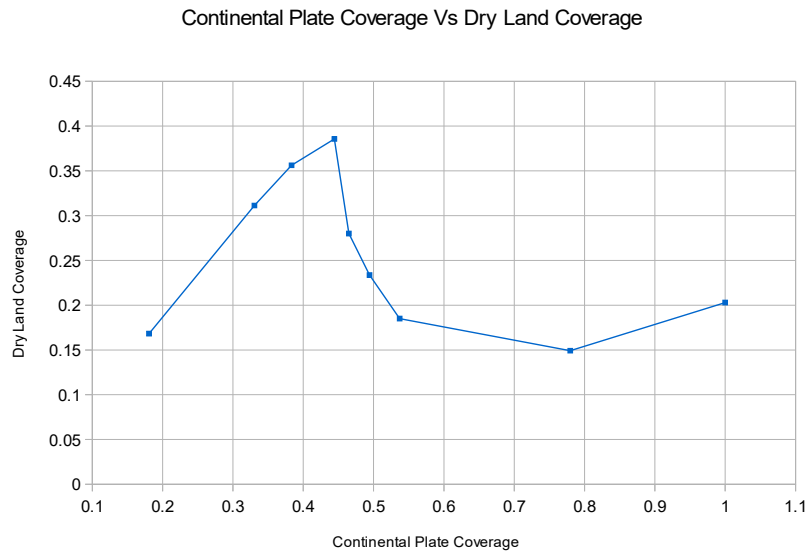


Figure 3.29: Continental plate percentage vs dry land percentage

Although the graph shows that in all possible cases, dry land is exposed to a significant degree and peaks at 44%. Only continental plates with sizes covering from 53.72% to 44.42% of the surface area of the earth are able to accommodate platforms and flat plains that offers feasible agriculture and shallow ocean with a submarine continental shelf which makes a biological transition from marine species to terrestrial ones possible given the endowed water budget on earth. Continental plates covering less than 44.42% of earth surface area has exposed,

subaerial continental shelf, high shore cliffs render transition from fish to amphibian species impossible. Continental plates covering more than 53.72% have high sea levels due to lower sea depth covering above the continental platform. The shoreline is much further inland, and the elevation rises sharply from the shore. In the best possible case, an intelligent tool-using species, fruit trees, and grass plant can evolve under such a configuration, but it is impossible to develop full-blown agricultural civilization because only very narrow strips of land along the shoreline has low enough elevation with moderate climate enabling cultivation.

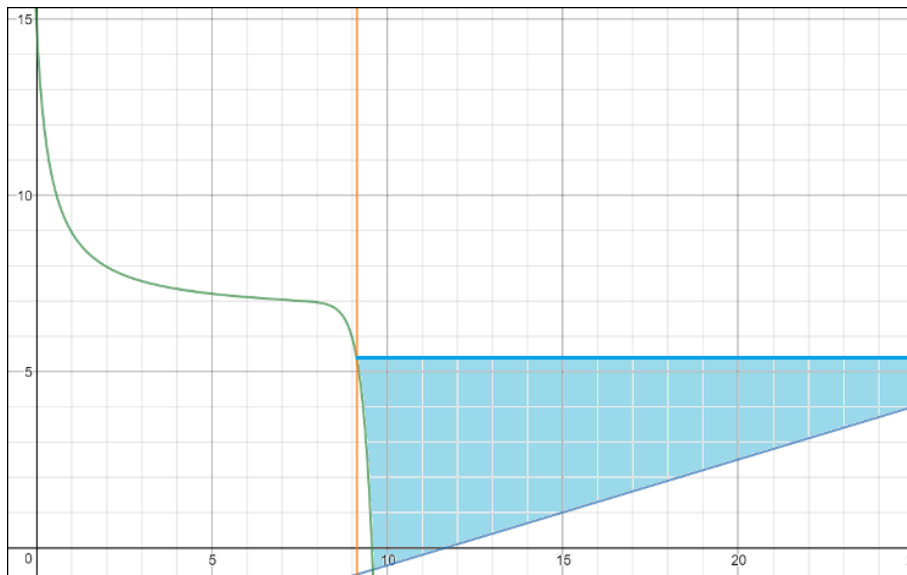


Figure 3.30: Planet with shoreline below the continental shelf

As a result, there are 9.3% out of all possible continental covering scenarios can provide the playground for intelligent species to realize its full potential given earth like water budget. Furthermore, parameters tweaking shows that the current continental configuration is susceptible to the total amount of water budget. Although ocean retreats during an ice age, at the peak of ice age 20,000 yrs BP, sea level was 120 meters lower, this only reduces the total mass of the ocean by 3%, unable to expose the continental shelf. Exposing the continental shelf requires a mass reduction by 5% or more. On the other hand, inundating continental shelf platform requires a mass increase by 5% or more. Since the total water budget available to earth enabling the exposure of dry lands ranges from 0 to 11 earth ocean worthy of water and is distributed around a mean of 1, the chance that earth water budget balances intricately enabling species to evolve on land and prosper is 45.33%. Then, the chance of having earth-like continental covering ratios and a similar level of ocean mass is merely 0.3596% assuming ocean to land surface coverage ratio stays roughly the same from 23% to 33%.

$$\frac{\int_{0.95}^{1.05} g_{ocean}(x) dx}{\int_0^{\infty} g_{ocean}(x) dx} = 0.003596 \quad (3.93)$$

We then generalize and applies the total probability for all possible cases. Any planet with a continental mass covering 18.08% or greater of the surface area provides the necessary condition for the emergence of intelligent life. For each possible continental distribution there lies a narrow range of water budget (from 5% reduction to 5% increase from the baseline), therefore, the total probability is 4.67%. There is two wats to arrive at this value. One approach is simply $\frac{0.1}{1.75} \cdot 0.82 = 0.0467$. Another approach is taking the integration of each land proportion, finding the mean, dividing by existing selected range, and times 0.82. Though we should use 9.3% instead of 82% for continental configurations as we stated earlier. We do want to illustrate later how glaciation can also narrow down the number of potential candidates based on continental configuration. In essence, there is more than one selection criteria that can exclude certain range of continental crusts from considerations.

Continental Proportion	Ocean to Land Ratio	Allowable Water Range
100.00%	20.29%	0.1~0.25
77.97%	14.92%	0.4~0.6
53.72%	18.50%	0.7~0.8
49.43%	23.36%	0.9~1.03
46.48%	28.00%	0.95~1.05
44.42%	38.56%	1~1.1
38.34%	35.62%	1.19~1.26
33.05%	31.13%	1.35~1.4
18.08%	16.83%	1.7~1.75

Table 3.3: Ocean to land ratio with required total water budget

In conclusion, from the previous mathematical model which shows all possible range of cases, dry land occupies at most 40% of the surface area of the planet given the total mass of surface ocean is similar to that on earth. Although nearly all planets do have an exposed land surface, their continental geology will be significantly different. Based on known geologic evidence and research, the first continents formed were much flatter than those today.[70] Although orogenic mountain building process also occurred, the highest mountains are probably around 3,000 meters in height above the sea level or even lower, since most of the continental plates first emerged have yet to merge into each other. On a planet dominated by continental plates land masses frequently bump into each other and creates magnificent mountain building regions. As a result, on a planet dominated by continental plates, as soon as one goes inland from the shoreline toward the continents interiors, the sea level rises sharply. With a sharp rise of the continental plates, tropical trees cannot thrive as the temperature drops quickly from the shoreline even if the trees grow near the equator. If we assume any typical intelligent species have to emerge from an environment that is relatively flat, and to cultivate agriculture before its transition into a technological species, then two thirds (island planets and continental planets with steep rises) of the planets may not be suitable candidates for the emergence of technological civilization despite possibly intelligent species living on it.

Finally, the solar system is one of the more metal-rich stars when it first formed 4.5 Gyr ago,

most of the planets revolving around their parent stars formed at the same age are poor in oxygen compares to earth. As a result, the upper limit of water formation on such a planet will be lower, implying ocean with a lower sea level. Under such a scenario, The percentage of exposed dry land will be greater and can exceed 40%. A few interesting facts follow. The shoreline could consistently touch the bottom of the continental shelf. The view of the planet can potentially be spectacular near the shoreline, where thousands of meters of cliff drops from the land to the sea. Rivers discharging into the ocean result in spectacular falls. This type of geology, just like we have shown in cases where the water budget on earth falls below 0.95 earth ocean mass, implies that almost no aquatic species on such a planet can evolve toward an amphibian type of creature. If one really stretches one's imagination, a flying fish type of creature may eventually develop flight and colonize the land, but such probability is astronomically low compares to transition from fish to amphibian where shorelines, lakes, and rivers naturally extend into the ocean. Furthermore, some of the greatest biological diversity is observed within the continental shelf, where the depth of the ocean is no more than a few hundred meters. Within this layer of the ocean, a complete ecosystem comprising food chains and symbiotic relationships develop and co-exist between the top layers of the water (photosynthesis) up to the bottom floor of the sea. Without the existence of continental shelf sea, it is hard to imagine the appearance of many multicellular life forms such as corals, crabs, lobsters, and fish which either directly or indirectly consumes sunlight as well as requiring anchoring on the ground, therefore, it is hard to imagine complex multicellular life (such as flying fish) to evolve at all. One can even stretch one's imagination even further, assume such planet had overcome the insurmountable barriers of high rise of the continents and conquered the land in an astronomically small chance. It is still hard to imagine such species to engage in inter-continental trade and undergoing through an Age of Exploration, which is one of the necessary recipes for the ushering into a technological industrial civilization. An intelligent species on such a planet will know the true meaning of the edge of the world not available in our dictionary.

3.11 Plate Tectonics

The debates have been on whether all terrestrial planets undergo plate tectonics. In fact, no other terrestrial planets undergo plate tectonics as observed on earth. Mars, Europa, Io, Enceladus drives internal heat from the core to the surface by through pipe volcano. Venus undergoes entire planetary resurface. This observation prompts many to propose the initiation of plate tectonics is probably unique to earth, and the number of possible planets that gave rise to the intelligent tool using species is small. However, studies done on the possibility of tectonic activity on super earth indicates that the presence of water on the terrestrial planets, essentially acting as a lubricant, enables tectonic subduction on plate boundaries.[53] Therefore, plate

tectonics should be universal on terrestrial planets within the habitable zone with the presence of considerable depth of ocean and plate tectonics is not a selection criteria for filtering the number of potentially habitable planets.

Although plate tectonics may be universal, one has to further investigate the level of intensity of the tectonic movement. If the geologic activity is intense with volcanism and earthquake, it is not conducive gives to the emergence of intelligent life. The model for tectonic movements, though very intricate and complex, can be simplified into a toy model based on two assumptions. First, the rate of tectonic plate creation is directly proportional to the heat release per unit area of the planet. That is, the greater the heat flux, the more active the plate tectonics. The formation of new crusts is a consequence by the convective magma inside the planet as a form of heat dissipation from the planet's original formation in the form of potential energy and radioactive elemental decay such as uranium and thorium. It is, then, no surprise that the young earth billions of years ago had more active geologic activities. Secondly, the rate of tectonic subduction is directly proportional to the gravity acted upon the plates. The oceanic mafic plate emerges from the site of its creation and gradually over the course of millions of years consolidated in density and increased in weight and sloped toward the subduction zone. The subduction zone, such as the Mariana trench, are some of the deepest places on earth, pulls the plate into the mantle upon its own weight, thereby completing the recycling of the oceanic plates. It is no surprise that planets with a higher mass also have a greater surface gravity and a greater surface heat flux. A third factor involving the thickness of the crust is sometimes also considered, but for the simplicity of our argument (a lack of data to correlate crust thickness based on the mass, composition, or the formation condition of the planet. Mars has a thicker crust with 10% earth mass, and Venus has comparable crust thickness to earth with comparable density, yet all three planets have comparable composition), we shall assume that the crust thickness is equivalent in all terrestrial planets of different masses. Finally, the presence of water as a lubricating agent is probably essential for carrying persistent tectonic activities.[53] The question becomes, given an increase in mass of a terrestrial planet, how will the speed of tectonic movement change and by how much. If we assume that all terrestrial planets have a similar density to earth,[83] then the following graph can be used to predict the surface gravity and surface area on terrestrial planets of other masses.

$$r_0 = \left(\frac{3}{4}x\right)^{\frac{1}{3}} \quad (3.94)$$

$$y_{plate} = \frac{1}{0.3029} \frac{\frac{4}{3}\pi r_0^3}{4\pi r_0^2} \quad (3.95)$$

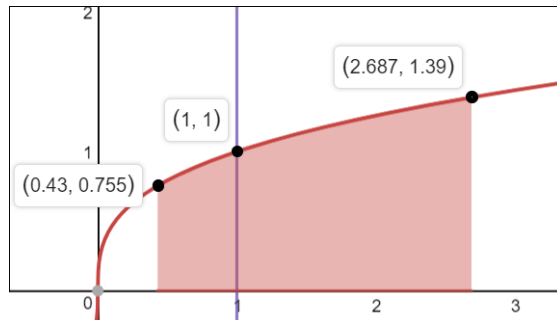


Figure 3.31: Geological intensity vs. terrestrial planet mass

The relationship of gravity and heat flux increase is plotted. One can quickly see, from the graph, that tectonics activity does not significantly increase as the mass of the planet increases. Based on the stellar to planetary mass ratio, the maximum attainable super earth size is about 2.687 earth mass. The surface gravity grows relatively slow compares to the increase in mass, that is, a terrestrial planet at the 2.687 earth mass will have a surface gravity at only 1.39 times that of the earth. Furthermore, the surface area will also be 1.39 times that of the earth, as a consequence, one can see that radiative convection on this planet will also create new crusts at 1.39 times the speed observed on earth while engulfing old crusts also at 1.39 times the speed on earth. As a result, for a terrestrial planet, put on a limit of no more than 2.687 earth masses, the plate tectonic movement cannot exceed more than 1.39 times the speed on earth. At this mass range, the speed of tectonic activity is moderately higher than earth. This does justify for the slight differential speed of evolution on different planets (we talked about how species can evolve quickly based on molecular biology but is held in check by the pace of geologic changes)⁴ but not sufficient enough to serve as a filter for limiting the number of habitable planets conducive to intelligent life.

⁴See Chapter 4 Section 4.5

4 Evolution

4.1 Water vs. Other Solvents

Some argue that water as the only solvent for life is probably too limiting, and by including other types of hydrocarbons such as ammonia and methane into consideration is also important. Upon closer examination, ammonia's molecules are composed of nitrogen and hydrogen. Even if nitrogen rarely interacts with other types of atoms, only 960 atoms out of every 1 million atoms in the Milky Way composed of nitrogen. Therefore, the maximum upper bound of ammonia creation is 960 pairs of ammonia molecules out of 1 million atoms. This directly pales in number with water with 10,112 pairs of molecules out of 1 million atoms at its upper bound. Ammonia makes up only 9.49% of the water budget in the galaxy at the most.

Furthermore, ammonia's melting and boiling points are between 195 K and 240 K. Chemical reactions generally proceed more slowly at a lower temperature. Therefore, ammonia-based life, if it exists, might metabolize more slowly and evolve more slowly than life on Earth. Ammonia is also flammable in oxygen, and could not exist sustainably in an environment suitable for aerobic metabolism. Ammonia could be a liquid at Earth-like temperatures, but at much higher pressures; for example, at 60 atm, ammonia melts at 196 K and boils at 371 K. However, the higher atmospheric pressure will guarantee more stabilizing climate and minimize the chance of fluctuating weather patterns. We shown in our discussion regarding the emergence of intelligent species in many ways, one kind of adaptation of intelligent life is its quick responses to ice age uncertainties.⁵

Methane, on the other hand, composed of hydrogen and carbon atoms. The maximum upper bound of methane creation is 4,472 pairs of molecules per 1 million atoms (carbon ready to bind with any other atoms freely). However, it has an even lower melting point at 90 K and boiling point at 112 K, and evolution will proceed even slower than ammonia-based life. With even higher atmospheric pressure, methane may be available at room temperature but as we have shown earlier thick atmosphere minimized the chance of ice ages (in addition to the fact methane is a greenhouse gas). Moreover, it is extremely flammable and may form explosive mixtures with air. It is violently reactive with oxidizers, halogen, and some halogen-containing compounds.

All other hydrogen chalcogenides such as hydrosulfuric acid (H_2S), hydroselenic acid (H_2Se), hydrotelluric acid (H_2Te), and hydropolonic acid (H_2Po) suffer the same handicaps listed earlier, and they are far rarer because sulfur, selenium, tellurium, and polonium are all rarer than nitrogen and carbon. At the same time, their boiling and melting points are all lower than water. Hydropolonic acid is the closest in terms of staying liquid at room temperature at 1 Atm, but it the rarest of all and very unstable chemically and tends to decompose into elemental polonium and hydrogen; like all polonium compounds, it is highly radioactive.

⁵See Chapter 5

Property	H ₂ O	H ₂ S	H ₂ Se	H ₂ Te	H ₂ Po
Melting point	0.0	-85.6	-65.7	-51	-35.3
Boiling point	100.0	-60.3	-41.3	-4	36.1

Table 4.1: Melting and boiling points of the list of hydrogen chalcogenides

In conclusion, if one wants to find all forms of life in all environment, then one should also include ammonia, methane, and other hydrocarbons into their targeted list, otherwise, targeting and selecting water as our filter criteria for finding the number of habitable planets hosting intelligent tool using species is sufficient.

4.2 Biocomplexity Explanation

The evolution of biological complexity is one important outcome of the process of evolution. Evolution has produced some remarkably complex organisms, and the assumption that life evolves toward greater complexity is one of the pillar assumptions in calculating the background evolutionary rate. However, it is well known that natural selection does not dictate the direction in any kind of way. Species are equally likely to evolve toward greater complexity with less offspring or evolve toward lower complexity and multiply faster and produce more offsprings if both opportunities are equally available. Then we confront the dilemma, why do we still see an evolution toward complexity as we observed.

Based on the mathematical model, two types of scenarios are possible to enable evolving toward greater complexity despite the non-directional evolution of life. If evolution possessed an active trend toward complexity (orthogenesis), as was widely believed in the 19th century,[82] then we would expect to see an increase over time in the most common value (the mode) of complexity among organisms.[84] Computer models show that the generation of complex organisms is an inescapable feature of evolution.[38][9] This is sometimes referred to as evolutionary self-organization. Self-organization is the spontaneous internal organization of a system. This process is accompanied by an increase in systemic complexity, resulting in an emergent property that is distinctly different from any of the constituent parts.

However, the idea of increasing production of complexity in evolution can also be explained through a passive process.[84] Assuming unbiased random changes of complexity and the existence of a minimum complexity leads to an increase over time of the average complexity of the biosphere.[62] This involves an increase in variance, but the mode does not change. The trend towards the creation of some organisms with higher complexity over time exists, but it involves increasingly small percentages of living things.

In this hypothesis, any appearance of evolution acting with an intrinsic direction towards increasingly complex organisms is a result of people concentrating on the small number of large, complex organisms that inhabit the right-hand tail of the complexity distribution and ignoring

simpler and much more common organisms. This passive model predicts that the majority of species are microscopic prokaryotes, which is supported by an estimates of 10^6 to 10^9 extant prokaryotes compared to the diversity estimates of 10^6 to $3 \cdot 10^6$, for eukaryotes.[71][85] Consequently, in this view, microscopic life dominates the Earth, and large organisms only appear more diverse due to sampling bias.

Nevertheless, a passive process can still over time lead to more complex organisms as a consequence of existing biological niches being occupied so only species with increasing novelty in addition to existing faculty can survive, and novelty and faculty lead to ever increasingly sophisticated responses between the Red Queen's predator and prey mechanism.

4.3 Probability on the Emergence of Prokaryotes from Amino Acids

Life emerged quickly as the condition of the earth becomes favorable. Just like many other significant milestones achieved later such as the Great Oxygenation Event (post the emergence of continental plates and shelf seas), the appearance of eukaryotes (post the Great Oxygenation event), and the emergence of complex multicellular organisms (post high oxygen build up in the atmosphere.). Life is very opportunistic and taking advantage of new niches. The earliest evidence of life occurred just 0.2 Gyr after the formation of the ocean, pointing toward and confirming the belief that life is easy to generate.[26]

But just how hard or how big a jump is it from generating an organic molecule to that of the first cell is the key question. We need to quantify the difficulty of abiogenesis. In order to quantify this jump, we count the number of atoms in each successive stage of evolution. We count the first amino acid (10 atoms), the first prokaryote ($9 \cdot 10^{10}$ atoms), the first eukaryote ($1 \cdot 10^{14}$ atoms), the start of multicellular life ($1 \cdot 10^{14}$ atoms), and the first multicellular fish ($7 \cdot 10^{27}$ atoms). We specify their emergence at 4.364 Gya, 3.95 Gya, 2.15 Gya, 0.85 Gya, and 0.45 Gya respectively. Counting the number of atoms is a simple and elegant way to capture the complexity of the organism obtained at each stage. Based on Galileo's squared cubed law, organisms not only follow the constraints and selection through natural selection but also subject to the law of physics. Organisms experience a totally different world as their size grows when certain forces dominant over some others, such as the strong capillary action at the microscopic level and gravity at the macroscopic level. A fish is not merely macroscopic-sized eukaryotic cell. As a result, organisms cannot simply just grow in size using their existing surviving strategy. Instead, it has to increase and alter their own information storage and protein creation in order to create new intercommunication protocol and cooperation to grow in size. It is exactly one observed from the transition of prokaryotes to eukaryotes (generally now believed to be the merging of archeon and bacteria) and the subsequent multicellular life forms which are only based on the innovation achieved at eukaryote level. From 3.95 Gya to 2.15 Gya, the number of atoms increased by a factor of 1.48 per 100 Myr. This is a relatively

stable period of growth,

$$T_{\text{prokaryote2eukaryote}} = 9 \times 10^{10} (1.48)^{18}$$

$$= 1.0446080939 \times 10^{14} \text{ atoms}$$

followed by a period of stasis from 2.15 Gya to 0.85 Gya. From 0.85 Gya to 0.45 Gya, the number of atoms increased by a factor of 1,200 per 100 myr.

$$T_{\text{eukaryote2fish}} = 1 \times 10^{14} (1,200)^{4.5} \quad (4.1)$$

$$= 7.1831611091 \times 10^{27} \text{ atoms}$$

This is what many generally termed the Cambrian explosion. It shows that evolution, under the right conditions (possibly adequate free oxygen and nitrogen) can accelerate fast. If one assumes that life at the earliest stage also followed a similar track of growth due to favorable conditions, then life could have evolved from simple amino acids to that of the prokaryotes in 0.424 Gyr starting at 4.264Gya.

$$T_{\text{amioacid2life}} = 10^1 (1,200)^{3.235} \quad (4.2)$$

$$= 9.1443182195 \times 10^{10} \text{ atoms}$$

If the increase factor is decreased to 223, or 18.6% the speed observed during the Cambrian explosion, then, we can push the start of evolution from simple amino acids to 4.364 Gya when earth's ocean just formed.

$$T_{\text{amioacid2life}} = 10^1 (223)^{4.24} \quad (4.3)$$

$$= 9.0534189785 \times 10^{10} \text{ atoms}$$

To further strengthen our argument, one can go a step closer. The viroid, supposedly the smallest pathogen known with a single-stranded RNA without a protein coat, represents the most plausible RNAs capable of performing crucial steps in abiogenesis, the evolution of life from inanimate matter. Many believed that viroid represents the living fossils of a class of species evolved during the RNA world of life evolutionary history which predates the current DNA world. Since viroids are capable of replication, it is then subject to natural selection. *Avocado sunblotch viroid* and *Coconut cadanf-casanf viroid*, two of the smallest of the viroids, consist only 246 nucleotides. Assuming each nucleotide contains 35 atoms, then the smallest structure subject to natural selection contains just 8,610 atoms. Though evolution itself is

directionless, the passive growth in complexity is nevertheless inevitable, and it will take only 228 Myr to evolve toward the complexity of prokaryotes if the rate of growth comparable to that of Cambrian explosion.

$$T_{viroid2life} = 8,610^1 (1,200)^{2.28} \quad (4.4)$$

$$= 9.0268534635 \times 10^{10} \text{ atoms}$$

In an RNA world or viroid world, different sets of RNA strands would have had different replication outputs, which would have increased or decreased their frequency in the population, i.e. natural selection. As the fittest sets of RNA molecules expanded their numbers, novel catalytic properties added by mutation, which benefitted their persistence and expansion, could accumulate in the population. Such an autocatalytic set of ribozymes, capable of self-replication in about an hour, has been identified. It was produced by molecular competition (in vitro evolution) of candidate enzyme mixtures.

It is possible that such a quick transition occurred because the available free energy in the early ocean limits the size of species. Nevertheless, the free energy is abundant enough to enable the growth from simple viroids to the prokaryotes.

We still have to show the probability of the aggregation from simple amino acids with 10 atoms to that of the smallest viroid with 8,610 atoms. Since this stage of evolution, is the earliest, and possibly does not or at the best only partially replicate its own data, the rule of natural selection is not applicable. Nucleotides, the basic unit of viroids, are the fundamental molecules that combine in series to form RNA. They consist of a nitrogenous base attached to a sugar-phosphate backbone. RNA is made of long stretches of specific nucleotides arranged so that their sequence of bases carries information.

The RNA world hypothesis holds that in the primordial soup (or sandwich), there existed free-floating nucleotides. These nucleotides regularly formed bonds with one another, which often broke because the change in energy was so low. However, certain sequences of base pairs have catalytic properties that lower the energy of their chain being created, enabling them to stay together for longer periods of time. As each chain grew longer, it attracted more matching nucleotides faster, causing chains to now form faster than they were breaking down. Using this hypothesis, we can derive the probability of abiogenesis. Assuming the most dominant bonding occurred between the pairing of two followed by the pairing of three and then the pairing of four..etc, then, the number of steps leading to the simplest viroid from amino acids requires $\log_n 861$ steps ($\frac{8610 \text{ atoms}}{10 \text{ atoms}} = 861$ nucleotides), where n is the pairing of two, three, or more chains of the molecular nucleotides. Pairing of fewer nucleotides leads to greater number of steps to the smallest viroid, but pairing between fewer nucleotides also comes with greater frequency. We further assumed that nucleotides can compose or groups of nucleotides can compose any number of atoms greater than 10. However, the occurrence frequency of pairing lowers in a

geometric way. So that the pairing between two nucleotides is 50%, pairing between three nucleotides is 25%.

Pairing number	Number of steps to viroid	Occurrence Frequency
2	9.74987	0.500
3	6.15148	0.222
4	4.87493	0.125
5	4.19904	0.040
6	3.77176	0.027

Table 4.2: The chance of pairing between nucleotides

The occurrence frequency distribution is described as:

$$\frac{2}{x^2} \tag{4.5}$$

and its integration up to the pairing between infinite number of nucleotides is 100%:

$$2 \int_2^{\infty} \frac{1}{x^2} dx = 1 \tag{4.6}$$

Then, in the simplest model, one can compute that:

$$2 \cdot \int_2^{\infty} \frac{1}{x^2} \frac{\log 861}{\log x} dx \tag{4.7}$$

$$= 5.18115739293$$

It shows that the expected number of steps leading to the simplest viroid requires, on average, 5.18 steps. If the chance of each step of successful bonding between the pairing of two, three, four up to n pairs is 50 percent, the total sum chance of all bonding leading to the smallest viroid is $\left(\frac{1}{2}\right)^{5.18} = 2.756\%$. We can call this the lower bound estimate because if one further assumes that considerable time between each step of aggregations, then, each step may have 100 percent chance leading to a longer chain. This not unreasonable since pairing between 2 nucleotides up to 7 nucleotides, just to illustrate, requires on average 5 steps of aggregation to reach the complexity threshold of viroids. Assuming 196 Myr time frame from the simplest amino acid to the viroids, it gives each step 39.38 Myr time to consolidate their bonds, that is, the building and creation of ever more complex molecules can be spaced out in a long time frame to guarantee its success. The primordial condition on earth is very different from that of today. Atmosphere composed of CO₂ and methane with intense atmospheric pressure, high temperature, high rate of volcanism and the recycling of crusts, and the ubiquity of hydrothermal vents. If life emerged around hydrothermal vents, then the energy intensity of early earth allowed a high frequency

of experiments at every local level which would take billions of years to produce the first viroid at today's rate. Therefore, the emergence of life can be an inevitable consequence of any early earth's chemical experiments and can only occur on a young, geologically active planet. In a sense, it is not that life is easy to produce, rather it depends on the frequency of nature's experiment.

If one takes the upper bound of total sum chance of all bonding leading to the smallest viroid is 100%, then *the median value of life emergence is 22.76%*.

Nevertheless, the true rate of life emergence can still lower than 22.76 percent based on various factors beyond the scope of this paper. We shall denote the additional probability on the emergence of life is an factor x in our final calculation to show the lower and upper bound of our model. The calculation does show, however, that life is not extremely implausible to start with.

4.4 Probability on the Emergence of Eukaryotes, Sex, and Multicellularity

From our mathematical model on the finding the average speed of evolutionary change⁶, we find that biological system can form new function or species relatively quickly and such changes and pace is largely driven by geologic changes. This can be generalized to simpler and earlier evolutionary times in the earth's past. *The emergence of Eukaryotes, for example, tightly followed the onset of the Great Oxygenation Event.* The Great Oxygenation Event, in turn, is driven by the emergence of continental plates for the first time in earth's geologic history as finally the earth has cooled enough. The process of Earth's increase in atmospheric oxygen content is theorized to have started with the continent-continent collision of huge land masses forming supercontinents, and therefore possibly the creation of the first supercontinent mountain ranges. These super mountains would have eroded, and the mass amounts of nutrients, including iron and phosphorus, would have washed into the oceans, just as we see happening today. The oceans would then be rich in nutrients essential to photosynthetic organisms,[70] which would then be able to respire mass amounts of oxygen. All eukaryotic cells use mitochondrion to process oxygen to obtain energy. Consensus agrees that the first proto-eukaryotic cell formed as archaea and prokaryotes merged into each other and to perform one specific function for the benefit of the whole. Merging also occurred in plant cell lineage with the addition of chloroplast at around the same time. This shows that symbiotic merger is a common occurrence. Mitochondrion bacteria utilizing oxygen must have formed only possible after the onset of free oxygen in the ocean. Soon as Mitochondrion bacteria formed and as it propagates through the earth's ocean, merging process logically follows. *The onset of Cambrian explosion, again, is a consequence of a significant rise in oxygen level.*[32] By Cambrian, cyanobacteria for the

⁶(Chapter 4, Section 4.5 "Speed of multicellular evolution")

first time have produced enough oxygen as its waste product not only filled the ocean's oxygen sink as well as the land's. As a result, the formation of ozone layer prevented the incoming of ultra-violet radiation from reaching the surface of the earth, and enough free oxygen available in the ocean and on the land reaching levels similar to that of today. The overabundance of oxygen provides enough fuel for the flourishing diversification of the Cambrian fauna.

Another major biological breakthrough, the emergence of sexual reproduction, is rather peculiar, it is first observed between the emergence of the eukaryotic cell (2.1 Gyr ago) and Cambrian explosion (0.58 Gyr ago) around 1.5 Gyr ago, in a period called the boring billion. When the supercontinent Rodinia and Columbia were maintained, and the climatic condition is generally stable, and no major biochemical and geologic changes occurred on earth. The viral origin of sexual reproduction posits that the cell nucleus of eukaryotic life forms evolved from a large DNA virus, (possibly a pox-like virus such as the lysogenic virus is a likely ancestor because of its fundamental similarities with eukaryotic nuclei. These include a double-stranded DNA genome, a linear chromosome with short telomeric repeats, a complex membrane-bound capsid, the ability to produce capped mRNA, and the ability to export the capped mRNA across the viral membrane into the cytoplasm. The presence of a lysogenic pox-like virus ancestor explains the development of meiotic division, an essential component of sexual reproduction.) in a form of endosymbiosis within a methanogenic archaeon. The virus later evolved into the eukaryotic nucleus by acquiring genes from the host genome and eventually usurping its role. Since it is estimated that viruses kill approximately 20% of marine microorganism' biomass daily and that there are 10 to 15 times as many viruses in the oceans as there are bacteria and archaea, they infect and destroy bacteria in aquatic microbial communities. They are one of the most important mechanisms of carbon recycling and nutrient cycling in marine environments. Then, *the chance of evolution of sexual reproduction is high*. The meiotic division arose because of the evolutionary pressures placed on the virus as a result of its inability to enter into the lytic cycle. This selective pressure resulted in the development of processes allowing the viruses to spread horizontally throughout the population. The outcome of this selection was cell-to-cell fusion. (This is distinct from the conjugation methods used by bacterial plasmids under evolutionary pressure, with important consequences.)[14] The possibility of this kind of fusion is supported by the presence of fusion proteins in the envelopes of the poxviruses that allow them to fuse with host membranes. These proteins could have been transferred to the cell membrane during viral reproduction, enabling cell-to-cell fusion between the virus-host and an uninfected cell. The theory proposes meiosis originated from the fusion between two cells infected with related but different viruses which recognized each other as uninfected. After the fusion of the two cells, incompatibilities between the two viruses result in a meiotic-like cell division.[15]

If the viral origin of sex is valid, then nature is constantly experimenting sexual reproduction as an alternative to binary fission. Therefore, we have found a congenit and reasonable mechanism for the emergence of sex. However, it is still likely that the evolution of sexual reproduction, though emerged, only reached its full potential and glories as a successful survival strategy as a

consequence of environmental resource pressure from the competition of prokaryotes. That is, the maintenance of such mechanism and its success requires investigation of organism's living environment. The fossil evidence of Stromatolites indicates that prokaryotes reached its greatest extent around 12 Gyr before its sharp decline. Sexual reproduction has been observed, indeed, related to environmental stress. Animals such as Hydra are capable of both sexual and asexual reproduction, depending on the environmental conditions. When resources and food are readily available, hydra reproduces by asexual reproduction in the form of binary fission. When food and environmental condition is harsh, it produces sperms and egg cell which falls to the bottom of the sea floor and gave to the birth of new hydra once the environmental condition becomes suitable again. Such mechanism may explain the maintenance of sexual reproduction. After the great oxygenation event, earth contains enough free oxygen making the evolution of eukaryotes possible but not enough to fuel its explosive growth. As a result, prokaryotes continue to flourish. As prokaryotes continue to flourish and compete for nutrients with eukaryotes, energy-hungry eukaryotes face a crisis. Eukaryotes then well adapt the strategy of sexual reproduction, which carried several advantages over asexual reproduction.

First, by sacrificing itself and disperses its own genetic material into the surrounding, it is able to preserve itself from intense resource competition with very little energy consumption and able to wait until the environmental condition becomes more suitable for its re-emergence. Secondly, sexual reproduction enables the faster emergence of new traits and genotypes, allows eukaryotes to diversify and enter new niches. In what termed as the Hill-Roberson Effect, the benefit of sexual reproduction becomes self-evident. In a population of finite size which is subject to natural selection, random linkage disequilibria will occur. These can be caused by genetic drift or by mutation, and they will tend to slow down the process of evolution by natural selection.[45] This is most easily seen by considering the case of disequilibria caused by mutation:

Consider a population of individuals whose genome has only two genes, a and b. If an advantageous mutant (A) of gene a arises in a given individual, that individual's genes will through natural selection become more frequent in the population over time. However, if a separate advantageous mutant (B) of gene b arises before A has gone to fixation, and happens to arise in an individual who does not carry A, then individuals carrying B and individuals carrying A will compete. If recombination is present, then individuals carrying both A and B (of genotype AB) will eventually arise. Provided there are no adverse epistatic effects of carrying both, individuals of genotype AB will have a greater selective advantage than aB or Ab individuals, and AB will hence go to fixation. However, if there is no recombination, AB individuals can only occur if the latter mutation (B) happens to occur in an Ab individual. The chance of this happening depends on the frequency of new mutations, and on the size of the population, but is in general unlikely unless A is already fixed, or nearly fixed. Hence one should expect the time between the A mutation arising and the population becoming fixed for AB to be much longer in the absence of recombination. Hence recombination allows evolution to progress faster.[45]

If these assumptions hold, it implies that the appearance of sexual reproduction, though partially attributed to environmental stress related to resource competition with existing prokaryotes, is an inevitable consequence of the evolution of more complex singled cell organism, especially as a logical consequence of viral origin of the eukaryotic cell nucleus. (Nature was trying repeatedly to create sexual recombination at the cellular level) The evolution of sexual reproduction, then, unlike the appearance of more complex eukaryotes and the appearance of complex multicellular life, does not require significant geologic and biochemical environmental changes as sexual reproduction itself does not consume more energy than the survival requirements of eukaryotes. Though with more stressful environmental conditions, it can appear faster in geological history as a successful survival strategy. It does not have to wait for 0.8 Gyr since the appearance of the first eukaryotes. Nevertheless, eukaryotic cells can resort to both asexual and sexual reproduction, and larger multicellular eukaryotes exclusively reproduces through sexual means as a means of cost control and adaptation to environmental uncertainties given the long lifespan of multicellular species and the amount of resources needed to maintain the body.

By elucidating the causes of the timing of the appearance of each major evolutionary changes, Several interesting predictions can be made. First of all, the appearance of eukaryotes is a consequence of cyanobacteria filling up the ocean's oxygen sinks. The filling of earth's oxygen sink, in turn, is contributed to the emergence of continental platforms from the ocean and the creation of the shelf sea.[70] As a result, every other condition being equal, a planet with lower sea levels (with a lower ocean surface to ocean volume ratio since nearly all cyanobacteria thrive near the surface of the ocean to convert sunlight) can lead to the appearance of eukaryotes much earlier than that we found on earth. Secondly, the diversification of multicellular eukaryotic organisms is a consequence of significant oxygen buildup which filled not only the ocean's oxygen sinks but as well as the land's. Therefore, a planet with greater portions of land masses (less surface covered by oceans) will take much longer time than what we observed on earth to evolve from eukaryotic cell to multicellular organisms. The reverse is also true, where a planet with higher sea level or entirely covered by the ocean is likely to take even greater delay than observed on earth to evolved oxygen-utilizing eukaryotes but quickly transitioned toward multicellular life forms. To be concise, *the proportion of ocean and land coverage of a planet determines the timing of the appearance of eukaryotes and multicellular life forms.* Thirdly, the size of the planet is a non-determining factor in which organisms evolve assuming the bacteria colony size on all habitable planets is comparable within a magnitude of difference. On smaller planets where the ocean surface area to land area ratio are similar to earth, fewer bacteria using sunlight as their energy source and produce oxygen as its waste to fill up smaller oxygen sinks, leading to a similar interval between the timing of each major evolutionary change. For super earths, there are more thriving bacteria producing more oxygen, but there are also more oxygen sinks in both ocean and exposed land to fill, leading to a similar interval between the timing of each major changes.

4.5 Speed of Multicellular Evolution

With the number of bases known in the human genome (3 billion base pairs) and the mutation rate of eukaryotes, one can calculate the theoretical upper bound on how fast human can evolve. In general, the mutation rate in unicellular eukaryotes and bacteria is roughly 0.003 mutations per genome per cell generation.[33][51][11] This means that a human genome accumulates around 64 new mutations per generation because each full generation involves a number of cell divisions to generate gametes.[33] Human mitochondrial DNA has been estimated to have mutation rates of $3 \times$ or 2.7×10^{-5} per base per 20-year generation [86] these rates are considered to be significantly higher than the rates of human genomic mutation at 2.5×10^{-8} per base per generation.[68] Using data available from whole genome sequencing, the human genome mutation rate is similarly estimated to be 1.1×10^{-8} per site per generation.[80]

1.1×10^{-8} per site per generation \cdot 3 billion base pairs = 33 base pairs. This implies that each child on average differs from their parents by 33 base pairs. If human lineages were limited to very few individuals for a very long period of time and no mutation repeats at the same base, $\frac{3 \text{ billion base pairs}}{33 \text{ base pairs}} = 90,909,090$ generations (1.818 billion years). Mutations would have turned every base pair once. However, Homo genus population from millions of years ago numbered 10,000 to 100,000 at least. With these many individuals per generation, mutations would have mutated every base within the population once only 181,818 years to 18,181 years! If bottleneck existed and only the most adaptable human survived, then, the emergence of Homo sapiens from ape-like creature can happen very quickly. Much quicker than the fossil record suggested. To make the argument even more convincing, the key genes for the development of the thumb, brain muscle, language development are now identified as few as just 100 different genes. Furthermore, many genes altered in Homo Sapiens compares to Chimpanzees are master switch genes, that controls other switch genes, this implies that by mutating certain key bases, an escalating number of bases are affected.

This calculation confirms the punctuated equilibrium model of evolution, where new species appeared suddenly within rock strata. This is also confirmed by adaptation of black and white moth in Britain during the industrial revolution, the domestication history of agricultural plants such as maize and animals such as pet goldfish, cats, and dogs. Then, it is certain that animal species can easily alter its morphology and form within a very short timescale but why is it not observed in nature? Does nature set a speed limit on how fast species should evolve or is it an interplay between nature and species themselves? *This is an important issue to address and resolve since by elucidating the mechanism and come forth with explanation with observed stasis of animal form in nature and its theoretical maximum limit of rapid evolution potential, we truly confirm the forces and factors shaping the evolutionary rate of speciation and the background evolutionary rate.* We use such measure to compute our years ahead against this background evolutionary rate and closest living arising extraterrestrial industrial civilization.

Stabilizing selection is occurring at many different levels. At the physical level, the square

cubed law and gravity applies to all biological species.[35] An animal can only be of a certain size while roaming on land and for arboreal species of primate living on trees must be even smaller, and birds which have to adapt to an aerial lifestyle have to be smaller still. As a result, nature's physical law places constraints on biological creatures which limit their evolutionary experiments into any random direction.

Primarily, ecological constraints set the limit on how fast evolution changes. Since breaking and rejoining continents and mountain creation occurs slowly over geologic timescale, allopatric, peripatric, and parapatric speciations, three of the four primary drivers of speciation condition can only occur over geologic timescale as well. As a result, individuals with unique mutations which are even beneficial if it underwent allopatric, peripatric, and parapatric speciations are not able to persist in a given population due to genetic recombination, genetic drift. Secondly, the climate changes gradually over geologic timescale, except those during the ice ages. As a result, a species suited well to a given climate and feeds on specific food will continue to survive and thrive in such climate, which perpetuates in geologic timescale. Any deviations do not confer any immediate benefit for such species, and such deviation is then not selected for by natural selection.

There also exists for the case that sexual selection favors those of its own species that conform to the norm. By choosing a devious individual, a partner risk itself in making the wrong decision at the cost of its own gene. This is demonstrated in *Homo sapiens* as well in which both sexes prefer to mate with the healthy, handsome, pretty and intelligent individuals of the opposite sex, thereby maintaining the uniformity of the gene pool. Therefore, devious members of the species do not even have an equal chance at interbreeding, further contributing their removal from a population's gene pool.

Secondly, a majority of the mutations are harmful, that is, newborn species tend to develop into different types of congenital symptoms that either succumb to such problem prior to birth or die shortly after birth. As a result, many paths of nature's experiment lead to dead ends. Semi-harmful mutations also exist. Newborns with extra teeth, two-toed feet, and six-toe feet have been reported.

Thirdly, with the absence of bottlenecks and isolated habitat scenarios, a large population of a given species breeds randomly with each other and remain constant in number from generation to generation. The Hardy-Weinberg principle states that within sufficiently large populations, the allele frequencies remain constant from one generation to the next unless the equilibrium is disturbed by migration(gene flow), genetic mutations, natural selection, mate choice, genetic drift, and meiotic drive. Mathematically it can be shown that the multinomial expansions for n allele frequencies at time iteration $t+1 =$ time iteration t when $t > 0$. Below is the mathematical proof for 2 alleles frequencies with binomial expansion.

$$f_t(A) = f_t(AA) + \frac{1}{2}f_t(Aa) \quad (4.8)$$

$$f_t(a) = f_t(aa) + \frac{1}{2}f_t(Aa) \quad (4.9)$$

$$f_1(AA) = p^2 = f_0(A)^2 \quad (4.10)$$

$$f_1(Aa) = pq + qp = 2pq = 2f_0(A)f_0(a) \quad (4.11)$$

$$f_1(aa) = q^2 = f_0(a)^2 \quad (4.12)$$

$$f_1(A) = f_1(AA) + \frac{1}{2}f_1(Aa) = p^2 + pq = p(p + q) = p = f_0(A) \quad (4.13)$$

$$f_1(a) = f_1(aa) + \frac{1}{2}f_1(Aa) = q^2 + pq = q(p + q) = q = f_0(a) \quad (4.14)$$

$$\begin{aligned} [f_{t+1}(AA), f_{t+1}(Aa), f_{t+1}(aa)] = \\ f_t(AA)f_t(AA) [1, 0, 0] + 2f_t(AA)f_t(Aa) \left[\frac{1}{2}, \frac{1}{2}, 0\right] + 2f_t(AA)f_t(aa) [0, 1, 0] \\ f_t(Aa)f_t(Aa) \left[\frac{1}{4}, \frac{1}{2}, \frac{1}{4}\right] + 2f_t(Aa)f_t(aa) \left[0, \frac{1}{2}, \frac{1}{2}\right] + f_t(aa)f_t(aa) [0, 0, 1] \end{aligned} \quad (4.15)$$

$$\begin{aligned} = \left[\left(f_t(AA) + \frac{1}{2}f_t(Aa)\right)^2, 2 \left(f_t(AA) + \frac{1}{2}f_t(Aa)\right) \left(f_t(aa) + \frac{1}{2}f_t(Aa)\right), \left(f_t(aa) + \frac{1}{2}f_t(Aa)\right)^2 \right] \\ = [f_t(A)^2, 2f_t(A)f_t(a), f_t(a)^2] \end{aligned} \quad (4.16)$$

Through genetic recombination, new arising mutation is quickly diluted. The law of large numbers is applicable, and only the mean behavior and morphology is maintained. By applying the Hardy-Weinberg Principle, one can also conclude that the genotypes within a given population stabilize within two generations of interbreeding and mixing.

Furthermore, genetic drift will quickly eliminate new arising mutations. When the allele frequency is very small, drift overpowers selection in large populations. For example, while disadvantageous mutations are usually eliminated quickly in large populations, new advantageous mutations are almost as vulnerable to lose through genetic drift as are neutral mutations. Not until the allele frequency for the advantageous mutation reaches a certain threshold will genetic drift have no effect.[23] The above statement can be stated in the following mathematical equation:

$$T_{fixed} = \ln \left(\frac{-10 \cdot N_e (1 - p) \ln (1 - p)}{p} \right) \quad (4.17)$$

where T is the number of generations, N_e is the effective population size, and p is the initial frequency for the given allele. The result is the number of generations expected to pass before

fixation occurs for a given allele in a population with given size (N_e) and allele frequency (p). If one plots the graph, one can quickly see that as the new arising allele has a very low frequency is equivalent of stating that the dominant allele has a very high frequency, which leads to the removal of the low-frequency alleles in a very short period of time.

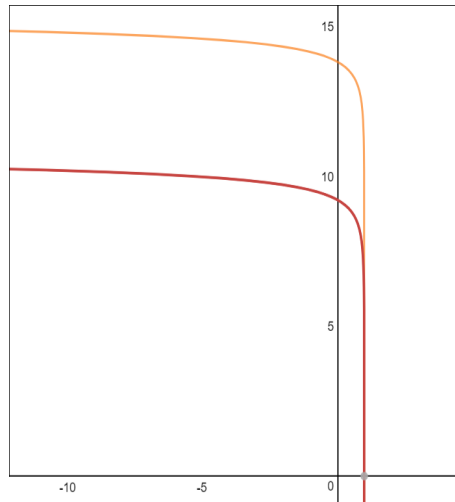


Figure 4.1: Allele frequency between 0 and 1 and expected fixations in generations for $n=10$ and $n=1000$

Therefore, given the large sampling size, beneficial mutations occur much more frequent in a large population but quickly diluted and drifted and selected away. Beneficial mutations occur much less likely in a small population, but it is likely to remain and fixed once it emerges. In the face of a bottleneck, beneficial mutations arising from a large population are selected by natural selection in the remaining surviving population, which generally diluted away in a pre-crisis large population, to become dominant and fixed in a given population thereafter.

We will illustrate this fact by the calculation taking punctuated equilibrium into account. Homo sapiens and Chimpanzee differs by 40 million base pairs. 35 million single nucleotide changes and 5 million insertion/deletion events are recorded. Therefore, one needs to flip $4 \cdot 10^7$ changes in order to turn an ape into a man. Each generation mutate by at most 33 random sites. We further assume that genetic drift plays minimal role so that new beneficial and harmful mutations are equally likely to be contributed to the gene pool. This implies that, on average, each individual flip 0.44 sites that are related to the evolution toward Homo sapiens.

$$\frac{4 \cdot 10^7}{3 \cdot 10^9} \cdot 33 = 0.44 \quad (4.18)$$

The rest 32.56 mutations have little to do with evolution toward Homo sapiens and so be labeled as neutral or harmful mutations.

We also assume that on average, 100,000 individuals thrive at any moment. Therefore, the total number of sites tried per generation evolving toward Homo sapiens is $100,000 \cdot 0.44 = 44,000$. Then the number of generation required to turn an ape into a man is 909 generations.

$$\frac{(4 \cdot 10^7)}{0.44 (100,000)} = 909.0909 \quad (4.19)$$

Assuming a generation time of 20 years in the Hominid lineage, the total number of years required to introduce 40 million base pairs of change is merely:

$$\frac{4 \cdot 10^7}{1 \cdot 0.44 \cdot 100000} \cdot 20 \quad (4.20)$$

$$= 18,181.8 \text{ Years}$$

Furthermore, the number of generations required to introduce all 40 million beneficial base modifications alone guaranteed the introduction of new non-beneficial mutations at some beneficial site within the entire group, due to high non-beneficial to beneficial mutation ratio (33 to 0.44). In 909 generations, the cumulative chance of beneficial gains mutated is then 50 percent and only 25,279,788 base altered in reality.

$$B_{base} = 100000 \cdot 0.44x \quad (4.21)$$

$$\int_0^{909} \left(\frac{B_{base}}{3 \cdot 10^9} \cdot (1) \cdot 10^5 \cdot 33 \right) dx = 0.4999 \quad (4.22)$$

Simulation shows that in 4,900 generations, the number of beneficial gains can eventually converges to 40 million base pairs despite the introduction of new non-beneficial mutations at some beneficial sites. This implies that it takes 98,000 years to introduce 40 million base pairs.

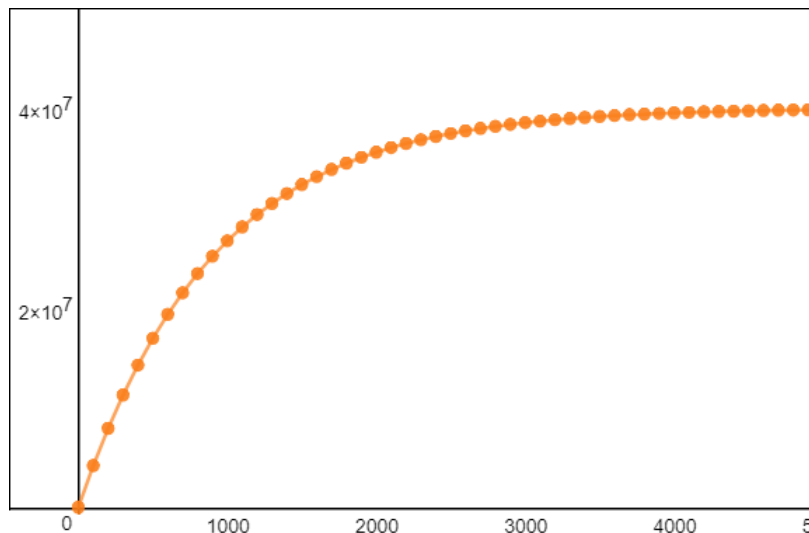


Figure 4.2: Number of generations to introduce 40 million base pairs

However, new allele introduced into a large population takes a long time before its fixation due

to genetic drift. Individuals possessed all 40 million base pair changes will be exceedingly rare within the population through sexual reproduction based on the Hardy-Weinberg principle. For a population of 100,000, one expect fixation to occur in 10^6 generations. With 20 years per generation, it implies that at least 20 million years of accumulated molecular changes by mutation rates required to turn Chimpanzee into Homo sapiens without the presence of directed selection. If one were to assume that 20 million years required after each generation, then it will take $4900 \cdot 2 \cdot 10^7 = 98$ Gyr, 21 times the age of earth. It certainly contradicts our observation because the divergence took place within 6 million years.

This implies that directional natural selection played role in the evolution of Homo sapiens by expediting the process. If the average beneficial mutation per individual is 0.44 per generation and the number of beneficial mutations obtained per generation is probabilistically distributed, then only those survived a directional population bottleneck event can reproduce. We assume that the probablistic distribution is:

$$g_{distr}(x) = \frac{3}{.95x^{1.85}Q_1\sqrt{2\pi}} e^{-\frac{(\ln 0.456x \cdot 9)^2}{2(Q_1)^2}} \quad (4.23)$$

$$Q_1 = 1.26$$

and only top 1% of the original 100,000 population survives. Then, it implies that

$$\frac{\int_{11.5}^{\infty} g_{distr}(x) dx}{\int_0^{\infty} g_{distr}(x) dx} \approx 1\% \quad (4.24)$$

The remaining top 1% population each had at least 11.5 beneficial mutations and a weighted average of 20.96 beneficial mutations toward the directional selection of Homo sapiens.

$$\frac{(\int_{11.5}^{\infty} x g_{distr}(x) dx)}{(\int_{11.5}^{\infty} g_{distr}(x) dx)} = 20.96 \quad (4.25)$$

Now, assuming the population recovery takes place by increasing each generation by 6%, then the total number of years expected for the surviving population to regain its loss after the bottleneck takes:

$$T_{double} = \frac{\log(100)}{\log(1.06)} \cdot 20 \quad (4.26)$$

$$= 1,580.66 \text{ Years}$$

So, a recovery takes place every 1,580 years. Moreover, T_{fixed} takes place in 10,000 years for a population of 1,000. In the fastest possible scenario, the very next bottleneck, directional selection event occurs immediately after its newly introduced genes becomes fixed within the

population and the population recovered from its initial loss. We further assumed that the bottleneck lasted as long as the fixation time and the population remained small (such as during a harsh glacial period, a super volcanic eruption, an extended drought, habitat isolation due to sea level changes). Any mutations that altered the beneficial gain will be removed by directional selection pressure during the bottleneck. Beneficial gains still proceed during the bottleneck period and we assumed the rate is at 0.44 per individual per generation. Since 10,000 years takes 500 generations, $500 \cdot 0.44 = 220$ beneficial mutations are gained per individual in all generations. Then:

$$T_{total} = T_{fixed} + T_{double} \quad (4.27)$$

Since $T_{fixed} > T_{double}$, T_{fixed} dominates. During the recovery phase of 1,580 years, directional selection pressure is removed and mutations are allowed to alter previous beneficial gain. It takes only 79 generations to reach a population of 100,000. The average population size during this period was only 21.5 percent of the normal level. Therefore, the number of beneficial bases altered are negligible.

$$\int_0^{79} \left(\frac{B_{base}}{3 \cdot 10^9} \cdot (0.215) \cdot 10^5 \cdot 33 \right) dx = 0.00081 \quad (4.28)$$

It remains a problem, if the onset of the next bottleneck event is delayed long enough on the order of 10,000 years. Then, new mutations are likely to overwhelm the beneficial gain of the previous round. This is where stabilizing selection comes to aid. During a period of geologic stasis, a stable environment ensure the stability of the gene pool, minimizing alteration on beneficial gains. Furthermore, genetic drift eliminates arising mutations quickly in large populations. Genetic recombination quickly diluted new arising mutation. Therefore, evolution toward human is composed of cycles of directional selection and stabilizing selection. That is, stabilizing selection acts on the population during the recovery phase and in between the bottleneck events.

Then, the fastest time possible to transition from Chimpanzee to Homo sapiens is:

$$\frac{4 \cdot 10^7}{(20.96 + 220) \cdot 1,000} \cdot 11,580 \quad (4.29)$$

$$= 1,922,310 \text{ Years} \quad (4.30)$$

Since $1.92 \text{ Myr} < 6 \text{ Myr}$, the calculation match reality. This also indicates that each bottleneck events do not immediately follow one and another. They are likely spaced out by 24,600 years to match 6 Myr. This speed is still not the theoretically fastest achievable. We assumed that the recovered population followed each directional bottleneck selection event still generates a probabilistic distribution centered on the mean of 0.44 beneficial mutations per individual per generation. However, it is more likely that the recovered population generates a probabilistic

distribution with a higher number of beneficial mutations across all ranges, as they shifted further toward the Homo sapiens' prototype and mutations occur at non-random patterns and tend to occur at selected concentrated sites such as master switch genes. Furthermore, a higher average number of beneficial mutations can also be justified, at least partially, by sexual selection. Sexual selection can be directed by both sexes. An alpha male with more human like traits able to exploit more resources leading to greater bargaining power with females and greater reproductive success. Then, the gene pool shifts toward both a higher number of beneficial mutations and a quicker convergence of its gene's fixation within a given population than random mating. If no alpha male is present at directing faster gene fixation, females can actively choose a selected group of males with enhanced features and fitness to mate with and refuse to mate with the inferior, typical, and average male. A caveat must be raised. This does not imply that sexual selection dominates directional selection. We simply assumed that directional selection, during a bottleneck event, has lifted the constraints placed upon by stabilizing selection so that directed evolutionary change are permitted to take place. The directed evolutionary change can be achieved by either sexual selection (faster), natural selection (slower), or both. When the directed evolutionary change has reached new constraint ceilings and environment reached new equilibrium as the bottleneck event ended, both sexual and directional selection will be replaced again by stabilizing selection. In the most extreme case imaginable, the mean number of beneficial mutations followed each recovery becomes 21 , 21^2 , 21^3 ... 21^n . As a result, the top 1% population of each round of selection contributes 21 , 21^2 , 21^3 ... 21^n beneficial genes individually, whereas 1,000 individuals survived each round and $T_{\text{fixed}} = 10,000$ years. During the bottleneck, each individual per generation contributes 21 , 21^2 , 21^3 ... 21^n beneficial mutations, and there are 500 generations.

$$(21 + 21 \cdot 500) + (21^2 + 21^2 \cdot 500) + \dots + (21^n + 21^n \cdot 500) = 501 \cdot 21 \cdot \frac{21^n - 1}{21 - 1} \quad (4.31)$$

$$501 \cdot 20.96 \left(\frac{20.96^{1.4279} - 1}{20.96 - 1} \right) \cdot 1,000 \text{ individuals} \approx 4 \cdot 10^7 \quad (4.32)$$

$$1.4279 \cdot 11,580 = 16,535 \text{ Years} \quad (4.33)$$

Then, in the most extreme case, it takes only 16,535 years to transition from Chimpanzee to Homo sapiens. In reality, the speed occur in nature falls within these ranges. Hence, we have mathematically shown that the evolution of Homo sapiens is directed by a series of directional punctuated bottleneck events with periods of stasis.

At this point, we can conclude that most species stabilized by slow changes in earth's climate and continent's configuration, during which time, stabilizing selection is favored over the directional and disruptive selection. Moreover, genetic recombination and genetic drift in a large, stable population will converge the gene pool toward uniformity. From this, we can conclude

that the earth's geologic changes played the most critical role in speciation, while genetic drift and recombination played a secondary role by reinforcing genomic uniformity while speciation opportunity does not arise.

Then, the question remains. How does a gradual change in geology sometimes lead to a sudden change in climate or habitat so that an existing species can no longer maintain its status quo and is mandated by disruptive, directional selection? This can be demonstrated by the separation of two continents, while South America and Africa start to split apart and the geologic process continued for tens of millions of years, certain sections of land bridges continue to connect to the two continents. The break up of two continents making migration across the two continents increasingly difficult but still possible. However, once the last landmass bridge is severed, land-based population exchange and gene flow stop completely, which is an one time, sudden disruptive change relative to the past. The reverse is true as well, the terror bird, a predatory bird lived on the island continent of South America, was suddenly forced to compete with northern invaders as the Isthmus of Panama was formed between North and South America. Although South America is drifting north toward North America for millions of years, the habitat of terror bird stabilized for millions of years with no apex predators to compete. Only when the two land masses connected physically by land, a sudden change in its habitat occurred.

When two bodies of water, once freely flow from one side to another, is increasingly blocked by land formation, the aquatic species flow is still possible throughout the plate creation process until the exchange of two bodies of water completely stopped. Then, a sudden change in species habitat takes place. A species formerly able to move freely between two bodies of water and access food resources are now constrained to just one. It may also well adapted to the water temperature at a given range are now forced to adapt to a different one because the water flow to equalize the temperature of bodies of water is no longer possible.

The reverse is also true when two bodies of water are separated by land bridges. Either side is well adapted to its local fauna and predators. As the land bridge stretched thinner and thinner by plate tectonics, two bodies of water are continued to be separated and maintained its status quo. When the land bridge separates the bodies of water disappeared, two bodies of water flow freely, causing temperature change, flow directional change, local fauna change, and exchange of animal species all occur within a very short timescale.

The formation of mountain ranges such as those in Tibetan plateau starts slowly. As mountain creation gradually increases in height, so do bird species adapt by flying higher to get across the mountain ranges. Despite the emergence of a physical barrier, gene flow continued on both sides of the range, so a species' gene pool maintained its uniformity. However, as the barrier continues to rise in height, there is a point reached when the cost of crossing over the mountain range searching for food outweigh the benefit of food access, then the gene flow stops, and speciation occurs at both sides of the mountain.

The reverse again is true. An ancient mountain range is gradually lowered due to weathering

and erosion. While species of animals for millions of years are kept to each side of the range, were suddenly able to cross over, leading to drastic habitat change.

A lake is gradually evaporated away in depth nevertheless is able to sustain an aquatic ecosystem until it is finally completely dry, leading to the extinction and destruction of the entire system. The reverse is also true. A freshwater lake is gradually gaining size and its habitat continue to thrive until it joins with the nearest ocean. Suddenly, saline water exchanges with freshwater, bringing invading species and change the entire ecosystem.

The gradual movement of continents and land formations also attribute to sudden climate change which perpetuated for millions of years. South America joined Antarctica before the opening of the Drake Passage. As long as a land bridge existed between them, the oceanic flow circulates both continents and is able to transform frigid polar flow into a warm tropical one and warms Antarctica as it returns. However, once the land bridge disappeared, frigid cold ocean circulates Antarctica, drastically alter the landscape of Antarctica, and turning it into an icy world.

Lastly, sympatric speciation requires a little more discussion, the first three types of speciation are all associated with geological change, yet sympatric speciation concerns that a single species diverged into two by selecting different survival strategies. It seems that sympatric speciation has little to do with geologic changes, but it is. Let consider a thought experiment. It is assumed that a species existed for a long time with increasing numbers and intraspecies competition develops two different feeding strategies on different types of fruits. However, if both types of fruit trees co-existed for a long time, it is likely that this species could have exploited two different niches long time ago instead of now. This contradicts with our assumption. Then if the fruit tree is just introduced now, it must be a consequence of three other types of speciation (from some other isolated environment), and it is just spreading its habitat into the fruit-eating species territory. The fruit tree can not just arise within the species territory because we have shown that stabilizing selection does not favor speciation in a static environment. Therefore, fruit-eating species speciation into two different subspecies by adapting different feeding strategy is an indirect consequence of allopatric, peripatric, and parapatric speciations, which in turn is a consequence of geologic change.

By now, it is clear that geologic movement continues, but its gradual, incremental quantitative change does not bring significant climate and habitat alteration until a critical threshold is reached, whether it is the joining of two separated landmass or the separation of the two. Thereafter, the incremental quantitative change led to a qualitative leap in the environment. Species then have to quickly adapt to avoid extinction. This is confirmed by the fossil record as sudden appearance and disappearance of genus and is the essence of punctuated equilibrium. As a result, *there is no such thing as the average Evolutionary rate of species. The final value of a computed evolutionary rate is actually the combined rate of geological change leading to drastic environmental alteration and the intrinsic rate of speciation in biological creatures.* This is conceptually similar to the final speed at which a box is moving across a rough surface,

which is broken down into the input force minus resistive friction. Nevertheless, a value can be obtained regarding this evolutionary rate, which is a factor between 1.23 to 4 per 100 million years. But one must understand that intrinsically biological creature is able to evolve to this rate at much shorter timescale than 100 million years. The rate of geological change leading to drastic environmental alteration is the brake on biological evolution, without drastic change and fluctuation in the environment, natural selection favors static, non-changing morphology and behavior. From this, we can again confirm the importance of ice age in contributing the rise of *Homo sapiens*, a period of chaotic, everchanging climate and weather patterns.

4.6 BER

Having elucidated the mechanism setting the nature's pace for evolution, we resort to calculating the background evolutionary rate. The background evolutionary rate prior to multicellularity is highly predictable. The onset of the great oxygenation event starts roughly 2 billion years after the appearance of photosynthesis, but the total time span can increase or decrease depending on the exoplanet's sea surface area to sea volume ratio in comparison to that of the earth. The onset of multicellularity starts roughly 1.5 billion years after the great oxygenation event, but the total time spent can increase or decrease depending on the exoplanet's land surface area to sea surface area ratio in comparison to that of the earth. However, we are more concerned about the background evolutionary rate at the multicellular stage of evolution. Alexei and Gordon have proved a method of calculation using DNA complexity, and they showed that genome complexity grows by 1.23 every 100 Myr. In chapter 6, we determined the background evolutionary rate by comparing the Encephalization quotient of mammals to that of reptiles. This rate is equivalent to 2.783 in 100 Myr. This implies that every 100 million years the biological diversity leading to greater EQ increase by 2.783.⁷ This is not a contradiction to our earlier discussion on the pace of evolution constrained by geology. We illustrated in Chapter 6, the increase in biodiversity does follow a positive feedback loop as greater biodiversity provides a greater ease at speciation and more niches opening during major geologic changes. Species will continue to emerge due to major geologic changes. The rate of major geologic changes will remain nearly constant throughout the history of multicellular life, but the number of newly emerged species and opened niches per each major geologic change increases exponentially.

4.7 Continent Cycle

Although the average rate of background evolutionary rate is now known, the evolutionary rate leading to greater diversity is non-uniform throughout the geologic history. This can be seen

⁷ (more on this please follow chapter 6 on section "YAABER for Evolution of *Homo Sapiens*").

from the biodiversity plot. It can be shown that biodiversity started to emerge in Cambrian and took a dive by Permian and continue to grow exponentially thereafter. The growth is especially fast since the Jurassic. The graph correlates well with the configurations of earth's continents' positions. The breaking up of Pannotia supercontinent certainly aided the start of multicellularity besides an increase in atmospheric oxygen, and as the continents merged to form Pangea supercontinent 300 million years ago at the start of Permian, the diversity not only stabilized but also dropped. The Permian-Triassic extinction, the deadliest one in earth's geologic history, caused the extinction of 90% of animal species. Pangea started to break up 170 million years ago during the mid-Jurassic. Thereafter, the diversity increased exponentially.

This slowing and speeding observed in geologic record cannot be associated with the rise and fall of oxygen level in the atmosphere. Although oxygen level is closely associated with the emergence of super-sized insects and enabled the appearance of multicellularity and speeded up biological evolution significantly, there is little correlation between biodiversity and atmospheric oxygen level. Cambrian, Ordovician, Silurian, and Devonian had oxygen level 63%, 68%, 70%, and 75% of modern level respectively, yet the biodiversity was increasing throughout this period. During the following Carboniferous and Permian era, the oxygen content was 163% and 115% of modern level respectively, yet biodiversity stabilized and even dropped.

Carbon dioxide level cannot correlate with biodiversity as well. Throughout all earth's history, fast and slow periods of biodiversity growth occurred during both high and low concentration of CO₂. During some high times of carbon dioxide level such as Cambrian (16 times modern level), Ordovician (15 times modern level), and Cretaceous (6 times modern level), biodiversity was increasing. During other high times of CO₂ levels such as Silurian (16 times modern level), Devonian (8 times modern level), Jurassic (7 times modern level), and Triassic (6 times modern level), biodiversity was stagnant or decreasing. At some low times of carbon dioxide level such as Permian (3 times modern level) and Carboniferous (3 times modern level), biodiversity stabilized. At other low times of CO₂ such as the Paleogene (2 times modern level), however, biodiversity increased exponentially.

Therefore, we can rule out the atmospheric composition played any significant role in the diversification and the rate of evolutionary change. If all terrestrial life-friendly planets go through similar continents-supercontinents cycle, then, we should expect that the background evolutionary rate on any particular planet follows a sinusoidal curve where the evolutionary rate and the diversification occur faster during the separation of continents, slows down. and even drops when continents merge. (the background evolutionary rate, the computed average of all habitable planets, however, will exhibit a smooth exponential curve since some planets at a given period go through evolutionary stasis while others are evolving rapidly). Nonetheless, biodiversity should follow the general increasing trend because new species of plants and animals establish in previously uninhabitable regions, altering the biochemistry and environment and rendering them habitable. This has repeatedly happened in earth's history. For example, the cyanobacteria's metabolic process has transformed the earth's atmosphere by providing free

oxygen. The establishment of land plants enabled the habitability by land animals later on. Moreover, new species opens new niches on existing habitable environment. For example, the evolution of fruit trees enabled the evolution of arboreal species in the primate family.

The loss of diversity can be expressed mathematically based on the configuration of continents. In the simplest model, island continents are surrounded by bodies of oceans, which brings precipitation to their shorelines. Marine climate further extends inland, however, the central part of the supercontinent remains dry and arid, receiving little precipitation with extreme temperature swings due to continental climate, reducing its chance to host a diversity of biological life. This simplified assumption generally applies to the climate currently observed on all continents across earth except the equatorial, tropical regions of the Amazon rain forest and central African jungle. Additionally, a perimeter surrounding each island continent with an extended continental shelf of shallow seas provides a great biodiversity for marine life. It has been measured that marine life biodiversity decreases with the depth, due to decreasing sunlight penetration disabling photosynthesis and decreasing temperature. If each island continent can be abstracted into the shape of a circle, then, one can make the following deductions.

Assuming each island continent size is small enough that is completely covered by marine climate to guarantee its biodiversity, and its radius is r . Then, the total size of m island continents composes a total region providing biodiversity:

$$i_{island} = m\pi r^2 \quad (4.34)$$

If m island continents merged into one supercontinent; then, the radius of the supercontinent is:

$$\pi R^2 = m\pi r^2 \quad (4.35)$$

$$R^2 = mr^2 \quad (4.36)$$

$$R = \sqrt{mr^2} \quad (4.37)$$

and assuming that biodiversity only extends a distance of d inland from the shoreline, then the total habitability of the supercontinent is given by the equation:

$$i_{supercontinent} = m\pi r^2 - \pi(\sqrt{mr^2} - d)^2 \quad (4.38)$$

$$i_{supercontinent} = m\pi r^2 - \pi(mr^2 - 2\sqrt{mr^2}d + d^2) \quad (4.39)$$

$$i_{supercontinent} = (m\pi r^2 - \pi mr^2) + 2\pi\sqrt{mr^2}d - \pi d^2 \quad (4.40)$$

$$i_{supercontinent} = 0 + 2\pi\sqrt{mr^2}d - \pi d^2 \quad (4.41)$$

$$i_{supercontinent} = \pi (2\sqrt{mr^2}d - d^2) \quad (4.42)$$

If one assumes that biodiversity extends a unit distance of 1 inland and each island continent's radius is also a unit distance, and omitting π , then the equation for total island continents diversity and supercontinents diversity can be simplified into:

$$i_{land} = m \quad (4.43)$$

$$y_{land} = 2\sqrt{m} - 1 \quad (4.44)$$

Moreover, one should also take continental shelf's marine biodiversity into account. Assuming the continental shelf extends a distance of R offshore, then the total zone of marine biodiversity for m island continents and supercontinent is given by:

$$z_{island} = m\pi (r + R)^2 - m\pi r^2 \quad (4.45)$$

$$z_{island} = m\pi (r^2 + 2Rr + R^2) - m\pi r^2 \quad (4.46)$$

$$z_{island} = m\pi (r^2 + 2Rr + R^2 - r^2) \quad (4.47)$$

$$z_{island} = m\pi (r^2 - r^2 + 2Rr + R^2) \quad (4.48)$$

$$z_{island} = m\pi (2r + R^2) \quad (4.49)$$

$$z_{supercontinent} = \pi (\sqrt{mr^2} + R)^2 - \pi (\sqrt{mr^2})^2 \quad (4.50)$$

$$z_{supercontinent} = \pi (mr^2 + 2\sqrt{mr^2}R + R^2) - \pi mr^2 \quad (4.51)$$

$$z_{supercontinent} = \pi mr^2 + 2\pi\sqrt{mr^2}R + \pi R^2 - \pi mr^2 \quad (4.52)$$

$$z_{supercontinent} = (\pi mr^2 - \pi mr^2) + 2\pi\sqrt{mr^2}R + \pi R^2 \quad (4.53)$$

$$z_{supercontinent} = \pi (2\sqrt{mr^2}R + R^2) \quad (4.54)$$

If one assumes that biodiversity extends a unit distance of 1 offshore and each island continent's radius is also a unit distance, and omitting π , then the equation for total island continents marine diversity and supercontinents marine diversity can be simplified into:

$$i_{sea} = 3m \quad (4.55)$$

$$y_{sea} = 2\sqrt{m} + 1 \quad (4.56)$$

combining land diversity with marine diversity, the following mathematical graph can be ex-

trapolated:

$$i_{total} = 4m \tag{4.57}$$

$$y_{total} = 4\sqrt{m} \tag{4.58}$$

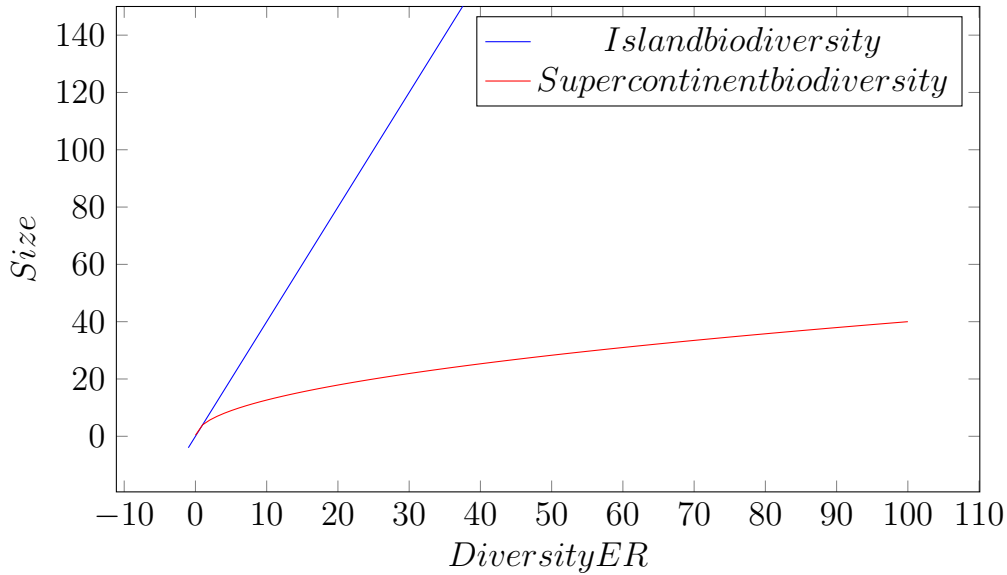


Figure 4.3: Biocomplexity of island continents and supercontinents vs land mass size

It shows that under ideal conditions, in all possible number of island continents leading up to supercontinents, island continents has as much as all their land areas nourished by moderate to adequate precipitation, moderated by sea currents to reduce temperature extremes. On the other hand, a supercontinent in size comparable to the total area of many island continents left vast stretches of its inland in arid, dry climate with huge temperature swings. Therefore, island continents provide a greater biodiversity than supercontinents in all ranges. Of course, taking into consideration the functioning of Hadley cell and its explanation for major dry, arid bands of latitudes stretching both the northern and the southern hemispheres, further refinements to the model are possible. Furthermore, instead of cutting off biodiversity at a certain distance inland, the drop in biodiversity is more likely to be gradual. However, the basic assumption that biodiversity correlates positively with separated island continents remains.

Of course, supercontinent such as those of Pangea must have had episodes of increased biodiversity, but such spurts of biological diversification do not alter the general trend of the epoch. After the Carboniferous rainforest collapse, first, local recovery simply filled the previously vacated niche. Since each local fauna recovered on its own and no two local fauna exchanged gene flows, self-imposed barrier existed between each region. As local fauna evolved and resorted to adaptive radiation and increased biological diversity (when new niches opened faster

than stabilizing genetic drift), the total diversity increased on the continent. However, as these species started to re-establish themselves among all others on the vast continent, they break the previously self-imposed barrier. Competition ensued and eventually led to stabilized or drop in the total biological biodiversity across the entire continent.

4.8 Continental Movement Speed

Having shown that continental cycles drive the cyclic pace of evolution, we now focus on the continental movement speed across all terrestrial planets. Continental movement speed varies between terrestrial planets of different sizes. The model for tectonic movement, though very intricate and complex, can be simplified into a toy model based on two assumptions. First, the rate of tectonic plate creation is directly proportional to the heat release per unit area of the planet. That is, the higher the heat flux, the more active the plate tectonics. The formation of new crusts is a consequence by the convective magma inside the planet in the form of heat dissipation from the planet's original formation in the form of potential energy and radioactive elemental decay such as uranium and thorium. It is, then, no surprise that young earth billions of years ago had more active geologic activities. Secondly, the rate of tectonic subduction is directly proportional to the gravity acted upon the plates. The oceanic mafic plate emerges from the site of its creation and gradually over the course of millions of years consolidated in density and increased in weight and sloped toward the subduction zone. The subduction zones, such as the Mariana trench, are some of the deepest places on earth, pulls the plate into the mantle upon its own weight, thereby completing the recycling of the oceanic plates. It is no surprise that planets with higher mass also has greater surface gravity and greater surface heat flux. A third factor involving the thickness of the crust is sometimes also considered, but for the simplicity of our argument (a lack of data to correlate crust thickness based on the mass, composition, or the formation condition of the planet. Mars has a thicker crust with 10% earth mass, and Venus has comparable crust thickness to earth with comparable density, yet all three planets have comparable compositions), we shall assume that the crust thickness is equivalent in terrestrial planet of different masses. The question becomes, given an increase in mass of a terrestrial planet, how will the speed of tectonic movement change and by how much. If we assume that terrestrial planets have a similar density to earth, then the following graph can be used to predict the surface gravity and surface area on terrestrial planets of other masses.

$$r_0 = \left(\frac{3}{4}x\right)^{\frac{1}{3}} \quad (4.59)$$

$$y_{plate} = \frac{1}{0.3029} \frac{\frac{4}{3}\pi r_0^3}{4\pi r_0^2} \quad (4.60)$$

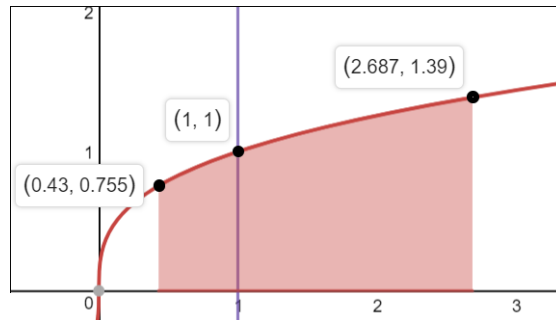


Figure 4.4: Geological intensity vs. terrestrial planet mass

The surface gravity grows relatively slow compares to the increase in mass, that is, a terrestrial planet at the mass of 2.687 times of earth will have a surface gravity at only 1.39 times that of the earth. Furthermore, the surface area will also be 1.39 times that of the earth. As a consequence, one can see that radiative convection on this planet will also create new crusts at 1.39 times the speed observed on earth while engulfing old crusts also at 1.39 times the speed on earth. As a result, for a terrestrial planet, put on a limit of no more than 2.687 earth mass, the plate tectonic movement cannot exceed more than 1.39 times the speed on earth. On the other hand, plate tectonics movement on planets with mass smaller than earth slows down significantly, with only a fraction observed on earth. We have deduced in the section regarding biodiversity cycle and its correlation with the continent-supercontinent cycle. It is shown the formation of supercontinent is not conducive to the maintenance of diversity relative to the island continent configurations. However, a drop in biodiversity is not only compensated by the breaking up phase of the supercontinent but with further increase in biodiversity. The first niche exploited by biological life on earth is the ocean, then life moved onto land as their next habitat, and then biological species created its own niche habitat in the form of forests and trees, and finally, biological creatures exploited the sky. One needs to stretch on more imagination to imagine what else is possible if the continental supercontinental cycle continues. For example, increased biodiversity and photosynthesis leads to a much denser atmosphere thus creating a new niche with lower density compares to the ocean but much higher density than the air we used to on earth today. Species semi-adapted to both flying and walking will become possible within such a niche. Seahorse like creatures swim through the air near the ground. Anything is possible. In the graph plotted below, we compare the upper limit at which the evolutionary rate can occur on super-earths analogs and the lower limit at which evolutionary rate can occur on mini-earths, the middle line is earth itself, assuming their multicellular life all started at the same time.

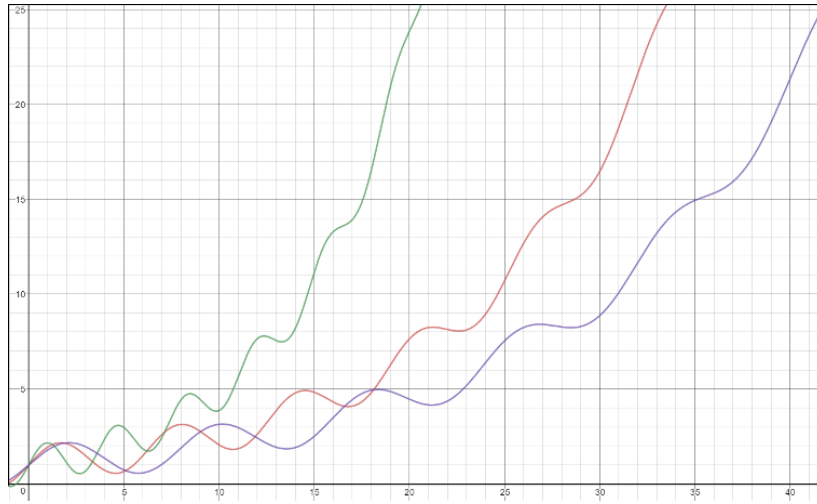


Figure 4.5: Super-earth, earth, sub-earth's idealized tectonic rates and their subsequent bio-complexity development

*It can be seen that super earth goes through a shorter cycle of continental drifts, as a result, achieves greater biodiversity at a faster rate than earth and faster background evolutionary rate compares to earth. On the other hand, mini-earth goes through a longer cycle of continental drifts, as a result, achieves greater biodiversity at a slower rate than earth and slower background evolutionary rate compares to earth. It is likely that life is sustained on such planet, will progress very slowly, since the movement of plates is the ultimate determining factor in biological evolution. It is also to be noted that, at times, especially toward the beginning of emergence, a mini earth's high point in biodiversity can eclipse that of the other super earth's low point in biodiversity, even though ultimately super earth led to a faster rate of evolution. In summary, by analyzing the different speed of evolutionary rate as a consequence of plate drift rate, we achieved a physical explanation for the abstract mathematical concept that background evolutionary rate varies. Some planets achieve emergence of superintelligence faster than others, and the sum total of all background evolutionary rate on all planets contributes to the **cosmic background evolutionary rate**, centered on the mean and represented as a probabilistic distribution with measurable standard deviation.*

5 Homo Sapien Emergence Probability

5.1 Why Human Did not Appear Earlier

Ice age and its fluctuating climate pattern act as tremendous accelerators on the emergence and the diversification new species. In order to quantify the magnitude of acceleration, we can resort to the annual cranial capacity growth rate of Australopithecus Afarensis at 405 cc to that of Neanderthal at 1600 cc, and one obtains 0.0000376248 percent. This compares to the rate of growth of EQ of early mammals at 1 to that of Chimpanzees at 2.35, at an annual evolutionary growth rate of 0.0000014046, or 26.786 times faster than the background evolutionary rate. To put in perspective, this increase in growth rate is comparable to human's rate of progress during post-Industrial Revolution compares to that of hunter-gatherers. In earlier ice ages, clearly illustrated from the formation of supercontinent Pangea and the Karoo ice, which drastically alter the humid climate from earlier epoch and earth entered a period of dry, cold climate. These ice ages also gave rise to novel adaptations but no adaptations of intelligent, tool-using species. Upon the drastic climatic change, amphibians which requires adaptation to moisture and close proximity to bodies of water to procreate the young evolved the mechanism of nurturing the young within hard-shelled eggs and gave rise to the reptiles. Moreover, the emergence of seed gave rise to Gymnosperms, which protects the plant seed from drying out, providing additional protection. Earliest species adapted to arboreal locomotion such as late Permian synapsid *Suminia getmanovi* and tree climbing dinosaurs such as *Deinonychus* exists during the early Cretaceous. However, neither species eventually transitioned to upright walking species with flexible hands. Besides the fact that no ice age with fluctuating climate pattern occurred since Permian before the Quaternary ice age, which is unable to turn arboreal species to a ground walking one, as in human's case. A very important and often overlooked fact is that the evolution of intelligence is not particularly beneficial for an organism adapting to its environment. When the total biological diversity is low in the earlier epochs of earth's history, organism's strategy is to maximize their body size, their running speed, their visual acuity. If any species adapts for flexibility, it may well be flexibility specialized in a particular way. For example, both chameleon and octopus can alter their skin color to fit its environment quickly, which hides the species from both predators and preys. But only as biological diversity bloomed during the Cenozoic era, with the abundance of fruit-bearing trees and wild berries to provide energy, furry animals with skin hide capable of providing warmth, and beehive to provide honey, can the evolution of intelligence benefits outweigh its costs. An intelligent species is able to combine different species' material based on its strength and characteristics to accomplish yet unseen impossible tasks, such benefit grows exponentially over time as the manipulative power and potential search space becomes ever greater. From this perspective, the evolution of intelligence, even though a passive evolutionary process not seeking any goal, will be inevitable. On a further note, the evolution of intelligent creatures in both ocean and

land are equally likely, as indicated by the EQ of dolphins and killer whales. However, only the cohort of terrestrial species have the chance to develop an industrial civilization, provided with a cataclysmic event such as the ice age (Ice age has a moderate effect on ocean temperature not as drastic climate shifts as those on land).

5.2 Ice Age as an Accelerator and Its Causes

Many have argued that the emergence of *Homo sapiens* is tightly intertwined with the current Ice Age. The quick, fluctuating climate and weather pattern made animal adaptations by means of natural selection difficult. At the onset of the current inter-glacial 10,000 BP, many major animal groups particularly the woolly mammoth became extinct. Though human hunters have played some role in accelerating its demise, its gigantic size and surviving strategy do not adapt well to a much humid, temperate epoch especially the interglacial summers. Throughout the last few ice ages, animals survived a glacial period can become extinct by the next interglacial, and the lucky ones survived the interglacial but ill-prepared for the harsh glacial period becomes extinct by the next one. *Homo* genus, on the other hand, adapts environment by tool usage, fire control, coordinated teamwork, and culture transmission of experience to the next generation. As a result, *Homo* genus not only survived each of the glacial and interglacial periods, and actually prospered.[8][42] Without the current ice age, the human ancestor likely remains on the trees in African tropical forests, and no evolutionary pressure forces them to roam the ground to search for food. They will either become extinct as a species or eventually adapt to walking on the ground tens of millions of years into the future. Since earth's continent continues to move, in millions of years further into the future, Africa plate will further shift north and join the Eurasian plate, causing fauna and environmental changes in current East and Sub-Sahara Africa. Therefore, in the absence of fast tectonic movement to drastically alter the living environment within a short geological period, an Ice Age acts as an accelerating contributing factor to the rise of *Homo Sapiens*. If Ice Age is critical to give rise to the intelligent species, we should resort to calculate the probability of any given geologic time period in which earth falls under one. The formation of earth's ice age is an interplay of solar radiation output, atmospheric composition (methane, carbon dioxide, and oxygen concentration), and the earth plates positions. The formation of Ice age occurred a few times during the earth's geologic past, some of which is attributed primarily to the changing atmospheric composition such as the Huronian, Cryogenian, and Karoo Ice Age.

Huronian glaciation extended from 2.4 billion years ago to 2.1 billion years ago caused by Cyanobacteria's evolution of photosynthesis. Their photosynthesis produced oxygen as a waste product expelled into the air. At first, most of this oxygen was absorbed through the oxidation of surface iron and the decomposition of life forms. However, as the population of the cyanobacteria continued to grow, these oxygen-sinks became saturated.[52] This led to a mass

extinction of most life forms, which were anaerobic, as oxygen was toxic to them. As oxygen filled the mostly methane atmosphere, and methane bonded with oxygen to form carbon dioxide and water, a different, thinner atmosphere emerged, and Earth began to lose heat. From our calculation on the continuously habitable zone, the earth was beyond the outer edge of the habitable zone with current atmospheric conditions and composition until 1.3 Gya. Without the presence of methane as a strong greenhouse gas, earth plummeted into an ice age until solar output eventually matched the loss of methane as a greenhouse gas.

The Karoo Ice Age was caused by the evolution of land plants from the earlier Devonian period which led to significantly higher oxygen content, and the global carbon dioxide went below the 300 parts per million level. However, it can be argued that without a significant presence of land mass near the south pole at the time, this ice age with biological origin can not perpetuate for long.

If we assumed that oxygen content and atmosphere density should reach levels comparable to that of earth on any other extraterrestrial planets enabling the emergence of intelligent species, then the ice age caused by biological process preparing for such prerequisite condition should be excluded from our investigation. The earth, after each of such preparatory changes, readjusted itself toward an ice-free world.

We can also assume that the sun's increasing radiation is slow compares to the geologic process, tectonic movement by at least a magnitude, then we can reasonably conclude that the movement of cratons and plates is the most significant contributing factor to the onset of an ice age.

Therefore, atmospheric changes and solar output can trigger and start an ice age, but in order to perpetuate one with a length comparable to a geologic period and an intensity comparable to our current glaciation, the configurations of plates are the necessary though insufficient condition.

The Quaternary glaciation is the most well-understood due to its recency. From the plate tectonics and ocean current theory, the long-term temperature drop is related to the position of the continents relative to the poles. This relation can control the circulation of the oceans and the atmosphere, affecting how ocean currents carry heat to high latitudes. Throughout most of the geologic time, the North Pole appears to have been in a broad, open ocean that allowed major ocean currents to move unabated. Equatorial waters flowed into the polar regions, warming them with water from the more temperate latitudes. This unrestricted circulation produced mild, uniform climates that persisted throughout most of the geologic time.

The formation of Antarctica ice sheet is a consequence of the formation of Drake passage that separates South America from Antarctica started 43 million years ago. The separation created the Antarctic Circumpolar Current that completely circles the continent. This current does not exchange with the warmer currents closer to the equator. Prior to the separation, currents alongside the southern continent flowed toward the equator, circled the entire South America continent before reaching Antarctica again with warmer currents. Over the course of millions of years, the cold Antarctic Circumpolar Current changed the continent's climate and cooled it

significantly. At the same time, North America continent, Greenland, and Eurasian continent moved north with the north pole in a small, nearly landlocked basin of the Arctic Ocean. A nearly landlocked ocean again can not exchange its colder currents with that of the warmer currents nearer the equator, resulting in the polar ice cap. Currents can also warm up regions. The Gulf Stream of Mexico which flows from the equator toward European continent helped Europe to be significantly warmer than the rest of the world at similar latitudes. Therefore, the role of currents in shaping climate is critical, and its direction is predicted by the position of continents. If one traces further back one can also find that the position of continents also played a significant role in earlier glaciation events. During the Karoo Ice Age from 360 million to 260 million years ago, Pangea supercontinent covers the entire south pole. Unlike Antarctica today, the shoreline to the south pole is significantly further away. Even in the absence of Antarctic Circumpolar Current at the time, warm currents and its effect on the climate is limited since its impact can only reach so much inland. Although the north pole is wide open, making current flow from tropics to the pole possible, North America and Angaran region of the supercontinent stretches well into 60 degrees in latitude north of the equator, making a complete exchange of ocean currents between the two hemispheres difficult.

Andean-Saharan glaciation occurred earlier during the Ordovician epoch showed a remarkably similar continent layout to that the Permian epoch, a vast supercontinent with a significant landmass covered the south pole.

From these encouraging observation, one can create a simplified model for the formation of Ice Age.

1. That is, when significant continental mass located at the poles
2. One craton located at the pole and separates from the rest by the ocean
3. A polar ocean is landlocked by the continents

It can be said if any one of the three conditions is fulfilled, then ice accumulation occurs on earth, a more severe form of ice age occurs when 2 or all 3 conditions are met. The Quaternary Ice Age is satisfied by condition 2 and 3.

5.3 Expected Ice Age Interval

Since earth shifts through continental cycles, the probability of ice age occurrence and its accelerated effects on evolution are essential in our discussion on the probability of the emergence of Homo sapiens if any planet already evolved flower plants and animals with capabilities similar to Reptiles, Birds, and Mammals. The onset of an early ice age on a planet with these prerequisite conditions will generate intelligent, tool-using species faster. Computing the probability of earth entering into any severe ice age as the one we observed right now, where both

poles covered in a significant depths of snow, is required. From our earlier discussion, we know that earth can enter into an ice age if there is two Antarctica sized plates sits on both poles. Glaciation initiates if there is significant continental mass covering the poles, as observed during Ordovician ice age and the Karoo ice age. Glaciation also initiates when one pole is covered by one Antarctica sized plate and another pole encircled by two or three Antarctica sized plates (our case observed today).

After listing the conditions for the creation of an ice age, we need to convert the complex everchanging continental movement of earth crusts into a much simpler problem we can tract and at the same time provide a reasonably good estimation. The configurations can be simplified into a toy mathematical model of the following configurations. First, dividing the surface of the earth into 34 blocks of equal sizes, where each block represents a plate. The number of subaerial blocks totaled 10, corresponding to 29 percent of the surface of earth emerged above water. Each block sized 3,872 km per side, with a total surface area of 14,992,384 km², this roughly comparable to the size of Antarctica. This is to show that over the geologic time period, any continent is free to move into any one of these 34 blocks of regions. Out of these 34 blocks of regions, only 1 block is reserved for the north pole and another one for the south pole, so the chances of moving into any one of these blocks is a matter of random combination. Furthermore, the nearest blocks to each of the pole, three of them circles the north pole, and another three circles the south pole. If a pole is unoccupied, yet all 3 adjacent blocks are occupied by the continents, then a current earth's north pole type of scenario emerges. On the other hand, if the south pole is occupied by a continent and all 3 adjacent blocks are unoccupied; then, current earth's Antarctica scenario emerges. If the pole is occupied, yet only 1 or 2 of the adjacent blocks is also occupied by a landmass; then, a south America attached to Antarctica scenario emerges and no ice accumulation at this pole. If all 3 adjacent blocks along with the pole block are occupied by landmass, then Pangea type of supercontinent configuration during the Karoo glaciation and the Andean-Saharan glaciation scenario emerges.

Moreover, Europe, Australia, South America, and Antarctica is represented as one block. Africa is represented by two blocks. North America is represented by only one block while its total surface area corresponds to 1.5 block sizes. However, it is not critical for our analysis because any land mass south of Canadian border can be discarded because we are only interested in a continental configuration which circled the pole and its discredited mass is added as an extra to Australia. Finally, Asia is represented by 3 blocks.

Then, one can see that the configuration of the blocks can be represented as a string of digits, where the leftmost digit represents the first block of the north pole. The second, third, fourth blocks represent the plates that surround the pole plate with a surface area size of Antarctica extending to 40 degrees south from the north pole, or 7,744 km south of north pole. The rest of digits represents different blocks comprising the mid-latitude Pacific Ocean and Atlantic Ocean. The last block represents Antarctica sits on top of South pole. Once we formulated the rule, we number our blocks from 1 to 34 and arrange them into 34th to the 1st digit of a binary number

representation.

Each region can be labeled as either 1 or 0. Each subaerial block can be represented as a digit of 1 (1 being occupied by a continent), and each submarine block can be represented as a digit of 0 (0 as being filled by the ocean). Total possible cases of 0's and 1's for such an arrangement can be represented by enumerating the binary number of 34 digits ranging in value from 1 to $2^{34}-1$. We then go through by hand or a computer program to pick and count the results which simulate ice age scenarios. *We take this total and divide by the total number of scenarios possible we end up with the probability of an ice age emergence.*

The enumerating table will be too large to exhibit. ⁸Fortunately, no exhaustively listing of possibility is needed. One can find the probability by picking the combinatorial results by giving different combinatorial configurations. For the combination of 10 chose out of 34, there are 131,128,140 total possibilities. This is the total number of possible land over ocean configurations.

$$\Pr(X = 10) = \binom{34}{10} = 131,128,140 \quad (5.1)$$

With both poles covered by Antarctica sized continents, there are 10,518,300 possibilities (choose 8 out of 32).

$$\Pr(X = 8) = \binom{32}{8} = 10,518,300 \quad (5.2)$$

With one pole covered by Antarctica sized plate and the other surrounded by large plates as it is observed today on earth, there are 475,020 possibilities (choose 6 out of 29). This case is symmetric in regards to north or south pole, so it is doubled to 950,040 possibilities. The choose base is 29 instead of 30 because 1 block of sea is surrounded by 3 blocks of land.

$$\Pr(X = 6) = 2 \binom{29}{6} = 950,040 \quad (5.3)$$

The Andean-Saharan ice age observed during the Ordovician and Karoo ice age observed during the Carboniferous have significant landmass buildup around the south pole, this suggests that large landmass centered around one pole also promotes glaciation, adding an additional 593,775·2 possibilities due to symmetry.

$$\Pr(X = 6) = 2 \binom{30}{6} = 1,187,550 \quad (5.4)$$

The total probability giving rise to glaciation can then be computed.

$\frac{12,655,890}{131,128,140} = 9.65\%$, or 1 out of 10.361.

If we take the average speed of plate movement around $9 \frac{\text{cm}}{\text{year}}$, and each block has a side length

⁸ however, a simpler case of total 10 blocks, or a binary number composed of 10 digits ranging from 1 to $2^{10}-1$ is listed at the end of the chapter.

of 3,872 km, then, $10.9267 \cdot 3,872 \text{ km} \cdot 1,000 \frac{\text{m}}{\text{km}} \cdot \frac{100 \text{ cm}}{1 \text{ m}} \cdot \frac{1 \text{ year}}{9 \text{ cm}} = 445,753,244 \text{ years}$

It implies that it takes about 10 different random combinations of earth plate to generate one glaciation phase, and each combination lasts 43 million years. If one compares this result with what we have observed from the paleogeological record, we found the timespan between Andean-Saharan ice age and Quaternary ice age closely match the computation. The Karoo ice age, then, is interesting, because it occurred between these two episodes. Two explanation can be made regarding this case.

First of all, the earth's continental movement was not completely random, and prior to Permian, a majority of the land masses were consistently located south of the equator. Consequently, two episodes of glaciations closely followed one and another by merely 60 million years apart. Secondly, the ice age was caused not primarily by the land mass configuration alone, as it is observed during the Quaternary. The evolution of land plants with the onset of the Devonian Period began a long-term increase in planetary oxygen levels. Giant tree ferns, growing to 20 m high, were secondarily dominant to the large arborescent lycopods (30–40 m tall) of the Carboniferous coal forests that flourished in equatorial swamps stretching from Appalachia to Poland, and later on the flanks of the Urals. Oxygen levels reached up to 35%,^[17] and global carbon dioxide got below the 300 parts per million level,^[72] which in today is associated with glacial periods. This reduction in the greenhouse effect was coupled with lignin and cellulose (as tree trunks and other vegetation debris) accumulating and being buried in the great Carboniferous Coal Measures. The reduction of carbon dioxide levels in the atmosphere would be enough to begin the process of changing polar climates, leading to cooler summers which could not melt the previous winter's snow accumulations. The growth in snowfields to 6 m deep would create sufficient pressure to convert the lower levels to ice.

Thirdly, the Karoo ice age had more moderate climatic effects than the current Quaternary ice age. With only one pole covered in ice, continents near the equators enjoyed milder climatic fluctuation than those observed today, as it is evident from the graph below.

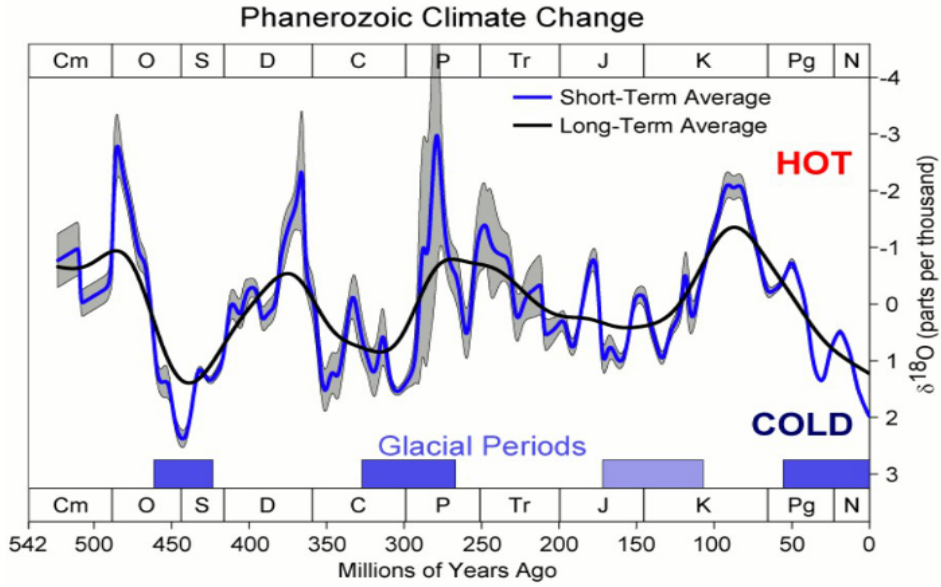


Figure 5.1: Earth's climate in the past 542 Myr

Nevertheless, we shall compute the probability of entering into an ice age at our current epoch by assuming that the last ice age ends 260 Mya. Since it would take another 472.35 Myr to guarantee the onset of the next glaciation which sets a limit to 212.35 Myr into the future, *the chance of entering another glaciation event at the current epoch is 55%*.⁹

Generalization can be made based on this model. Our model indicates the probability leading to glaciation with 29% land coverage and 71% ocean coverage. Applying the same approach, one can find the probabilities distribution of different land and ocean coverage.

$$P(n, k) = \frac{n!}{k!(n-k)!} \quad (5.5)$$

$$T_0 = P(34, x) \quad (5.6)$$

$$T_1 = P((34 - 2), (x - 2)) \quad (5.7)$$

$$T_2 = 2P((34 - 5), (x - 4)) \quad (5.8)$$

$$T_3 = 2P((34 - 4), (x - 4)) \quad (5.9)$$

$$G(x) = \frac{3,872 \cdot 10^3 \cdot 10^2}{9 \cdot 10^8} \left(\frac{(T_1 + T_2 + T_3)}{T_0} \right)^{-1} \quad (5.10)$$

⁹This is a special case from a whole range of permissible values, the final generalized results show to be 70%, please check section 5.4

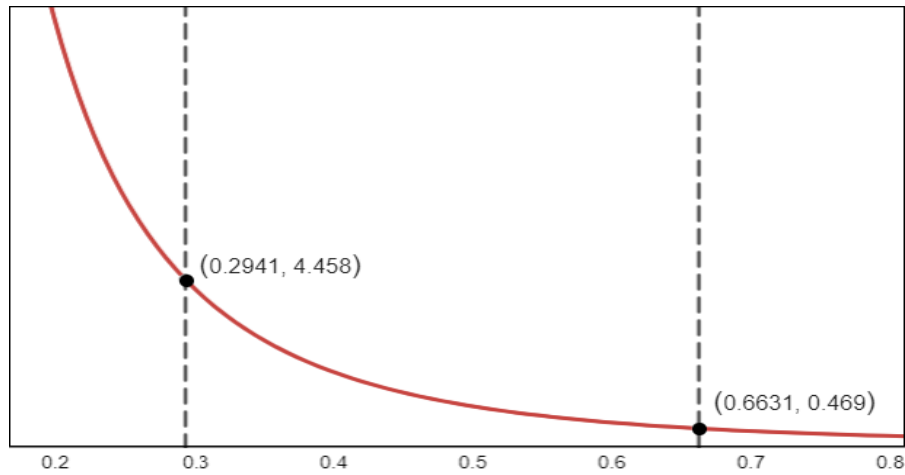


Figure 5.2: Dryland percentage coverage and the expected timing of the next glaciation event for 100% dryland coverage to 0% dryland coverage

In general, smaller land coverage results in a smaller probability of glaciation and more land coverage results in a higher probability of glaciation. On a hypothetical planet with scattered island continents, glaciation occurs at much longer intervals, and the accelerated evolution of *Homo sapiens* cannot occur. On the other hand, on a hypothetical desert planet, where land covers more than 66.3 percent of the planet surface, glaciation dominates the planet at every epoch, with 100% probability in any given time. Extreme, extended period of glaciation impedes the evolution and development of complex multicellular life, as it is evidenced by the Cryogenian ice age prior to Cambrian explosion. Atmospheric oxygen is already reaching a significant proportion at the start of the glaciation, but multicellular evolution was kept in check by advancing snowball earth.

We investigated the distribution of the percentage of ocean coverage given different total surface areas of lightweight granite continental plate in Chapter 3. It is shown that earth analogs (with both land and sea coverage on their surface in a delicate proportion to allow a transition from ocean-based multicellular life to a terrestrial one) are, in general, covered by at most 38% dry land mass. As a result, all habitable planets leading to intelligent, tool-using species experience almost no glaciation to only occasional glaciation events, with planets having greater land masses more likely developing intelligent, tool-using species on land. Since we derived the relationship between continental plate percentage to oceanic plates and the total ocean coverage in Chapter 3, we now have to derive the range of ocean to land coverage most likely results in an ice age at the current epoch just like we observed on earth. We take 12.92 blocks out of 34 blocks, or 38% as the upper limit because the computed results show that terrestrial land mass can at most extend to 38% of land coverage in all possible configurations. The lower limit is obtained by assuming if the current epoch has a certain chance of an ice age occurring (between 0 and 1) and by pushing on the expected onset of an ice age at 100% probability further into the future to the mean expected appearance time of intelligent, tool-using species on all terrestrial

planets. It is computed to be 334.4 Myr into the future (see Chapter 7). Then, the appearance of an ice age occurring at an interval greater than the mean appearance time on all terrestrial planets do not contribute at all, at accelerating the emergence of intelligent, tool-using species. We found that 8 out 34, or dry land covering less than 23.53% of the planetary surface satisfies the aforementioned condition. We then reached the conclusion that dry land coverage ranges from 23.53% to 38% can broadly be labeled as ice age capable configurations along the y-axis. This is translated into continental plates cover range from 26% to 50% of the planetary surface along the x-axis. This amounts to 24.44% of all possible configurations. However, earlier in Chapter 3 we have shown that island continents (less than 18.2% coverage) are not conducive to agricultural activities; hence, unsuitable for a hunter gatherer to transition to a full-blown industrial civilization. *As a result, the adjusted value excluding this 18.2% from the overall range selection is 29.88%.*

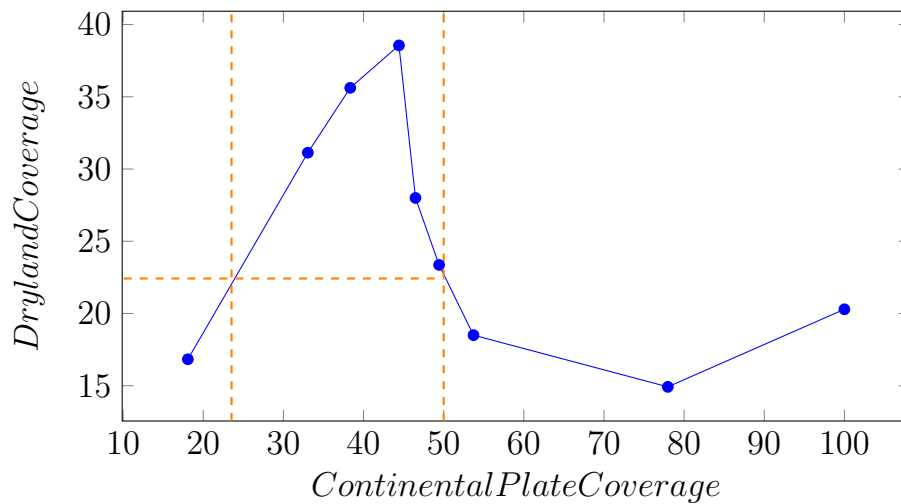


Figure 5.3: The range of dryland coverage percentage that renders glaciation possible

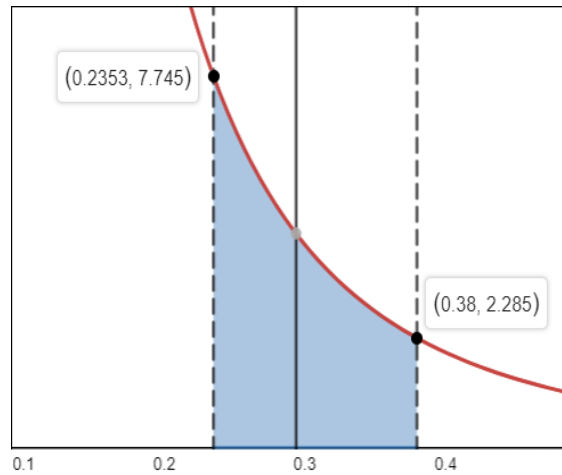


Figure 5.4: The expected timing of next glaciation event for the lower (23.53% dryland coverage) and upper bound (38% dryland coverage) coverage enabling glaciation. At the lower bound, every 228.5 Myr guarantees an ice age. At the upper bound, every 774.5 Myr guarantees an ice age, and currently 260 Myr passed since the last ice age, guaranteeing the appearance of another ice age in at most in 514.5 Myr.

Of course, the rate of emergence is non-uniform within ice age capable range from 23.53% to 38% of dry landmass coverage. The rate of emergence depends on the proportion of island continents to supercontinents at any given time. That is, more island continent configurations leads to greater biodiversity. We used a toy model representing the earth's surface by composing 9 blocks fitted in a 3 by 3 grids and assumed that land coverage ranges from 0 to 100% by running the combinations of placing 0, 1, 2, and up to 9 blocks of dryland over 9 blocks of sea. We define an island continent as an individual land block that does not touch any other land block at the top, bottom, left, and right side. Two land blocks can touch each other diagonally but it is not counted as a connected landmass because each block is well surrounded by the ocean. We define a supercontinent as three land blocks connected with each other by the top, bottom, left, or right side. Three blocks of drylands translated into 33% of land coverage, roughly equivalent to the proportion of earth's total land coverage to the surface area. Any land configurations composing more than three blocks eventually leading to a desert planet scenario is treated as a megacontinent. On the other hand, land configurations composing two blocks are labeled as mini-supercontinent, comparable to the size of Gondwana observed on earth.

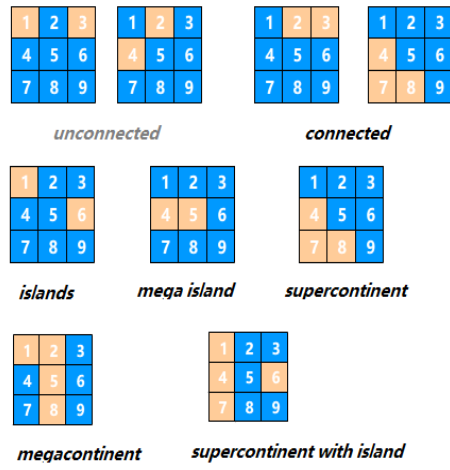


Figure 5.5: The graphically illustrated possible scenarios from the model

We first enumerated all possible combinatorial cases and the result is presented below:

Cases	Sea	land configurations	Number	Subtotal
no land	9	0	1	1
$\frac{1}{9}$ land	8	1	9	9
$\frac{2}{9}$ land	7	1+1	24	36
		2	12	
$\frac{3}{9}$ land	6	1+1+1	22	84
		2+1	40	
		3	22	
$\frac{4}{9}$ land	5	1+1+1+1	6	126
		2+2	12	
		3+1	44	
		2+1+1	28	
		5+4	36	
$\frac{5}{9}$ land	4	1+1+1+1+1	1	126
		4+1	36	
		3+2	16	
		3+1+1	16	
		2+2+1	8	
		5	49	
$\frac{6}{9}$ land	3	5+1	20	84
		4+2	8	
		3+3	4	
		4+1+1	4	
		6	48	
$\frac{7}{9}$ land	2	6+1	4	36
		7	32	
$\frac{8}{9}$ land	1	8	9	9
all land	0	9	1	1

Table 5.1: Island continent and supercontinent breakdown by percentage of land coverage

Under each case, we compute the probability of island continent formation and the supercontinent formation. Each island continent is awarded with 1 point and the multiplied by its appearance frequency within each case. A supercontinent with a size of 2 blocks is awarded with

$\frac{2}{3}$ point, a supercontinent with a size of 3 blocks is awarded with 1 point, and supercontinent with a size of 4 blocks is awarded with $\frac{4}{3}$ point. Some configurations contain a mixture of island continents and supercontinents. The probability is then computed for both island continents and supercontinents multiplied by their appearance frequency under each configuration and is added to the total probability of hosting an island continent and supercontinent under each case respectively.

The finalized curve fitting for both island continent formation probability and supercontinent formation probability is listed in the graph below:

$$y_{super} = (1.75 \tanh 2.9 (x - .65) + 1.68) \quad (5.11)$$

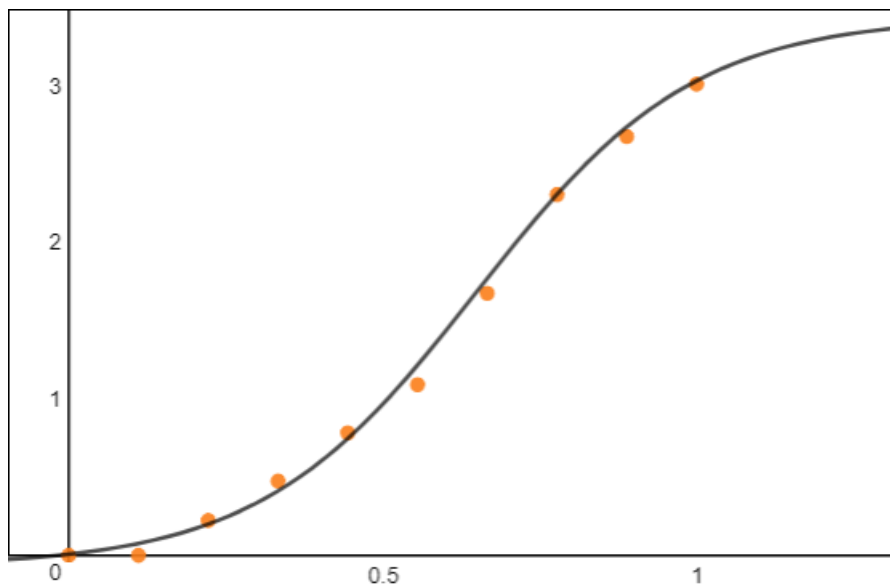


Figure 5.6: Supercontinent formation probability

$$g_0(x) = \left(\frac{0.0061}{x^{3.5} Q_{10} (2\pi)^{0.1}} e^{-\frac{(\log(x)+0.04)^2}{2 \cdot (Q_{10})^2}} \right)^{0.91} \quad (5.12)$$

$$S_{down} = 0.5 (\tanh (-7 (x - 0.7)) + 1) \quad (5.13)$$

$$y_{island} = g_0(x) \cdot S_{down} \quad (5.14)$$

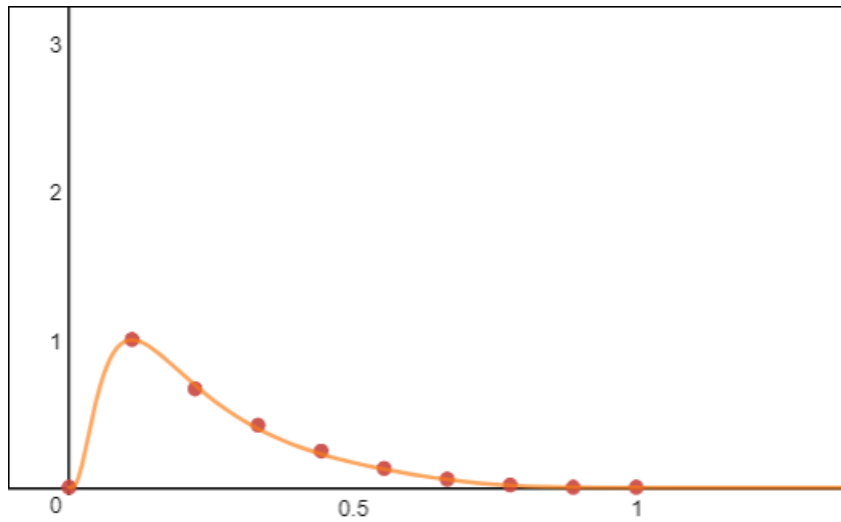


Figure 5.7: Island continent formation probability

Both graph plotted along the same axis shows that the unscaled probability is much in favor for supercontinent formation with dryland coverage greater than 33.02%. It also shows that island continent formation rate reaches its zenith at 11.08% of dryland coverage over the surface area. The crossover point occurs at 33.02% in which any less coverage by dryland results in more chance in island continent configuration and more land coverage results in more chance of supercontinent formation. In earth's case, continent's configurations are in slight favor of island continent configurations over supercontinent configurations at a chance of $\frac{0.484}{0.484+0.324} = 59.9\%$. This is confirmed through geologic history where earth goes through periodic continent and supercontinent cycles in which each period lasts half as long as the other one.

We then re-run the toy model with 4 and 4 grids, and achieved similiar results as our 3 by 3 grids. In earth's case, continent's configurations are still in a slight favor over island continent configurations over supercontinent configurations at a chance of $\frac{0.484}{0.484+0.324} = 55.36\%$, slightly lower than the previous value.

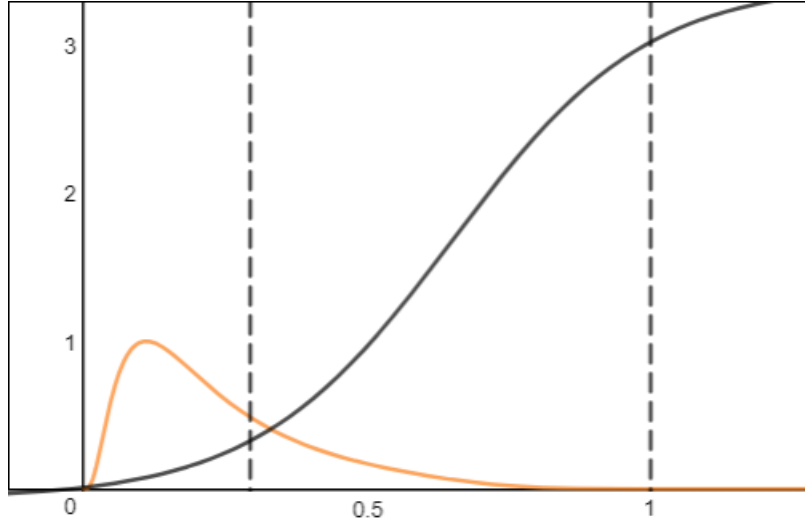


Figure 5.8: Island continent and supercontinent formation probability combined

We then apply our earlier equations accounting for the biodiversity for island and supercontinent configuration

$$y_{diversity}(x) = T_{tectonics} \left(\left(\frac{y_{island}}{y_{super} + y_{island}} \right) \cdot 34x + \left(\frac{y_{super}}{y_{super} + y_{island}} \right) (\sqrt{34x}) \cdot D_{perim} \cdot D_{inland} \right) \quad (5.15)$$

$$D_{perim} = \sqrt{0.5 - 2(x - .75)} \quad (5.16)$$

$$D_{inland} = \sqrt{0.5 - 2(x - .75)} \quad (5.17)$$

$$T_{tectonics} = \left((1 - (x + 1))^7 + 1 \right)^{50} \quad (5.18)$$

Whereas one takes the island continent formation chance divided by the composite chance of both super and island continent and multiplied by island continent biodiversity curve $34x$ and combines with the supercontinent formation chance divided by the composite chance and multiplied by supercontinent biodiversity curve $\sqrt{34x}$.

Supercontinent biodiversity is further multiplied by D_{perim} and D_{inland} . We derived earlier that the total biodiversity of supercontinent can be expressed as:

$$\pi \left(2\sqrt{mr^2}R + R^2 \right) + \pi \left(2\sqrt{mr^2}d - d^2 \right) \quad (5.19)$$

Whereas the continental shelf extends a distance of R offshore and non-extreme habitat extends a distance of d inland, and assuming $R=d$, then we have:

$$\pi (2\sqrt{mr^2R}) + \pi (2\sqrt{mr^2d}) \quad (5.20)$$

$$\Rightarrow \pi (2\sqrt{mr^2} (R + d)) \quad (5.21)$$

$$\Rightarrow r\sqrt{md} \quad (5.22)$$

One notices that the total biodiversity of supercontinent is directly proportional both the radius and the the distance d . This implies that that the biodiversity is also proportional to the perimeter of the supercontinent. The perimeter of the supercontinent increases until its coverage exceeds 50% of planetary surface. With coverage beyond 50%, the continent shore line decreases as the surface area of ocean decreases. This relationship is captured by D_{perim} . As a result, as the dryland coverage approaches 100%, the biodiversity drops in 0. Furthermore, as the size of the ocean coverage decreases, milder tropical storms are rains are less likely to bring precipitation to vast stretches of dryland. Therefore, the non-extreme habitat range also decreases. We find that D_{inland} is a good approximation to the drop of ocean's effect on land. The equation is obtained at one extreme by assuming at an ocean coverage at 71% of the planetary surface guarantees a diverse biocomplexity on land by ensuring the maintenance of the water cycle. On the other extreme, the Mediterranean Sea covering 2.5 million km^2 , or about $\frac{1}{200}$ th the surface area of earth, evaporated within a thousands years during the Messinian salinity crisis 6 Mya. We assumed that the curve touches the point (0.995, 0.1), that is, there is about 10% chance that a Mediterranean Sea sized ocean coverage is able to maintain the water cycle because the Mediterranean Sea was not completely dry during the period and Mediterranean Sea is much shallower than a typical ocean.

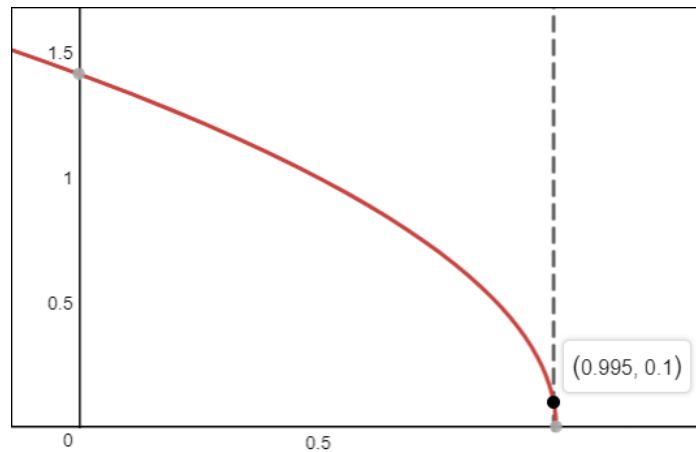


Figure 5.9: Total biodiversity curve between 0 to 58.82 percent dryland coverage

Finally, the overall diversity is multiplied by the factor $T_{tectonics}$ because we assume that a significant presence of water, acting as a lubricant, is critical in ensuring mechanism of plate tectonics, which in turn is essential in generating biodiversity in the first place. We simply assumed that no plate tectonics is possible when the entire planet is covered by 75.6% of

Land	Glaciation cycle length	Permissible range	Glaciation chance	Emergence events per glaciation cycle	Chance within a breaking up phase	Emergence rate
21.99%	2.00·Earth	0.7650	0.605	1.7255	0.6602	26.36%
24.86%	1.50·Earth	0.6670	0.655	1.0500	0.6028	18.44%
26.84%	1.25·Earth	0.6640	0.652	0.9066	0.5603	17.59%
28.29%	1.10·Earth	0.5905	0.690	0.7800	0.5263	15.22%
29.41%	1.00·Earth	0.5100	0.700	1.0000	0.5000	17.85%
30.69%	0.90·Earth	0.3700	0.812	0.5000	0.4690	7.82%
32.99%	0.75·Earth	0.3000	0.834	0.3333	0.4263	4.74%
38.00%	0.50·Earth	0.1588	0.875	0.5000	0.3025	4.20%

Table 5.2: The chance of appropriate ice age timing breakdown

The results are plotted and a step function is used for curve fitting due to the difficulty at constructing an exact fit.

$$P_{iceage} = \begin{cases} 0.00564x^4 - 0.631x^3 + 26.5x^2 - 496.3x + 3508 & 0 < x < 28.29 \\ 1.7907 \cdot 10^{14} (0.35808)^x + 4.2 & 28.29 < x < 29.34 \end{cases} \quad (5.23)$$

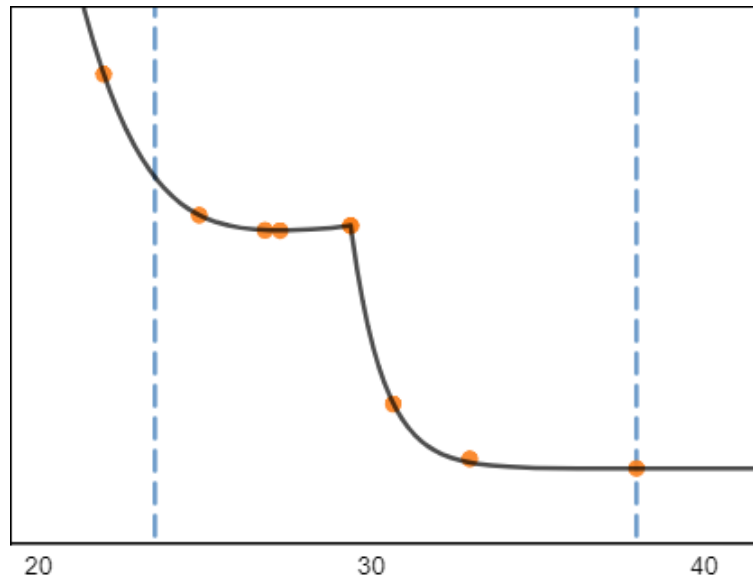


Figure 5.11: The chance of appropriate ice age timing curve between 15 to 50 percent dryland coverage

One can draw several conclusions based on the data. First of all, the percentage of permissible range of supercontinent cycle placement within its glaciation cycle grows as the duration of

the hiatus between episodes of glaciation grows. As a consequence, greater land mass coverage with shorter, more frequent ice age cycle results lower percentage of permissible ranges which only occur at the late times of the cycle. Therefore, the weighted chance of glaciation within the permissible placement decreases as the land mass coverage decreases. Emergence events per glaciation cycle, in general, tends to increase as the cycle length grows, as the length of continent cycle becomes shorter than the length of the glaciation cycle. However, a mismatch on the length of continent and glaciation cycle can adversely effect events per cycle such that there always exists some continent cycle places itself completely on the non-permissible range when others are placed within the permissible range. This is especially true for 32.99% land coverage in which only 1 emergence event is possible out of every 3 glaciation cycle. Finally, assuming one already fixed the continent cycle to be within the permissible range of the glaciation cycle, the chance of an earth-like habitable planet currently falls on the breaking up phase of the cycle grows as the land mass coverage shrinks. We assumed that the duration of continent cycle stays the same but the ratio of island to supercontinent configuration varies. As a result, the chance of island configurations which promote greater biodiversity dominates over the supercontinent configurations with smaller land coverage. The composite effect on biodiversity and evolutionary rate for different dryland coverage are then:

$$P_{iceage} \cdot \left(\frac{y_{diversity}(x)}{y_{diversity}(10)} \right)^4 \quad (5.24)$$

with the plotted graph:

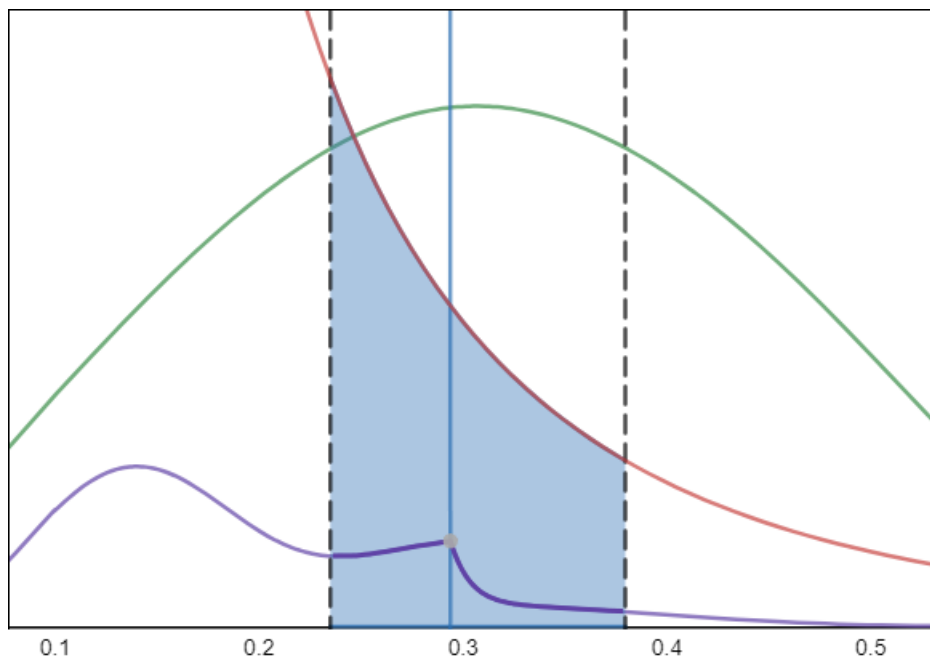


Figure 5.12: The composite effect curve on biodiversity and evolutionary rate between 0 to 60 percent dryland coverage

The biodiversity is compared with the baseline of 29% dryland coverage as earth's case and

raised to the 4th power. The reason for quadrupling the ratio (or some power) is that an increasing biodiversity has a non-linear effect in creating further biodiversity and accelerate evolutionary change. Starting at the Quaternary glaciation, the Hominid lineage retained opposable thumb, gained bipedalism, omnivorous diets, enlarged brain, and language communication. The lineage also lost almost all of its hair. Out of these attributes, at least the retainment of the opposable thumb, the evolution of omnivorous diets and the enlarged brain is strengthened by the increasing biodiversity of the Cenozoic era.[69] Opposable thumb in a non-arboreal habitat seem useless. However, freed hands can gather a diverse range of resources such as nectar, fruits, nuts, and grass plant roots only available since the Cenozoic and directly influenced the evolution of omnivorous diets. Feeding on omnivorous diet expedite the evolution of a larger head. With a larger cranial capacity capable of abstract and creative thinking, Hominid is able to take the advantage of its increasingly biological diverse environment by experimenting with different combination of resources. In turn, the continual success of the conscious thinking leads to further evolution of dexterous hands and a greater tolerance to a diverse range of food in a positive feedback loop. Furthermore, limited resources will prevent an arising civilization to fulfill its full potential. The Aztecs and Incas were transitioning into an agricultural society. However, a lack of domesticable games such as horses and oxes with considerable muscle strength significantly hamper the rate of their progress. With less abundant resources for manipulation and exploitation, the traits of intelligent, tool making species are less selected for by evolution since its full-blown potential cannot be realized.

Based on the final composite results, the overall chance on the appropriate ice age timing accelerating the emergence of intelligent species is approximately the same across 23 to 29 percent of dryland coverage and drops considerably beyond 31 percent. There is a slight peak around 29% land mass coverage, but in general a widening mismatch on the length of continent and glaciation cycle in both directions (especially smaller duration between glaciations) can increasingly adversely effect emerging events per cycle. A greater chance in finding oneself within an island configuration can offset the decline in number of events per cycle for smaller land coverage. However, a greater permissible placement range in smaller land coverages decreases the weighted chance of glaciation also increasingly adversely effect the chance of overall emergence. By now, one should rationalize the importance of an ice age and its non-trivial chance across all land ranges. If earth did not enter an ice age, the retainment of the opposable thumb, the evolution of bipedalism, omnivorous diets, enlarged brain, and language communication can still happen as the total biodiversity increases. However, it will occur at a much slower pace. The early bipedal Hominid lineages such as *Australopithecus Africanus* was exclusively vegetarian, based on their dental fossil records. They may nevertheless use hands to exploit more non-meat food resources, but they were not evolving toward an omnivorous diet. The unpredictable change of climate during a glaciation can cause a drastic change of fauna in their habitat within a generation's time, and the adoption of an omnivorous diet can be a choice between life and death. Hominid can only obtain their energy from meat in certain seasons at

one extreme and only plants in certain seasons at the other extreme and anything in between. An adoption of omnivorous diet, again, is no guarantee of a quick transition toward a larger brain. If the environment is stable, natural selection places less emphasis on the emergence of a larger brain since planning, memory, abstract, creative thinking is less useful under the regime of a stable climate. As a result, an omnivorous diet will lead to a larger brain but at a much slower pace. This fact is observed in many bird species. Many omnivorous birds such as crow has EQ between human and other species. In the case of flying birds, their living range is significantly larger than land-based mammals. With the initiation of ice age, birds can choose new habitat by crossing mountain ranges, rivers, seas, and open oceans and settle into regions with more stable climate. Therefore, birds experience less selectional pressure toward the evolution of a large brain with the ability to gather information and plan for the future. Hominids, on the other hand, have no choice in the face of chaotic climate to evolve larger brain to survive since they are confined by geologic barriers of mountains, seas, rivers, and deserts.

5.4 Supercontinent Cycle and Ice Age

We have discussed earlier (Chapter 4) that the formation of supercontinent stabilizes the rate of speciation, that is making newer species more difficult to emerge. In earth's case, a cycle of the formation of the supercontinent and breaking up into smaller ones repeats. The most recent supercontinent Pangea was formed 300 million years ago and started to break up 175 million years ago. Secular continental configuration is transitioning from fragmentation toward reunification, and for the past 175 million years earth's continents were scattered as island continents, but such scattering pattern is about to end. The Indian subcontinent and South America continent have already joined with Eurasia and North America respectively. Africa will join with Europe 50 million years into the future, forming the first supercontinent in 200 million years. Within 250 million years, Pangea Ultima will form and join all the continents together again; thus completing a supercontinent cycle in 550 million years. With the scattered continent configuration ending, the window of speciation opportunity closes, making future emerging species' life prospect difficult. The emergence of angiosperm (later fruit trees) and birds synchronized in time with the breaking up of Pangea, angiosperm and birds species later diversified and developed into a symbiotic relationship during the Cenozoic, along with pollinators such as bees and butterflies. Thanks to such diversification of fruit trees, arboreal primate species is able to evolve opposable thumbs, binocular vision, and partial bipedalism. Since the chance of glaciation onset at the current epoch is 1 in 2, and the onset of glaciation could have delayed as long as 235 million years into the future (in a more likely scenario), a hypothetical bipedal ape (non tool-use, non fire-control *Australopithecus Afarensis* type) then walks on the ground will face predators not only confined to Africa but the Eurasia and Indian subcontinent. Under such a scenario, the bipedal ape can be outcompeted by predators and gone extinct.

If glaciation occurred earlier during the breaking up of Pangea (though glaciation more likely to occur now than earlier, so this is the less likely scenario), the harsh climate could delay the emergence and diversification of birds and angiosperm despite greater speciation opportunity. As a result, diversification of the fruit tree and emergence of primates will occur now instead of at the earlier Cenozoic epoch. By the time a bipedal ape (non tool-use, non fire-control *Australopithecus Afarensis* type) evolved 50 million years into the future as Africa continent shifts north, it will again face predators not only confined to Africa but the Eurasia, Americas, and Indian subcontinent. More importantly, the rejoining of the continents eventually reduces the living space of all species as the interiors of the merging supercontinent subject to more climate the temperature fluctuation extremes. As a result, human will face significant challenges under such scenario.

Therefore, we have three constraints on the secular placement of the supercontinent cycle on the existing glaciation cycle, and we define a complete cycle as a breaking up phase of a supercontinent followed by a rejoining phase.

1. The previous glaciation must occur at or before the onset of the current breaking up phase of the cycle, minimizing possible disturbances on the biodiversity increase during the island continent phase.
2. It is assumed that in the last 200 Myr on any earth like planet, it requires, on average, 170 Myr to generate the biodiversity as we observed on earth today.
3. The following glaciation must occur at or before the biodiversity reaches its maximum and began returning toward a supercontinent configuration.

With the constraints listed above, the possible secular placement of supercontinent cycle ranges from 0 Myr to 221 Myr after the termination of the previous glaciation. It can be no later than 221 Myr because we assumed that it takes 179 Myr to generate the biodiversity of the Cenozoic at the current epoch. The following glaciation is guaranteed to occur 400 Myr after the previous one and lasts another 50 Myr, completing an ice age cycle in 450 Myr. Therefore, $400 \text{ Myr} - 179 \text{ Myr} = 221 \text{ Myr}$ is the latest possible placement. Then, one can see that only $\frac{221 \text{ Myr}}{400 \text{ Myr}} = 51.1\%$ of the possible glaciation cycle can potentially foster the emergence of an intelligent creature. This implies that the emergence of intelligence can only occur at the later phase of any glaciation cycle when the chance of the next glaciation reaches from 40% to 100%. *Therefore, on average, the chance of glaciation contributing to the emergence of human is 70%.* This is a revision from our prediction from section 5.3. This is more generalized and more accurate than our earlier calculation for earth's unique secular placement of supercontinent cycle over the glaciation cycle (89 Myr following the Karoo ice age).

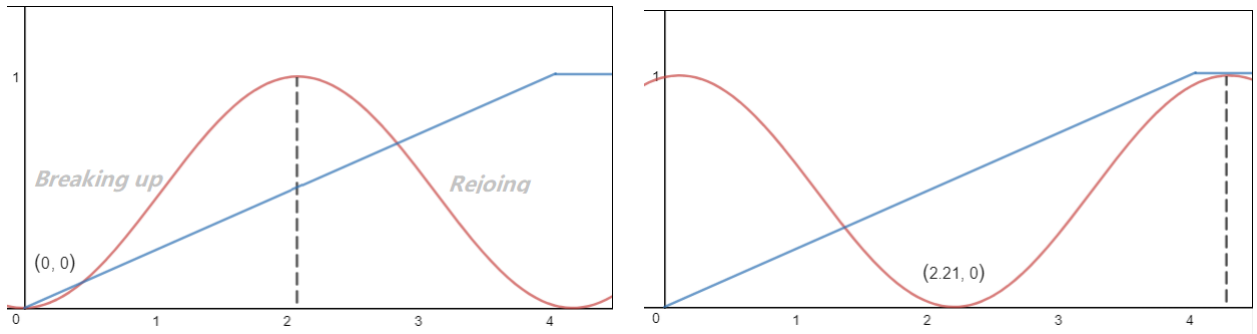


Figure 5.13: The permissible placement range for the supercontinent cycle: from immediately after the last glaciation up to 221 Myr after the previous glaciation

Within a breaking up phase of the supercontinent cycle, the probability of giving the emergence of intelligence is non-uniform. Three critical factors the rate of the biodiversity increase, the biocomplexity transformation, and the increasing chance of the next onset of ice age determine the final probabilistic outcome on the chance of emergence. We define the biodiversity increase as the derivative of the supercontinent cycle. As the breaking up phase initiates, the rate of biocomplexity increases. The rate of increase decreases to 0 as the breaking up phase terminates, and the maximum is reached at the midpoint.

$$w_{continent} = 0.5 \sin 1.5 (x + 2.25) + 0.5 \quad (5.25)$$

$$y_{diversitychange} = \frac{d}{dx} w_{continent} \quad (5.26)$$

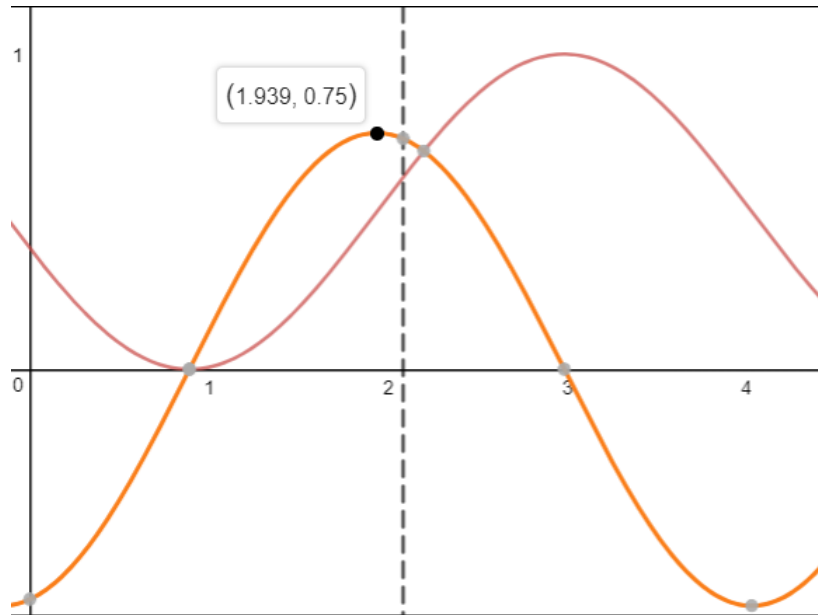


Figure 5.14: According to this simplified model, the rate of biodiversity change turns positive at 170 Mya in the mid Jurassic when Pangea started to break apart and peaked at 193.9 Myr after the Karoo ice age, or 66.1 Mya at the end of Cretaceous, and the rate of biodiversity change turns negative again in 38.6 Myr when Africa joined with Europe and Asian joined with North America.

The biocomplexity transformation factor, which is discussed in Chapter 6 and Chapter 7, basically states that the total biodiversity increases over time at the rate of 2.76 per 100 Myr. That is, the number of species within all genera and new genera increases by 2.76 folds in 100 Myr. Finally, one applies the increasing chance of the onset of the next glaciation. The composite curve pushes the maximum likelihood of the emergence to 160 Myr after the start of the breaking up phase.

$$y_{emergeman} = \frac{1}{0.75} \frac{d}{dx} w_{continent} \cdot \left(\frac{1}{30} \cdot 2.76^x \right) y_{ice} \quad (5.27)$$

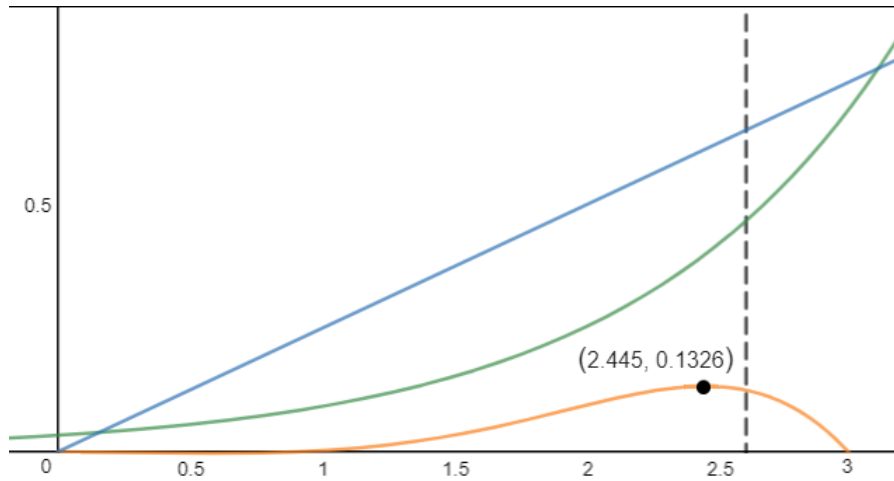


Figure 5.15: The rescaled biocomplexity transformation factor and glaciation occurrence probability curve applied to the simplified model of the rate of biodiversity change shows that the peak of the likelihood of the emergence of man is 15.5 Mya, at the mid Miocene.

This is fairly close to our current time. Since the constraint requires that the next glaciation to occur 170 Myr after the diversification of species, preparing for the emergence of intelligence, up to the time when the breaking up phase ends, then we derived the probability on the appropriate timing for the onset of ice age acting as an accelerator at this period ± 15 Myr to be 21.20%.

$$y_{emergeman} = \frac{1}{0.75} \frac{d}{dx} w_{continent} \cdot \left(\frac{1}{30} \cdot 2.76^x \right) \quad (5.28)$$

$$\frac{\int_{2.3}^{2.6} y_{emergeman} dx}{\int_{0.742}^{2.836} y_{emergeman} dx} \quad (5.29)$$

$$= 0.21199314716 \quad (5.30)$$

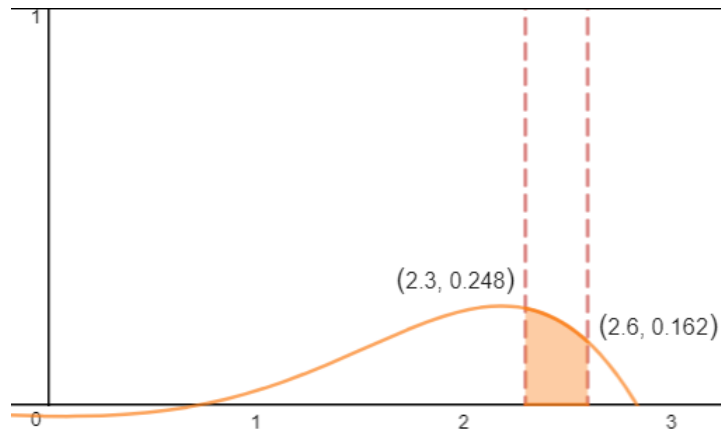


Figure 5.16: The emergence of intelligence toward the late times of the breaking up phase is favored

This shows that, regardless of the temporal placement of supercontinent cycle relative to the glaciation cycle within the permissible ranges, the emergence of intelligence toward the late times of the breaking up phase is favored. Nevertheless, there is a nearly 80% chance of glaciation happening earlier during the breaking up phase of the cycle if it were to occur at all (but its chance of occurrence is lower than the average chance of glaciation within the permissible range of 70%), disrupting the chance of the emergence of human.

One yet to address the fact that the highest probability of emergence predicted to occur earlier at mid Miocene. This implies that all earth like planet undergoing a breaking up phase which initiated 170 Mya should emerge earlier than us. This seemingly contradiction is resolved if one considers the timing of the emergence of Homo sapiens. If Homo sapiens emerged 15 to 1 Mya, at a time when Africa was still separated by the sea from Asia, the Bering strait were wider, and the isthmus of Panama still did not yet exist, they will have much more difficulty in migration and colonization of the surface of the planet. One can then speculate, on many planets that are undergoing similiar transformation as earth but with earlier emergence, the intelligent species, though fully emerged, is stucked on their own continent, still separated by wide bodies of ocean, and have to wait for another 15 Myr to 1 Myr before they rejoin and cross over. As a result, they arose early but their domination of the planetary surface proceed at the same time as ourselves. Furthermore, the factors enabling human domination is actually bidirectional. Majority of domesticated crops and animals originated outside of human's native Africa. Ancestors of dogs, horses and camels first evolved in North America and crossed into Asia and later Africa 8 Mya. Cats and chickens evolved in Asia. Only sheeps, goats, and buffalo were found in both Asia and Africa. All major crop plants originated from North America except potato evolved in South America. In fact, the spread of grassland may well be a consequence of fauna migration out of North America. Without the rejoining of the continents, grassland may not even evolve in Africa by 2 Mya. This is intriguing because it shows that it is not a coincide that we find ourselves dominating the planet at a particular time

as it is now. Whereas the island continent configuration is just starting to transition toward a supercontinent configuration and all continents are just barely connected to each other. Having determined the permissible secular placement of continent cycle relative to the glaciation cycle and the probability of the occurrence of life within the breaking up phase of the cycle. We can now think the glaciation cycle and the supercontinent cycle as one interwoven cycle. The current time, represented as a point on the interwoven cycle, can occur at the breaking up phase or the rejoining phase of the continent cycle. For the simplicity of the model, we assume that each phase lasts half as long of the entire cycle, though, we have shown earlier in Section 5.3, that 29% of dryland coverage results in 59% breaking up configuration and 41% supercontinent configurations. As a result, the chance that current time period falls on a breaking up phase on all earthlike planet is simply 50%.

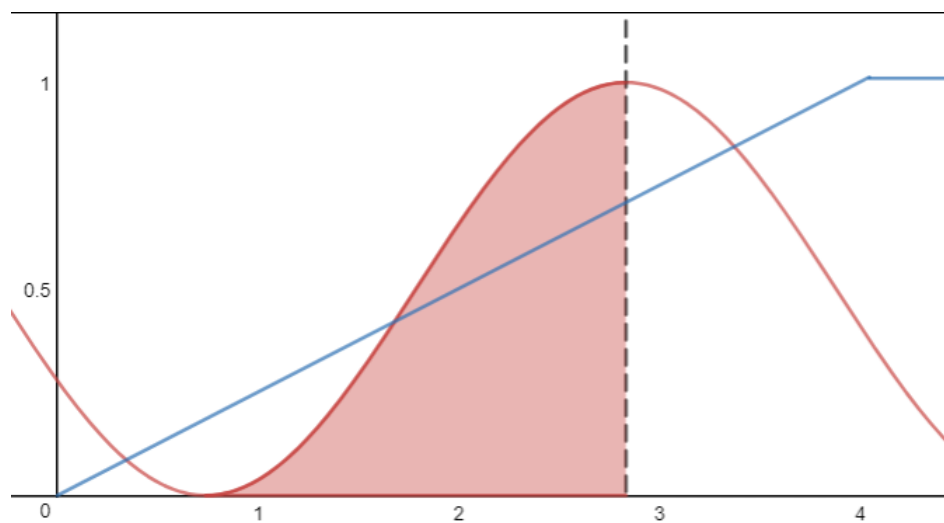


Figure 5.17: The chance of current time falling on the beaking up phase of the supercontinent cycle is 50%

In order to illustrate the possible cycles on planet covered by less or more land, the following sinusoidal wave and their graph is shown. It can be seen that as dryland coverage decreases, the phase of island configuration dominates over the supercontinent phase, and vice versa. Of course, in reality, the cycles are not necessarily perfectly sinusoidal, but the macro trend stays. Moreover, it is also to note the probability of glaciation increases slower throughout the glaciation cycle in the case of less dryland coverage, and the probability of glaciation approaches 1 throughout all periods in the case of more dryland coverage.

$$y_{\text{nearlyoceanplanet}} = 2(0.5 \sin x + 0.45)^{0.2} + 1.13$$

$$y_{\text{earthtypical}} = 1.55 \sin x + 1.55$$

$$y_{\text{nearlydesertplanet}} = 5.6 \cdot 10^{-15} (1.55 \sin x + 1.55)^{30}$$

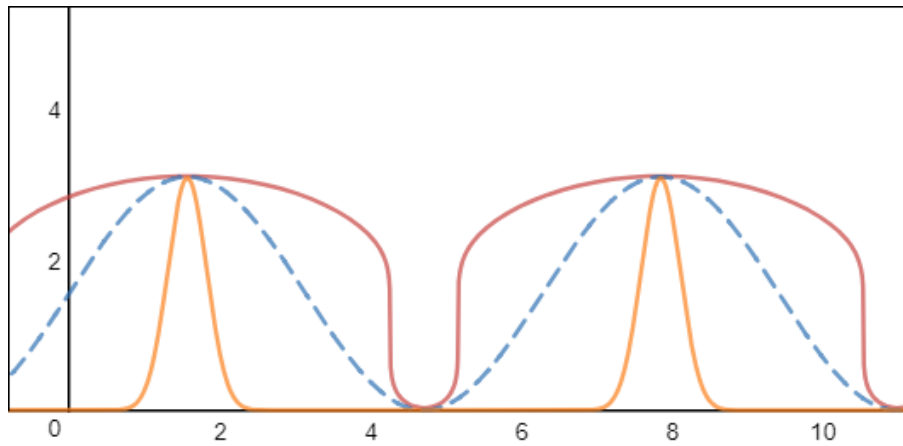


Figure 5.18: Nearly ocean planet, earth typical (dashed), and nearly desert planet continent cycle

As a result, one can confirm that glaciation at the right time and its subsequent consequence on habitat change otherwise taking geologic time scale serves as an accelerator rather than a detractor. If one assumes that the emergence of hominid line 15 Mya is the start of the opportunity window for the onset of an ice age acts as an accelerator, then the opportunity window ends with Africa colliding into Eurasia and the closing the Mediterranean ocean in 15 million years.

$$P_{\text{permissibleRange}} \cdot P_{\text{endofbreakingphase}} \cdot P_{\text{chanceinbreakingphase}} \tag{5.31}$$

$$0.511 \cdot 0.212 \cdot 0.50 \tag{5.32}$$

$$= 0.054166 \tag{5.33}$$

Then, only 5.4166% of an expected ice age interval will ice age results in accelerated evolutionary pace.

5.5 The Probability of the Hominid Lineage

In order to compute the probability of giving rise to Hominid lineage, we can not simply pick our denominator as the current total number of living species of birds, mammals, and reptiles. Neither can we use computational molecular biology, we have shown already that species can adapt and evolve quickly to changing environment (Chapter 4). A suitable sequence of quick environmental change can accelerate the evolution of Homo sapiens in timescale much faster than even those we have observed. If earth's environment is the brake, the pacemaker, and the cookie cutter of evolution, then the success and the pervasiveness of each trait leading to Homo sapiens adapted to each niche is the key in understanding our likelihood of emergence.

What we really need to evaluate is the probability of each particular trait that is critical for the emergence of an intelligent tool-using species. Since each trait is largely independent of other traits, then the probability of *Homo sapiens* can be defined as the product of the probabilities of each trait. Caveats must be thrown, however, because the probability of each trait inevitably depends on current cohorts of species which adapted to the current climate, the probability of animals possessing these traits can fluctuate throughout different epochs of earth's history. (Even if one were to use the current data samples, the megafaunal mass extinctions of 10,000 BP may have distorted our calculation since extinctions across all major land masses are correlated with the arrival of human.) Each of these traits has been observed in at least one species since Mesozoic, but no species possessed all of them at once until the emergence of man. This observation indicates that each trait is a local evolutionary maximum where life converged to quickly and arose early. Certain traits, such as opposable thumbs and bipedal locomotion, can be inversely correlated. That is, advancing forest gives more opportunity to thriving arboreal residents but squeezes the living space of land-based bipeds on grasslands. If it holds, then, the total probability giving rise to *Homo sapiens* does not deviate in orders of magnitudes throughout all time periods because certain characteristics become more common at the expense of rendering other traits rarer. However, in the long run, more species are appearing from geologic data records, and if more species are appearing within every niche, then the total probability should remain constant if every other condition stays the same. Ultimately, to adequately sample the probability of each trait throughout the entire Mesozoic and Cenozoic, its mean value, and its relationship with climate change, and the general trend over time is critical. The most tantalizing problem though is that, even by sampling data across all time period, our picture may remain incomplete in regards to the actual probability giving rise to intelligent, tool-using species. It is possible that in the real course of evolution, not all possible paths and combinations were adopted by nature. In fact, nature only tried the combination of a particular subset of opposable thumb (excluding those of panda and tree frog and favoring the primate family). It tried a particular type of bipedal locomotion (excluding bipedal locomotion observed in birds, hopping animals such as the kangaroo), a particular type of language communication using larynx vocalization, and a particular type of brain structure (mammalian brain with neocortex). It is also possible for nature to adapt all possible combinations but it requires significantly more time than we observed and requires a length of period beyond the habitability of the planet. All of these are problems for future paleontologists and researchers and is beyond the scope of this paper.

5.5.1 Binocular Vision

The first trait we need to compute for its probability is the binocular vision. Binocular vision creates depth perception and is found in Primates for fruit searching and arboreal locomotion. Carnivora and birds of prey used depth perception for prey capture.

Mammal	Species	Bird	Species
Primate	450	Accipitriformes	261
Carnivora	286	Cathartidae	7
Bats	1,240	Strigiformes	200
—	—	Coraciimorphae	6
—	—	Cariamiformes	1
—	—	Falconiformes	75
Sum Total			2,526

Table 5.3: Species breakdown by binocular vision

There are 450 extent Primate species (including *Homo sapiens*), 286 extant species of Carnivora, and 1,240 species of bats. For the birds of prey, there are 261 species of Accipitriformes (1 species of Sagittariidae, 4 species of Pandionidae, 256 species of Accipitridae), 7 species of Cathartidae (New World vultures), 200 species of Strigiformes (owls), 6 species of Coraciimorphae, 1 species of Cariamiformes, and 75 species of Falconiformes (one species of Cariamidae, 63 species of Falconidae, 11 species of Polyborinae). We have an added total of 2,526 species with binocular vision.

5.5.2 Large Cranial Capacity

Next, we compute the total number of species possessing a large cranial capacity in a ratio relative to their body mass, or what one calls as high EQ. For certain animals where EQ cannot be obtained, those that passed the mirror test, which supposedly tests self-awareness, is used as a criterion for inclusion. There are 56 extant species of dolphins (with 3 species of the humpback whale, fin whale, and sperm whale). 120 species of Corvidae (including crows, raven, and magpies). 167 species of tegu lizards. 79 species of monitor lizards. 600 species of anolis lizards, 200 species of owls, 41 species of falcons, and 7 species of Hominidae, totaling 1,270 species.

Mammal	Species	Bird	Species	Reptile	Species
Dolphin	56	Corvidae	120	Tegu lizard	167
Hominidae	7	Owl	200	Monitor lizard	79
—	—	Falcons	41	Anolis lizard	600
Sum Total					1,270

Table 5.4: Species breakdown by cranial capacity

5.5.3 Language

Next, we compute the number of species possessing language communication skills. Communication can take place within water such as those generated by dolphins and whales, and in the air such as birds and bats. Species with simple alarm calls are not included in the list. The species included are those that evolved relatively more complex call systems that beyond a mere reflex, that is, it is able to synthesize new sounds based on different combination of

existing patterns and symbols. The diverse array of sound symbol manipulation may reflect an advanced overall neural developments such as human, or merely an advanced functioning of a particular organ such as the the tongue of greyparrots' used mating and social signaling. There are 1 species of Hominidae, 51 species of dolphin, 44 species of whales, 4,000 species of birds, 1,240 species of bats, totaling 5,336 species.

Mammal	Species	Bird	Species
Hominidae	1	Song birds	4,000
Dolphin	51	—	—
Whales	44	—	—
Bats	1,240	—	—
Sum Total			5,336

Table 5.5: Species breakdown by language communication

5.5.4 Bipedal

Next, we compute the number of species capable of bipedal locomotion. There are 59 species of macropods, 20 species of kangaroo rats and mice, 3 species of springhares, 5 species of hopping mice, 1 species of pangolins, 1 Hominidae, and all species of birds (10,000 species), totaling 10,089 species.

Mammal	Species	Bird	Species
Macropods	65	Birds	10,000
Kangaroo rats and mice	22	—	—
Springhares	2	—	—
Hopping mice	4	—	—
Pangolins	8	—	—
Hominidae	1	—	—
Sum Total			10,089

Table 5.6: Species breakdown by bipedal locomotion

5.5.5 Thumbs

Next, we compute the number of species possessing opposable thumbs. All such species have adapted to arboreal locomotion. There are 145 species of old world monkeys, 7 species of Hominidae, 18 species of gibbons, 2 species of giant pandas, 6 species of pencil-tailed tree mice, 4 species of Vandeleuria, 9 species of hopping mice, 28 species of Phalangeridae, 1 species of koala, 103 species of opossums, and 30 species of tree frogs, totaling 353 species.

Mammal	Species	Mammal	Species
Old world monkeys	145	Pencil-tailed tree mouse	6
Hominidae	7	Vandeleuria	4
Gibbons	18	Hopping mouse	9
Giant panda	2	Phalangeridae	28
Opossums	103	Koalas	1
Sum Total			353

Table 5.7: Species breakdown by opposable thumbs

5.5.6 Social

Next, we compute the number of species that developed social organizations. The social organization has to be complex enough to extend beyond the immediate family members. The ability to organize and cooperate for the common good is a necessary step before the adaptation to a much more complex organization as those created by *Homo sapiens*. There are 3 species of phodopus, 1,240 species of bats, 21 species of cockatoos, 42 species of Callitrichidae, 18 species of tamarins, 22 species of marmosets, 45 species of corvus, 53 species of dophins, 4 species of elephants, 1 species of starling, 103 species of gerbils, 1 species of guinea pigs, 7 species of hominidae, 7 species of horse, 4 species of hyenas, 1 species of killer whales, 63 species of rabbits, 1 species of lion, 1 species of meerkat, 1 species of orange-fronted parakeet, 3 species of paracheirodons, 152 species of Tetra, 21 species of penguins, 10 species of Psittacidae, 1 species of sea otter, 64 species of rats, 1 species of wolves, and 1 species of Zebra finch. The number of social species totaled 1,901 species. It is 3,586 species if one considers all primates and 1,000 species of migratory birds as social animals.

Mammal	Species	Mammal	Species	Bird	Species
Phodopus	3	Gerbil	103	Cockatoos	21
Bats	1240	Guinea pigs	1	Corvidae	120
Primate	445	Hominidae	1	Starling	1
dwarf mongoose	1	Horse	1	Orange-fronted parakeet	1
naked mole rat	1	Hyena	4	Penguin	21
Dolphin	53	Killer whales	1	Psittacidae	148
Elephants	4	Rabbits	1	Zebra finch	1
Meerkats	1	Lion	1	Stork	19
Sea otter	1	Rats	64	Crane	15
Wolf	1	Mole rats	1	Migratory birds	1,000
Elephant seals	2	Zebra	3	Common pheasant	1
Red deer	1	Wildebeests	2	Greater rhea	1
African bufallo	1	Sheep	1	-	-
Bison	1	Goat	1	-	-
Lion	1	-	-	-	-
Sum Total					3,586

Table 5.8: Species breakdown by prosocial characteristics

5.5.7 Omnivorous Feeding

Finally, we compute the number of species possessing omnivorous feeding behaviors.

First, we count the number of omnivorous mammals. Among mammals, there are 1 species of pig, 11 species of badgers, 8 species of bears, 4 species of coati, 20 species of civets, 17 species of hedgehogs, 103 species of opossums, 12 species of skunks, 6 species of sloths, 285 species of squirrels, 1 species of raccoon, 25 species of chipmunks, 30 species of mice, 64 species of rats, 7 species of Hominidae, 385 species of tree shrews, and 43 species of Erinaceidae, 103 species of Gerbil, totaling 1,125 species. The majority of mammals are either herbivores or insectivores, the proportion of omnivores are lower than birds.

Species	Number	Species	Number	Species	Number
Pig	1	Opossum	103	Mouse	30
Badger	11	Skunk	12	Rats	64
Bear	8	Sloth	6	Hominidae	7
Coati	4	Squirrels	285	Tree shrews	385
Civet	20	Raccoon	1	Erinaceidae	43
Hedgehog	17	Chipmunk	25	Gerbil	103
Sum Total					1,125

Table 5.9: Omnivorous mammal species

Secondly, we count the number of omnivorous birds. We do not have an accurate description of all species of birds with an omnivorous diet, but we do have the catalog of species of birds that have more specialized dieting habits. Therefore, we will work our way backward. Among carnivores, there are 60 species of eagles, 200 species of owls, 31 species of shrikes. Among Crustacivores, there are 1 species of crab plover and 212 species of rails. 16 species of detritivores. Among folivores, there are 1 species of hoatzin and 6 species of mousebirds. Among frugivores, there are 26 species of turacos, 240 species of tanagers, 42 species of birds-of-paradise. Among granivores, there are 146 species of geese and 25 species of grouses, 142 species of estrildid finches. Among herbivores, there are 8 species of whistling ducks, 1 species of ostrich, and 1 species of mute swan. Among insectivores, there are 177 species of cuckoos, 83 species of swallows, 150 species of thrushes, 25 species of drongos, and 240 species of woodpeckers. Among Nectarivores, there are 1,039 species of hummingbirds, 132 species of sunbirds, and 58 species of lorikeets. Among piscivores, there are 4 species of darters, 5 species of loons, 8 species of pelicans, 20 species of penguins, and 19 species of storks. Among sanguinivorous, there are 2 species of oxpeckers and 1 species of sharp-beaked ground finch. Among Saprovores, there are 16 species of vultures and 37 species of crows. The number of non-omnivorous bird species totaled 3,174. Since there are 10,000 species of birds, the number of omnivorous bird species totaled 6,826, proportionally significantly higher than mammals.

Carnivores		Crustacivores		Detritivores	
Eagles	60	Crab plover	1	–	16
Owls	200	Rails	212	–	–
Shrike	31	–	–	–	–
Folivores		Frugivores		Granivores	
Hoatzin	1	Turacos	26	Geese	146
Mousebirds	6	Tanager	240	Grouse	25
–	–	Birds-of-paradise	42	Estrildid finches	142
Herbivores		Insectivores		Nectarivores	
Whistling ducks	8	Cuckoo	177	Hummingbirds	1,039
Ostrich	1	Swallows	83	Sunbirds	132
Mute swan	1	Thrush	150	Lorikeets	58
–	–	Drongos	25	–	–
–	–	Woodpecker	240	–	–
Piscivores		Sanguinivorous		Saprovores	
Darter	4	Oxpecker	2	Vultures	16
Loon	5	Ground finches	1	Crow	37
Pelican	8	–	–	–	–
Penguin	20	–	–	–	–
Stork	19	–	–	–	–
Sum Total					3,174

Table 5.10: Non-omnivorous birds

Thirdly, we count the number of omnivorous reptiles. Turtles (327 species) are predominantly omnivorous. They are exclusively carnivorous before reaching adulthood and herbivorous once reaching adulthood. Tortoises (155 species), or land-based turtles, are herbivorous. 98 percent of lizards (the rest are herbivores), snakes, and worm lizards are carnivorous, totaling 9,600 species. All species of Crocodylia (25 species) are carnivorous.

Omnivorous	Species	Carnivores	Species	Herbivores	Species
Turtles	327	Snakes	–	2% of Lizards	30
–	–	98% of Lizards	–	–	–
–	–	Worm lizards	–	–	–
Sum Total					10,108

Table 5.11: Reptile species breakdown by feeding behaviors

Among 10,108 species of reptiles, only 327 species are omnivorous. Reptiles are predominantly carnivorous.

The total number of omnivorous species then numbered 8,175 species.

Before we proceed, we do need to verify that the traits are independent from each other. In order to confirm, one needs to take a combinatorial approach and find the product of the probability of two traits out of all listed and denote the probability as $P_{predicted}$. One then needs to manually examine the species that indeed share both traits and divided by the total number of species we counted, which is 25,483 and denote the probability as P_{actual} . One could take the combinatorial up to the product of no more than three traits because the product of thumb, brain, and binocular vision yields the predicted number of species among 25,483 is only 1.67. If one were continue to multiply with additional traits, it will take a larger cohorts of all extent species to verify the prediction which is not unavailable to us. If $P_{predicted} = P_{actual}$, it implies that the two traits are exactly independent from each other as mathematics would predict. If $P_{predicted} > P_{actual}$, it implies in reality these two traits are more unrelated than mathematics would predict. if $P_{predicted} < P_{actual}$, it implies that two traits are dependent on each other, so they are not independent variables. We define relatedness by $R = \frac{P_{actual}}{P_{predicted}}$ and ranked them in the order of the most related to the least. Finally, we want to find the total product of all R, as:

$$T = \prod_{n=0}^m R_n \quad (5.34)$$

Whereas:

$$T \neq \frac{P_{actual}(Trait_0, Trait_1, Trait_2 \dots Trait_n)}{\prod_{n=0}^m Trait_n} \quad (5.35)$$

T does not equal to the number of observed species over the total product of the probabilities of all traits. In can be illustrated from a simple example by assuming one wants to define T as the total product of all R for cross examination of the traits of omnivorous, binocular, bipedal, and social.

$$R_0 = \frac{P_{actual}(O_m, b_{inocular})}{O_m \cdot b_{inocular}} \quad (5.36)$$

$$R_1 = \frac{P_{actual}(O_m, b_{ipedal})}{O_m \cdot b_{ipedal}} \quad (5.37)$$

$$R_2 = \frac{P_{actual}(O_m, S_{ocial})}{O_m \cdot S_{ocial}} \quad (5.38)$$

$$T = \prod_{n=0}^m R_n = \frac{P_{actual}(O_m, S_{ocial}) \cdot P_{actual}(O_m, b_{ipedal}) \cdot P_{actual}(O_m \cdot b_{inocular})}{O_m^3 \cdot S_{ocial} \cdot b_{ipedal} \cdot b_{inocular}} \quad (5.39)$$

$$T \neq \frac{P_{actual}(O_m \cdot S_{ocial} \cdot b_{ipedal} \cdot b_{inocular})}{O_m \cdot S_{ocial} \cdot b_{ipedal} \cdot b_{inocular}} \quad (5.40)$$

Trait 1	Trait 2	$P_{predicted}$	P_{actual}	R
thumb	binocular	0.00137	0.00679	4.94412
social	binocular	0.01395	0.06636	4.75719
social	thumb	0.00195	0.00667	3.42227
social	language	0.02844	0.09453	3.32407
omnivorous	bipedal	0.12861	0.26790	2.08308
language	binocular	0.02003	0.04140	2.06663
brain	binocular	0.00472	0.00973	2.06087
bipedal	language	0.08001	0.15701	1.96229
omnivorous	language	0.06565	0.10719	1.63269
social	brain	0.00670	0.00712	1.06242
omnivorous	thumb	0.00450	0.00432	0.95927
social	bipedal	0.05571	0.05298	0.95088
omnivorous	social	0.04571	0.03487	0.76279
bipedal	brain	0.01886	0.01421	0.75317
language	brain	0.00963	0.00685	0.71125
bipedal	binocular	0.03924	0.02162	0.55096
thumb	brain	0.00066	0.00027	0.41625
omnivorous	brain	0.01548	0.00498	0.32204
thumb	language	0.00280	0.00075	0.26633
omnivorous	binocular	0.03220	0.00263	0.08165
thumb	bipedal	0.00548	0.00039	0.07155

Table 5.12: Cross examination

The ranking indicates that opposable thumbs, binocular vision, social, and language are not independent from each other. They are more likely to find on the same species occupying the arboreal niche. Social & language are highly related because the majority of the song bird species are social. Omnivores & bipedalism and language & bipedalism are related because the majority of the bipedal species are song birds feeding on an omnivorous diet. Language & binocular vision are related because mini bats using echolocation and binocular vision to capture its tiny insect prey comparable to its own body size. Large cranial capacity & binocular vision is related because predatory bird species feeding on meat also requires considerable flexible intelligence to catch its prey comparable to its own body size. High protein intake also enables predatory birds to gain a larger brain, completing a positive feedback loop. On the other end of the spectrum, one finds that bipedalism & brain are more unrelated than prediction since most bipedal bird does not have a large brain. Language & brain is not as related because many mini-bats species uses echolocation for survival but no large brain is needed to capture insects which are proportionally small compare to its own body size. Bipedalism & binocular vision is unrelated mainly because most birds species are non-predatory on other bird species. Additionally, all bat species with binocular vision are non-bipedal. Thumb & brain is unrelated because the majority of the intelligent species such as dolphins, corvidae, owls do not possess thumb and does originate from arboreal habitats. Omnivorous diet & brain are not related since high protein intake with meat guarantees more energy can be invested to the development of the brain. Human is utterly an exception in this case. Some speculate that human's initial enlargement of the brain is due to extraction of bone marrow by using tool. This is a rather peculiar route at achieving a larger brain rather than the typical path of first becoming a carnivore. Thumb & language are not related because many species with a highly developed auditory capacity such as song birds and mini-bats do not possess opposable thumbs. Language seems to be evolved in the settings of dim light environment (echolocation in nocturnal bats and dolphin) and social interactions (song birds, raven, and human) in species experiencing lesser predatory pressures. Most arboreal primates are diurnal and social but quiet to avoid predation in open day light. The benefit of language communication must outweigh the cost of broadcasting one's location. This can be achieved in species subject under fewer predations, or species formed a very strong defense system against predators. Omnivorous diets & binocular vision are unrelated because binocular vision is essential and critical on the survival of predatory carnivorous species. Binocular vision is evolved in the arboreal habitat, and primates using binocular vision to thrive on the trees and feeds on a frugivorous diet. Therefore, frugivorous diet and carnivorous diet are the peaks in a landscape of binocular vision utilization and omnivorous diet sits in the deep valley. There is no evolutionary pressure for omnivores to acquire depth perception for capturing its prey. Ultimately, thumb and bipedal are highly unrelated because all bird species does not possess a thumb and all mammalian species possessing opposable thumb thrives in an arboreal habitat. Finally, we find the total product of all traits cross-examined:

$$T = \prod_{n=0}^m R_n = 0.07 < 1 \quad (5.41)$$

and we find the total product is less than 1, this implies that though some of the traits cross-examined are dependent on each other, so they are not independent variables. Other traits such as thumb & bipedalism is so rare in nature that these two traits are highly unrelated than mathematics would predict. Therefore, the overall result concludes that all traits possessed by human is largely independently related from each other.

We then apply the traits cross examination for 3 traits combined (we only listed some of the most related and the least related):

Trait 1	Trait 2	Trait 3	$P_{predicted}$	P_{actual}	R
binocular	thumb	social	0.0002	171	34.7279
binocular	language	social	0.0028	1055	14.6860
binocular	cranial	bipedal	0.0019	242	5.0794
cranial	language	social	0.0014	175	5.0543
binocular	cranial	thumb	0.0001	7	4.1993
language	bipedal	omnivorous	0.0260	2731	4.1239
language	social	omnivorous	0.0092	890	3.7794
cranial	thumb	social	0.0001	7	2.9580
cranial	social	omnivorous	0.0022	121	2.1804
bipedal	social	omnivorous	0.0181	923	2.0003
binocular	bipedal	thumb	0.0005	1	0.0722
binocular	social	omnivorous	0.0045	8	0.0693
bipedal	thumb	social	0.0008	1	0.0508
language	thumb	omnivorous	0.0009	1	0.0432
binocular	cranial	language	0.0010	1	0.0411
language	bipedal	thumb	0.0011	1	0.0354
bipedal	thumb	omnivorous	0.0018	1	0.0220
binocular	bipedal	social	0.0055	1	0.0071
binocular	language	omnivorous	0.0065	1	0.0060
binocular	language	bipedal	0.0079	1	0.0049
binocular	bipedal	omnivorous	0.0127	1	0.0031

Table 5.13: Cross examination

The results shows both more correlated features and more independent features at both extremes. Binocular & thumb & social traits defines the primates. Binocular & language & social defines bats. Binocular & cranial & bipedal defines predatory birds. Binocular & cranial & thumb defines the Homininid. At the other extremes, binocular & bipedal & omnivorous is rare in any species because predatory birds always eat meat, omnivorous bird not binocular, chimps are not bipedal. Binocular & language & bipedal is rare because predatory birds do

not communicate, song birds do not possess binocular vision, hominid are not bipedal except human. Binocular & language & omnivorous are rare because song birds do not possess binocular vision. Binocular & bipedal & social are rare because predatory birds not social. Bipedal & thumb & omnivorous rare because birds did not evolve from the trees and possess no thumb. Language & bipedal & thumb are rare because birds do not possess thumbs and primates generally are quiet. Binocular & cranial & language is rare because most Homininid produces no speech, predatory birds possess limited language capability, bats has small brain, dolphin has no binocular vision. Language & thumb & omnivorous is rare because birds possessed only wings and most primates are non-omnivorous. Bipedal & thumb & social are rare because birds only possess wings, and primates except human are non-bipedal.

The overall result concludes that all traits possessed by human is largely independently related from each other.

$$T = \prod_{n=0}^m R_n = 3.5791 \cdot 10^{-14} < 1 \quad (5.42)$$

There is 25,483 total number of extant species of birds, mammals, and reptiles (5,450 species of mammals, 9,925 species of birds, and 10,108 species of reptiles). So the total probability is computed as the follows:

$$p = \frac{1}{\prod_{n=0}^m Trait_n} \quad (5.43)$$

$$p = \left(\frac{25,483}{2,526} \right) \left(\frac{25,483}{1,214} \right) \left(\frac{25,483}{353} \right) \left(\frac{25,483}{10,089} \right) \left(\frac{25,483}{5,150} \right) \left(\frac{25,483}{8,278} \right) \left(\frac{25,483}{3,586} \right) \quad (5.44)$$

$$\begin{aligned} p &= \frac{1}{4,179,613.11129} \quad (5.45) \\ &= 2.3925659466 \times 10^{-7} \end{aligned}$$

Once we computed the total probabilities of all traits that made Homo sapiens unique as a tool using intelligent species, we find that nature needs to experiment on average 7,081,064 times to create a species similar to the Hominid family. One also needs to compute the total number of species of birds, reptiles, and mammals arose since the Cenozoic. At this stage, we simply took the number of fossil species along the genus Homini, which numbered 13 species and one extant living species and use it as the filter factor for every 2.85 million years. That is, on average one of out of every 13 species survived to the current day for every 2.85 million years. Then, the total number of species (birds, mammals, reptiles) ever lived since Cenozoic is 7,555,486 $(25,096 \text{ species} \cdot \frac{66 \text{ myr}}{2.85 \text{ myr}} \cdot 13)$ species, which serves as the upper bound. We apply the same methodology to the entire family of Hominidae lineage, which contains 7 extant species and 69 extinct ones. It can be inferred that on average one out of every 10.857 species survived for

every 14 million years. This means that the total number of species ever lived since Cenozoic is 1,284,534 ($25,096 \text{ species} \cdot \frac{66 \text{ myr}}{14 \text{ myr}} \cdot 10.857$), which serves as the lower bound. On average, then, there should be around 2,345,199 species of our selected cohorts ever lived since the Cenozoic based on a weighted average. This number falls below the probability of giving rise to Homo sapiens. In fact, it predicts the rise of Homo sapiens type of intelligent species 104.13 million years into the Cenozoic based on the current BER. Careful examination reveals that the ordering of the evolved characteristics of a human-like creature is important. In fact, at least two traits a large, complex brain and bipedal locomotion cannot be the initial conditions of a human-like creature. At the same time, certain traits such as the evolution of opposable thumb have to occur before the emergence of large brain and bipedalism. Other traits, such as language, sociality, and binocular vision can happen either before or after the evolution of opposable thumb. Bipedal locomotion as observed in kangaroo and birds offers great advantages that these species will not sacrifice their existing beneficial feature to trade for a lesser one just for the sake of evolving opposable thumbs. From a mathematical perspective, in order for bipeds to evolve toward a tree climbing one, it has to give up a huge local optimum choice, climbing a high cost hill before getting into another local optimum, which is somewhat an inferior choice than the one it started. In case of the large brain, or high EQ, all organism evolved high EQ requires some carnivorous diet. A species with high EQ adapt to arboreal lifestyle have to forego its carnivorous or omnivorous diet to become almost exclusively herbivorous. Such lifestyle eventually led to a reduction of EQ by natural selection, a large brain relative to body mass can no longer be maintained because the energy intake has been lowered. In some species such as the genus Homo and Elephant, the switch can be even more absurd. For species with such a large brain and body mass, trees branches, in general, do not have the strength to support. As a result, out of the seven traits listed, two of them can to be excluded from the list as non-starting initial conditions. Since ordering matters, the rest of possible choices with anyone as the initial starting traits that lead to homo sapiens can be expressed as a simple permutation $n!$. $5!$ equals 120 possible paths leading to Homo sapiens. However, $7!$ equals 5,040 possible paths is also important. It shows that only $\frac{1}{42}$ out of all paths leading to Homo sapiens (not starting with big brain and bipedalism). If we consider at least some species with large EQ with a small light body can somehow adjust such as anolis lizards, we can also consider excluding bipedal trait only, that leaves us $6!$ which equals 720 possible paths leading to Homo sapiens, showing $\frac{1}{7}$ out of all paths leading to Homo sapiens. *We treat those two cases as the upper and the lower bound determined that on average there is $\frac{1}{14}$ chance leading to Homo sapiens out of a total path of 5,040.* This conclusion has significant importance. We stated earlier that it would take only 104.13 million years for the emergence of Human-like creatures if ordering and steps of successive trait gaining are not important. Now, we added the ordering, then, we would expect, it takes 1.457 billion years (104.13 Myr multiplied by the factor 14) to guarantee the evolution of the next Homo Sapiens at the current BER (Background Evolutionary rate). This result correlates well with our computation, human's progress compares to the BER, as

YAABER at 1.6788 billion years (chapter 6). When one needs to compute the probability of Homo sapiens' emergence, one can arrive at the following conclusion.

List of cases	Years required at current BER	Years required in reality	Chance Factor
Ordering non-important	104.13 Myr	70.88 Myr	1
Ordering important	1.457 Gyr	270.2 Myr	×14
Ordering important with Ice age			
Ordering important with the shortest path	104.13 Myr	70.88 Myr	1
Ordering important with the shortest path with Ice age	≤ 65 Myr	≤65 Myr	×0.55

Table 5.14: List of possible ordering cases

If the ordering of traits for the emergence of Homo sapiens is not important, one would expect the emergence in the first 104.13 million years into the Cenozoic at the current BER (70.88 Myr in reality when accelerated BER in the future taking into the account)

Since the ordering is important, it would take 1.457 billion years at the current BER to guarantee the emergence of an intelligent tool-using species with meandering and repeated gains and losses of traits at current BER. Moreover, the speed of emergence will be faster in the future as BER also increases (the number of new species appearing in a 100 million year period should increase and lead to a shorter time of emergence by nature's trial and error). It would take, in reality, only 270.2 million years into the future (Chapter 7 Section 7.5 "Complexity Transformation") for the emergence.

When the ordering is important and nature took the shortest path, one would expect the emergence in the first 104.13 million years into the Cenozoic at the current BER (70.88 Myr in reality when accelerated BER in the future taking into account)

Finally, if ordering is important and the planet enters an ice age, and it takes the shortest path, then, one would expect the arrival of intelligent species within 65 million years. In the last case scenario, the probability of the emergence of Homo sapiens is reduced by more than 14 folds, and possibly as much as 100 folds compares to the case whereas ordering is important and takes the longest path.

Homo sapiens, inevitably rise within the next 1.457 billion years at current BER. However, an early arrival in the first 65 million years of Cenozoic is rather a rarity, a chance of less than 1 in 14, not even counting the probability of emergence of fruit tree as a pre-condition and the appearance of grass plant as the other.

5.6 The Probability of Alternative Intelligence

We will now cross-examine our results with that of other species. Assuming humans are gone, determining the timing for the emergence of next intelligent, tool-using species.

In order to calculate the probability of the rise of the intelligent, tool-using species, we do need to list the major features of *Homo sapiens* that distinguishes us from the rest of other species. We have stated earlier, that our species is differentiated from the rest by large cranial capacity, manifested as having high EQ, opposable thumbs, bipedal locomotion, binocular vision, omnivorous diet, language communication, and social organization. We have discussed earlier that each of the listed traits are independently evolved. That is, the opposable thumb does not increase the chance of evolving toward a high EQ or an omnivorous diet. Each trait can stand alone as an independent variable. We have calculated the number of species currently thriving possessed each of these traits divided by the total number of species of mammals, reptiles, and birds. The computed probability for each trait possessed by the cohorts under consideration gives us a general overview how successful a trait (whether evolved only once or repeatedly by convergent evolution) is ensuring the survival of the species in question at the current time.

This probability is time biased; that is, we can only compute the probability for the current geologic period. Because fossil records are incomplete, it is hard if not impossible to compute the average probability for each trait totaled under each epoch. We do need to take some faith in that data is unbiased through natural selection at different epoch may favor one type of traits or behavior more over the other. All major traits and behavior have been explored and established by the Mesozoic such as bipedalism, flight, increasingly large brain; therefore, the probability computed may not truly reflect the usefulness of the trait across all times. But the margin of error should be within the error of tolerance and validate and strengthening our argument.

Secondly, this probability is location biased. This probability is observed and only observed on earth, the only habitable planet we are currently able to investigate. Aside from temporal and spatial limitation of our data, the total probability of the emergence on *Homo sapiens* can be computed by multiplication of the probability of each independent variable.

What does the multiplication mean in this case? To state simply, the multiplication implies the chance that a species have well adapted into environment₁ with its possessed trait₁ with given probability p_1 has at some later time either voluntarily or involuntarily changed into habitat₂ and evolved trait₂ (behavior₂). Since habitat₂ and trait₂ adapted to environment₂ can be known based on existing species, and we can label it with probability P_2 . Then, the total chance that this species possessed trait₁ and trait₂ then is simply $P_1 \cdot P_2$. If the species possessed n traits, then the total probability for the emergence of that species is $P_1 \cdot P_2 \cdot P_3 \dots P_n$. A caveat to this problem is that one can not over-interpret the mathematical formula to real evolutionary settings. As a matter of fact, $P_1 \cdot P_2 \cdot P_3 \dots P_n \neq P_n \cdot P_{n-1} \cdot P_{n-2} \dots P_1$

To understand their inequivalence, *that is the ordering in the multiplication is important*, as we stated earlier. Let us use real examples to illustrate the asymmetry.

Human evolution toward intelligent, tool-using creature went under the following sequence:

First, the earliest primate adapted arboreal lifestyle and evolved partially opposable thumb. Then it evolved binocular vision, social organization, bipedal locomotion, omnivorous diet, enlarged cranial capacity, and finally language communication.

For eagles, the sequence would be bipedal locomotion, binocular vision, enlarged cranial capacity. For certain songbirds, it would be bipedal locomotion, omnivorous diet, enlarged cranial capacity, social organization, and language communication.

In order to evolve the additional trait of an opposable thumb, birds have to first devolve into a quadrupedal terrestrial species. However, birds have no chance to claim the ground casually given the number of fast running predators. It is only to occur if a mass extinction kills all land-based predators. If it succeeds, then it has to become first smaller in size, then climbs back on trees, and then descend from the trees.

The greatest challenge is that there is no short route to achieve the next major trait leading to intelligent, tool use species, instead of seemingly taking just one additional step, it has to take many more steps before it can fully gain a given trait. One may object that there is a possible short route by bird evolving opposable claws on its wings. However, early ancestors of birds all had claws on wings. As soon as flight ability and specialized beak fully evolved, they are able to survive by adopting these traits, and claws become unnecessary. It is possible that if angiosperm based fruit tree evolved earlier, there is a chance that some of the bird species may maintain their claws by gliding from tree to tree and using their claws to extract fruit. This shows that the timing of the appearance of new ecological niche is critical to the emergence of an associated trait. If a niche does not exist, even potentially very beneficial traits are removed by selection.

For a different case, one can consider that of dolphin, which evolved fins and tails adapting to the ocean, then carnivorous diet, and then social organization, enlarged cranial capacity, and finally language communication. However, in order to gain traits such as bipedal locomotion, it has to first return to dry land.

Vertebrates evolved onto land seem happened only once because existing land predators quickly kill transitional forms. However, a transition back to water is easier. It is because ancestors of dolphin could use their legs in the shallow water and swim and retract back to land when it is necessary. Therefore, their legs served a dual purpose until it is completely transitioned toward the fins. The reverse, however, is difficult, fins are adopted in the aquatic environment but almost helpless once on land. As a result, their fins, an existing trait cannot be used in a different setting, making a transition difficult.

The only scenario in which a dolphin reclaim on land if a major extinction event occurs and all land predators and herbivores no longer able to compete with aquatic competitors.

Once it regained its hold on the land, it has to revolve quadrupedal locomotion. By living on

land, it has to adopt different vocalization range because their voice generated underwater is difficult to duplicate in the medium of air. Because it no longer able to chase its source food, it has to re-adapt into a herbivorous diet, reducing their caloric consumption and their cranial capacity. Furthermore, in order to gain opposable thumbs, it has to reduce its size and climb on trees. As a result, by gaining an additional trait required to become intelligent tool user, it has to not only go through many more meandering steps, and significantly decreasing its chance of becoming one, it has also to lose many of the traits it gained before.

If species such as birds and dolphins' YAABER (read more about in chapter 6) is plotted against the rest of animal cohorts, these species can be said to have YAABER millions even tens of millions of years ahead of the average value. However, they could not keep ahead forever because it takes many more steps to gain the additional features to become intelligent tool-using species. As a result, they either become stagnant in their position while the rest of the species catch up in millions of years or they readapt into a new niche and loses existing traits associated with intelligent tool-using species and their YAABER retract.

If we summarize the major breakthroughs since the Cambrian explosion, we have the following major evolutionary events leading to intelligent, tool-using species:

Event Name	Epoch
Multicellularity	Pre-Cambrian
Evolution of Vertebrate*	Cambrian
Plants moved on land*	Ordovician
Tetrapod moved on land*	Devonian
Evolution of amniote egg-bearing tetrapod*	Carboniferous
Evolution of Mammals*	Triassic~Jurassic
Evolution angiosperms*	Cretaceous
Evolution of opposable thumbs (primate)*	Paleocene
Evolution of binocular eyes (primate)*	Paleocene
Evolution of bipedalism (ape)*	Neogene
Omnivorous diet (Homo)	Neogene
Enlarged brain	Neogene
Language communications	Neogene

Table 5.16: Major evolutionary innovation and their first emergence

After the evolution of bipedalism in the ape lineage, the evolution rate started to race ahead of the background rate. Therefore, We consider 9 asterisked cases as the frequency of major evolutionary change by the background evolutionary rate for a period spanning from 542 million years ago to 3.2 million years ago. There is a period of supercontinent Pangea which lasted 170 million years with no increase in diversity. Discounting this time period, so on average, 45.42 million years a major change occurs either by the tetrapod lineage themselves or plant

lineage opens new biological niche, notice that such timing correlates well with the average time tectonic movement transitioned from an existing configuration to a new one from our previous derivations.

Song Birds: (Number of years expected to become intelligent, tool-using species)

Event Name	Years
A major extinction event	108.4 Myr (average mass extinction gap observed)-66 Myr = 42.4 Myr
Regain foothold on land	45.42 Myr
Regained quadrupedalism	45.42 Myr
Climb on Tree (opposable thumb)	45.42 Myr
Binocular vision, (Bipedalism if glaciation happened)	45.42 Myr (100% at the initiation of the next glaciation)
Expected time required	212.3 Myr
The reign of Pangea Ultima Supercontinent	130 Myr (supercontinent not conducive to evolutionary complexity and diversity)
Bipedalism	45.42 Myr
Max time required	399.5 Myr

Table 5.18: A hypothetical evolutionary trajectory for song bird gaining ascendance

Dolphin: (Number of years expected to become intelligent, tool-using species)

Event Name	Years
A major extinction event	108.4 Myr (average mass extinction gap observed)-66 Myr = 42.4 Myr
Regain foothold on land	45.42 Myr
Adapt different vocalization range	45.42 Myr
Reduce body size	45.42 Myr
Climb on Tree (opposable thumb), (Binocular vision and Bipedalism if glaciation happened)	45.42 Myr (100% at the initiation of the next glaciation)
Expected time required	212.3 Myr
The reign of Pangea Ultima Supercontinent	130 Myr (supercontinent not conducive to evolutionary complexity and diversity)
Binocular vision	45.42 Myr
Bipedalism	45.42 Myr
Max time required	444.92 Myr

Table 5.19: A hypothetical evolutionary trajectory for dolphin gaining ascendance

A careful reader may point out extra time is required because one needs to wait for the emergence of crop plants, and especially grass plant family. However, over the course of another 212.3 Myr, it is expected that grass plants have been evolved as the biodiversity grows among all genera, and it is assumed that once it is evolved, its form persisted and the transition from hunter-gatherer to agricultural societies possible. It is also taken for granted that the metallicity of the home planet is high enough so that at least project PACER type of nuclear fusion is economically feasible to sustain the expanding industrial civilization.

In retrospect, *Homo sapiens* and earth itself took one of the shortest paths possible (by first hanging on trees) to achieve an industrial civilization, and it is likely the typical path of any early intelligent extraterrestrial intelligence's path to attain ascendance. *Homo sapiens* is fortunate because many traits evolved have already been used in earlier niches and served dual purposes during transitional periods and none of the critical traits gained earlier enabling an intelligent tool user have been lost. (other than none essential traits such as tail, hair growth). *This luck may also partially be attributed to the meteorite impact at Yucatan 66 mya.* Without the extinction of dinosaurs, the chance of tree climbing frugivores diminishes. Although lizards and chameleons are arboreal, they retained their reptilian feeding behavior of predominantly carnivorous diet even today. Since no major species adapted the arboreal niche, they can only feed on insects or tiny creatures and unable to utilize fruits as an energy source. As a result, their own sizes decrease to lower the energy requirements based on their energy intake. Birds,

on the other hand, feed on fruits but they fasten themselves using claws, and no development of opposable thumb is necessary. Reptilian arboreal frugivores may eventually emerge but possibly much later than the emergence of primates.

5.7 Probability of the Emergence of Homo Sapiens within the Genus Homo

We have defined the probability of the emergence of bipedalism, opposable thumb, binocular vision, large cranial capacity, and complex communication into a single intelligent, tool-using species.

Basically, we have defined the probability giving rise to any species within the genus of Homo. However, not all members of the genus are created equal. All earlier ancestral species possessed all traits described as human except complex language communication.

Earlier we have shown that the number of species possessing language communication skills totaled 5,336 species, which is a 5,336 out of 25,483 chance. Then, the probability indicates that the chance Homo sapiens emerges from the hominid lineage is at 20.939%, or 1 out of 4.7756 chance.

Next, we cross-examine this result with real data. We simply took the number of fossil species along the genus Homini, which numbered 13 species and one extent living species and use it as the filter factor in the last 2.85 million years. That is, on average one of out of every 13 species survived to the current day.

Species Name	Existence	Species Name	Existence
<i>H. habilis</i>	2.8 Mya	<i>H. rhodesiensis</i>	0.4 Mya ~ 0.12 Mya
<i>H. naledi</i>	2 Mya	<i>H. helmei</i>	0.259 Mya
<i>H. ergaster</i>	1.9 Mya ~ 1.3 Mya	<i>H. neanderthalensis</i>	0.25 Mya ~ 0.028 Mya
<i>H. rudolfensis</i>	1.9 Mya	<i>H. sapiens sapiens</i>	0.195 Mya ~ now
<i>H. gautengensis</i>	1.9 Mya ~ 0.6 Mya	<i>H. tsaichangensis</i>	0.19 Mya ~ 0.01 Mya
<i>H. erectus</i>	1.9 Mya ~ 0.07 Mya	<i>H. sapiens idaltu</i>	0.16 Mya
<i>H. antecessor</i>	1.2 Mya ~ 0.8 Mya	<i>H. floresiensis</i>	0.094 Mya ~ 0.013 Mya
<i>H. heidelbergensis</i>	0.6 Mya ~ 0.3 Mya	Cro-magnon	0.05 Mya
<i>H. palaeojavanicus</i>	0.5 Mya	Denisovans	0.041 Mya
<i>H. cepranensis</i>	0.5 Mya ~ 0.35 Mya		

Table 5.20: List of discovered species within the genus Homo

This is 1 out of 13 chance, or 7.69% of the emergence of truly intelligent, tool-using species that ultimately transitioned into an industrial civilization. This probability is lower than purely derived based on the chance of evolving additional complex language as an adaptation of communication. This suggests that it is harder to evolve into Homo sapiens even with language as an additional trait taking into account. *This suggests that a factor of $\frac{13}{4.7756}$, or 1 out of 2.722*

(36.73%) should be applied further to the emergence of truly intelligent, tool-using species that ultimately transitioned into an industrial civilization. This shows that the rise of Homo Sapiens is not inevitable even if bipedalism, opposable thumb, binocular vision, and large cranial capacity is evolved within the lineage in the presence of an ice age. This is at least partially justified because even our closest cousin, Neanderthals did not exhibit complex ritualistic behavior, extensive artworks, and very likely being displaced by the migration of Homo sapiens. It can also be assumed, if the earth's evolutionary history rewind and unfold again from the start of Cenozoic even with the onset of an ice age, there is a chance that Homo sapiens will not emerge.

5.8 Probability of Fruit Trees

Of course, Primates is not the first family of species to embark on this shortest route out of many possible trait combinations to attain ascendance, by first adapting to the arboreal niche. Many had attempted but failed. The earliest documented from the fossil records traced back to Permian. This adaptation was not successful because the species can not fully adapt to an arboreal lifestyle. Tree species of the late Paleozoic are dominated by gymnosperms, hard to chew and woody. Even if it did adapt to such niche, the energy content obtainable from such source is very low. This can be reflected from the energy content such as lettuce, spinach in contrast to fruit such as pear, almond, apricot, apple, pear, and banana. Creatures living on such low energy content diet cannot evolve enlarged cranial capacity and its body size likely remained small.

The next attempt came in Cretaceous of the late Mesozoic. *Deinonychus*, a species of bipedal dinosaur's claws has been investigated, and its strength was not significant enough cause fatal harm to prey, but its likely adapted to arboreal climbing. Although it is likely that it lived on trees before reaching adulthood, it had an exclusive niche on the ground as an adult. This showed that just before the emergence of angiosperm, gymnosperms do not offer significant ecological niche to any potential explorers. *Deinonychus* went extinct 74 million years ago, before the KT boundary.

Therefore, the emergence of Primates is strongly depended on the diversification of fruit trees, and if fruit tree evolved independently from the rise of primates, then we need to multiply the chance of the emergence of fruit trees into the probability giving rise to Homo sapiens.

Fruit tree's speciation, continuation, and dispersion are almost entirely independently evolved from the emergence of Primates. Primates, at most, played a marginal role in the dispersion of fruit tree.

First, fruit tree pollination is regulated by both biological and physical factors. Physical factors such as wind and gravity played an important role in flower pollination. More importantly, biological vectors such as insects (bees, fruit flies, butterflies, ants, and beetles) developed a

symbiotic relationship with the plants. In fact, plant response to ant adaptation has evolved hundreds of times independently, indicating a strong correlating, non-independent relationship. The dispersion of fruit tree species is done by both physical and biological vectors. Fruit seed can be dispersed by wind, river flow, ocean currents, and gravity. Some seeds are even dispersed by exploding mechanism. Biological vectors are dominated by birds, mammals, and insects. Birds frequently eat fruits and scattered seeds through their digestive tract. Hairy mammals carried sticky seeds along with them on their fur. Insects carried seeds as a form of food for storage in their nests such as ants, giving a chance for the seeds to germinate. Primates disperse seeds by both digestions and sticking to their fur. However, as we observed, even with the absence of primates, fruit trees will continue to diversify.

Given a complete list of all fruit trees, it accounted for a total of 667 species, out of total 295,383 species of angiosperms, one can see that 1 in 442.853 chance gives rise to fruit trees. This number is significantly lower than the portion of cohorts of birds, mammals, and reptiles surviving on the arboreal niche. Even by the most conservative estimate based on the number of primates, 256 species out of the total of 25,616 cohorts of mammals, reptiles, and birds lived on trees, 1 in 100 species adapted the arboreal niche. This implies that arboreal habitat is exceptionally nourishing despite their rare occurrence as species in the angiosperm family. However, we will not include fruit tree as a filter criterion for the emergence of *Homo sapiens*. First, tree accounted for 25% of all plant species' diversity, indicating its commonality. Second, angiosperm is differentiated from gymnosperm by enclosing seeds into fruit bodies; therefore, fruit-bearing is a universal trait among all angiosperms.

5.9 Probability of Crop Plants

In Chapter 6, we discuss how and why the emergence of crop plants play a crucial role in the transition from hunter-gatherer to a feudal society, which enabled the development of city-states and the continuation of civilizations. The passage and the accumulation of knowledge and technology eventually ushered in the industrial revolution. Crop plants allowed the harvest of solar energy at an unprecedented scale and resulted in a population explosion and the division of labor. It is, therefore, essential to compute the lower and upper bound on the probability of the emergence of crop plants essential for human lives.

To establish an upper bound of all plant species that are able to feed a very large population base, we count the number of species within all the family groups that contains all the crop species that gave us the agricultural revolution.

10,035 of them belongs to the family of Poaceae, also called true grasses, are a large and nearly ubiquitous family of monocotyledonous flowering plants. With more than 10,035 domesticated and wild species, the Poaceae are the fifth-largest plant family. This family includes rice, wheat, barley, oats, rye, sorghum, millet, and maize, providing more than half of all calories eaten by

humans.[4][76] Of all crops, 70% are grasses, and are members of this family.[30]

The Fabaceae family contains 19,500 species, also known as the bean family, contains soybean, pea, alfalfa, and peanut. Both peanut and soybean have a higher level of energy content than rice and wheat, enabling these crops to nourish complex agricultural societies with significant population base.

Solanaceae family contains 2,460 species, some of the most important species within this family that contribute to the rise of complex agricultural civilization are the potato and the eggplant. Pepper and tomato are also members of this family, but it is not in our interest of research since tomato and pepper do not contain enough energy content to aid a large population base.

Polygonaceae family contains 1,200 species and includes buckwheat, a high energy content seed. The total number of species, therefore, is 31,995 for all three families. We assume since all member species within such family group is more genetically closely related to each other, these species all have a significant chance of evolving into crops for the benefit of the agricultural society than the other comparing groups.

Since all living species of flowering plants contain 295,383 species; therefore, *1 out of every 8.898 plant species are potentially domestic-able and give rise to agricultural revolution.* It shows that the rise of Homo sapiens is much rarer than the rise of domestic-able plants. Indeed, there are several species such as maize, rice, potato, and beans that are able to independently sustain an agricultural society. If one of such species does not exist, one or more alternative can be used as a substitute. However, Homo sapiens cannot be substituted by any other species such as *Homo Neanderthals*. This shows that the requirements for domesticable plant species are simply able to store a significant amount of energy (very relaxed), the requirements for an environment-altering and self-altering species is much more stringent (very rigorous). Unlike accounting for the probability of the rise of Homo sapiens, we can not just multiply the probability of the emergence of crop species with extinction rates of angiosperms (which is again roughly 100 within 10 million years for 1% survival rate of any species within a 10 million years temporal window). It is because a very suitable species could arise before the emergence of human, and it could lead to agricultural revolution because it is passively selected and breed-ed by earlier arising intelligent species. We can only assume that given our current temporal window, the number of crop species is an average, typical of all temporal period since Cenozoic era.

We may be still interested in calculating the lower bound of the probability of crop producing species. In order to calculate such lower bound, we have to sum up all species for each type of major crops on earth.

Oats contains 17 wild species and 5 cultivate ones as indicated from the Avena genus. There are 19 species within the rice genus Oryza. There are 9 species within the rye genus Secale. There are 28 species within sorghum's genus Sorghum. 4 species of Zizania or wild rice. 15 species of buckwheat under the genus of Fagopyrum. 23 species of Wheat. 38 species within the genus Hordeum which contains barley 6 species within the genus Zea which comprises maize. 27 species within the genus Glycine which contains soybean. 3 species within the genus Pisum

which includes pea. 80 species within the genus *Arachis* which includes peanuts. 2,000 species within the genus *Solanum* which contains potato and eggplant. The total number of species is; therefore, 2,274 species. Since all living species of flowering plants include 295,383 species; therefore, *1 out of every 129.89577 plant species are potentially domestic-able and give rise to agricultural revolution at the lower bound.*

5.10 Probability of Angiosperm

After one examined the probability of crop plants and fruit trees, one needs to take a closer examination of angiosperms, the class of flowering plants. The emergence and diversification of angiosperm seem to be a natural, logical consequence of the evolutionary change, serving as an exemplary case for exponentially increasing biological species diversity. Upon closer examination, the increase may be ahead of the average rate of growth, and this may have set ourselves apart from the rest of the habitable planets. Given for example, the earlier dominant class of seed plants the gymnosperms includes only 1,500 species. One can not argue that gymnosperm is outcompeted by angiosperms because 80% of all temperate and high latitude forests are composed of gymnosperms. Even earlier plants such as ferns, the very first vascular plants, contains 34,000 species. The total number of plant species, before the emergence of angiosperms, are roughly in proportion to the number of vertebrate animal species. With the emergence of angiosperms, the number of plant species dramatically outpace the number of vertebrates. The vast increase in plant diversity enables the emergence of primates and agricultural revolution. Using our exponentially increasing evolutionary transformation factor¹⁰, one should expect an increase of 3,700 species to 100,000 species of angiosperms at most. The lower bound is derived by assuming that angiosperm is a branching of gymnosperm and over the course of 100 Myr the lineage diversity is $1,500 \cdot 2.7$. The upper bound is derived by taking into account the total number of land plant species in all clades and multiplied by the transformation factor and subtracting existing number of non-angiosperms. If one takes the intermediate value at 20,000, comparing to the number of angiosperm species of 250,000, the plant diversity on earth is then, 260 Myr ahead of the average rate of expected evolution diversity. That is, the chance of this happening is $(\frac{1}{2.7})^{2.6}$, or 7.55882 percent. Additionally, *if one were to give it a margin of tolerance, we can set the chance at 26% to 27%, which is exactly 3.6 times greater chance than 7.55% and exactly 3.6 times rarer than 100%.*

¹⁰See Chapter 7 Section 7.5 “Complexity Transformation”

6 The Distribution Model

6.1 Mathematical Model for Human Evolution

To capture all possible scenarios and represent them abstractly we need the tool of mathematics. Knowing that life can potentially be abundant on all habitable exoplanets, and yet highest attainable life form similar to human composed of different attributes each stands independently evolves through local evolutionary forces. Then, we can expect a Gaussian/log normal distribution of all extra-terrestrial life forms in the Milky Way and beyond. Normal distribution should be used because of its most general form, under the conditions (which include finite variance), states that averages of random variables independently drawn from independent distributions converge in distribution to the normal, that is, become normally distributed when the number of random variables is sufficiently large. Physical quantities that are expected to be the sum of many independent processes (such as measurement errors) often have distributions that are nearly normal.[63].

Binocular vision, bipedal locomotion, opposable thumbs and grabbing fingers, little to no tails, omnivorous diet, land-dwelling, and big brain are each independent attributes observed across many different genera and species of animals on earth. The only partially correlated attributes in human are the big brain and sophisticated manipulation of language communication. To further demonstrate that binocular vision is not a byproduct of a big brain, we found mice, which resembles the earliest ancestor of mammals before adaptive radiation 65 million years ago, had partial depth perception. Carnivorous cats, a different genus of mammal, also have binocular vision for catching prey yet much smaller Encephalization quotient compares to human. Birds such as owls and eagles evolved through the Cenozoic era. Both have binocular visions. On the other hand, dolphins with highest Encephalization quotient other than Homo Sapiens, do not have binocular vision. Bipedal locomotion does not directly correlate with a big brain. Ostrich, and extinct Dodo bird and bipedal dinosaurs most have $EQ < 1$, *Troodon* from the late Cretaceous may be an exception compares to its contemporary cohorts; however, its EQ is still less than 1. *Australopithecus Afarensis* of the Hominid lineage had highly developed bipedal locomotion but with a small cranial capacity of 350 cc. Opposable thumb has evolved on many tree-dwelling animals ranging from tree shrews, monkeys, to amphibian tree frogs, and reptilian Chameleon. Most of these animals have Encephalization quotient comparable to 1 or even lower. Therefore, the gripping power of fingers and claws contributes little to the expansion of brain, and vice versa. Animals with little to no tails may first appear a significant achievement of hominid lineage, but a closer examination reveals that early ancestors of amphibian frog-like creatures already shed their tails after fully metamorphosed into an adult in the Carboniferous epoch, some 325 Mya. Later, some species of sea turtles become tailless during the Mesozoic, and some mammals species also evolved to become tailless. Primates lineage certainly re-evolved long and thick tails to balance on trees, in a sense regressed from the average norm

of the evolutionary prototype of the mammalian ancestor. We also found raven and magpie which has a feathered tail, score high on self-cognition and measured Encephalization quotient; Dolphin lives in the ocean and has no legs but a tail used for aquatic propulsion. Therefore, brain size has no strong correlation with tail size. Brainy animals could have a long, short, or no tail. Human eats both vegetables, fruits, and meat, yet many species of insects, birds, mammals have shown to exhibit similar behavior. Dolphin and cetacean have some of the highest brain sizes among all living animals but they live in the ocean, and they lack bipedal locomotion, grabbing fingers, and are carnivorous.

So each of these attributes is evenly likely distributed among different species of animals, then, we expect human to be the rightmost outlier in the normally distributed data set because we possess all these attributes. Some have argued that we are not evolving toward higher intelligence and one can well devise a normal distribution dataset with criteria, so that elephant with long nose becomes the rightmost outlier.[61] The argument is valid that datasets can be rearranged to show the differential importance of each attribute or particular species of animal's possessed characteristics enables it to be plotted as the rightmost outlier in the distribution. However, what unique about Homo sapien is that our set of biological attributes enables us to change and adapt at a rate much faster than natural selection. So that over time, our position shifts further to the right and becoming ever more and increasingly outlying compares to the mean value. That is, our position on the distribution changes while other animals held stationary in sub-geologic time scale (at time scale too short to observe significant biological evolutionary changes $x < 10^7$ yrs). It is true that evolution does not dictate a predetermined path to industrial civilization. However, with increasing biodiversity on earth, which is evident from the graph below, that as certain animals adapted to certain niches become saturated, a new differentiated species must develop new attributes or more exaggerated existing features to occupy new niches and avoid competition. As biodiversity increases along with gradual geological change periodically leading to drastic change, the chance and propensity for nature evolving both brainy, long feathered, great wingspan, long-nosed, or some combinations with these attributes increases. In summary, an extra-terrestrial civilization's host planet must have a great diversity of animals species and genera sufficiently guarantee the rise of an organism sharing all functional equivalent attributes of Homo sapiens.

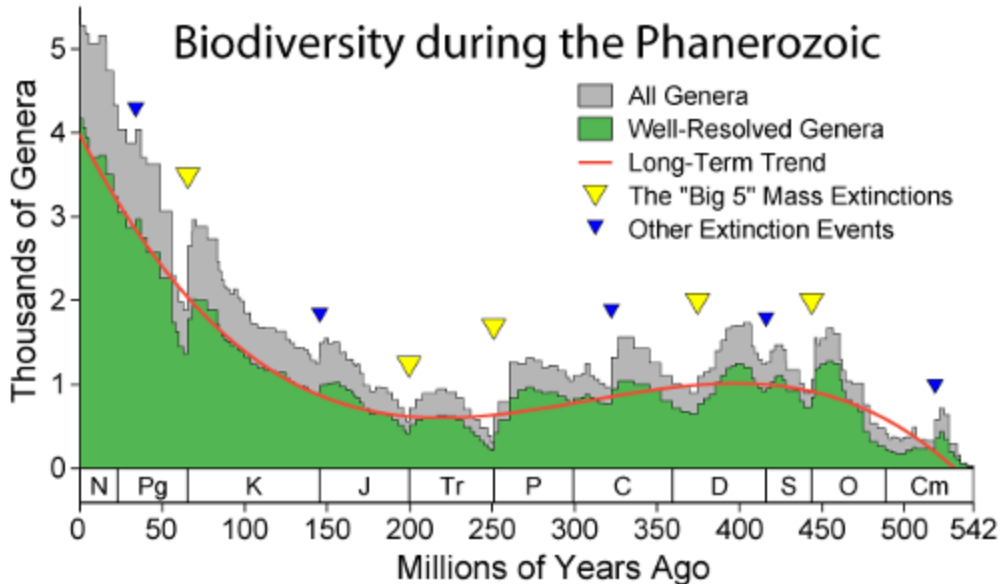


Figure 6.1: Historical trend of biocomplexity change

It is important to emphasize, that once an organism achieves fully anatomical or functional equivalent of *Homo sapiens*, they will alter their environment in degrees according to the level of mastery of the sophistication of technology, so that natural selection has less an effect on them than other animals. Yet as long as they remain biologically unaltered, they will subject to biological constraints on food, resources, temperature swings, aging, sickness, and death. As a result, a log-normal distribution or a heavy-tail distribution will fit better in model and forecasting. Furthermore, for simplifying our analysis, we can divide our data sets by temporal epochs of evolutionary development. For example, *evolving from common mammalian ancestor up to anatomical and functional Homo sapiens can be captured and modeled by approximately Gaussian Normal Distribution. Evolving from hunter-gatherers up to post-singularity civilization follows lognormal or a heavy tail distribution. A post-singularity civilization follows a uniform probability distribution.* More will be discussed in detail in later sections regarding analysis simplification. For the simplicity of our argument, we will use normal and log normal distribution in our discussion for now.

6.2 Background Rate

After we have selected our mathematical prototype model, how do we calculate the mean, the standard deviation of such Gaussian normal/lognormal distribution given limited data available on astrobiology? For now, fortunately and unfortunately, the best data we can gather is from the earth itself and paleontology. We choose an average mammal with encephalization quotient=1 as the average/median attained evolutionary sample from all habitable exoplanets. Then, we have to use bio-informatics, genomic, epigenetic, and functional complexity to calculates

how much more accelerated biological progression occurred in the Hominid lineage since its divergence from the main lineage following the K-T extinction event 65 million years ago. The following table lists some common animals by their encephalization quotient and other essential characteristics possessed by Homo sapiens. Where each animal obtains a score under each category, and their summed final score is listed in the very right column.

Animal	Brain	Bipedal	Binocular Vision	Language	Landbased	Thumb	Omnivorous	No Tail	Total
Homo sapiens sapiens	1.00	1	1	1	1	1	1	1	8
Bottlenose dolphin	0.73	0	0	0.6	0	0	0	0	1.33
Chimpanzee	0.52	0.2	1	0.3	1	0.5	1	1	5.52
Crow	0.51	0.5	0	0.3	1	0.3	1	0.75	4.36
Tegu lizard	0.49	0	0.25	0	1	0.3	0	0	2.04
Monitor lizard	0.49	0	0.25	0	1	0.3	0	0	2.04
Anole	0.49	0	0.5	0	1	0.3	0	0	2.04
Killer whale	0.49	0	0	0.4	0	0	0	0	0.89
African grey parrot	0.49	0.5	0	0.6	1	0.3	0.1	0.8	3.79
African elephant	0.49	0	0	0.3	1	0	0	0.85	2.64
Rhesus macaque	0.21	0	1	0.1	1	0.5	0.3	0.3	3.41
Wolverine	0.21	0	1	0	1	0	0	0.8	3.01
Manta ray	0.20	0	0	0	0	0	0	0.5	0.7
Walrus	0.20	0	0	0	0.5	0	0	0	0.7
Hummingbird	0.20	0.3	0	0	1	0	0	0.75	2.25
Giraffe	0.19	0	0	0	1	0	0	0.85	2.04
Baboon	0.18	0	0	0.15	1	0.5	1	0.2	3.03
Cat	0.18	0	1	0.1	1	0.1	0	0.7	3.08
Giant cuttlefish	0.18	0	0.2	0	0	0	0	0	0.38
Dog (husky)	0.18	0	1	0.2	1	0	0	0.8	3.18
Elephant fish	0.17	0	0	0	0	0	0	0	0.17
Giant octopus	0.15	0	0	0	0	0.2	0	1	1.35
Horse	0.14	0	0	0	1	0	0	0.9	2.04
Gorilla	0.14	0	1	0.1	1	0.4	0	1	3.64
Pig	0.14	0	0.7	0.1	1	0	1	0.9	3.84
Zebra	0.12	0	0	0	1	0	0	0.9	2.02
Sulcata tortoise	0.09	0	0.2	0	0.2	0	0	0.9	1.39
Cattle	0.09	0	0	0.1	1	0	0	0.85	2.04
Lion	0.09	0	1	0	1	0	0	0.85	2.94
Rabbit	0.08	0.1	0	0	1	0	0	0.95	2.13

Mouse	0.07	0.1	0.6	0.1	1	0.2	1	0	3.07
Sperm whale	0.07	0	0	0.2	0	0	0	0	0.27
Hippopotamus	0.05	0	0	0	0.65	0	0	0.9	1.6
Rat	0.05	0	0.6	0.1	1	0.2	1	0	2.95
Nile crocodile	0.04	0	0.35	0	0.8	0.1	0	0	1.65
Saltwater crocodile	0.04	0	0.35	0	0.8	0.1	0	0	1.65

Rearranging their final scores from high to low, we have some expected and surprise results

Animal	Brain	Bipedal	Binocular Vision	Language	Landbased	Thumb	Omnivorous	No tail	Total
Homo sapiens sapiens	1.00	1	1	1	1	1	1	1	8.00
Chimpanzee	0.52	0.2	1	0.3	1	0.5	1	1	5.52
Crow	0.51	0.5	0	0.3	1	0.3	1	0.75	4.36
Pig	0.14	0	0.7	0.1	1	0	1	0.9	3.84
African grey parrot	0.49	0.5	0	0.6	1	0.3	0.1	0.8	3.79
Gorilla	0.14	0	1	0.1	1	0.4	0	1	3.64
Rhesus macaque	0.21	0	1	0.1	1	0.5	0.3	0.3	3.41
Dog (husky)	0.18	0	1	0.2	1	0	0	0.8	3.18
Cat	0.18	0	1	0.1	1	0.1	0	0.7	3.08
Mouse	0.07	0.1	0.6	0.1	1	0.2	1	0	3.07
Baboon	0.18	0	0	0.15	1	0.5	1	0.2	3.03
Wolverine	0.21	0	1	0	1	0	0	0.8	3.01
Rat	0.05	0	0.6	0.1	1	0.2	1	0	2.95
Lion	0.09	0	1	0	1	0	0	0.85	2.94
African elephant	0.49	0	0	0.3	1	0	0	0.85	2.64
Hummingbird	0.20	0.3	0	0	1	0	0	0.75	2.25
Rabbit	0.08	0.1	0	0	1	0	0	0.95	2.13
Tegu lizard	0.49	0	0.25	0	1	0.3	0	0	2.04
Monitor lizard	0.49	0	0.25	0	1	0.3	0	0	2.04
Anole	0.49	0	0.5	0	1	0.3	0	0	2.04
Giraffe	0.19	0	0	0	1	0	0	0.85	2.04
Horse	0.14	0	0	0	1	0	0	0.9	2.04
Cattle	0.09	0	0	0.1	1	0	0	0.85	2.04
Zebra	0.12	0	0	0	1	0	0	0.9	2.02
Nile crocodile	0.04	0	0.35	0	0.8	0.1	0	0	1.65
Saltwater crocodile	0.04	0	0.35	0	0.8	0.1	0	0	1.65

Hippopotamus	0.05	0	0	0	0.65	0	0	0.9	1.60
Sulcata tortoise	0.09	0	0.2	0	0.2	0	0	0.9	1.39
Giant octopus	0.15	0	0	0	0	0.2	0	1	1.35
Bottlenose dolphin	0.73	0	0	0.6	0	0	0	0	1.33
Killer whale	0.49	0	0	0.4	0	0	0	0	0.89
Manta ray	0.20	0	0	0	0	0	0	0.5	0.70
Walrus	0.20	0	0	0	0.5	0	0	0	0.70
Giant cuttlefish	0.18	0	0.2	0	0	0	0	0	0.38
Sperm whale	0.07	0	0	0.2	0	0	0	0	0.27
Elephant fish	0.17	0	0	0	0	0	0	0	0.17

leveraged results considering all essential biological attributes contributed to the rise of Homo sapiens versus other animals, we found human score 8 on top and followed by Chimpanzee, which is somewhat expected, and then followed by crow. Most surprisingly, dolphin scored extremely low on the ranking despite their big brain because dolphin pretty much failed on every other category essential for the emergence of functional equivalent of the human species. Each listed attribute is essential for a capable biological species to adapt eventually to an industrial civilization.

Needless to say, a big brain is a requirement for comprehension of the environment, abstract concepts, new idea construction, and communication and complex ideas comprehension through language.

Binocular vision enables depth perception. Without depth perception, it is very difficult to develop geometric theories, advanced mathematics and creating tools that fit one part into another. Our brain is evolved and fine-tuned with binocular vision so that we have an innate understanding of geometry, shapes just like bats marvelously able to interpret rebounding high-frequency sound for obstacle detection.

An omnivorous diet is essential for the development of industrial civilization. First of all, carnivorous and omnivorous animals tend, on average, have greater cranial capacity because they are able to obtain more proteins from their intake, especially when they had similar biological attributes and lives in similar habitats. This is illustrated in omnivorous crow which has EQ score of 4.5 compares to vegetarian African Grey Parrot at 3.75, and omnivorous Chimpanzee at 4.8 compares to vegetarian Gorilla at 2.1. Dolphins and killer whales both are carnivorous and have sufficient protein to support their large brains. Omnivores feed on meat. Animals feeding on meat requires greater flexibility, agility, planning, and canniness to catch its prey. Those are the essential quality selected by natural evolution is also essential for the successful development of a civilization. Most importantly, omnivores are also adapt well to vegetables and starch. In order to transition from a hunter-gatherer society to an industrial society, an intermediate agricultural society phase requires each member of the species consume

a significant amount of vegetation such as rice, wheat, and rye. A species can only digest meat can not significantly expand their population beyond scattering hunter-gatherer bands; therefore, trap on a stable local maximum level of energy extraction from the locality and unable to form into flourishing an industrial civilization.

Bipedal locomotion is essential because highly advanced technological society (ladder, building, tunnels, bridges, airplane, and auto) requires a biological hand to construct. Walking on hind legs freed the arms to perform that tasks. However, opposable thumb is not a consequence of bipedalism. Tree shrews have grabbing power without standing upright. Neither do ostrich and birds with bipedal locomotion developed opposable thumbs. It is the independent development of bipedal locomotion in combination with opposable thumb brings significant advantage to human. Human with a dexterous hand is able to manipulate and create objects, but to carry and move tools over long distances, requires bipedal locomotion which freed the forelimb for carrying. Later toolset and contemporary artifacts/edifices of *Homo sapiens* require creations which made up many parts originating from great distances from each other. It is utterly unthinkable that human is able to achieve greater technological improvements if bipedal locomotion is not evolved and forelimb is not freed to carry these parts across great distances, so tools creation can only be confined locally. Human can surely hold tool parts in their mouth to carry over great distance, but human jaw muscles are adapted for an omnivorous diet. If human had been exclusively carnivorous, greater jaw muscle would able to hold greater goods over large distances without bipedal locomotion and developed into an intelligent species almost identical to human except walking on four legs. However, we have just concluded that a carnivorous species cannot successfully transform its mode of living from a hunter-gatherer to an agricultural society. As a result, no transformation into industrial civilization is possible. On the other hand, Omnivorous but non-bipedal tree shrews with dexterous hands can develop tools using their hands, but its living range will be limited to the trees. Its forelimbs and hind legs are not well adapted to walk over great distances, so no complex tool making (requires materials from far away) is possible for this species. Most importantly, by limiting its own living range on the trees, it will never transition from hunting and gathering lifestyle to that of an agricultural mode of living (agriculture crops requires flat land for cultivation not on the trees. One could argue these animals can cultivate their host trees so that it becomes its own living habitat as well as crop producing warehouse. So a sort of horticultural revolution is possible. This reasoning is flawed in 2 ways. First, trees take a significant growth cycle because they are not perennial. Artificial breeding and selection will take extremely long time to see significant improvement in food production, and the costs outweigh the effort to start such a transition. Secondly, a tree, no matter how finely tuned, will not produce as much food compares to staple crops, so energy return versus energy invested will always be less than a human agricultural society. A significant amount of energy is invested by the tree in its own maintenance of its trunk, bark, branches, and roots. As a result, the population supported by such a horticultural revolution will still hold lower population density in a given region than

one started by human agricultural revolution. Horticulture society is also unable to undergo crop rotation which increases food intake diversity. If a tree with weaker trunk is selected by the species to breed in exchange for greater energy return in the forms of fruit production, then the specie is on a suicide journey because its own survival is dependent on the sturdiness of the tree trunk itself to escape from land predators) even if it achieves characteristics just like human such as omnivorous diet (have the potential to expand its population density significantly), big brain, language, opposable thumb, land dwelling (the potential to use fire), binocular vision except not developing bipedal locomotion on flat land surfaces. It is noted that monkeys have greater grabbing power on their hands than even human. Paradoxically, stronger grabbing power trades with lesser precision control in tool making. Therefore, bipedal locomotion, once freed monkeys opposable thumb from branch grabbing, refined it for sophisticated tool making. So hand evolved ever more manipulative of objects as a self-reinforcing positive feedback loop. A luxury neither enjoyed by quadrupedal nor arboreal species. Therefore, one can argue that there is a positive correlation between refined opposable thumbs at human level precision and bipedal locomotion but opposable thumb as an independently evolved feature must already present at the time when bipedal locomotion is evolved. Indeed, human lineage developed quickly after the emergence of convincing bipedal locomotion found in fossil remains of *Australopithecus Afarensis*. As a result, Gaussian normal, lognormal distribution should be right skewed, and at least sub log-normal distributed even just consider the data set from average mammalian sample to the emergence of anatomical Homo sapiens. For the simplicity of our argument and calculation, we shall treat the data as Gaussian normally distributed for now.

Furthermore, an animal has to be a land dweller. The use and control of fire enabled human to first transition from stone to bronze tools, and then to iron tools. With iron molding technology, human eventually constructed steel furnace and ushered in the industrial revolution. If human evolved in the ocean, no matter how smart we become, we would never be able to contain fire (fire manipulation is not possible underwater by all means) inside a furnace and transition from biological muscle power to steam power. Curiously enough as a thought experiment, it is possible that a hypothetical smart aquatic species with dexterous hands can utilize the steam vents from the ocean floor by casting a stone furnace around it and do useful work. However, such device cannot store an energy source and can not be transferred from one location to another. So their device resembles a localized medieval waterclock rather than a steam engine even though they capture energy from steam emitted by vents so be called a steam-powered engine. However, one should not be confused by the language verbiage tricks from its intrinsic property.

The opposable thumb is, of course, essential for the development and continued progress of human civilization. We have already mentioned that bipedal locomotion truly freed human hands for other tasks. Human hands create tools, and bipedal locomotion helps human to carry these tools over great distances. Palm with one opposable thumb may not be the only

functional equivalent to a dexterous biological appendage enabling technological civilization. A hand with two or more opposable thumbs, or some other anatomically bendable structure is possible. It is likely such landscape of possibilities can also be quanta-sized by mathematics, but it is beyond the scope of this paper.

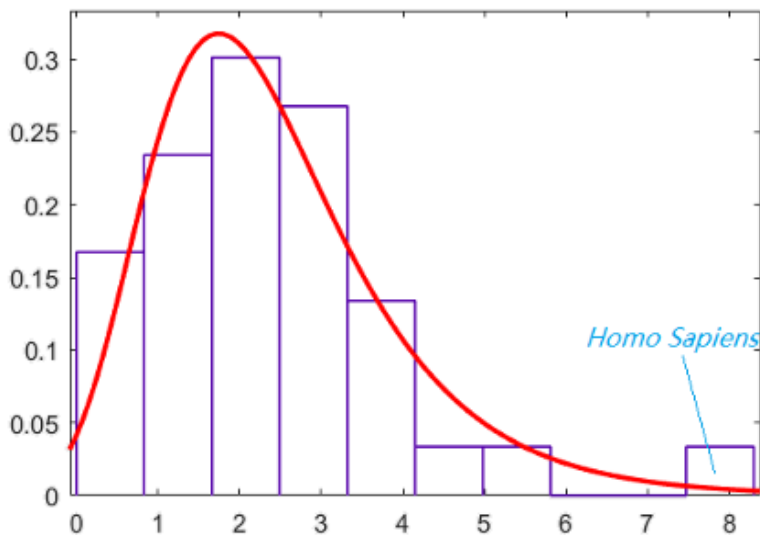


Figure 6.2: Lognormal distribution of species possessing different number of Homo sapiens' traits

The total attributes plotted for probabilistic distribution shows skewed normal/lognormal with human as an extreme outlier. By now, we have confirmed that animals on earth follow normal/lognormal distributed attributes curve, then we have to compute human attributes as an outlier, how much more advanced or faster we evolved compared to the average rate of evolution. We need to set a background evolutionary rate. We do not know the mean overall evolutionary rate within our galaxy and beyond, but we can choose different mean rate based on cohorts of animals here on earth. Mammals, birds, and reptiles are chosen because they are most similar to human and more evolved than fish, amphibians, and invertebrates. If we can show that human emergence is rare even if assuming species functional equivalent to an average mammal, birds, and reptiles roamed on all Earth-like planets, then we set an upper bound and complied better with the principle of Mediocrity.

6.3 Counting YAABER

Here we introduce the equation for calculating the deviation value of Homo sapiens from the mean mammalian average. We introduce a concept called **Years Ahead Against the Background Evolutionary Rate**. Or **YAABER**. This is an estimation of how many years into the future using the current rate of evolution observed in which the average model organism we

compare and contrasts to will diversify and evolve into a species comparable to human today with a probability of 1. We have already shown that the emergence of human at the current epoch on earth, even among the current cohorts of avian, mammalian, and reptilian lineage, is much closer to 0 than 1. With increasing bio-diversity, the chance of emerging functionally human equivalent species in any habitable planet will approach 1 in some number of years into the future. Keen readers might quickly point out that Earth has only $5 \cdot 10^9$ years of an effective land dwelling evolutionary window remaining, so the window might be too short to guarantee the emergence of human functional equivalent again on earth or any other planets. I would like to point out and remind them in that somewhat the Sun is the more massive of the GFK spectral class stars, stars with lower mass, not as small as a red dwarf, have significantly longer time span for biological evolution. ¹¹

$$e_n = e_{n-1} + \sum_{i=0}^m f(k_i, e_i) \quad (6.1)$$

$$f(k_i, e_i) = \begin{cases} k_i & k_i > 0 \\ 0 & k_i = 0 \\ -k_i & -k_i < 0 \end{cases} \quad (6.2)$$

The equation above is a recursive summation, where the term e_n is recursively defined until it reaches e_0 , the base case. The term e_n is defined as the mean cohort average we are comparing against with. We currently defined e_n as the mammalian ancestor of 65 Mya with close similarity to mouse today, along with surviving bird ancestors and reptilian ancestors following the K-T extinction event. Then, e_{n-1} can be defined as the last common ancestor between reptiles and mammals, some 225 Mya. e_{n-2} can be defined as the last common ancestor between amphibians and reptiles. e_{n-3} can be defined as the last common ancestor of amphibians and fish. e_{n-4} can be defined as the last common ancestor between fish and vertebrates. e_{n-5} can be defined as the last common ancestor of vertebrates and invertebrates. e_{n-6} can be defined as the last common ancestor of multicellular eukaryotes and unicellular eukaryotes. e_{n-7} can be defined as the last common ancestor between eukaryotes and prokaryotes. Finally, e_0 can be defined as the last common ancestors for all life forms on earth. However, each term of e does not need to be assigned to a major lineage split in the evolutionary tree of life. It can well be represented by the last common ancestor between subspecies where one of the subspecies led to the human ancestor. For example, *Homo Habilis* can be used as the term e_n , and *Homo Erectus* as the term e_{n-1} , *Australopithecus Afarensis* as the term e_{n-2} . It is not very practical to use this approach, however, because we will soon see that any evolutionary features take time to evolve and we need greater temporal time span to derive mathematically significant value. The first order

¹¹See Chapter 2

approximation of our computed values closely approaches the actual value if each successive ancestors leading up to human were computed in the recursive summation. Higher resolution in temporal aspects leads to more precise computations but takes much significant time, and not all missing links are well-documented.

This recursive summation can be simplified in our discussion to

$$e_n = \sum_{i=0}^m f(k_i, e_i) \quad (6.3)$$

$$f(k_i, e_i) = \begin{cases} k_i & k_i > 0 \\ 0 & k = 0 \\ -k_i & -k_i < 0 \end{cases} \quad (6.4)$$

This is possible because we assume that all habitable planets have biological and functional equivalent creatures to terrestrial mammals, reptiles, and birds roaming on its surfaces to comply better with the principles of Mediocrity. Then, we are only interested in how many Years Ahead Against the Background Evolutionary Rate since the Cenozoic era. If ancestors of mammals and reptiles are used as the typical average model organisms on all terrestrial planets relative to Homo Sapiens, then their value for YAABER will be larger indeed. We do need to pay closer attention to the defined function f . In order to appreciate all cases listed and defined for the function, we need to draw a 2 by 3 matrix for each different cases.

K_i	e_0	e_1
$K_i > 0$	Ancestors lacked the trait, but descent evolved the trait	Ancestors possessed the trait, but descent outperformed the ancestor
$K_i = 0$	Both ancestor and descent lacked the trait	Both ancestors and descent possessed the trait
$K_i < 0$	Ancestor lack the trait, but descent has further lost the trait	Ancestor possessed the trait, but descent has lost the trait

Table 6.3: A table lists the YAABER value for a list of traits possessed by a particular species compared against the basal mammalian ancestors when that trait is also absent from the ancestor is grouped under column e_0 , and a list of traits possessed by a particular species compared against the basal mammalian ancestors when that trait is already present in the ancestor is grouped under column e_1

K_i	e_0	e_1
$K_i > 0$	Homo sapiens' complex language, tool usage	Homo Sapiens' bigger brain, fixed bipedal locomotion, and binocular vision
$K_i = 0$	Homo sapiens' lack of feather, bird-like wings	Homo sapiens' Omnivorous diet
$K_i < 0$	Naked mole rats with little to no vision, bats with poor eyesight	Dolphin's lack of bipedal locomotion and the use of tail

Table 6.4: With listed examples of specific traits drawn from Homo sapiens, naked mole rats, bats, and dolphins

The matrix shows different cases of features possessed by Homo sapiens, bats, rats, and dolphins versus the prototypic mammal's features. Traits under e_0 such as complex language and tool usage are completely absent from prototypic mammals, surviving reptiles, and bird species 65 Mya, the complex language and tool usage exhibited by humans converted into K_i value then will be counted positively to the final Years Ahead Against the Background Evolutionary Rate. Traits listed under e_1 such as cranial capacity, partial binocular vision, forms of bipedal locomotion is found in birds, and mammals from 65 Mya, but Homo Sapiens has a greater cranial capacity. Therefore, its K_i value is counted positively toward the final YAABER. Mammals 65 Mya did not possess bird-like wings and feather, so the trait falls under e_0 , and Homo Sapiens do not possess feathers and wings 65 million years later, so no value is counted toward the YAABER. On the other hand, Mammals 65 Mya had an omnivorous diet, as it is listed under e_1 , Homo Sapiens 65 million years later also had an omnivorous diet. Therefore, no value is added toward the YAABER. It is important to note, however, primates, from 30 million years ago, had a predominantly, insectivorous diet. As a result, a negative value is added toward the final YAABER if we had used primate as an intermediary ancestor in our recursive summation computation in case of computation with a higher resolution. However, this negative value is canceled later in the equation because Homo Sapiens re-evolved omnivorous diet and an equally positive value is added to the final YAABER. Therefore, omnivorous diet had a total contribution toward YAABER of zero, just as we have computed without taking primates as an intermediary consideration in our recursive summation. Mammals 65 Mya lacks adequate color detection found in birds and reptiles. Therefore, color-detection and poor vision for mammals 65 Mya falls under e_0 . it is possible, such as naked mole rat living exclusively underground and bats lived predominately inside caves and active during the night, had even poorer vision. As a result, the color vision attributes of naked mole rats and bats had contributed negatively

toward the final YAABER. Finally, mammals, birds, reptiles 65 Mya in general walked with legs, so this trait falls under e_1 , yet dolphin 65 million years later evolved legs into a tail, therefore, contributed negatively toward the YAABER.

Having shown the definition of the function f , we now proceed to define each computed value of K .

First and foremost, we need to compute the cranial compacity increase of Homo Sapiens against the Background Evolutionary rate observed in an average bird, reptile, and mammals since the start of the Cenozoic era.

As we have seen earlier, omnivorous diet contributed nothing toward the final YAABER because mammals from 65 Mya had an omnivorous diet, this is equally valid conclusion for Homo sapiens evolved bipedal locomotion because birds 65 Mya had evolved bipedalism and bipedal dinosaurs roamed earth since Triassic lasted up until the K-T extinction event.

Homo sapiens also has no tail. This attribute does not contribute any value to the YAABER because amphibian frogs and reptilian turtles had adapted with little to no tail during the Carboniferous and Mesozoic era.

Homo sapiens has opposable thumbs. This attribute do not contribute to the final YAABER because genus Phyllomedusa (tree frogs), and primate ancestors from 65 Mya had at least partial gripping power.

Homo Sapiens unique language skill does seem to contribute positively to the final YAABER, however, human language, as demonstrated by experiments, originated from the Broca's and Wernicke's areas of the brain. The abstract thinking behind complex language and symbol manipulation lie under the frontal cortex. Essentially, language is a by-product of a big brain. We need to exercise extreme cautiousness to avoid double counting values to the final YAABER. Human language, viewed from the perspective of the range of vocalization capable by the larynx and vocal chord, seem to suggest more evolved than others, this view is unfortunately undermined by African Grey Parrot such as Alex, which demonstrated stunningly accurate imitation of human sound in different tones.

Finally, someone may point out that other attributes such as being warm-blooded, having a placenta and having hair may contribute positively to the final YAABER. However, warm-blooded, hairiness and bearing young inside one's body is present in mammals 65 Mya. Being warm blooded is even demonstrated in dinosaurs in some degree during the Mesozoic epoch.

In conclusion, Homo sapiens' great cranial capacity attribute contribute more than the majority toward the final YAABER, (conforms with our intuition). Though other attributes are also essential for the transformation of a biological species into an industrial one, they do not contribute significantly in our calculation toward the final YAABER since these attributes have been evolved in birds, reptiles, and mammals 65 Mya or earlier. Nevertheless, the unique combination is only evolved in the human lineage and their presence along with a large brain created a self-reinforcing positive feedback loop enabling greater cranial capacity. That is, the growth of the cranial capacity as a trait to reach our current size is only possible when other

traits help to magnify the advantage and fulfill the potential offered by an advanced brain and makes the a directional selection toward an ever larger brain feasible. Therefore, by simply calculating the cranial growth size we also elegantly included the evolutionary pace of others complementary traits against the background average. It is This also confirms that greater cranial capacity is a less well-adapted feature by evolution, it does not immediately gain a great benefit to the organism otherwise it would have evolved much earlier such as bipedal locomotion or flying.

6.4 YAABER for Evolution of Homo Sapiens

If we choose an average mammal with encephalization quotient=1 as the median attained evolutionary sample from all habitable exoplanets, then, we can determine the background evolutionary rate by comparing the encephalization quotient of mammals to that of the reptiles. In general, average mammals' encephalization quotient is a magnitude higher than the reptiles. Since the earliest mammals evolved 225 million years ago in the age of reptiles, we can assume that the median of EQ has grown 10 folds since 225 Mya (Tikitherium) in the age of mammals after the diversification. The definition of mammals is defined as synapsids that possess a dentary-squamosal jaw articulation and occlusion between upper and lower molars with a transverse component to the movement or, equivalently in Kemp's view, the clade originating with the last common ancestor of Sinoconodon and living mammals. Then, we are able to define the **BER**, the background evolutionary rate of the earth.

$$\begin{aligned}
 q &= 10^{\left(\frac{1}{225,000,000}\right)} - 1 \\
 &= 1.0233711656 \times 10^{-8}
 \end{aligned}
 \tag{6.5}$$

This rate is equivalent to 2.783 in 100 Myr. This implies that every 100 million years the biological diversity leading to greater EQ increase by 2.783.

The background evolutionary rate is also cross-checked with the number of neurons in different species. This is somewhat tricky because one has to pick the right data points to compare with. For example, octopus has 500 million neurons and emerged 323.2 Mya, and lemur contains 254,710,000 neurons but emerged 55 Mya by the earliest. If one compares those two data points, the Background Evolutionary Rate seems to increase negatively. In reality, octopus is probably one of smartest species during the Carboniferous epoch and lies as the furthest point lying to the right from the median value for the cohorts of all animal species at the time. Lemur, on the other hands, lies much closer to the median value in the Cenozoic.

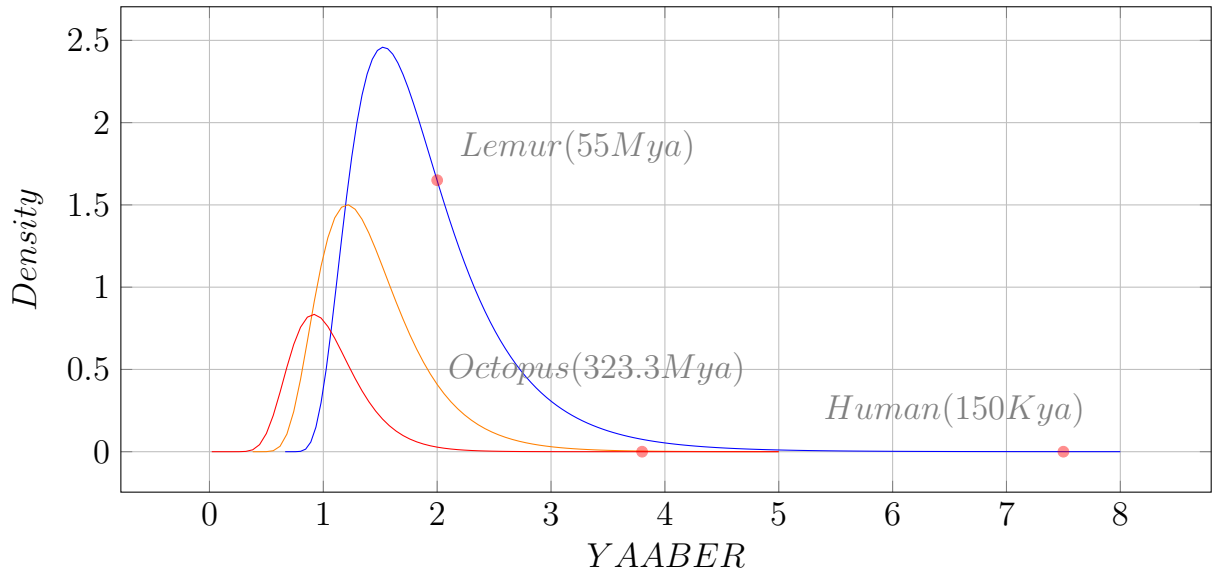


Figure 6.3: Hypothetical biocomplexity probability distribution of Cambrian, Carboniferous, and Cenozoic

Moreover, the size of two species across different epochs has to be similar in size. No one would expect two species such as an ant and whale have the same number of neurons even if the EQ of the two species are the same. We eventually selected two data points to compare with. Frog with 16,000,000 neurons which emerged 200 Mya during the Early Jurassic to that of short-tailed shrew and house mouse emerged in the early Cenozoic with 52,000,000 neurons and 71,000,000 neurons respectively. Both frog and mouse has comparable size and yields a BER of 2.3, which is not too different from our earlier calculated result.

$$16,000,000 (2.3)^{1.6} \tag{6.6}$$

$$= 60,657,501.871 \text{ neurons}$$

Once we calculated the BER, we can compute the YAABER for the primate lineage leading up to *Australopithecus afarensis*, the first bipedal walking ape. Primates, on average, have an EQ of 1.8 with 55 Myr of evolution. Then, we can compute the Evolutionary rate for the primate lineage and use it to calculate the YAABER.

$$k_{primate} = 1.8 \left(\frac{1}{55,000,000} \right) - 1 \tag{6.7}$$

$$= 1.0687030372 \times 10^{-8}$$

$$T_{prim} = \frac{k_{primate}}{q} \cdot (55,000,000 - 3,900,000) \tag{6.8}$$

$$= 53,363,556.6803 \text{ YAABER}$$

We can see that the YAABER for Primates is 53.4 Myr ahead of the mammalian average, that is, it will take this long for the mammal's average EQ reaches parity with the current primate level using current rate of evolutionary growth. The evolutionary rate from the emergence of *Australopithecus afarensis* to Homo Sapiens is computed based on the growth of cranial capacity of the species, which is equivalent to EQ, but just with more precision and the YAABER calculated to be an additional 140.61 Myr ahead of the evolutionary rate.

$$k_{\text{homosapien}} = 0.0000003762 \tag{6.9}$$

$$T_{\text{homo}} = \frac{k_{\text{homosapien}}}{q} \cdot (3,900,000 - 75,000) \tag{6.10}$$

$$= 140,610,274.003 \text{ YAABER}$$

6.5 YAABER for Hunter Gatherer

After Homo sapiens emerged as a new species in Africa by 195,000 years ago, the species spent the rest of 185,000 years as hunter-gatherers. In fact, it is the mode of life just like any of its predecessor species. Because the species eventually transitioned into an agricultural one and the changes occurred during this period was much faster than the epigenetic and functional modularity changes occurred in the hominid lineage. The toolset of the species transitioned from Paleolithic to Mesolithic and eventually into Neolithic stone tools. Around 45,000 BC a profound cultural change occurred where behaviors comparable to modern man has been observed from the archaeological remains. Human started to practice ritualistic burials, painted cave art, sculpted effigies, and started extensive trade networks. The domestication of animals started around 30,000 BC starting with the wolf and eventually led into a full-blown agricultural revolution. Human anatomical structure, however, changed little if not at all. As a result, we need to resort to some other parameters to measure the rate of progress compares to the background evolutionary rate, and add this value to the final YAABER. Evolution can be rethought as a form of passive manipulation of matter and energy. Starting from the hunter-gathering phase of human existence, the species actively manipulates matter and energy by using tools. In essence, we need to measure the rate of change in energy manipulation, passive or active. Then, in order to quantify the change occurred during this period of human as hunter-gatherers, the best we can use is to measure the rate of energy acquisition growth during this phase of human evolution and the most direct way to measure it is through measurement on the rate the human population growth. At the emergence of our species, 50,000 individuals lived in East Africa. Mt.Toba eruption had further reduced our numbers to 20,000 around 70,000 BC. Then, from 70,000 BC to 10,000 BC, human population increased to 5,000,000

around the world just before the start of the Neolithic revolution. Human population is one of the more reliable means to quantify the pace of change during this period. First of all, human, anatomically similar, consumed a similar amount of calories per day extracted from its immediate surroundings, the energy consumption discrepancy between genders or race (if it existed) can be deemed negligible. Secondly, human as hunter-gatherers still subject to the laws of natural selection. If human had exhausted a local supply of food resources and without able to locate newer ones, they would die. The population of a given animal species is fixed in a sub geological time scale as hunter-gatherers. If human has been completely subject under the law of natural selection, we should have observed human population stagnates or fluctuates around a mean value. However, human population during this period was continually increasing. This trend of growth suggests that the total amount of energy extractable by man in its immediate surrounding is increasing and the total energy consumption is also increasing. By utilizing better tools with greater precision and more clear communicating language, humans are more capable of hunting big games previously deemed too dangerous to be accessible, collecting nutrients and energy from nuts too sturdy to crack and consume. Despite a possible hunter-gatherers' version of Malthusian catastrophe awaiting for them, they constantly worked around ecological constraints by exploiting new food niches. The tools sets become a powerful extension of human biological capability, which even at the very best, takes hundreds of thousands of years to evolve. Yet the evolution of tool sets can be accomplished in tens of thousands of years using successive generation of advanced tool sets.

Therefore, measuring the total population growth rate of humans since its emergence is the first order approximation of the actual growth rate occurred during this period if one considers every aspect of human advancement in arts, language, culture, trade, and toolset innovations contributes toward the overall growth of this period. It is an excellent approximation because every human progress eventually can be measured in the advancement of the welfare and well-being of the species, and its total population is a direct manifestation of such transformation.

$$k_{hunter} = 0.0000931043 \quad (6.11)$$

$$T_{hunter} = \frac{k_{hunter}}{q} \cdot (75,000 - 5,000) + \frac{k_{homosapien}}{q} \cdot (75,000 - 5,000) \quad (6.12)$$

$$= 639,419,520.507 \text{ YAABER}$$

We can now use the rate of population growth per year divided over the background evolutionary rate (BER) of growth per year, and we arrived at 9,097.803. This number implies that even as a hunter-gatherer, we are advancing 9,097.803 times faster than biological evolution through natural selection. We did not include 195 Kya to 75 Kya because human population was reset following a major bottleneck possibly connected to Mt.Toba eruption. The intu-

ition we have over cave man for their slow reaction and dim wit seems to be more a cultural myth and construct. Of course, we should not neglect the rate of human evolution itself, the passive manipulation of matter and energy encoded into our DNA. This still applies despite the shortness of hunter-gatherer period. But as the second term indicates, it only adds an insignificant amount of change (2,573,259 years) compares to the human-directed cultural and technological evolution (636,846,261 years), or just 0.402% of the total YAABER of this period. From this point onward, consciously directed energy change dominates over passive manipulation by natural selection, which requires a geological timescale to add significant value to the YAABER. Because human cultural and technological changes occurred in $x < 10^5$ years, biological contribution to the YAABER still exists but becomes very insignificant.

6.6 YAABER for Feudal Society

No one should underestimate the importance of plant diversity in providing opportunity for species diversification. This importance has been observed in geologic past many times. The formation of Pangea supercontinent ushered in a period of cold, dry climate. This change in climate triggered the evolution of seed plants. By enclosing seed within hard shell, plants are able to populate further inland and to places less hospitable to earlier plant species. Following the speciation of seed plant, reptiles emerged within 20 Myr, also adapted to drier environment and exploited this new ecological niche opened by seed plants. Breaking of the Gondwana supercontinent during the Cretaceous gave the emergence of angiosperm. The emergence of angiosperm created the arboreal niche. The arboreal niche provides the living space for primates and birds. Finally, the advent of grass plants made human civilization possible. The transition from hunter-gatherer to agricultural civilization happened almost simultaneously around the world at the start of the last inter-glacial period. Domestications of wild rice, wheat, rye, and barley enabled energy acquisition to be magnitudes higher than a hunter-gatherer. The shortness of time span required to transition from hunter-gatherers to agricultural society seems to suggest as long as mild climate persists (interglacial) then agriculture revolution seems to be inevitable. However, I would suggest that many intelligent species on many Earth-like planets may never evolve into an agricultural society, consequently, maintained their mode of living throughout its entire existence as hunter-gatherers and never able to transform into an industrial one. Grass plants are unique in their annual growth cycle and little investment in their self-maintenance and a significant portion of investment in their seeds. As a result, high levels of energy density is stored in seed kernels. Its biological adaptation evolved in the recent millions of years, a very recent biological innovation that was possibly co-evolved with herbivores which are the ancestors of goats, cows, sheeps, and horses. Ancestors of humans, however, lived on the trees throughout this time when grass evolved and co-evolved with herbivores on land. *Therefore, the advent of grass plants is an independent evolutionary event from*

the emergence of intelligent Homo sapiens. Our ingenuity and dexterity eventually exploited this biological innovation. Therefore, in a sense, we took a free ride from the hard working symbiotic relationship and evolutionary feedback loop between herbivores on land and grass plants persisted millions of years before we walked on the ground. During the latter part of the agricultural revolution, grass also provides the ingredients of papermaking, which made information dissemination much more efficient and cheap and prepared for the transition into an industrial civilization. The following table is a list of seeds and their energy content based in kilo-calories.

Species Name	Energy	Species Name	Energy	Species Name	Energy
Sunflower Seed	2445	Fig	310	Beet	180
Maize	1528	Raspberry	220	Carrot	173
Rice	1528	Apple	218	Onion	166
Broad Beans	1425	Pineapple	209	Cabbage	103
Sorghum	1419	Blackberry	180	Spinach	97
Wheat	1369	Grapefruit	138	Turnip	84
Cassava	670	Lemon	121	Bell pepper	84
Soybean	615	Pumpkin	109	Tomato	74
Yam	494	Eggplant	104	Radish	66
Sweet Potato	360	Cucumber	65	Lettuce	55
Pea	339	–	–	–	–
Potato	322	–	–	–	–
Average	1042.83	Average	167.4	Average	108.2

Table 6.5: Edible plants and their energy content

One can see that rice plants top the list along with sunflower seeds and pine seeds and followed by fruits and then by vegetables such as spinach and lettuce. Although pine seeds have comparable energy content to that of the rice plants, pine trees are perennials and takes a long growth cycle to reach maturity. Then a much smaller amount of energy it captured is stored into its final seed product, a significant portion is invested into its bark, trunk, and leaves maintenance. Therefore, pine trees, from hunter-gatherers' perspective can be too costly to be domesticated. In fact, the cost of domestication is so prohibitively expensive that it will fail to start in the first place. A transition from hunter-gatherer to an agricultural civilization on a planet dominated with pine like trees or lacking a biological equivalent of grass plants on earth will be almost impossible. One may argue, that given enough time, in the scale of tens of millions of years (which will still be a magnitude or two faster than natural selection), pine trees may possibly be successfully domesticated. However, 99% of species went extinct within 10 million years. Therefore, the timescale involved to transform a pine-like tree into a grass plant is impractical. On the other hand, a planet may be dominated with fruits growing on tomato, zucchini like annual plants, a transition to an agricultural civilization is then possible but its population density will be significantly lower than that is attainable on earth. Furthermore, a planet dominated by the sea with scattered island masses will have little carrying capacity

even if rice like plants are plenty and their intelligent species transitioned successfully from hunter-gatherers to agriculturalists. Finally, an agricultural society will be much smaller in size on a planet dominated by land with a few seas and a significant supply of grass plants yet a majority of the land are occupied by desert, ice sheets, or high lands, or all of them combined. Of course, we might find the completely the reverse to be true, where abundant land filled with grass plants and technologically capable species. The point of the thought experiment is to appreciate the number of possibilities given the billions of habitable planets confirmed to exist. Given the enormous amount of available data points, each planet, representing a data point of slightly different values from each other if they are ever possibly be sorted from high to low, will form the Gaussian distribution, the lognormal curve in our model for ex-terrestrial civilizations' advancement index distribution.

A planet dominated by grasslands or highlands with scattered spots capable of agriculture will be particularly interesting. Since highland and grasslands are less suitable for raising the type of plants similar to wheat and rice, pastoral nomads may become the dominant mode of living among its most intelligent creatures. A pastoral society shares some characteristics of the agricultural society in that it is able to raise a higher number of people through animal breeding yet they also roam in order to secure water and strategical resources like hunter-gatherers. The primary disadvantage of such society is its difficulty in fostering scientific and investigative science since it requires a high level of specialization to produce the tools (which requires stationary factories to build and hardly can be moved from place to place) over successive generations with dictated improvements and refinements. A pastoral society primarily concerned with its own subsistence and emphasize self-independence can produce little work specialization beyond a family and tribal complexity. Most interestingly, as observed in the history of earth repeatedly, that the competition between pastoral and agricultural society was intense. The earlier examples are the Huns which looted and attacked the agricultural based Han dynasty, and the Germans and Gothic people attacked the Romans. A later example is the Mongols which attacked the Song dynasty in East Asia and Europe and Arabic Empire in the Western Eurasia continent. Though all agricultural society survived the onslaught and eventually transformed into industrial civilizations, the destruction is nevertheless substantial. Given the sheer size of agricultural land on earth and limited pastoral land and the destructive power possessed by those smaller pockets of pastorals, it is possible that on a planet dominated by grasslands, agricultural society follows cycles of prosperity and bust triggered by the onslaught of the pastorals and can hardly survive at all. Its science follows periods of progress and then regress as information and knowledge are lost due to war and destruction. It is also possible that some pastorals eventually become agriculturalists themselves as they occupied the land once owned by previous agriculturalists. However, as they become the agriculturalists themselves, their fate followed the similar trajectory of their predecessors. Therefore, its civilization can hardly transform into an industrial one and is trapped at the stage of development of pastoral society and agricultural society.

To measure the rate of progress compares to the background evolutionary rate, and add this value to the final YAABER, we resort to both population growth from 10,000 BC with yields per acre. Population data is well-extrapolated and documented for the past 10,000 years. We sample our data from three periods. The first one ranges from 5,000 BC at the start of the full transition from hunter-gatherer to agricultural to 1,000 BC when city-states began merging into empires. We call the first period the period of city-states. Then, from 1,000 BC to AD 1600, it includes the classical, Roman, the middle ages, and the early modern period. Finally, the age of exploration spans from 1600 to 1750. We compute the population growth rate of each period (obtain the annual rate of growth) and then use them to compute the final YAABER.

$$k_{citystates} = 0.000576 \quad k_{middle} = 0.000943 \quad k_{exploration} = 0.00207$$

$$\begin{aligned} T_{citystates} &= \frac{k_{citystates}}{q} (5000 - 1000) + \frac{k_{hunter}}{q} \cdot (5000 - 1000) + \frac{k_{homosapien}}{q} \cdot (5000 - 1000) \\ &= 261,676,514.841 \text{ YAABER} \end{aligned} \tag{6.13}$$

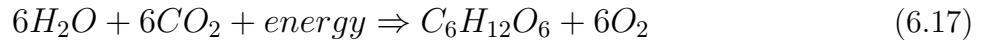
$$\begin{aligned} T_{middle} &= \frac{k_{middle}}{q} (1000 + 1600) + \frac{k_{hunter}}{q} \cdot (1000 + 1600) + \frac{k_{homosapien}}{q} \cdot (1000 + 1600) \\ &= 263,330,587.241 \text{ YAABER} \end{aligned} \tag{6.14}$$

$$\begin{aligned} T_{exploration} &= \frac{k_{exploration}}{q} (1750 - 1600) + \frac{k_{hunter}}{q} \cdot (1750 - 1600) + \frac{k_{homosapien}}{q} \cdot (1750 - 1600) \\ &= 31,711,082.539 \text{ YAABER} \end{aligned} \tag{6.15}$$

$$\begin{aligned} t &= T_{citystates} + T_{middle} + T_{exploration} \\ &= 556,718,184.622 \text{ YAABER} \end{aligned} \tag{6.16}$$

We found that the rate of increase is another 556.7 million years faster than the evolutionary background rate of growth. That brings us to another good question. Will agricultural productivity continue to increase without steam power or any machine power in general? To answer this question, we need to know if any growth constraints persist in biological plants themselves. Since all biological products we consume ultimately derives its energy content from that of the sun, then biological conversion efficiency can be measured, and the highest attainable conversion sets the upper bounded constraints on agricultural, domestic selection and breeding.

Photosynthesis can be described by the simplified chemical reaction:



where $C_6H_{12}O_6$ is glucose (which is subsequently transformed into other sugars, cellulose, lignin). The value of the photosynthetic efficiency is dependent on how light energy is defined – it depends on whether we count only the light that is absorbed, and on what kind of light is used. It takes eight photons to utilize one molecule of CO_2 . The Gibbs free energy for converting a mole of CO_2 to glucose is 114 kcal, whereas eight moles of photons of wavelength 600 nm contains 381 kcal, giving a nominal efficiency of 30%. [88] However, photosynthesis can occur with light up to wavelength 720 nm so long as there is also light at wavelengths below 680 nm to keep Photosystem II operating. Using longer wavelengths means less light energy is needed for the same number of photons and therefore for the same amount of photosynthesis. For actual sunlight, where only 45% of the light is in the photosynthetically active wavelength range, the theoretical maximum efficiency of solar energy conversion is approximately 11%. In actuality, however, plants do not absorb all incoming sunlight (due to reflection, respiration requirements of photosynthesis and the need for optimal solar radiation levels) and do not convert all harvested energy into biomass, which results in an overall photosynthetic efficiency of 3 to 6% of the total solar radiation. [2] If photosynthesis is inefficient, excess light energy must be dissipated to avoid damaging the photosynthetic apparatus. Energy can be dissipated as heat (non-photochemical quenching), or emitted as chlorophyll fluorescence.

Quoted values sunlight-to-biomass efficiency:

Plant	Efficiency
Plants, typical	0.1% [3], 0.2~2% [5]
Typical crop plant	1~2% [3]
Sugarcane	7~8% peak [3]

Table 6.6: Photosynthetic efficiency

The following is a breakdown of the energetics of the photosynthesis process from Photosynthesis by Hall and Rao: [31]

Starting with the solar spectrum falling on a leaf, 47% lost due to photons outside the 400–700 nm active range (chlorophyll utilizes photons between 400 and 700 nm, extracting the energy of one 700 nm photon from each one) 30% of the in-band photons are lost due to incomplete absorption or photons hitting components other than chloroplasts. 24% of the absorbed photon energy is lost due to degrading short wavelength photons to the 700 nm energy level. 68% of the utilized energy is lost in conversion into d-glucose. 35–45% of the glucose is consumed by the leaf in the processes of dark and photorespiration.

Stated another way: 100% sunlight split into 47% non-bioavailable photons as waste, leaving

53% (in the 400–700 nm range). Then, 30% of remaining photons are lost due to incomplete absorption, leaving 37% as the absorbed photon energy. Out of which, 24% is lost due to wavelength-mismatch degradation to 700 nm energy, leaving 28.2% of sunlight energy collected by chlorophyll. Out of this collected sunlight, 32% efficient conversion of ATP and NADPH to d-glucose, leaving 9% of sunlight collected as sugar. Out of 35 to 40% of sugar is recycled/consumed by the leaf in dark and photo-respiration, leaving 5.4% net leaf efficiency. Finally, many plants lose much of the remaining energy on growing roots. Most crop plants store 0.25% to 0.5% of the sunlight in the product (corn kernels, potato starch, etc.). Sugar cane is exceptional in several ways, yielding peak storage efficiency of 8%.

According to the cyanobacteria studies, the total photosynthetic productivity of earth is between 1,500 and 2,250 TW, or from 47,300 to 71,000 exajoules per year. Using this source’s figure of 178,000 TW of solar energy hitting the Earth’s surface,[74] the total photosynthetic efficiency of the planet is 0.84% to 1.26%.

Based on these studies, a typical plant yields a photosynthetic efficiency of 1% and typical crop plant yields at 1.5% and maximum upper bound at 6~8%. Therefore, we can apply the yield per acre growth rate observed from the past two millennia to see at which year into the future had industrial civilization not occurred the agricultural revolution would reach its ultimate potential. Yields per acre data have been accurately preserved for the past three millenniums, especially in China. During each dynasty, one of the most important tasks of the imperial court of China is to take the census and measure the average yield per acre on different types of crops. Using this data,[101] we can back-extrapolate the yield per acre at 10,000 BC and its rate of energy acquisition to that of the evolutionary background. From the table below, we have collected and sampled the yield per acre record from the Eastern Zhou dynasty (771 BC - 256 BC) to Qing dynasty (AD 1644 - AD 1911).

Dynasty	Year	Wheat Yield	Rice Yield
East Zhou	476 BC	0.2	–
Han	8	0.6	0.4
Wei & Jin	300	0.6	0.6
East Jin	400	–	0.9
North & South Dy	500	1.2	–
Tang	800	0.6	0.9
Song	1127	0.6	1.2
Yuan	1300	1.2	2.4
Ming & Qing	1644	1.2	2.4

Table 6.7: Historical yields per acre

Regression on wheat yield:

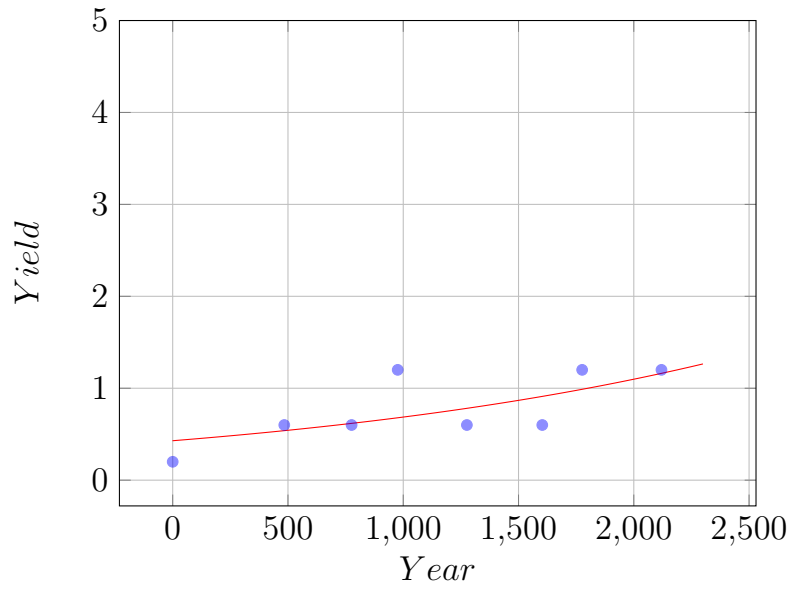


Figure 6.4: Regression on wheat yield over 2000 years

$$y = 0.429(1.00048)^x \tag{6.18}$$

with an annual growth rate of 0.048%.

Regression on rice yield:

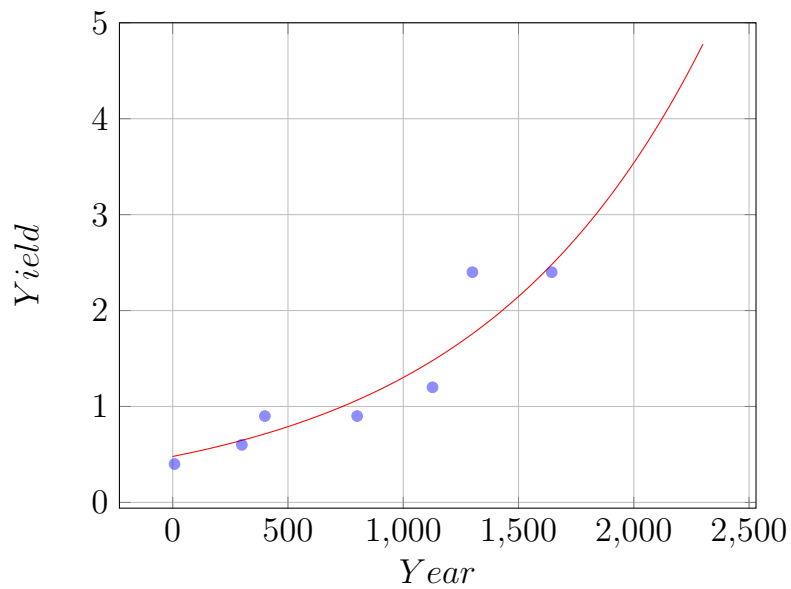


Figure 6.5: Regression on rice yield over 2000 years

$$y = 0.480857(1.00102)^x \tag{6.19}$$

with an annual growth rate of 0.102%.

Simply using these rates, one finds the final value to be 1,509 years (rice) and 2,732 years (wheat) into the future to reach 7% efficiency. That is, if industrial revolution had not occurred and human and livestock based muscle power dominated agricultural revolution continues; then, we would expect, on average, another 2,120 years of a steady rise of world total energy output harvested by man and then the growth can no longer be maintained. In the long run, if industrial civilization never occurred, artificial breeding may eventually raise the photosynthetic efficiency to 30% based on chemical constraints placed in nature. Then, it is still possible to extend a sense of continued progress in human affairs in terms of population growth for another 4,000 years given the standard agricultural economic growth rate per year, and possibly as long as 40,000 to 400,000 years if domestic selections to yield higher photosynthetic efficient crop plant proved to be difficult. Thereafter, the human society would stagnate at this level of development. But how can such society never develops industrial civilization if hundreds of thousands of years of agricultural civilization persisted? There are many possible scenarios barred them from further development. First of all, the planet may lack a significant amount of uranium in its crust so that transitioning into a sustainable industrial civilization is not possible. The Faint Young Sun paradox proposes that earth was warm even in the early phase of sun's formation. Many pointed out that greater amount of radioactive material was present at the earlier days of the planet and released heat to compensate the dimming sun in its early days, and we continue to enjoy active earth with internal heat from the abundance of uranium in our earth' crust. Uranium presence may be a necessary but insufficient condition for life formation. This assumption is undermined, however, it is now generally agreed that tidal heating contributes toward a third of the internal heat budget of the earth. That is, uranium contributes some but not all of the internal heat. On a super earth, with even greater tidal heating in its core, even greater amount of heat can be released and keep the planet warm throughout all periods so that the planet remains warm despite its deficiency in uraniums. Furthermore, some terrestrial planets, even born at the same time as the sun, likely to be more metal-poor in uranium. In both of these scenarios, intelligent life may use fossil fuels to develop an industrial civilization but found themselves unable to maintain it because the cost of EROEI for uranium extraction is prohibitively expensive or simply non-existent. As we have shown earlier it is also possible that the planet is by dominated by highlands or oceans. It is also possible, though much fewer cases throughout the cosmos, fossil fuels were not well-preserved on a planet even though uranium is abundant in its crusts. Without the cheap, accessible fossil fuel to kickstart an industrial revolution, intelligent life on such a planet stuck at the level of development of agricultural society. One should not underestimate the level of complexity and energy budget available to such a stagnant civilization. A fully matured agricultural society which utilizes all possible land mass to capture solar energy at the maximum photosynthetic efficiency can yield total energy output comparable to our industrial civilization. Let's do some thought experiment, given the total available arable land on earth today, and assume the theoretical maximum photosynthetic

efficiency is reached, and we arrived at 31 TJ of energy for such a civilization! However, we will show that even though they are able to achieve such level of energy budget, their society still deemed as non-progressing because all these energy is diverted into the direct consumption by livestock, biomass, and the extremely well-fed species itself. (can still be under-nourished if high population is required to maintain such large energy output) However, no high-density energy driven technology such as airplanes, computers are possible, and no computer and Moore's law to observe. This brings us to one of the most critical assumptions in our overreaching hypothesis. *That is, almost all intelligent species evolved on all existing habitable planets are stagnant in its development, that is, it does not shift its position relative to the mean cosmic evolutionary rate of the static, non-moving normal distribution model bounded by geologic time frame, ($x < 10^7$) years.* This is very counter-intuitive to our common sense. Since the rise of Homo sapiens, we learned nothing but change and progress strived and achieved by man. These assumptions, then, implies that human progress is transitory, and ephemeral, and likely either to end soon or not sustainable.

Then, to solve the assumptions that human progress is transitory and ephemeral, and likely either to end soon or not sustainable we need to introduce the uniform distribution model in an AI led technological civilization. For a civilization which successfully transitioned into a sustainable industrial one powered by nuclear fusion and entered a cosmic expansionary phase, a different scenario awaits and at the same time, does not violate the assumption stated above. The resolution of the dilemma regarding an ever-progressing and expanding cosmic civilization in our static, non-moving normal distributed model is discussed below.

6.7 YAABER for Industrial Society

Human started the transition from biological muscle dominated society into a fossil fuel based industrial machine civilization in the 18th century. Thanks to James Watt's steam engine, fuel driven devices made progress much faster than agricultural revolution. It is estimated that one gallon of oil is equivalent to 2,000 manual labor hours.[46] With such level of cheap, abundant energy available, an intelligent species is able to exploit uranium in its crust, if available, and make it affordable to transition into a sustainable industrial civilization driven by nuclear fusion. As we have stated in our opening pages, once a civilization developed fusion and gained adequate knowledge on the development of fusion spaceship, it is just a matter of time before it expands and uses the energy of the sun and other stars. Then, its position relative to the cosmic evolutionary rate continually shift, and YAABER will continue to increase in our static, non-moving normal/lognormal distribution model. To illustrate this dilemma in our model, let's start by calculating how much progress Homo sapiens obtained since 1800 given the rate of economic growth rate, reflected in net energy usage, is 1.5% increase per year. It is noted by British economists and labeled as White's law, that the economic growth is closely intertwined

with the growth rate of energy usage. In essence, measuring total energy output can be one of the most straightforward ways to measure the amount of progress achievable, not significantly different from our earlier analysis on hunter-gatherer society and agricultural society. It is only this time; fossil fuel-based energy budget substituted the solar based one. With a much greater amount of energy budget and capable tools (agricultural machinery, construction cranes, tunnel diggers, railroads, trains, cargo planes and ships) to convert it into useful work, the diversity and complexity of the society backed by the species increases.

We then calculate this rate with our background evolutionary rate from AD 1750 to AD 2100 over the course of 350 years, and we arrived at 375.9 million years.

$$k_{earlyindustrial} = 0.00507 \quad (6.20)$$

$$\begin{aligned} T_{earlyindustrial} &= \frac{k_{earlyindustrial}}{q} (1900 - 1750) + \frac{k_{hunter}}{q} \cdot (1900 - 1750) + \frac{k_{homosapien}}{q} \cdot (1900 - 1750) \\ &= 75,683,398.2669 \text{ YAABER} \end{aligned} \quad (6.21)$$

From 1750 to 1900, during the early industrial period, the population was growing slower than the full blown one in the 20th century because only a handful of countries (UK, US, France, Germany) were undergoing industrialization. Moreover, none of them had completed their transformation at the time. The overall slower growth rate is reflected from the population growth rate at the time, lower than 1.5% per annum.

$$k_{industrial} = 0.0132 \quad (6.22)$$

$$\begin{aligned} T_{industrial} &= \frac{k_{industrial}}{q} (2100 - 1900) + \frac{k_{exploration}}{q} (2100 - 1900) + \frac{k_{hunter}}{q} \cdot (2100 - 1900) \\ &\quad + \frac{k_{homosapien}}{q} \cdot (2100 - 1900) \end{aligned} \quad (6.23)$$

$$= 300,252,362.322 \text{ YAABER}$$

For the latter part of the industrial phase, it spans from 1900 to 2100. We choose 2100 as the expected time by which the society either stops grow and transitions into a steady state biological led industrial civilization due to increasing limits on resources or transitions into an industrial civilization led by non-biological superintelligence.

Either way, by AD 2100 we will have made another 375.9 million years of progress compares to the cosmic evolutionary rate in 350 years! Note that agricultural society contributed an insignificant portion of 40.4 million years into the final YAABER, because throughout this transition, agriculture still maintained its steady progression toward its maximum utilization

rate, and likewise, a tiny portion of YAABER itself.

If we continue to extrapolate this trend, we would expect another 150 million years added to the final YAABER by the 22nd century and 300 million years to YAABER by the end of the 23rd century. Within a few centuries, the contribution to YAABER by industrial civilization would dominate the entire calculation. This implies by simply maintaining our current level of industrial progress, we would expect soon to be one of the only one possible industrial civilization within the observable universe within a diameter of 93 billion light years predicted by the distribution function, and soon magnitudes above the observable universes diameter. However, such an argument implies something very special about industrial civilization itself, and within a few millennium of development, we expect ourselves to be the only one in the entire universe in terms of development, this is in contradiction with the principles of mediocrity. Even if industrial civilization is not as frequent as the number of habitable Earth-like planets, claiming ourselves as the only one present ourselves as a variant version of the rare earth hypothesis (in fact, a rare industrial civilization hypothesis.) On the other hand, if we conform to the principle of mediocrity, then, we would expect our growth-based economic model to be unsustainable. In reality, are our industrial civilization capable of continued economic growth for the next few centuries or are we facing a transition to no growth based stagnant industrial civilization or an industrial collapse? Or can we reconcile these dilemmas?

A key insight is to distinguish two states of an industrial civilization. *One is that led and maintained predominantly by intelligent biological species. Another is that led and maintained predominantly by post-biological intelligence risen from the industrial revolutionary process itself.* This insight is crucial to understanding and resolving the inconsistency in our model for prediction. The increasingly dominant role of post-biological intelligence in industrial civilization is not well-appreciated and even taken seriously until the Law of Accelerating Returns, a generalized form of the Moore's Law, which states that the speed of central processing unit in the semiconductor industry doubles every 18 months. Using this model, it is predicted that machine with the equivalent of human-level intelligence is roughly at the cost of \$1,000 by 2019 and a thousand times faster by 2029, and a billion times by 2045; hence, a term is labeled as the Technological Singularity. If the trend of post-biological intelligence overtaking and dominating in any evolving industrial civilization is typical, by the principle of mediocrity, then, it implies that every industrial civilization, with its abundant cheap energy, will transform its technology at such a fast speed. Within a sub-geologic timescale, transition toward a post-biological industrial civilization is then inevitable. Once a post-biological industrial civilization transition is complete, it is no longer represented as a data point in our static, non-moving Gaussian distribution model. A post-biological civilization is not subject to the biological constraints placed upon a biological species. Despite human's ingenuity, human requires certain biological assumptions to survive on. Human can only survive unprotected between a temperature range between negative 30 and positive 50 degrees Celsius at 1-atmosphere pressure. Human cannot survive at 100% level of pure oxygen at the standard 1 Atm. A further study was done by

NASA for oxygen tolerance at different atmospheric pressures. At longer time frame, human needs significant amount water to maintain its bodily functions. At even longer time frame, human requires the gravitational environment to maintain healthy bones and frames. Even with satisfying conditions mentioned above, human continued economic growth will eventually raise the global temperature generated from the heat waste product of the industrial process. Since humans are biological and maintain their physical energy from primary crops and live-stocks, rising temperature guarantees a global warming scenario, which is catastrophic to the lives of human themselves. This global warming scenario is way more general trend than the CO₂ emission from fossil fuel, which is already generating heated debate within the society. The heat waste is generated by even the so-called green energy alternatives. Since a continued growing civilization ultimately requires a transition into nuclear power, the heat waste in the forms of hot water dumped into waters and streams will eventually raise the global temperature, albeit at a slower rate than the CO₂ emission observed by burning fossil fuel. The rising global temperature is an inevitable consequence of economic growth based on the second law of thermodynamics. In such a case, biologically based industrial civilization will eventually face a choice of growth or sustainability. It will still be able to maintain its level of development or somewhat lower level of energy consumption. Otherwise, it is essentially non-growing in terms of energy usage. That is, its position stays relatively static to the cosmic evolutionary rate. Some may argue that by turning the moon into a giant solar energy collector and beaming energy back to earth or by building all nuclear power plants on the moon will solve the heat waste problem. However, eventually, the final energy product, excluding the heat waste, has to be delivered back to earth to be consumed, the heat accumulation will eventually contribute to a warming up. To appreciate how quickly human can alter its environment compares with nature, we can do a calculation on a solar collector on the moon with a growth rate of 1.5% per year, in 400 years, it will able to capture and deliver 4% of total sunlight received on earth annually to earth via laser. This additional 4% of solar energy increase is equivalent to the sun's increase in luminosity in 440 million years into the future. That is, very consistent with our analysis that 400 years of industrial revolution contributes to 515.94 million years to YAABER. A stagnant civilization in terms of energy usage does not imply a stagnation in progress. It may well be diverting its resources into information technology and bioinformatics. In such a scenario, this civilization stagnates for a few hundred years before a transition into a post-biological industrial one. Within a timescale of 10⁷ years, its stagnation will not even show up in the model.

We can then calculate the upper bound of a biological based industrial civilization if we take the report on the maximum allowable temperature range increase to be 4 percent warmer in terms of total solar insolation. Assuming alternative nuclear energy is adopted, the increase in heat waste will guarantee an increase of 4 percent by AD 2400. Given that currently, the average waste heat of the earth per square meter is 0.028 $\frac{\text{Watt}}{\text{m}^2}$ and an industrial growth rate of annual 1.5%. Of course, faster growth rate and concentration in urban areas will run into

the limit much earlier.

$$\begin{aligned}
 T_{wasteheat} &= 0.028 \cdot (1.015)^{400} & (6.24) \\
 &= 10.8037600757 \frac{\text{watt}}{\text{m}^2}
 \end{aligned}$$

Temperature is not the only limitation placed upon on biological based industrial civilization. Since crops require land to grow and harvest energy, photosynthetic efficiency, as mentioned before, and the total amount of arable lands and even total lands available becomes the limiting constraints. We can perform some calculations on the limits based on earth. Assuming the entire earth adopts to an urbanized lifestyle and maintained a population density comparable to Tokyo and the remaining crop lands maintain the natural photosynthetic efficiency, then, we would expect world's carrying capacity at 54 billion and urban metropolitan size of the country of Brazil and takes 137.5 years to reach this level with 1.5% annual growth rate.

$$P_{agrimitarea} = 5.4053866714 \times 10^{10} \text{ km}^2 \quad (6.25)$$

$$\begin{aligned}
 A_{agrimitarea} &= 5.4053866714 \times \frac{10^{10}}{6,224.66} & (6.26) \\
 &= 8,683,826.37991 \text{ km}^2 \text{ Metropolitan Area}
 \end{aligned}$$

$$T_{agrimit} = (1.015)^{137.5} \quad (6.27)$$

$$= 7.74605915486 \text{ 7Billion}$$

the units above is 7 billion, the current population of the world.

With GMO enabled crop to reach its ultimate biological conversion efficiency, it is possible to support a population of 711.8 billion and urban area size of all continents except Antarctica, and it takes 310 years to reach this level with 1.5% annual growth rate.

$$P_{agrimeaarea} = 7.1181844926 \times 10^{11} \quad (6.28)$$

$$\begin{aligned}
 A_{agrimeaarea} &= 7.1181844926 \times \frac{10^{11}}{6224.66} & (6.29) \\
 &= 114,354,591.136 \text{ km}^2 \text{ Metropolitan Area}
 \end{aligned}$$

$$T_{agrimea} = (1.015)^{310.43} \quad (6.30)$$

$$= 101.68420451 \text{ 7Billion}$$

the units above is 7 billion, the current population of the world.

It is interesting to note that further expansion was not possible even though photosynthetic efficiency can be continually raised because growing population requires land to dwell. The costs (occupying agricultural space) of a continued rise in population eventually overtaking the benefit of having people producing the agricultural products in the first place.

Even if temperature and land space were not considered to be constraints, what are the possible limits to an expanding biological based industrial civilization? In which case, the total surface area, converted into the urban landscape and people feed based on vertical horticultural food grown from LED lights, can support at most 8,992 billion, and it will take 326 years to reach this level assuming 1.5% annual population growth rate.

$$\begin{aligned}
 P_{all} &= 148940000 \cdot 6224.66 \cdot \frac{0.97}{1} \\
 &= 8.9928783459 \times 10^{11} \text{ people}
 \end{aligned}
 \tag{6.31}$$

Is it possible to transform into a scale II civilization that harnesses the host star output energy? We still need to make certain assumptions about the biologically based human. The minimum requirement is to reside on a solid mass that contains a considerable amount of gravity which in turn is able to hold onto an atmosphere. If such scenario is true, it remains whether photosynthesis can be carried out by nuclear fusion instead of the sun as the sun itself is to be converted into thousands of Earth-sized planet where each can hold the 700 billion carrying capacity of the earth. We also assume that hydrogen harvested from the sun can be converted into metallic hydrogen, and helium can be converted into metallic helium. In order to turn one sun into millions of Earth-sized planet, we soon find that overcoming the sun's gravitational binding energy is way greater than a 540 billion human can generate to start with, economically prohibitively expensive.

$$\begin{aligned}
 T_{sun} &= \frac{(6.87 \cdot 10^{41})}{\frac{540}{70} \cdot (6.8 \cdot 10^{19})} \\
 &= 1.3096405229 \times 10^{21} \text{ years}
 \end{aligned}
 \tag{6.32}$$

It will take $1.3 \cdot 10^{21}$ years of all energy generated by 540 billion people to tear the sun apart. If we assumed maximum upper bound on human population covering the entire surface of earth, and they tear Jupiter apart instead, it would still take them $1.3 \cdot 10^{19}$ years to accomplish this task.

$$\begin{aligned}
 T_{jupiter} &= \frac{(6.87 \cdot 10^{41}) \left(\frac{318}{333000} \right)}{101.68 \cdot (6.8 \cdot 10^{19})} \\
 &= 9.4884478128 \times 10^{16} \text{ years}
 \end{aligned}
 \tag{6.33}$$

As a result, the splitting of the sun to create earth analogs remain a science fiction to biological-

based industrial civilization.

Apart from the natural limitation placed upon human, human self-directed decision making can also render its own industrial civilization collapse. Most commonly mentioned examples are the nuclear holocaust, grey goo nano-technological catastrophe, and social degeneration. In each of these cases, the position of the civilization shifts toward the left, or toward the cosmic mean evolutionary rate. The derivative of the bell curve will be negative in the direction of positive increase from the mean. Fossil fuel depletion before a successful transition into a nuclear-based civilization will also render a civilization-wide collapse, indicated by the M. Hubbert's peak oil theory.

In conclusion, the increasingly diminishing chance of observed biological led industrial civilization in the bell curve model is a combination of the above-mentioned factors. In particular, a phase transition sometimes occurs during its development where the cost of transitioning into a post-biological one is lower than that of the biological led one. If we consider earth is typical, and all intelligent species act rationally according to the principle of economics, we would expect most biological based industrial civilization transition into a post-biological one in 300 years after the start of the industrial revolution on their home planet. This reconciles with the principles of mediocrity. Because it shows that after 300 years of progression, those civilizations which graduate into a post-biological one should be common rather than extremely rare. It also implies that a biological led industrial civilization which does not transition but keeps expanding without improving upon themselves is foolhardy and consequently, rare in the cosmos. A post-biological industrial civilization does not mean, however, that all components of the society are exclusively post-biological. Just as the economy of United States today labeled as a developed industrial economy, it does not imply that it does not perform agricultural activities. In fact, United States contains the largest agricultural activity in the world. Because over 95% of economic activities have no direct relation with agricultural activity, the direction and progression of the economy are determined by the decision making in the industrial sector. In a sense, a biological led industrial civilization's position on the bell curve resembles a supernovae's brightness in a galaxy.

All stars within a galaxy shine significantly fainter than the sum of all stars within the galaxy and their brightness can be modeled by power law/lognormal distribution. Their brightness grows very slowly as they burn slowly on the main sequence, but within the timeframe of human affairs, their brightness stays constant, non-changing. Yet a supernovae's luminosity position shifts quickly within the spans of weeks to the right of the curve by a few standard deviations and then fades quickly to the left of the mean as a white dwarf, a neutron star, or black hole. The progress of humanity on the evolutionary distribution curve is conceptually similar. A biological human-led industrial civilization shifts its position quickly on the bell curve, reaches an extreme right-handed outlying value, many sigmas above the mean, but also quickly drops from the model altogether as it successfully transitioned into a post-biological industrial civilization or retracts its position and returns to a non-moving position as an agricultural civilization, or

non-growth based industrial civilization.

In conclusion, the total amount of time on average a civilization spends as a biologically directed industrial civilization in growth mode is what we needed to add to the final YAABER. In our case, from the start of the utilization of the steam engine until the utilization of sustainable nuclear fusion and the advent of strong AI. Without nuclear fusion and even with Strong AI, the industrial civilization will collapse and eventually retracts to an agricultural one. With only nuclear fusion, civilization is earthbound (at most add a terraformed Mars), and the society eventually stops grow and transition into a steady state biological led industrial civilization. Only when both nuclear fusion and strong AI are realized, the society transitioned into an industrial civilization led by non-biological superintelligence and expands into the universe. Since we have formalized the project PACER since the 1960s and expecting the emergence of technological singularity around 2045, we are not underestimating the YAABER under the age of industrialization by setting our computed boundary at 2100. That is, nearly all civilization made their full transition from biologically led civilization to a post-biological one within this time frame or stagnate into a steady state faced by the biological and resource constraints. Then, the sum total of the entire YAABER from all period is 1.766 Gyr.

$$\begin{aligned} t &= T_{prim} + T_{homo} + T_{hunter} + T_{citystates} + T_{middle} + T_{exploration} + T_{earlyindustrial} + T_{industrial} \\ &= 1.7660472964 \times 10^9 \text{ YAABER} \end{aligned} \tag{6.34}$$

7 Model Predictions

7.1 Number of Habitable Earth

From the previous Chapter 2 and 3, we have enumerated and demonstrated different criteria that restrict the number of habitable planets and eventually the number of planets that gives to the emergence of industrial civilization. We will now list the figures after each selection criterion.

Term	Probability	Number
P_0		1,347,261,098
Galactic Habitable	25.76%	346,987,961
Binary	86.81%	301,212,727
Habitable Zone	9.20%	27,714,025
Eccentricity	95.76%	26,538,951
Appropriate Mass	65.18%	17,298,416
Rotation	78.00%	13,492,764
With a Moon	55.92%	7,545,521
Non-locked Moon	21.91%	1,652,960
Metallicity & Wet Earth	30.63%	506,230
Ocean Budget	45.33%	229,450
Dry Land Ratio	4.67%	10,719
N_{earth}		10,719

Table 7.1: Number of Habitable Earth

The number of terrestrial planets within the Milky Way galaxy obtained based on Lineweaver's method that emerges between 5 Gya and 4 Gya is 1.347 Billion.

The number of planets within the galactic habitable zone is 347 Million.

The habitability of binary, ternary, and multiple systems reduces the number to 301 Million.

The habitable zone restricts planets to be between 0.840278 AU and 1.0887 AU total radius for terrestrial planets' formation zone of solar mass stars. The total radius for terrestrial planet formation zone and the band of habitability expands and shrinks according to stellar mass, but the ratio remains fixed for different stellar mass. Therefore, the number of terrestrial planets within the habitable zone is 27.7 Million.

Terrestrial planet with moderate eccentricity so that its orbit falls within the comfortable range of the band of habitability is 26.5 Million.

Out of these planets, the terrestrial planet mass ranges between 0.43 to 2.6875 earth mass is 17.3 Million.

Out of these planets during its final merging process, the rotation is fast enough so that the day and night cycle after 4.5 Gyr of evolution is less than 7 days is 13.49 Million.

Out of these planets that the final generated moon does not eventually fall back onto the planet itself is 7.54 Million.

Out of the planets that have a satellite, the satellite is light enough that it does not tidally lock with its parent planet during the emergence of civilization 5 Gyr after its initial formation is 1.65 Million.

Out of these planets that are covered by water, or as wet planets, is numbered 0.5 Million:

Out of the wet planets, those planets that allow the exposure of dry land in some proportion is 0.229 Million.

Finally, those planets that have the right proportion of ocean water so that a submerged continental shelf enables the smooth transition from ocean-based life to a land-based life form is 10,719.

Very lastly, the number of low mass binaries (Chapter 2) is 843,478. One applies all the previous filter mentioned except the filter criteria for the habitability of binary system and the habitability within the habitable zone since they were already computed from the previous round and we obtain 80 habitable planets.

Therefore, there are, in total, *10,799 habitable planets within the Milky Way* at the current epoch that can potentially lead to intelligent life.

The Composite Probability on the Emergence of Industrial Civilization

Term	Probability	Number
N_{earth}		10,799
Life	22.76%	2,458
Angiosperm	26.03%	640
Fastest Emergence of Man	7.14%	46
Glaciation by Land Ratio	29.88%	14
Current Glaciation	70.00%	10
Permissible Placement of Continent Cycle over Glaciation Cycle	5.4166%	0.52
Emergence of Man	36.74%	0.19
Industrial	10.12%	1/51.9626296708
$N_{\text{industrial}}$		1/51.96

Table 7.2: Number of Civilizations

Now, having derived the number of habitable planets, out of these planets where life has actually developed from the assemblage of amino acids is 2,458.

Out of those that developed life, the biodiversity of angiosperms or the primary producers has reached the level of complexity observed on earth is 640.

Out these planets, the evolution of intelligent species embarked the shortest starting path by acquiring opposable thumbs first as an arboreal species, which is partially attributed by the accidental asteroid hitting earth 66 Mya and clearing the niches for the mammalian adaptive radiation is 46.

Out of these planets, the probability that they possessed a land mass of the right proportion that enables the periodic ice age as an evolutionary accelerator is no more than 14.

Out of these planets, the chance of the planets that are currently undergoing ice age reduces the number to no more than 10.

Out of these planets, the chance of the planets hosting an glaciation at the appropriate timing enabling the fastest emergence of man is less than 1.

Out of these planets with fluctuating climate pattern, the actual emergence of intelligent, tool-using species is no more than 0.19.

Finally, the number of intelligent species that actually go on to transition into agricultural society and then to an industrial one, mostly constrained by the probability of the emergence of major, high-calorie crop plants is just 0.019.

$$N_{earth} \cdot P_{life} \cdot P_{angiosperm} \cdot P_{startwiththumbasteroid} \cdot P_{iceagebyratio} \cdot P_{iceagenow} \cdot P_{man} \cdot P_{industrial} \quad (7.1)$$

$$= 0.0192448159221$$

This concludes that the probability of the emergence of an industrial civilization is as rare as at least 1 in almost 52 galaxies at the current epoch.

$$(N_{earth} \cdot P_{life} \cdot P_{angiosperm} \cdot P_{startwiththumbasteroid} \cdot P_{iceagebyratio} \cdot P_{iceagenow} \cdot P_{man} \cdot P_{industrial})^{-1} \quad (7.2)$$

$$= 51.962045469848$$

7.2 The Model

After we have laid the foundations regarding the number of habitable terrestrial planets within the 5 Gya to 4 Gya window, the chance of emergence of Homo sapiens on those planets, and the concept of background evolutionary rate, and the Years Ahead against the Background Evolutionary Rate. We can finally introduce our distribution function.

The total number of extraterrestrial industrial civilization is given by the log-normal distribution function:

$$F(x) = \frac{N_0}{Y_{aaber} \cdot (B_{er})^x Q \sqrt{2\pi}} e^{-\frac{(\ln(Y_{aaber}(B_{er})^x))^2}{2(Q)^2}} \quad (7.3)$$

Where Y_{aaber} is the years ahead of the current evolutionary rate (YAABER), B_{er} is the background evolutionary rate BER. N_0 is a number derived based on the number of terrestrial planets within the Milky way galaxy determined based on N_{earth} (2,458 planets with life emerges), and it has to satisfy the condition that:

$$N_{earth} = \int_{-\infty}^{\infty} F(x) dx \quad (7.4)$$

B_{er} is raised to the power of x, which is the number of years into the future or the past in the unit of 100 million years. If one wants to investigate the number of civilizations emerged from 200 Mya to 100 Mya within the galaxy, one can apply the following formula.

$$N_{earth} = \int_1^2 F(x) dx \quad (7.5)$$

If one wants to investigate the number of civilizations within the Milky way galaxy emerged between now and 100 Myr into the future, one can apply the following formula.

$$N_{earth} = \int_{-1}^0 F(x) dx \quad (7.6)$$

The exponentially increasing term of B_{er} complexity transformation does not indicate the progressiveness/advancement of biological evolution of the exoplanet toward a goal of creating human-like intelligent creatures. *It's a curve simply indicating that biological complexity and diversity increases exponentially over time.* With increasing specialization and adaptation to new niches and sustaining on existing biological substrates, the chance of creatures with a large head, manipulative appendages, walked on hind legs increases. Once such creature is able to manipulate nature and pass on their knowledge from generation to generation, it will break through the ecological constraints placed upon them and transform into a post-biological one in a brief time scale compares to the geologic one. It is more accurate to state that the B_{er} biological complexity transformation term indicates as time progresses, more different varieties of new species is able to fulfill unimaginable niches or non-existent niches at past, though most of the new species, if not of all of them, just adapt to new niches without manipulating, and disrupting their niche and others, unlike human-like creatures will do.

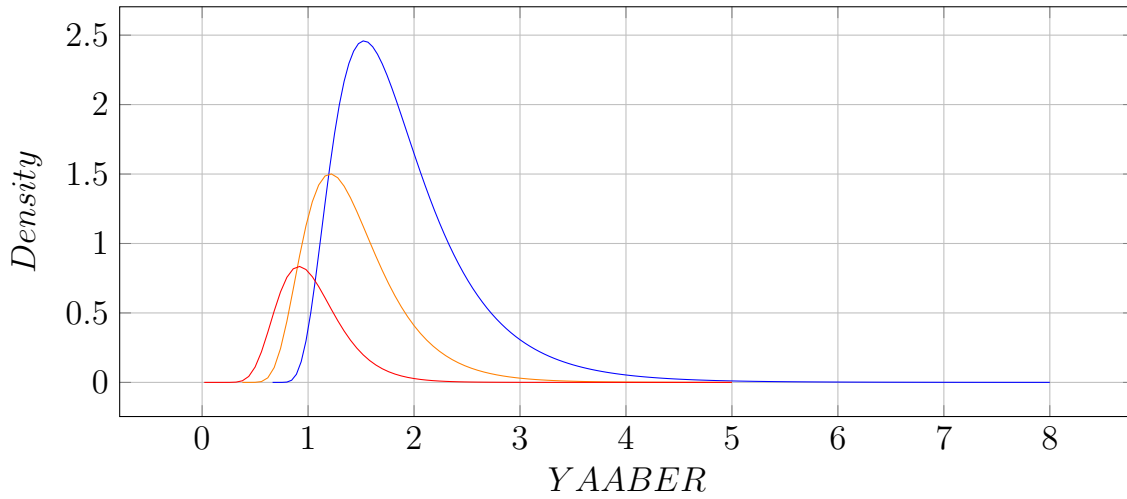


Figure 7.1: Biocomplexity increase overtime

By getting the values for each term (YAABER, BER) from earlier calculations and a parameterized value for deviation Q , we can plug in the values and solve the distribution.

$$g_1 = \frac{1,796.2}{17.6604 \cdot (2.7825594149)^x Q \sqrt{2\pi}} e^{-\frac{(\ln(17.6604(2.7825594149)^x))^2}{2(Q)^2}} \quad (7.7)$$

$$Q = 0.8207342$$

We parameterized N_0 to be 1,796.2 because this value can sum up the total number of habitable terrestrial planets to be N_{earth} with life emerges.

$$N_{\text{earth}} = \int_{-\infty}^{\infty} g_1 dx \quad (7.8)$$

$$= 2,458.06241223$$

We cross-examine our results by summing up the total probability for the emergence of potentially intelligent industrial civilizations within the Milky way from the past up to now, and the result needs to be that Homo sapiens led industrial civilization is as rare as 1 in 52 galaxies, based on previous chapters results.

$$t_{\text{galaxy}} = \left(\int_0^{\infty} g_1 dx \right)^{-1} \quad (7.9)$$

$$= 51.9626442221 \text{ galaxies}$$

We obtained the average distance between the galaxies by taking the volume of the local supercluster (Virgo) and divide by the number of milky way mass (assuming each galaxy has, on average, one Milky Way mass) the cluster possesses and arrived at 11.85 million light years in radius (23.7 million light years in diameter). That is it takes a spheric volume with radius 11.85 million light years to host a single galaxy. We then use this result to show

$$\begin{aligned} & \frac{(t_{galaxy} \cdot 1,185^3)^{\frac{1}{3}}}{100} \\ & = 44.2196632886 \text{ Mly} \end{aligned} \tag{7.10}$$

That it takes a spherical volume with a radius 44.21 million light years to host an industrial civilization at our current level of development. Therefore, it takes twice the radius, *88.44 million light years, on average, to reach our nearest industrial neighbor.*

The number of human-like civilizations in the universe, then, can be estimated to be:

$$\begin{aligned} t_{alien} &= \int_0^\infty g_1 dx \cdot \left(\frac{1,379,900}{1,185} \right)^3 \\ &= 30,387,610.4231 \text{ civilizations} \end{aligned} \tag{7.11}$$

30.39 million extraterrestrial industrial civilizations assuming the size of the universe is determined by the amount of time light is capable of traveling since the start of the universe.

And if one were to consider the comoving distance of all light signals from the most distant corners just as its light is reaching us now, we have:

$$\begin{aligned} t_{alien} &= \int_0^\infty g_1 dx \cdot \left(\frac{4,570,000}{1,185} \right)^3 \\ &= 1.1038302874 \times 10^9 \text{ civilizations} \end{aligned} \tag{7.12}$$

That is a staggering *1.103 billion extraterrestrial industrial civilizations* within our observable universe. Since we have no knowledge about the size of the universe, and ***if the universe is infinitely vast in size, then the number of extraterrestrial industrial civilizations is also infinitely large in number.***

$$t_{alien} = \int_0^\infty g_1 dx \cdot \left(\frac{\infty}{1,185} \right)^3 = \infty \tag{7.13}$$

If the universe is finitely bounded and based on the current estimate of its size, one can estimate the number of extraterrestrial industrial civilizations to be:

$$t_{alien} = \left(\frac{1}{4.4 \cdot 10^7} \right)^3 \cdot 3.621 \cdot 10^6 \cdot 10^{10^{122}} \tag{7.14}$$

Next, we compute *the earliest arising industrial civilization within a 13.799 billion light years radius to be 232.74 Mya.* Due to the nature of exponential growth in biological complexity, all 30 million extraterrestrial industrial civilizations have arisen no earlier than the mid-Triassic. If one were to assume that the rate of extraterrestrial industrial emergence was uniform as an

upper bound speed estimation, that implies *a new industrial civilization emerges every 7.659 years* in the observable universe within the last 232.74 Myr.

$$t_{galaxy} = \left(\int_{2.3274}^{\infty} g_1 dx \right)^{-1} \quad (7.15)$$

$$= 1.5794901823 \times 10^9 \text{ galaxies}$$

$$\frac{(t_{galaxy} \cdot 1,185^3)^{\frac{1}{3}}}{10^5} \quad (7.16)$$

$$= 13.8003677831 \text{ Gly}$$

Next, we compute *the earliest arising industrial civilization within the comoving distance of 46 billion light years radius to be 270.95 Mya*. Due to the nature of exponential growth in biological complexity, all 1.103 billion extraterrestrial industrial civilizations have arisen no earlier than the late Permian. If one were to assume that the rate of extraterrestrial industrial emergence was uniform as an upper bound speed estimation, that implies *a new industrial civilization emerges every 0.2108 years (2 months 16 days)* in the observable universe within the last 270.95 Myr.

$$t_{galaxy} = \left(\int_{2.0845}^{\infty} g_1 dx \right)^{-1} \quad (7.17)$$

$$= 5.8724730647 \times 10^{10} \text{ galaxies}$$

$$\frac{(t_{galaxy} \cdot 1185^3)}{10^5} \quad (7.18)$$

$$= 46.0601514367 \text{ Gly}$$

Since civilizations are already emerging and assuming that the earliest detectable signal traveled at the light speed or their expanding near the speed of light, then one can compute the total space occupied by all expanding extraterrestrial industrial civilizations. Due to the nature of exponential growth, the majority of the civilizations emerges recently than much further in the past. We take the weighted average over all time periods and find that average expanding industrial civilization expanding near the speed of light traveled 7.28 million years in all directions since its first emergence, indicating that on average, each civilization only had enough time to colonize its home galaxy since its emergence. Then, the total space currently occupied by any expanding civilization is given by:

$$s_{spaceoccu} = \int_0^{\infty} g_1 dx \cdot \left(\frac{1,379,900}{1,185} \right)^3 \left(\frac{0.0728901767}{137.9900} \right)^3 \quad (7.19)$$

$$= 0.00447879015807$$

This shows that only 0.4479% of all space within the universe is occupied by all expanding

industrial civilizations at the most. This indicates that the chance we are within one of their expanding bubbles are very small and can be used to argue as the reason for the silent sky. Due to the expansion of these spheres, the distance between all expanding civilizations is somewhat smaller, and this can be calculated to be:

$$d_{between0} = \left((1 - s_{spaceoccu}) \cdot \frac{4}{3} \pi (1,379,900)^3 \cdot \left(\frac{1}{t_{alien}} \right) \left(\frac{1}{\pi} \right) \left(\frac{1}{\frac{4}{3}} \right) \right)^{\frac{1}{3}} \quad (7.20)$$

$$= 44.1535476198 \text{ Mly}$$

In contrasts to a universe with non-expanding civilizations with mean sphere radius of 44.21 million light years, the radius of one with expanding civilization has shrunk by 66,115.6688 light years, or 132,231.3626 light years in contact distance, about the diameter of the Milky Way.

More interestingly, we are interested in predicting the arrival time of all industrial civilizations, or in other words, the time of the first contact, or when the seemly empty universe is filled with civilizations.

$$\int_0^{\infty} g_1 dx \cdot \left(\frac{13,799}{11.85} \right)^3 \left(\frac{0.365223 + 0.0729}{137.99} \right)^3 + \int_{-0.365223}^{\infty} g_1 dx \cdot \left(\frac{13,799}{11.85} \right)^3 \left(\frac{0.0729}{137.99} \right)^3 \quad (7.21)$$

$$\approx 1.00$$

We performed the same calculation on the comoving distance of the universe:

$$\int_0^{\infty} g_1 dx \cdot \left(\frac{45,700}{11.85} \right)^3 \left(\frac{0.365223 + 0.0729}{457} \right)^3 + \int_{-0.365223}^{\infty} g_1 dx \cdot \left(\frac{45,700}{11.85} \right)^3 \left(\frac{0.0729}{457} \right)^3 \quad (7.22)$$

$$\approx 1.00$$

The results are the same.

In order to find the time of the first contact, not only one has to consider the additional space existing civilizations are gaining near the speed of light but also those civilizations that are emerging from all potentially habitable planets. The results show that *36.52 million years into the future, the entire universe will be filled with expanding industrial civilizations* if one assumes that all life on all these planets nearly all reached the stage of biocomplexity similar to mammals, reptiles, and birds observed on earth, and emerging civilizations expand near the speed of light. This time frame can be extended easily assuming the average expansionary speed of all civilizations is merely at a fraction of the speed of light or the emergence of industrial civilization is rarer than we assumed, which we will discuss later. The expansion is dominated by earlier arising expanding civilizations (the left term of the equation), in fact, it represents 94.31% of all space ultimately occupied. Therefore, one can state that from earth's vantage

point, we are more likely to connect with someone comes further far away emerged long ago than someone emerged close by and recently.

Having computed the average size of our sphere of dominance, we then proceed to answer the questions. Out of the existing expanding civilizations, has anyone connected with someone else? In order to answer this question, one takes the fraction of the universe occupied by expanding civilizations to the n^{th} power and multiply by the total number of civilizations in order to find the number of pairs of connected civilizations:

$$t_{alien1connect} = t_{alien} \cdot (s_{spaceoccu})^1 = 136,099.73049 \quad (7.23)$$

$$t_{alien2connect} = t_{alien} \cdot (s_{spaceoccu})^2 = 609.562133436 \quad (7.24)$$

$$t_{alien3connect} = t_{alien} \cdot (s_{spaceoccu})^3 = 2.73010088396 \quad (7.25)$$

This shows that a little more than a half of a quarter million civilizations have contacted with at least one neighbor and 2 civilizations have contacted with at least 3 neighbors, and no civilizations have contacted more than 3 neighbors within a sphere of radius of 13.799 Billion light years. This indicates that the vast majority of expanding civilizations 99.55% have not met or contacted with any neighbor.

Now we proceed to perform the same calculation for the comoving distance of the observable universe.

$$t_{alien1connect} = t_{alien} \cdot (s_{spaceoccu})^1 = 4,943,824.22749 \quad (7.26)$$

$$t_{alien2connect} = t_{alien} \cdot (s_{spaceoccu})^2 = 22,142.3512933 \quad (7.27)$$

$$t_{alien3connect} = t_{alien} \cdot (s_{spaceoccu})^3 = 99.1709450491 \quad (7.28)$$

$$t_{alien4connect} = t_{alien} \cdot (s_{spaceoccu})^4 = 0.444165852653 \quad (7.29)$$

Because the comoving space occupies a much greater volume, there are 4.943 million extraterrestrial industrial civilizations have connected with at least one neighbor and 99 civilizations connected with up to 3 neighbors. Again, 99.55% of all civilizations have not met or contacted with any neighbor.

7.3 The Wall of Semi-Invisibility

The wall of semi-invisibility can be defined as follows, there exists such a set of inverse of integrations (CDF) such as $\frac{1}{\int_x^\infty g_1(x)dx}$ for any member such as g_1 within a set of probabilistic

distribution functions (we yet to find the most accurate function to model exoplanet biodiversity distribution) in which the y-intercept is non-zero and rises sharply when $x > 0$. We show that the cumulative distribution function (CDF) for our current distribution function is bounded by the PDF itself. That is, values for CDF within ranges between -2 to ∞ is straightly less than the values for PDF within the same range. This is possible due to variance $Q=0.8207342$. It is expressed mathematically as the follows:

$$g_1(x) > \int_x^\infty g_1(x) dx \quad (7.30)$$

The relationship of CDF over PDF is expressed by the formula:

$$\frac{\int_x^\infty g_1(x) dx}{g_1(x_0)} \quad (7.31)$$

and its ratio is plotted below:

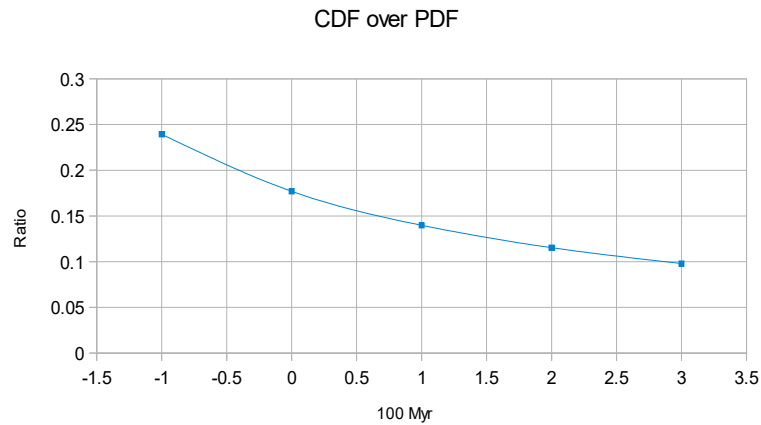


Figure 7.2: Cumulative distribution function (CDF) over probabilistic distribution function (PDF)

It shows that across all time periods under our considerations, ranging from 200 Myr into the future to 300 Mya, CDF is straightly a fraction of PDF and as one looks further back in time, the ratio further drops following the inverse of power. Having demonstrated that CDF is bounded by PDF, we can now use PDF to illustrate the concept of the wall of semi-invisibility by plotting the following equation to show the radius size required to find an earlier arising extra-terrestrial civilization:

$$\frac{\left(\frac{1}{g_1} \cdot (1,185)^3\right)^{\frac{1}{3}}}{10^5} \quad (7.32)$$

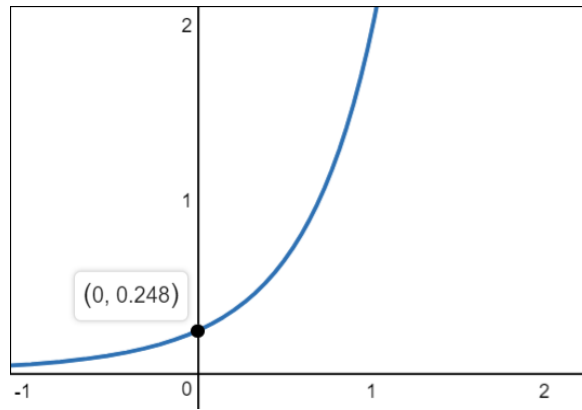


Figure 7.3: Nearest civilization

The nearest current existing arising extra-terrestrial civilizations is a non-zero distance away, yet its earliest detectable signature is still needed to reach earth by the distance in light years involved. One can observe from the graph that currently the intercept posits at $(0, 0.248)$. The intercept with the y-axis is the distance of the closest arising extra-terrestrial industrial civilization to earth in the present time. Then, the nearest arising extra-terrestrial industrial civilization is located at least 22.4 million light years away at the present time. It will take another 22.4 million years for the signal of the earliest of such civilization to reach us.

To seek civilization evolved even earlier that could have signals reached us by now, one can ideally accomplish this task by looking ahead at a greater distance. (However, we can not gain any bonus points now by looking further deep into the space because the probability of earlier civilization arising, in geologic time scale, is dependent on time, and shaped by the complexity transformation factor. It is not governed by an uniform distribution which can only be applied and approximated within a very short timescale peering into the past where changes based on the complexity transformation factor are negligible, as one look further back in time the chance of civilization arising decreases). However, the rising curve is so steep that in order to find a civilization evolved d years ahead relative to us, one has to look at a sphere size with radius $d+t$, where t is much greater than d in light years plus the non-zero distance to our nearest industrial civilization neighbor, implying that our search space will consist of mostly of regions where signals emitted before the rise of such a civilization.

Dividing the previous equation by x , we find the ratio $(d+t)$ to t and plot the graph:

$$\frac{\left(\frac{1}{g_1} \cdot (1,185)^3\right)^{\frac{1}{3}}}{10^4 \cdot x} \quad (7.33)$$

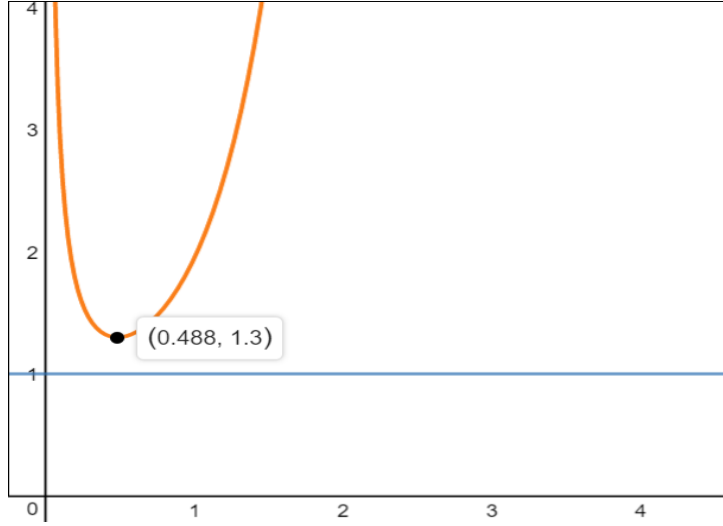


Figure 7.4: Threshold test for the wall of semi-invisibility

One can see that as long as $\frac{(d+t)}{d} > 1$, $t > 0$. That is, in order to seek a civilization evolved d years earlier, one has to look some positive value t light years in addition to d light years in distance. The graph shows that $d+t$ first decreases up to 1.3 times the size of d at 48.8 Myr and then increases quickly thereafter. It also means that by looking further into the distant region, the probability of additional extraterrestrial signal detection is at least $(1.299)^3$ or 2.192 times harder than finding signals by extending one's lookout distance and looking for earlier arising civilizations. If we have a small chance of finding signals in the most likely case, then the chance is even slimmer by looking further into the distance and the past. If PDF already satisfy the requirement in which the minimum value of $\frac{(d+t)}{d} > 1$, $t > 0$, then we also know that *the CDF, bounded by PDF, must also satisfy the requirement in which the minimum value $\frac{(d+t)}{d} > 1$, $t > 0$, thus, even in our most conservative case of extra-terrestrial civilization emergence estimation, the wall of semi-invisibility exists.*

It is called the wall of semi-invisibility because given by the distributive probability, a sphere size of radius $d+t$ will guarantee to find the an earlier arising civilization d light years before of our present time. However, it is still possible that such a civilization can be found much closer with a distance less than $d+t$, or even significantly less than d , however, if $\frac{d}{(d+t)}$ is close to 0; then, the chance of observing such civilization is minimal if non zero.

The probability density function of all arising extra-terrestrial industrial civilization arising can be more accurately approximated, if one plots the integration for different values of g_1 as the cumulative probability of having one arising civilization x years into the past as follows:

$$N_{galaxy} = \left(\int_x^{\infty} g(x) dx \right)^{-1} \quad (7.34)$$

$$\frac{(N_{galaxy} (1, 185)^3)^{\frac{1}{3}}}{10^4} \quad (7.35)$$

Then, the approximate curve fitting for the list of values for correspondingly 10 Mya, 20 Mya, 30 Mya, 40 Mya, 50 Mya, 75 Mya, and 100 Mya is approximately:

$$P_{cdf}(x) = \frac{\left(\frac{1}{g(x)} (1,185)^3\right)^{\frac{1}{3}}}{10^4} \cdot 1.85 \quad (7.36)$$

and can be more precisely expressed as the 4th order polynomial as:

$$P_{cdf}(x) = ax^4 + bx^3 + cx^2 + dx + f \quad (7.37)$$

$$a = 1.716, b = -0.61 \quad c = 1.332, d = 0.773 \quad f = 0.442 \quad (7.38)$$

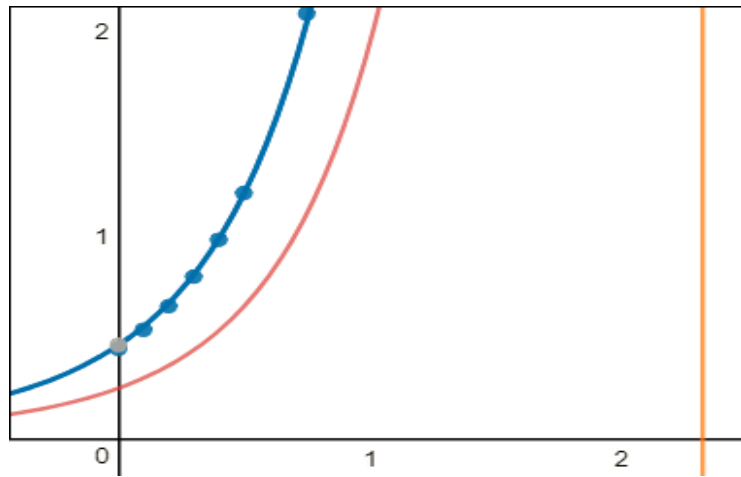


Figure 7.5: The best fit for the CDF of g_1

This is the best fit for the CDF of g_1 . Then, the probability density function of all arising extra-terrestrial industrial civilization arising is:

$$\left(\frac{x}{P_{cdf}(x)}\right)^3 \quad (7.39)$$

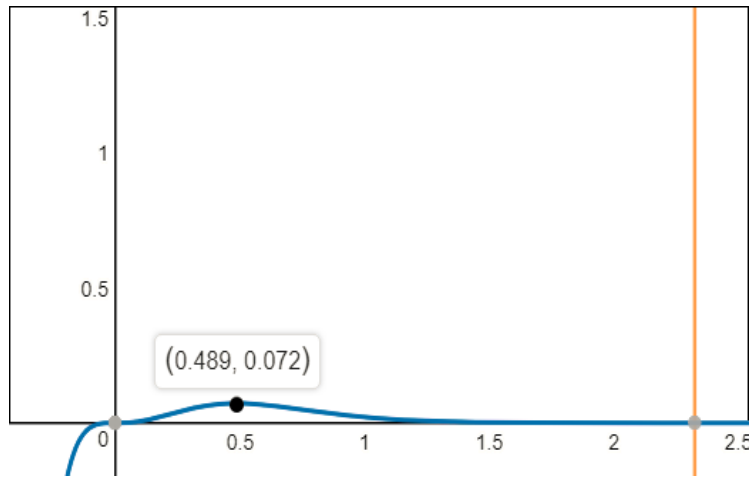


Figure 7.6: PDF of extraterrestrial detection

Whereas the chance of observing extraterrestrial peaks at 48.9 million light years away at merely 7.2%. The weighted average of the chance of detection is then just 2.066% (assuming one does not need to look at distance further than 232.7 Mya because we have shown that no civilization arises within the observable universe prior to 232.7 Mya). This shows that the wall of semi-invisibility is fairly opaque:

$$\frac{\left(\int_0^{2.327} \left(\frac{x}{P_{cdf}(x)} \right)^3 dx \right)}{2.327} \quad (7.40)$$

$$= 0.0206630151645$$

One can also see that:

$$E = \frac{(P_{cdf}(0))^3}{(P_{cdf}(x))^3} \quad (7.41)$$

$$\left(\frac{x}{P_{cdf}(0)} \right)^3 \cdot E = \left(\frac{x}{P_{cdf}(x)} \right)^3 \quad (7.42)$$

That is, the current signal detection chance at any lookout distance is the lookout spherical volume size in proportion to the emergence spherical volume size of 44.16 Mly at the current time multiplied by the emergence rate of the past relative to the current emergence rate of spherical volume size of 44.16 Mly observed from earth at that distance.

Finally, we want to stress that we assume the light travel distance and angular diameter distance is approximately one of the same. That is, $d_T(z) \approx d_A(z)$. This is a valid assumption because signals traveled at such low redshift $z \leq 0.017$ and close distance to earth, the light travel distance is not significantly distorted by the expansion of spacetime. The error rate is less than 0.8568%; therefore, the delay of extraterrestrial's light signal's arrival is at the most by

0.8568%.

Having demonstrated the concept of the wall of semi-invisibility, we shall further refine our argument by presenting a proof. We start by imagining one were to parameterize the PDF, so it further shifts to the right such as the plot below:

$$g_1 = \frac{17,960,000,000.2}{17.6604 \cdot (2.7825594149)^x Q \sqrt{2\pi}} e^{-\frac{(\ln(17.6604(2.7825594149)^x))^2}{2(Q)^2}} \quad (7.43)$$

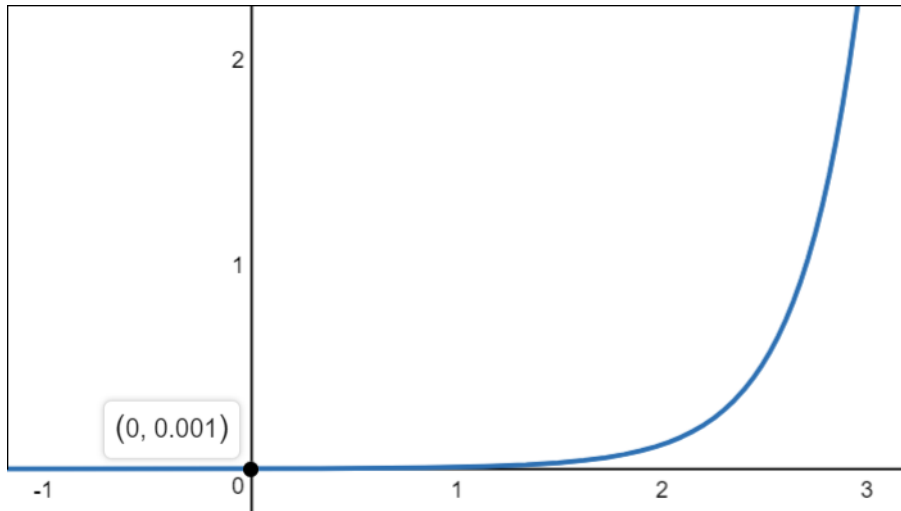


Figure 7.7: A hypothetical case for nearest civilization much closer

But it is obvious that the function cannot be right shifted so that the intercept occurs at a much closer distance to earth, for example at (0, 0.001). In such a hypothetical scenario, the closest arising industrial civilization is located at 100,000 light years away at the present time (so it would take another 100,000 years for the signal to reach us). Since the curve remains almost flat (the probability of arising civilization does not decrease as one traces further back in time, the probability of arising extra-terrestrial industrial civilization then approximately follows a uniform distribution), one expects to find earlier arising civilizations by simply looking ahead in greater distance, say 140,000 light years to the edge of the Milky Way. A civilization formed earlier should already exist given the greater sample size to look at. This is also expressed mathematically by the plots of $\frac{(d+t)}{d}$,

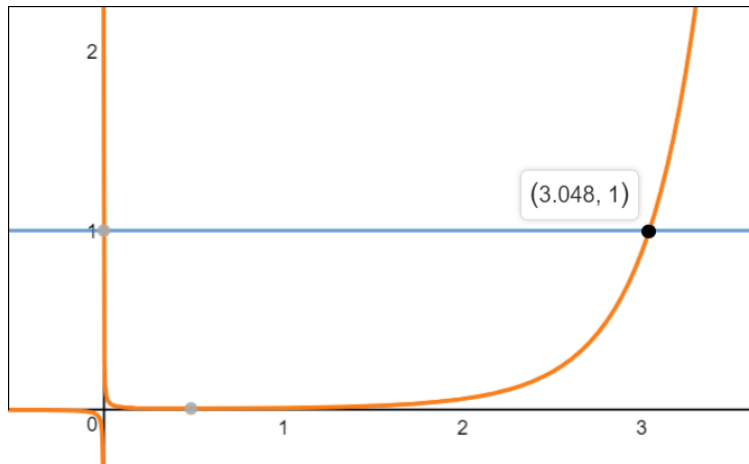


Figure 7.8: Threshold test fails for the hypothetical case

We find that current time up to 304.8 Mya into the past, $\frac{(d+t)}{d} < 1$. This implies as one looks further away into space, more signals of extraterrestrial civilization should be detectable. But this is contradicted by our current observation. We have pretty much ruled out the signatures of extra-terrestrial industrial civilization in our galaxy.

First, a proof by contradiction is outlined below regarding the above principle. Assume in a universe where one among all habitable planets transform into an industrial civilization every n years and the rate of transformation stays constant, that is, the probability is a uniform distribution given that every time period has an equal chance of transforming just one planet, it does not transform more or less.

7.3.1 Base Case:

We first establish three criteria that needed to be fulfilled:

1. The emergence rate has to follow an uniform distribution from a temporal perspective.
2. The emergence rate has to follow an uniform distribution from a spatial perspective.
3. The density distribution of planets within the universe follow an uniform distribution.

We will show that it is impossible to fulfill the three criteria at the same time, as result, it is impossible for the emergence rate to follow an uniform distribution from both a spatial and temporal aspect.

Assume that within a volume with a radius of $r = 1$ contains one transforming sample and assumed it is located at the edge of the radius of 1 light year, so with a radius of $r = 2$, the volume has grown by 8 folds, within this same volume, one can hold 8 transforming samples.

If the emergence rate follows an uniform distribution from a temporal perspective, as one looks back in time, there is 1 transforming planet per every time period. Then we know that at a radius of $r = 1$, the planet's transforming signal at the current time (current time period) will reach us next year. Now extending the radius to 2, we know that one of the transforming

planet's signal from 1 year ago (last time period) also will reach us next year from 2 light years away. So we will receive the signal confirmation from two of the planets at various distances from earth at the same time. However, this temporal placement violates uniform distribution from the spatial perspective (criterion 2).

If the emergence rate follows an uniform distribution from a spatial perspective, the rate of emergence is fixed at 1 planet per every 1 light year radius in each layer. Then we know that at a radius of $r = 1$, the planet's transforming signal at the current time (closest layer) will reach us next year. Extending the radius to 2, the 7 remaining planets' transforming signal from 1 year ago (second closest layer) also will reach us next year from 2 light years away. So we will receive the signal confirmation from all of the planets at various distances from earth at the same time. However, this led to a contradiction because the assumption is that 8 planets take 8 years to transform not 2 years, violating uniform distribution from the temporal aspect as we stated earlier (criterion 1). If all 8 transformed, as one looks back in time, the number of emergence detection increases and does not stay constant.

To resolve this contradiction, we have two solutions.

1. None of the 6 remaining planets have evolved into an advanced civilization prior to last year (they will transform in the future)
2. They have already arisen 7, 6, 5, 4, 3, and 2 years ago respectively. (they transformed in the past)

Both solutions are equally likely until we try to fit these solutions into real observation.

Since we assumed that advanced life has existed long before man, then we shall use 2) as our solution to resolve the contradiction. That is, if advanced life evolved according to an uniform distribution from the temporal aspect, life evolved on the remaining 6 planets 2 to 7 years ago located 2 light years away, and their signal should have already reached us between now and 5 years ago 1 year apart from each other. We should find significant evidence regarding their existence. However, this is contradicted by our current observation. There is no evidence of their existence. Moreover, such emergence pattern still violates an uniform distribution from a spatial perspective. The uniform distribution from the spatial perspective predicts 7 emerging civilizations per layer all in one time period.

To keep up with our observation and continually assuming life on the 6 planets arose in the past and conforming to criteria 1 and 2, the universe needs just one new appearing transforming planet readily to be visible from the past light cone's event horizon as r (the lookout radius) increases, the probability of planet with industrial civilization rising has to be decreased by a factor of:

$$\frac{1}{\left(\frac{\frac{4}{3}\pi(x)^3}{\frac{4}{3}\pi(1)^3}\right)} = \frac{1}{x^3} \tag{7.44}$$

Whereas x light years in radius, there exists $\frac{\frac{4}{3}\pi(x)^3}{\frac{4}{3}\pi(1)^3}$ planets occupying a volume space of $\frac{4}{3}\pi(x)^3$ and only 1 of them (assuming the spatial volume for one transforming planet is $\frac{4}{3}\pi(1)^3$) emerged x years ago.

From this, we can extrapolate that the probability of an alien civilization formation in the universe falls at least by a factor of

$$\frac{1}{x^3} \tag{7.45}$$

as one further traces back in time. Each of six planets has to be placed $r = \{3, 4, 5, 6, 7, 8\}$ light years respectively from earth and arose 2 to 7 years ago respectively and to expect all signals reaching us next year. This would satisfy uniform distribution from both the temporal and the spatial aspect. Each time period is transforming one layer away from earth, and each layer contains only 1 planet. Therefore, uniform distribution from spatial perspective predicts 1 emerging civilization per layer; and uniform distribution from temporal perspective predicts 1 emerging civilization per time period. Unfortunately, this still led to a contradiction because the remaining 6 planets have to be placed within 2 light years from earth based on our initial assumption. Otherwise, the density of the universe is non-uniform and the density is concentrated around earth, violating criterion 3.

Therefore, we are forced to recognize that we have to take proposition 1) as our solution. As a result, none of the 6 remaining planets have evolved into an advanced civilization prior to last year. By adopting this final solution, we also abandoning criterion 2. The emergence rate does not follow an uniform distribution from a spatial perspective.

Moreover, 6 remaining planets are not transforming at the rate of 1 per year into the future as an uniform distribution would predict. It is assumed, based on the model, all remaining 6 planets located at 2 ly must completely transforming into an industrial one now as the emergence rate density reaches 1 transforming sample $\frac{1}{(1)^3} = 100\%$ per a distance of $r = 1$ ly at the current time (in other words, 100% total emergence at the current time). Therefore, we also abandoning criterion 1. The emergence rate does not follow an uniform distribution from a temporal perspective. At the end, we are only adhering to criterion 3, the the density of planets within the universe is uniformly distributed.

Furthermore, we have both empirically confirmed and demonstrated in the earlier section that it takes a radius of a significantly larger size d light years to host one emerging civilization at the current time. (0 years ago). As a result, the current emergence rate is $\frac{1}{d^3}$ and its emergence rate density per 1 ly radius is strictly less than

$$\frac{1}{d^3} < \frac{1}{1^3} \tag{7.46}$$

and the majority of the transforming samples take place not now, but is further delayed up to d years into the future. That is, the rest of the samples supposed to transform currently are

instead transforming between now and d years into the future.

Furthermore, in order to keep up with the observation of having just one appearing sample readily visible from the past light cone as the lookout radius increases assuming the radius > 2 , the probability of planet with industrial civilization rising in the future has to be increased by a factor of x^3 correspondingly to be on the same signal detection curve. Therefore, we have shown that most of the civilization not only emerges in the future but the probabilistic emergence follows a non-uniform distribution from both spatial and temporal perspective, and the vast majority of the planets are transforming closer to d years into the future.

7.3.2 Inductive Step:

In general, if one were to inspect a sphere with radius x, then $f(x)$ more planets have yet to evolve into industrial civilization in the future as stated in the equation below:

$$f(x) = x^3 - x \tag{7.47}$$

We can then run a proof by induction. Assume that $f(k)$ planets with a radius k so that

$$f(k) = k^3 - k \tag{7.48}$$

is true, then

$$f(k + 1) = (k + 1)^3 - (k + 1) \tag{7.49}$$

must be true.

From empirical observation, we find that increasing the radius by 1 increases the number of habitable planets with future emerging civilization by $3k^2+3k$.

Radius	Yet to Emerge	Difference	Formula	Total Planets	Emerging Planets
1	0		$3 \cdot 0^2 + 3 \cdot 0$	1	1
2	6	6	$3 \cdot 1^2 + 3 \cdot 1$	8	2
3	24	18	$3 \cdot 2^2 + 3 \cdot 2$	27	3
4	60	36	$3 \cdot 3^2 + 3 \cdot 3$	64	4
5	120	60	$3 \cdot 4^2 + 3 \cdot 4$	125	5
6	210	90	$3 \cdot 5^2 + 3 \cdot 5$	216	6
7	336	126	$3 \cdot 6^2 + 3 \cdot 6$	343	7
8	504	168	$3 \cdot 7^2 + 3 \cdot 7$	512	8

Table 7.3: $3k^2+3k$

$$\Rightarrow f(k) + 3k^2 + 3k \quad (7.50)$$

$$\Rightarrow (k^3 - k) + 3k^2 + 3k \quad (7.51)$$

$$\Rightarrow k^3 + 3k^2 + 2k \quad (7.52)$$

$$\Rightarrow k^3 + 3k^2 + 3k + 1 - (k + 1) \quad (7.53)$$

$$\Rightarrow (k + 1)^3 - (k + 1) = f(k + 1) \quad (7.54)$$

Q.E.D

However, we can not simply run induction by just add 1 step because as k becomes large, adding the radius by 1 only increase 1 habitable planet which means zero habitable planets yet to emerge.

$$\lim_{x \rightarrow \infty} \frac{(x + 1)^3}{x^3} \quad (7.55)$$

$$= \lim_{x \rightarrow \infty} \frac{(x^3 + 3x^2 + 2x + 1)^3}{x^3} \quad (7.56)$$

$$= \lim_{x \rightarrow \infty} 1 + \frac{3}{x^1} + \frac{2}{x^2} + \frac{1}{x^3} = 1 \quad (7.57)$$

So we will run induction by adding k steps.

Induction by adding k steps

Assume that f(k) planets with a radius k so that

$$f(k) = k^3 - k \quad (7.58)$$

is true, then

$$f(k + k) = (2k)^3 - (2k) \quad (7.59)$$

must be true.

From empirical observation, we find that increasing the radius by k increases the number of habitable planets with future emerging civilization by $7k^3 - k$.

Radius	Yet to Emerge	Difference	Formula	Total Planets	Emerging Planets
1	0		0	1	1
2	6	6	$7 \cdot 1^3 - 1$	8	2
4	60	54	$7 \cdot 2^3 - 2$	64	4
8	504	444	$7 \cdot 4^3 - 4$	512	8
16	4,080	3576	$7 \cdot 8^3 - 8$	4,096	16
32	32,736	28656	$7 \cdot 16^3 - 16$	32,768	32
64	262,080	229344	$7 \cdot 32^3 - 32$	262,144	64
128	2,097,024	1834944	$7 \cdot 64^3 - 64$	2,097,152	128

Table 7.4: $7k^3-k$

$$\Rightarrow f(k) + 7k^3 - k \quad (7.60)$$

$$\Rightarrow (k^3 - k) + 7k^3 - k \quad (7.61)$$

$$\Rightarrow 8k^3 - 2k \quad (7.62)$$

$$\Rightarrow (2k)^3 - (2k) = f(k + k) \quad (7.63)$$

Q.E.D

One can also notice that if the emergence criterion requires emergence radius to be k instead of 1 while $r = k$, then

$$f(k) = \left(\frac{k}{k}\right)^3 - \left(\frac{k}{k}\right) = 0 \quad (7.64)$$

which is the same as our base case when $r = 1$ with emergence radius =1.

$$f(1) = \left(\frac{1}{1}\right)^3 - \left(\frac{1}{1}\right) = 0 \quad (7.65)$$

While $r = 2k$ and emergence radius to be k:

$$f(2k) = \left(\frac{2k}{k}\right)^3 - \left(\frac{2k}{k}\right) = 6 \quad (7.66)$$

which is the same as our base case when $r = 2$ with emergence radius =1.

$$f(2) = \left(\frac{2}{1}\right)^3 - \left(\frac{2}{1}\right) = 6 \quad (7.67)$$

This proves that the equation is self-similar.

How likely is that we are at a particular point in time where all extra-terrestrial signal is about to reach from each of its respective distance to earth originated n years ago? If we take the decreasing function, we will find that such function rises sharply within $r = 4$ light years.

This implies that the universe's alien civilization arising curve is extremely steep, that is, in the past billions of years, almost none of the life-bearing planets transformed, yet in the most recent 4 years, all remaining planets will transform. This implies that there is something extraordinary about the next 4 years in the entire universe, violating the mediocrity principle.

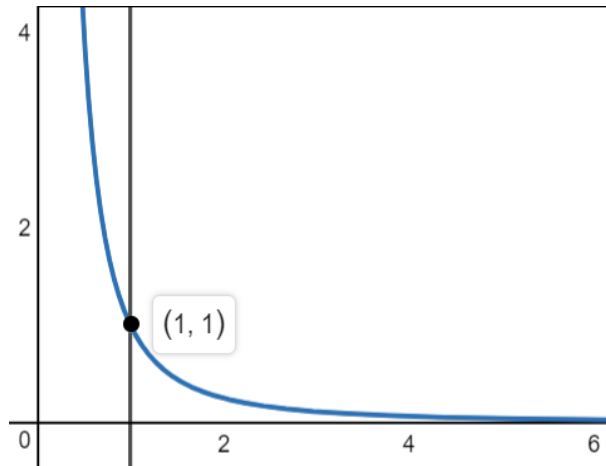


Figure 7.9: Assuming all extraterrestrial civilization arises sharply in the next 4 years in the universe

Civilizations' technological gap between the Maya and the Spanish is well within the order of thousands of years even between societies on the same planet within the same species, so it is highly improbable that all planets converge and transform on a such short timescale. We can gradually decrease the factor to a variable x , so that longer time span into the future is taken into consideration in which all remaining life-bearing planets give rise to industrial civilizations, if we assume that such emergence takes at least as long as the geologic process timeframe on earth (we set it at 44.2 million years, corresponding to the radius requirement for the emergence of one industrial civilization), then, the nearest extra-terrestrial civilization must also be at least tens and hundreds of million light-years away.

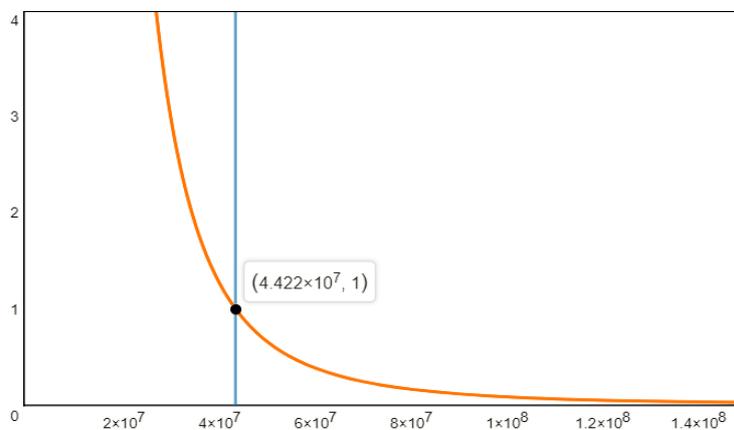


Figure 7.10: Assuming all extraterrestrial civilization arises sharply in the next 44.2 Myr in the universe

$$y = \frac{1}{\left(\frac{x}{44,219,659}\right)^3} \quad (7.68)$$

The solution for $y=1$ for this expanded case is:

$$1 = \frac{1}{\left(\frac{x}{44,219,659}\right)^3} \quad (7.69)$$

$$1 = \left(\frac{x}{44,219,659}\right)^3 \quad (7.70)$$

$$x^3 = 44,219,659^3 \quad (7.71)$$

$$x = 44,219,659 \quad (7.72)$$

That is, the new equation requires 44.2 Myr time-frame for all planets to be emerged previously takes only 1. Previously by using the factor $\frac{1}{x^3}$, it is shown that within 1 light year radius, there is 1 transforming sample. Now, it takes 44,219,659 light year distance to host one transforming sample. Then, the next 44,219,659 years can accomodate the timing for the emergence of the rest of the civilizations instead of squeezing all of the rest to be all emerged within 1 year.

The final solution implies several vital points:

1. The rate of alien civilization formation in the universe is a decreasing function with a factor within the order of $y = \frac{1}{x^3}$ as the upper bound and $y=0$ as the lower bound as one further traces back in time.
2. We are relatively early arising civilization compares to the rest of the life-nurturing planets. (The emergence rates remain very flat prior and very flat after for a long time before its final surge.)
3. In order to cope with the principle of mediocrity, the silent sky can be explained by both 1) and 2). We likely neither the earliest nor the latest comer given by random sampling. We are especially unlikely to be late, proved with current observation. It will also be a strong violation against the principle of mediocrity if we are so late just before the emergence rate of all intelligent lives arises sharply yet almost no intelligence arrives before us if the signal detection curve approaches the value of $\frac{1}{x^3}$ if d is small or close to 1 instead of $\frac{1}{\left(\frac{x}{d}\right)^3}$ whereas d is a large number. Because it would imply something extraordinary for the next decade, hundreds, or thousands of years in a universe that can last for trillions of years but converges toward some very tiny transformation temporal window. The consequence of satisfying both conditions requires that the nearest extra-terrestrial civilization must also be at least tens and hundreds of million light years away,

which is reinforced from our earlier calculation.

Having derived the theoretical upper bound curve, one now checks if our PDF is bounded strictly by the theoretical upper bound. In order to derive the theoretical upper bound to reflect the reality, rescaling is required to convert every unit into a $\frac{100 \text{ myr}}{100 \text{ mly}}$ light year distance. One then divides a sphere of arbitrary size over another sphere with 44.22 my light years in radius (the minimum size required for the emergence of one industrial civilization). We simplify the expression can be derived:

$$\frac{\frac{4}{3}\pi (100x)^3}{\frac{4}{3}\pi (44.22)^3} = \frac{(100x)^3}{(44.22)^3} = 11.565x^3 \quad (7.73)$$

This factor can be expressed in a more generalized form as:

$$\left(\frac{100}{\left(\frac{\left(\int_0^\infty g(x) dx \right)^{-1} (1,185)^3}{10^2} \right)^{\frac{1}{3}}} \right)^3 x^3 \quad (7.74)$$

Whereas $g(x)$ is the distribution function integrated over all previous time period for the cumulative chance of observing extraterrestrials and the radius required to find one arising industrial civilization with a 100% chance. As a result, by altering $g(x)$, the factor can vary from $11.565x^3$. This expression is the total number of emerging civilizations per 100 million light years in diameter in proportion to the number of emerging civilizations within a 44.22 million light years diameter. One also knows that our earlier discussion the upper bound requires that at every time period there is at most one emerging civilization, whose signal just about to reach us. Then, for every unit of x translating into $\frac{100 \text{ myr}}{100 \text{ million}}$ light years, there are at most

$$\frac{1}{11.565x^3} \quad (7.75)$$

civilizations are trying to but not yet reached us.

The decreasing factor becomes $\frac{1}{11.565x^3}$ instead of $\frac{1}{x^3}$; that is, the probability of the emergence of industrial civilization has to be further decreased by a factor of $\frac{1}{11.565x^3}$, establishing a more stringent upper bound.

$$y_d = \frac{1}{11.565 (x)^3} \quad (7.76)$$

whereas the best approximate curve fitting for the integration of $g(x)$ was expressed as the 4th order polynomial as:

$$\frac{\left(\int_x^\infty g(x) dx\right)^{-1} (1,185)^3}{10^2} = P_{cdf}(x) = ax^4 + bx^3 + cx^2 + dx + f \quad (7.77)$$

$$a = 1.716, b = -0.61 \quad c = 1.332, d = 0.773 \quad f = 0.442 \quad (7.78)$$

and we express the rate of extraterrestrial civilization emergence as:

$$E = \frac{(P_{cdf}(0))^3}{(P_{cdf}(x))^3} \quad (7.79)$$

As one looks further into the past, the rate of civilization emergence decreases.

Then, the rate of extraterrestrial civilization emergence E crosses the point (0, 1).

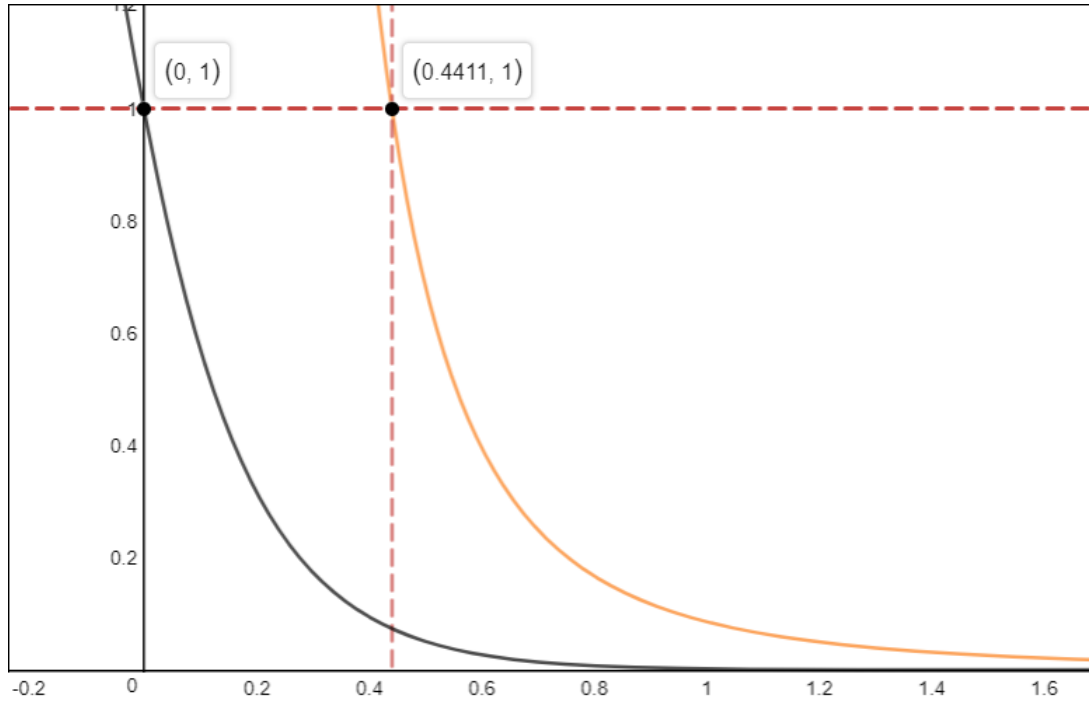


Figure 7.11: The cosmic distribution CDF of g_1 is bounded by the upper bound curve with the nearest civilization at 44.11 Mly away

Finally, the ratio is formulated as:

$$d_0 = \log\left(\frac{y_d}{E}\right) \quad (7.80)$$

Then, both curves when $x > 0$ can be compared. The finalized equations above checks the ratio of the theoretical upper bound to the CDF, in the approximate curve fitting to our PDF.

In order to clarify our plots for our reader, we would like to further discuss about the graph

above, first let us focus on the emergence curve $E = \frac{(P_{cdf}(0))^3}{(P_{cdf}(x))^3}$. One can think of the point (0, 1) as at the current time, we know mathematically through our derivation that the emergence rate is 1 at a radius of 44.2 Mly away, but this is not yet verified currently, it will take another 44.2 Myr for the light to reach us to verify our assumption. The point (0.442, 0.0733) denotes the emergence rate we currently observe and verify from a radius 44.2 Mly away. The signals we currently receiving from 44.2 Mly away is the emergence rate of 44.2 Myr ago. At that time, the emergence rate is 0.0733 for a radius of 44.2 Mly, or merely $\frac{1}{13.64}$ th of today's. This is a much lower chance than guaranteeing spotting an extraterrestrial industrial civilization, so there is a $\frac{12.64}{13.64} = 92.69\%$ not spotting one. Distance d denotes 44.2 Mly in radius, that is, in order to guarantee finding a civilization emerged 44.2 Mly earlier, the coverage radius has to increase to $d+t$. This is another perspective to explain our threshold test of $\frac{d+t}{d}$ discussed earlier in the section. Hence, one can see the emergence curve can be more clearly interpreted from a temporal aspect, but the x coordinate of the emergence rate of the past can also be interpreted as the distance away relative to earth from a spatial perspective.

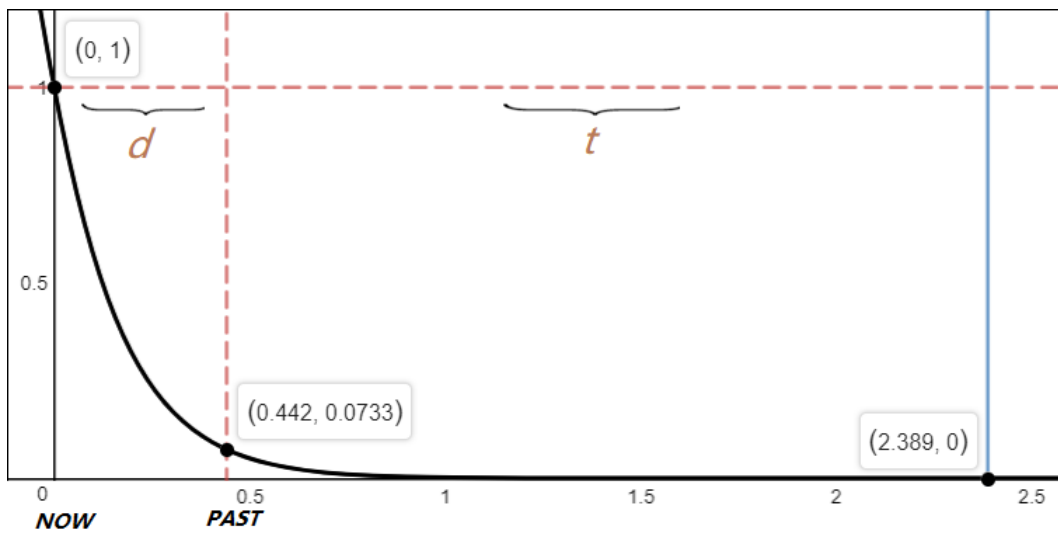


Figure 7.12: The physical explanation for the emergence curve

Now, we focus on light signal detection curve $y_d = \frac{1}{11.565x^3}$. This curve passes through the point (0.4416, 1) because we assumed that it takes a radius of 44 Mly to host one emerging civilization. Therefore, this point sits on the signal detection curve which guarantees exactly one positive detection at any distance. The factor requirement guaranteeing a single positive detection increases by the cubed as the lookout distance decreases and decreases by the cubed as the lookout distance increases. *The curve does not care how to guarantee one signal detection is achieved or if it is achievable in reality.* It is simply used as a point of reference to show that, relative to the current one positive detection per 44 Mly radius, the amount of value needed to be adjusted to maintain one positive detection for any lookout distance from the earth.

The point (0, 1) denotes at a distance of 0 ly away at the current time, the signal detection will occur 44.16 Myr into the future. We will confirm the fact that there is one arising alien industrial civilization currently unobservable at the distance of 44.16 Mly away at the current time. The point (0.4416, 1) denotes that the signal which will confirm the existence of one arising extraterrestrial per 44 Mly radius is being emitted by the expanding alien civilization now at a distance of 44.16 Mly away. The point touches the dashed line $y=1$ because we assumed that it takes a radius of 44.16 Mly for one emerging civilization at the current time.

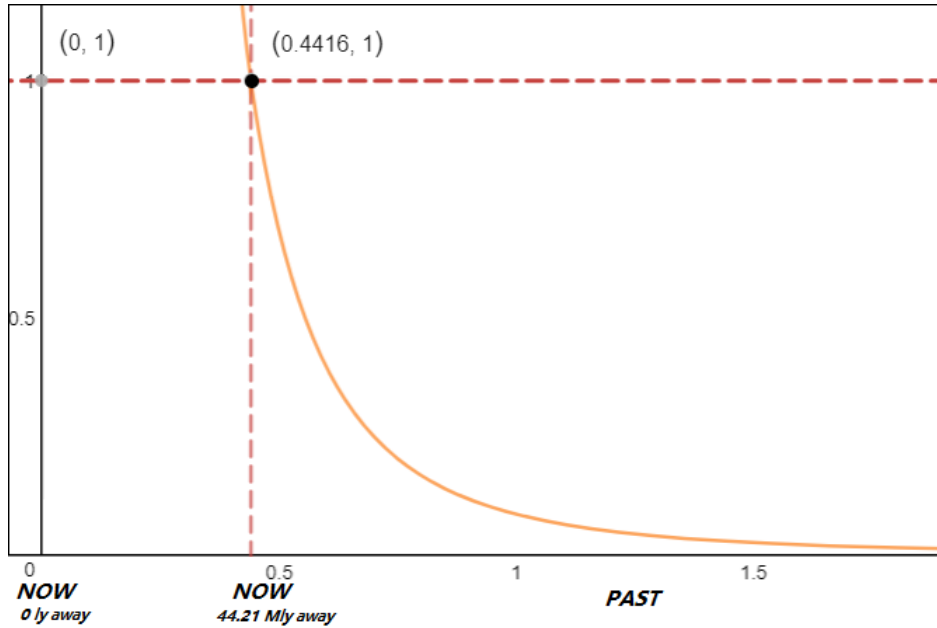


Figure 7.13: The physical explanation for the signal light arrival curve

Finally, we can arrange the emergence curve and signal detection curve on the same graph. The meaning of $\frac{y_d}{E}$ (signal detection curve over the emergence curve) is the following. The curve represents the number of times the detectable chance/number (always <1) of the actual observed civilization of the past at any lookout radius needs to be increased to guarantee exactly 1 detectable civilization at the current time at any lookout distance. Even at the current time, the most attainable emergence rate is 1 per 44 Mly radius. In other words, within a lookout radius of 1 ly, the chance of detection is $1 \cdot \left(\frac{1 \text{ ly}}{44 \text{ Mly}}\right)^3$. The chance is much closer to 0 than 1. Therefore, the number of times on the current detection chance of one positive signal needed to be increased to guarantee one positive detection must be high. *The curve does not care how to guarantee one signal detection is achieved.* It can be achieved through a change in the emergence rate holding the lookout volume size constant, or it can be achieved through a change in volume size holding the emergence rate constant, or through both an change in volume and the emergence rate.

The inverse of the number of detectable civilization at any arbitrary distance proportional to a 44 Mly radius is actually equivalent to y_d from our initial definition of the signal detection curve so that their product equals 1.

$$\left(\frac{x}{P_{cdf}(0)}\right)^{-3} = y_d = \frac{1}{11.565x^3} \quad (7.81)$$

As a result, one can multiply $\frac{y_d}{E}$ by $\frac{\left(\frac{x}{P_{cdf}(0)}\right)^3}{\left(\frac{x}{P_{cdf}(0)}\right)^3}$:

$$\frac{y_d \cdot \left(\frac{x}{P_{cdf}(0)}\right)^3}{E \cdot \left(\frac{x}{P_{cdf}(0)}\right)^3} = \frac{1}{\left(\frac{x}{P_{cdf}(x)}\right)^3} \quad (7.82)$$

We interpret the numerator $y_d \cdot \left(\frac{x}{P_{cdf}(0)}\right)^3$ as the scale factor required to fix the appearance number of civilization to 1 regardless of the search radius one initially seek. Fixing the number of detectable civilization to 1 is the invariant.

This achieved by expanding the lookout radius to 44 Mly when the initial lookout distance < 44 Mly. Since it is not possible to increase the emergence rate higher than 1 per 44 Mly radius at the current time. It is not possible to host a civilization less than 44.21 Mly currently. The only way to guarantee the appearance number is to expand the lookout radius to 44 Mly.

It is achieved by reducing the past emergence rate to $\frac{1}{x^3}$ relative to the emergence rate of 44 Mly radius when the initial lookout distance $x > 44$ Mly since the search volume is now greater than 44^3 Mly^3 and the number of civilization detection increases beyond 1 if the emergence rate of the past is fixed at 1 per 44 Mly radius. We can verify that fixing the appearance number is not achieved through fixing the lookout radius to 44 Mly even the initial lookout radius > 44 Mly. This is confirmed by the following inequality for $x > 44.15$ Mly:

$$\frac{x \left(\frac{1}{E \cdot \left(\frac{x}{P_{cdf}(0)}\right)^3} \right)^{\frac{1}{3}}}{0.4415} \neq \frac{0.4415 \left(\frac{1}{E \cdot \left(\frac{x}{P_{cdf}(0)}\right)^3} \right)^{\frac{1}{3}}}{0.4415} \quad (7.83)$$

The left term states the *actual* lookout radius size in the ratio of 44.15 Mly required for one civilization detection at an arbitrary distance. The right term states the *predicted* lookout radius size (if one fixes the appearance number by fixing the lookout volume to 44^3 Mly^3 even if the initial lookout volume $> 44^3 \text{ Mly}^3$) in the ratio of 44.15 Mly required for one civilization detection at an arbitrary distance.

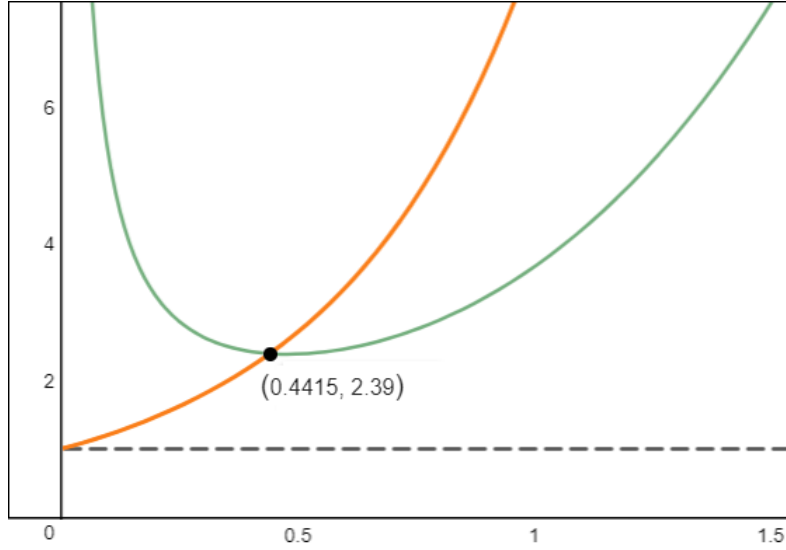


Figure 7.14: The the actual look out radius vs predicted if one fixes the appearance number by fixing the look out volume

In fact, those two curve differs by a factor of :

$$\frac{x \left(\frac{1}{E \cdot \left(\frac{x}{P_{cdf}(0)} \right)^3} \right)^{\frac{1}{3}}}{0.4415} = \frac{0.4415 \left(\frac{1}{E \cdot \left(\frac{x}{P_{cdf}(0)} \right)^3} \right)^{\frac{1}{3}}}{0.4415} \cdot \left(\frac{1}{y_d} \right)^{\frac{1}{3}} \quad (7.84)$$

and the factor:

$$\left(\frac{1}{y_d} \right)^{\frac{1}{3}} = \left(\frac{x}{P_{cdf}(0)} \right) > 1 \quad (7.85)$$

is always greater than 1 for $x > 44.15$ Mly. $\left(\frac{x}{P_{cdf}(0)} \right)$ is the rescale factor for the radius expansion beyond 44.15 Mly, which raised to the cubed and multiplied with a decreasing emergence rate $\frac{1}{x^3}$ to guarantee the appearance number of 1 detectable civilization along an arbitrary distance from earth. Hence, we have verified that fixing the appearance number is not achieved through fixing the lookout radius.

We interpret the denominator $E \cdot \left(\frac{x}{P_{cdf}(0)} \right)^3$ as the emergence rate from the past x years ago relative the emergence rate at the current time multiplied by the ratio of any lookout volume to the current emergence volume of 44 Mly radius yields the apparent number of detectable civilization (always < 1) at the current time from any distance of x light years away. This is equivalent to the probability density function of all arising extra-terrestrial industrial civilization $\left(\frac{x}{P_{cdf}(x)} \right)^3$

Because

$$\left(\frac{x}{P_{cdf}(x)}\right)^3 < 1 \quad (7.86)$$

Then:

$$\frac{1}{\left(\frac{x}{P_{cdf}(x)}\right)^3} > 1 \quad (7.87)$$

The above equation indicates that the lookout volume has to be increased by this factor in order to gain 1 positive detection, and the lookout radius has to increase by:

$$\sqrt[3]{\frac{1}{\left(\frac{x}{P_{cdf}(x)}\right)^3}} > 1 \quad (7.88)$$

The lookout radius of x light years is to be rescaled by the factor $\sqrt[3]{\frac{1}{\left(\frac{x}{P_{cdf}(x)}\right)^3}}$ to a larger size because the currently observed emergence rate signal from any lookout radius is strictly from the past. The past offers a lower chance of emergence. Furthermore, an observer can not alter the emergence rate but can increase the lookout distance, therefore, the lookout radius has to expand beyond x light years to accommodate one positive detection. This is equivalently:

$$\sqrt[3]{\frac{1}{\left(\frac{x}{P_{cdf}(x)}\right)^3}} = \frac{(d+t)}{d} = \frac{\left(\frac{1}{P_{cdf}(x)} \cdot (1,185)^3\right)^{\frac{1}{3}}}{10^4 \cdot x} \quad (7.89)$$

On a further note, the factor required to rescale the lookout radius size first shrinks as the emergence rate derived from the past signal reaching earth is catching up with the continuous drop of the signal detection threshold curve of $\frac{1}{x^3}$. However, as one inspects beyond 44.2 Mly radius, despite a continuous drop of the signal detection threshold curve of $\frac{1}{x^3}$ at every point, the emergence rate derived from the past signal reaching earth is smaller still, as a result, the factor required to rescale the search radius to guarantee passing the signal detection threshold actually increased.

With a full comprehension of the model, we show that the boundary checking is conceptually equivalently to our earlier threshold test, except that the boundary checking is expressed as the log of the threshold test ratio raised to the cubed:

$$\left(\frac{y_d}{E}\right)^{\frac{1}{3}} = \frac{\left(\frac{1}{P_{cdf}(x)} \cdot (1,185)^3\right)^{\frac{1}{3}}}{10^4 \cdot x} \quad (7.90)$$

The final curve is plotted below:

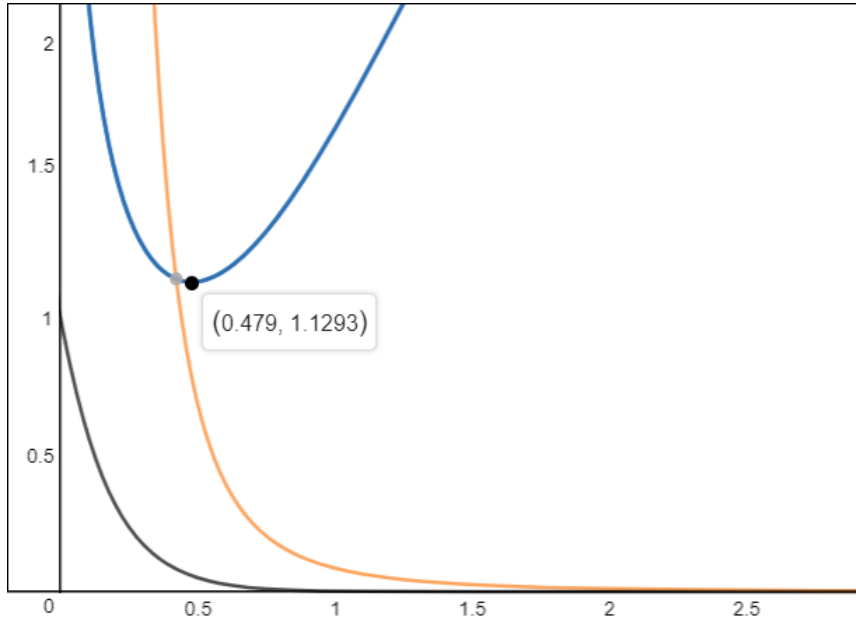


Figure 7.15: The logarithmic ratio of upper bound curve divided by the the cosmic distribution PDF $g(x)$

The curve indicates that the ratio is strictly positive for all values of $x > 0$, this indicates for all additional look ahead distance, the emergence rate of extraterrestrial civilization is much smaller than our theoretical maximum upper bound. In other words, the emergence rate of civilization decreases much faster than $\frac{1}{11.565x^3}$ as one looks further back in time.

Using this equation, we can also find the lower bound for BER. *The Background evolutionary rate cannot dip below 1.5319, that is, the biological complexity per 100 Myr on all planets increases by at least a factor of 1.5319 assuming 1 civilization emerges per 44.22 million light years radius.*

$$\Rightarrow g(x) = \frac{1796.2}{17.66 \cdot (1.6975)^x Q\sqrt{2\pi}} e^{-\frac{(\ln(17.66(1.6975)^x))^2}{2(Q)^2}} \quad (7.91)$$

$$P_{cdf}(x) = 0.05x^4 + 0.055x^3 + 0.199x^2 + 0.344x + 0.355 \quad (7.92)$$

$$\Rightarrow g(x) = \frac{0.5176 \cdot 1796.2}{17.66 \cdot (1.5666)^x Q\sqrt{2\pi}} e^{-\frac{(\ln(17.66(1.5666)^x))^2}{2(Q)^2}} \quad (7.93)$$

$$P_{cdf}(x) = 0.0276x^4 + 0.045x^3 + 0.166x^2 + 0.346x + 0.419 \quad (7.94)$$

$$\Rightarrow g(x) = \frac{0.439 \cdot 1796.2}{17.66 \cdot (1.5386)^x Q\sqrt{2\pi}} e^{-\frac{(\ln(17.66(1.5386)^x))^2}{2(Q)^2}} \quad (7.95)$$

$$P_{cdf}(x) = 0.024x^4 + 0.043x^3 + 0.159x^2 + 0.346x + 0.436 \quad (7.96)$$

$$\Rightarrow g(x) = \frac{0.4215 \cdot 1796.2}{17.66 \cdot (1.5319)^x Q\sqrt{2\pi}} e^{-\frac{(\ln(17.66(1.5319)^x))^2}{2(Q)^2}} \quad (7.97)$$

$$P_{cdf}(x) = 0.0229x^4 + 0.0419x^3 + 0.158x^2 + 0.346x + 0.441 \quad (7.98)$$

As one lowers the BER, the appearance horizon of the nearest extraterrestrial civilization draws closer, one has to readjust the PDF $g(x)$ so that the appearance horizon restores to 44.21 Mly. Each step requires a new curve fit for the CDF $P_{cdf}(x) = ax^4 + bx^3 + cx^2 + dx + f$ to the newly adjusted PDF $g(x)$. As a result, many rounds of iterations are required to finally converge on the lower bound for BER where the nearest civilization is located at 44.21 Mly away. We stopped at the 4th iteration where the computational precision reaches 100 K years.

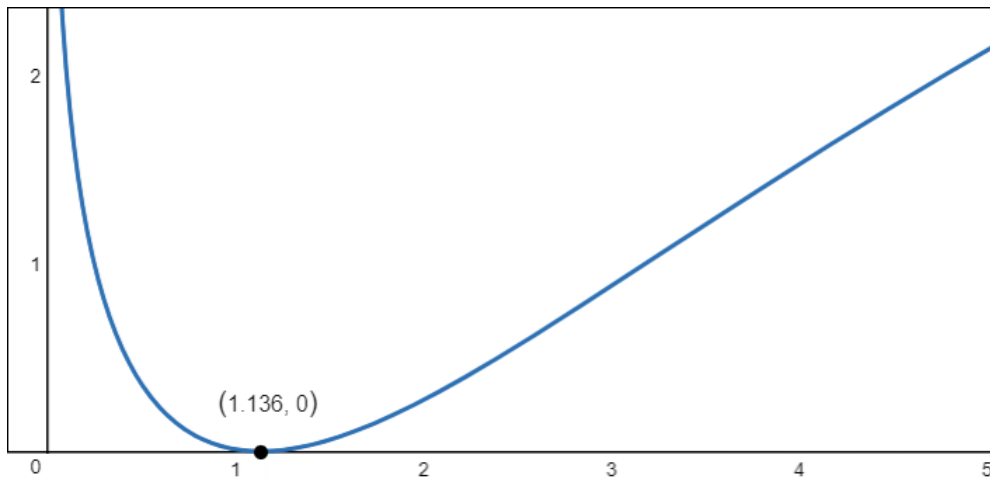


Figure 7.16: Assuming $BER \geq 1.5319$ and the emergence rate of 1 per 44.21 Mly light year radius, the cosmic distribution falls slower than the upper bound curve

However, by tweaking the emergence rate down to 1 civilization per 100 million light year radius, it is possible to reduce BER down to as low as 1.2087.

We start by initiating conditions:

$$\frac{\frac{4}{3}\pi (100x)^3}{\frac{4}{3}\pi (100)^3} = \frac{(100x)^3}{(100)^3} = x^3 \quad (7.99)$$

$$\left(\frac{100}{\left(\frac{(\int_0^\infty g(x)dx)^{-1} (1,185)^3}{10^2} \right)^{\frac{1}{3}}} \right)^3 x^3 \approx x^3 \quad (7.100)$$

$$P_{cdf}(x) = ax^4 + bx^3 + cx^2 + dx + f \quad (7.101)$$

$$a = 3.89, b = -1.38 \quad c = 3.019, d = 1.7531 \quad f = 1.001 \quad (7.102)$$

$$E = \frac{(P_{cdf}(0))^3}{(P_{cdf}(x))^3} \quad (7.103)$$

$$y_d = \frac{1}{(x+0)^3} \quad (7.104)$$

$$d_0 = \log\left(\frac{y_d}{E}\right) \quad (7.105)$$

$$\Rightarrow g(x) = \frac{0.08582 \cdot 1796.2}{17.66 \cdot (1.3321)^x Q\sqrt{2\pi}} e^{-\frac{(\ln(17.66(1.3321)^x))^2}{2(Q)^2}} \quad (7.106)$$

$$P_{cdf}(x) = 0.0058x^4 + 0.02x^3 + 0.105x^2 + 0.347x + 0.656 \quad (7.107)$$

$$\Rightarrow g(x) = \frac{0.02424 \cdot 1796.2}{17.66 \cdot (1.2327)^x Q\sqrt{2\pi}} e^{-\frac{(\ln(17.66(1.2327)^x))^2}{2(Q)^2}} \quad (7.108)$$

$$P_{cdf}(x) = 0.002x^4 + 0.01x^3 + 0.076x^2 + 0.347x + 0.9 \quad (7.109)$$

$$\Rightarrow g(x) = \frac{0.01768 \cdot 1796.2}{17.66 \cdot (1.2133)^x Q\sqrt{2\pi}} e^{-\frac{(\ln(17.66(1.2133)^x))^2}{2(Q)^2}} \quad (7.110)$$

$$P_{cdf}(x) = 0.00158x^4 + 0.01x^3 + 0.07x^2 + 0.347x + 0.97 \quad (7.111)$$

$$\Rightarrow g(x) = \frac{0.016345 \cdot 1796.2}{17.66 \cdot (1.2087)^x Q\sqrt{2\pi}} e^{-\frac{(\ln(17.66(1.2087)^x))^2}{2(Q)^2}} \quad (7.112)$$

$$P_{cdf}(x) = 0.00148x^4 + 0.0097x^3 + 0.069x^2 + 0.347x + 0.993 \quad (7.113)$$

Again, many rounds of iterations are required to finally converge on the lower bound for BER where the nearest civilization is located at 100 Mly away. We stopped at the 4th iteration where the computational precision reaches 100 K years.

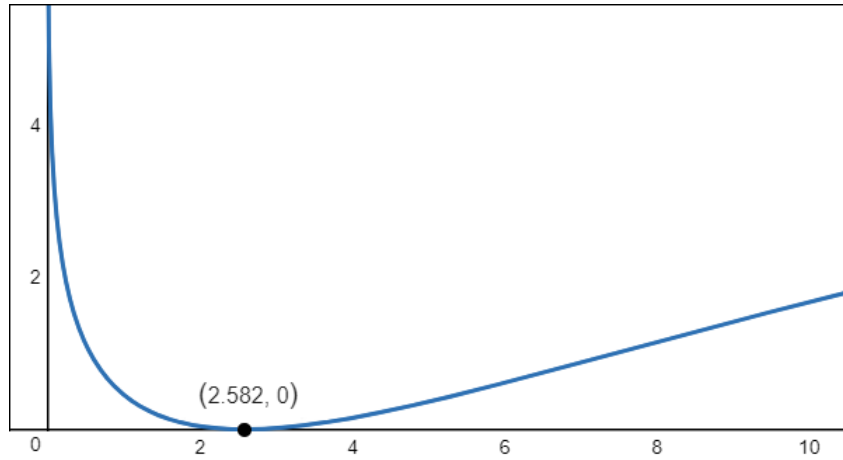


Figure 7.17: Assuming $BER \geq 1.2087$ and the emergence rate of 1 per 100 Mly light year radius, the cosmic distribution falls slower than the upper bound curve

Next, we shall test and confirm that PDF is bounded by any arbitrarily large values.

The test for convergence is presented below:

$$E = \frac{(P_{cdf}(0))^3}{(P_{cdf}(x))^3} = \frac{(a(0)^4 + b(0)^3 + c(0)^2 + d(0) + f)^3}{(ax^4 + bx^3 + cx^2 + dx + f)^3} \quad (7.114)$$

$$E = \frac{f^3}{(ax^4 + bx^3 + cx^2 + dx + f)^3} \quad (7.115)$$

$$y_d = \frac{1}{\left(\frac{10^4}{\left(\left(\int_0^\infty g(x) dx \right)^{-1} (1185)^3 \right)^{\frac{1}{3}}} \right)^3} = \frac{(1185)^3}{\left(\int_0^\infty g(x) dx \right) \cdot 10^{12} x^3} \quad (7.116)$$

Limit test for convergence:

$$\frac{E}{yd} = \frac{f^3}{(ax^4 + bx^3 + cx^2 + dx + f)^3} \cdot \frac{(\int_0^\infty g(x) dx) \cdot 10^{12} x^3}{(1185)^3} \quad (7.117)$$

$$\lim_{x \rightarrow \infty} \frac{f^3}{\left(\frac{ax^4 + bx^3 + cx^2 + dx + f}{x}\right)^3} \cdot \frac{(\int_0^\infty g(x) dx) \cdot 10^{12}}{(1185)^3} \quad (7.118)$$

$$\lim_{x \rightarrow \infty} \frac{1}{\left(\frac{ax^3}{f} + \frac{bx^2}{f} + \frac{cx}{f} + \frac{d}{f} + \frac{1}{x}\right)^3} \cdot \frac{(\int_0^\infty g(x) dx) \cdot 10^{12}}{(1185)^3} \quad (7.119)$$

$$\lim_{x \rightarrow \infty} \frac{\frac{1}{x^9}}{\left(\frac{ax^3}{fx^3} + \frac{bx^2}{fx^3} + \frac{cx}{fx^3} + \frac{d}{fx^3} + \frac{1}{xx^3}\right)^3} \cdot \frac{(\int_0^\infty g(x) dx) \cdot 10^{12}}{(1185)^3} \quad (7.120)$$

$$\lim_{x \rightarrow \infty} \frac{\frac{1}{x^9}}{\left(\frac{a}{f} + \frac{b}{fx} + \frac{c}{fx^2} + \frac{d}{fx^3} + \frac{1}{x^4}\right)^3} \cdot \frac{(\int_0^\infty g(x) dx) \cdot 10^{12}}{(1185)^3} \quad (7.121)$$

$$\lim_{x \rightarrow \infty} \frac{\frac{1}{x^9}}{\left(\frac{a}{f}\right)^3} \cdot \frac{(\int_0^\infty g(x) dx) \cdot 10^{12}}{(1185)^3} \quad (7.122)$$

$$0 \cdot \lim_{x \rightarrow \infty} \frac{(\int_0^\infty g(x) dx) \cdot 10^{12}}{(1185)^3} \quad (7.123)$$

$$0 \cdot \lim_{x \rightarrow \infty} \int_0^\infty g(x) dx \quad (7.124)$$

We substitute $\int_0^\infty g(x) dx$ with g_1 because we have shown earlier that $\int_0^\infty g(x) dx < g_1$ for $-2 < x < \infty$.

$$0 \cdot \lim_{x \rightarrow \infty} g_1 \quad (7.125)$$

$$0 \cdot \lim_{x \rightarrow \infty} \frac{1796.2}{17.66 \cdot (B_{er})^x Q \sqrt{2\pi}} \cdot e^{-\frac{(\ln(17.66(B_{er})^x))^2}{2(Q)^2}} \quad (7.126)$$

$$0 \cdot \lim_{x \rightarrow \infty} \frac{1796.2}{17.66 \cdot (B_{er})^x Q \sqrt{2\pi}} \cdot \frac{1}{e^{\frac{(\ln(17.66(B_{er})^x))^2}{2(Q)^2}}} \quad (7.127)$$

$$0 \cdot \lim_{x \rightarrow \infty} \frac{1796.2}{17.66 \cdot (B_{er})^x Q \sqrt{2\pi}} \cdot \lim_{x \rightarrow \infty} \frac{1}{e^{\frac{0.5}{(Q)^2} (\ln(17.66) + x \ln(B_{er}))^2}} \quad (7.128)$$

$$0 \cdot \lim_{x \rightarrow \infty} \frac{1796.2}{17.66 \cdot (B_{er})^x Q \sqrt{2\pi}} \cdot \lim_{x \rightarrow \infty} \frac{1}{e^{\frac{0.5}{(Q)^2} ((\ln(17.66))^2 + 2x \ln(B_{er}) \ln(17.66) + x^2 \ln(B_{er})^2)}} \quad (7.129)$$

$$0 \cdot \lim_{x \rightarrow \infty} \frac{1796.2}{17.66 \cdot (B_{er})^x Q \sqrt{2\pi}} \cdot \lim_{x \rightarrow \infty} \frac{1}{e^{\frac{0.5x^2}{(Q)^2} \left(\frac{(\ln(17.66))^2}{x^2} + \frac{2}{x} \ln(B_{er}) \ln(17.66) + \ln(B_{er})^2 \right)}} \quad (7.130)$$

$$0 \cdot 0 \cdot 0 \quad (7.131)$$

The test for convergence shows that the ratio of PDF g_1 to theoretical upper bound converges to 0 as x approaches infinity, concluding that our CDF is bounded by PDF, which is then strictly bounded by the theoretical upper bound of the wall of semi-invisibility.

7.4 Complexity Equivalence

Now, using our existing lognormal distribution, we will investigate the property of biodiversity/civilization complexity equivalence.

From the previous derivation, we know that currently, Homo sapiens led industrial civilization occurs once in every 52 galaxies.

$$\begin{aligned} t_{galaxy} &= \left(\int_0^\infty g_1 dx \right)^{-1} \\ &= 51.9626294477 \end{aligned} \quad (7.132)$$

Using this equation, we can extrapolate the first arising industrial civilization within the Milky Way galaxy to be 77.88 million years into the future:

$$\begin{aligned} t_{galaxy} &= \left(\int_{-0.7788}^\infty g_1 dx \right)^{-1} \\ &\approx 1.00 \end{aligned} \quad (7.133)$$

If next industrial civilization arising from the Milky way will occur 77.88 Myr into the future, what does it mean? Since we know that our YAABER is the total sum of YAABER for hominid lineage evolution + hunter-gatherer transition + agricultural transition + industrial transition, at what stage of development could the next industrial civilization be at today if we observe it directly through a telescope? It is tempting to conclude that they are only 77.88 Myr behind us. Therefore, they are probably just stuck in steam-powered or 19th-century Victorian era development for the next 77.88 Myr. This conclusion, upon close inspection, is absurd. Since industrial civilization is categorized into two stages, first the increase usage of fossil fuel led to economic growth and energy utilization growth and second the replacement of fossil fuel by nuclear fusion power so that the industrial civilization can be maintained indefinitely at a steady state on the home planet or grow exponentially by expanding into the cosmic neighborhood. This led to one conclusion, fossil fuel based industrial civilization, like that of the steam-powered based Victorian era is a transient short one either facing collapse or fully transitioned into an expansionary cosmic civilization. Since we predict by high probability and log-normally distributed temporal arrival, then we can rule out that this next arising civilization is on its way to transition into a sustainable industrial civilization, and we also know that this planet has endowed enough radioactive material so that nuclear fusion can be developed once industrial civilization is kick-started. That is, this planet has all the necessary ingredients to successfully transition once they develop steam engine. If we assume that most civilization is not foolhardy enough once industrial civilization is developed and destroy themselves along the way, then it is unlikely that this planet is on a race with earth to obtain galactic industrial civilization status but fails because it destroys itself and has to wait for another 77.88 Myr of evolution for the next creature to take over.

Let's take a step further back, is it possible that this planet has developed into an agricultural society and maintained a steady state for the next 77.88 Myr. Although agricultural society evolves much slower than an industrial one, 77.88 Myr is more than enough time even from geological perspective to evolve basal mammals into Homo sapiens with the presence of an ice age. It is possible that this agricultural society was well maintained, but at some point in its 77.88 Myr of progression, population pressure will force it to utilize fossil fuel. It is also highly likely that climate change and catastrophic events such as an asteroid collision within this time window will render the agricultural society extinct since agricultural society are severely limited by ecological constraints. It is possible that an agricultural society lasted for 77.88 Myr or even more years before transitioning to an industrial one, but such case is highly unlikely.

This leaves us with the following intriguing scenarios. First, grass-like plants capable of sustaining vast population have evolved, but there is no human-like creature exists on the planet. This is interesting because this implies that the stage is set for the main player yet the main player still has to show up. 77.88 Myr fits reasonably well as a geological time frame for the evolution of creatures comparable to the human level in every possible way if not better given favorable conditions. If earth observers are patient enough, up to the first 40 Myr of continuous

observation of this planet, nothing other than plenty of grass-like plants, creatures with great potential being utilized as farm animals in an agricultural society have evolved. However, another 10 Myr of observation found the emergence of creatures similar to human and left their arboreal habitat and roamed their grounds. By the last 1 million years, they utilized fire and tools and by 100 Kyr before the 77.88 Myr predicted, they started to transition into an agricultural society, and 500 years before the 77.88 Myr time window ends they developed steam engine and ushered in industrial civilization, 200 years before the window closes they developed nuclear fusion and ushered in technological singularity. By the time the window closes, they are already expanding 200 light years in radius from their home planet.

Secondly, human-like creatures have evolved on this planet but maintained a hunter-gatherer mode of subsistence because grass-like plants yet to evolve on this planet. In this case, the protagonist has arrived early, but the stage and all necessary equipment are not yet ready for him/her to perform. Homo sapiens are benefited from a fast transition from hunter-gatherers to an agricultural one after 100,000 years at the start of the current inter-glacial. However, human-like creatures on other planets may not be as lucky as we are. It is possible on a planet where human-like creatures have evolved and used stone tools and banded together and is able to dominate their landscape as the apex predator. However, they are not able to transition to an agricultural society because high energy crop species such as wheat, rye, oats, and rice are not available. They could maintain their population about a few million around the globe but not any further. They have to wait for high yield crop plants to evolve on their own before they can transition. One may underestimate the difficulty of transition between hunter-gatherer to that of agricultural society. Human ingenuity is crucial but limited in its ability to manipulate nature. Human's artificial breeding and selection of domesticated plants and animals simply exaggerated a trait already existed in their genome, but human has no power to add and remove genes at their will. Furthermore, the hunter-gatherers are unlikely even to contemplate to domesticate their environment because the cost over return is so high that any attempts will be detrimental to their survival based on their conservative hunter-gathering lifestyle. If one were to observe such planet from earth, one might be delighted to find creatures similar to us and optimistically predict that such creature will arise and expand into the universe less than geological timescale. However, one will be disappointed by the fact these creatures are not evolving toward other modes of living though they utilized fire and tools. By the last 1 million years before the predicted end of the appearance window, grass plants have finally evolved on their planet. By 100 Kyr before appearance window, they started to transition into an agricultural society, and 500 years before the 77.88 Myr time window ends they developed the steam engine and ushered in industrial civilization, 200 years before the window closes they developed nuclear fusion and ushered in the technological singularity. By the time the window closes, they are already expanding 200 light years in radius from their home planet.

Thirdly, it is possible that sub-earths, which we have shown earlier, should have slower tectonic plate movements, which translates to a slower pace of evolution on such a planet. As a result,

some of their developmental trajectory will be similar to earth except at a slower pace. That is, the emergence of an intelligent species and grass plants occur roughly at the same time. Almost like earth's history unfolding at a slow motion, an observer looking at such a planet will find neither human-like creatures nor any grass plants. However, near the end of the temporal window, both the intelligent creature and grass plants have emerged and ushered into an industrial civilization.

Lastly, it is possible that the planet has a comparable mass to earth with a similar pace of tectonic plate movement and it has the right placement of the continent cycle over the glaciation cycle. However, its cycle is delayed by 77 Myr. As a result, it is currently undergoing a similar biodiversity transition as we had experienced during the late Cretaceous. Therefore, the life history unwinds at the same pace as it is observed on earth except it is played with some significant delay. Obviously, one will neither human-like creatures nor any grass plants.

In all cases, an extended period of waiting time is needed before the emergence of industrial civilization, from the mathematical point of view, they are identical, all have to wait for 77.88 Myr before their arrival on the cosmic stage. I call this equivalence the complexity equivalence; that is, from a mathematical and modeling perspective those four scenarios are quantitatively equal. The assumption that all existing habitable planets' Years against Background Evolutionary Rate does not change at sub-geologic timescale is satisfied in all cases. They both appear non-moving until the very last million years where a fast transition occurs and rapidly shifted its position on the distribution curve. However, it remains speculative which of those scenarios is more likely and if it is possible to give a more precise probability treatment for each of the cases.

One then can compute the emergence probability of Homo sapiens and that of the emergence of crop plants. Since the emergence of human at the current epoch requires not only the probability of right ordering of the attainment of major traits, but it also requires the probability of ice age formation. Overall, the probability of human emergence is 1 out of 502 during the latter part of a supercontinent cycle. The emergence of crop plants, on the other hand, ranges from 1 out of 8.898 to 1 out of 129. It is not hard to conclude that the probability of human emergence is rarer than the emergence of crop plants at the odds ranges from 56.4 to 1 at the upper limit to 3.89 to 1 at the lower limit. As a result, we can conclude for every habitable planet we found that has the potential to evolve into the next expanding industrial civilization. We found that only between 25.7% and 1.773% of all planet has the necessary ingredients such as the presence of crop plants yet no human-like creatures on them. Additionally, we mentioned cases whereas both the crop plants and human like creatures yet to emerge. This gives us high confidence that if we are able to pinpoint the exact planet to observe our next arising industrial civilization within the galaxy, we will be disappointed by most of the time, not finding any human-like creature on that planet at all!

7.5 Complexity Transformation

The probabilistic distribution accounts both temporal and spatial aspects of civilization's attainable complexity. If we assume that our civilization is 1.76604 Gyr ahead of BER, and the appearance rate is within a radius of 88 million light years, a civilization assumed to arose 100 million years ago comparable to human civilization's development at our current stage implies that it is 5.099 billion years ahead of BER at the time of its appearance.

$$Y_{aaber} = \int_0^x (B_{er})^x dx \quad (7.134)$$

$$\int_0^{(2.883+1)} (2.782559)^x dx \quad (7.135)$$

12

$$= 5.9918450163 \text{ Gyr YAABER}$$

Such level of complexity translates into the appearance rate within a radius of 734.3 million light years in radius, indicating its rarity and exponential growth in difficulty in attaining biological complexity in an earlier epoch. Moreover, 5.099 billion years ahead of BER can also be understood as human civilization continued in its development path into the near future, so that it is increasingly improbable that in our vicinity giving rise to a civilization at the level of complexity as ours. It is also applicable to any other extraterrestrial civilization is attaining its complexity ahead of current human development. However, a caveat should be raised to interpret the numbers literally. We have shown earlier that once a biological-based species achieving control of nuclear fusion and able to maintain industrial civilization paradigm into the indefinite future, it is only a matter of time before the civilization becomes multi-planetary, and the majority of the decision making will be transitioned to that of artificial intelligence, completely renouncing the biological constraints placed onto the species. Though an industrial civilization may remain on biological substrates and continue its expansion as a biological species directed one, there must exist a mean time frame by which time the industrial civilization transitioned into a post-biological one. No one is yet sure what that time horizon is, but many argued that the foreseeable technological singularity is the cause of such a transition, and it is typical in all technological civilization's path of development, though the time of technological singularity is widely debated. On the other hand, we have discussed in Chapter 6 the limits of growth to biological beings directed civilization. With an annual growth rate of 2%, growth can be maintained at most for another 300 years for biologically led industrial civilizations.

If we compute for a civilization attained our current human level of technological progress 40 million years into the future, one can find that only 1.1425 Gyr ahead of BER. It means that as more habitable planets evolved with more biologically diverse species. The chance of arising

¹²2.883 stands for 288.3 Myr needed to catch up with a YAABER of 1.766 Gyr

human civilization increases and the attainment of human-like civilization is not as remarkable as it is now or it was in the past.

$$Y_{aaber} = \int_0^{x-0.4} (B_{er})^x dx \quad (7.136)$$

$$\int_0^{(2.883-0.4)} (2.782559)^x dx \quad (7.137)$$

$$= 11.4257100978 \text{ Gyr YAABER}$$

The number can also be interpreted differently. One can argue that 1.1425 Gyr ahead means that a civilization attained a level of sophistication comparable to Age of Exploration on earth, that is, they thoroughly explored their planet and developed sophisticated agricultural society but yet to transform or unable to transform into an industrial one. It can also be interpreted as a planet with all the necessary ingredients to nurture an advanced technological civilization such as the appearance of grass plants, plenty of open fields, fruit trees, massive endowment of fossil fuels and uranium sources, but yet to wait for the appearance of an intelligent, tool manipulating species, as we have discussed this in section “Complexity equivalence”. In either case, the radius of the sphere for the appearance of this civilization is only 14.9 million light years and is less than ours, because there are more civilizations or planets attained at the level of biological complexity and diversity lower than observed on earth.

The biological complexity growth rate (the background evolutionary rate) per 100 million years is one of the most interesting aspects of the entire model. This number can vary widely from 1.203 up to 4.51, depending on the derivation methods used. According to Alexei and Sharov, the genome complexity (the number of sites of functional codons) of living organisms doubles every 250 million years which translated to 1.203 per 100 million years. This is the lower bound of growth curve estimates. We have shown earlier, under the section 7.3 “Wall of Semi-Invisibility”, in order for BER to hold a value of 1.203, the rate of emergence has to be lowered so that it can satisfy the condition required by the theoretical upper bound. If we take the rate of EQ growth from typical reptiles in the early Triassic to that of the mammals in the early Cenozoic, with an increase of 10 folds, we found that the growth rate per 100 million years is 2.78, which is the one we used (see Chapter 6 and Chapter 4). Interestingly, assuming the first cell arise between 4.28 Gyr and 3.8 Gyr, then the complexity attained by the multicellular animal from single celled prokaryotes purely based on the total cell numbers assumed a growth rate of 2.973 per 100 million years. It is essential, again, to stress this growth rate not the intrinsic biological rate of change attainable by molecular mutation and recombination. Genome evolution has been shown and stated (see Chapter 4) can be much faster. However, most of the time, the pace of evolution is kept in check by the earth’s external environment, which favors stabilizing selection. Therefore, the background evolutionary rate itself can be misleading. It is, instead, the rate of geologic change and its dominant effect on the species, in which the rate of evolution is predominantly controlled by earth’s rate of the

geologic process rather than living organism's genome mutation rate.

7.6 Darwin's Great-Great Grandson's Cosmic Voyage

We discussed complexity equivalence and complexity transformation. Now we want to use these concepts to illustrate interesting consequences. Although YAABER for ourselves is 1.76604 Gyr, this is the YAABER compares to the current cosmic evolutionary rate, for the average cohorts of all planets currently developed biological diversity and complexity to guarantee the emergence of human-like creatures does not take 1.76604 Gyr into the future. To understand this, one should realize as the time goes by, the cosmic background evolutionary rate is speeding up, as a result, one needs to wait less time to see all earth analogs develop intelligent creatures found on earth. This can be calculated based on the following derivation:

$$Y_{aaber} = \int_0^x (B_{er})^x dx \quad (7.138)$$

$$\Rightarrow \left[\frac{(B_{er})^x}{\ln(B_{er})} \right]_0^x \quad (7.139)$$

$$\Rightarrow \left[\frac{(B_{er})^x}{\ln(B_{er})} \right] - \left[\frac{(B_{er})^0}{\ln(B_{er})} \right] \quad (7.140)$$

$$\Rightarrow Y_{aaber} = \frac{(B_{er})^x}{\ln(B_{er})} - \frac{1}{\ln(B_{er})} \quad (7.141)$$

$$\Rightarrow Y_{aaber} + \frac{1}{\ln(B_{er})} = \frac{(B_{er})^x}{\ln(B_{er})} \quad (7.142)$$

$$\Rightarrow \ln(B_{er}) Y_{aaber} + 1 = (B_{er})^x \quad (7.143)$$

$$\text{Taking both sides with log:} \quad (7.144)$$

$$\Rightarrow \ln(\ln(B_{er}) Y_{aaber} + 1) = x \ln(B_{er}) \quad (7.145)$$

$$\Rightarrow x = \frac{\ln(\ln(B_{er}) Y_{aaber} + 1)}{\ln(B_{er})} \quad (7.146)$$

$$y = \frac{\ln(\ln(B_{er}) Y_{aaber} + 1)}{\ln(B_{er})} \quad (7.147)$$

That is, by taking the integration from now to x years into the future, the sum of cumulative biodiversity throughout x years into the future is the YAABER one current possessed.

By substituting B_{er} with our current estimate 2.782599 per 100 Myr.

$$y = \frac{\ln(\ln(2.782599)(17.6604) + 1)}{\ln(2.782599)} \quad (7.148)$$

$$= 2.88095041828$$

$$= 288.095041828 \cdot 10^9 \text{ Myr}$$

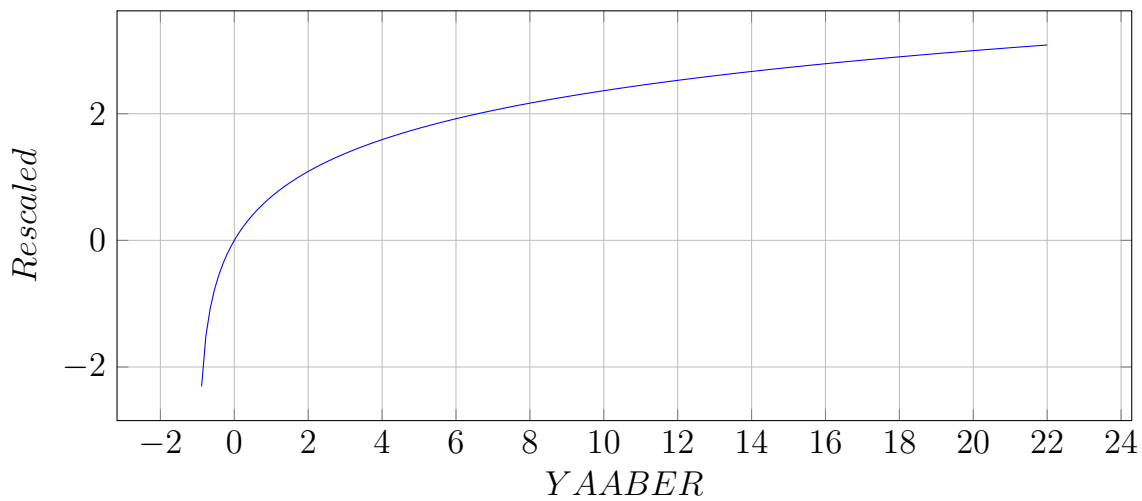


Figure 7.18: Biocomplexity transformation curve

And it can be found that it will take just 288.1 Myr instead of 1.76604 Gyr.

Assuming extraterrestrial civilization expands very slowly, so we will no expect to encounter any in the next 288 Myr. Then, what will Darwin's great-grandson see if he takes on a cosmic expedition to gather astrobiological data? If he takes on a near light speed travel vessel that properly shielded himself from radiation and make a quick stop at each destination and then quickly hops to the next one. He is set to travel 288.1 Million light years from stationary perspective while he only aged 50 years or so. As a result, he will able to collect enormous data in 50 years of time. His first observation was from the life hosting exoplanets within our Milky Way galaxy. All of such planets are devoid of human-like creatures. He probably observed some creatures that share some similarity to some aspects of human, but none of them possessed full potential as human. He stayed within the Milky way for the first 6 days and left to explore more distant galaxies. Throughout most of his career, the first 45 years of his expedition, he observed the similar patterns in other galaxies as that he observed in the Milky Way, though he did observe that a few planets already possessed human-like creatures and full-blown agricultural society and transitioning into industrial and eventually into post-biological society. The first one he observed transcending occurred 10 years into his journey. Majority of them, however, are not. However, in the last few years of his career, he observed that almost every life hosting planet visited is possessing by at least one human-like species and is rapidly evolving into a human-like society. At first, it appears some of these creatures stagnated at the hunter-gatherer stages because it lacks crop plants, but sooner or later the plants co-evolved and ushered in agricultural revolution. In the last few days of his career, every other planet he visited is evolving into an agricultural one. In the last few hours of his

career, every other planet he visited is turning into an industrial one, finally, in the last few minutes of his career, every other planet he visited is transforming into a post-biological life form and replacing him as the expedition team leader as the descendants of the Darwin's from each of their home planet emerges and continue their expedition in the cosmos.

7.7 Upper Bound & Lower Bound

We have already shown that the closest extraterrestrial industrial neighbor lies 88 million light-years away and the universe will be filled by expanding cosmic expansionists in 37 million years from now by the earliest. However, it is possible other filter criteria not covered in previous chapters worthy mentioning and can push the time frame to a later time period.

One issue not addressed previously is the position of the star within the Milky Way. The Sun's position is favorable not only because it posits on the galactic habitable zone but also in between the spiral arms and its orbits around the galaxy minimizes its crossing over the spiral arms. The greater density of interstellar medium and closer proximity to other stars during arm crossing can result in greater catastrophic events. Studies have been shown the relationship between Sun's spiral arm crossing in the past and extinction event. More studies are required in this area, and if Sun's position is indeed more favorable, the number of habitable planets within the galaxy has to be reduced significantly.

The sun, unlike many stars in the galaxy, seems to have stayed in its orbit since its inception. Recently, finding pointed out that up to half of the stars within the galaxy has migrated from their birth site to other locations either as inward or outward migration. The frequency of each type of migration and the average age at which the stars migrated and the spectral class profile breakdown of the stars require more examination. If migration indeed occurs frequently, a habitable planet can shift beyond the galactic habitable zone. Other stars may shift into the galactic habitable zone but with a shortened window of habitability, so that complex, multicellular life does not have enough time to evolve before the host star evolves off the main sequence.

The sun, unlike some other stars, has a low galactic orbital eccentricity. Other stars, can have higher eccentricity. Though these stars do not migrate during their main sequence lifetime, it nevertheless ventures beyond the galactic habitable zone. More data on stellar eccentricity is needed before conclusion can be drawn. If indeed a significant portion of stars favoring eccentric orbit around the galaxy, a substantial number of habitable planets needs to be reduced.

All of the factors mentioned above can generally be grouped into the category of a filter of the galactic habitable zone. Recent studies, however, have shown that such region may not exist. The galactic center actually hosts the highest probability of habitable planets given the density of stars per unit volume. Neither inward, outward, horizontal, or vertical movement of stars significantly alter the habitability of the system. The study concludes that 1.2% of

all stars within the galaxy are habitable. Since the study was done with metallicity and the habitable zone used as selection criteria, we multiply the metallicity factor (see Chapter 2 & 3) and habitable zone filter to yield 13.04%. This implies that the rarity of the emergence of industrial civilization is reduced by a factor of 1.975. Together along with the factor for galactic habitable zone at $\frac{1}{3.882}$ to yield a total factor of 7.667 (Chapter 2). This partially justifies the original Lineweaver's model for earth production in an unexpected way, which has to increase by a factor of 27.313 in order to comply with the number of stars in the galaxy, albeit the justification is not a consideration in the original model.

The size of dinosaurs and some prehistoric creatures posed a challenge to biology. Based on Galileo's squared cubed law, no animals at the size of gigantic dinosaur can survive today given the current atmospheric pressure and condition (with various causes such as difficulty pumping blood into its brain given its height).[36] Pterodactyl, given its size and wingspan, cannot sustain horizontal upward flight movement. That is, pterodactyl can glide from the cliffs to the shores, but it will have great difficulty in getting back to the edge of a cliff. A resolution to such paradox has been pointed out. The atmospheric pressure and atmospheric density potentially have to be several times higher than today, enabling the evolution of gigantic creatures with aided buoyancy. If air density fluctuates, then the evolution of fruit trees can be a consequence of evolutionary adaptation as the benefit to evolving fruits is significantly higher on planets with thinner atmosphere.[102][36] Basically, the plants are begging and luring animals to carry its seed away by rewarding them with their fruits. In an environment with a dense atmosphere, plants can disperse their seeds simply using mechanical means such as wind and rewarding animals with dispersion can be complementary. Therefore, angiosperms may not develop as easily on planets with denser atmosphere as it is observed on earth. Without the presence of fruit trees and the creation of the arboreal niche, the opposable thumb cannot develop, and no tool using species will exist. Currently, it is believed that earth had three atmospheres in its geologic history, the first was shrouded with primordial hydrogen, the second one composed mainly of carbon dioxide and methane, and our current one composed mainly nitrogen and oxygen. Preceding atmospheres were significantly denser than the current one. However, it is believed that the ocean, comprising the universal solvent water, along with life, is responsible for converting a huge share of carbon dioxide into carbonated stone such as the dolomite and limestone, and reducing the density to the current level. The onset of plate tectonics and carbon cycle may also significantly contributed toward a thinner atmosphere of today. Therefore, it is generally assumed that the density of atmosphere on all habitable planets converges toward similar conditions. This conclusion, however, can change as more is learned. If earth's atmosphere condition is typical and atmospheric pressure did fluctuate in geologic history, then the timing of the fluctuation can determine the emergence of intelligent tool using creatures. If fluctuation is the norm, then sooner or later fruit-bearing plants will emerge and arboreal niche will appear on such a planet to enable the emergence of opposable thumbs.

In one of the most frequently cited solutions to the Fermi Paradox, many argued all industrial

civilizations tend to destroy themselves through nuclear conflict or out of control nanotechnology and Artificial intelligence. Although this explanation has been ruled out due to non-mutual exclusivity, It is possible that not all industrial civilization succeeded in transforming into an expanding one. Even on our home planet, during the cold war era, had precariously avoided several incidents that could have initiated World War III. Since there is no tool to measure the likelihood a civilization to destroy themselves, it is hard to quantify this parameter.

Among civilizations which succeeded in transitioning into an AI controlled nuclear fusion powered civilization, a significant fraction may just choose not to expand. The civilization may or may not aware the existence of other extraterrestrial industrial neighbors. For various reasons, it is more inward-focused and consuming energy in a steady state fashion. Many futurists have hypothesized this type of civilization, which essentially harvests the energy of their home star and power their citizens with the abundance of wealth and material goods. It is also possible that the civilization immerses itself in a full-virtual reality that is qualitatively better than the real world it has to deal with.

It is also possible that civilization does expand, but on average expands at much slower speed than the speed of light. As a result, it takes a significant amount of time for each other to connect even if they intentionally wanted to do so. This theory is somewhat undermined because it has been shown that even with modest nuclear fission rockets using the technology we currently attained, we can reach 50% speed of light. It is further undermined by our discussion under relativistic economics (Chapter 8), it is shown that post-singularity society has a high incentive and the most significant economic gain by expanding nearing the speed of light.

All of the aforementioned factors could potentially render the emergence of an expanding civilization near the speed of light less likely. Therefore, we can group these factors into a single term called term x . Depending on the magnitude of term x , it can then be shown the limits and lower bound on the emergence of extraterrestrial industrial civilizations. To illustrate our point, we shall use results based on Gowanlock [65] to give the upper bound estimate for the number of extraterrestrial civilizations. According to Gowanlock, the concept of galactic habitable zone needs to be revised, it is found that no particular region of the galaxy is inhabitable for life, and the overall 0.3% of all stars may be capable of supporting complex life on a non-tidally locked planet. In a clear contrasts to our earlier calculation showing that 25.76% falls within the galactic habitable zone (Chapter 2), the calculation seem to suggest that one reduce the number of habitable planet by a factor of 85.867. However, the original study already taking planetary habitable zone and metallicity selection into effect, so we need to remove them from our calculation to yield the percentage we are interested. We have done calculation earlier showing that 9.20% of planets falls within the planetary habitable zone and 25% of stars falls within the metallicity selection criteria. As a result, the adjusted percentage indicates that Gowanlock predicts that 13.04% of all stars may be capable of supporting complex life. Then, a list of parameters we have discussed earlier can be recalibrated as the follows:

Term	Number
N_{earth}	5,466
Emergence rate	1 in 102.65 Galaxies
Nearest neighbor	110.97 Mly
Aliens by observable universe	15,382,548
Aliens by co-moving universe	558,771,232
Earliest within observable universe	225.27 Mya
Earliest within co-moving universe	263.90 Mya
Total space occupied	0.2267%
Distance between	55.48 Mly
Total filled up time	47.709 Myr
Connect with 1 neighbor (observable)	34,876
Connect with 2 neighbors (observable)	79
Connect with 3 neighbors (observable)	0
Connect with 1 neighbor (co-moving)	1,266,854
Connect with 2 neighbors (co-moving)	2,872
Connect with 3 neighbors (co-moving)	7

Table 7.5: Estimates based on upper bound

7.8 Subluminal Expansion

We have assumed that intelligent life of those undergone post-biological transition prefers to propagate and expands at closely approximate or at the speed of light.(see Chapter 8) What if the civilization chooses to expand at sub-luminal speed? If the civilization starts to expand at subluminal speed, from our relativistic economics model (see Chapter 8), it can be shown that sooner or later such civilization will adapt to speed close to the light speed. If for some reason, they remain at slow expansionary speed, they can be observed in the sky as an astronomical phenomenon. If such phenomenon occurs and expands at speed less than the expansionary speed of the universe based on its redshift index Z compares to earth, then, it will gradually disappear from our view. If it expands at the same speed as the expansionary speed of the universe from our vantage point, then its size will remain fixed. The most likely scenario is that its expansionary speed is faster than the expansionary speed of the universe from our vantage point of view. If the speed is as close to the speed of light as possible, the observation of such phenomenon will be one of the worst news for humanity because it implies that its physical arrival to earth is imminent. Since it takes millions of light years for the signal to travel to earth, and during these millions of years, the civilization is likely expand from a sub-luminal speed toward speed c . The delay in the observance of an extra-terrestrial artificial phenomenon and its physical arrival is simply the time used by the civilization to optimize its expansionary

speed from subluminal to speed c . This may take from a few millenniums to just a few days (in a post-singularity scenario). This will make earth extremely ill-prepared for such an encounter. The sky will appear as utterly devoid of any artificial signals and phenomenon (like what we have observed now so far) to a spot or spots of interests. Then, suddenly the entire sky will be filled with artificial phenomenon with delays in just days, months, years, decades, centuries, or millenniums, all tiny time scale compares to cosmological timescale.

7.9 Observational Equations

In order to mathematically state the Fermi paradox as a set of equations, one has first to define the probability of arising industrial civilization within a sphere of unit radius r , which can be any arbitrary value. We have simply set it as the sphere radius of the observable universe within 13.8 billion light years. The total chance of observing one, two, three, and up to n number of extra-terrestrials summarily is simply:

$$\left(\int_0^\infty g_1 dx\right)^1 + \left(\int_0^\infty g_1 dx\right)^2 + \left(\int_0^\infty g_1 dx\right)^3 + \dots + \left(\int_0^\infty g_1 dx\right)^n \quad (7.149)$$

$$= \sum_{k=1}^n \left(\int_0^\infty g_1 dx\right)^k \quad (7.150)$$

The maximum number of observable extraterrestrials can be then easily derived based on the measured radius, and we have shown earlier that no extra-terrestrial civilization met more than three other extraterrestrial civilizations within the radius of the observable universe.

Then, we have the equation for the total number of extraterrestrials regardless of the time of their emergence with a fixed given radius of r , and r_0 is simply the weighted average of the radius of galaxies taking the empty space between them into considerations:

$$N_{all}(r) = \sum_{k=1}^n \left(\int_0^T g_1 dx\right)^k \left(\frac{\frac{4}{3}\pi r^3}{\frac{4}{3}\pi r_0^3}\right) \quad (7.151)$$

$$= \sum_{k=1}^n \left(\int_0^T g_1 dx\right)^k \left(\frac{r}{r_0}\right)^3 \quad (7.152)$$

$$T = 13.8 \text{ Gyr} \quad r_0 = 11.85 \text{ Mly}$$

If r applies to the size of the observable universe, the equation states the number of all extra-terrestrial industrial civilization ever arise regardless they are current observable or not. That is, currently arising extra-terrestrial civilization 1 billion light years away is not directly observable, yet it can be calculated from the equation. Though the universe at its inception was infinitely

dense, the chance of extra-terrestrial civilizations forming was infinitely small. As a result, the total number of arising extra-terrestrial within the size of observable universe is finite (again, the universe expanded quickly so that only finite amount of mass is distributed within the space-time fabric of the observable universe, the total number of arising extra-terrestrials can remain infinite for the entire size of the universe)

$$N_{past}(r) = \int_0^T \sum_{k=1}^n \left(\int_r^T g_1 dx \right)^k \left(\frac{4\pi r^2}{\frac{4}{3}\pi r_0^3} \right) dr \quad (7.153)$$

where each step of $dr = r$ as the lower bound for $\int_r^T g_1 dx$

The second equation states that since the expansion of the universe, the total sum of signals ever has reached us from the past at each distance from earth. That is, a distance of 0 from us implies all signals starting from the big bang up to today will be counted toward the total sum. A distance of 13.8 billion light-years from us implies only a few years if not a few minutes of signals following the big bang is counted toward the total sum. Of course, the model is still an excellent approximation of the real situation because earth's or sun's and Milky Way's position cannot be assumed to be fixed. However, such local movement is small enough that does not alter the general calculation. (i.e. sun's revolution's diameter of 60,000 light years is 0.000217391% of the diameter of the universe. So the model is 99.999782% correct.

$$N_{now}(r) = \int_0^T \sum_{k=1}^n \left(\int_r^{r+d} g_1 dx \right)^k \left(\frac{4\pi r^2}{\frac{4}{3}\pi r_0^3} \right) dr \quad (7.154)$$

where $d \leq 0.000000036$ and $(r + d) \leq T$

The third equation states that since the expansion of the universe, the total sum of signals that are currently reaching us from the past at each distance from earth. We define currently as the recent 50 years of observation. This is converted to $d \leq 0.000000036$. That is, a distance of 0 from us implies all signals just occurred will be counted toward the total sum. A distance of 13.8 billion light-years from us implies just that moment of the big bang is counted toward the total sum. Since signals from the more distant past imply that the bio-complexity transformation factor was much lower; therefore, the chance of observing any extra-terrestrial decreases with greater distance, as we have already discussed.

To clarify the difference between the above three equations, we need to reuse diagram from Chapter 1. The size of the rectangle is the total number of extra-terrestrial civilizations given the age and the size of the observable universe, corresponding to the first equation. The size of the shaded triangle corresponds to the second equation. The tiny hypotenuse of the rectangle is the sum of all signals currently reaching earth.

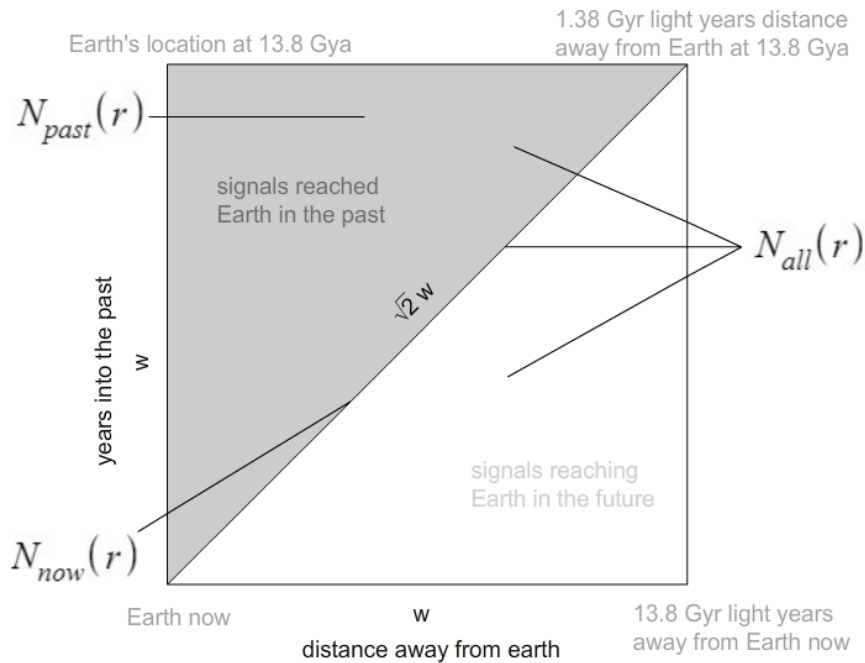


Figure 7.19: Signal detection landscape of time vs distance

It can be shown that as the width and height increase toward infinity, the ratio of the third equation toward both the second and the third approaches 0. This implies that the fraction of currently observed signals in the universe is tiny compares to all signals ever received. The total fraction currently observed, in fact, is 0.0056% of all signals since the Big Bang. The relationship between the three equation can be then formulated as the follows:

$$N_{all}(r) \geq N_{past}(r) \geq N_{now}(r) \quad (7.155)$$

This is the Fermi Paradox stated from purely mathematical perspective. That is, arising extra-terrestrial civilization are not observable if they currently lie outside of our past light cone. Given the vast amount of signals have reached us from the past (50% of all signals ever created within the observable universe and our starting assumption that a civilization utilizing nuclear fusion is sustainable) and the lack of any evidence earth and its cosmic vicinity is colonized, the lack of signals implies again that we can receive such signal only in the future if at all. *Therefore, if cosmic transition bound to occur, then Fermi Paradox is an observational one, and a natural consequence of all extra-terrestrial civilization arising in the relatively recent past, and almost all arising extra-terrestrial industrial civilization at the current epoch facing the similar paradox.*

Having derived the general form of our equation, we can re-estimate the distance to the nearest extraterrestrial industrial civillization by the following equation:

$$N_{galaxy} = \left(\int_0^\infty g(x) dx + \int_0^\infty (g(x))^2 dx + \int_0^\infty (g(x))^3 dx + \dots \int_0^\infty (g(x))^\infty dx \right)^{-1} \quad (7.156)$$

$$\frac{\left(N_{galaxy} (1,185)^3 \right)^{\frac{1}{3}}}{10^4} = 43.362 \text{ Mly} \quad (7.157)$$

That is, the nearest civilization now lies somewhat closer at 43.363 million light years away instead of at 44.21 million light years away, or 0.848 million light years closer, by simply considering the extra possibility of seeing more than one extraterrestrial industrial civilizations within our sphere of influence. This is deemed as the more precise result compared to our earlier one.

8 Relativistic Economics

8.1 Overview

The outlook is very different for a post-biological directed industrial civilization. We have already shown eventually post-biological intelligence have a good chance dominating the earth and the solar system beyond. This transition can be quick, as advocated by the Singularitytarians, where machine intelligence overtakes humans within decades, or can be slow based on generational commitment in biological technology and fine-tuning. In either case, a transition is quick compares to the geological timescale of $x < 10^7$ years. As a result, post-biological species is able to adapt to a much wider range of habitats and environments, its energy acquisition can be efficient, and no crop plants is needed. To appreciate the expansionary economics in the cosmic scale, we need to introduce the concept of relativistic economics and finance, a generalized form of finance applied at the cosmic scale to deal with cosmic investment and growth. Immense distance renders conventional communication and transportation impossible. Relativistic mass and speed, energy acquisition and incubation period become the conventions. As a result, relativity is required to deal with the problems associated with them. The equations are applicable to both biological led expanding industrial civilization as well as to post-biological expanding industrial civilization. Though the numbers from the calculations differ and we are discussing them below.

Economic growth is a very complex interaction between interest rates, prices, investment, savings, and over the long run, on technology growth. Since technology is the utilization of extracted energy, and it helps to ensure greater energy acquisition. (such as early oil well and the consequent development of oil rigs and drills based on the abundance of cheap energy and their later use in horizontal drilling and fracking, previously deemed unprofitable without refined technology) Technology sophistication and energy acquisition correlates positively and reinforce each other. Yet technology is hard to quantify into abstract mathematical numbers or concepts, and the total use of energy can be measured at any given time. As a result, we make an assumption that energy consumption is a measure of the level of economic development as for an individual or for a group, as in accordance with White's law. Then, we can measure the rate of economic growth of a civilization based on the total growth of its energy usage. Whether the energy increase achieved through increased per capita energy consumption, increased population, socialistic system, capitalistic system, or any other possible sociological system do not alter our basic assumption. For the sake of simplicity, we shall adopt the assumption that the total energy usage is the consequence of population growth while the per capita energy consumption stays constant.

For Relativistic Economics: the inequality expressed between the Final Return on Migration and initial costs, we have an equation in the simplest conceptual form for investors:

Final Return on Investment - Preparation Cost - Migration Cost > 0

Whereas the Final return on investment can be more conceptually materialized into:

$$R_{final} = \frac{1}{m} \cdot (E_{stable} \cdot P_{growth} + E_{growth}) \cdot P_{migration} \quad (8.1)$$

R_{final}	Final Return on Investment, units in Joules
E_{stable}	Maximum allowable energy acquisition for stabilized 1 billion years, units in Joules
P_{growth}	Perceived rate of subjective value depreciation on the finalized stable return over 1 billion year period during the expansionary phase at the destination
E_{growth}	The total energy acquisition for the expansionary phase before the maximum energy extraction level is reached, units in Joules.
m	Number of participants
$P_{migration}$	Perceived rate of subjective value depreciation on the overall return due to the migration waiting phase toward the destination before any return is initiated. (So investors' subjective value of return is lower than the actual return.)

Preparation Cost (for both earthbound and shipbound investors) can be more conceptually materialized into:

$$C_{prepare} = \epsilon_{lost} \cdot m \cdot T_{preparation} \cdot P_{preparation} \quad (8.2)$$

$C_{prepare}$	Preparation cost on earth, units in Joules
ϵ_{lost}	Energy saved (unavailable currently) for preparation purposes per participants per year, units in Joules
m	Number of participants
$T_{preparation}$	The total preparation time required to save enough energy to send the ship at certain speed, units in years
$P_{preparation}$	Perceived rate of subjective value depreciation on the total costs required to commence the trip during the preparation phase (so investors' subjective value of costs is lower than its actual costs)

Migration Cost for shipbound investors can be more conceptually materialized into:

$$C_{migrate} = \epsilon_{lost} \cdot m \cdot T_{migration} \cdot P_{migration} \quad (8.3)$$

$C_{migrate}$	Migration cost for the ship, units in Joules
ϵ_{lost}	Energy (generating-energy opportunity) lost due to migration time spent on ship per participants per year, units in Joules
m	Number of participants
$T_{migration}$	The total migration time in the ship's reference frame at certain speed, units in years
$P_{migration}$	Perceived rate of subjective value depreciation on the final return during the migration phase. (so that investors' subjective value of costs is lower than the actual costs.)

We also need to introduce two units of conversion so to simplify our equations down the road. Total relativistic energy required for an unit mass departure at a certain speed:

$$K_{rel} = \frac{1}{\sqrt{1 - \frac{v^2}{c^2}}} - 1 \quad (8.4)$$

It is also expressed in our calculation as:

$$K_{rel} = \frac{1}{\sqrt{1 - \frac{x^2}{100^2}}} - 1 \quad (8.5)$$

Total time required for migration at certain speed in shipbound investors' reference frame:

$$T_{rel} = \frac{d}{v} \sqrt{1 - \frac{v^2}{c^2}} \quad (8.6)$$

It is also expressed in our calculation as:

$$T_{rel} = \frac{d}{\frac{x}{100}} \sqrt{1 - \frac{x^2}{100^2}} \quad (8.7)$$

c = Speed of light

d = The current cosmological distance from the origin to the destination, units in light years

v = The migration traveling speed, units in a fraction of the speed of light

For earthbound investors, the equation is expressed as:

$$E_{arth} = \frac{\epsilon}{m} \left[\left(\sum_{k=0}^{10^9} M (p)^k \right) p^{\frac{\ln(\frac{M}{m})}{\ln a}} + \frac{\ln(\frac{M}{m})}{\ln a} \sum_{k=0} m (ap)^k \right] p^{\left(\frac{m \cdot K_{rel}}{\epsilon} + \frac{d}{v} \right)} - m\epsilon \left[\sum_{k=0}^{\frac{m \cdot K_{rel}}{\epsilon}} p^k \right] \quad (8.8)$$

m = The initial number of participants

M = The final number of population owned/controlled by the initial participants as the founders

a = The economic growth rate (population growth rate)

p = The perceived rate of subjective depreciation on returns

ϵ = The amount of energy can be produced each year per capita, units in Joules

For shipbound investors, the equation is expressed as:

$$S_{hip} = \frac{\epsilon}{m} \left[\left(\sum_{k=0}^{10^9} M (p)^k \right) p^{\frac{\ln(\frac{M}{m})}{\ln a}} + \frac{\ln(\frac{M}{m})}{\ln(a)} \sum_{k=0} m (ap)^k \right] p^{\left(\frac{m \cdot K_{rel}}{\epsilon} + T_{rel} \right)} - m\epsilon \left[\sum_{k=0}^{\frac{m \cdot K_{rel}}{\epsilon}} p^k \right] - m\epsilon \left[\sum_{k=0}^{T_{rel}} p^k \right] \quad (8.9)$$

These equations are the abstract manifestation of the following concepts. First of all, we assume that inhabitants on earth achieve economic stabilization and no further room for economic growth is possible. (this assumption can be relaxed to show that incentive of stellar migration is strong as long as the rate of return is lower on earth than migration to another star system, but our discussion is based on the simplicity of our model). The first term (the summation part) of the equation simply means that the perceived value of eventual return in the form of energy when a group of individuals given by a total population of m , migrated to a new hospitable planet. (observed through telescope before migration, so no terraforming costs involved) This migrated population then grows exponentially based on a fixed energy growth rate until their descendants fill the entire planet with population M . We assume that their descendants are loyal to the founders and reaping the economic benefit of their initial investment with an energy budget of $M \cdot \epsilon$. The final objective value on return is then $\frac{M}{m} \cdot \epsilon$. Then, it is easy to show that a small group of founders will be willing to take risks to migrate, and much less likely for the population of the entire planet to migrate to a different earth because little to no

return is achievable (assuming all earth analogs holds similar carrying capacity). The growth rate maintains at the rate of a until it reaches population M , a term of p is the perceived value loss over a longer period of time. That is, biological creatures with limited lifespan hold a considerable perceived value of loss over a return that takes a significant time to achieve. In the economic endowment theory, the owner valued possession lost is twice as costly as its intrinsic value. In other words, the owner had expected to possess the item into the indefinite future while he has a perceived value of a loss of 50%. That is, his value placed on the current item is 1 at the current year, and only $\frac{1}{2}$ for the next year which yet to pass, and only $\frac{1}{4}$ for the third year, $\frac{1}{8}$ for the fourth year, and so on, then the sum of all years then is 2. If we assume one's view on his eventual return on the investment follows the similar perceived value of a loss, then p can be substituted with 0.5. This implies that human put very little attention toward any gain or loss three years into the future, and their concerns for any gain or loss over time decreases geometrically. However, a post-biological or even just more well-educated populace may place more emphasis toward the future by having a longer lifespan or more knowledge and awareness for long-term well-being. As a result, the perceived value of eventual return is greater when p is greater.

When the product of economic growth rate a and p is less than 1, given by the limit test, we have a convergent series which sums up to:

Limit test for convergence:

$$\sum_{k=1}^n m (ap)^k \rightarrow \lim_{n \rightarrow \infty} \left| \frac{a_{n+1}}{a_n} \right| \rightarrow m \lim_{n \rightarrow \infty} \frac{|ap|^{n+1}}{|ap|^n} \rightarrow m |ap| < 1 \rightarrow |ap| < \frac{1}{m} \quad (8.10)$$

$$\text{where } m=1: |ap| < 1$$

$$\text{when } ap < 1 \text{ and } p < 1$$

$$E_{arth} = \frac{\epsilon}{m} \left[M \frac{1 - p^{10^9}}{1 - p} p^{\frac{\ln(\frac{M}{m})}{\ln a}} + m \frac{1 - ap^{\frac{\ln(\frac{M}{m})}{\ln a}}}{1 - ap} \right] p^{\left(\frac{m \cdot K_{rel}}{\epsilon} + \frac{d}{v} \right)} - m \epsilon \frac{1 - p^{\frac{m \cdot K_{rel}}{\epsilon}}}{1 - p} \quad (8.11)$$

$$S_{hip} = \frac{\epsilon}{m} \left[M \frac{1 - p^{10^9}}{1 - p} p^{\frac{\ln\left(\frac{M}{m}\right)}{\ln a}} + m \frac{1 - ap \frac{\ln\left(\frac{M}{m}\right)}{\ln a}}{1 - ap} \right] p^{\left(\frac{m \cdot K_{rel}}{\epsilon} + T_{rel}\right)} - m\epsilon \frac{1 - p^{\frac{m \cdot K_{rel}}{\epsilon}}}{1 - p} - m\epsilon \frac{1 - p^{T_{rel}}}{1 - p} \quad (8.12)$$

when $ap \geq 1$

$$m \frac{1 - (ap)^n}{1 - ap} < \sum_{k=0}^n m (ap)^k \quad (8.13)$$

$$M \frac{1 - p^n}{1 - p} < \sum_{k=0}^n Mp^k \quad (8.14)$$

This is a special case of our summation, and very likely the solution of the perceived value of eventual return led by biologically expanding industrial civilization, which is what we are currently. The value for p can still be higher than 0.5 but must be lower than 1. This shows that for biological led civilization with a deep discount toward very far future, the total benefit for the eventual return on migration cannot be realized. For example, a team of one thousand migrated to the new terrestrial planet and populated up to 10 billion people in 814 years with an annual growth rate of 2% and a final theoretical return of 10,012,437.41 folds of the original investment. However, with $p = 0.98$, then, the perceived value of eventual return is only 50 folds, this is 200,249 folds difference! For a post-biological being which attains biological or even permanent immortality, its p infinitely approaches 1. As a result, its perceived value of eventual return will infinitely approach the theoretical value.

To make the matter even worse, the eventual return is further delayed by the amount of time at gathering the energy to send the spaceship to the distant planet and the amount time spent traveling from the origin to the destination for shipbound investors, the perceived value of the eventual return is a tiny fraction of the theoretical. The waiting time contributes toward an exponentially decreasing function where the perceived value on the return decreases exponentially as the waiting time increases.

For shipbound investors, the second term is the amount of time used to gather the energy required to send the spaceship to the destination, it plays close relationship with the third term in the equation, the amount of time used in travel to the destination. A group of one thousand can quickly prepare their trip to the destination without gathering too much energy manifested by their current energy budget that they can buy with their savings as ϵ . However, a slow spaceship will cost them thousands of years to reach their destination. On the other hand,

these 1,000 people can gather the energy they needed so that they can reach their destination in a very short time from the perspective both stationary observers on earth and the travelers themselves at a significant fraction of the speed of light. Traveling at a significant speed up to fractions of the light speed requires a tremendous amount of energy which can take the organizers thousands of years to complete. Therefore, it lies the dilemma, that no interstellar colonization is possible in a biological led industrial civilization. Or is it? Though groups of individuals and companies may not have the adequate time and resources to invest in such a project. All populations on earth as a whole may and possibly can, but we just showed that the entire population has little to no incentive to migrate at once. However, two ways can guarantee a migration scheme. The first of which is a lottery system. A lottery system can be activated planet-wide where each participant in the lottery have a tiny chance of migration. A small fraction of the energy used by each individual is invested into one interstellar project at a time, times the total population on earth. Then, the energy requirements can be fulfilled after a few rounds of the lottery and may take up to a thousand years. At the end of the lottery draw, 1,000 lucky winners are sent to the new habitable planet. The lottery can then be repeated over and over again and sending winners to the next closest habitable planet yet to be occupied. However, the interval between each successful lottery draw will be longer and longer because it takes more and more energy to get the winners to the destination further and further away. Newly colonized planets will able to perform their own version of lottery draws and send their descendants to those planets nearest to them, and they will have an advantage over lottery players on earth because they are closer to some of the unoccupied planets hence shorter waiting time for the next successful lottery draws.

Lottery approach is great. It shows that it is possible that when a market's perceived value of eventual return is too low one can still manage to colonize the stars. One shortcoming of the lottery approach, however, is that the selected winners are not necessarily the best fitted for a migration. If their winning ticket can be traded with someone else, the one really willing to go might get it. However, we just showed that the price for trade would be extremely high because it takes the entire world population to contribute 1,000 member team. So the most willing to go may not have the amount required to pay. Even if the most willing to go can always come up with the sum to pay, he or she may not have the most biological fit body to survive the trip and procreate upon the destination.

As a result, a second alternative, a government-funded project through taxation is another approach to stellar migration. A forward-looking, futuristic government which are well-aware the benefit of spreading and leveraging the risks of the extinction of human civilization will able to put fourth a thousand year plan where each year specific portion of taxes is contributed to the construction of interstellar vessels and gathers the necessary energy to send the spaceship to the destination. The government also builds facility and trains selected individuals from the pool of entire population who are screened and to be best fitted for the travel and procreation upon the destination.

The cons of government-sponsored projects are corruption, authoritarianism, and the unlikelihood of its survival in very long terms. It is noted that all human-led institutions suffer inefficiency in the forms of miscommunication and misallocation. The success of the state-run project requires a highly controlled population with solidarity. It is conceivable a strong government and sacrificing population is possible given a significant existential threat to the entire population; however, it is becoming increasingly difficult to assert authoritarian control of the masses given the ubiquity of the internet and without any extinction-level threat to the humanity. Furthermore, no government projects can last for thousands of years so far in documented human history. The construction of the pyramids took a few centuries of extensive development, and the construction and maintenance of the great wall of China lasted only a few centuries during the Han dynasty and the Ming dynasty.

Nevertheless, it can be shown that even with biological led industrial civilization, interstellar colonization is possible and desirable. Now let us focus on determining the speed at which our current level of industrial development can expand at the cosmic scale.

Assuming the subjective rate of depreciation is 0.95 and plotting the equation with a short distance to a destination within a few light years (20 lyr), one quickly concludes that the perceived economic incentives for earthbound investors and shipbound investors differ though both perceives positive return over a range of fractions of the speed of light. Their difference mainly stems from earthbound investors more inclined to making shorter preparation time and shipbound investors inclined for cruising at a higher speed to save trip time. Their curves also share crossover point at a specific fraction of the speed of light. At the crossover point, the earthbound investors perceived economic return agree with shipbound investor's perceived economic return value.

$$T_{relu} = \frac{1}{\frac{x}{100}} \sqrt{1 - \frac{x^2}{100^2}} \quad (8.15)$$

$$y_{ship0} = m \frac{1 - (1.02p)^{\frac{\ln(\frac{100}{m})}{\ln(1.02)}}}{1 - (1.02p)} p^{(mK_{rel} + 20T_{relu})} - \frac{1 - p^{mK_{rel}}}{1 - p} - \frac{1 - p^{20T_{relu}}}{1 - p} \quad (8.16)$$

$$y_{earth0} = m \frac{1 - (1.02p)^{\frac{\ln(\frac{100}{m})}{\ln(1.02)}}}{1 - (1.02p)} p^{\left(mK_{rel} + \frac{20}{100}\right)} - \frac{1 - p^{mK_{rel}}}{1 - p} \quad (8.17)$$

$$p = 0.95 \quad (8.18)$$

$$m = 4 \quad (8.19)$$

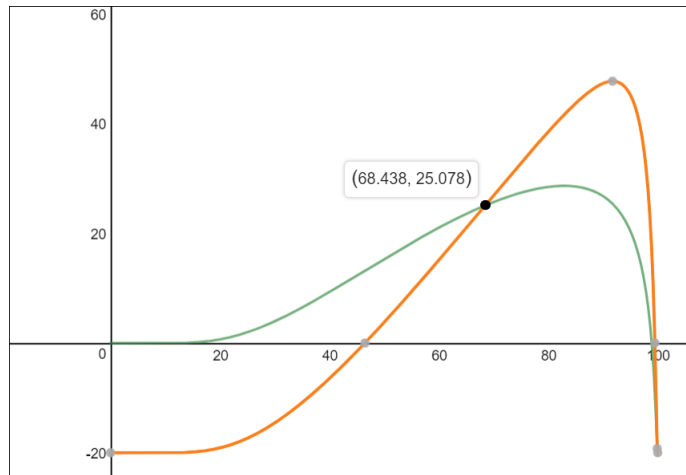


Figure 8.1: Earthbound vs. Shipbound perceived economic return

However, the most profitable speed of travel is not the crossover points; rather, it is the maximum value of the sum of both curves for earthbound and ship bound investors.

$$y_{ship0} + y_{earth0} \tag{8.20}$$

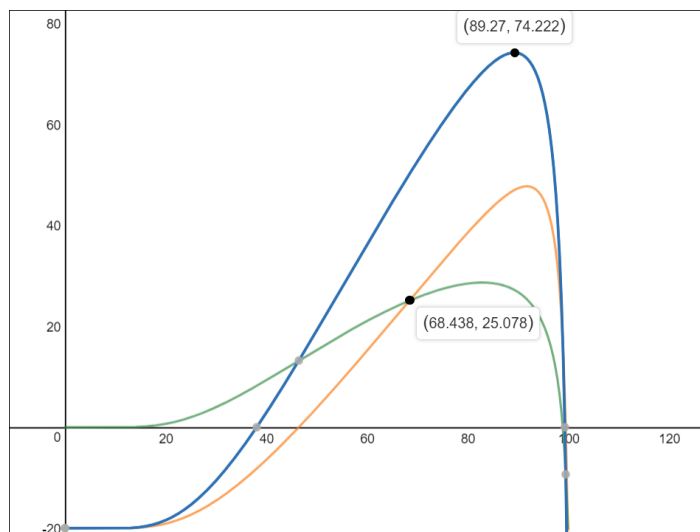


Figure 8.2: Composite perceived economic return and their maximum value

By setting every other variable constant except for the destination travel distance, one can also see the trend that economic wise, it is more profitable to send colonization fleet (both for the earth and shipbound investors) at a higher speed when the destination is further away even with more time and investment opportunity foregone domestically.

$$y_{20} = \left(m \frac{1 - (ap) \frac{\ln\left(\frac{100}{m}\right)}{\ln(a)}}{1 - (ap)} \right) p \left(\frac{mK_{rel}}{1} + \frac{20}{\frac{x}{100}} \right) - \frac{1 - p \left(\frac{mK_{rel}}{1} \right)}{1 - p} \quad (8.21)$$

$$y_8 = \left(m \frac{1 - (ap) \frac{\ln\left(\frac{100}{m}\right)}{\ln(a)}}{1 - (ap)} \right) p \left(\frac{mK_{rel}}{1} + \frac{8}{\frac{x}{100}} \right) - \frac{1 - p \left(\frac{mK_{rel}}{1} \right)}{1 - p} \quad (8.22)$$

$$y_3 = \left(m \frac{1 - (ap) \frac{\ln\left(\frac{100}{m}\right)}{\ln(a)}}{1 - (ap)} \right) p \left(\frac{mK_{rel}}{1} + \frac{3}{\frac{x}{100}} \right) - \frac{1 - p \left(\frac{mK_{rel}}{1} \right)}{1 - p} \quad (8.23)$$

$$p = 0.9 \quad a = 1.08 \quad (8.24)$$

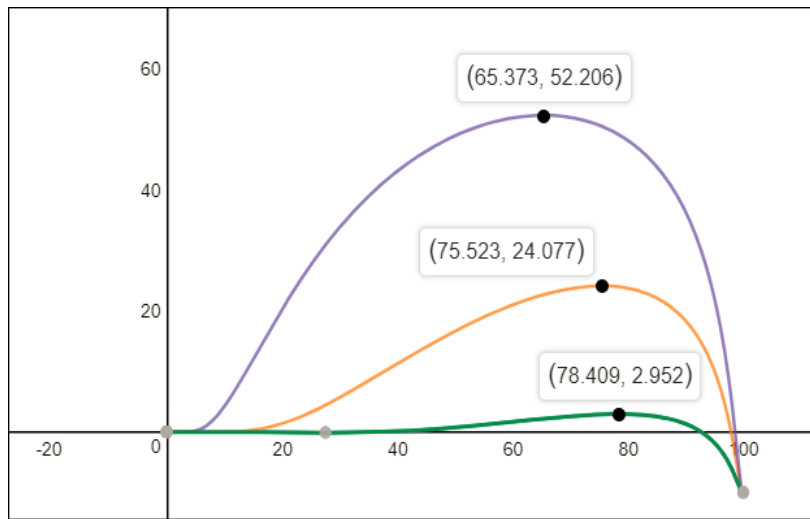


Figure 8.3: Earthbound investors' perceived economic return to a colonizing destination 3, 8, and 20 light years from earth

We model the cases for destination 3, 8, and 20 light years away respectively for earthbound investors, as the distance increases, the maximum economic return is achieved at higher colonization speed. We then model the cases for destination 3, 8, and 20 light years away respectively for shipbound investors. As the distance increases, the maximum economic return is achieved at higher colonization speed, but shipbound investors prefer higher speed than earthbound observers at the comparable distance because relativistic time dilation significantly shortens the waiting time before the start of colonization. (shipbound investors

have more opportunity lost while they are aboard the ship.) In both models, the preparation time before the departure is short in comparison to the trip time.

$$y_{ship05} = m \frac{1 - (1.02p)^{\frac{\ln(\frac{100}{m})}{\ln(1.02)}}}{1 - (1.02p)} p^{(mK_{rel} + 3T_{relu})} - \frac{1 - p^{mK_{rel}}}{1 - p} - \frac{1 - p^{3T_{relu}}}{1 - p} \quad (8.25)$$

$$y_{ship10} = m \frac{1 - (1.02p)^{\frac{\ln(\frac{100}{m})}{\ln(1.02)}}}{1 - (1.02p)} p^{(mK_{rel} + 8T_{relu})} - \frac{1 - p^{mK_{rel}}}{1 - p} - \frac{1 - p^{8T_{relu}}}{1 - p} \quad (8.26)$$

$$y_{ship30} = m \frac{1 - (1.02p)^{\frac{\ln(\frac{100}{m})}{\ln(1.02)}}}{1 - (1.02p)} p^{(mK_{rel} + 20T_{relu})} - \frac{1 - p^{mK_{rel}}}{1 - p} - \frac{1 - p^{20T_{relu}}}{1 - p} \quad (8.27)$$

$$p = 0.95 \quad (8.28)$$

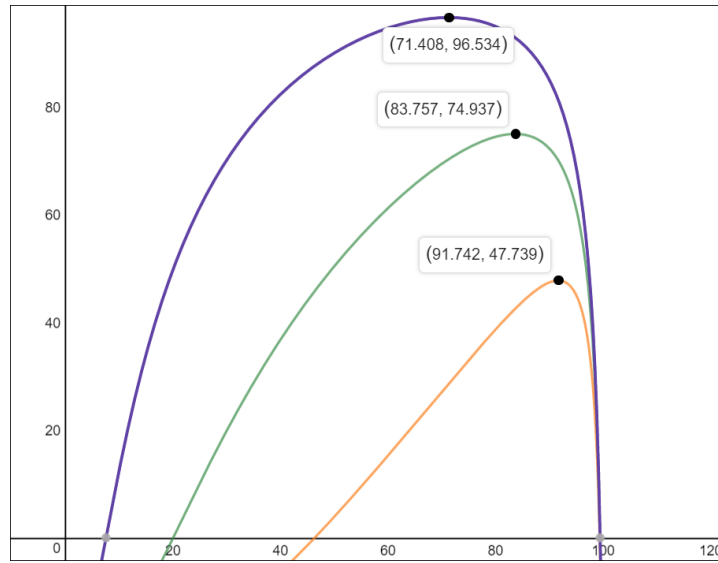


Figure 8.4: Shipbound investors' perceived economic return to a colonizing destination 5, 10, and 30 light years from earth

On the other hand, by setting every other variable constant except for the travel speed, one can also see the trend that economic wise, higher speed (up to 0.9c) renders long-distance colonization target more profitable. The additional time and investment opportunity foregone domestically at the energy and material preparation for the trip are justified. We modeled the speed at 0.1c, 0.5c, and 0.9c, the greatest distance for which a trip is profitable is 1.748 ly, 14.278 ly, and 17.538 ly respectively.

$$y_{earthdist0.1c} = \left(m \frac{1 - (ap) \frac{\ln\left(\frac{100}{m}\right)}{\ln(a)}}{1 - (ap)} \right)^p \left(\frac{m}{\sqrt[1]{1 - \frac{10^2}{100^2}} + \left(\frac{x}{100}\right)} \right) - \frac{1 - p \left(\frac{m}{\sqrt[1]{1 - \frac{10^2}{100^2}}} \right)}{1 - p} \quad (8.29)$$

$$y_{earthdist0.5c} = \left(m \frac{1 - (ap) \frac{\ln\left(\frac{100}{m}\right)}{\ln(a)}}{1 - (ap)} \right)^p \left(\frac{m}{\sqrt[1]{1 - \frac{50^2}{100^2}} + \left(\frac{x}{100}\right)} \right) - \frac{1 - p \left(\frac{m}{\sqrt[1]{1 - \frac{50^2}{100^2}}} \right)}{1 - p} \quad (8.30)$$

$$y_{earthdist0.9c} = \left(m \frac{1 - (ap) \frac{\ln\left(\frac{100}{m}\right)}{\ln(a)}}{1 - (ap)} \right)^p \left(\frac{m}{\sqrt[1]{1 - \frac{90^2}{100^2}} + \left(\frac{x}{100}\right)} \right) - \frac{1 - p \left(\frac{m}{\sqrt[1]{1 - \frac{90^2}{100^2}}} \right)}{1 - p} \quad (8.31)$$

$$p = 0.9 \quad a = 1.08 \quad (8.32)$$

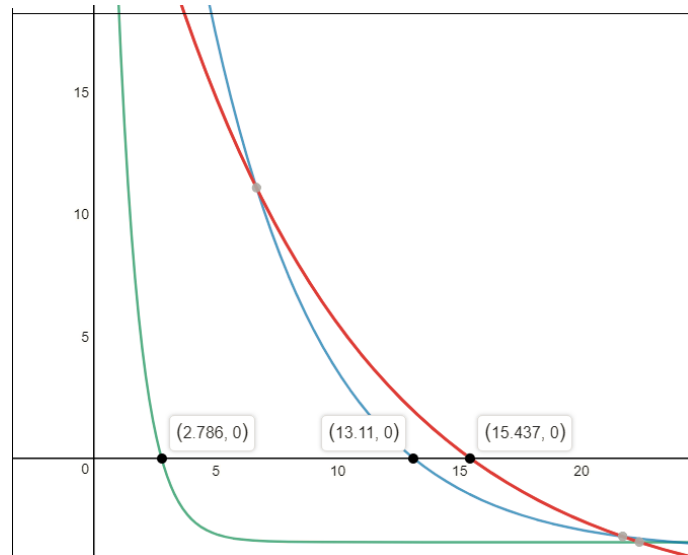


Figure 8.5: The greatest distances at which a colonizing destination provides a positive economic return for 0.1c, 0.5c, and 0.9c respectively

One can also fix the travel speed and destination distance and check for the economic return for different portions of the population involved in investing. We modeled our results for a target

at 10 ly and 20 ly away respectively and travel speed of 0.5c.

$$y_{rate10} = \left(x \frac{1 - (ap) \frac{\ln\left(\frac{100}{x}\right)}{\ln(a)}}{1 - (ap)} \right) p \left(\frac{xK_{relu}(50)}{100} + \frac{10}{100} \right) - x \frac{1 - p \left(\frac{xK_{relu}(50)}{100} \right)}{1 - p} \quad (8.33)$$

$$y_{rate20} = \left(x \frac{1 - (ap) \frac{\ln\left(\frac{100}{x}\right)}{\ln(a)}}{1 - (ap)} \right) p \left(\frac{xK_{relu}(50)}{100} + \frac{20}{100} \right) - x \frac{1 - p \left(\frac{xK_{relu}(50)}{100} \right)}{1 - p} \quad (8.34)$$

$$K_{relu}(x) = \frac{1}{\sqrt{1 - \frac{x^2}{100^2}}} - 1 \quad (8.35)$$

$$p = 0.9 \quad a = 1.08 \quad (8.36)$$

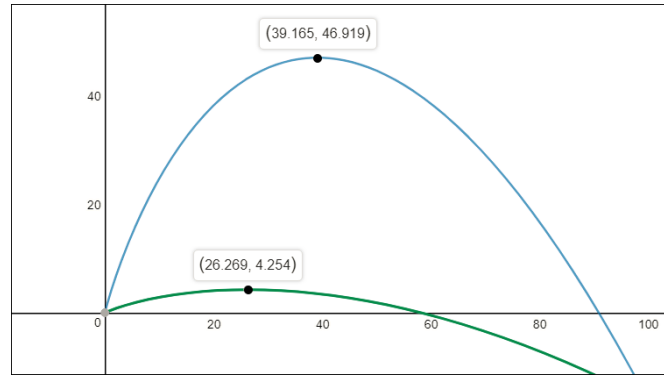


Figure 8.6: Optimal population participation rates for destination 10 light years away and 20 light years away

One finds that it is most profitable if 31.97% of the entire population participates in the colonization effort if the target distance is 10 ly away and 21% of the entire population participates in the colonization effort if the target distance is 20 ly away.

One can also vary the cost for the trip preparation, when the trip preparation cost is high, only a smaller portion of the entire population can afford such a trip to remain profitable (at the cost of the majority of the rest). We modeled our results for a target at 10 ly away, traveling speed of 0.5c, and the preparation cost proportional to the number of initial investors, and in the second case, the preparation cost is 100 times proportional to the number of initial investors.

$$y_{ratecost1} = \left(x \frac{1 - (ap) \frac{\ln(\frac{100}{x})}{\ln(a)}}{1 - (ap)} \right) p \left(\frac{xK_{relu}(50)}{100} + \frac{10}{50} \right) - x \frac{1 - p \left(\frac{xK_{relu}(50)}{100} \right)}{1 - p} \quad (8.37)$$

$$y_{ratecost100} = \left(x \frac{1 - (ap) \frac{\ln(\frac{100}{x})}{\ln(a)}}{1 - (ap)} \right) p \left(\frac{xK_{relu}(50)}{100} + \frac{10}{50} \right) - 100x \frac{1 - p \left(\frac{xK_{relu}(50)}{100} \right)}{1 - p} \quad (8.38)$$

$$p = 0.9 \quad a = 1.08 \quad (8.39)$$

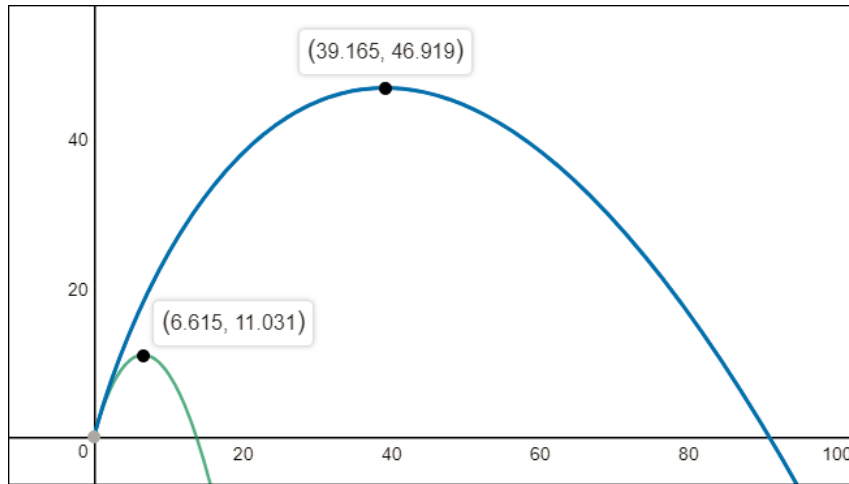


Figure 8.7: Optimal population participation rates for destination 10 light years away with preparation cost of 1 and 100

Having conceptualized the model, now we focus on applying the model for predictions based on reality. From the previous chapter, we have shown that out of all habitable planets within the Milky Way galaxy, only 41,930 planets¹³ with ages between 5 Gyr and 4 Gyr whereas it is likely that a significant buildup of oxygen has commenced with the onset of photosynthetic bacteria. Based on the size of the galaxy, we are able to determine that the nearest habitable planet be 1,777 light years in distance.

$$D_{nearest} = 2 \cdot \left(\frac{3 (140,000)^2 \cdot 2,000}{4 \cdot 41,930} \right)^{\frac{1}{3}} \quad (8.40)$$

¹³This is from an earlier calculation, new results shown to be 10,719. Adjustment to the value of depreciation will be done, but the results remain similar

$$D_{nearest} = 1,776.79566109 \text{ ly} \quad (8.41)$$

Then, one can set up realistic scenarios and plots for earth and ship bound investors and their final economic returns.

8.2 Earthbound Democracy

It can be shown that for earthbound investors comprising the entire population of earth (assuming a maximum carrying capacity of 60 billion a little higher than our lowest maximum carry capacity calculation in Chapter 6) investing into the colonization of the nearest habitable planet can only doubling their initial investment. We assume that a team of 1,000 people (each 70 kg on average and carrying necessary subsistence, recyclable material 20 times their body mass) represents the entire earth will be sent to colonize the nearest habitable planet. Once the planet being colonized, the entire human race benefits from the investment in equal share. Due to the long distance involved, we found that the rate of subjective depreciation cannot be lowered than 0.9999999, that is, $p > 0.9999999$ in order for the trip to be profitable. This implies either earthbound investors have to have extremely long lifespan themselves, so they valued extreme long-term future prospects. More realistically, it can be interpreted as long-standing culture emphasizing on inter-generational commitment in colonization effort. As

a result, the second term of $R_{earth} \sum_{k=1}^{\frac{\ln\left(\frac{P_{earth}}{m_g}\right)}{\ln(1.02)}} m (ap)^k$ can not be substituted by our special case $m_g \frac{1-(1.02p)^{\frac{\ln\left(\frac{P_{earth}}{m_g}\right)}{\ln(1.02)}}}{1-(1.02p)}$ because $1.02p > 1$. We simply using a software iteration to approximate this term and we obtained $3.09 \cdot 10^{12}$ Joules of energy.

$$R_{earth} = P_{earth} \left(\frac{1 - p^{10^9}}{1 - p} \right) p \frac{\ln\left(\frac{P_{earth}}{m_g}\right)}{\ln(1.02)} + \frac{\ln\left(\frac{P_{earth}}{m_g}\right)}{\ln(1.02)} \sum_{k=1} m (ap)^k \quad (8.42)$$

$$R_{earth} = 5.97 \cdot 10^{19} \text{ J} \quad (8.43)$$

$$K_{rel} = \frac{1}{\sqrt{1 - \frac{x^2}{100^2}}} - 1 \quad (8.44)$$

$$T_{rel} = \frac{d}{\frac{x}{100}} \sqrt{1 - \frac{x^2}{100^2}} \quad (8.45)$$

$$p = 0.999999999999 \quad (8.46)$$

$$P_{earth} = 60 \cdot 10^9 \text{ people} \quad (8.47)$$

$$m_g = 1,000 \text{ people} \quad (8.48)$$

$$m = 70\text{kg} \cdot m_g \cdot 20 \quad (8.49)$$

$$d = 1,776 \text{ ly} \quad (8.50)$$

Whereas j represents the energy output per capita based on the total energy output of the World in 2008 divided by the total population of the world:

$$j = \frac{6.8 \cdot 10^{19} \text{ J}}{6.5 \cdot 10^9 \text{ people}} \quad (8.51)$$

The final return is expressed as: (whereas $10^{10} \cdot j$ represents the maximum energy can be contributed to the space exploration in one year by the entire earth assuming the population ceiling is in the order of 10 billion derived from Chapter 6)

$$y_{earthreal} = \ln \left(\frac{j}{P_{earth}} \cdot R_{earth} \cdot p \left(\frac{mc^2 K_{rel}}{10^{10} j} + \frac{d}{\left(\frac{x}{100}\right)} \right) - j_t \frac{1 - p \left(\frac{mc^2 K_{rel}}{10^{10} j} \right)}{1 - p} \right) \quad (8.52)$$

8.3 Earthbound Investing Nearest Galaxy

We can extend the above scenario into intergalactic colonization. We assume that a team of 1,000 people (each 70 kg on average and carrying necessary subsistence, recyclable material 20

times their body mass) represents the entire earth will be sent to colonize the nearest galaxy with 41,930 habitable planets.¹⁴ We assume the average separation distance of 11.85 million light years in distance (Andromeda galaxy is much closer than the typical distance between galaxies since it is on its course with a collision with the Milky Way). Due to the immense distance involved, we found that the rate of subjective depreciation cannot be lowered than 0.9999925 in order for the trip to be profitable. This indicates that a biological led species with a culture of an extremely strong commitment to inter-generational colonization is theoretically possible though highly unlikely.

$$y_{earthmilky} = \ln \left(\frac{j}{P_{earth}} \cdot R_{milky} \cdot p \left(\frac{mc^2 K_{rel}}{10^{10} j} + \frac{d}{100} \right) - j_t \frac{1 - p \left(\frac{mc^2 K_{rel}}{10^{10} j} \right)}{1 - p} \right) \quad (8.53)$$

$$R_{milky} = P_{milky} \left(\frac{1 - p^{10^9}}{1 - p} \right) p \frac{\ln \left(\frac{P_{milky}}{m_g} \right)}{\ln(1.02)} + m_g \frac{1 - (1.02p) \frac{\ln \left(\frac{P_{milky}}{m_g} \right)}{\ln(1.02)}}{1 - (1.02p)} \quad (8.54)$$

$$R_{milky} = 5.97 \cdot 10^{24} \text{ J} \quad (8.55)$$

$$d = 11,850,000 \text{ ly} \quad (8.56)$$

Whereas j_t represents the energy output per 1 earth based on the total energy output of the World in 2008 times 10, that is, assuming the population ceiling is in the order of 10 billion derived from Chapter 6. Whereas P_{milky} represents the total population in the galaxy eventually achievable based on the number of habitable planets conducive to intelligent, multicellular life within the galaxy.

$$j_t = 10 \cdot 6.8 \times 10^{19} \text{ J} \quad (8.57)$$

$$P_{milky} = 10^5 \cdot P_{earth} \quad (8.58)$$

$$p = 0.999999999999 \quad (8.59)$$

Most interestingly, the economic return for a single planet committed to intergalactic colonization is higher than interstellar colonization at every possible travel speed. This may feel counter-intuitive, given the amount of resources and energy a civilization has to forfeit in the near term in order to prepare for such a colonization. This is possible when the subjective rate of depreciation cost is minimized by the greater emphasis on the commitment to inter-generational

¹⁴This is from earlier calculation, new results shown to be 10,719. Adjustment to the value of depreciation will be done, but the results remain the same

colonization. Hence, in theory, we have shown that biological led industrial civilization can expand in the universe even if the decision making is based on the economic return of earthbound investors.

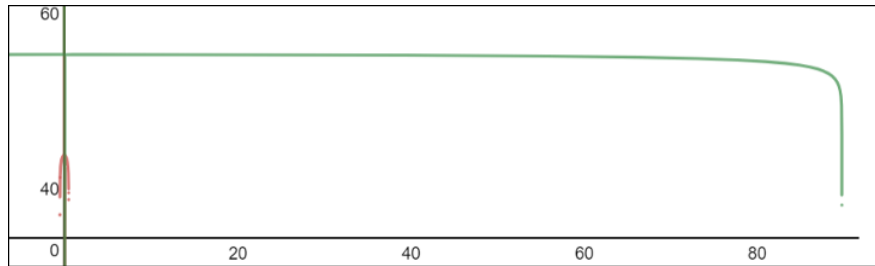


Figure 8.8: Democratic earthbound investors for nearest galaxy > democratic earthbound investors

We can also see that as the carrying mass of the ship changes, the maximum speed achievable for reaping positive economic return changes inversely. This is easily understood as greater mass requires greater kinetic energy and resource preparation in the first place, whereas the cost of preparation outweighs the time lost waiting for its arrival to commence colonization.

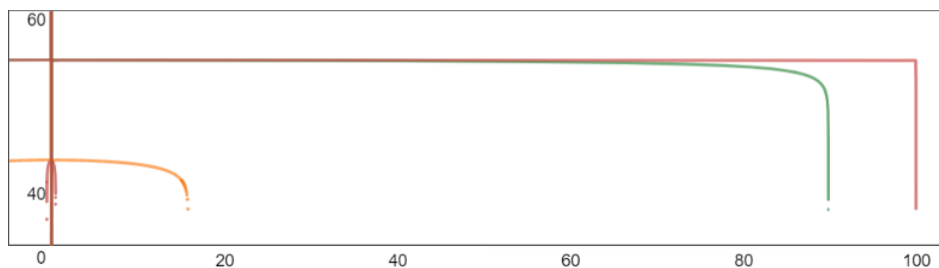


Figure 8.9: With smaller loads, positive economic returns justify traveling at higher speed

8.4 Galaxy Bound Investing Nearest Galaxy

As a logical extension to the previous case, one can also model the case where the entire colonized galaxy is ready to colonize the next nearest galaxy. Under such a scenario, the entire galaxy's energy and material preparation can be utilized to send a group of selected 1,000 explorers which will colonize another 41,930 habitable planets¹⁵ of the nearest galaxy, and the return is equally shared among the galaxy empire. We also assumed that 10 years' total energy productions (10^{10} people per planet $\cdot 10^5$ planets $\cdot 10$ years) from the entire galaxy is used to prepare for such a migration.

¹⁵This is from an earlier calculation, new results shown to be 10,719. Adjustment to the value of depreciation will be done, but the results remain the same

$$y_{milk2milk} = \ln \left(\frac{j}{P_{milky}} \cdot R_{milky} \cdot p \left(\frac{mc^2 K_{rel}}{10^{16}j} + \frac{d}{100} \right) - 10^5 \cdot j_t \frac{1-p \left(\frac{mc^2 K_{rel}}{10^{16}j} \right)}{1-p} \right) \quad (8.60)$$

$$p = 0.999999999999999 \quad (8.61)$$

$$d = 11,850,000 \text{ ly} \quad (8.62)$$

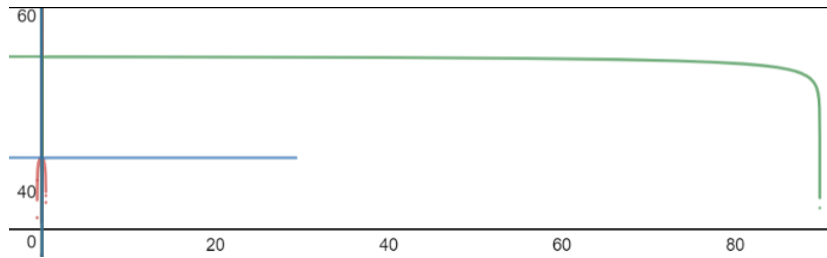


Figure 8.10: Democratic earthbound investors for the nearest galaxy > democratic galaxy bound investors for the nearest galaxy > democratic earthbound investors for the nearest habitable planet

The graph shows that it is less profitable for the entire galaxy to invest to the nearest galaxy and equally share the return, but it is more profitable than a single planet based civilization to invest to the nearest habitable planet.

8.5 Earthbound Ruling Class

Earthbound investors comprising a small population (assuming 1,000 individuals) investing into the colonization of the nearest habitable planet can yield much more return on their initial investment. We assume that 1,000 explorers (each 70 kg on average and carrying necessary subsistence, recyclable material 20 times their body mass) represent this group of 1,000 individuals will be sent to colonize the nearest habitable planet. Once the planet being colonized, only this group of 1,000 individuals investing will benefit from the investment in an equal share. We assume that this group of individuals have an extreme authoritative control over the populace in general and is able to raise the resources in preparation by taxing the entire population for given amount of years. As a result, the economic incentives for this group of people to start such colonization initiative will be significantly higher than as the entire population of earth. Despite much greater promised return on investment, the waiting time is still considerably significant. As a result, we found that the rate of subjective depreciation cannot be

lowered than 0.996773 in order for the trip to be profitable. This implies that this group of people as the ruling class must still maintain its commitment to inter-generational colonization projects as well as its authoritative control over the population. Comparing the plots with the earlier democratic case where the entire population receives an equal share of return, the greatest economic return occurs at the higher speed. This is achievable because a small group of individuals' cost of preparation from their own perspective is significantly lower compares to their final return (at the expense and the sacrifice of the general populace with or without complaints), so they could spend significantly longer time period at energy gathering for the preparation phase. Hence, it is able to achieve a higher expansionary speed. The graph shows that a group of 1,000 people taxed or borrowed general populace of earth in terms of energy and material resource at 10 times of the current world population and the maximum economic return for different fractions of the speed of light for migration (black curve $y_{earthlow}$). Furthermore, a second curve $y_{earthhigh}$ represents the case of taxing the general populace assuming it stays at the same level of population ceiling but a higher level of per capita energy output and the economic return for different speeds of light. The ultimate per capita achievable as biologically led industrial civilization can be computed as the follows. We have shown that the ultimate barrier to economic growth is the accumulation of waste heat which reaches the threshold of catastrophe in 400 years from now assuming an annual growth rate of 1.5% (See Chapter 6). Since we already shown that the population ceiling at 10 times of our current population, therefore, the GDP per capita of the world can increase by 38.58 folds. In other words, the GDP per capita (assuming current GDP (PPP) per capita is \$15,800) can reach at most \$609,564 at the current dollar prices per year with a population base of 60 billion.

$$\frac{(1.015)^{400}}{10} = 38.58 \quad (8.63)$$

$$y_{earthhigh} = \ln \left(\frac{j}{m_g} \cdot R_{earth} \cdot p \left(\frac{mc^2 K_{rel}}{38.58 j t} + \frac{d}{100} \right) - m_g \cdot j \frac{1-p \left(\frac{mc^2 K_{rel}}{38.58 j t} \right)}{1-p} \right) \quad (8.64)$$

$$y_{earthlow} = \ln \left(\frac{j}{m_g} \cdot R_{earth} \cdot p \left(\frac{mc^2 K_{rel}}{10^{10} j} + \frac{d}{100} \right) - m_g \cdot j \frac{1-p \left(\frac{mc^2 K_{rel}}{10^{10} j} \right)}{1-p} \right) \quad (8.65)$$

$$p = 0.9978 \quad (8.66)$$

$$d = 1,776 \text{ ly} \quad (8.67)$$

$$j_t = 10 \cdot 6.8 \times 10^{19} \text{ J} \quad (8.68)$$

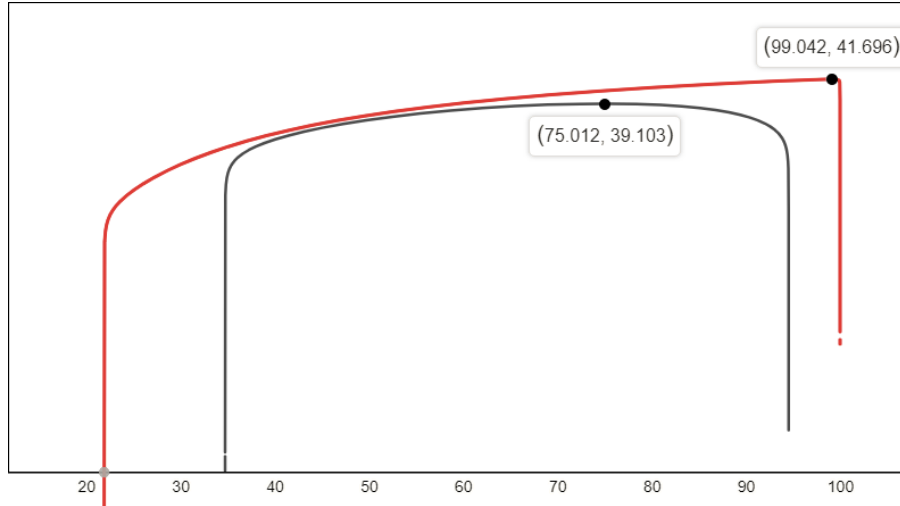


Figure 8.11: Higher GDP per capita renders near light speed travel economically profitable for earthbound ruling class

It can be seen that higher GDP (PPP) per capita (or otherwise conceptually equivalent as more energy available for each individual at their disposal) and its preparation during the fuel acquisition phase allows the migration to infinitely approaching the speed of light that would be otherwise unprofitable under low GDP per capita scenarios. Therefore, any ruler of the earth's intention to maximize GDP per capita can be justified not by the will of the people but by an ambition of space colonization alone.

8.6 Shipbound with Energy Gathering Case

Having discussed earthbound investors, we can now move onto the ship bound investors. If the ship-bound investors participate in the original energy gathering, then their subjective rate of value depreciation is comparable to a small group of earthbound investor (The earthbound ruling class case) and must be prepared with multi-generational commitments. It is still somewhat higher than earthbound ruling class case because relativistic time dilation made their trip to destination shorter.

$$y_{shiphigh} = \ln \left(\frac{j}{m_g} \cdot R_{earth} \cdot p \left(\frac{mc^2 K_{rel} + T_{rel}}{38.58 j_t} \right) - m_g \cdot j \frac{1-p}{1-p} \left(\frac{mc^2 K_{rel}}{38.58 j_t} \right) - m_g \cdot j \frac{1-p^{T_{rel}}}{1-p} \right) \quad (8.69)$$

$$y_{shiplow} = \ln \left(\frac{j}{m_g} \cdot R_{earth} \cdot p \left(\frac{mc^2 K_{rel} + T_{rel}}{10^{10} j} \right) - m_g \cdot j \frac{1-p}{1-p} \left(\frac{mc^2 K_{rel}}{10^{10} j} \right) - \left(m_g \cdot j \frac{1-p^{T_{rel}}}{1-p} \right) \right) \quad (8.70)$$

$$p = 0.998 \quad (8.71)$$

The graph shows that a group of 1,000 individuals taxed or borrowed the general populace of earth in terms of energy and material resource and the maximum economic return for different fractions of the speed of light for migration (green curve $y_{shiplow}$). Furthermore, a second curve $y_{shiphigh}$ represents the case of taxing the general populace assuming it stays at the same level of population ceiling but a higher level of per capita energy output and the economic return for different speeds of light. It can be seen that high GDP per capita and its preparation during the fuel acquisition phase allows the migration to infinitely approaching the speed of light that would be otherwise unprofitable under short preparation scenarios.

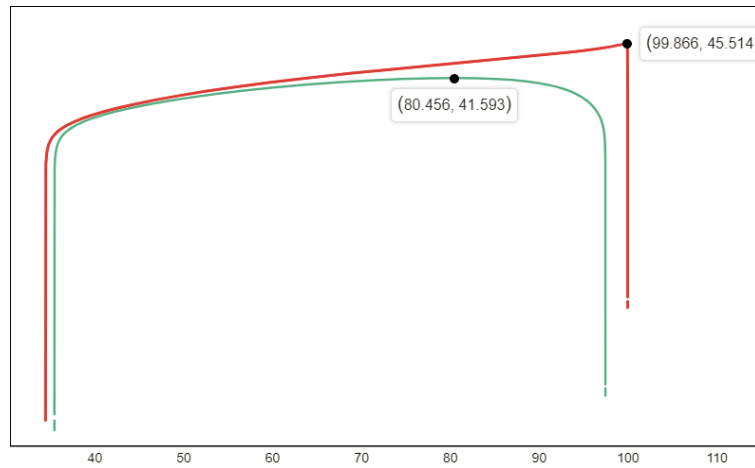


Figure 8.12: Higher GDP per capita renders near light speed travel economically profitable for shipbound ruling class

8.7 Shipbound as Lottery Winners Case

If the final explorers were comprising individuals picked at random from the general populace every few generations as the energy gathering for colonization preparation completes. Then, the subjective rate of depreciation can be much lower and is only limited by the travel time and travel speed (the cost of time lost in getting to destination that can be used to invest on earth)

$$y_{shiplottery} = \ln \left(\frac{j}{m_g} \cdot R_{earth} \cdot p^{T_{rel}} - m_g \cdot j \frac{1 - p^{T_{rel}}}{1 - p} \right) \quad (8.72)$$

$$p = 0.998 \quad (8.73)$$

and it can be shown that its subjective economic return is higher than the Ship bound with Energy and the Earthbound Ruling class cases when $p = 0.998$ and at speed $> 0.3684c$.

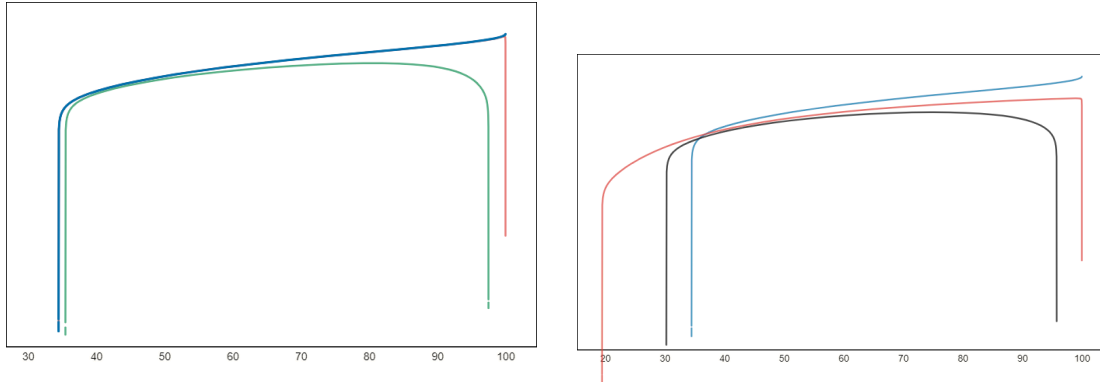


Figure 8.13: Shipbound lottery winners' perceived economic return (blue curve) is strictly higher than both shipbound and earthbound ruling class cases

Comparing all these scenarios and one finds that the economic return in the order of most profitable to the least as the follows: shipbound lottery winners $>$ shipbound ruling class investors \approx earthbound ruling class investors $>$ democratic earthbound investors for the nearest galaxy $>$ democratic galaxybound investors for the nearest galaxy $>$ democratic earthbound investors for the nearest planet. Interestingly enough, the economic return through the democratic process results in both extremes, the lottery winners and the democratic earthbound investors.

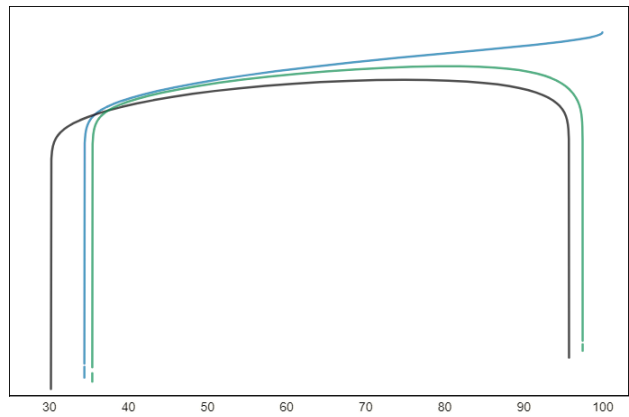


Figure 8.14: Shipbound lottery winners > shipbound ruling class investors > earthbound ruling class investors when $p = 0.9987$ and at the current GDP per capita

Democratic Earthbound investors investing into the nearest habitable planet case is not profitable unless its subjective depreciation value reaches ($0.99999999999 \leq p < 1$). However, at such value of p all three previous cases converge toward the same value on the graph shown below.

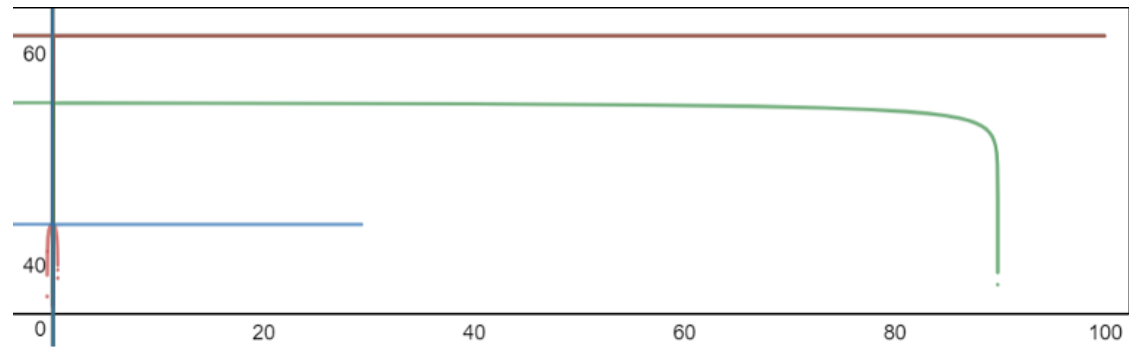


Figure 8.15: (Shipbound lottery winners = shipbound ruling class investors = earthbound ruling class investors) > democratic earthbound investors for nearest galaxy > democratic galaxy bound investors for nearest galaxy > democratic earthbound investors when $p = 0.99999999999$

8.8 Post-Singularity

We just showed how slow we could expand by using our current level of industrial development. How about a post-biological one? How fast would they expand in the universe? In a few millennia, assuming technological singularity does not occur in this century, human should have full control over their genes and biological development. It implies that Homo sapiens may have artificially diverged into different species each occupying different niches where some can be much smaller than our current size and some others much larger. If we are artificially evolving toward smaller size and at the same time able to convert energy more efficiently directly

into our body discarding the digestive system, we can build a much smaller spaceship and much less fuel to travel to a habitable planet. At the same time, if we are able to achieve significantly longer lifespan, our p will also approach toward 1. As a result, the post-biological creatures calculated final return value increasingly approaches the theoretical value. If it is foreseeable that Homo sapiens to genetically modify ourselves; then, there is no reason to doubt extra-terrestrials would not do the same. On the other end of the spectrum, a robotic led industrial civilization as predicted by the singularity led to even more extreme toward the theoretical limit. Artificial intelligence, which is immortal even in the face of accidents because of its own copied backup of itself, will use the following equation when calculating return on their colonization investment.

In a post-singularity society, assuming the mass required to carry intelligence and information processing shrinks significantly so that it takes significantly less time at energy and material gathering phase, then the economic return is certainly much higher than biological led species, and the most optimal strategy is cruising near the speed of light. We can illustrate a possible scenario. We denote the mass requirement is simply less than 1 out of 10^{10} of current biological human form, or about the mass of 100 cells in the human body.[97] The GDP/Energy per capita requirements for sustaining itself becomes $\frac{1}{10^{10}}$ th of current human level per AI (so the opportunity cost at ship preparation and migration phase becomes negligible), yet each AI is capable of significantly expand its energy per capita by transforming into other gigantic forms on earth and generate energy at the order of 10^4 of the current GDP per capita on earth for the trip preparation. The return on the colonized destination is the total biological population limit times current GDP/Energy per capita for 10 billion years. Finally, one assume for immortalized AI based life form, $p=0.997$.

$$y_{shipAI} = \ln \left(j \cdot R_{earth} \cdot p \left(\frac{10^{-10} mc^2 K_{rel} + T_{rel}}{10^4 j} \right) - \frac{j}{10^{10}} \frac{1-p}{1-p} \left(\frac{10^{-10} mc^2 K_{rel}}{10^4 j} \right) - \frac{j}{10^{10}} \frac{1-p^{T_{rel}}}{1-p} \right) \quad (8.74)$$

$$y_{earthAI} = \ln \left(j \cdot R_{earth} \cdot p \left(\frac{10^{-10} mc^2 K_{rel} + \frac{d}{100}}{10^4 j} \right) - \frac{j}{10^{10}} \frac{1-p}{1-p} \left(\frac{10^{-10} mc^2 K_{rel}}{10^4 j} \right) \right) \quad (8.75)$$

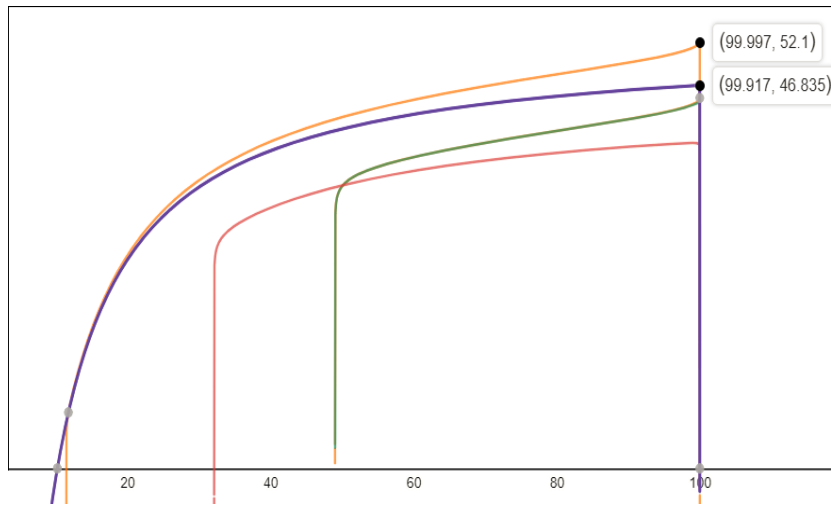


Figure 8.16: Shipbound AI > Earthbound AI > Shipbound lottery winners > Shipbound ruling class investors > Earthbound ruling class investors

This can be compared in the graph above, whereas both the earthbound AI investor and shipbound AI investors' economic return tops any biological species led scenarios.

All of these calculations showed that it is lucrative for AI to colonize the universe with a very low cost and a high reward for an expansion. These sets of equations can be further expanded to accommodate the expansion of the universe. The universe's space-time is stretching with speed relative to the observer at $74 \frac{\text{km}}{\text{sec}}$ for every million parsecs. So for long journeys committed, the expansion of the universe will add additional travel time before one can reach its destination, and any destination becomes unreachable beyond the cosmic event horizon which is moving away from us as fast or faster than the speed of light. As a result, there is an upper limit as to how far we could travel even at the speed of light because destinations beyond the horizon will remain forever unreachable.

In order to account for the cosmic expansion rate and the Hubble constant, cosmological distance has to be rescaled into the real distance:

$$T_{rel} = \frac{E(d, v)}{v} \sqrt{1 - \frac{v^2}{c^2}} \tag{8.76}$$

whereas $E(d, v)$ is a function that handles the conversion for a cosmological distance of d for any given constant migration speed of v . The derivation of $E(d, v)$ is later defined in Chapter 9. As a result, the generalized formula becomes:

$$E_{arth} = \frac{\epsilon}{m} \left[\left(\sum_{k=0}^{10^9} M (p)^k \right) p^{\frac{\ln(\frac{M}{m})}{\ln a}} + \sum_{k=0}^{\frac{\ln(\frac{M}{m})}{\ln a}} m (ap)^k \right] p^{\left(\frac{m \cdot K_{rel}}{\epsilon} + \frac{E(d,v)}{v} \right)} - m\epsilon \left[\sum_{k=0}^{\frac{m \cdot K_{rel}}{\epsilon}} p^k \right] \quad (8.77)$$

when $ap < 1$

$$E_{arth} = \frac{\epsilon}{m} \left[M \frac{1 - p^{10^9}}{1 - p} p^{\frac{\ln(\frac{M}{m})}{\ln a}} + m \frac{1 - ap^{\frac{\ln(\frac{M}{m})}{\ln a}}}{1 - ap} \right] p^{\left(\frac{m \cdot K_{rel}}{\epsilon} + \frac{E(d,v)}{v} \right)} - m\epsilon \frac{1 - p^{\frac{m \cdot K_{rel}}{\epsilon}}}{1 - p} \quad (8.78)$$

when $ap \geq 1$

$$m \frac{1 - (ap)^n}{1 - ap} < \sum_{k=0}^n m (ap)^k \quad (8.79)$$

$$M \frac{1 - p^n}{1 - p} < \sum_{k=0}^n M p^k \quad (8.80)$$

However, one should not ignore the migration cost term from a stationary observer's perspective, which describes the time spent traveling. Although AI based life form can travel near the speed of light and the time experienced under their inertial frame of reference is always a very very tiny fraction of the time of experienced by a stationary observer, appearing with little cost occurred during their travel. Nevertheless, the time spent traveling is the cost of opportunity lost.

8.9 Expansion Speed from Outsider's Perspective

If an extraterrestrial civilization expands near the speed of light, from their perspective, almost no time has elapsed, but from an observer on earth which is stationary relative to them, their speed of expansion is just the speed of light at the best. In order to illustrate how slow such expansion appears to be one needs to resort to calculations. One can comprehend the speed

of economic growth occurred since the Industrial Revolution. If we use the world population growth as a measure of growth in energy consumption and the rate of so defined social progress, then from AD 1900 the world population of 16.5 Billion increased to 61.27 Billion in AD 2000, it can be shown that the rate of growth is 1.32 percent per year. If one steps back prior to the Industrial Revolution and computes the period of Age of Exploration from year AD 1600 to AD 1750 and the population grows from 580 million to 791 million, we find that the annual growth rate is 0.207 percent. The annual growth rate from classical Greece from 1000 B.C up to AD 1600 is 0.0943 percent. During this period the world population grows from 50 million to 580 million resulting in 10 fold increase in 2,600 years. From the onset of the full transition from hunter-gatherers to agricultural societies at 5000 B.C with a population of 5 million to that of city-states at 1000 B.C. of 50 million, the annual growth rate is 0.0576 percent. Finally, we find the annual rate of growth during the hunter-gatherer period of Homo sapiens' migration out of Africa from 70,000 BC following the Mount Toba bottleneck with 15,000 individuals to the transition of agricultural society at 5 million to be 0.00931043 percent. Based on this results, we can roughly quantify the rate of progress human society is achieving in each time period. We can see that the transition from hunter-gatherer to that of the agricultural is a major one, in which the annual growth rate jumped 6.187 times. During the following classical and the Middle Ages, the annual growth only increase by 1.63 times. Agricultural lands and farming tools are continually improving but the growth are not significant. During the following Age of Exploration, the annual rate of growth increased by another 2.195 times thanks to Columbian exchange, which enabled crops from America to be cultivated around the world, increasing the varieties of food domestication. However, only the Industrial Revolution brought the annual rate of growth to another 6.377 fold increase, comparable and surpassed the magnitude of change observed from hunter-gatherers to that of the agricultural society. Upon the Industrial paradigm, new modes of production such as Communism and Capitalism both claims to increase the efficiency and annual growth rate, which may not necessarily reflect from population growth, but rather gave the rise of the standards of living per capita. This is especially evident from the economic growth of China, which has kept to grow at the pace of 8 percent per year for the last 30 years, another 6 folds increase from the average speed of growth of Industrial Era. By now, we have a clear appreciation of the rate of change at each period of human society's progress, we shall resort to the calculation for the speed of galaxy colonization, if one expands very close to the speed of light, one can traverse the entire Milky Way galaxy in 140,000 years. If every star is harnessed for its energy just as our sun by constructing Dyson spheres and the total stellar mass of the Milky Way is estimated to be $5.515 \cdot 10^{10}$ solar masses, so we start with one solar mass, our sun, ended up harnessing $5.515 \cdot 10^{10}$ solar mass of energy in 140,000 years. We found that the annual rate of growth from a stationary observer's perspective to be 0.01767 percent per year, whereas a majority of the time is the cost of expanding from one star system to the next. This rate is 1.898 times faster than Homo Sapiens' speed of "progress" during our hunter-gatherer period. If our future technology can only reach a fraction of the

speed of light, then, the speed of expansion can be slower than our hunter-gatherer period. Furthermore, once Milky Way galaxy is colonized, one has to traverse another 2.13 million light years to reach our nearest neighbor, the Andromeda Galaxy, and 2.64 million years to reach the Triangulum Galaxy. If we take into account of the entire cosmic expansion, then amortized annual rate of growth is merely 0.0010719 percent. This shows that even expanding near the speed of light the speed of cosmic expanders appears to be just 11.5% the annual growth rate of hunter-gatherers. Nevertheless, this speed is significantly faster than that of biological evolution. For the case of *Australopithecus Afarensis*' emergence at 3.9 million years ago to that of the emergence of Neanderthal 250K years ago, the cranial capacity increased from 405 cc to 1600 cc, corresponding to an annual increase rate of 0.00003762 percent, or about 3.51 percent of the upper growth bound of a cosmic expander.

Then, we can conclude that from the expander's perspective, almost no time is lost in gaining energy usage and information utilization from one's home planet to this civilization's expansionary limit bounded by their expansionary industrial extra-terrestrial neighbors. This is an almost infinite increase in terms of economic size in almost no time from the perspective of expanding civilization near the speed of light. Therefore, they have the full economic incentive to expand. Though they have to know that such expansion is once only, and they have to resort to sustainability immediately afterward. However, from earth observers' perspective, such expansion is slow, as we have already shown how slow it is. It is so slow that it appears that such civilization's economic growth rate is as slow as the hunter-gatherers. Therefore, any expanding alien civilization expanding even at the speed of light will appear extremely slow from stationary observer's perspective.

To see this further let's set up another example. Assuming a future robotic civilization arising from the solar system decided to colonize a distant galaxy 1 billion light-years away and travels at 99.999% speed of light and it takes about 1 year of time in their reference frame. From the stationary observer's point of view, 1 billion years have passed since they started their journey. During this 1 billion years, an enormous amount of energy from the stars have been converted from usable to the un-usable energy given by the second law of thermodynamics. If the destination is even further out at 10 billion years, lots of stars have been born, burned, and died and the energy can be gathered but lost is a foregone opportunity cost no one can afford to lose. As the rate of star formation slows down into the future, every GFK stars and its energy released is precious. (Of course, such scenario is naturally applicable to biological led sustainable industrial civilization but it is not practical to do so. The energy acquisition required even to the Andromeda galaxy lying 2.3 million light-years away is so tremendous that even a lottery based system activated on earth will take thousands of years to gather the energy requirements for a team of 1000, as our previous discussion has shown.)

8.10 Worm Hole

As a result, an extreme distant journey by AI based life form would be deemed wasteful even if it can be done at ease. Furthermore, as we have shown earlier, the cosmic evolutionary rate, albeit slow, comparable to the rate of change attributed to the rise of Homo sapiens and their civilization. In just half billion years of time, every terrestrial planet habitable to life, with their increasing biological diversity, will give rise to intelligent creatures comparable to human and their future robotic form. An earth-based robotic life form spent billion years travel to claim their territory may encounter the resistance and defeat from the rising robotic civilizations at those distant locations from earth.

This seems to imply that AI-based life form or any lightweight matter based life form of the future will unlikely to attempt any long distance journey. In fact, their descendants may scatter vast reaches of the universe, but communications and trades only occur at the very local level, whereas the time lost while spent on traveling is bearable. As a result, no galactic empire is possible and only islands of isolation is possible even if they all descended from the same original ancestor.

Fortunately, the future seems to be much more interesting, and the scenario above is unlikely to hold. Though the expanding cosmic civilization may start their empire by sending back and forth spaceships between their controlled planets, it will sooner or later adopt and construct wormholes to expedite their travel and journey. Although wormhole is still a theoretical construct and in recent years various papers have pointed out that less and less energy (in fact negative energy) is required to maintain the operations of such tunnels. In the very beginning, calculations have shown that the energy requirements for the construction of Alcubierre drive and wormholes require the equivalent energy of the entire observable universe. Recent papers have suggested minimal amount energy can maintain a wormhole about the size of a human.[54] For post-biological intelligence which can alter its size and energy requirements for travel, even smaller energy is required to maintain microscopically sized wormholes. More recently, negative energy has also been obtained in experiments[64]; therefore, the construction and low-cost maintenance of wormhole seems to be possible.

The construction of wormholes does not violate the theory that arising extraterrestrial industrial civilizations require time to reach us limited by the speed of light. Although a completed wormhole allows travel time less than the speed of light traveling on a flat space-time fabric, the construction of such wormhole itself cannot exceed the speed of light. It is still under research as to how short a wormhole can be required to connect any arbitrary point in space and time. As more and more progress is done in the future on theoretical physics and practical engineering, it can be shown that the wormhole constructed can be increasingly shorter in length yet able to connect to more distant locations. In our model, we simply assume that the wormhole is able to take a traveler to a different destination with a cost in time and maintenance C and where $C <$ the cost spend travel near the speed of light on a flat space-time

fabric. Under the most extreme assumption, we can have $C = 0$; that is, it takes no time to traverse to distant points in the universe. If we take these assumptions, we can derive the following cost and benefit analysis using cost amortization for n trips between two points of cosmological distances.

Without wormhole for earthbound investors:

$$\lim_{n \rightarrow \infty} \left(\frac{1}{n} \sum_{k=0}^n \frac{\epsilon}{m} \left[M \frac{1-p^{10^9}}{1-p} p^{\frac{\ln(\frac{M}{m})}{\ln a}} + \sum_{k=0}^{\frac{\ln(\frac{M}{m})}{\ln a}} m (ap)^k \right] p^{\left(\frac{m \cdot K_{rel}}{\epsilon} + \frac{E(d,v)}{v} \right)} - m\epsilon \frac{1-p^{\frac{m \cdot K_{rel}}{\epsilon}}}{1-p} \right) \quad (8.81)$$

$$= \frac{\epsilon}{m} \left[M \frac{1-p^{10^9}}{1-p} p^{\frac{\ln(\frac{M}{m})}{\ln a}} + \sum_{k=0}^{\frac{\ln(\frac{M}{m})}{\ln a}} m (ap)^k \right] p^{\left(\frac{m \cdot K_{rel}}{\epsilon} + \frac{E(d,v)}{v} \right)} - m\epsilon \frac{1-p^{\frac{m \cdot K_{rel}}{\epsilon}}}{1-p} \quad (8.82)$$

With wormhole for earthbound investors:

$$\lim_{n \rightarrow \infty} \left(\frac{1}{n} \sum_{k=0}^n \frac{\epsilon}{m} \left[M \frac{1-p^{10^9}}{1-p} p^{\frac{\ln(\frac{M}{m})}{\ln a}} + \sum_{k=0}^{\frac{\ln(\frac{M}{m})}{\ln a}} m (ap)^k \right] p^{\left(\frac{m \cdot K_{rel}}{\epsilon} + \frac{E(d,v)}{v} \right)} - m\epsilon \frac{1-p^{\frac{m \cdot K_{rel}}{\epsilon}}}{1-p} \right) \quad (8.83)$$

$$= \frac{\epsilon}{m} \left[M \frac{1-p^{10^9}}{1-p} p^{\frac{\ln(\frac{M}{m})}{\ln a}} + \sum_{k=0}^{\frac{\ln(\frac{M}{m})}{\ln a}} m (ap)^k \right] \quad (8.84)$$

and economic return with wormhole for earthbound investors $>$ economic return without wormhole for earthbound investors

$$\begin{aligned}
& \frac{\epsilon}{m} \left[M \frac{1-p^{10^9}}{1-p} p^{\frac{\ln(\frac{M}{m})}{\ln a}} + \sum_{k=0}^{\frac{\ln(\frac{M}{m})}{\ln a}} m (ap)^k \right] \geq \\
& \frac{\epsilon}{m} \left[M \frac{1-p^{10^9}}{1-p} p^{\frac{\ln(\frac{M}{m})}{\ln a}} + \sum_{k=0}^{\frac{\ln(\frac{M}{m})}{\ln a}} m (ap)^k \right] p^{\left(\frac{m \cdot K_{rel}}{\epsilon} + \frac{E(d,v)}{v}\right)} - m\epsilon \frac{1-p^{\frac{m \cdot K_{rel}}{\epsilon}}}{1-p} \quad (8.85)
\end{aligned}$$

Without wormhole for shipbound investors:

$$\begin{aligned}
& \lim_{n \rightarrow \infty} \frac{1}{n} \left(\sum_{k=0}^n \frac{\epsilon}{m} \left[M \frac{1-p^{10^9}}{1-p} p^{\frac{\ln(\frac{M}{m})}{\ln a}} + \sum_{k=0}^{\frac{\ln(\frac{M}{m})}{\ln a}} m (ap)^k \right] p^{\left(\frac{m \cdot K_{rel}}{\epsilon} + T_{rel}\right)} \right. \\
& \left. - m\epsilon \frac{1-p^{\frac{m \cdot K_{rel}}{\epsilon}}}{1-p} - m\epsilon \frac{1-p^{T_{rel}}}{1-p} \right) \quad (8.86)
\end{aligned}$$

$$\begin{aligned}
& = \frac{\epsilon}{m} \left[M \frac{1-p^{10^9}}{1-p} p^{\frac{\ln(\frac{M}{m})}{\ln a}} + \sum_{k=0}^{\frac{\ln(\frac{M}{m})}{\ln a}} m (ap)^k \right] p^{\left(\frac{m \cdot K_{rel}}{\epsilon} + T_{rel}\right)} \\
& - m\epsilon \frac{1-p^{\frac{m \cdot K_{rel}}{\epsilon}}}{1-p} - m\epsilon \frac{1-p^{T_{rel}}}{1-p} \quad (8.87)
\end{aligned}$$

With wormhole for shipbound investors:

$$\lim_{n \rightarrow \infty} \frac{1}{n} \left(\sum_{k=0}^n \frac{\epsilon}{m} \left[M \frac{1-p^{10^9}}{1-p} p^{\frac{\ln(\frac{M}{m})}{\ln a}} + \sum_{k=0}^{\frac{\ln(\frac{M}{m})}{\ln a}} m (ap)^k \right] p^{\left(\frac{m \cdot K_{rel}}{\epsilon} + T_{rel} \right)} - m\epsilon \frac{1-p^{\frac{m \cdot K_{rel}}{\epsilon}}}{1-p} - m\epsilon \frac{1-p^{T_{rel}}}{1-p} \right) \quad (8.88)$$

$$= \frac{\epsilon}{m} \left[M \frac{1-p^{10^9}}{1-p} p^{\frac{\ln(\frac{M}{m})}{\ln a}} + \sum_{k=0}^{\frac{\ln(\frac{M}{m})}{\ln a}} m (ap)^k \right] \quad (8.89)$$

and economic return with wormhole for shipbound investors > economic return without wormhole for shipbound investors

$$\frac{\epsilon}{m} \left[M \frac{1-p^{10^9}}{1-p} p^{\frac{\ln(\frac{M}{m})}{\ln a}} + \sum_{k=0}^{\frac{\ln(\frac{M}{m})}{\ln a}} m (ap)^k \right] \geq \frac{\epsilon}{m} \left[M \frac{1-p^{10^9}}{1-p} p^{\frac{\ln(\frac{M}{m})}{\ln a}} + \sum_{k=0}^{\frac{\ln(\frac{M}{m})}{\ln a}} m (ap)^k \right] p^{\left(\frac{m \cdot K_{rel}}{\epsilon} + T_{rel} \right)} - m\epsilon \frac{1-p^{\frac{m \cdot K_{rel}}{\epsilon}}}{1-p} - m\epsilon \frac{1-p^{T_{rel}}}{1-p} \quad (8.90)$$

and one can conclude, that within a wormhole network, economic return within wormholes for shipbound investors = economic return with wormhole for earthbound investors.

Although spaceship based empire and wormhole based empire bear similar cost at the very beginning, a wormhole based empire soon or later can be shown to be superior in cost and investment.

It is showed that as the number of trips and trades completed increases and eventually going toward infinity, a spaceship based empire continue to subject under relativistic economics and cost foregone in energy gathering and opportunity lost during space travel. However, a

wormhole based empire's trade and communication will more and more resemble the classical economics familiar to us all on earth today. Information and exchanges are delayed by at most the cost C , and if C infinitely approaches 0, then the cost of communication and trades between any points on a wormhole network will also approaches 0. Therefore, the construction and the expansion of wormhole network itself will still subject to the law of relativistic economics, but the economic activities performed upon an established, matured network of wormholes within a galactic empire will resemble that of the classical economics on earth.

The construction of wormhole at the cosmic scale and its cost amortization analysis bears striking resemblance to the construction of bridges across a river, railroad system connecting two distant points, and urban subways connecting different districts.

Before a bridge is constructed, cars and train carriages have to be lifted and then lowered onto a barge and shipped to the other side. The time and energy costs involved is similar in concept to the amount of time required to gather energy needed for a spaceship's departure. Barges are generally slow-moving; therefore, the amount of time spent on traversing the surface of a body of water is conceptually similar to the time and opportunity cost of space travel at any speed. The construction of wormhole is at least as costly and as fast as the speed of light and possibly much slower, and the construction of bridge requires years and in the short run, no more cost-effective than barge and ferry. In the long run, a completed bridge offers unprecedented advantage where trains, cars, and people can be carried over with a tiny fraction of the original travel time and a significant cost reduction.

Before the advent of the railroad, merchants usually trade and sell items that only last very long time such as jewelry, clothing, porcelain and dried goods such as spices, tobacco, and coffee. Fresh goods such as vegetables and cakes can only be traded locally within the time frame before the perishable goods lose their value. The railroad system and later air freight service have completely changed the landscape of market exchange. Now fruits and vegetables from distant corners can be reached at local supermarkets. At the cosmic scale, whereas biological human, which lifespan is measured in decades, becomes the perishable goods in the cosmic level trade network, which may be dominated by matter and artificial intelligence. Biological human is confined to their own star system or their galaxy but not much beyond. With the advent of extensive wormhole networks, not only biological human can easily visit other habitable planets without subjecting to the constraints of relativistic economics, other biological creatures arising from alien planets can be brought back here at home. The issue of biological quarantine and seclusion is a different problem (a specific dwarf planet or part of Mars can be set up to host such exotic zoo), but it is to show that perishables can then easily be transported from one place to another.

Finally, the construction of wormhole can be compared with the urban subway system. The subway system is essentially a 3 dimensional tube underground connecting to two points above the ground otherwise impossible to connect due to the existence of buildings and communities. The cost of bus waiting and bus ride in a busy city is conceptually comparable to the time

required for the energy gathering for the departure of the spaceship and the time required for getting there. It takes less time to wait for the slow bus where it stops at very stations, but it takes a significant amount time to reach your destination. Or you can take the fast bus which takes much more waiting time at the station to catch one. In both cases, buses are subject to congestion. The underground system, on the other hand, travels between two points with the least distance, conceptually similar to shortcuts on space-time fabric. In many cities in the world, the construction of subway system eventually lowers the load of bus rides and in some cases even eliminates some lines and routes altogether, this again conceptually predicts that the adoption of cosmic wormhole network will at first reduce space travel on a flat spacetime and may eventually eliminate such travel altogether.

A further elaboration is needed, in that as the internal connecting stars and its harvest-able energy within the wormhole network increases and always exceeds all the exploratory frontier required energy costs. (Think of the total number of nodes within the wormhole network as the volume of the expanding sphere times a diluting factor f and the total number of frontier nodes to the expanding sphere as the total surface area times the diluting factor f . As the radius of the sphere increases, the volume always increases faster than the surface area), then the time required to gather energy to expand the frontier subject to laws of relativistic economics decreases. As a result, one would expect the frontier to be connected and integrated into the existing sphere faster and faster until almost no cost is involved in expanding (waiting interval between each expansion is shortened to 0). Therefore, the costs subject to the relativistic economics becomes almost insignificant and economic incentives for expansion can be almost modeled by the classical economics defined on earth.

$$\Rightarrow \frac{4\pi r^2 \cdot f}{\frac{4}{3}\pi r^3 \cdot f} \quad (8.91)$$

$$\Rightarrow \frac{3}{r} \quad (8.92)$$

$$\Rightarrow \lim_{r \rightarrow \infty} \frac{3}{r} \quad (8.93)$$

$$\Rightarrow 0 \quad (8.94)$$

Furthermore, at the start of the cosmic expansion, the construction of wormhole network is so costly that even a planet-wide or solar system wide government can hardly afford. The government can only afford to sent teams of explorers to nearby stellar systems every 1,000 years or so through an annual lottery system or government taxation, assuming it is a biological led thriving technological civilization.

A calculation is performed to indicate the prohibitive initial cost to market entry:

For a wormhole based economics, assuming $p = 0.997$ and assuming that one end of the wormhole is attached to the exploratory ship and the other end attached to the earth, then earth-

bound investor's economic return exactly matches with the shipbound investors' return. That is, the first time when wormhole was constructed, their economic return curve is one of the same.

$$y_{wormearth} = \ln \left(\frac{j}{m_g} \cdot R_{earth} p^{\left(\frac{mc^2 K_{rel}}{38.58 j t} + T_{rel} \right)} - m_g \cdot j \frac{1-p}{1-p} - m_g \cdot j \frac{1-p^{T_{rel}}}{1-p} \right) \quad (8.95)$$

$$y_{wormship} = \ln \left(\frac{j}{m_g} \cdot R_{earth} \cdot p^{\left(\frac{mc^2 K_{rel}}{38.58 j t} + T_{rel} \right)} - m_g \cdot j \frac{1-p}{1-p} - m_g \cdot j \frac{1-p^{T_{rel}}}{1-p} \right) \quad (8.96)$$

$$y_{shiphigh} = \ln \left(\frac{j}{m_g} \cdot R_{earth} \cdot p^{\left(\frac{mc^2 K_{rel}}{38.58 j t} + T_{rel} \right)} - m_g \cdot j \frac{1-p}{1-p} - m_g \cdot j \frac{1-p^{T_{rel}}}{1-p} \right) \quad (8.97)$$

$$y_{wormearth} = y_{wormship} = y_{shiphigh} \quad (8.98)$$

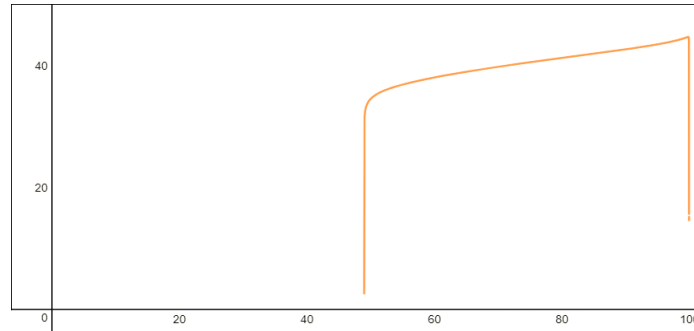


Figure 8.17: At the first time when worm hole is constructed, economic return of wormhole expansion = shipbound investors = earthbound investors' economic return when $p=0.997$

It can be shown that biological led species have much lower economic incentive to initiate wormhole construction compares to a post-singularity society due to greater mass requirements for colonization. If biologically led species ever were led to create wormhole infrastructure, it is far more likely and lucrative to be based on the control and the interest of a small group of people. That is, the start of wormhole network construction is prohibitively expensive and restricted to the privileged.

$$y_{shipAI} = \ln \left(j \cdot R_{earth} \cdot p \left(\frac{10^{-10} mc^2 K_{rel} + T_{rel}}{10^4 j} \right) - \frac{j}{10^{10}} \frac{1-p}{1-p} \left(\frac{10^{-10} mc^2 K_{rel}}{10^4 j} \right) - \frac{j}{10^{10}} \frac{1-p^{T_{rel}}}{1-p} \right) \quad (8.99)$$

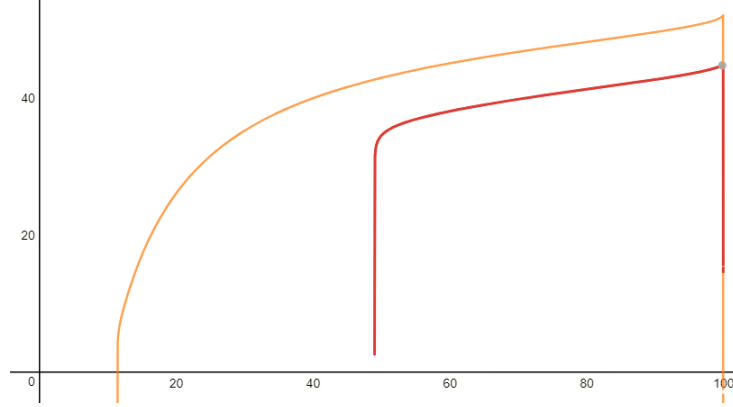


Figure 8.18: Shipbound AI's perceived economic return > Shipbound human investors' return when $p = 0.997$

Once the wormhole is established, traveling within the wormhole more or less is comparable to traveling at subluminal speed and finite distances on earth. For traversing an established wormhole, depending on the distance that is reduced, one can also find the most optimal cruising speed within the wormhole. Assuming that the distance within the wormhole compares to the external physical universe has reduced by a million fold and a hundredfold respectively for an AI based investor, then the equation is given by:

$$y_{earthAIopt1} = \ln \left(j \cdot R_{earth} \cdot p \left(\frac{10^{-10} mc^2 K_{rel} + \frac{d}{10^6}}{10^4 j} \right) - \frac{j}{10^{10}} \frac{1-p}{1-p} \left(\frac{10^{-10} mc^2 K_{rel}}{10^4 j} \right) \right) \quad (8.100)$$

$$y_{earthAIopt2} = \ln \left(j \cdot R_{earth} \cdot p \left(\frac{10^{-10} mc^2 K_{rel} + \frac{d}{100}}{10^4 j} \right) - \frac{j}{10^{10}} \frac{1-p}{1-p} \left(\frac{10^{-10} mc^2 K_{rel}}{10^4 j} \right) \right) \quad (8.101)$$

and the plot shows that the optimal cruising speed at 0.23831c for a wormhole reducing the travel distance $d=1,776$ ly by a million fold. This result can be conclusively derived by taking the derivative of $y_{earthAIopt1}$ and finding its x-intercept:

$$0 = \frac{d}{dx} (y_{earthAIopt1}) \cdot 1,000 \quad (8.102)$$

$$y_{earthAIwormoptimalspeed} = \left(\left(\frac{y_{earthAIopt1}}{52.12} \right)^{590,000} \right) \quad (8.103)$$

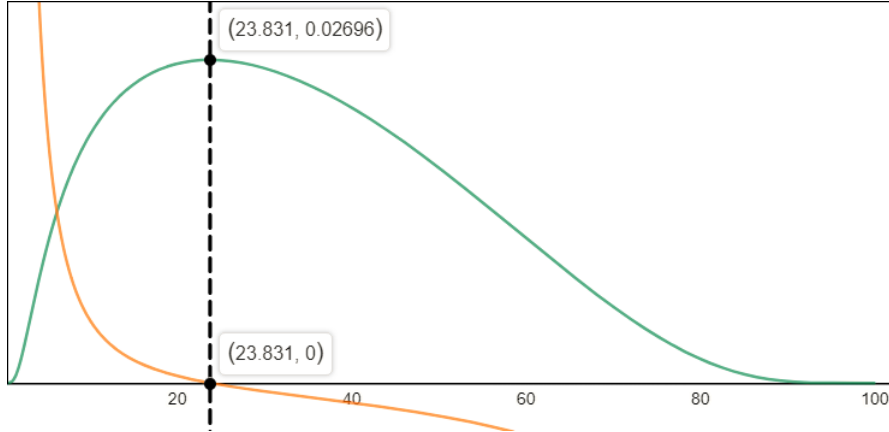


Figure 8.19: The most optimal travel speeds for a wormhole which reduces the travel distance by a million folds.

and the optimal cruising speed at 0.98258c for a wormhole reducing the travel distance $d=1,776$ ly by a hundredfold. It can also be shown when the wormhole reduces the travel distance to a destination to 0. Then the optimal speed is also 0.

$$0 = \frac{d}{dx} (y_{earthAIopt1}) \cdot 10^{-292.5} \quad (8.104)$$

$$y_{earthAIwormoptimalspeed} = \left(\left(\frac{y_{earthAIopt2}}{52.12} \right)^{590,000} \right) \quad (8.105)$$

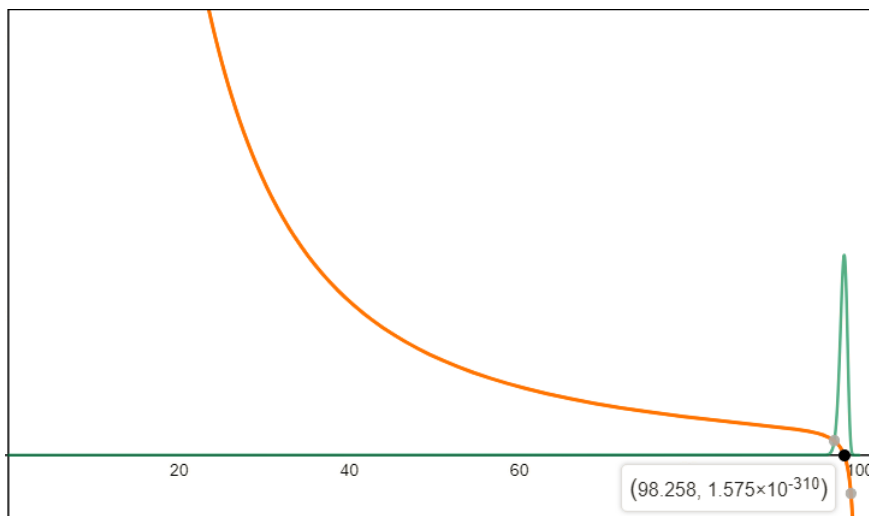


Figure 8.20: The most optimal travel speeds for a wormhole which reduces the travel distance by a hundred folds.

Toward the end of network expansion, increasingly smaller groups of individuals grouped as firms, non-profit groups are able to harness the energy needed within the entire wormhole network in a relatively short time to fund their expansion. As a result, the cost of expansion becomes so small that smaller groups of people or even individuals can play the role of cosmic expansion and make a profit. This is strikingly similar to the development of internet infrastructure here observed on earth in the past few decades. The original internet was conceived in 1969 by the US government codenamed DARPA, as a backup network of connected machines in case of Soviet nuclear attack. The initial cost of construction was so high that only government has the resources and incentive to implement such a network in the first place. As the internet expands, the scale of economics dictates falling costs of additional network expansion.

As a result, telecommunication companies with a group of people at a size much smaller than the entire government enters the market and deployed vast stretches of fiber and optical network during the 90s and 00's which provides the backbone of the fast internet we enjoyed today. As the internet infrastructure matured, increasingly more and more start-ups and even individuals entered the market as entrepreneurs and made profits based on their idiosyncratic ideas that fulfill specific market needs. All thanks to the low cost of entry.

A calculation is performed to indicate the falling cost of market entry (We have discussed earlier in the section how the ratio of surface expanding nodes to internal nodes decreases):

$$\Rightarrow \frac{4\pi r^2 \cdot f}{\frac{4}{3}\pi r^3 \cdot f} \tag{8.106}$$

$$\Rightarrow \frac{3}{r} \tag{8.107}$$

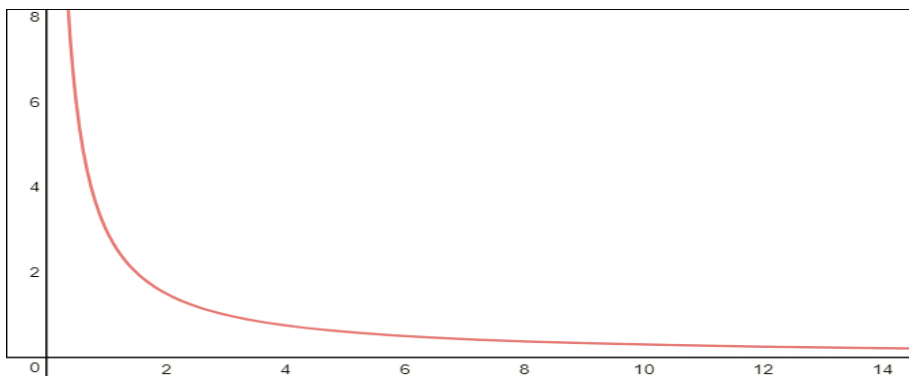


Figure 8.21: Falling cost of market entry as the network enlarges

As the wormhole network expands and matures, an entire earth's biological population can then easily obtain the material and energy requirement for migration to a new planet by borrowing from other planet based civilization within the galaxy. The cost of preparation then can be minimized to 0, and a positive economic return available to the entire population becomes

possible. The equation below shows that both the energy acquisition cost term (borrowing resources through wormhole waste no time) and the travel distance is reduced to $\frac{1}{50}$ th of the original. $10^{21} \cdot j$ is used as the total energy budget per year because one assumes AI harnessed every stars energy. Furthermore, the cost of depreciation can be reduced from 0.99999999999 to 0.997.

$$y_{biowormmmature} = \ln \left(\frac{j}{P_{earth}} \cdot R_{earth} \cdot p \left(\frac{mc^2 K_{rel}}{10^{21}j} + \frac{d}{100} \right) \right) \quad (8.108)$$

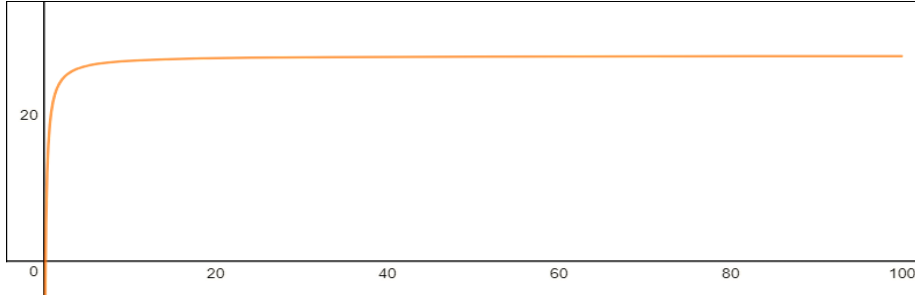


Figure 8.22: Economic return for earthbound democracy vs various speed of light

This, in theory, implies that the construction of wormholes is most likely initiated by AI with tiny mass, followed by biological species led by a dictatorial civilization, and least likely by biological species led democracy. Once the infrastructure is in place, colonization efforts is feasible by biological species led democracy.

There is one major striking difference, though that distinguishes the wormhole network from that of the internet network. The ultimate frontier of a wormhole network touches the nearest expanding extra-terrestrial civilization. Since we can not predict the intention of an unmet unknown civilization, a cosmic civilization uses all its resources to guard its frontier just as national borders we observed on earth today.

Therefore, a cosmic civilization may have to use macroeconomic measures to prohibit or discourage individuals or corporation expanding near the edge of the wormhole expansion, where the theoretical boundary to meet the nearest expanding extra-terrestrial industrial civilization can be calculated using aforementioned equations with concrete observational data from our galaxy and beyond.

8.11 Worm Hole Maintenance Cost

Finally, we shall devote ourselves to the calculation of the maintenance of the wormhole network. It is shown that in order to maintain a wormhole, disregarding the effect of cosmic space expansion within a relatively short time period of fewer than 100 million years. We also assume that the nearest industrial civilization is 88.43 million ly away. As a result, as long as the

economic return is positive within the 88.43 million ly radius, then wormhole network can be maintained perpetually. We first consider the case for a biological led intergalactic civilization. We know earlier that the number of habitable planets at the current epoch is 10,719. Therefore, the average distance between all stars within a galaxy sphere (not the size of the galaxy but the weighted size including mostly empty space between galaxies in a 3 dimensional space) is 1,074,888 ly.

$$\frac{\left(\frac{4}{3}\pi (11,850,000)^3\right)}{\left(\frac{4}{3}\pi (537,444)^3\right)} = 10,719.0277 \quad D_0 = 537,444 \cdot 2 = 1,074,888 \text{ ly}$$

There are two approaches to construct the wormhole network. In the first case, assuming each additional 1,074,888 ly from earth, in the order of x^3 total number of habitable planets can be connected by the shortest path between adjacent neighbors originating from earth, whereas x stands for the radius of our interest. This spiral ring is further connected with all habitable planets of an additional 1,074,888 ly further away. Then, the total length of wormhole network needs to be maintained is the average distance between all planets times the number of planets and the sum of all short segments originated from planets on each layer that connects to the ring to the nearest layer beneath it. If we follow the clockwise direction of the spiral configuration, each planet connects with the next planet on the same layer (equal distance relative to earth), the length of the segment serving intra-layer connection is $2R_{bio}$. Each planet further connects with a corresponding planet extending further out from earth at the next layer. The length of segment serving inter-layer connection is also $2R_{bio}$. As a result, The sum total of all segments leading from any particular planet is $4R_{bio}$. The total number of nodes within a radius of x is $\left(\frac{x}{R_{bio}}\right)^3 - 1$. D_{ly} is the distance of 1 light year in kilometers. Whereas j_t represents the energy output per 1 earth based on the total energy output of the World in 2008 times 10, that is, assuming the population ceiling is in the order of 10 billion derived from Chapter 6. $T_{convert}$ stands for the number of seconds in a year since we computed our energy output based on its annual quota.

$$y_{biowormmupper} = \ln \left(38.5j_t \cdot \left(\frac{x}{R_{bio}}\right)^3 - T_{convert} \cdot r_{bioupper} \cdot D_{ly} \left(4R_{bio} \left(\left(\frac{x}{R_{bio}}\right)^3 - 1 \right) \right) \right) \quad (8.109)$$

$$R_{bio} = 537,444 \text{ ly}$$

$$T_{convert} = 365 \text{ days} \cdot 24 \text{ hours} \cdot 60 \text{ minutes} \cdot 60 \text{ seconds}$$

$$D_{ly} = 9.4607 \cdot 10^{15} \text{ m}$$

Then, the first term stands for the total energy output of all planets within the network, and the

second term stands for the total length of the worm hole network in meters. We are interested in finding the value of $r_{bioupper}$ so that the first term and the second term sums up to 0. Setting $y_{biowormupper} = 0$, we can solve for the cost of maintenance by rearranging our equation, whereas $D_{nearest}$ is the nearest extraterrestrial to earth in light years:

$$D_{nearest} = 0.442196590976 \cdot 2 \cdot 10^8 = 88,439,318.1952 \text{ ly} \quad (8.110)$$

$$r_{bioupper} = \frac{38.5j_t \cdot \left(\frac{\left(\frac{D_{nearest}}{2} \right)^3}{R_{bio}} \right)}{D_{ly} \cdot \left(4R_{bio} \left(\left(\frac{\left(\frac{D_{nearest}}{2} \right)^3}{R_{bio}} \right) - 1 \right) \right) \cdot T_{convert}} \quad (8.111)$$

$$= 6.4313677804 \times 10^{-8} \text{ J}$$

It is then can be found that as long as the cost of maintenance does exceed $6.4313677804 \times 10^{-8} \text{ J}$ per second for every meter length of the wormhole, or $6.4313677804 \times 10^{-8} \text{ Watt}$ for every meter length, the network will be maintained. This is less than the kinetic energy of a flying mosquito. This suggests that it is highly unlikely biologically led industrial civilization ever takes on worm hole expansion.

In a more simplified version, however, the spiral ring originating from earth is still necessary to connect all habitable planets within each layer distanced away from earth. However, the number of segments connects to each layer can be reduced to just one long pipe extends from earth to the outermost layer with a length of 44.21 million ly that intercepts with the spiral ring. If we follow the clockwise direction of the spiral configuration, each planet connects with the next planet on the same layer (equal distance relative to earth), the length of the segment serving intra-layer connection is $2R_{bio}$. Each planet further connects with a corresponding planet extending further out from earth at the next layer. The length of segment serving inter-layer connection is also $2R_{bio}$. The long pipe is simply the radius of the sphere we are investigating and is denotes as length x . The total number of nodes within a radius of x is $\left(\frac{x}{R_{bio}} \right)^3 - 1$. D_{ly} is the distance of 1 light year in kilometers.

Then the equation simplifies to:

$$y_{biowormlower} = \ln \left(38.5j_t \cdot \left(\frac{x}{R_{bio}} \right)^3 - T_{convert} \cdot r_{biolower} \cdot D_{ly} \left(2R_{bio} \left(\left(\frac{x}{R_{bio}} \right)^3 - 1 \right) + x \right) \right) \quad (8.112)$$

Setting $y_{biowormlower} = 0$, we can solve for the cost of maintenance by rearranging our equation:

$$r_{biolower} = \frac{38.5j_t \cdot \left(\frac{\left(\frac{D_{nearest}}{2} \right)}{R_{bio}} \right)^3}{D_{ly} \cdot \left(2R_{bio} \left(\left(\frac{\left(\frac{D_{nearest}}{2} \right)}{R_{bio}} \right)^3 - 1 \right) + \frac{D_{nearest}}{2} \right) \cdot T_{convert}} \quad (8.113)$$

$$= 1.2862352901 \times 10^{-7} \text{ J}$$

and we solved for the lower bound and found that as long the cost of maintenance as does exceed $1.2862352901 \times 10^{-7} \text{ J}$ per second for every meter length of the wormhole, or $1.2862352901 \times 10^{-7} \text{ Watt}$ for every meter length the wormhole network will be maintained. This is comparable to the kinetic energy of a flying mosquito. This suggests that it is highly unlikely biologically led industrial civilization ever takes on worm hole expansion. Both equations are plotted below is the breakeven point of wormhole network:

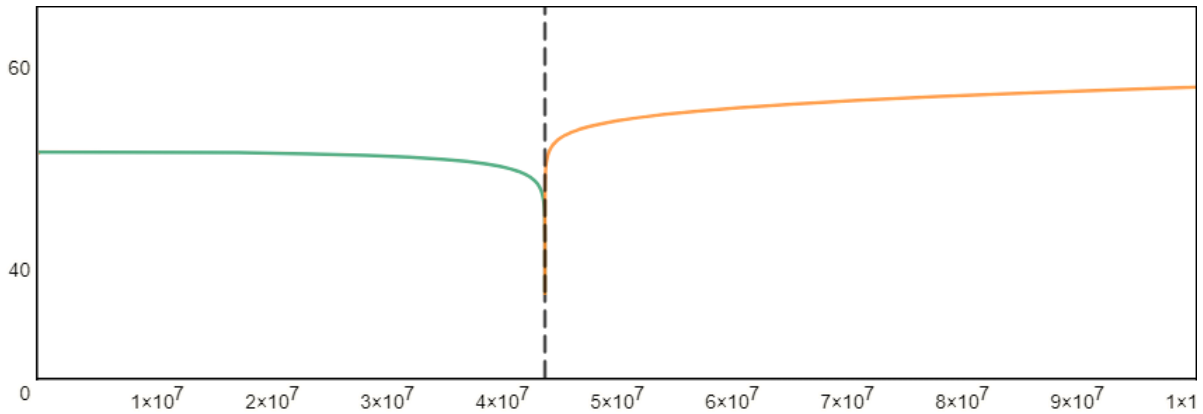


Figure 8.23: Biologically-based expanding civilization's wormhole network's economic return turns to negative (green curve) at a distance of 88.4 million ly (upper bound cost limit) or greater and becomes positive (black curve) at 88.4 million ly (lower bound cost limit) or greater.

For machine led civilization, every star is a target for energy acquisition. As a result, we take the galaxy sphere and divide by the number of stars and find the average distance between stars to be $583 \cdot 2 = 1167 \text{ ly}$.

$$R_{AI} = \frac{3}{4\pi} \left(\frac{\frac{4}{3}\pi (11,850,000)^3}{477.093 \cdot 10^9} \right)^{\frac{1}{3}} \quad (8.114)$$

$$= 583.612962426 \text{ ly}$$

$$y_{AIwormupper} = \ln \left(0.5^{3.5} \cdot P_{sol} \cdot \left(\frac{x}{R_{AI}} \right)^3 - r_{AIupper} \cdot D_{ly} \left(4R_{AI} \left(\left(\frac{x}{R_{AI}} \right)^3 - 1 \right) \right) \right) \quad (8.115)$$

$$D_{ly} = 9.4607 \cdot 10^{15} \text{ m}$$

$$P_{sol} = 3.8 \cdot 10^{26} \text{ J}$$

Since AI is capable of harvesting every star's resources, then P_{sol} is the solar output per second and is multiplied by $0.5^{3.5}$ because the weighted average mass of stars in the galaxy is 0.5 solar mass and the power output of the star is raised to the 3.5th power of its mass. With the shorter colonization distance, the upper bound maintenance cost can be set as high as 1,520,794.10354 J per second for every meter length of the wormhole. This means that every meter of wormhole network cost can be as high as 1,520,794.10354 Watt for every meter length, or 2,039.42 horse power for every meter length and remain profitable.

$$r_{AIupper} = \frac{0.5^{3.5} \cdot P_{sol} \cdot \left(\frac{\left(\frac{D_{nearest}}{2} \right)}{R_{AI}} \right)^3}{D_{ly} \cdot \left(4R_{AI} \left(\left(\frac{\left(\frac{D_{nearest}}{2} \right)}{R_{AI}} \right)^3 - 1 \right) \right)} \quad (8.116)$$

$$= 1,520,794.10354 \text{ J}$$

the lower bound maintenance cost can be set as high as 3,041,588.20681 J per second for every meter length of the wormhole. This means that every meter of wormhole network cost can be as high as 3,041,588.20681 Watt for every meter length or 4,078.836 horse power for every meter length and remain profitable.

$$y_{AIwormlower} = \ln \left(0.5^{3.5} \cdot P_{sol} \cdot \left(\frac{x}{R_{AI}} \right)^3 - r_{AIlower} \cdot D_{ly} \left(2R_{AI} \left(\left(\frac{x}{R_{AI}} \right)^3 - 1 \right) + x \right) \right) \quad (8.117)$$

$$r_{AI\ lower} = \frac{0.5^{3.5} \cdot P_{sol} \cdot \left(\frac{\left(\frac{D_{nearest}}{2} \right)^3}{R_{AI}} \right)}{D_{ly} \cdot \left(2R_{AI} \left(\left(\frac{\left(\frac{D_{nearest}}{2} \right)^3}{R_{AI}} \right) - 1 \right) + \frac{D_{nearest}}{2} \right)} \quad (8.118)$$

$$= 3,041,588.20681 \text{ J}$$

The combined graph is plotted below:

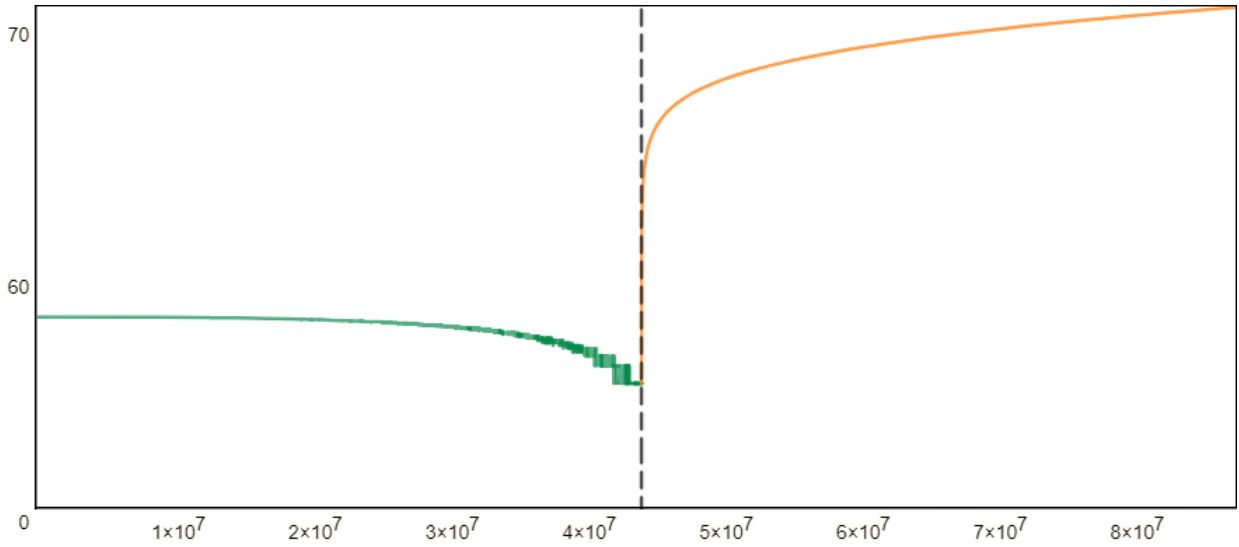


Figure 8.24: AI-based expanding civilization’s wormhole network’s economic return remains positive (green curve) at a distance of 44.2 million ly with the upper bound maintenance cost limit and starts to become positive (orange curve) at 44.2 million ly distance at the lower bound maintenance cost limit.

The economic return of the wormhole network can be strongly correlated with the size of the network itself. If maintenance cost can become sufficiently small, one can see that economic return value increases as the monotonically as the radius of the network increases and incorporates more and more energy resources into the network which outweigh the cost of network maintenance. Therefore, we have proved that there is a perpetual motive for the expansion of such network to gain additional economic return from the expander’s perspective. In our case sceario, we simply reduce our AI wormhole network upper bound maintenance cost by just even 1.0000001 and results monotonically increasing positive returns.

$$y_{Allowercost} = \ln \left(0.5^{3.5} \cdot P_{sol} \cdot \left(\frac{x}{R_{AI}} \right)^3 - r_{Allowercost} \cdot D_{ly} \left(4R_{AI} \left(\left(\frac{x}{R_{AI}} \right)^3 - 1 \right) \right) \right) \quad (8.119)$$

$$r_{Allowercost} = \frac{0.5^{3.5} \cdot P_{sol} \cdot \left(\frac{\left(\frac{D_{nearest}}{2} \right)}{R_{AI}} \right)^3}{D_{ly} \cdot \left(2R_{AI} \left(\left(\frac{\left(\frac{D_{nearest}}{2} \right)}{R_{AI}} \right)^3 - 1 \right) + \frac{D_{nearest}}{2} \right) \cdot 1.0000001} \quad (8.120)$$

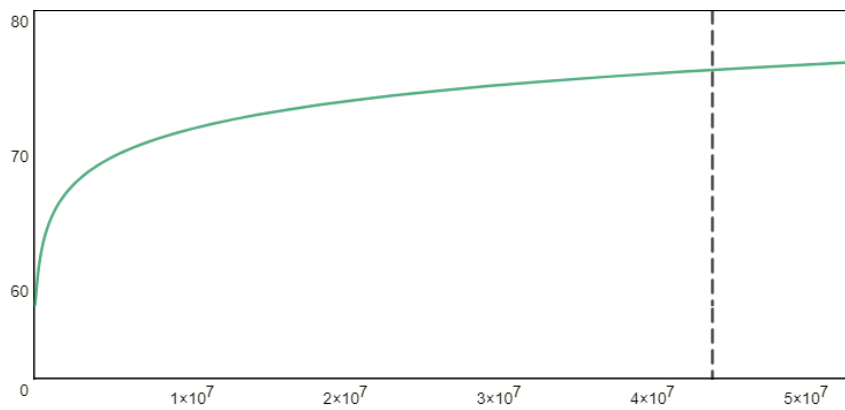


Figure 8.25: The economic return on wormhole construction vs its radius

9 The Principle of Universal Contacts

9.1 $E(d, v)$ Derivation and the Limit of Our Reach

If the construction of wormholes are economically lucrative and feasible, then what are the limits of wormhole expansion can be carried out by a single civilization?

In order to answer this question, we now discuss the derivation for the function of $E(d, v)$, that handles the conversion for a cosmological distance of d for any given constant migration speed of v .

Due to the expansionary nature of the universe, if earth based civilization starts its expansion at most the speed of light now and tries to catch the furthest point that they can reach in every direction, then we need to calculate what is the furthest distance reachable given various speeds. Since all galaxies are moving away and the further away they are located, the faster they recede from earth's observers, there is a point and beyond even one travels at the speed of light can never reach. As you approaching this point and beyond, it recedes faster and faster from you.

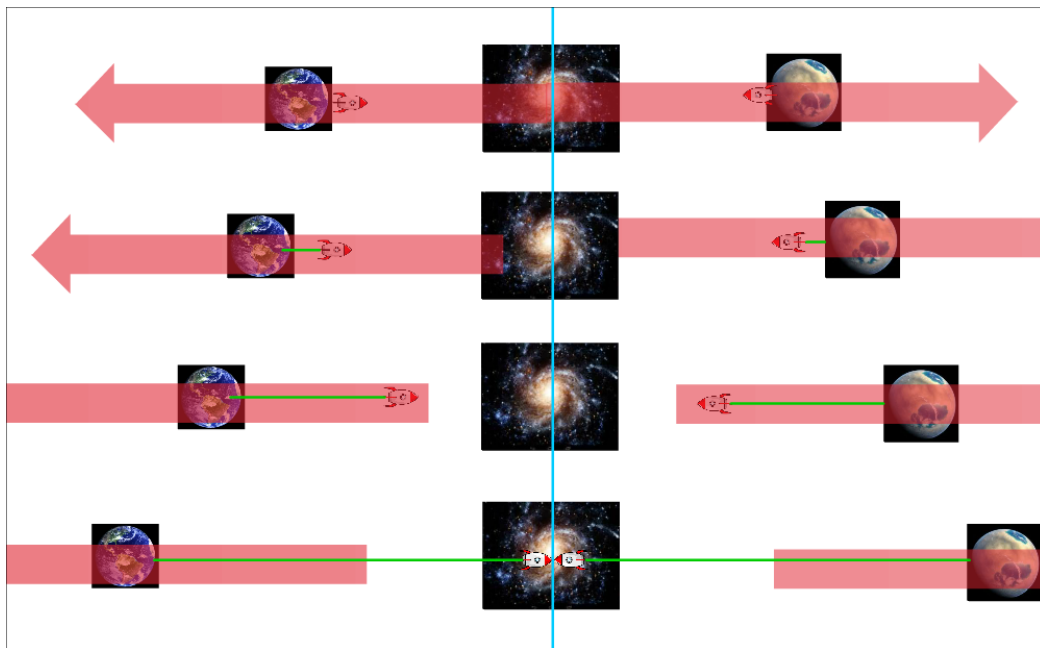


Figure 9.1: Illustration of an expanding universe

This point can be calculated from a recursive function sequence listed below. Based on the Hubble constant, which states that objects every 1 million parsecs (327 million light years) apart recedes at a uniform speed of $74 \frac{\text{km}}{\text{sec}}$. We take the time required to reach object located at this point in space given a specified speed v , and then we calculate the amount of distance the object located at this point has receded further away since our catching this point started

(the total time elapsed). With this distance known, one can calculate how much more time required again for our traveler to catch up to the object. In the third round of calculation, once again we calculate the amount of distance the object has receded further away since our catching this object started during the second round, the steps are repeated until one finally catches the object. The calculation to be performed is best represented by a recursive function as the receding speed increases along the path of expansion.

The recursive nature of the equation requires, in the greatest precision, infinite number of steps of recursion at every round of calculation. For example, each second, hour, and a day the distant object is moving a tiny bit faster away than the previous second, hour, or day due to its distance becomes further distant from earth. We can simplify our calculation by applying approximation and then deriving the closed form from data points.

First of all, we define the unit of cosmic expansion as the amount of distance can be traveled due to cosmic expansion by a celestial object located at 1 million parsecs away in one year and convert that distance in terms of light years. We take $74 \frac{\text{km}}{\text{sec}}$ multiply by 60 seconds, 60 minutes, 24 hours, and 365 days and divide by the number of km in a light year.

$$E = \left(\frac{74 \cdot 60 \cdot 60 \cdot 24 \cdot 365}{9.4607 \cdot 10^{12}} \right) \quad (9.1)$$

$$E = 0.000246669273944 \quad (9.2)$$

This result will be further divided by 3.262 to rescale to the unit of 1 million light years.

Then, the total distance needs to be traveled before reaching the destination is defined by: where up to j rounds of successive catch-ups is needed to reach the receding object.

$$E(d, v) = G_{\text{escape}}(d, 0, v) + G_{\text{escape}}(x_1, 1, v) + G_{\text{escape}}(x_2, 2, v) + \dots + G_{\text{escape}}(x_j, j, v) \quad (9.3)$$

$$E(d, v) = G_{\text{escape}}(d, 0, v) + \sum_{n=1}^{G_{\text{escape}}(x_j, j, v)=0} G_{\text{escape}}(x_n, n, v) \quad (9.4)$$

And the first round (as well as any other rounds) in the recursive function for finding how much the object receded can be further divided in the current round of catch-up into another sum of series of mini-steps:

Whereas d is the distance in light years of the object one tries to reach, k is the total number of mini-steps to update before the specified distance d is reached. The number k can be as large as infinity or much smaller, depending on the resolution and the precision one needs to reach in the calculation. In our simulation, the k we used is 30,000 mini-steps. Each step units in light years.

$$G_{escape}(d, 0, v) = S(0) + S(1) + S(2) + \dots + S(k) = \sum_{n=0}^k S(n) = x_1 \quad (9.5)$$

Time factor $\frac{c}{v}$ is the time scale factor for a given speed v to tranverse a distance of $\frac{d}{k}$ in units of light years.

$$S(0) = \frac{Ed}{3.262} \cdot \left(\frac{c}{v}\right) \left(\frac{d}{k}\right) \quad (9.6)$$

$$S(1) = \frac{E(d + S(0))}{3.262} \cdot \left(\frac{c}{v}\right) \left(\frac{d}{k}\right) \quad (9.7)$$

$$S(2) = \frac{E(d + S(0) + S(1))}{3.262} \cdot \left(\frac{c}{v}\right) \left(\frac{d}{k}\right) \quad (9.8)$$

$$S(k) = \frac{E(d + S(0) + S(1) + \dots + S(k))}{3.262} \cdot \left(\frac{c}{v}\right) \left(\frac{d}{k}\right) \quad (9.9)$$

The second round in the recursive function can be subdivided into another sum of series of mini-steps which is almost identical to the first round except that the distance d one tries to reach is replaced by the total distance the object has shifted further away during the trip time that took the ship from earth to the object's original location in the first round of catch up. It is denoted as x_1 , equivalently as $G_{escape}(d, 0, v)$.

$$G_{escape}(x_1, 1, v) = S(0) + S(1) + S(2) + \dots + S(k) = \sum_{n=0}^k S(n) = x_2 \quad (9.10)$$

$$S(0) = \frac{EG_{escape}(d, 0, v)}{3.262} \cdot \left(\frac{c}{v}\right) \left(\frac{G_{escape}(d, 0, v)}{k}\right) \quad (9.11)$$

$$S(1) = \frac{E(G_{escape}(d, 0, v) + S(0))}{3.262} \cdot \left(\frac{c}{v}\right) \left(\frac{G_{escape}(d, 0, v)}{k}\right) \quad (9.12)$$

$$S(2) = \frac{E(G_{escape}(d, 0, v) + S(0) + S(1))}{3.262} \cdot \left(\frac{c}{v}\right) \left(\frac{G_{escape}(d, 0, v)}{k}\right) \quad (9.13)$$

$$S(k) = \frac{E(G_{escape}(d, 0, v) + S(0) + S(1) + \dots + S(k))}{3.262} \cdot \left(\frac{c}{v}\right) \left(\frac{G_{escape}(d, 0, v)}{k}\right) \quad (9.14)$$

We repeat this process until the last step j (at this step we finally reached our targeted object) is simulated:

$$G_{escape}(x_j, j, v) = S(0) + S(1) + S(2) + \dots + S(k) = \sum_{n=0}^k S(n) = x_{j+1} \quad (9.15)$$

$$S(0) = \frac{EG_{escape}(x_{j-1}, j-1, v)}{3.262} \cdot \left(\frac{c}{v}\right) \left(\frac{G_{escape}(x_{j-1}, j-1, v)}{k}\right) \quad (9.16)$$

$$S(1) = \frac{E(G_{escape}(x_{j-1}, j-1, v) + S(0))}{3.262} \cdot \left(\frac{c}{v}\right) \left(\frac{G_{escape}(x_{j-1}, j-1, v)}{k}\right) \quad (9.17)$$

$$S(2) = \frac{E(G_{escape}(x_{j-1}, j-1, v) + S(0) + S(1))}{3.262} \cdot \left(\frac{c}{v}\right) \left(\frac{G_{escape}(x_{j-1}, j-1, v)}{k}\right) \quad (9.18)$$

$$S(k) = \frac{E(G_{escape}(x_{j-1}, j-1, v) + S(0) + S(1) + \dots + S(k))}{3.262} \cdot \left(\frac{c}{v}\right) \left(\frac{G_{escape}(x_{j-1}, j-1, v)}{k}\right) \quad (9.19)$$

We have now completed the mathematical description of the recursion. Assuming E, the Hubble constant stayed constant for all time periods. From the simulation, it is shown that traveling at the speed of light; the furthestmost location can be reached from earth is 91 billion light-years away. Unfortunately, the expansion of the universe is expanding. As a result, the Hubble constant is also changing as one trying to catch the furthestmost point one can reach. The expansion of the universe is modeled after the equation below:

$$f(x) = 0.822x^{\frac{2}{3}} + 0.0623 \left(e^{0.645x} - 1 \right) \quad (9.20)$$

At early times we expect the scale factor to be dominated by matter, and this gives a $x^{\frac{2}{3}}$ dependence. At late times we expect the scale factor to be dominated by dark energy and this gives an exponential dependence on x. The graph shows this nicely, with the changeover being somewhere around half a Hubble time.[77]

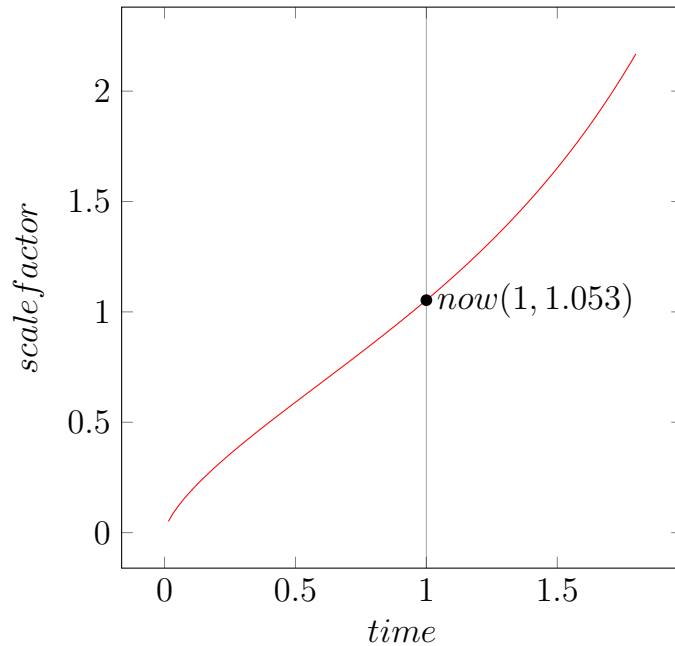


Figure 9.2: The scale factor of the universe

We take the derivative of the equation above and yields the following equation, which is the rate of change for the expansion of the universe:

$$R(y) = 0.0965891e^{1.55039x} + \frac{0.548}{\sqrt[3]{x}} \quad (9.21)$$

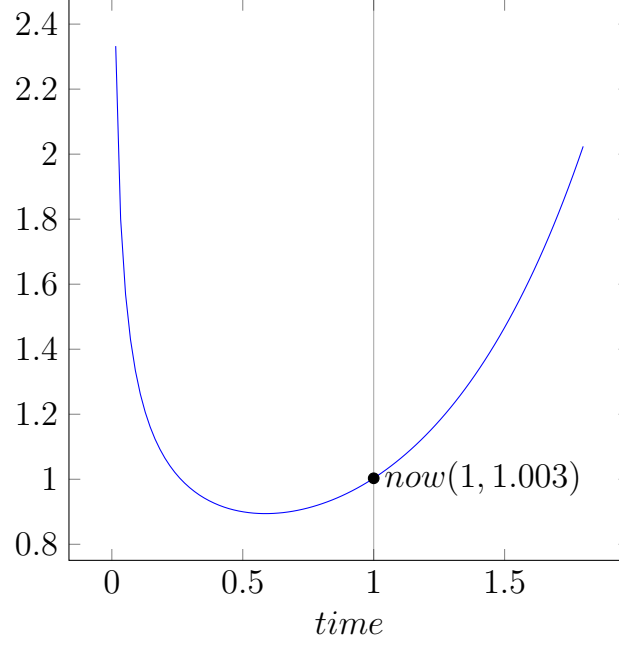


Figure 9.3: The derivative of the scale factor

and we add $R(y)$ as a scale factor to the Hubble constant, now the expansion speed changes with time.

$$E(y) = \frac{74 \cdot R(y) \cdot 60 \cdot 60 \cdot 24 \cdot 365}{9.4607 \cdot 10^{12}} \quad (9.22)$$

We then need to modify the first term of the existing recursive function as:

$$G_{escape}(d, 0, v) = S(0) + S(1) + S(2) + \dots + S(k) = \sum_{n=0}^k S(n) = x_1 \quad (9.23)$$

$$S(0) = \frac{E(T_{current})d}{3.262} \cdot \left(\frac{c}{v}\right) \left(\frac{d}{k}\right) \quad (9.24)$$

$$S(1) = \frac{E\left(T_{current} + \frac{d}{k}\left(\frac{c}{v}\right)\right)(d + S(0))}{3.262} \cdot \left(\frac{c}{v}\right) \left(\frac{d}{k}\right) \quad (9.25)$$

$$S(2) = \frac{E\left(T_{current} + \frac{2d}{k}\left(\frac{c}{v}\right)\right)(d + S(0) + S(1))}{3.262} \cdot \left(\frac{c}{v}\right) \left(\frac{d}{k}\right) \quad (9.26)$$

$$S(k) = \frac{E\left(T_{current} + d\left(\frac{c}{v}\right)\right)(d + S(0) + S(1) + \dots + S(k))}{3.262} \cdot \left(\frac{c}{v}\right) \left(\frac{d}{k}\right) \quad (9.27)$$

Whereas T_{current} stands for the current time, 13.8 Gyr since the Big Bang. Since one divides distance d into k steps to gain precision, the Hubble constant is re-adjusted at each step. At step 0, the Hubble constant remains the same as now. At step 1, the Hubble constant is updated with the current time plus the time it takes to complete the first mini-step with speed v . At mini-step 2, the Hubble constant is updated with the current time plus the time it takes to complete the first two mini-steps with speed v . At step k , the Hubble constant is updated with the current time and the time it takes to complete the first k mini-steps with speed v . The precision of the updates depends on both the number of mini-steps and the speed v . If the number of mini-steps is held constant, then the precision is positively related with travel speed. The faster the speed, the shorter time lapse between each mini-steps (and shorter time lapse for the current round of catch-up overall), the greater the precision on the Hubble constant. The second round of the recursive function is rewritten as:

$$G_{\text{escape}}(x_1, 1, v) = S(0) + S(1) + S(2) + \dots + S(k) = \sum_{n=0}^k S(n) = x_2 \quad (9.28)$$

$$S(0) = \frac{E\left(T_{\text{current}} + d\left(\frac{c}{v}\right)\right) G_{\text{escape}}(d, 0, v)}{3.262} \left(\frac{c}{v}\right) \left(\frac{G_{\text{escape}}(d, 0, v)}{k}\right) \quad (9.29)$$

$$S(1) = \frac{E\left(T_{\text{current}} + d\left(\frac{c}{v}\right) + \frac{G_{\text{escape}}(d, 0, v)}{k} \left(\frac{c}{v}\right)\right) (G_{\text{escape}}(d, 0, v) + S(0))}{3.262} \left(\frac{c}{v}\right) \left(\frac{G_{\text{escape}}(d, 0, v)}{k}\right) \quad (9.30)$$

$$S(2) = \frac{E\left(T_{\text{current}} + d\left(\frac{c}{v}\right) + \frac{2G_{\text{escape}}(d, 0, v)}{k} \left(\frac{c}{v}\right)\right) (G_{\text{escape}}(d, 0, v) \dots + S(1))}{3.262} \left(\frac{c}{v}\right) \left(\frac{G_{\text{escape}}(d, 0, v)}{k}\right) \quad (9.31)$$

$$S(k) = \frac{E\left(T_{\text{current}} + d\left(\frac{c}{v}\right) + G_{\text{escape}}(d, 0, v) \left(\frac{c}{v}\right)\right) (G_{\text{escape}}(d, 0, v) \dots + S(k))}{3.262} \left(\frac{c}{v}\right) \left(\frac{G_{\text{escape}}(d, 0, v)}{k}\right) \quad (9.32)$$

Whereas the Hubble constant is updated at each step by taking into consideration the total time consumed in the previous round of calculation and the time it takes to complete the n previous steps with speed v at the current round of calculation.

and the k^{th} round of catch up can be rewritten as:

$$G_{\text{escape}}(x_j, j, v) = S(0) + S(1) + S(2) + \dots + S(k) = \sum_{n=0}^k S(n) = x_{j+1} \quad (9.33)$$

$$S(0) = \frac{E \left(T_{\text{current}} + d \left(\frac{c}{v} \right) + \dots + G_{\text{escape}}(x_{j-2}, j-2, v) \left(\frac{c}{v} \right) \right)}{3.262} \\ G_{\text{escape}}(x_{j-1}, j-1, v) \cdot \left(\frac{c}{v} \right) \left(\frac{G_{\text{escape}}(x_{j-1}, j-1, v)}{k} \right) \quad (9.34)$$

$$S(1) = \frac{E \left(T_{\text{current}} + d \left(\frac{c}{v} \right) + \dots + G_{\text{escape}}(x_{j-2}, j-2, v) \left(\frac{c}{v} \right) + \frac{G_{\text{escape}}(x_{j-1}, j-1, v)}{k} \left(\frac{c}{v} \right) \right)}{3.262} \\ (G_{\text{escape}}(x_{j-1}, j-1, v) + S(0)) \cdot \left(\frac{c}{v} \right) \left(\frac{G_{\text{escape}}(x_{j-1}, j-1, v)}{k} \right) \quad (9.35)$$

$$S(2) = \frac{E \left(T_{\text{current}} + d \left(\frac{c}{v} \right) + \dots + G_{\text{escape}}(x_{j-2}, j-2, v) \left(\frac{c}{v} \right) + \frac{2G_{\text{escape}}(x_{j-1}, j-1, v)}{k} \left(\frac{c}{v} \right) \right)}{3.262} \\ (G_{\text{escape}}(x_{j-1}, j-1, v) + S(0) + S(1)) \cdot \left(\frac{c}{v} \right) \left(\frac{G_{\text{escape}}(x_{j-1}, j-1, v)}{k} \right) \quad (9.36)$$

$$S(k) = \frac{E \left(T_{\text{current}} + d \left(\frac{c}{v} \right) + \dots + G_{\text{escape}}(x_{j-2}, j-2, v) \left(\frac{c}{v} \right) + G_{\text{escape}}(x_{j-1}, j-1, v) \left(\frac{c}{v} \right) \right)}{3.262} \\ (G_{\text{escape}}(x_{j-1}, j-1, v) + S(0) + S(1) + \dots + S(k)) \cdot \left(\frac{c}{v} \right) \left(\frac{G_{\text{escape}}(x_{j-1}, j-1, v)}{k} \right) \quad (9.37)$$

By adopting this function, simulation is run for the speed of $0.1c$, $0.2c$, $0.3c$, $0.4c$, $0.5c$, $0.6c$, $0.7c$, $0.8c$, $0.9c$, and c and the maximum distance reachable to double digits precision. The resulting graph is plotted below and the closed form derived based on the 4th order polynomial regression analysis is obtained:

$$y = ax^4 + bx^3 + cx^2 + dx + f \tag{9.38}$$

$$a = -4.1028 \cdot 10^{-8} \quad b = 0.0000186725 \quad c = -0.00438047$$

$$d = 0.918646 \quad f = -0.00850667$$

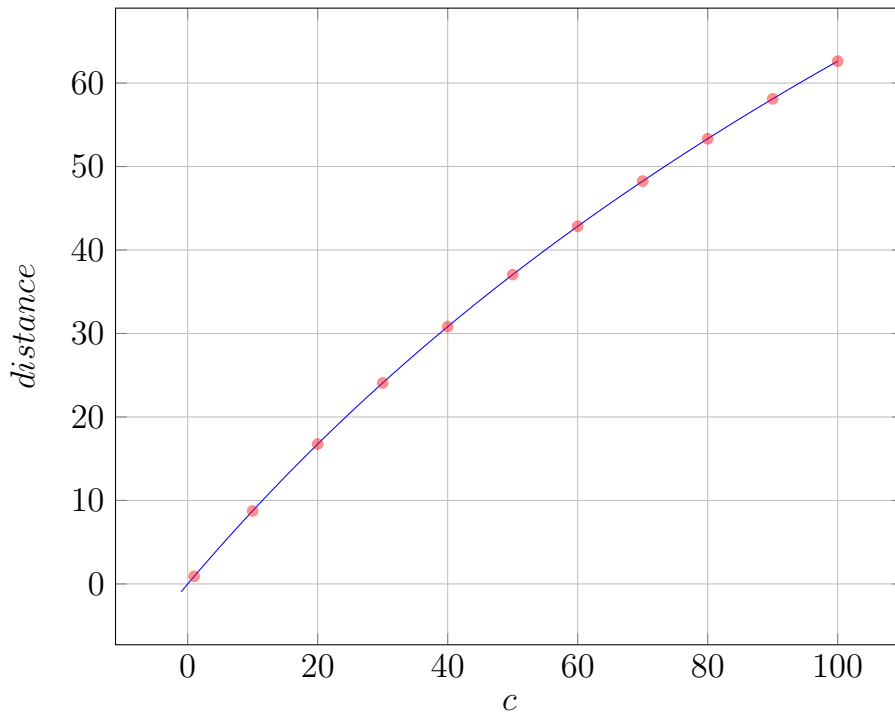


Figure 9.4: Reachable distance vs speed of light

The plot indicates that as the speed approaches c , the maximum distance reachable decreases. This is not surprising as one with a higher speed is able to reach distance further away, objects located further away are also moving away faster. The target location is also moving away faster relative to earth. As a result, the actual distance one needs to travel grows significantly as one tries and capable of reaching distance further away. The net consequence is that the furthest distances reachable grow sublinearly as the speed increases. Therefore, the limit of our reach is 6.266 billion light years by comoving distance, or at the redshift about $z = 1.5$. This is the upper limit of spatial distance we can ever reach if we travel at the speed of light. This is the current comoving distance from earth. It is not the observed signal distance from such location. Since it takes 6.266 billion light years to reach us from this location currently, its currently observable snapshot of itself must be from less than 6.266 billion light years ago because it was closer to earth. Therefore, from the perspective an earth observer, the furthest he/she can reach is less than 6.266 billion light years. We can use our equation $E(d, v)$ with a modified condition that computes the co-moving distance of the object where light is emitted.

We set $v = c$ and $E_{comoving}(d, v) = 6.266$ Gly to back-derive the apparent distance d .

$$E_{comoving}(d, v) = G_{escape}(d, 0, v) + \sum_{n=1}^{t=T_{current} \& G_{escape}(x_{j,j}, v)=d} G_{escape}(x_n, n, v) \quad (9.39)$$

$$S(0) = \frac{E\left((T_{current} - d) + d\left(\frac{c}{v}\right) + \dots + G_{escape}(x_{j-2}, j-2, v)\left(\frac{c}{v}\right)\right)}{3.262} \\ (d + G_{escape}(d, 0, v) + \dots + G_{escape}(x_{j-1}, j-1, v)) \cdot \left(\frac{c}{v}\right) \left(\frac{G_{escape}(x_{j-1}, j-1, v)}{k}\right) \quad (9.40)$$

$$S(k) = \frac{E\left((T_{current} - d) + \dots + G_{escape}(x_{j-2}, j-2, v)\left(\frac{c}{v}\right) + G_{escape}(x_{j-1}, j-1, v)\left(\frac{c}{v}\right)\right)}{3.262} \\ (d + G_{escape}(d, 0, v) + \dots + G_{escape}(x_{j-1}, j-1, v) + S(0) + S(1) + \dots + S(k)) \cdot \left(\frac{c}{v}\right) \left(\frac{G_{escape}(x_{j-1}, j-1, v)}{k}\right) \quad (9.41)$$

Alternatively, one can use the sets of equations for calculating the comoving distance based on the redshift, whereas z is the redshift, $\Omega_m = 0.286$ is the total matter density, $\Omega_\Lambda = 0.714$ is the dark energy density, $\Omega_k = 1 - \Omega_m - \Omega_\Lambda$ represents the curvature, H_0 is the Hubble parameter today, and $d_H = \frac{c}{H_0}$ is the the Hubble distance.

$$E(z) = \sqrt{\Omega_r(1+z)^4 + \Omega_m(1+z)^3 + \Omega_k(1+z)^2 + \Omega_\Lambda} \quad (9.42)$$

whereas comoving distance is:

$$d_C(z) = d_H \int_0^z \frac{dz'}{E(z')} \quad (9.43)$$

Transverse comoving distance:

$$d_M(z) = \begin{cases} \frac{d_H}{\sqrt{\Omega_k}} \sinh\left(\sqrt{\Omega_k} d_C(z)/d_H\right) & \text{for } \Omega_k > 0 \\ d_C(z) & \text{for } \Omega_k = 0 \\ \frac{d_H}{\sqrt{|\Omega_k|}} \sin\left(\sqrt{|\Omega_k|} d_C(z)/d_H\right) & \text{for } \Omega_k < 0 \end{cases} \quad (9.44)$$

Angular diameter distance:

$$d_A(z) = \frac{d_M(z)}{1+z} d_A(z) = \frac{d_M(z)}{1+z} \quad (9.45)$$

The finally derived results indicates that a redshift $z = 0.5037$ satisfies the condition for a current comoving distance of 6.266 billion light years, and angular diameter distance is 4.1503 Gyr. That is, the furthest object reachable appears to be at 4.1503 billion light years away. By setting hubble constant to 69.6 km/s instead of 74 km/s to keep it consistent with the first result, our own equation $E(d, v)$ indicates 4.2343 Gyr in apparent distance. The discrepancy results from different values of Ω_m and Ω_Λ .

Careful analysis indicates that this conclusion is only partially right. Although it is true that by the time the signals transmitted at 4.2 Gly away at the 4.2 Gya reaches earth, the original object that gave the signal's comoving distance will shifted to 6.266 Gly away, it will happen in the future because the light travel time is longer than 4.3 Gly due to the expansion of the universe. That is, the signals transmitted from 4.2 Gly away at 4.2 Gya is still on its way and have not reached us. In fact, this object's comoving distance is only 5.7 Gly at the current time. As a result, one needs to find the object that currently at a comoving distance of 6.266 Gly. Through back extrapolation, we found that the distance is at 4.642 Gly. However, light transmitted at 4.642 Gly away at 4.5 Gya still yet to reach us, so we must find an earlier snapshot of this object at a closer distance to earth. We compute the comoving distance of this object vs time and find the 4th order polynomial to great precision.

$$A_{62.7}(x) = 2.02 \cdot 10^{-9}x^4 + -4.2 \cdot 10^{-6}x^3 + 0.005141x^2 + 0.419x + 2894.93 \quad (9.46)$$

We then run the simulation and find that only signals transmitted at 5.7948 Gya and from this object when it was located at 4.276196 Gly away by comoving distance are currently reaching earth.

We then compute the various comoving distance of objects vs time as well as the signals transmitted time and its comoving distance. The graph shows that the intersections between the red curve and the blue curves determine the age and the comoving distance of the signals transmitted which we are currently receiving.

$$A_{2.8}(x) = 6.3618 \cdot 10^{-11}x^4 + 216.576 \quad (9.47)$$

$$A_{9.3}(x) = 7.47 \cdot 10^{-11}x^4 + 0.127x^{1.2} + 349.085 \quad (9.48)$$

$$A_{23.9}(x) = 1.1216 \cdot 10^{-10}x^4 + 9.52 \cdot 10^{-4}x^2 + 1329.15 \quad (9.49)$$

$$A_{37.9}(x) = 1.3281 \cdot 10^{-9}x^4 - 2.9 \cdot 10^{-6}x^3 + 3.56 \cdot 10^{-3}x^2 + 1800.73 \quad (9.50)$$

$$A_{50.3}(x) = 1.7281 \cdot 10^{-9}x^4 - 3.7 \cdot 10^{-6}x^3 + 4.58 \cdot 10^{-3}x^2 + 0.086x + 2371.12 \quad (9.51)$$

$$A_{74.9}(x) = 2.7513 \cdot 10^{-9}x^4 - 6.1 \cdot 10^{-6}x^3 + 7.49 \cdot 10^{-3}x^2 - 0.21x + 3592.25 \quad (9.52)$$

$$A_{94.3}(x) = 3.919 \cdot 10^{-9}x^4 - 9.2 \cdot 10^{-6}x^3 + 0.0112x^2 - 1.144x + 4712.45 \quad (9.53)$$

$$A_{149.8}(x) = 6.3863 \cdot 10^{-9}x^4 - 1.45 \cdot 10^{-5}x^3 + 0.0165x^2 - 0.42x + 6997.63 \quad (9.54)$$

$$y_{determinant} = -5.1264 \cdot 10^{-9}x_{11}^4 + 1.04 \cdot 10^{-5}x - 0.0123x + 0.06x_{11} + 6920.44 \quad (9.55)$$

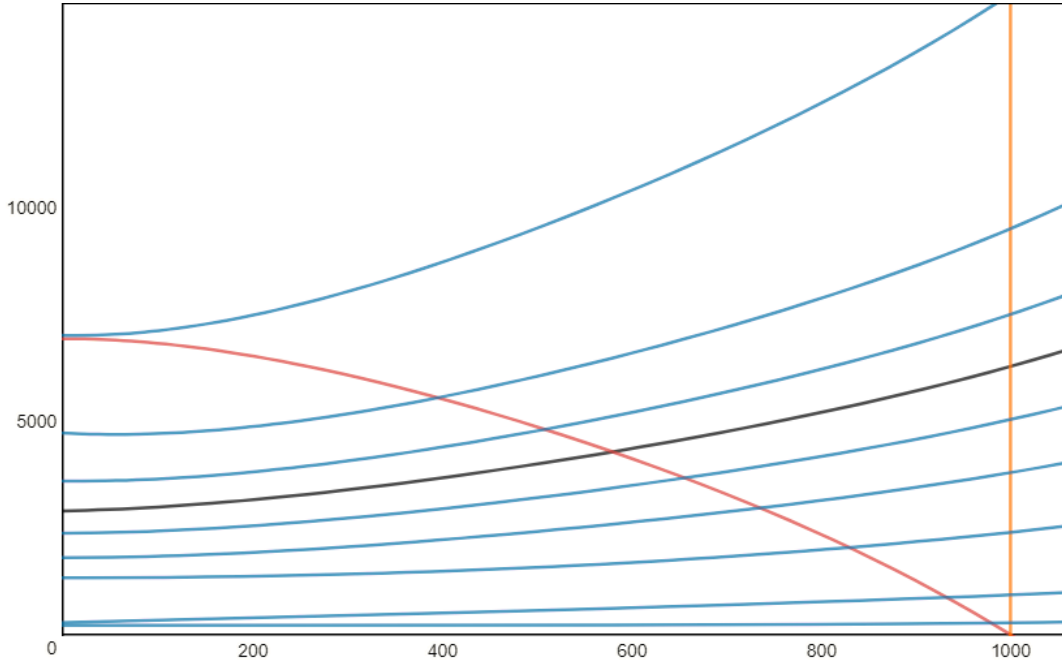


Figure 9.5: The age and the comoving distance of the signals determinant, 1000 = current time, vertical axis represents lookout distance in 1 Myr and horizontal axis represents lookback time in units of 10 Mly. The black curve represents the catchable limit in which the current comoving distance at 6.266 Gly.

Certainly, this is a very limited range provided that the observable universe in 27.6 billion light years in diameter and 98 billion light years in diameters in terms of comoving distance.

9.2 Connected/Disconnected

Given that each expanding civilization can only expand up to 6.266 billion light-years in radius, we can then deduce a different kind of future of the universe. The one which we are already familiar is the observation and calculation done in recent years and more distant past by general relativity. The universe can be regarded either as acceleratingly open, open, flat, or closed based on its spacetime geometry, the effects of gravity, and the role of dark matter and dark energy. We now know that dark energy is playing an increasing role in the acceleration of the expansion of the universe, and likely that our universe will remain accelerating open to the indefinite future.

Knowing the cosmic distribution of intelligent species scattered within the cosmos, we come up with two different possibilities for the future of the universe: connected or disconnected.

In order for the universe to be connected, three possible scenarios are presented:

1. Given that the current emergence rate of expanding civilization is high so that more than one expanding civilization lies within the 12.532 Gy light years (6.266 Gy ly times 2) distance from earth since we know that the outermost limit of the reaches by expanding civilization originating from earth can only reach 6.266 Billion light years in radius. At the same time, the Background evolutionary rate BER is significantly higher than 1 so that even more expanding civilization emerges within the 12.532 Gy light years radius from earth in the future.
2. If the Background evolutionary rate BER is 1 or very close to 1, so that almost no other extraterrestrial civilizations arise in the future, then the current emergence rate permits the nearest arising civilizations have to be within 12.532 Gy light years radius from earth.
3. If the current emergence rate is so low that it takes a radius of more than 12.532 Gy light years, then the Background evolutionary rate BER must be high enough so that the expanding civilization eventually appears within 12.532 Gy light year radius.

The universe is disconnected if:

1. If the current emergence rate is so low that it takes a radius of more than 12.532 Gy light years, and the Background evolutionary rate BER is 1 or even less than 1, as the number of civilization emerges decreases as time passes.

Knowing the above constraints, we can back extrapolate whether our observable universe is connected or disconnected from the rest by observing the local fauna genome complexity on each habitable planets within the Milky Way galaxy. Once we confirm our YAABER and BER for habitable planets within our and neighboring galaxies falls into the first three scenarios,

then we will have a high confidence that our part of the universe will be connected with the rest.

Nevertheless, we have a great confidence in predicting the universe seem to be connected even without visiting and collecting samples from each of the habitable planets.

Our current model predicts that the nearest extraterrestrial civilization lies 88.44 million light-years away. This conclusion, satisfies both scenarios 1 and 2, regardless of the Background Evolutionary Rate.

Now, assuming that the emergence of life on earth is unique and early that the emergence rate is much lower and the radius of emergence is larger than 12.532 Gy light years. If we take our observation on earth's biological development, then the universe is still connected because BER is much higher than 1, satisfying scenario 3. Since habitable planets only exist at 5.0 Gya at the earliest, given the prevalence of Gamma-ray bursts from the metal-poor past of cosmic history and the gradual development of spiral arms away from the galactic central cores, then the timing and the emergence of life on all habitable planet should be in a similar stage. Since oxygen readily reacts with other elements, no free oxygen will be available on any proto earth-like planet in its early evolutionary stages. Only when photosynthesis evolved among the bacteria type of living organisms on such a planet and gradually filled the oxygen sinks in both the oceans and the lands will eukaryotic cell and multicellular life becomes possible. Furthermore, the buildup of oxygen is directly related to the rise of continental plates, which is a logical consequence of the gradual cooling of a Earth-like planet. As a result, oxygen buildup can only become possible 2 to 3 Gyr after the formation of earth analogs. Since 5 Gyr has passed on the earliest possible planet to host life, and the average age of earth like habitable planets are younger than earth. Then it is very likely that currently earth-like planets with an average, a typical age of 3 Gyr form continental plates and start the buildup of oxygen and the evolution of the eukaryotic type of cell (oxygen-consuming cell). It takes another 2 billion years for the eukaryotic cell to evolve into multicellular life form including invertebrates, anthropods, vertebrate fish, amphibians, reptiles, mammals, and birds. Additionally, it will take on average another 0.8 Gyr to reach human-like creature given that evolution of Homo sapiens is rather rare. 0.54 Gyr of multicellularity on earth + 0.26 Gyr of YAABER (1.76 Gyr of YAABER based on the current BER but it is translated into 0.26 Gyr into the future by taking the complexity transformation into consideration. Check Chapter 7 Section 7.4). Then, 2.8 Gyr into the future, a typical earth analog hosts earth like civilization and begins its expansion, and the average distance between each civilization will be within the size of their home galaxy.

Knowing that the universe is connected, then one can also calculate the minimum possible speed that one can expand to remain connected with each other. For biological led species, colonization at a slower speed gives the species more choices even if it is not the most economic optimal one. (Obviously, less burden on taxpayers as we have shown from Chapter 8)

Finding the minimum expansionary speed to remain connected under scenario 2 one needs to specify the minimum distance between our nearest neighbors. If our neighbor lies x light years

away and $0 < x < 12.532$ Gy light years, then the minimum speed requirements for a connected universe is (assuming both moves toward each other) derived from the inverse of the closed form for distance vs. speed:

$$y = D(x) = ax^4 + bx^3 + cx^2 + dx + f \quad (9.56)$$

$$S_{peed} = D^{-1}\left(\frac{y}{2}\right) \quad (9.57)$$

$$\frac{x}{2} = ay^4 + by^3 + cy^2 + dy + f \quad (9.58)$$

and we can illustrate it graphically by assuming that the nearest neighbor is 6.8 Gy light years away at the current comoving distance and both sides are rushing toward each other. Then both sides need to cover 3.4 Gy light years of distance. As a result, both sides need to travel at least at the speed of $0.45011c$ to stay connected.

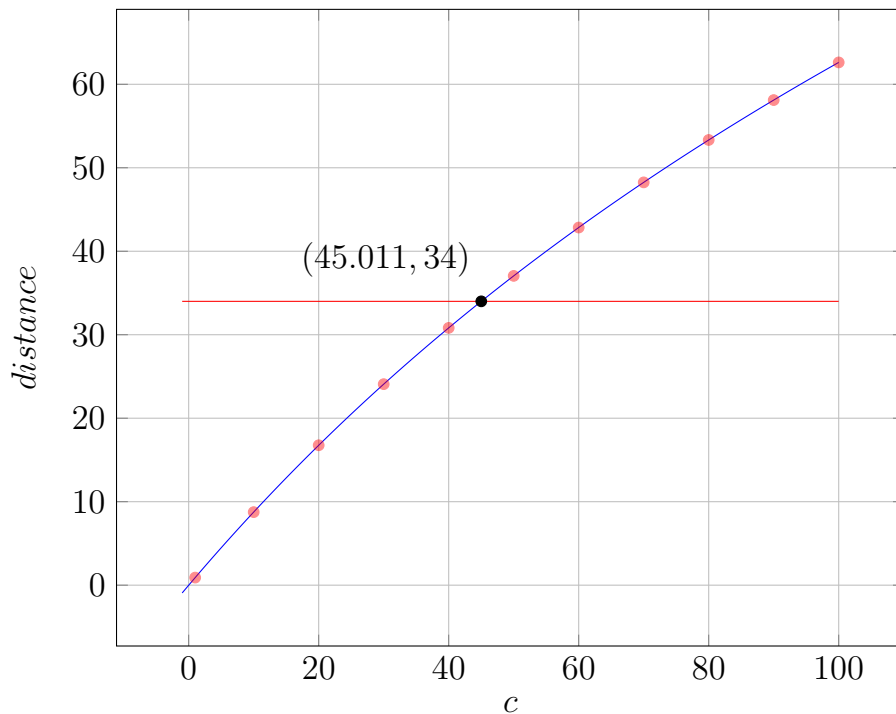


Figure 9.6: Reachable distance vs speed of light

Finding the minimum speed of expansion under scenario 3 requires first knowing the time at which the emergence rate falls below 12.532 Gy light years radius. Then, one needs to specify the exact distance between the neighbor to connect. Assuming it takes x years waiting time for the emergence of expanding civilization to fall below 12.532 Gy light year radius, and the Background evolutionary rate drops to 0 afterward so no closer civilization will appear. This can be possible if the condition of creating earth-like planets is much more stringent than what we have proposed and the growing metallicity of the galaxy prevents future arising terrestrial planets in general. Then, depending on the distance between us and our neighbor x years into the future, one can derive the minimum speed required for our own expansion. The speed will

always be less than the expansion speed of our neighbor since we started now and spent the entire waiting time expanding toward the edge of our sphere of influence.

For various travel distance, the final rescaled distance before catching the target destination varies with speed, the plotted graph for a distance of 0.875 Gy light years, 2.4 Gy light years, 3.675 Gy light years, and 52 Gy light years respectively is presented. Each is represented by a different gradient curve, and their closest approximated closed form is listed below:

$$D_8(v) = (x - 0.0875)^{-0.71} + 8.29 \quad (9.59)$$

$$D_{24}(v) = (x - 0.24874)^{-1.505} + 27.874 \quad (9.60)$$

$$D_{38}(v) = (x - 0.363)^{-2.5} + 52.855 \quad (9.61)$$

$$D_{52}(v) = (x - 0.17318)^{-8.9} + 88 \quad (9.62)$$

One can easily interpret that at the slower speed the total distance one has to travel increases up to the point where the minimum speed required to catch the target destination. For targets at greater distances, the minimum speed required to catch the destination increases accordingly. With the known distance of target destination and the rescaled final distance, one can also determine the total time spent cruising toward such destination, which can be obtained by simply add adding a speed factor, an example is given for a travel distance of 0.875 Gy light years:

$$D_{8.75}(v) = (v - 0.0875)^{-0.71} + 8.29 \quad (9.63)$$

$$T_{8.75}(v) = \frac{1}{v} \left((v - 0.0875)^{-0.71} + 8.29 \right) \quad (9.64)$$

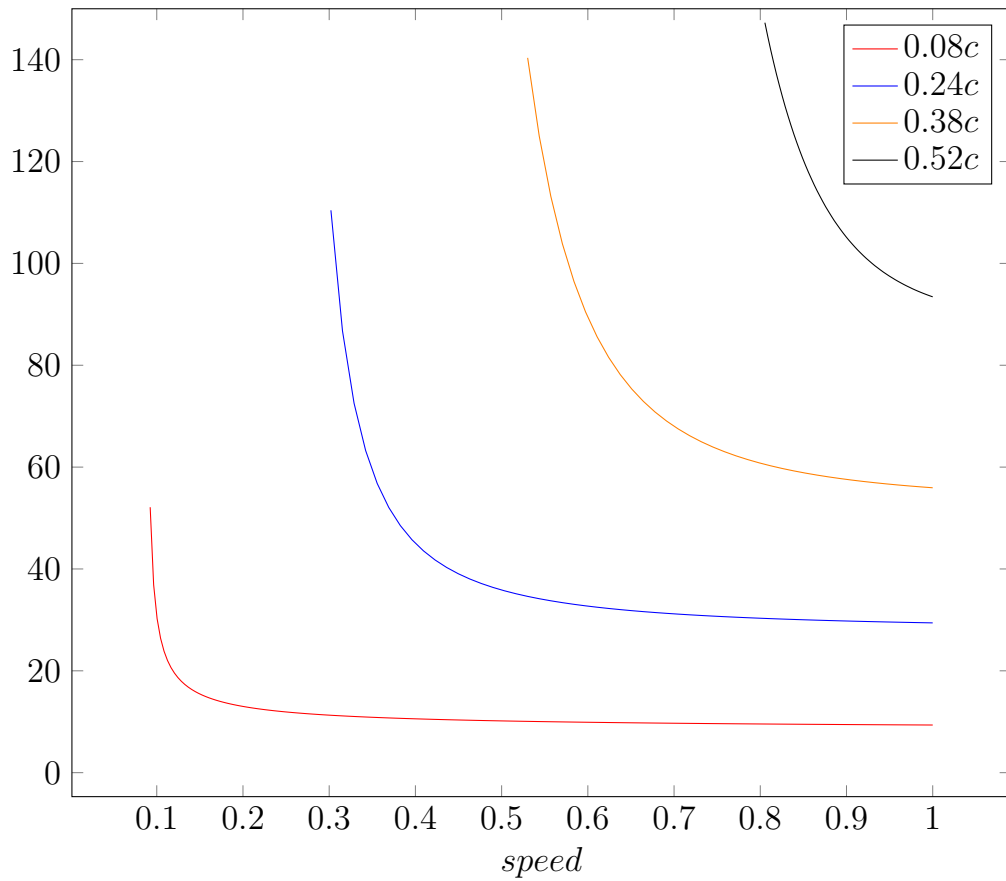


Figure 9.7: Speed vs dist traveled

and can be generalized to any distance as:

$$D_x(v) = (v - a)^{-b} + c \quad (9.65)$$

$$T_x(v) = \frac{1}{v} \left((v - a)^{-b} + c \right) \quad (9.66)$$

As a result, one obtains the final distance to be traveled and the total time spent traveling for a given distance d and travel speed v . The inverse relationship between the travel speed v and travel distance d is derived based on the $E(d, v)$ recursive function as we derived earlier.

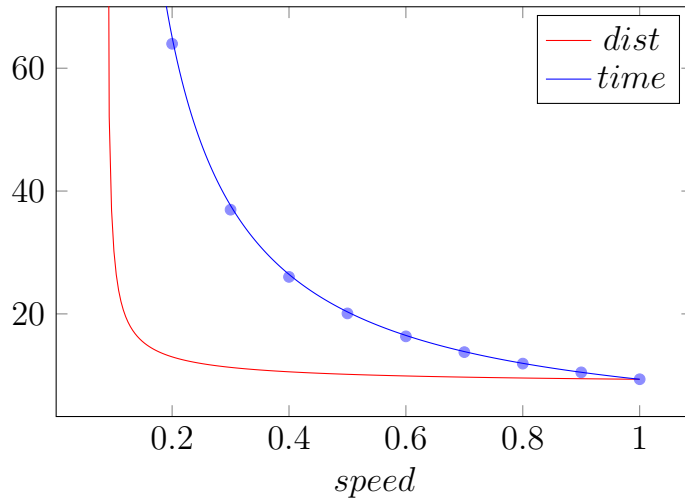


Figure 9.8: Distance and time

Then, one adds the waiting time for the emergence of the extraterrestrial neighbor and derives one's own minimum speed required to reach the destination.

and it can be shown that:

$$T(d, v) = \frac{1}{v} \cdot E(d, v) \quad (9.67)$$

$$S_{speed} = \frac{E(D_{emerge}, v)}{T(D_{emerge}, v) + T_{wait}} \quad (9.68)$$

Whereas S_{speed} is the minimum speed in which the universe can be connected. D_{emerge} is the emerging distance of the closest neighbor D light years away. $E(D_{emerge}, v)$ is the actual distance one needs to travel with a speed of v so that $\max_{\min v} E(D_{emerge}, v) < \infty$. That is, the minimum expansion speed required so that one can remain connected with one's neighbor. $T(D_{emerge}, v)$ is the total time it takes for it to be connected with its neighbor at the minimum speed v . T_{wait} is the waiting time in years before your neighbor emerges at a distance of D_{emerge} light years away.

However, a caveat has to be thrown. We assumed the T_{wait} is significantly less than the current age of the universe and distances between the nearest neighbor's redshift $Z < 0.5$. So that the overall cost reduction of a leisure expansion at a slow speed can be justified and outweigh potential costs of a slight increase in travel time and distance due to the expansion of the universe.

That is, having a head start over your neighbor is always advantageous. You can expand more slowly than your neighbor by starting expansion during the waiting period to reach the halfway distance between you and your emerging neighbor. Or you can expand at the full speed and expand well into your neighbors' supposed space.

$$S_{speed} = \frac{E(D_{emerge}, v)}{T(D_{emerge}, v) + T_{wait}} \leq \frac{E(D_{emerge}, v)}{T(D_{emerge}, v)} \quad (9.69)$$

In the most likely scenario 1, in which we assume not only life on all habitable planet formed 4 Gyr ago or earlier have attained the status of multicellularity but actually evolved and filled on ecological niches and our nearest neighbor is 88.44 million light-years away and no other intelligence arises again. We solve the minimum speed requirement for the recursive function reaching its maximum finite value with specified constraint of 88.44 million light years (to have the universe connected):

$$\max_{\min v} E(88.44\text{Mly}, v) < \infty \quad (9.70)$$

we found that:

$$E(88.44\text{Mly}, 0.00492c) < \infty \quad (9.71)$$

Then, we need to only expand at most 0.00492c, about 0.492 percent of the speed of light in order for the universe to be connected. Of course, this is an over-estimation because the background evolutionary rate at 2.7 will guarantee the eventual emergence of expanding civilization within our own galaxy, rendering the closest civilization within reach even with conventional rocket speeds. The easiest way to verify the connectedness of the universe shall be relying on the next generation digital instrumentation to measure the atmospheric content of all potentially habitable planets. If any, or even most of the habitable planet we find have detected traces of oxygen, then it is likely that Eukaryotic type of organisms must already be present on them. If the oxygen concentration is comparable to earth or even higher, then multicellular life is likely to flourish.

9.3 Cosmic Nash Equilibrium

Most excitingly, if all arising extra-terrestrial industrial civilizations adopt wormhole based trade networks, then it can be shown that every expanding extra-terrestrial industrial civilization constructs their own networks before its contact with any nearby civilization. Once it does make contact with another, they can connect their network with that of the other. How the standard is enforced and agreed upon remain into the details of the technical specification, much like the ISO protocol or the 4G wireless network discussed in recent years. If the universe is indeed infinite or indeed extremely large, then, as predicted before, there can be infinitely many intelligent extra-terrestrial industrial civilizations expanding and adopting wormhole networks. When all these networks are connected, then an infinitely vast universe can be traversed from edge to edge in a finite amount of time if the cost of C is small. It will remain whether such network can be maintained into the indefinite future given the accelerating expansion of the universe or enough energy to maintain it indefinitely. It is to show, however, that *it*

is theoretically sound that an expanding cosmic civilization, by constructing its own wormhole network, will eventually have a chance to meet every other alien civilization within the universe in a finite amount of time, and every other alien civilization can also meet each other. I call this the Principle of Universal Contacts.

Do extra-terrestrial industrial civilizations have to expand even given the incentives we have described above? Is there any other reason or incentive for them to expand? It seems that Nash Equilibrium, at the cosmic scale, can also play a role in the decision each civilization will make. If we formulate a utility function f where the maximization of the function is the total diversity of all possible industrial civilizations arising from all possible planets, then, every civilization should not expand and simply wait for their neighboring stars incubating the next industrial civilization. However, once a civilization is able to calculate how much ahead they are in terms of YAABER against the cosmic mean evolutionary rate, it will be able to calculate their nearest neighbor. In our case, if we assume that the avian, reptilian, and mammalian level of genome complexity is the average of all terrestrial habitable planets, then our nearest neighbor is 88.44 million light-years away. Due to the speed of light, we will not be able to communicate with them prior; therefore, one has to ask for the optimal strategy one has to play knowing the presence of other players while with the absence of other information. The game choices are presented in the boxes below:

	Earth Expands	Earth did not Expand
Alien Expands	$(-\frac{R}{2}, -\frac{R}{2}) *$	$(0, R)$
Alien did not Expand	$(-R, 0)$	$(0, 0)$

Table 9.1: Cosmic nash equilibrium strategies

It can be shown that the expansionary strategy is the cosmic Nash Equilibrium. If our neighbor expands at the same time as we are making decision, we also need to expand so that we will maintain our sphere of influence with a radius that is at the best half the distance between earth and the next extra-terrestrial civilization's origin. If our neighbor does not expand, then we have at best a sphere of influence with a radius the distance between earth and the nearest extra-terrestrial civilization. Of course, such expansionary strategy's gain is at the expense of potential and future arising technological civilizations suppressed locally by the dominant early forming industrial civilizations. So an expanding civilization causes a lose at the cosmic scale with a negative value for biodiversity.

Furthermore, a Nash Equilibrium is also played against all players across all temporal periods. It is almost inevitable that a rational player will probably know that there are possibly earlier arising civilizations within its neighborhood, but by whatever reasons choose not to expand, and there are definitely going to be future arising civilizations may either choose to expand or not to expand. Since the player itself has no absolute understanding of its vicinity until it is fully explored, its best strategy is to expand because it can not communicate with the past nor

can it communicate with the future without the cost of sacrificing its first-mover advantage. The civilization has only two choices. It can wait or travel near the speed of light until the next industrial civilization arises in the neighborhood.

As a result, a rational player will not wait until it meets its closest neighbor and will expand according to Nash Equilibrium

from both temporal and spatial point of view. If we assume every arising extra-terrestrial industrial civilization is a rational player, then we can predict that the universe will be segregated by early arising industrial civilizations' sphere of influence and no particular civilization is significantly dominating since the earliest possible arising industrial civilization in the observable universe cannot be older than 0.232 Gyr (See Chapter 7). In other words, the universe is segregated into more or less even sized sphere of influence of different extra-terrestrial civilizations. Since wormholes are constructed, information and decision making between each player can be carried out with a cost of at most C . Since the universe is assumed to exist for a long time into the future, then it is expected that players in this multi-player game will seek cooperation for repeated transactions.

9.4 Looking Back in Time

Relativistic expansion of the wormhole network in coordination with other extraterrestrial industrial civilizations brings some remarkable results worthy examining. Wormhole network can be conceptually treated as a pipe with an entrance and an exit. One attaches the entrance of the wormhole at earth at the current time and stretches the wormhole near the speed of light toward the edge of our sphere of influence. Since the entrance and the exit of a wormhole stay connected at the same age, then our exit is not only 250 Myr light years in distance from our home planet but also at least 250 Myr years into the future. The wormhole network not only serves as a network connecting points in space, but it is also connecting points in time, as naturally indicated by its nature of connecting both space and time. Whats more interesting is at the point when you leave your wormhole network and enters into your neighbors. Strange things happen. Assuming that traversing the wormhole itself takes a negligible amount of time and you started your journey immediately at the completion of the wormhole, then by crossing into your neighbors' network you can quickly reach their home planet, by doing so, you are not only traversing distance but also time. At the edge of two wormhole networks, you are 250 Myr light years in distance from our home planet and at least 250 Myr years into the future. As you stare back at earth, you saw earth as it is now, because signals of earth's light travel along with the expansionary phase of the wormhole for a period of 250 Myr. However, as you reach the home planet of the alien civilization, you are 500 Myr light years in distance from our home planet but your time is now the same as you started your travel from earth. Staring backward at the earth, which is 500 Myr light years away, you see the earth from its Permian era before

the rise of Dinosaurs. Whereas the light from 250 Myr ago (it is not 500 Myr ago because it took us 250 Myr just to reach our civilization's boundary) just reaching you right now. If you don't travel nearly as far as to the home planet of the alien civilization and just simply cross into their territory, you can stare back to see every point of human civilization's development. We can view the earth as it was a century ago, a millennium ago, the start of the agricultural revolution, or our migration out of Africa, as watching a silent film. *I call this ability to skip ahead of signals escaped from the earth and staring back into our historical past Photographic Time Travel, Passive Time Travel, or Time Travel Mirage*, that is, you can observe the past events but not able in any way to affect it. Though this is not time travel in the purest sense, it is very comforting to validate its possibility. Photographic time travel brings some interesting consequences for cooperating extraterrestrial civilizations. As each civilization expands toward its civilization's boundary, it will be able to collect enough information about its intelligent neighbor since all of its evolutionary history is well within our grasp, quasi-military intelligence gathering type of manner; therefore, one knows well about their neighbors' vulnerabilities and comparative advantages. Similarly, our neighbor also knows our past history as it approaches our border. As a result, both sides will know the possible intention of the other, rendering war-like behavior less likely. More importantly, our neighbor will have a huge incentive to peacefully enter our network to collect historical information about their past and vice versa. In a sense, the information capture and storage of a civilization's past is probably one of the primary incentive to trade in an information market of the global cosmic interconnecting wormhole network.

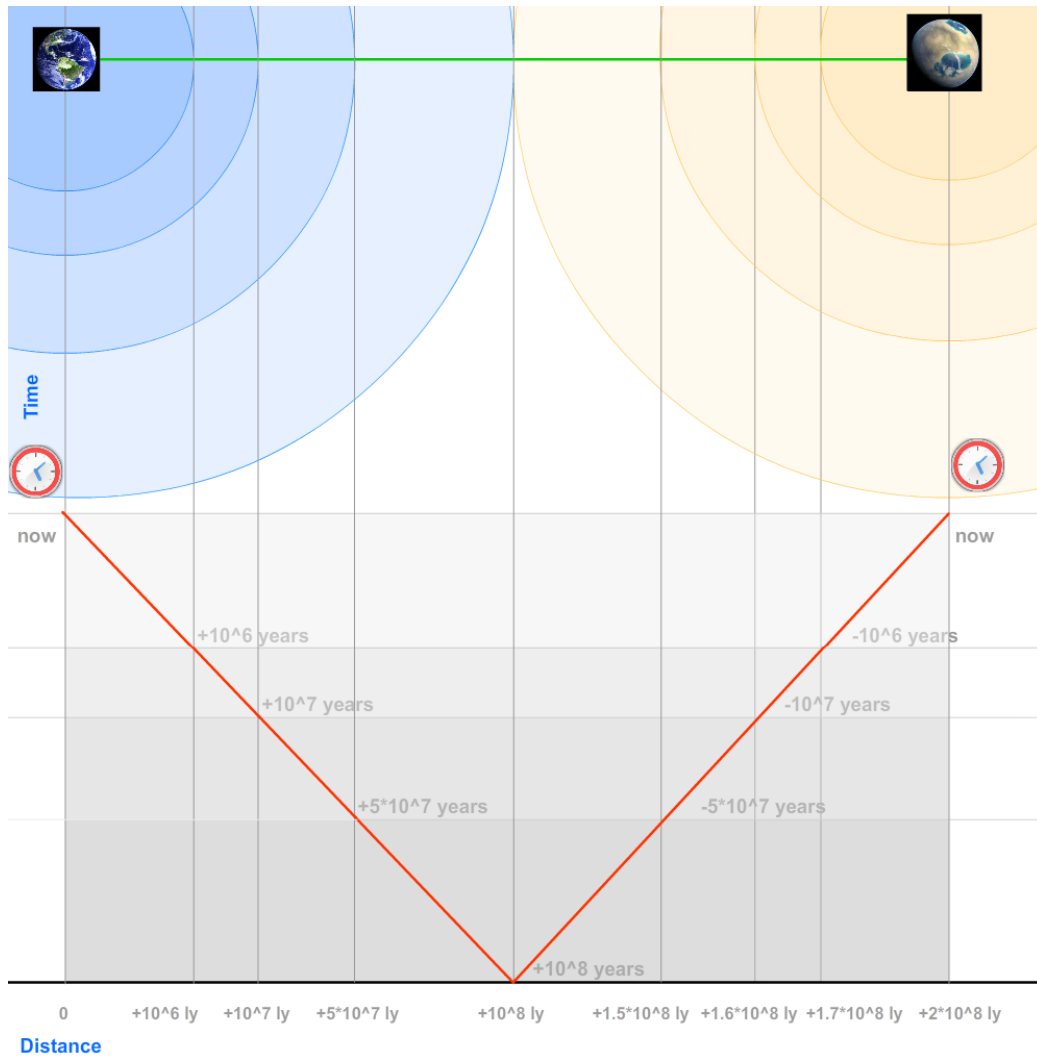


Figure 9.9: Photographic time travel

If the nearest civilization is 200 Myr years away, how can one be sure that earth's reflected lights and signals are visible given the enormous distance involved? In order to answer this question, one has to resort to the law of Telescope. In order to render the image of earth from a given distance, enough photons leaving earth must be captured. If the angle between two distant points is θ , the light in question has a wavelength of λ , and the size of your telescope is D across, then the smallest resolvable angle is approximately[73]:

$$\theta = \frac{\lambda}{D} \quad (9.72)$$

A telescope of an arbitrarily large size can be constructed by networking many smaller ones together. If something that's a large distance L away, and that is a size S across, takes up an angle of approximately:

$$\theta = \frac{S}{L} \quad (9.73)$$

So, if you want to be able to see something, you need [73]:

$$\frac{S}{L} \geq \frac{\lambda}{D} \quad (9.74)$$

Assuming visible light has a wavelength of $\lambda = 0.5 \cdot 10^{-6}$ m, and a viewing distance of $L = 2 \cdot 10^8 \cdot 63,241 \cdot 1.495 \cdot 10^{11}$ m (200 Myr in units of meters), and a human appearance size of 0.3 m, we can solve for the size of the telescope required.

$$D = \frac{\lambda L}{S} \quad (9.75)$$

$$\begin{aligned} & \frac{(2 \cdot 10^8 \cdot 63,241.0771 \cdot 1.49597871 \cdot 10^{11} \cdot 0.5 \cdot 10^{-6})}{0.3 \cdot (1.49597871 \cdot 10^{11}) (63,241.0771)} \\ & = 333.333 \text{ ly} \end{aligned} \quad (9.76)$$

By using the equation above, one finds that the size and diameter of the telescope (a spherical one to capture enough photons) have to be 333 light years across to resolve fine details of human size.

$$\begin{aligned} & \frac{(2 \cdot 10^8 \cdot 63241.0771 \cdot 1.49597871 \cdot 10^{11} \cdot 0.5 \cdot 10^{-6})}{3 \cdot 10^7 \cdot (1.49597871 \cdot 10^{11})} \\ & = 0.211 \text{ AU} \end{aligned} \quad (9.77)$$

If one intends just to capture an image of earth, the requirement is significantly smaller, at merely 0.21 Astronomical unit, or just 31,535,768 km.

Compares to the size and extent of one's civilization's sphere of influence, the cost of construction should be negligible. If we use the scientific budget of United States as the rule of thumb as to what percentage of the expanding galactic civilization is willing to invest in historical data collection, then we expect a diversion of 1% of their galactic resources at its construction (assuming a galaxy disc with 100,000 ly disc radius and 9,800 ly disc height). We can expect the civilization builds 11,962,697 stations of telescopes with 333 light years diameter across. Each galaxy would host on average 19,904 stations. (there are 601 galaxies in a 100 million light years diameter)

$$\begin{aligned} N_{telescopeingalaxy} &= \frac{(\pi \cdot 100,000^2 \cdot 9,800)}{\left(\frac{4}{3}\right) \pi (333.333)^3} \cdot \left(\frac{1}{100}\right) \\ &= 19845.0595351 \end{aligned} \quad (9.78)$$

Each telescope's received signal is reassembled and connected through the wormhole network so that signal delay can be minimized. Therefore, telescopes based on Photographic Time Travel is both theoretically feasible and economically practical from their perspective.

To generalize, we can further extrapolate when the average speed of expansion of all industrial civilizations within the universe is at a small fraction of the speed light c instead of nearing

the speed of light. Then, one crosses the boundary between our and our neighbor's civilization and staring back at earth will not be able to see our earth from our past, because light from the past already traveled much further away. Assume the wormhole network connects to n^{th} degree neighbors from our nearest neighbor or neighbor of the first degree of separation, then, one can traverse the network and track earth's prehistory from our n^{th} degree neighbor. The equation is given by:

$$N_{thneighbor} = \frac{(T_{waitconnect} \cdot c - T_{nearestdist})}{R_{avg}} \quad (9.79)$$

Where $T_{waitconnect}$ is the average time it takes for expanding civilizations to complete the construction of interconnecting wormholes. $T_{waitconnect}$ is then multiplied by c to derive the amount of distance traversed by photons at the speed of light since our expansion started. $T_{nearestdist}$ stands for the distance between earth and our nearest neighbor in light years. R_{avg} stands for the average diameter size of a civilization in light years. A prudent thinker may point out that $T_{waitconnect}$ should be the time it takes for the human civilization to complete the network and joining with the rest or the slowest time an n^{th} degree neighbor connects to the $n+1^{\text{th}}$ degree neighbor to form the bridge from earth to the civilization center of $n+1^{\text{th}}$ degree neighbor. However, an extremely slow expanding civilization will be outpaced by their neighbor so that territories they supposed to occupy will be occupied and developed by their neighbor. As a result, $T_{waitconnect}$ stands for the average

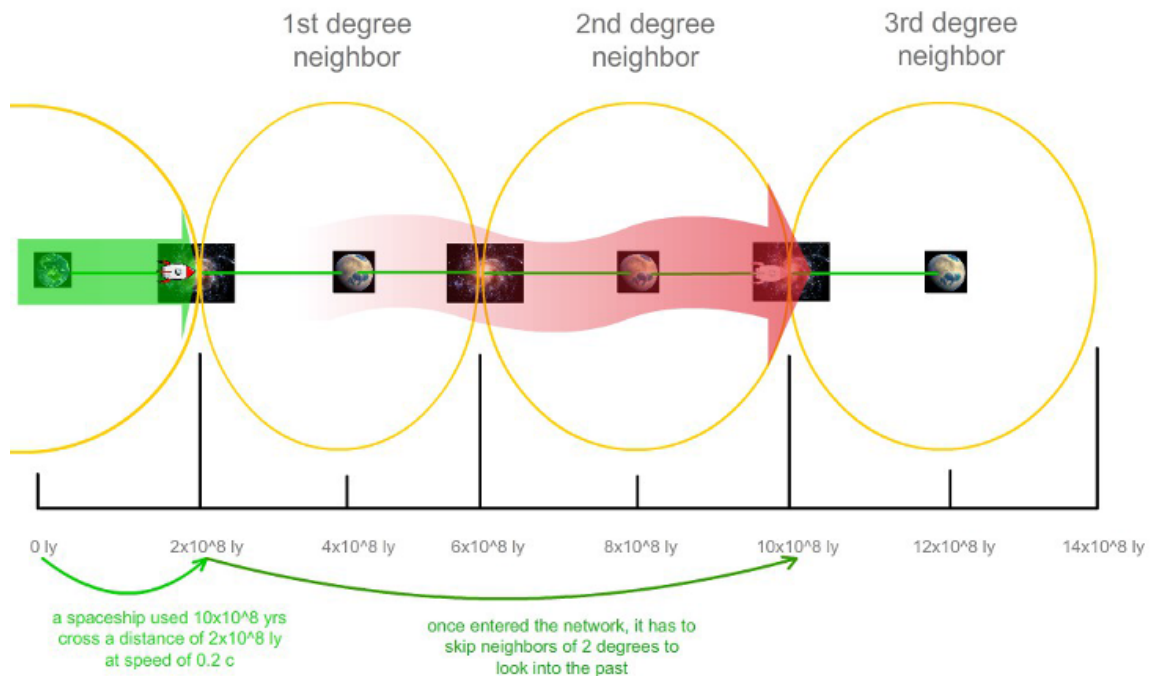


Figure 9.10: Reaches the n^{th} neighbor

time of cosmic wormhole network development and expansion. Although all civilization may reach a consensus from the economic perspective to develop the network not close to the speed

of light such as $0.9999c$, but rather at $0.1c$. In both cases, each civilization's past will be capturable from some remote distance, but the costs are not the same. The closer one has to travel to view one's past, the smaller the size of the telescope required. The further one has to travel to view one's past, the larger the size of the telescope required. Therefore, civilization before they met each other, will formulate models of cost and benefit analysis, to maximize their return. Nevertheless, viewing one's older past such as earth from the Hadean, and Archean era will require a higher cost to reach the same finite detail and resolution of eras close to today.

10 Conclusion

10.1 Extra-terrestrials vs. Time

Finally, we predict the pattern of future arising extra-terrestrial industrial civilizations based on the Background evolutionary rate of gradually increasing biological complexity and habitable planets formation model. We rescaled the earth formation rate function and right shifted it to 4 Gyr later to indicate that only after 4 Gyr of evolution will multicellular life evolve on any habitable planets. Then we formulated an inverse tangent function that matches the background evolutionary growth curve but tapers off as the mean biocomplexity at the time on any habitable planet reaches parity with the progress of Homo sapiens led industrial civilization. We also discounted any habitable planet that moved off the main sequence that renders the planet uninhabitable (We assumed that once a planet attained biocomplexity on parity with Homo sapiens, the habitability continues for another 1.3 Gyr at most with a weighted average including stars with mass less than the sun, with a total window of habitability of 5.8 Gyr). Lastly, the expansion of the universe is also taking into account.

The rate of habitable planet formation rate:

$$f_{earth}(x) = 2.655 \ln \left(1.1814 \cdot \left(-1.0454(x-0.274) + (1.73(x-0.48))^{\frac{1}{2.8}} \right) \right) \quad (10.1)$$

Biocomplexity growth diversity curve:

$$P_{biocomplexity}(x) = 0.75 \tanh 180(x - 1.013) + 0.75 \quad (10.2)$$

Universe expansion factor:

$$f_{cosmicexpansion}(x) = 0.822(x)^{\frac{2}{3}} + 0.0623 \left(e^{\frac{x}{0.645}} - 1 \right) \quad (10.3)$$

$$\frac{1}{f_{cosmicexpansion}(x)} \quad (10.4)$$

Total habitable planets minus those moved off the main sequence:

$$F_{earth} = \int_0^x [f_{earth}(x) - f_{earth}(x - 0.0942)] dx \quad (10.5)$$

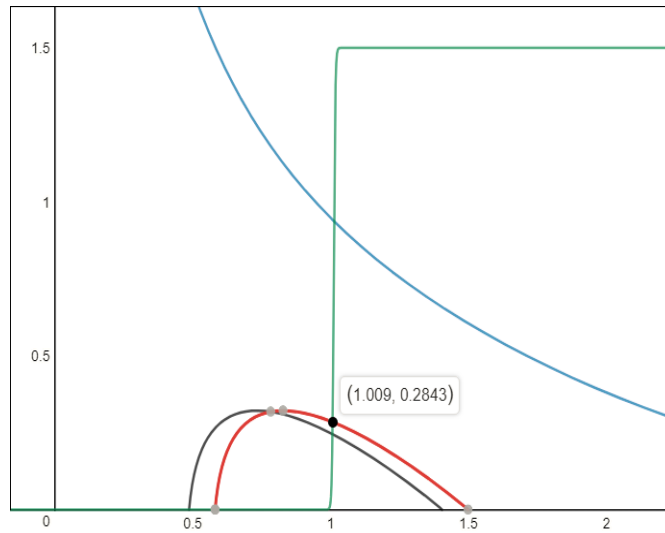


Figure 10.1: The rate of habitable earth production, the rate of habitable earth destruction, the rate of cosmic biological evolution, and the rate of cosmological spacetime expansion

The final plot for the total number of extra-terrestrial civilization ever will arise is listed below.

$$N_{civilization}(x) = \frac{F_{earth} \cdot P_{biocomplexity}(x)}{f_{cosmicexpansion}(x)} \quad (10.6)$$

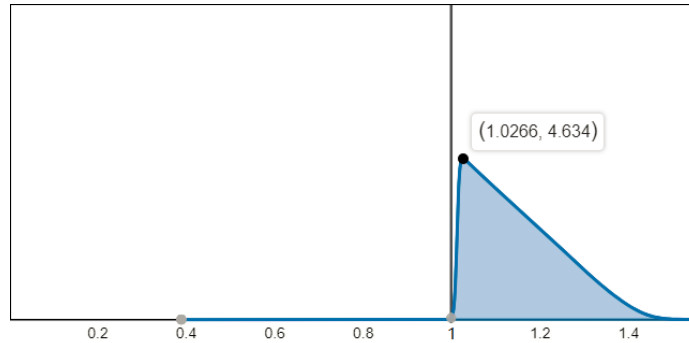


Figure 10.2: The number of extraterrestrial civilizations emergence in the future, note the rate decrease to zero in 1.5 times the time since the Big bang.

The peak of the number of extra-terrestrial industrial civilization production is reached at 367.08 Myr (taking the curve max at $(1.0266-1) \cdot 13.8 \text{ Gyr} = 0.36708 \text{ Gyr}$) into the future. The model confirms our earlier discussion and the assumption that life can be started locally here on earth in a relatively easy process. As the universe is becoming less energetic, threats from cosmic regulating mechanisms such as Gamma Ray Bursts, and Quasar-like super black holes were dominant in the cosmic past since the Big Bang decreased. Our position is somewhat advantageous or early compares to the mean, and this is to accommodate our observation. As a result, one should expect that the temporal window is open and the universe is just becoming

ripe for nurturing extra-terrestrial industrial civilizations and expecting a peak production in about 364.32 Myr. The number of future arising civilizations is primarily bounded by the star and planet formation rate, as the rate of production decreased to zero in 2 billion years, the last civilization emerges no later than 6.9 billion years into the future. The expansion of the universe does play some role at minimizing the number of arising civilizations within the observable universe, but the effect is minor since the number of arising civilization dropped to 0 before the extremely rapid expansion of the universe starts.

Finally, one can also predict that the extraterrestrial civilization distribution function itself is:

$$g_1 = \frac{N_0(x)}{17.6604 \cdot (2.7825594149)^x Q_1 \sqrt{2\pi}} e^{-\frac{(\ln(17.6604(2.7825594149)^x))^2}{2(Q_1)^2}} \quad (10.7)$$

$$\int_{x_1}^{x_2} N_{civilization}(x) \cdot dx = \int_{x_1}^{x_2} g_1 \cdot dx \quad (10.8)$$

unlike our earlier model which assumes that the total number of extraterrestrial civilizations is fixed within the temporal window of 5 Gya to 4 Gya, we now shows that the total number of extraterrestrial civilizations over the entire epoch also changes depends on the time period x_1 to time period x_2 under consideration.

As of now, the theory can be summarized to be based on the following key facts and inferences drawn from them:

There is a tremendous number of exoplanets (fact).

Earth, one among many, experienced increasing biological complexity through evolution (fact).

Given enough number of planets and enough time, somewhere else life emerges (inference).

Nature does not set limit on human progress (fact).

Near light speed, fast travel is possible (fact).

There is no known evidence of extraterrestrials visited earth or changing the universe (fact).

We must be arrived relatively early and the emergence rate decreases further back in time (inference).

With a lack of data regarding neighbors' behaviors, based on game theory, the optimal strategy for any civilization is to expand (fact).

There is a tendency for expanding civilizations to eventually universally connect (inference).

10.2 Final Thoughts

We have shown that any given extraterrestrial industrial civilization is highly likely to expand even if the most optimal energy and information utilization efficiency is reached locally given by Jevon's paradox. Furthermore, we have followed the Copernican principle as closely as possible by assuming currently all Earth-like habitable planets contain multi-cellular life forms evolved

to the level of complexity and diversity comparable to the avian, mammalian and reptilian lineages observed on earth. We could not follow the Copernican principle in the strictest sense and assume all habitable planets have evolved into industrial civilizations because it is already contradicted by our current observation in our local galaxy clusters with a high level of confidence (null results from 50 years of SETI and recent WISE data from 100,000 nearby galaxies). On a larger scale, we found that we are possibly the first industrial civilization within the local supercluster. Given the extremely low probability of creating Earth-like conditions and evolving human-like creatures as the initial conditions. Coupled with suitable planet fauna (grass plants), it enables agricultural revolution. Finally, having abundant radioactive material so that project Pacer type of nuclear fusion device and sustaining an industrial civilization without facing collapse because the sun evolved with higher metallicity compared to earlier generations of earth harboring host stars. We followed the assumption led by Alexei and Sharov that the information complexity encoded in genome has been steadily increasing since the emergence of life along with the first terrestrial planets 9.3 Gyrs ago. As a result, we have shown that no extraterrestrial industrial civilization could possibly arrive earlier than 232.74 Mya in the observable universe and no earlier than 26.3 Gya in the entire universe even assuming that the entire universe is 10^{96} larger we observed. As a result, we have eliminated the need to survey sky deeper than 232.74 Mya light years further out from the earth. We also showed the wall of semi-invisibility constrained by the known physical limit on the speed of light. That is, in order to detect the next appearing extra-terrestrial industrial civilization, one has to look further out into more distant regions of sky where the snapshot taken occurs at the time when such extra-terrestrial industrial civilization has not yet been evolved. By calculating and locating the distance between earth-bound observers for even earlier arising industrial civilizations, the distance involved in guaranteeing their appearance, measured in light years, eventually always grows faster than their first arising date measured in years compares to the current time measured in light years. This is the strong case for observational Fermi Paradox. Since we yet to thoroughly survey our sky and detect any signs of extra-terrestrial civilization, there remains a small possibility that detection is possible within our past light cone and we can follow the Copernican principle even more closely by assuming more fractions of the habitable planets have evolved into industrial civilizations and appearing at a closer distance to earth. However, we have shown again that such civilization likely to expand near the speed of light so that no prior warning and observation can be made from earth's vantage point. That is, the delay between the extra-terrestrials' first detection in the sky as an astronomical phenomenon and their physical arrival is shorter than cosmic timescale and even possibly human cultural time scale. This completes the second case of observational Fermi Paradox.

Both cases imply that the expansion can already be well underway yet we could not possibly make any detection.

We have also shown that given the sheer size of the universe, the number of arising industrial civilizations is probably infinite in number. If each is driven by economic incentive and optimal

strategy according to cosmic Nash equilibrium outlined, they will expand and construct their wormhole networks at or close to the speed of light. Eventually, every industrial civilization in the universe is likely to meet each other and connect with each other. If such scenario is possible, then one can reach to a much more, possibly close to infinitely distanced ($3.621 \cdot 10^6 \cdot 10^{10^{122}}$ light years if bounded) corners of the universe (much larger than the size of our observable universe) in a finite amount of time. Obviously, the question of size of the universe can be confirmed. In such a cosmically engineered universe, one should be able to traverse into neighbor's network and witness the birth of one's own civilization through snapshot time travel.

This paper also set up a guideline for various disciplines. It is comprehensible that the future descendants of earth-based industrial civilization will calculate our cosmic evolutionary rate faithfully to millions of decimal precision just as we have calculated the value of π . In order to reach a more precise value for our Years against Background Evolutionary Rate, biologists should continue to find and predict the precise number of species of animals, plants, unicellular, and multi-cellular alike here on earth. Paleontologists should continue to refine their excavation of ancient fossil specimens especially those of the hominid lineage so that the probability of *Homo sapiens* as a species' emergence can be calculated to a great precision. Astro-biologists in the upcoming decades should observe the atmospheric signatures of habitable exoplanets closely and in the upcoming centuries to record and measure the local indigenous habitable planets' bio-complexity and diversity via robots. Astronomers will continue to survey the sky for megastructures with artificial origin. Eventually, we should have enough detailed knowledge about our own position in the cosmic family well before we ever make the first contact with our nearest industrial civilization neighbor.

This is the second edition of the original published version dated Feb 26th, 2018. Significant revisions are made. Word usage, equation corrections, mistakes, typos, and clarifications were updated throughout the chapters. Major revisions are done to Chapter 4 Section 4.7 “Continent Cycle”(added equation derivation steps), Chapter 5 Section 5.3 “Expected Ice Age Interval” (added substantial new content and equations), Section 5.4 “Supercontinent Cycle and Ice Age”(added substantial new content and equations), 5.5 “The Probability of the Hominid Lineage” (added equations and corrected and added tables) Chapter 7 Section 7.1 “Number of Habitable Earth”(updates on the probability on Number of Civilizations), Section 7.3 “The Wall of Semi-Invisibility” (corrected mistakes and added substantial new content and equations), Section 7.4 “7.4 Complexity Equivalence”(added content), Section 7.9 “Observational Equations” (corrected mistakes), Chapter 8 Section 8.2 “Earthbound Democracy” (corrected mistakes added new content and equations), Section 8.5 “Earthbound Ruling Class”(corrected mistakes on equations and graphs), Section 8.6 “Shipbound with Energy Gathering Case”(corrected mistakes on equations and graphs), Section 8.11 “Worm Hole Maintenance Cost” (corrected mistakes on calculations and graphs), Chapter 9 Section 9.1 “E(d, v) Derivation and the Limit of Our Reach”(clarification on previous equations and explanations), Section 9.2 “Connected/Disconnected” (developed more robust explanations), and Section 9.4 “Looking Back in Time” (clarification on previous equations).

Acknowledgments

It has been almost 14 years since I first read about the Fermi Paradox. It has always remained a fascination for me over the possibility of extraterrestrials. I have also been a keen follower of the Kepler mission and the related topics of exoplanets. However, I have never dreamed and imagined to undertake a project like this all by myself from start to finish. What really prompted me to start working on this project was my accidental rediscovery of nuclear fusion using the Project Pacer approach in July 2014. Prior to this date, I always believed that the Fermi Paradox implies a pessimistic future for the humanity. That is, every civilization eventually exhausts its limited fossil fuel stock and dies out. My rediscovery of nuclear fusion gives me hope for the sustainability of the modern industrial infrastructure. Most importantly, being the youngest and an industry outsider I personally knew to have discovered such approach, I become confident enough to believe that I may have the talent and potential to tackle the even greater Fermi Paradox. Over the last few years, I used all of my free time besides work to contemplate over many different issues across many disciplines. Notes have been piled up. As I solidified problems and calculated precision up to my ability, I am finally presenting my results to all. My research serves as a starting framework, and I am eager to collaborate with others across all disciplines to make the calculation more precise and proofs more rigorous. I am thankful for those that helped to shape my academic career including but not limited to: Kenneth J. Goldman, Richard J. Smith, Paul Rothstein, Weixiong Zhang, Bill Smart, Chenyang Lu, David C. Butler, Jon Turner, Lihao Xu, and Xinwen Zhang. This book is also dedicated to my mother and my deceased father.

References

- [1] The nebular theory of the origin of the solar system. [Online]. Available:
- [2] “Renewable biological systems for unsustainable energy production.” *FAO Agricultural Services Bulletins* (1997).
- [3] “What is photosynthesis?”
- [4] *Dimensions of Need: An atlas of food and agriculture*, 1995.
- [5] “converting sunlight into algal biomass wageningen university project,” 2005-2008.
- [6] (2015, September) Earth-like exoplanets may have magnetic fields capable of protecting life. [Online]. Available: <https://exoplanets.nasa.gov/news/217/earth-like-exoplanets-may-have-magnetic-fields-capable-of-protecting-life/>

- [7] (2015, November) Tiny red dwarf star has a magnetic field several hundred times stronger than our sun. [Online]. Available: <https://scitechdaily.com/tiny-red-dwarf-star-has-a-magnetic-field-several-hundred-times-stronger-than-our-sun/>
- [8] (2016, March) Climate effects on human evolution. [Online]. Available: <http://humanorigins.si.edu/research/climate-and-human-evolution/climate-effects-human-evolution>
- [9] C. T. C. Adami C, Ofria C, “Evolution of biological complexity,” *PNAS.*, vol. 97, pp. 4463–8.
- [10] B. Alcott, “Jevons’ paradox,” *Elsevier Ecological Economics*, vol. 54, pp. 9–21, 2005. [Online]. Available: <https://www.sciencedirect.com/science/article/pii/S0921800905001084>
- [11] V. G. Anastassia Makarieva, “On the dependence of speciation rates on species abundance and characteristic population size,” *Journal of Biosciences*, vol. 29, March 2004. [Online]. Available: <http://www.ias.ac.in/article/fulltext/jbsc/029/01/0119-0128>
- [12] R. L. ARMSTRONG, “The persistent myth of crustal growth,” *Australian Journal of Earth Sciences*, vol. 38, pp. 613–630, 1991. [Online]. Available: <http://www.mantleplumes.org/WebDocuments/Armstrong1991.pdf>
- [13] K. Atobe and S. Ida, “Obliquity evolution of extrasolar terrestrial planets,” *Icarus*, 2006. [Online]. Available: <https://arxiv.org/pdf/astro-ph/0611669.pdf>
- [14] P. Bell, “Viral eukaryogenesis: was the ancestor of the nucleus a complex dna virus?” *J Molec Biol.*, vol. 53, p. 251–6, 2001.
- [15] ———, “Sex and the eukaryotic cell cycle is consistent with a viral ancestry for the eukaryotic nucleus,” *J Theor Biol.*, vol. 243, p. 54–63, 2006.
- [16] Y.A. .W. Benz, “Formation and composition of planets around very low mass stars,” *Astronomy and Astrophysics manuscript*, vol. ms rev v3, 2016. [Online]. Available: <https://arxiv.org/pdf/1610.03460v1.pdf>
- [17] R. A. Berner, *Atmospheric oxygen over Phanerozoic time*, 1999.
- [18] N. Bostrom, “Existential risks: analyzing human extinction scenarios and related hazards,” *Journal of Evolution and Technology*, vol. 9, 2002. [Online]. Available: <https://ora.ox.ac.uk/objects/uuid:827452c3-fcba-41b8-86b0-407293e6617c>
- [19] Britannica. Principle of mediocrity. [Online]. Available: <https://www.britannica.com/topic/principle-of-mediocrity>

- [20] A. I. S. K. C. J. Hawkesworth, “Evolution of the continental crust,” *Nature*, vol. 443, 2006.
- [21] R. M. Canup, “On a giant impact origin of charon, nix, and hydra,” *The Astronomical Journal*, vol. 141, no. 2, 2010. [Online]. Available: <http://iopscience.iop.org/article/10.1088/0004-6256/141/2/35/meta>
- [22] J. Catanzarite and M. Shao, “The occurrence rate of earth analog planets orbiting sunlike stars,” p. 19, 2011. [Online]. Available: <https://arxiv.org/ftp/arxiv/papers/1103/1103.1443.pdf>
- [23] M. Cavalli-Sforza, L. Luca, *The History and Geography of Human Genes*, 1996.
- [24] G. Chabrier, “Galactic stellar and substellar initial mass function,” 2003. [Online]. Available: <https://arxiv.org/pdf/astro-ph/0304382.pdf>
- [25] B. K. G. Charles H. Lineweaver, Yeshe Fenner, “The galactic habitable zone and the age distribution of complex life in the milky way,” *Science*, January 2004. [Online]. Available: <https://arxiv.org/ftp/astro-ph/papers/0401/0401024.pdf>
- [26] T. M. D. Charles H. Lineweaver, “Does the rapid appearance of life on earth suggest that life is common in the universe?” *ASTROBIOLOGY*, vol. 2, no. 3, 2002. [Online]. Available: <http://www.mso.anu.edu.au/~charley/papers/LineweaverDavis.pdf>
- [27] R. W. M. Charles J. Call, “A novel fusion power concept based on molten-salt technology: Pacer revisited,” *Nuclear Science and Engineering*, 1990. [Online]. Available: <http://www.ralphmoir.com/wp-content/uploads/2012/10/novFus90.pdf>
- [28] N. R. M. Cin-Ty A. Lee, “Rise of the continents,” *GEOCHEMISTRY*, 2015. [Online]. Available: <https://static1.squarespace.com/static/54b9bb6fe4b07b4a7d145b55/t/5596e6b9e4b059fd6c6117e3/1435952825168/117-Lee-McKenzieNewsandViews2015.pdf>
- [29] ckersch. (2015, February) Is there a theoretical maximum size for rocky planets? [Online]. Available: <https://worldbuilding.stackexchange.com/questions/9948/is-there-a-theoretical-maximum-size-for-rocky-planets>
- [30] G. Constable, *Grasslands and Tundra.*, 1985.
- [31] K. K. R. David Oakley Hal, *Biochemistry (2nd ed.)*, 1999.
- [32] C. D. David T. Johnstona, Simon W. Poultonc, “An emerging picture of neoproterozoic ocean chemistry: Insights from the chuar group, grand canyon, usa,” *JOURNAL OF MAGNETIC RESONANCE IMAGING*, 2009. [Online]. Available: <http://nrs.harvard.edu/urn-3:HUL.InstRepos:10059265>

- [33] C. D. Drake JW, Charlesworth B, “Rates of spontaneous mutation,” *Genetics*, vol. 148, p. 1667–86, April 1998.
- [34] S. G. Engle and E. F. Guinan, “Red dwarf stars: Ages, rotation, magnetic dynamo activity and the habitability of hosted planets,” *the Pacific Rim Conference on Stellar Astrophysics ASP Conference Series*, 2011. [Online].
- [35] D. Esker. (2009) Dinosaurtheory - the blue planet-the fallacy of an unchanging world. [Online].
- [36] ——. (2009) Dinosaurtheory - the thick mesozoic atmosphere. [Online].
- [37] B. G. et al., “Synchronous locking of tidally evolving satellites,” *Icarus*, vol. 122, pp. 166–192. [Online]. Available: <https://www.sciencedirect.com/science/article/pii/S0019103596901177>
- [38] K. K. Furusawa C, “Origin of complexity in multicellular organisms,” *Phys. Rev. Lett*, vol. 84, pp. 6130–3.
- [39] K. S. G. Schubert, “Planetary magnetic fields: Observations and models,” *Elsevier - Physics of the Earth and Planetary Interiors*, vol. 187, pp. 92–108, 2011. [Online]. Available: <http://www.maths.gla.ac.uk/~rs/res/B/PlanetDyn/Schubert2011.pdf>
- [40] . A. K. Gaspard Duch, “Stellar multiplicity,” *Annu. Rev. Astron. Astrophys.*, vol. 1056-8700, 2013. [Online]. Available: <https://arxiv.org/pdf/1303.3028.pdf>
- [41] C. H. L. . D. Grether, “What fraction of sun-like stars have planets?” *University of New South Wales*. [Online]. Available: <http://www.mso.anu.edu.au/~charley/papers/LineweaverGrether03.pdf>
- [42] B. Handwerk. (2014, September) How climate change may have shaped human evolution. [Online]. Available: <https://www.smithsonianmag.com/science-nature/how-climate-change-may-have-shaped-human-evolution-180952885/?no-ist>
- [43] J. D. Haqq-Misra and S. D. Baum, “The sustainability solution to the fermi paradox,” *Elsevier Ecological Economics*, 2009. [Online]. Available: <https://arxiv.org/ftp/arxiv/papers/0906/0906.0568.pdf>
- [44] B. Harder. (2002, March) Inner earth may hold more water than the seas.
- [45] A. G. Hartl, D. L. Clark, *Principles of Population genetics, 4th ed.*, 2007, vol. 243.
- [46] R. Heinberg, *The Party’s Over: Oil, War and the Fate of Industrial Societies*, June 2005.
- [47] M. Hubbert, “Energy resources: a report to the committee on natural resources of the national academy of sciences–national research council,” December 1962.

- [48] S. S. D. J. T. Wright, R. Griffith, “The g infrared search for extraterrestrial civilizations with large energy supplies. ii. framework, strategy, and first result,” *The Astrophysical Journal*, June 2014. [Online]. Available: <https://arxiv.org/pdf/1408.1134.pdf>
- [49] A. M. W. Jason X. Prochaska, Eric Gawiser, “The age-metallicity relation of the universe in neutral gas: The first 100 damped Ly α systems,” *Astrophysical Journal Letters*, 2003. [Online]. Available: <https://arxiv.org/pdf/astro-ph/0305314.pdf>
- [50] Jim2B. (2015, April) What is the minimum planetary mass to hold an atmosphere over geologic time scales? [Online]. Available: <https://worldbuilding.stackexchange.com/questions/13583/what-is-the-minimum-planetary-mass-to-hold-an-atmosphere-over-geologic-time-scal>
- [51] D. C. John W. Drake, Brian Charlesworth, “Rates of spontaneous mutation,” *GENETICS*, no. 4, pp. 1667–1686, April 1998. [Online]. Available: <http://www.genetics.org/content/148/4/1667>
- [52] R. Kopp, *The Paleoproterozoic snowball Earth: A climate disaster triggered by the evolution of oxygenic photosynthesis*, June 2005.
- [53] J. Korenaga, “On the likelihood of plate tectonics on super-earths: Does size matter?” *The Astrophysical Journal Letters*, p. L43–L46, April 2010. [Online]. Available: <https://people.earth.yale.edu/sites/default/files/korenaga10b.pdf>
- [54] S. Krasnikov, “The quantum inequalities do not forbid spacetime shortcuts,” May 2003. [Online]. Available: <https://arxiv.org/pdf/gr-qc/0207057.pdf>
- [55] P. Kroupa, “The initial mass function of stars:evidence for uniformity in variable systems,” *SCIENCE*, vol. 295, p. 82–91, 2002. [Online]. Available: <https://arxiv.org/pdf/astro-ph/0201098.pdf>
- [56] A. Kukla, *Extraterrestrials: A Philosophical Perspective*, 2009. [Online]. Available: <https://worldbuilding.stackexchange.com/questions/9948/is-there-a-theoretical-maximum-size-for-rocky-planets>
- [57] J. H. Kunstler, *The Long Emergency: Surviving the End of Oil, Climate Change, and Other Converging Catastrophes of the Twenty-First Cent*, March 2006.
- [58] R. Kurzweil. (2001, March) The law of accelerating returns. [Online]. Available: <http://www.kurzweilai.net/the-law-of-accelerating-returns>
- [59] K. Lewis, “Moon formation and orbital evolution in extrasolar planetary systems - a literature review,” *EPJ Web of Conferences*, vol. 11, no. 04003, 2011. [Online]. Available:

- [60] C. H. Lineweaver, “An estimate of the age distribution of terrestrial planets in the universe: Quantifying metallicity as a selection effect,” *Icarus*, vol. 187, p. 13, 2001. [Online]. Available: <https://arxiv.org/pdf/astro-ph/0012399.pdf>
- [61] C. H. LINEWEAVER, “Paleontological tests: Human-like intelligence is not a convergent feature of evolution,” *65th International Astronautical Congress, Toronto, Canada, IAF*, N/A. [Online]. Available: <https://arxiv.org/ftp/arxiv/papers/0711/0711.1751.pdf>
- [62] M. J. Longo Giuseppe Montévil Maël. Dinneen, “Computation, physics and beyond.” *Lecture Notes in Computer Science*, vol. 97, pp. 289–308.
- [63] A. Lyon, *Why are Normal Distributions Normal?*, 2014.
- [64] M. E. M. M. A. Khamehchi, Khalid Hossain, “Negative-mass hydrodynamics in a spin-orbit-coupled bose-einstein condensate,” *The Astrophysical Journal*, April 2017. [Online]. Available: <https://arxiv.org/pdf/1612.04055.pdf>
- [65] D. R. P. M. G. Gowanlock and S. M. McConnell, “A model of habitability within the milky way galaxy,” p. 40, 2011. [Online]. Available: <https://arxiv.org/pdf/1107.1286.pdf>
- [66] I. D. Milan M. Cirkovic, Branislav Vukotic, “Galactic punctuated equilibrium: How to undermine carter’s anthropic argument in astrobiology,” *Astrobiology*, 2009. [Online]. Available: <https://arxiv.org/ftp/arxiv/papers/0912/0912.4980.pdf>
- [67] N/A, “Properties of the pluto-charon binary,” February N/A. [Online]. Available: <https://authors.library.caltech.edu/51983/7/Canup.SOM.pdf>
- [68] C. S. Nachman MW, “Estimate of the mutation rate per nucleotide in humans,” *Genetics*, vol. 156, p. 297–304, September 2000.
- [69] Nicholson-W. (2000, March) Setting the scientific record straight on humanity’s evolutionary prehistoric diet and ape diets. [Online]. Available: <http://www.beyondveg.com/nicholson-w/hb/hb-interview1f.shtml>
- [70] P. F. R. Nicolas Flament, Nicolas Coltice, “A case for late-archaeon continental emergence from thermal evolution models and hypsometry,” *Earth and Planetary Science Letters*, vol. 275, November 2008. [Online]. Available:
- [71] A. Oren, “Prokaryote diversity and taxonomy: current status and future challenges,” *Philos. Trans. R. Soc. Lond. B Biol. Sci.*, vol. 359, p. 623–38.
- [72] D. J. B. Peter J. Franks, Dana L. Royer, *New constraints on atmospheric CO₂ concentration for the Phanerozoic*, July 2014, vol. 31.

- [73] T. Physicist. (2013, April) What kind of telescope would be needed to see a person on a planet in a different solar system? [Online]. Available: <http://www.askamathematician.com/2013/04/q-what-kind-of-telescope-would-be-needed-to-see-a-person-on-a-planet-in-a-different-solar-system/>
- [74] B. I. Pisciotta JM, Zou Y, *Light-Dependent Electrogenic Activity of Cyanobacteria*, 2010, vol. 5.
- [75] P.Z.Myers. The mediocrity principle. [Online]. Available:
- [76] J. G. Raven P.H, *Carol J. Mills, ed. Understanding Biology (3rd ed.)*, 1995.
- [77] J. Rennie. (2014, 18) “how does the hubble parameter change with the age of the universe?” general relativity - how does the hubble parameter change with the age of the universe? - physics stack exchan. [Online]. Available: <http://physics.stackexchange.com/questions/136056/how-does-the-hubble-parameter-change-with-the-age-of-the-universe>
- [78] A. K. P. Richard L. Magin PhD, John K. Lee BS, “Biological effects of long-duration, high-field (4 t) mri on growth and development in the mouse,” *JOURNAL OF MAGNETIC RESONANCE IMAGING*, vol. 12, pp. 140–149, 2000. [Online]. Available: <http://www.brl.uiuc.edu/Publications/2000/Magin-JMRI-140-2000.pdf>
- [79] ———, “Biological effects of long-duration, high-field (4 t) mri on growth and development in the mouse,” *JOURNAL OF MAGNETIC RESONANCE IMAGING*, vol. 12, pp. 140–149, 2000. [Online]. Available: <http://www.brl.uiuc.edu/Publications/2000/Magin-JMRI-140-2000.pdf>
- [80] S. A. Roach JC, Glusman G, “Analysis of genetic inheritance in a family quartet by whole-genome sequencing,” *Science*, vol. 328, p. 636–9, April 2010.
- [81] R. L. Rudnick, “Making a continental crust,” *Review Article*, N/A. [Online].
- [82] M. Ruse, *Monad to man: the Concept of Progress in Evolutionary Biology*.
- [83] C. A. H.-M. S Seager, M Kuchner, “Mass-radius relationships for solid exoplanets,” *The Astrophysical Journal*, vol. 669, no. 1279 1297, 2007. [Online]. Available: <http://seagerexoplanets.mit.edu/ftp/Papers/Seager2007.pdf>
- [84] C. SB, “Chance and necessity: the evolution of morphological complexity and diversity,” *Nature*, vol. 409, pp. 1102–9.
- [85] H. J. Schloss P, “Status of the microbial census,” *Microbiol Mol Biol Rev.*, vol. 68, p. 686–91, 2004.

- [86] E. L. Schneider S, “Estimation of past demographic parameters from the distribution of pairwise differences when the mutation rates vary among sites: application to human mitochondrial dna,” *Genetics*, vol. 152, p. 1079–89, July 1999.
- [87] R. G. Sharov Alexei A, “Life before earth,” vol. [1304.3381], March 2013. [Online]. Available: <https://arxiv.org/abs/1304.3381>
- [88] L. Stryer, “Biochemistry (2nd ed.),” *Science*, vol. 328, p. 448, 1981.
- [89] A. S. Stuart Armstrong, “Eternity in six hours: Intergalactic spreading of intelligent life and sharpening the fermi paradox,” *Elsevier Acta Astronautica*, vol. 89, March 2013. [Online]. Available: <https://pdfs.semanticscholar.org/847d/8dabb12f67124868af0876c77538e4fd1c60.pdf>
- [90] H. K. Suzan Bongers, Pauline Slottje, “P227 long term exposure to static magnetic fields in mri manufacturing and risk of developing hypertension,” *BMJ Journal*, September 2016.
- [91] A. Szoke and R. W. Moir, “Peaceful nuclear explosions a practical route to fusion power,” *Technology Review*, July 1991. [Online]. Available: <http://www.ralphmoir.com/wp-content/uploads/2012/10/pracFus91.pdf>
- [92] J. Tainter, *The Collapse of Complex Societies*, 1988.
- [93] L. N. Trefethen, “Predictions for scientific computing fifty years from now,” *Oxford University Computing Laboratory*, p. 10, June 1998. [Online]. Available: <http://eprints.maths.ox.ac.uk/1304/1/NA-98-12.pdf>
- [94] A. J. C. Tsvi Piran, Raul Jimenez, “Formation and composition of planets around very low mass stars,” 2016. [Online]. Available: <https://arxiv.org/pdf/1508.01034.pdf>
- [95] R. J. Tsvi Piran, “On the role of grbs on life extinction in the universe,” November 2014. [Online]. Available: <https://arxiv.org/pdf/1409.2506.pdf>
- [96] J. P. Vallee, “Observations of the magnetic fields inside and outside the solar system: From meteorites (~ 10 attoparsecs), asteroids, planets, stars, pulsars, masers, to protostellar cloudlets (< 1 parsec),” January 1998. [Online]. Available: <https://ned.ipac.caltech.edu/level5/March03/Vallee/paper.pdf>
- [97] V.G.Gurzadyan, “Kolmogorov complexity, string information, panspermia and the fermi paradox,” p. 5, 2005. [Online]. Available: <https://arxiv.org/pdf/physics/0508010.pdf>
- [98] B. Vukotic and M. M. Cirkovic, “On the timescale forcing in astrobiology,” *Serb. Astron. J.*, no. 175, p. 7, May 2007. [Online]. Available: <https://arxiv.org/pdf/0712.1508.pdf>

- [99] A. Williams. (2014, August) Scientists detect evidence of 'oceans worth' of water in earth's mantle. [Online]. Available: <https://www.astrobio.net/news-exclusive/scientists-detect-evidence-oceans-worth-water-earths-mantle/>
- [100] M. I. Y Takashima, J Miyakoshi, "Genotoxic effects of strong static magnetic fields in dna-repair defective mutants of drosophila melanogaster," *Journal of radiation*, vol. 45, pp. 393–397, 2004.
- [101] Y. Yu, "China's historical average crop yields per acre survey," *China Academic Journal Publishing House*, p. 13, 2013. [Online]. Available: <https://wenku.baidu.com/view/dfee90bc6bec0975f465e2d3.html>
- [102] C. Yukna. Mysteries of the dinosaur epoch cases solved? [Online].
- [103] S. S. Zhu, "Gravitational effect on the final stellar to planetary mass ratio," February 2018.